EMERGING INFECTIOUS DISEASES®

CDC Centers for Disease Control and Prevention

Crimean-Congo Hemorrhagic Fever

May 2024

Vladimir Donatovich Orlovsky (1842–1914) *Harvest* (1882). Oil on canvas, 24.4 in x 39.4 in/62 cm x 100 cm. National Art Museum of Ukraine, Kyiv, Ukraine. Photo credit: Alfredo Dagli Orti. Digital image from Art Resource, New York, New York, USA.

EMERGING INFECTIOUS DISEASES®

Emerging Infectious Diseases is published monthly by the Centers for Disease Control and Prevention, 1600 Clifton Rd NE, Mailstop H16-2, Atlanta, GA 30329-4018, USA. Telephone 404-639-1960; email, eideditor@cdc.gov

EMERGING INFECTIOUS DISEASES®

Crimean-Congo Hemorrhagic Fever **May 2024**

On the Cover

Vladimir Donatovich Orlovsky (1842–1914) *Harvest* (1882). Oil on canvas, 24.4 in x 39.4 in/62 cm x 100 cm. National Art Museum of Ukraine, Kyiv, Ukraine. Photo credit: Alfredo Dagli Orti. Digital image from Art Resource, New York, New York, USA.

About the Cover p. 1063

Synopses

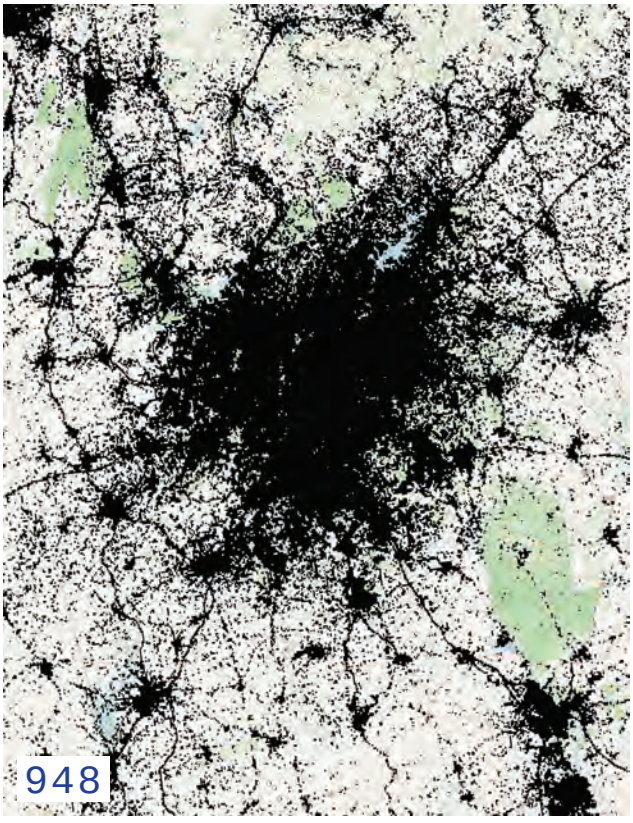

Research

EMERGING INFECTIOUS DISEASES®
May 2024

Dispatches

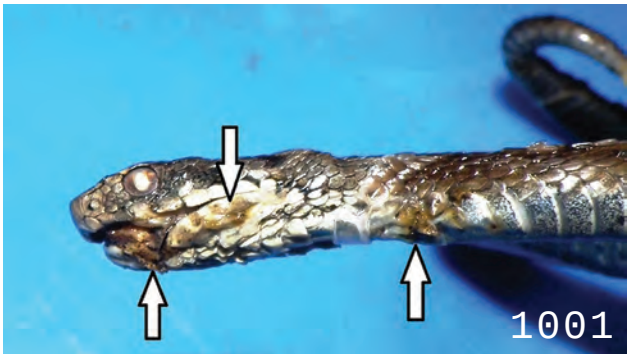

Research Letters

EMERGING INFECTIOUS DISEASES®
May 2024

About the Cover

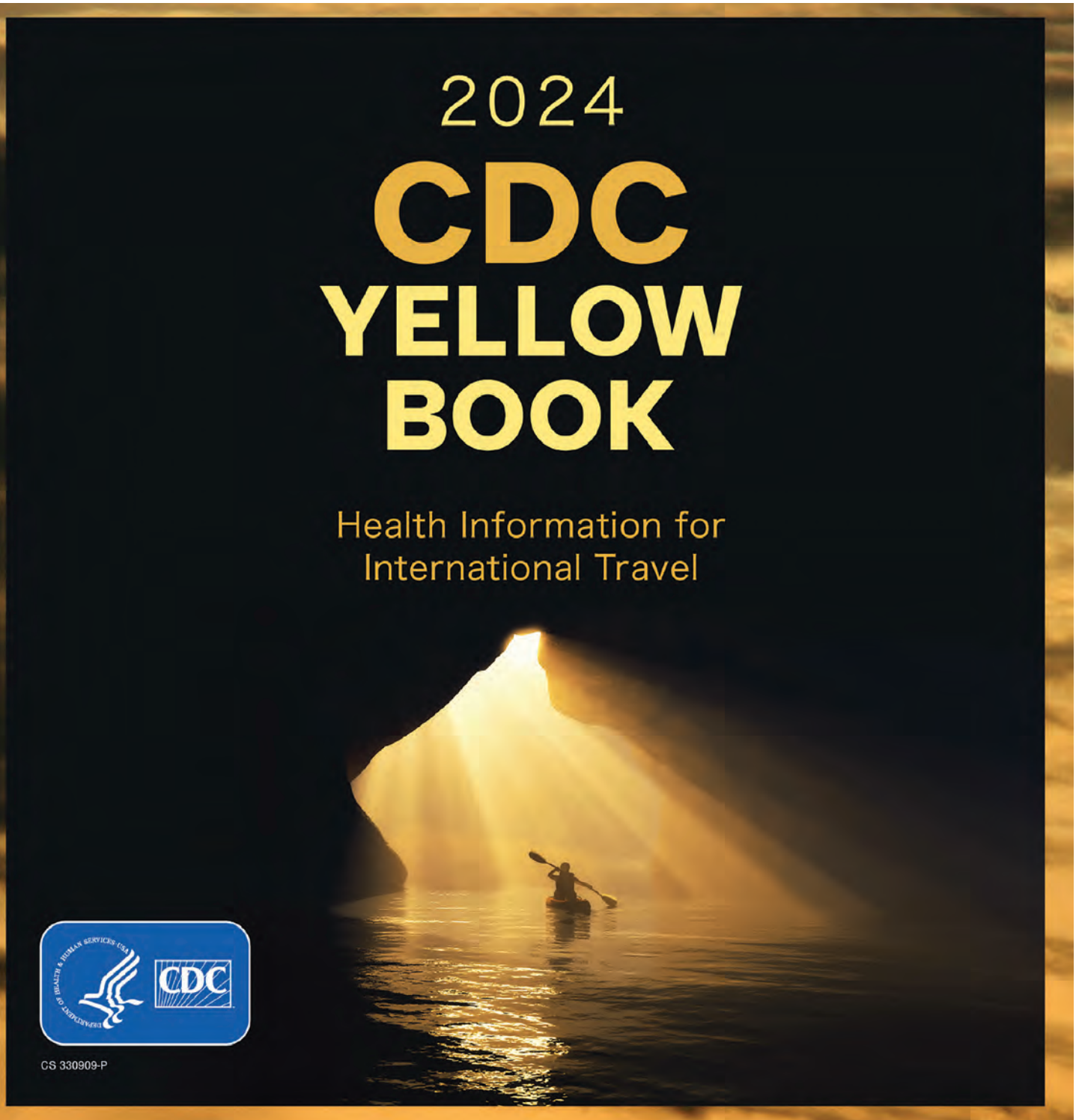

Launch of CDC Yellow Book 2024 – A Trusted Travel Medicine Resource

CDC is pleased to announce the launch of the CDC Yellow Book 2024. The CDC Yellow Book is a source of the U.S. Government's recommendations on travel medicine and has been a trusted resource among the travel medicine community for over 50 years. Healthcare professionals can use the print and digital versions to find the most up-to-date travel medicine information to better serve their patients' healthcare needs.

The CDC Yellow Book is available in print through Oxford University Press and online at www.cdc.gov/yellowbook.

Crimean Congo-Hemorrhagic Fever Virus for Clinicians—Virology, Pathogenesis, and Pathology

Maria G. Frank, Gretchen Weaver, Vanessa Raabe;[1] State of the Clinical Science Working Group of the National Emerging Pathogens Training and Education Center's Special Pathogens Research Network

Crimean-Congo hemorrhagic fever (CCHF), caused by CCHF virus, is a tickborne disease that can cause a range of illness outcomes, from asymptomatic infection to fatal viral hemorrhagic fever; the disease has been described in >30 countries. We conducted a literature review to provide an overview of the virology, pathogenesis, and pathology of CCHF for clinicians. The virus life cycle and molecular interactions are complex and not fully described. Although pathogenesis and immunobiology are not yet fully understood, it is clear that multiple processes contribute to viral entry, replication, and pathological damage. Limited autopsy reports describe multiorgan involvement with extravasation and hemorrhages. Advanced understanding of CCHF virus pathogenesis and immunology will improve patient care and accelerate the development of medical countermeasures for CCHF.

Crimean-Congo hemorrhagic fever (CCHF) was clinically categorized as a disease during World War II when, after being exposed to ticks, ≈200 soldiers from the Soviet Union stationed in the Crimean Peninsula during 1944–1945 developed hemorrhagic fever symptoms, as part of an illness initially termed Crimean hemorrhagic fever. Similar clinical features had been described in present-day Tajikistan and Uzbekistan as early as the 12th Century (*1*,*2*). An enveloped, single-stranded RNA virus isolated from an infected patient in 1967 was named Crimean hemorrhagic fever virus. Another virus (Congo virus) was identified following a hemorrhagic fever outbreak in the current Democratic Republic of the Congo (formerly Zaire) in 1956 (*2*). In the early 1970s, the name was changed to Crimean-Congo hemorrhagic fever virus (CCHFV), after Crimean hemorrhagic fever virus and Congo viruses were found to be serologically indistinguishable in 1967.

Human CCHFV infection mainly occurs through the bite of an infected tick or exposure to blood or tissue from infected animals; human-to-human transmission, particularly in healthcare settings, has been reported (*3*–*5*). Approximately 10,000–15,000 CCHF cases are estimated to occur worldwide each year, but more definitive numbers are difficult to ascertain. Uncertainty arises because up to 88% of cases are thought to be subclinical (*6*–*8*), unrecognized, or occur in locations with limited disease surveillance or laboratory testing capability; also, the case definition for CCHF is not standardized across endemic regions (*9*,*10*). A recent worldwide systematic review and meta-analysis, using data collected during 1974–2020, reported an overall case-fatality rate of 11.7% for humans with acute CCHFV infection (defined as presence of live virus, viral antigen, or RNA), a prevalence of 22.5% (n = 35,198), recent infection (defined as presence of IgM) seroprevalence of 11.6% (n = 27,173), and an overall past infection (defined as presence of IgG) seroprevalence of 4.3% (n = 74,900) in humans (*11*).

CCHFV is an enveloped, multisegmented, single-stranded, negative-sense RNA virus (genus *Orthonairovirus*, order Bunyavirales, family Nairoviridae). The viral genome exists as 3 single-stranded, negative-sense RNA molecules, leading to a complex replication program. Replication of the trisegmented CCHFV genome is error prone, leading to antigenic drift

Author affiliations: Denver Health and Hospital Authority, Denver, Colorado, USA (M.G. Frank); University of Colorado School of Medicine, Denver (M.G. Frank); University of Massachusetts Chan Medical School, Worchester, Massachusetts, USA (G. Weaver); New York University Grossman School of Medicine, New York, New York, USA (V. Raabe)

DOI: https://doi.org/10.3201/eid3005.231646

[1]Current affiliation: Pfizer Inc., New York, New York, USA. These materials reflect only the personal views of the author and may not reflect the views of her employer.

[2]Members of this group are listed at the end of this article.

resulting in 7 distinct genotypes (*12*). CCHFV binds to an unknown cell receptor; however, the low-density lipoprotein receptor (LDLR) has recently been proposed as critical for CCHFV cell entry (*13*). The virus can enter a wide range of human cells, triggering damage both directly as a result of viral infection and indirectly by modifying vascular permeability and eliciting a proinflammatory immune response (*14*).

Disease because of CCHFV infection is limited to humans, although asymptomatic transient viremia lasting up to 15 days has been documented in multiple livestock and wild animals (*15*). Severe or fatal human disease correlates with an exuberant proinflammatory immune response leading to vascular dysfunction, disseminated intravascular coagulation, multiorgan failure, and shock (*16*). Detection of IgM, usually present as early as 4–5 days after illness onset, and IgG, usually present 7–9 days after illness onset, correlate with declining viremia (*17*). However, antibody response to CCHFV does not correlate with disease outcomes or protection through vaccination (*17*).

This first article in a 3-part series summarizing the main aspects of CCHF is meant to provide clinicians with an overview of the virology, pathogenesis, and pathology of CCHF. The second article focuses on epidemiology, clinical features, and prevention and control of CCHF (*18*) and the third on diagnostic testing and management of CCHF (*19*).

Methods

The focused review for this paper involved MeSH (National Center for Biotechnology, https://www.ncbi.nlm.nih.gov/mesh) and PubMed (https://pubmed.ncbi.nlm.nih.gov) search strings customized for CCHF/CCHFV. We focused our review on human data from the past 10 years when available; we included older data or data from animal cases where appropriate. We conducted title, abstract, and full text reviews of relevant manuscripts, reviews, and book chapters. We also completed bibliography scans on reviewed articles and meta-analyses.

Virology

CCHFV virions are pleiomorphic, but mostly spherical, and measure 80–120 nm in diameter (*2*). The natural cycle of CCHFV involves both domestic and wild animals as hosts, with ticks from *Hyalomma* (CCHFV's main vector), *Rhipicephalus*, and *Dermacentor* genera as vectors and reservoirs (*12*). The natural cycle includes transovarial (vertical) and transstadial (horizontal) transmission among ticks and transmission between ticks and their vertebrate hosts. Humans are considered dead-end or accidental hosts for the virus because they are not a source of infection for ticks. CCHFV virions contain a trisegmented, negative-sense RNA genome comprised of the small (S) segment, which encodes the nucleocapsid protein (NP) and nonstructural protein (NS); medium (M) segment, which encodes membrane glycoproteins Gn and Gc as well as several NS; and large (L) segment, which encodes the RNA-dependent RNA polymerase (RdRp) (*7*,*20*,*21*).

The S segment (NSs) encodes the NP, which is composed of a globular domain and protruding arm, and a small NS (*12*). The NP interacts with viral RNA to form ribonucleoprotein (RNP) complexes. The NP also performs endonuclease activity that promotes viral replication, transcription, and assembly, and interacts with host heat shock proteins during intracellular replication of the virus (*22*,*23*). It has been postulated that both NP and NS might have a role in cellular apoptosis as well (*22*).

The M segment encodes a polyprotein that results in 2 transmembrane glycoproteins, Gn and Gc, and NS, such as GP160/85 that is further processed into GP38, a mucin-like domain (MLD), and M-segment nonstructural protein (NSm) after cleavage (*12*,*21*,*22*). Gn and Gc stud the virion lipid envelope as spikes. Gc is assumed to be responsible for binding to cellular receptors and has recently been described binding to the LDLR present in various human cells; of note, the LDLR density is directly correlated with CCHFV infectivity (*13*). Gc has been identified as the target for neutralizing antibodies generated during the infection course as well (*17*). Gn contributes to membrane fusion (*17*). MLD and GP38 may play roles in glycoprotein processing and incorporation into virions (*23*). Both NSs and NSm have been postulated to have roles in interferon antagonism (*17*,*24*).

The L segment encodes a single, large protein containing RdRp enzyme and cap-snatching mechanisms required for genome replication (*23*,*26*). The RdRP protein also harbors an ovarian tumor protease (OTU) that may function as an inhibitor of the multiple host-cell antiviral mechanisms in the interferon-signaling pathway (*12*,*27*,*28*).

As for most viruses in the Nairoviridae family, the replication cycle for CCHFV commences after the binding of the viral glycoprotein, Gc for CCHFV, to a host cell receptor, potentially LDLR, leading to receptor-mediated endocytosis (*13*). Reduced pH in the endosome provokes a change in glycoprotein morphology with consequent fusion of endosomal membrane and envelope resulting in release of ribonucleoprotein into cytosol. The genomic ribonucleoprotein acts as the template for

RdRp-generating virus mRNA, which is translated into viral proteins and cRNA which serves as the template for genomic viral RNA (vRNA) production. New ribonucleoprotein is formed by association of vRNA, RdRp, and capsid proteins; glycoprotein translation and cleavage into Gc and Gn precursors occur in the endoplasmic reticulum. Further processing and maturation of glycoproteins happens in Golgi complex completing assembly of new virions. Once virion assembly and transport to plasma membrane is complete, virions are released through exocytosis (*1*,*12*,*29*,*30*).

CCHFV is a genetically diverse virus with 20% sequence divergence of S segment, 31% of M segment, and 22% of L segment of virus isolates (*12*). Based on S segment sequence data, 7 CCHFV genotypes correlate with the geographic area of parent virus identification, hence the terminology used by Atkinson to name the different genotypes: Africa 1–3, Asia 1 and 2, and Europe 1 and 2 (*29*,*31*). Those lineages correlate with Carroll's denomination into 6 clades: I (Africa 3), II (Africa 2), III (Africa 1), IV (Asia 1 and 2), V (Europe 1), and VI (Europe 2) (*32*,*33*). Research has shown that CCHFV evolves and acquires genetic diversity through various mechanisms. The virus can accumulate mutations through antigenic drift from a common ancestor. Further, the multisegmented genome enables reassortment events when coinfection with 2 different strains occurs, resulting in a dramatic antigenic shift. Reassortment is especially concerning because it can increase through expanded travel and long-range transport of infected ticks or animals. Finally, there is evidence of recombination between RNA segments of different strains (*12*). Although there is greater genetic diversity within M segment than L and S segments, resulting in Gn and Gc nucleotide diversity, this difference does not render a greater antigenic variety (*12*,*33*).

It has been proposed that differences between viral lineages and their adaptation to regional hosts might affect the severity of human illness (*12*). The AP92 strain of CCHFV was recovered from a *Rhipicephalus* sp. tick in Greece in 1979 (*34*). Based on indirect epidemiologic data, AP92 is thought to be avirulent or have very low virulence in humans. Similar strains have recently been isolated in Turkey and other areas from patients with mild CCHF (*34*–*36*). In contrast, patients in South Africa infected with a reassorted CCHFV strain (M segment mapped to Asian clades, S and L segments mapped to African clades) suffered a higher mortality rate when compared with patients infected with the nonreassorted endemic CCHFV strains (*37*).

Pathogenesis

Although CCHF pathogenesis and immunobiology are not yet fully understood, multiple processes seem to contribute to viral entry, replication, and immune response (Figure). After transmission from an infected tick, CCHFV passes through the epithelium

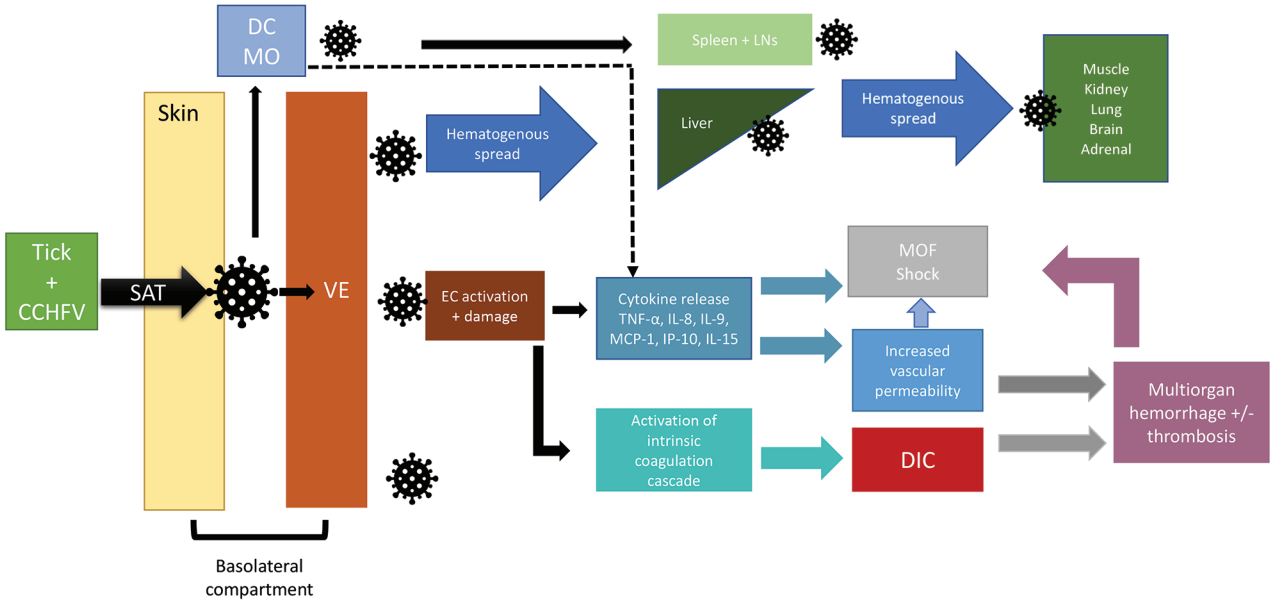

Figure. Flowchart showing an abbreviated proposed pathway for Crimean-Congo hemorrhagic fever virus pathogenesis. CCHFV, Crimean-Congo hemorrhagic fever virus; DC, dendritic cell; DIC, disseminated intravascular coagulation; EC, endothelial cell; IL, interleukin; LN, lymph nodes; MCP, monocyte chemoattractant protein; MO, macrophage; MOF, multiorgan failure; SAT, saliva-assisted transmission; TNF, tumor necrosis factor; VE, vascular endothelium.

into the basolateral compartment of the skin, where it infects endothelial cells of local capillaries and small blood vessels, dendritic cells, and macrophages (*38*). Viral entry is mediated by the Gc component of the envelope protein, which binds to a host cell receptor, likely LDLR, for entry (*13*,*17*).

The shorter CCHF incubation period associated with tick-mediated exposure, as compared with exposure to blood and tissue of infected animals, has been attributed to tick saliva–assisted transmission (SAT) mediating viral entry and replication. Tick saliva contains a mixture of peptide and nonpeptide molecules, as well as water, ions, host proteins, and exosomes (*39*,*40*). Multiple tick saliva components may contribute to SAT by counteracting host-derived vasoconstrictors, inhibiting multiple host cell responses including wound healing, complement pathways, platelet aggregation, local coagulation pathways, and promoting local analgesia by means of bradykinin inhibition (*40*–*42*). The specific tick saliva components mediating SAT might vary depending on the specific tick species.

In vitro, CCHFV replicates in human cell lines from adrenal, bone marrow, brain, cervix, liver, lung, lymphocytes, kidney, muscle, and vascular endothelium (*35*). In vivo, after initial entry and replication, CCHFV spreads hematogenously, leading to potential infection in multiple organs: adrenals, liver, lungs, spleen, and kidneys (*14*,*44*,*45*). Infection of glial cells and astrocytes has been documented in humanized mouse models, but not to date in human patients (*46*).

CCHFV infection results in both direct cellular damage, such as apoptosis, and indirect damage, such as increased vascular permeability through upregulation of soluble adhesion molecules (i.e., E-selectin, vascular cell adhesion molecule 1 [VCAM 1], intracellular adhesion molecule 1 [ICAM 1], and vasoactive molecules) (*14*,*43*). Vascular endothelial damage promotes platelet aggregation and degranulation leading to subsequent activation of the intrinsic coagulation cascade which, in severe cases, culminates in disseminated intravascular coagulation (*14*). CCHFV infection also leads to the release of proinflammatory cytokines which can lead to immune-mediated damage. Robust proinflammatory response has been associated with severe cases and fatal outcomes (*17*). Specifically, positive associations between disease severity and poor prognosis have been correlated with elevated levels of interleukin (IL) 8, IL-9, IL-15, IP-10, TNF-α (tumor necrosis factor-α), and MCP 1 (monocyte chemoattractant protein 1) (*17*). In contrast, RANTES (regulated upon activation, normal T cell expressed and secreted; also called CCL-5 [chemokine ligand 5]) levels appear to have a negative correlation with severity of CCHF (*17*). CCHFV is an interferon-susceptible virus; infected cells delay induction of type-1 interferon, giving the virus time to replicate and spread systemically (*47*).

Immune correlates of protection against and resolution of CCHF remain unknown. IgM and IgG responses are associated with declining viremia, and the generation of an antibody response is associated with better disease outcomes. However, the role of antibodies in controlling infection remains unclear (*17*). It is well documented that severe CCHF cases have minimal humoral immune response (*12*,*48*). Conversely, survivors develop CCHFV-specific humoral and cellular immunity, and to date, reported human reinfection has not been documented (*17*,*27*,*49*,*50*). Studies from CCHFV-infected nonhuman primates suggest that antibody titers and neutralizing activity do not correlate well with severity of disease or outcomes (*45*).

Pathology

To date, few autopsy or necropsy reports of CCHF patients have been published. Histopathologic reports on 2 skin biopsies noted diffuse extravasation of erythrocytes into the epithelial interstitium, associated with hemorrhages in the skin (Appendix reference *51*, https://wwwnc.cdc.gov/EID/article/30/5/23-1646-App1.pdf). Anecdotally, a liver biopsy obtained during a nosocomial outbreak in South Africa in 1984 showed interhepatocyte infiltration of erythrocytes with diffuse extravasation (Appendix reference *51*). Using electron microscopy, evidence of pericapillary edema and autolysis of hepatocytes, as well as intracytoplasmatic virions in epithelial cells of hepatic sinusoids and portal vessels, were observed (Appendix reference *51*). Evidence of hepatic lesions ranged from disseminated necrosis to multiple necrotic foci. Of note, the foci of viral antigen demonstrated by immunofluorescence was disproportionate to the severity of necrosis, suggesting injury mechanisms other than direct viral cytopathic effect. Thrombus formation in central and portal veins was found in patients with more severe liver involvement (Appendix reference *52*). More recent reviews of liver pathology using immunohistochemistry demonstrated infection of Kupffer cells, hepatic endothelial cells, and hepatocytes, with mononuclear portal inflammation, and necrosis characterized by hemorrhage (*14*). A marked splenic lymphoid apoptosis and lymphocyte depletion with dilated sinusoids were also described (*14*).

Petechial hemorrhage of serosa, liver and spleen capsule, and intestinal hyperemia are visible by macroscopic exam (*12*). Necropsy from an autochthonous case in Spain, in addition to hepatocyte necrosis, demonstrated cytoplasmic macrovesiculation and microvesiculation, complete epithelial denudation of the colon, occasional microthrombi, and bone marrow hemorrhages (Appendix reference *53*). A study from Turkey of 5 confirmed and 14 suspected CCHF cases demonstrated hemophagocytosis with unclear clinical significance in the bone marrow of 7 patients (Appendix reference *54*).

Conclusions

CCHFV is an enveloped, single-stranded RNA, tick-borne virus. The virus life cycle and molecular interactions are complex and not fully described. Although pathogenesis and immunobiology are not yet fully understood and research is needed to fill the gaps, it is clear multiple processes contribute to viral entry, replication, and pathological damage, and limited autopsy reports describe multiorgan involvement with extravasation and hemorrhages. Broadening knowledge about CCHFV pathogenesis and immunology will enable improved patient care and accelerate the development of medical countermeasures for CCHF.

Members of the State of the Clinical Science Working Group of the National Emerging pathogens Training and Education Center's Special Pathogens Research Network: Richard T. Davey, Jr., Noreen A. Hynes, Mark G. Kortepeter, Nahid Bhadelia, Kerry Dierberg, Aneesh K. Mehta, Corri B. Levine, Peter C. Iwen, Denis A. Bente, Justin Chan, and Adam Beitscher.

Acknowledgments

Authors thank the following authors who completed a previous version of this manuscript: Nahid Bhadelia, Kerry Dierberg, and Mark G Kortepeter.

Research reported in this publication was financially supported by the Department of Health and Human Services Office of the Assistant Secretary for Preparedness and Response.

About the Author

Dr. Frank is a hospitalist and medical director of Denver Health Hospital Authority's Biocontainment Unit and a professor of medicine at the University of Colorado School of Medicine. Her research interests include medical management of special pathogens and involvement of general internists in disaster responses.

References

1. Whitehouse CA. Crimean-Congo hemorrhagic fever. Antiviral Res. 2004;64:145–60. https://doi.org/10.1016/j.antiviral.2004.08.001
2. Hoogstraal H. The epidemiology of tick-borne Crimean-Congo hemorrhagic fever in Asia, Europe, and Africa. J Med Entomol. 1979;15:307–417. https://doi.org/10.1093/jmedent/15.4.307
3. Tsergouli K, Karampatakis T, Haidich AB, Metallidis S, Papa A. Nosocomial infections caused by Crimean-Congo haemorrhagic fever virus. J Hosp Infect. 2020;105:43–52. https://doi.org/10.1016/j.jhin.2019.12.001
4. Pshenichnaya NY, Nenadskaya SA. Probable Crimean-Congo hemorrhagic fever virus transmission occurred after aerosol-generating medical procedures in Russia: nosocomial cluster. Int J Infect Dis. 2015;33:120–2. https://doi.org/10.1016/j.ijid.2014.12.047
5. Joubert JR, King JB, Rossouw DJ, Cooper R. A nosocomial outbreak of Crimean-Congo haemorrhagic fever at Tygerberg Hospital. Part III. Clinical pathology and pathogenesis. S Afr Med J. 1985;68:722–8.
6. Whitehouse CA, Ergonul O, editors. Crimean-Congo hemorrhagic fever: a global perspective. Dordrecht (the Netherlands): Springer; 2007.
7. Mishra AK, Hellert J, Freitas N, Guardado-Calvo P, Haouz A, Fels JM, et al. Structural basis of synergistic neutralization of Crimean-Congo hemorrhagic fever virus by human antibodies. Science. 2022;375:104–9. https://doi.org/10.1126/science.abl6502
8. Formenty P. Introduction to Crimean-Congo haemorrhagic fever. 2019 [cited 2023 Jul 1]. https://cdn.who.int/media/docs/default-source/documents/health-topics/crimean-congo-haemorrhaigc-fever/introduction-to-crimean-congo-haemorrhagic-fever.pdf
9. Al-Abri SS, Abaidani IA, Fazlalipour M, Mostafavi E, Leblebicioglu H, Pshenichnaya N, et al. Current status of Crimean-Congo haemorrhagic fever in the World Health Organization Eastern Mediterranean Region: issues, challenges, and future directions. Int J Infect Dis. 2017;58:82–9. https://doi.org/10.1016/j.ijid.2017.02.018
10. Hawman DW, Feldmann H. Recent advances in understanding Crimean-Congo hemorrhagic fever virus. F1000Res. 2018;7:F1000 Faculty Rev-1715. https://doi.org/10.12688/f1000research.16189.1
11. Belobo JTE, Kenmoe S, Kengne-Nde C, Emoh CPD, Bowo-Ngandji A, Tchatchouang S, et al. Worldwide epidemiology of Crimean-Congo hemorrhagic fever virus in humans, ticks and other animal species, a systematic review and meta-analysis. PLoS Negl Trop Dis. 2021;15:e0009299. https://doi.org/10.1371/journal.pntd.0009299
12. Bente DA, Forrester NL, Watts DM, McAuley AJ, Whitehouse CA, Bray M. Crimean-Congo hemorrhagic fever: history, epidemiology, pathogenesis, clinical syndrome and genetic diversity. Antiviral Res. 2013;100:159–89. https://doi.org/10.1016/j.antiviral.2013.07.006
13. Xu ZS, Du WT, Wang SY, Wang MY, Yang YN, Li YH, et al. LDLR is an entry receptor for Crimean-Congo hemorrhagic fever virus. Cell Res. 2024;34:140–50. https://doi.org/10.1038/s41422-023-00917-w
14. Akıncı E, Bodur H, Leblebicioglu H. Pathogenesis of Crimean-Congo hemorrhagic fever. Vector Borne Zoonotic Dis. 2013;13:429–37. https://doi.org/10.1089/vbz.2012.1061
15. Nurettin C, Engin B, Sukru T, Munir A, Zati V, Aykut O. The seroprevalence of Crimean-Congo hemorrhagic fever in wild and domestic animals: an epidemiological update for domestic animals and first seroevidence in wild animals

from Turkiye. Vet Sci. 2022;9:462. https://doi.org/10.3390/vetsci9090462
16. Saksida A, Duh D, Wraber B, Dedushaj I, Ahmeti S, Avsic-Zupanc T. Interacting roles of immune mechanisms and viral load in the pathogenesis of Crimean-Congo hemorrhagic fever. Clin Vaccine Immunol. 2010;17:1086–93. https://doi.org/10.1128/CVI.00530-09
17. Rodriguez SE, Hawman DW, Sorvillo TE, O'Neal TJ, Bird BH, Rodriguez LL, et al. Immunobiology of Crimean-Congo hemorrhagic fever. Antiviral Res. 2022;199:105244. https://doi.org/10.1016/j.antiviral.2022.105244
18. Frank MG, Weaver G, Raabe V; State of the Clinical Science Working Group of the National Emerging pathogens Training and Education Center's Special Pathogens Research Network. Crimean-Congo hemorrhagic fever virus for clinicians—epidemiology, clinical manifestations, and prevention. Emerg Infect Dis. 2024;30:854–863. https://doi.org/10.3201/eid3005.231647
19. Frank MG, Weaver G, Raabe V; State of the Clinical Science Working Group of the National Emerging Pathogens Training and Education Center's Special Pathogens Research Network. Crimean-Congo hemorrhagic fever virus for clinicians—diagnosis, clinical management, and therapeutics. Emerg Infect Dis. 2024;30:864–873. https://doi.org/10.3201/eid3005.231648
20. Wang Y, Dutta S, Karlberg H, Devignot S, Weber F, Hao Q, et al. Structure of Crimean-Congo hemorrhagic fever virus nucleoprotein: superhelical homo-oligomers and the role of caspase-3 cleavage. J Virol. 2012;86:12294–303. https://doi.org/10.1128/JVI.01627-12
21. Golden JW, Fitzpatrick CJ, Suschak JJ, Clements TL, Ricks KM, Sanchez-Lockhart M, et al. Induced protection from a CCHFV-M DNA vaccine requires $CD8^+$ T cells. Virus Res. 2023;334:199173. https://doi.org/10.1016/j.virusres.2023.199173
22. Sanchez AJ, Vincent MJ, Nichol ST. Characterization of the glycoproteins of Crimean-Congo hemorrhagic fever virus. J Virol. 2002;76:7263–75. https://doi.org/10.1128/JVI.76.14.7263-7275.2002
23. Freitas N, Enguehard M, Denolly S, Levy C, Neveu G, Lerolle S, et al. The interplays between Crimean-Congo hemorrhagic fever virus (CCHFV) M segment–encoded accessory proteins and structural proteins promote virus assembly and infectivity. PLoS Pathog. 2020;16:e1008850. https://doi.org/10.1371/journal.ppat.1008850
24. Leventhal SS, Wilson D, Feldmann H, Hawman DW. A look into Bunyavirales genomes: functions of non-structural (NS) proteins. Viruses. 2021;13:314. https://doi.org/10.3390/v13020314
25. Honig JE, Osborne JC, Nichol ST. Crimean-Congo hemorrhagic fever virus genome L RNA segment and encoded protein. Virology. 2004;321:29–35. https://doi.org/10.1016/j.virol.2003.09.042
26. Reguera J, Weber F, Cusack S. Bunyaviridae RNA polymerases (L-protein) have an N-terminal, influenza-like endonuclease domain, essential for viral cap-dependent transcription. PLoS Pathog. 2010;6:e1001101. https://doi.org/10.1371/journal.ppat.1001101
27. Kalkan-Yazıcı M, Karaaslan E, Çetin NS, Hasanoğlu S, Güney F, Zeybek Ü, et al. Cross-reactive anti-nucleocapsid protein immunity against Crimean-Congo hemorrhagic fever virus and Hazara virus in multiple species. J Virol. 2021;95:e02156–20. https://doi.org/10.1128/JVI.02156-20
28. Kaushal N, Baranwal M. Mutational analysis of catalytic site domain of CCHFV L RNA segment. J Mol Model. 2023;29:88. https://doi.org/10.1007/s00894-023-05487-7
29. Lasecka L, Baron MD. The molecular biology of nairoviruses, an emerging group of tick-borne arboviruses. Arch Virol. 2014;159:1249–65. https://doi.org/10.1007/s00705-013-1940-z
30. Hawman DW, Feldmann H. Crimean-Congo haemorrhagic fever virus. Nat Rev Microbiol. 2023;21:463–77. https://doi.org/10.1038/s41579-023-00871-9
31. Atkinson B, Chamberlain J, Logue CH, Cook N, Bruce C, Dowall SD, et al. Development of a real-time RT-PCR assay for the detection of Crimean-Congo hemorrhagic fever virus. Vector Borne Zoonotic Dis. 2012;12:786–93. https://doi.org/10.1089/vbz.2011.0770
32. Atkinson B, Latham J, Chamberlain J, Logue C, O'Donoghue L, Osborne J, et al. Sequencing and phylogenetic characterisation of a fatal Crimean-Congo haemorrhagic fever case imported into the United Kingdom, October 2012. Euro Surveill. 2012;17:20327. https://doi.org/10.2807/ese.17.48.20327-en
33. Carroll SA, Bird BH, Rollin PE, Nichol ST. Ancient common ancestry of Crimean-Congo hemorrhagic fever virus. Mol Phylogenet Evol. 2010;55:1103–10. https://doi.org/10.1016/j.ympev.2010.01.006
34. Papadopoulos O, Koptopoulos G. Isolation of Crimean-Congo haemorrhagic fever (CCHF) virus from *Rhipicephalus bursa* ticks in Greece. Acta Hell Microbiol. 1978;23:20–8.
35. Elevli M, Ozkul AA, Civilibal M, Midilli K, Gargili A, Duru NS. A newly identified Crimean-Congo hemorrhagic fever virus strain in Turkey. Int J Infect Dis. 2010;14(Suppl 3):e213–6. https://doi.org/10.1016/j.ijid.2009.07.017
36. Midilli K, Gargili A, Ergonul O, Elevli M, Ergin S, Turan N, et al. The first clinical case due to AP92 like strain of Crimean-Congo hemorrhagic fever virus and a field survey. BMC Infect Dis. 2009;9:90. https://doi.org/10.1186/1471-2334-9-90
37. Burt FJ, Paweska JT, Ashkettle B, Swanepoel R. Genetic relationship in southern African Crimean-Congo haemorrhagic fever virus isolates: evidence for occurrence of reassortment. Epidemiol Infect. 2009;137:1302–8. https://doi.org/10.1017/S0950268808001878
38. Papa A, Tsergouli K, Tsioka K, Mirazimi A. Crimean-Congo hemorrhagic fever: tick-host-virus interactions. Front Cell Infect Microbiol. 2017;7:213. https://doi.org/10.3389/fcimb.2017.00213
39. Nuttall PA, Labuda M. Tick-host interactions: saliva-activated transmission. Parasitology. 2004;129(Suppl):S177–89. https://doi.org/10.1017/S0031182004005633
40. Nuttall PA. Tick saliva and its role in pathogen transmission. Wien Klin Wochenschr. 2023;135:165–76. https://doi.org/10.1007/s00508-019-1500-y
41. Ali A, Zeb I, Alouffi A, Zahid H, Almutairi MM, Ayed Alshammari F, et al. Host immune responses to salivary components—a critical facet of tick-host interactions. Front Cell Infect Microbiol. 2022;12:809052. https://doi.org/10.3389/fcimb.2022.809052
42. Šimo L, Kazimirova M, Richardson J, Bonnet SI. The essential role of tick salivary glands and saliva in tick feeding and pathogen transmission. Front Cell Infect Microbiol. 2017;7:281. https://doi.org/10.3389/fcimb.2017.00281
43. Dai S, Wu Q, Wu X, Peng C, Liu J, Tang S, et al. Differential cell line susceptibility to Crimean-Congo hemorrhagic fever virus. Front Cell Infect Microbiol. 2021;11:648077. https://doi.org/10.3389/fcimb.2021.648077
44. Bente DA, Alimonti JB, Shieh WJ, Camus G, Ströher U, Zaki S, et al. Pathogenesis and immune response of Crimean-Congo hemorrhagic fever virus in a STAT-1

knockout mouse model. J Virol. 2010;84:11089–100. https://doi.org/10.1128/JVI.01383-10
45. Haddock E, Feldmann F, Hawman DW, Zivcec M, Hanley PW, Saturday G, et al. A cynomolgus macaque model for Crimean-Congo haemorrhagic fever. Nat Microbiol. 2018;3:556–62. https://doi.org/10.1038/s41564-018-0141-7
46. Spengler JR, Kelly Keating M, McElroy AK, Zivcec M, Coleman-McCray JD, Harmon JR, et al. Crimean-Congo hemorrhagic fever in humanized mice reveals glial cells as primary targets of neurological infection. J Infect Dis. 2017;216:1386–97. https://doi.org/10.1093/infdis/jix215
47. Wahid B, Altaf S, Naeem N, Ilyas N, Idrees M. Scoping review of Crimean-Congo hemorrhagic fever (CCHF) literature and implications of future research. J Coll Physicians Surg Pak. 2019;29:563–73. https://doi.org/10.29271/jcpsp.2019.06.563
48. Akinci E, Bodur H, Sunbul M, Leblebicioglu H. Prognostic factors, pathophysiology and novel biomarkers in Crimean-Congo hemorrhagic fever. Antiviral Res. 2016;132:233–43. https://doi.org/10.1016/j.antiviral.2016.06.011
49. Goedhals D, Paweska JT, Burt FJ. Long-lived CD8+ T cell responses following Crimean-Congo haemorrhagic fever virus infection. PLoS Negl Trop Dis. 2017;11:e0006149. https://doi.org/10.1371/journal.pntd.0006149
50. Karaaslan E, Çetin NS, Kalkan-Yazıcı M, Hasanoğlu S, Karakeçili F, Özdarendeli A, et al. Immune responses in multiple hosts to nucleocapsid protein (NP) of Crimean-Congo hemorrhagic fever virus (CCHFV). PLoS Negl Trop Dis. 2021;15:e0009973. https://doi.org/10.1371/journal.pntd.0009973

Address for correspondence: Maria G. Frank, Denver Health and Hospital Authority, 194 South Ulster St, Denver, CO 80230, USA; email: maria.frank@dhha.org, maria.frank@cuanschutz.edu

Crimean-Congo Hemorrhagic Fever Virus for Clinicians—Epidemiology, Clinical Manifestations, and Prevention

Maria G. Frank, Gretchen Weaver, Vanessa Raabe;[1] State of the Clinical Science Working Group of the National Emerging Pathogens Training and Education Center's Special Pathogens Research Network[2]

Medscape CME Activity

In support of improving patient care, this activity has been planned and implemented by Medscape, LLC and Emerging Infectious Diseases. Medscape, LLC is jointly accredited with commendation by the Accreditation Council for Continuing Medical Education (ACCME), the Accreditation Council for Pharmacy Education (ACPE), and the American Nurses Credentialing Center (ANCC), to provide continuing education for the healthcare team.

Medscape, LLC designates this Journal-based CME activity for a maximum of 1.00 ***AMA PRA Category 1 Credit(s)™***. Physicians should claim only the credit commensurate with the extent of their participation in the activity.

Successful completion of this CME activity, which includes participation in the evaluation component, enables the participant to earn up to 1.0 MOC points in the American Board of Internal Medicine's (ABIM) Maintenance of Certification (MOC) program. Participants will earn MOC points equivalent to the amount of CME credits claimed for the activity. It is the CME activity provider's responsibility to submit participant completion information to ACCME for the purpose of granting ABIM MOC credit.

All other clinicians completing this activity will be issued a certificate of participation. To participate in this journal CME activity: (1) review the learning objectives and author disclosures; (2) study the education content; (3) take the post-test with a 75% minimum passing score and complete the evaluation at https://www.medscape.org/qna/processor/71557?showStandAlone=true&src=prt_jcme_eid_mscpedu; and (4) view/print certificate. For CME questions, see page 1067.

NOTE: It is Medscape's policy to avoid the use of brand names in accredited activities. However, in an effort to be as clear as possible, the use of brand names should not be viewed as a promotion of any brand or as an endorsement by Medscape of specific products.

Release date: April 19, 2024; Expiration date: April 19, 2025

Learning Objectives

Upon completion of this activity, participants will be able to:

1. Assess the epidemiology of Crimean-Congo hemorrhagic fever (CCHF)
2. Distinguish the typical clinical pattern of CCHF
3. Analyze specific clinical characteristics of CCHF
4. Evaluate symptoms or signs that might discriminate CCHF from other viral hemorrhagic infections

CME Editor

Jill Russell, BA, Technical Writer/Editor, Emerging Infectious Diseases. *Disclosure: Jill Russell, BA, has no relevant financial relationships.*

CME Author

Charles P. Vega, MD, Health Sciences Clinical Professor of Family Medicine, University of California, Irvine School of Medicine, Irvine, California. *Disclosure: Charles P. Vega, MD, has the following relevant financial relationships: served as a consultant or advisor for Boehringer Ingelheim; GlaxoSmithKline.*

Authors

Maria G. Frank, MD; Gretchen Weaver, MPH; Vanessa Raabe, MD, MSc.

Author affiliations: Denver Health and Hospital Authority, Denver, Colorado, USA (M.G. Frank); University of Colorado School of Medicine, Denver (M.G. Frank); University of Massachusetts Chan Medical School, Worchester, Massachusetts, USA (G. Weaver); New York University Grossman School of Medicine, New York, New York, USA (V. Raabe)

DOI: https://doi.org/10.3201/eid3005.231647

[1]Current affiliation: Pfizer Inc., New York, New York, USA. These materials reflect only the personal views of the author and may not reflect the views of her employer.

[2]Members of this group are listed at the end of this article.

Crimean-Congo hemorrhagic fever (CCHF) is a tickborne infection that can range from asymptomatic to fatal and has been described in >30 countries. Early identification and isolation of patients with suspected or confirmed CCHF and the use of appropriate prevention and control measures are essential for preventing human-to-human transmission. Here, we provide an overview of the epidemiology, clinical features, and prevention and control of CCHF. CCHF poses a continued public health threat given its wide geographic distribution, potential to spread to new regions, propensity for genetic variability, and potential for severe and fatal illness, in addition to the limited medical countermeasures for prophylaxis and treatment. A high index of suspicion, comprehensive travel and epidemiologic history, and clinical evaluation are essential for prompt diagnosis. Infection control measures can be effective in reducing the risk for transmission but require correct and consistent application.

Human Crimean-Congo hemorrhagic fever (CCHF) infection mainly occurs after the bite of an infected tick or exposure to blood or tissues from infected animals; human-to-human transmission, particularly in healthcare settings, has also been reported. Approximately 10,000–15,000 cases of CCHF occur annually worldwide, although more definitive numbers are difficult to ascertain; up to 88% of cases are thought to be subclinical (*1*–*3*), unrecognized, or occur in locations with limited disease surveillance or laboratory testing capability (*4*,*5*). A recent meta-analysis of CCHF-endemic areas reported an overall acute infection prevalence of 22.5%, recent infection seroprevalence of 11.6%, and an overall past infection seroprevalence of 4.3% in humans (*6*).

CCHF causes clinical manifestations in humans ranging from asymptomatic infection to severe hemorrhagic fever. The case-fatality rate (CFR) during outbreaks is typically 5%–30% (*1*), but CFRs of up to 62% have been reported (*7*). Disease caused by CCHF virus (CCHFV) is limited to humans, but asymptomatic transient viremia (lasting ≤15 days) has been documented in livestock and wild animals (*8*). Severe or fatal disease causes proinflammatory immune response that leads to vascular dysfunction, disseminated intravascular coagulation, multiorgan failure, and shock (*9*). The detection of IgM (present as early as day 4–5 of illness) and IgG (present after days 7–9 of illness) correlates with declining viremia, but fatal cases often show no or very late immune response (*10*). However, antibody response to CCHFV does not correlate with disease outcome or protection from vaccines, which, combined with a paucity of available animal models (*11*), makes research on vaccines and treatments challenging. No vaccines or treatments for CCHF have been approved by the US Food and Drug Administration.

This second article in a 3-part series summarizing the main aspects of CCHF is intended to provide clinicians with an overview of the epidemiology, clinical features, and prevention and control of CCHF. The first article focuses on the virology, pathogenesis, and pathology of CCHF (*12*) and the third on diagnostic testing and management of CCHF (*13*).

Methods

The focused review for this paper involved MeSH (National Center for Biotechnology [NCBI], https://www.ncbi.nlm.nih.gov/mesh) and PubMed (https://pubmed.ncbi.nlm.nih.gov) search strings customized for CCHF and CCHFV. We focused our review on the past 10 years and used human data when available; we included older relevant data and animal data where appropriate. We conducted title, abstract, and full text reviews of relevant manuscripts, reviews, and book chapters. We also completed bibliography scans on review articles and meta-analyses.

Epidemiology

CCHF is the most geographically widespread tickborne disease, identified in >30 countries in Africa, Asia, the Middle East, and Europe located south of the 50th parallel north (Figure 1). The annual incidence is estimated to be 10,000–15,000 cases worldwide but has been slowly and steadily rising (*3*). That increase in incidence is thought to be caused by the expanding range of its main vector, *Hyalomma* ticks, and by increased testing (*6*). Most cases occur after tick bites; the second most common means of exposure is through bodily fluids and tissue from infected animals; and last, human-to-human transmission can occur in the healthcare setting.

In recent years, CCHF has been documented in previously unaffected countries, such as Spain and Jordan (*14*–*17*). Although tickborne transmission is the main route for human CCHF, contact with viremic animals, infected humans, or contaminated surfaces (e.g., nosocomial transmission) can also lead to human illness. Persons at the highest risk for CCHF include farmers living in CCHF-endemic areas, participants in recreational activities (e.g., hiking, camping) in endemic areas, slaughterhouse workers, veterinarians, and healthcare workers, who are now considered the second most affected group (*3*,*18*). Transmission to household contacts is uncommon, although horizontal transmission from mother to child has been reported (*19*). Sexual

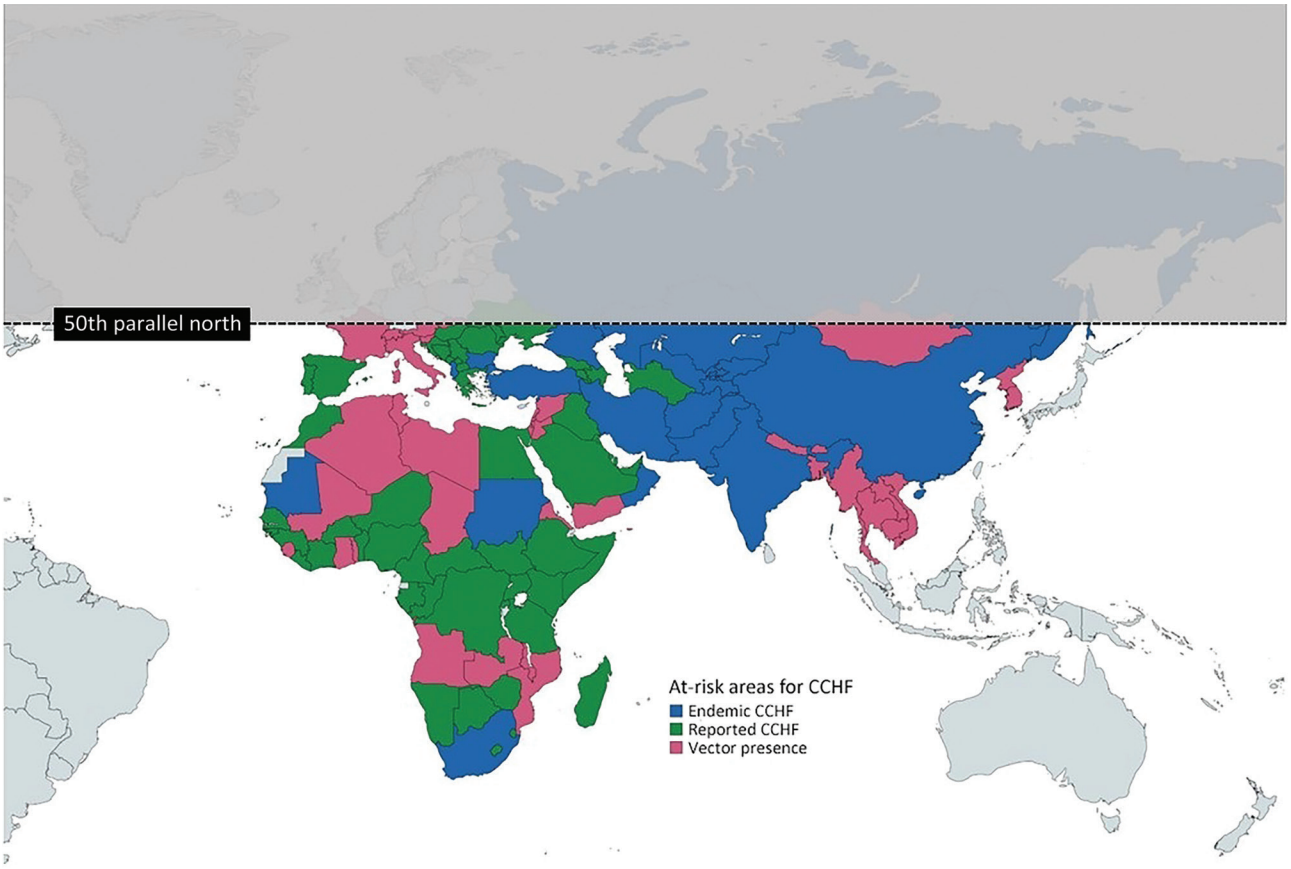

Figure 1. Geographic distribution of CCHF and *Hyalomma* spp. ticks. CCHF, Crimean-Congo hemorrhagic fever.

transmission has been proposed; however, presence of CCHFV in semen or vaginal fluids has yet to be confirmed (*20*). Similarly, airborne transmission has been hypothesized to occur in association with nosocomial and laboratory-acquired CCHF clusters, despite a lack of direct evidence (*21*–*23*). Nosocomial infections are symptomatic in 92.4% of cases, and in 76.5% of those patients, hemorrhagic disease develops; these cases tend to have high mortality (CFR 32.4%) (*23*).

Clinical Features

Incubation Period

The typical incubation period for CCHF is 3–7 days (range 1–13 days); incubation period is shorter (1–5 days) after a tick bite and longer (5–13 days) after exposure to infected blood or tissues (*14*). The accelerated viral dissemination after a tick bite is thought to be caused by a tick saliva–enabling effect, known as saliva-activated transmission, related to bioactive molecules in tick saliva causing antihemostatic, anti-inflammatory, and immunomodulatory effects on the vertebrate host (*14*,*24*).

Clinical Spectrum of Infection

Clinical manifestations of CCHF range from asymptomatic (≤88%) (*3*) infection or mild, nonspecific febrile illness to severe hemorrhagic disease with multiorgan failure leading to death (*14*). CCHF case definitions vary across endemic regions; the case definition proposed in Ergonul et al. (*1*) includes suspect, probable, and confirmed cases (Figure 2).

Clinical Course

CCHF is characterized by an incubation period, as described, followed by prehemorrhagic, hemorrhagic, and convalescent phases (Table; Figure 3). Most patients will recover and transition to the convalescent period; patients who die typically succumb to the disease by day 10.

The prehemorrhagic phase frequently lasts 1–5 days and is usually characterized by nonspecific symptoms. Those symptoms include sudden onset of fever, which lasts for an average of 4–5 days, and nonspecific signs and symptoms such as diarrhea, dizziness, headache, myalgia, nausea, vomiting, and weakness. Headache occurs in almost 70% of patients and tends to be severe. Two thirds of patients describe the

Suspected Case	Probable Case	Confirmed Case
Patient with fever, myalgia, malaise, and diarrhea and History of residence in CCHF-endemic area and recent tick exposure OR residence in or travel to CCHF-endemic area	Suspected case and >1 of leukopenia thrombocytopenia, or elevated AST, ALT, or LDH	Probable case and Evidence of CCHFV in patient's bodily fluids or tissue: · Positive CCHFV IgM in serum · Positive PCR for CCHFV in blood or body fluids

Figure 2. Crimean-Congo hemorrhagic fever case definitions, modified from Ergonul et al. (*1*). ALT, alanine aminotransferase; AST, aspartate aminotransferase; CCHF, Crimean-Congo hemorrhagic fever; CCHFV, CCHF virus; LDH, lactate dehydrogenase.

pain as mimicking a migraine crisis, including throbbing and being accompanied by nausea, vomiting, photophobia, and phonophobia (*25*); half of patients describe the headache as worsening with activity. Characteristically, those patients might also develop upper body (face, neck, and chest) hyperemia, conjunctivitis, and congested sclera. Because of the lack of specificity in clinical manifestations, a high index of suspicion on the basis of a thorough exposure and travel history is essential for recognition.

The hemorrhagic illness phase typically begins 3–5 days after symptom onset and is usually short, lasting 1–3 days. This phase begins with a petechial rash of the skin and mucous membranes and might progress to more severe hemorrhagic features at multiple sites, including ecchymoses; cerebral hemorrhage; bleeding from the nasopharynx, gastrointestinal tract (hematemesis and melena), and genitourinary (hematuria) tract; menometrorrhagia; and hemoptysis (*14*). Epistaxis is present in ≤50% of patients in the hemorrhagic phase, hematemesis in ≤35% of patients, hematuria, melena and hematochezia in 10%–20% of patients, and intraabdominal or intracerebral bleeding in 1%–2% of cases (*1*). Large ecchymoses are present in 30%–45% of patients, and although they are not pathognomonic, their presence should suggest CCHF over other viral hemorrhagic fevers. Hepatosplenomegaly is common and described in up to one third of patients (*1*). Severe disease during this phase is often characterized by anemia, thrombocytopenia, evidence of coagulation abnormalities (prolonged prothrombin time [PT] and activated partial thromboplastin time [aPTT]) and disseminated intravascular coagulation. Liver enzymes, including alanine aminotransferase (ALT) and aspartate aminotransferase (AST), are typically elevated. Renal insufficiency and hypotension are common in severe cases (*14*,*26*,*27*).

During the hemorrhagic phase, patients might experience neurologic and neuropsychiatric symptoms such as agitation, confusion, delusions, neck stiffness, headache, photophobia, and, in rare cases (2.8%), myoclonic jerks (*28*). Involvement of the central nervous system has been suspected; however, a recent prospective study showed no cases with encephalitis or brain abnormalities on magnetic resonance imaging despite a high percentage of patients experiencing fever (94.4%) and headache (66.7%). None of the 36 patients in the case series showed brain changes over the course of their disease, although no cerebrospinal fluid analysis was performed in the study, so presence of viral meningitis could not be ruled out (*28*,*29*). Those findings in humans are in contrast with a study of humanized mice infected with CCHFV in which autopsies showed gliosis, meningitis, and meningoencephalitis, suggesting direct viral infection of the central nervous system (*11*,*17*,*30*).

Cardiopulmonary manifestations include myocardial infarction, myocarditis (*31*), pulmonary edema, and pleural effusions. Engin et al. (*32*) evaluated 44 consecutive CCHF patients using transthoracic echocardiography and reported that patients with severe CCHF had statistically (but not necessarily clinically) significant lower ejection fraction of the left ventricle (50% vs. 55%) and higher systolic pulmonary pressures and were more likely to have pericardial effusion than were nonsevere CCHF patients. Whether myocardial dysfunction is a result of immune-related or direct viral cytotoxic effect on the myocardium is unclear.

Literature case reports of CCHF-associated acute pancreatitis and acute nonsuppurative parotitis during the hemorrhagic phase of illness can be found, but no virologic confirmation in tissue was obtained in those cases (*33*,*34*). A case of acute epididymo-orchitis during the prehemorrhagic phase has also been reported (*35*). Most deaths occur in the second week of illness and are associated with rapidly developing refractory shock that leads to multiorgan failure and severe coagulopathy with evidence of acute and severe hepatopathy (*14*,*36*,*37*).

The convalescent phase of CCHF usually starts on day 10–20 of illness and can last up to 1 year. Most patients recover without complications or sequelae. Among those patients with symptomatic convalescence, they frequently experience fatigue and malaise, hair loss, anorexia, and polyneuritis. Tachycardia and dyspnea have also been described. Memory and visual and auditory impairment have also been described (*1*,*21*). A study from Turkey reported that 48.4% of patients studied exhibited symptoms of posttraumatic stress disorder (PTSD) and 18.5% had PTSD after recovery (*38*). PTSD and PTSD symptoms were more common among patients who had required intensive care unit stays (*38*).

To date, relapses of CCHF and reinfections with CCHFV, particularly of patients being reexposed in endemic areas, have not been described (*10*,*14*,*39*). Nonetheless, duration of protective immunity has not yet been elucidated.

Special Populations

More than 40 cases of CCHF in pregnant women have been reported and are associated with high maternal mortality (CFR 34%) compared with nonpregnant patients (CFR 4%–14% depending on the reporting country); mortality rates were higher in the second half of pregnancy, but the difference was not statistically significant. Fetal and neonatal mortality (58%) is associated with spontaneous abortion or maternal death. Exposure to bodily fluids (i.e., blood, amniotic fluid) during cesarean section or vaginal delivery confers a high risk for transmission; up to 14.8% of deliveries have resulted in transmission to healthcare workers (*40*). It is key to consider HELLP (hemolysis, elevated liver enzymes, low platelets) syndrome in the differential diagnosis of pregnant patients suspected to have CCHF (*1*).

Most pediatric cases of CCHF are the result of a tick bite, and patients more frequently exhibited rash, abdominal pain, and myalgia, leading to a different differential diagnosis than seen in adults. Tonsillopharyngitis is a common finding in pediatric patients (*41*). Elevated AST, ALT, and lactate dehydrogenase, as well as leukopenia and thrombocytopenia, are common among pediatric patients admitted for

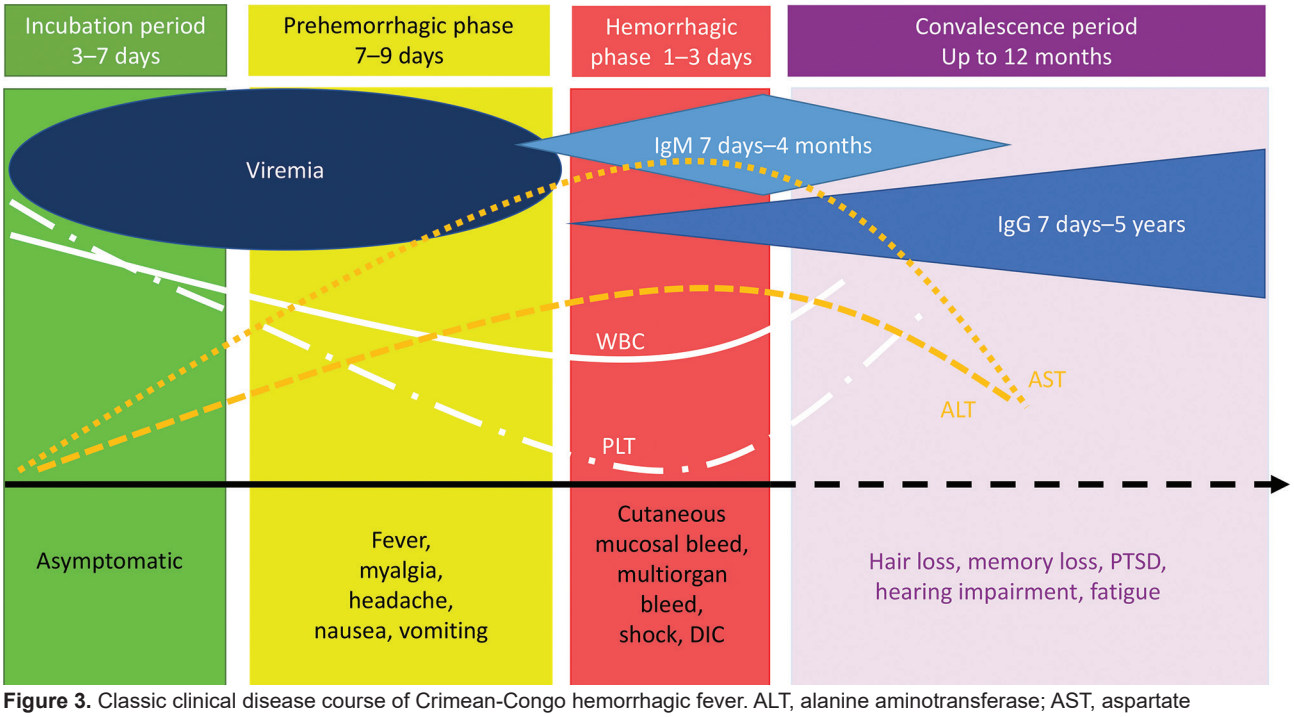

Figure 3. Classic clinical disease course of Crimean-Congo hemorrhagic fever. ALT, alanine aminotransferase; AST, aspartate aminotransferase; DIC, disseminated intravascular coagulation; PLT, platelet count; PTSD, posttraumatic stress disorder; WBC, white blood cell count.

Table. Clinical phases of Crimean-Congo hemorrhagic fever*

Clinical phase	Duration	Clinical features	Laboratory features
Incubation	3–7 d (3–5 d after tick bite, 5–7 d after exposure to blood or tissue)	Not applicable	Normal-mildly decreased PLT
Prehemorrhagic	1–7 d	Fever, headache, myalgia, dizziness, nausea, vomiting, diarrhea, hyperemia of upper body, conjunctivitis	Viremia (positive PCR), mild leukopenia, mild thrombocytopenia, elevated CK, mild elevation of AST, ALT, and LDH
Hemorrhagic	Begins at day 3–5 of illness	Petechial rash (skin, conjunctiva, mucosa), large cutaneous ecchymoses, gastrointestinal and genitourinary bleeding, hepatosplenomegaly, if fatal (days 5–14 of illness) secondary to MOF, bleeding, shock DIC	Decreasing viremia, in most cases resolved by day 9 of illness, positive serum IgM against CCHFV, leukopenia, anemia, profound thrombocytopenia, marked elevation of AST, elevation of ALT, elevated PT, aPTT, D-dimer and FDP, schistocytes
Convalescence	Up to 1 y	Weakness, malaise, hair loss, anorexia, polyneuritis, impaired memory, vision impairment, hepatic and renal insufficiency	Thrombocytosis, slow decrease in AST and ALT, slow resolution of renal and liver function, positive serum IgG against CCHFV

*ALT, alanine aminotransferase; aPTT, activated partial thromboplastin time; AST, aspartate aminotransferase; CCHFV, Crimean-Congo hemorrhagic fever virus; CK, creatine phosphokinase; DIC, disseminated intravascular coagulation; FDP, fibrinogen degradation products; LDH, lactate dehydrogenase; MOF, multiorgan failure; PT, prothrombin time.

CCHF management (*1*). A case of acute CCHF-related myocarditis in a 13-year-old was reported; symptoms resolved completely after the convalescent period (*31*). The clinical course for reported pediatric cases was milder and shorter than for adults (*41*).

Pediatric cases of hemophagocytic lymphohistiocytosis (HLH) secondary to CCHF have been described (*42*,*43*). Secondary HLH, although rare, can be associated with malignancies, severe infections, medications, and autoimmune disorders and has been thought to be secondary to a hyperinflammatory syndrome (*44*). Most patients will have a combination of fever, hepatosplenomegaly, pancytopenia, hypertriglyceridemia, hypofibrinogenemia, a variety of neurologic symptoms, and evidence of hemophagocytosis in pathology examination of bone marrow or other tissues (*44*). Because of the high rates of illness and death associated with HLH, its early recognition is key for timely treatment consideration (such as corticosteroids, intravenous immunoglobulin, immunomodulators, and therapeutic plasma exchange) (*43*,*44*).

Disease Severity and Mortality Risk Factors

CFR estimates range from 5% to 60% in case series depending on geographic region. Multiple factors, such as healthcare resource availability, difference in circulating strain virulence, risk for co-infections, and the clinician's threshold for early CCHF testing, can affect outcomes (*14*,*37*,*45*).

Several CCHF disease severity assessment models have been proposed. In 1989, Swanepoel et al. (*36*) proposed a model that predicted a ≥90% fatal outcome if patients had any of the following: leukocytosis (leukocytes ≥10,000/mm^3), thrombocytopenia (platelets ≤20,000/mm^3), AST ≥200 U/L or ALT ≥150 U/L, aPTT ≥60 seconds, or fibrinogen ≤110 mg/dL. In 2006, Ergonul et al. (*46*) defined severe CCHF as the presence of any of thrombocytopenia (<20,000/mm^3), AST ≥700 U/L or ALT ≥900 U/L, aPTT >60 seconds, or fibrinogen <110 mg/dL, in addition to the presence of melena, hematemesis, or somnolence. In both models, criteria were based on signs and symptoms that appeared within 5 days after symptom onset (*36*,*47*).

Bakir et al. (*47*) developed a scoring system for CCHF severity to aid in predicting clinical course and mortality risk through a severity grading score (SGS). The variables used in the SGS system are age, routinely collected and available laboratory markers (PT, aPTT, international normalized ratio [INR], AST, ALT, lactate dehydrogenase, and leukocyte and platelet counts), and other clinical features (hepatomegaly, organ failure, bleeding), each with associated point values. Point values predicted mortality risk (low, SGS ≤4; medium, SGS 5–8; high, SGS ≥9): patients with a high SGS at admission were at high risk for death (sensitivity 96%, specificity 100%), whereas a low score showed no association with mortality; mortality risk was 20% in the medium risk group (*47*).

In 2022, Bakir et al. (*37*) published a comparison of models' performance in predicting death in CCHF patients. The authors compared the sequential organ failure assessment score, the qSOFA (quick sepsis-related organ failure assessment), APACHE II score, and SGS. All models except qSOFA were adequate for predicting death when applied at admission; however, all models performed well at 72 hours and 120 hours after admission (*37*).

CCHF viremia levels have been correlated with disease severity, and viral loads equal or above 10^8 copies/mL and 10^9 copies/mL are significantly associated with high mortality from CCHF (*48*,*49*). However, CCHF viral load measurements are not routinely available to the bedside clinician.

Differential Diagnoses

The differential diagnosis for CCHFV infection might vary geographically and is based on known occupation and environmental exposures, immunization status, season, and the geographic location (current and recent) of the patient. Options include, but are not limited to, brucellosis, COVID-19, ehrlichiosis, influenza, leptospirosis, Lyme disease, malaria, Q fever, rickettsiosis, salmonellosis, tickborne encephalitis, viral hepatitis, and other viral hemorrhagic fevers (*1*). Obtaining a thorough history, including animal, environmental, insect, occupational, and travel exposures, is critical for assessing the likelihood of CCHF as a potential diagnosis.

Infection Prevention and Control

Infection prevention and control measures against CCHF aim to minimize exposure. Such measures apply to community, occupational, and healthcare settings.

Community Settings

The risk of acquiring CCHF in the community is primarily related to exposure to ticks or infected animals. Thus, prevention efforts focus on prevention of tick-to-human transmission (e.g., wearing protective clothing, avoiding locations with high tick burden) and animal-to-human transmission (e.g., use of gloves and other protective clothing for direct contact with animals' bodily fluids and their tissues in CCHF-endemic areas) (*3*,*18*).

CCHFV does not typically cause disease in animals, although tick infestation of domestic, farm, and wild animals can increase the risk for transmission to humans. Reducing activities in tick-infested areas and implementing pest-management strategies in both domestic and farm animals are key for preventing CCHF transmission in agricultural communities (*18*). Other proposed community strategies to mitigate the effects of CCHF include regulating and monitoring livestock migratory activities, media campaigns focusing on simple CCHF prevention measures and community engagement, easy-to-access training modules for healthcare workers, and increased communication between veterinarian and medical health experts (*3*,*50*).

Temporal trends in incidence could help guide the timing of community mitigation efforts for maximum impact. CCHF follows a seasonal pattern and is positively associated with monthly average temperature, monthly cumulative rainfall, and decreased relative humidity (Appendix reference *51*). In addition, increases in CCHF cases often occur during or around the time of the annual celebration of Eid al-Adha. Rural livestock brought to urban areas for slaughter for the festivities might carry CCHFV (either through infected ticks or because livestock are viremic at the time of slaughter) (*50*). Geographic areas where risk for CCHF is higher can be targeted for control strategies using a predictive tool to estimate the prospective number of CCHF cases for the next 2 years (*3*,*50*).

Occupational Settings (Nonhealthcare)

Persons whose occupations expose them to animals or raw animal tissues and fluids, such as butchers, farmers, slaughterhouse workers, veterinarians, and veterinary clinic staff, are at increased risk for CCHF exposure (*3*; Appendix reference *52*). Availability and use of PPE when handling animals, animal carcasses, or animal body fluids, as well as the quarantining of livestock potentially carrying CCHFV or CCHFV-infected ticks before transport and slaughter, can also minimize human exposure in those occupations (*18*).

Healthcare Settings

Education on identifying signs and symptoms of CCHF early, rapidly isolating suspect cases, and informing the appropriate authorities, as well as on obtaining information on relevant epidemiologic history or exposures, is essential to reducing risk for nosocomial transmission. Human-to-human transmission is most often documented in the nosocomial setting and is thought to occur through exposure to blood and bodily fluids of infected patients. Numerous case series have described clusters of CCHF among healthcare workers in Pakistan, Russia, Turkey, Mauritania, Iran, and elsewhere; failures in infection prevention and control have been implicated (*22*; Appendix references *53*–*57*). In 1 study, the seroprevalence of healthcare workers who cared for CCHF patients was 3.78%, compared with 0% for healthcare workers with no known exposure to CCHF (Appendix reference *55*). A delay in clinical suspicion of CCHF and subsequent delay in implementing infection control measures has also been reported as a contributing factor in nosocomial transmission (Appendix reference *58*).

Persons who are suspected of having CCHF should be isolated immediately to minimize the risk for nosocomial transmission, appropriate PPE should

be used when providing care, and relevant public health authorities should be informed (*3*). Healthcare worker PPE for the management of CCHF patients is generally based on recommendations for other viral hemorrhagic fevers, mainly filoviruses, such as Ebola virus disease. Both the World Health Organization (https://www.who.int/health-topics/crimean-congo-haemorrhagic-fever) and the US Centers for Disease Control and Prevention (https://www.cdc.gov/vhf/crimean-congo/index.html) apply infection control approaches for Ebola virus disease to management of patients with suspected or confirmed CCHF. That guidance includes detailed recommendations on placing and isolating patients, collecting and processing laboratory specimens, managing waste, and cleaning and disinfecting the environment (https://www.cdc.gov/vhf/ebola/clinicians/evd/infection-control.html).

Needlestick injuries and splash exposures to mucous membranes are considered common mechanisms of exposure for nosocomial CCHFV transmission from blood. Other body fluids might potentially transmit CCHFV; CCHFV RNA can be detected in saliva and urine early in the clinical course. Further research regarding timing of viral presence in other bodily fluids is necessary (Appendix references *59*,*60*). Policies and procedures for isolation, discharge criteria, and guidance on the potential risk for transmission after discharge should take into account the potential for persistent viral shedding (*20*; Appendix references *59*–*61*). The patient should be placed in a single room, when available, immediately upon suspicion of CCHF. Although airborne transmission has been proposed in some nosocomial clusters, definitive evidence is lacking to recommend universal use of N95 respirators for the care of CCHF patients; however, N95 respirators or equivalent should be worn during aerosol-generating procedures (*22*). As has been noted for other viral hemorrhagic fever diseases, the patient's severity of illness seems to correlate with increased risk for infections in healthcare workers (Appendix reference *61*). Despite availability of infection prevention and control guidelines, a recent survey of 23 international centers taking care of CCHF patients in endemic countries noted high variability in healthcare workers' use of PPE; all centers reported a high-risk exposure in the previous 5 years (Appendix references *61*,*62*).

Conclusion

CCHF is the most geographically widespread tick-borne disease, identified in >30 countries in Africa, Asia, the Middle East, and Europe located south of the 50th parallel north. It poses a continued public health threat; estimated annual incidence is 10,000–15,000 cases worldwide. Farmers, persons participating in outdoor recreational activities, slaughterhouse workers, veterinarians, and healthcare workers in CCHF-endemic areas are at risk for infection. Clinical manifestations of CCHF range from asymptomatic infection or mild, nonspecific febrile illness to severe hemorrhagic disease with multiorgan failure ultimately leading to death; reported CFR in some case series is as high as 60% (*7*). A high index of suspicion, comprehensive travel and epidemiologic history, and clinical evaluation are essential for prompt diagnosis. Infection control measures can be effective in reducing the risk for transmission both within community and healthcare settings; however, correct and consistent application is required effectively achieve this goal.

Members of the State of the Clinical Science Working Group of the National Emerging pathogens Training and Education Center's Special Pathogens Research Network: Richard T. Davey, Jr., Noreen A. Hynes, Mark G. Kortepeter, Nahid Bhadelia, Kerry Dierberg, Aneesh K. Mehta, Corri B. Levine, Peter C. Iwen, Denis A. Bente, Justin Chan, and Adam Beitscher.

Acknowledgments

We thank the authors who completed a previous version of this manuscript: Nahid Bhadelia, Kerry Dierberg, and Mark G. Kortepeter.

Research reported in this publication was supported by the Department of Health and Human Services Office of the Assistant Secretary for Preparedness and Response.

About the Author

Dr. Maria G. Frank is a hospitalist and medical director of Denver Health Hospital Authority's Biocontainment Unit and a professor of medicine at the University of Colorado School of Medicine. Her research interests include medical management of special pathogens and involvement of general internists in disaster response.

References

1. Ergonual O, Whitehouse CA. Crimean-Congo hemorrhagic fever: a global perspective. The Netherlands: Springer; 2007.
2. Mishra AK, Hellert J, Freitas N, Guardado-Calvo P, Haouz A, Fels JM, et al. Structural basis of synergistic neutralization of Crimean-Congo hemorrhagic fever virus by human antibodies. Science. 2022;375:104–9. https://doi.org/10.1126/science.abl6502
3. World Health Organization. Introduction to Crimean-Congo hemorrhagic fever [cited 2023 Jul 1]. https://cdn.who.int/media/docs/default-source/documents/health-topics/

crimean-congo-haemorrhaigc-fever/introduction-to-crimean-congo-haemorrhagic-fever.pdf
4. Al-Abri SS, Abaidani IA, Fazlalipour M, Mostafavi E, Leblebicioglu H, Pshenichnaya N, et al. Current status of Crimean-Congo hemorrhagic fever in the World Health Organization Eastern Mediterranean Region: issues, challenges, and future directions. Int J Infect Dis. 2017;58:82–9. https://doi.org/10.1016/j.ijid.2017.02.018
5. Hawman DW, Feldmann H. Recent advances in understanding Crimean-Congo hemorrhagic fever virus. F1000 Res. 2018;7:7. https://doi.org/10.12688/f1000research.16189.1
6. Belobo JTE, Kenmoe S, Kengne-Nde C, Emoh CPD, Bowo-Ngandji A, Tchatchouang S, et al. Worldwide epidemiology of Crimean-Congo hemorrhagic fever virus in humans, ticks and other animal species, a systematic review and meta-analysis. PLoS Negl Trop Dis. 2021;15:e0009299. https://doi.org/10.1371/journal.pntd.0009299
7. Khan AS, Maupin GO, Rollin PE, Noor AM, Shurie HH, Shalabi AG, et al. An outbreak of Crimean-Congo hemorrhagic fever in the United Arab Emirates, 1994–1995. Am J Trop Med Hyg. 1997;57:519–25. https://doi.org/10.4269/ajtmh.1997.57.519
8. Nurettin C, Engin B, Sukru T, Munir A, Zati V, Aykut O. The seroprevalence of Crimean-Congo hemorrhagic fever in wild and domestic animals: an epidemiological update for domestic animals and first seroevidence in wild animals from Turkey. Vet Sci. 2022;9:9. https://doi.org/10.3390/vetsci9090462
9. Saksida A, Duh D, Wraber B, Dedushaj I, Ahmeti S, Avsic-Zupanc T. Interacting roles of immune mechanisms and viral load in the pathogenesis of Crimean-Congo hemorrhagic fever. Clin Vaccine Immunol. 2010;17:1086–93. https://doi.org/10.1128/CVI.00530-09
10. Rodriguez SE, Hawman DW, Sorvillo TE, O'Neal TJ, Bird BH, Rodriguez LL, et al. Immunobiology of Crimean-Congo hemorrhagic fever. Antiviral Res. 2022;199:105244. https://doi.org/10.1016/j.antiviral.2022.105244
11. Garrison AR, Smith DR, Golden JW. Animal models for Crimean-Congo hemorrhagic fever human disease. Viruses. 2019;11:11. https://doi.org/10.3390/v11070590
12. Frank MG, Weaver G, Raabe V; State of the Clinical Science Working Group of the National Emerging pathogens Training and Education Center's Special Pathogens Research Network. Crimean-Congo hemorrhagic fever virus for clinicians—virology, pathogenesis, and pathology. Emerg Infect Dis. 2024;30:847–853. https://doi.org/10.3201/eid3005.231646
13. Frank MG, Weaver G, Raabe V; State of the Clinical Science Working Group of the National Emerging Pathogens Training and Education Center's Special Pathogens Research Network. Crimean-Congo hemorrhagic fever virus for clinicians—diagnosis, clinical management, and therapeutics. Emerg Infect Dis. 2024;30:864–873 https://doi.org/10.3201/eid3005.231648
14. Bente DA, Forrester NL, Watts DM, McAuley AJ, Whitehouse CA, Bray M. Crimean-Congo hemorrhagic fever: history, epidemiology, pathogenesis, clinical syndrome and genetic diversity. Antiviral Res. 2013;100:159–89. https://doi.org/10.1016/j.antiviral.2013.07.006
15. Lorenzo Juanes HM, Carbonell C, Sendra BF, López-Bernus A, Bahamonde A, Orfao A, et al. Crimean-Congo hemorrhagic fever, Spain, 2013–2021. Emerg Infect Dis. 2023;29:252–9. https://doi.org/10.3201/eid2902.220677
16. Shahhosseini N, Wong G, Babuadze G, Camp JV, Ergonul O, Kobinger GP, et al. Crimean-Congo hemorrhagic fever virus in Asia, Africa and Europe. Microorganisms. 2021;9:9. https://doi.org/10.3390/microorganisms9091907
17. Spengler JR, Bente DA. Crimean-Congo hemorrhagic fever in Spain—new arrival or silent resident? N Engl J Med. 2017;377:106–8. https://doi.org/10.1056/NEJMp1707436
18. Hawman DW, Feldmann H. Crimean-Congo hemorrhagic fever virus. Nat Rev Microbiol. 2023;21:463–77. https://doi.org/10.1038/s41579-023-00871-9
19. Saijo M, Tang Q, Shimayi B, Han L, Zhang Y, Asiguma M, et al. Possible horizontal transmission of Crimean-Congo hemorrhagic Fever virus from a mother to her child. Jpn J Infect Dis. 2004;57:55–7.
20. Pshenichnaya NY, Sydenko IS, Klinovaya EP, Romanova EB, Zhuravlev AS. Possible sexual transmission of Crimean-Congo hemorrhagic fever. Int J Infect Dis. 2016;45:109–11. https://doi.org/10.1016/j.ijid.2016.02.1008
21. Hoogstraal H. The epidemiology of tick-borne Crimean-Congo hemorrhagic fever in Asia, Europe, and Africa. J Med Entomol. 1979;15:307–417. https://doi.org/10.1093/jmedent/15.4.307
22. Pshenichnaya NY, Nenadskaya SA. Probable Crimean-Congo hemorrhagic fever virus transmission occurred after aerosol-generating medical procedures in Russia: nosocomial cluster. Int J Infect Dis. 2015;33:120–2. https://doi.org/10.1016/j.ijid.2014.12.047
23. Tsergouli K, Karampatakis T, Haidich AB, Metallidis S, Papa A. Nosocomial infections caused by Crimean-Congo hemorrhagic fever virus. J Hosp Infect. 2020;105:43–52. https://doi.org/10.1016/j.jhin.2019.12.001
24. Nuttall PA, Labuda M. Tick-host interactions: saliva-activated transmission. Parasitology. 2004;129(Suppl) :S177–89. https://doi.org/10.1017/S0031182004005633
25. Aksoy D, Barut H, Duygu F, Çevik B, Kurt S, Sümbül O. Characteristics of headache and its relationship with disease severity in patients with Crimean-Congo hemorrhagic fever. Agri. 2018;30:12–7.
26. Flick R, Whitehouse CA. Crimean-Congo hemorrhagic fever virus. Curr Mol Med. 2005;5:753–60. https://doi.org/10.2174/156652405774962335
27. Cevik MA, Erbay A, Bodur H, Gülderen E, Baştuğ A, Kubar A, et al. Clinical and laboratory features of Crimean-Congo hemorrhagic fever: predictors of fatality. Int J Infect Dis. 2008;12:374–9. https://doi.org/10.1016/j.ijid.2007.09.010
28. Öztoprak B, Öztoprak İ, Engin A. Is the brain spared in Crimean-Congo hemorrhagic fever? An MR-SWI study to reveal CNS involvement. Eur Radiol. 2018;28:3893–901. https://doi.org/10.1007/s00330-018-5310-9
29. Spengler JR, Kelly Keating M, McElroy AK, Zivcec M, Coleman-McCray JD, Harmon JR, et al. Crimean-Congo hemorrhagic fever in humanized mice reveals glial cells as primary targets of neurological infection. J Infect Dis. 2017;216:1386–97. https://doi.org/10.1093/infdis/jix215
30. Ahmeti S, Berisha L, Halili B, Ahmeti F, von Possel R, Thomé-Bolduan C, et al. Crimean-Congo hemorrhagic fever, Kosovo, 2013–2016. Emerg Infect Dis. 2019;25:321–4. https://doi.org/10.3201/eid2502.171999
31. Gülhan B, Kanık-Yüksek S, Çetin İİ, Özkaya-Parlakay A, Tezer H. Myocarditis in a child with Crimean-Congo hemorrhagic fever. Vector Borne Zoonotic Dis. 2015;15:565–7. https://doi.org/10.1089/vbz.2015.1769
32. Engin A, Yilmaz MB, Elaldi N, Erdem A, Yalta K, Tandogan I, et al. Crimean-Congo hemorrhagic fever: does it involve the heart? Int J Infect Dis. 2009;13:369–73. https://doi.org/10.1016/j.ijid.2008.07.019
33. Bastug A, Kayaaslan B, But A, Aslaner H, Sertcelik A, Akinci E, et al. A case of Crimean-Congo hemorrhagic fever

complicated with acute pancreatitis. Vector Borne Zoonotic Dis. 2014;14:827–9. https://doi.org/10.1089/vbz.2014.1623
34. Kaya S, Yilmaz G, Ertunç B, Koksal I. Parotitis associated with Crimean Congo hemorrhagic fever virus. J Clin Virol. 2012;53:159–61. https://doi.org/10.1016/j.jcv.2011.10.008
35. Aksoy HZ, Yilmaz G, Aksoy F, Koksal I. Crimean-Congo hemorrhagic fever presenting as epididymo-orchitis. J Clin Virol. 2010;48:282–4. https://doi.org/10.1016/j.jcv.2010.06.002
36. Swanepoel R, Gill DE, Shepherd AJ, Leman PA, Mynhardt JH, Harvey S. The clinical pathology of Crimean-Congo hemorrhagic fever. Rev Infect Dis. 1989;11 (Suppl 4):S794–800. https://doi.org/10.1093/clinids/11.Supplement_4.S794
37. Bakir M, Öksüz C, Karakeçili F, Baykam N, Barut Ş, Büyüktuna SA, et al. Which scoring system is effective in predicting mortality in patients with Crimean Congo hemorrhagic fever? A validation study. Pathog Glob Health. 2022;116:193–200. https://doi.org/10.1080/20477724.2021.2012921
38. Gul S, Gul EU, Yesilyurt M, Ozturk B, Kuscu F, Ergonul O. Health-related quality of life and the prevalence of post-traumatic stress disorder among Crimean-Congo hemorrhagic fever survivors. Jpn J Infect Dis. 2012;65:392–5. https://doi.org/10.7883/yoken.65.392
39. Mendoza EJ, Warner B, Safronetz D, Ranadheera C. Crimean-Congo hemorrhagic fever virus: past, present and future insights for animal modelling and medical countermeasures. Zoonoses Public Health. 2018;65:465–80. https://doi.org/10.1111/zph.12469
40. Pshenichnaya NY, Leblebicioglu H, Bozkurt I, Sannikova IV, Abuova GN, Zhuravlev AS, et al. Crimean-Congo hemorrhagic fever in pregnancy: a systematic review and case series from Russia, Kazakhstan and Turkey. Int J Infect Dis. 2017;58:58–64. https://doi.org/10.1016/j.ijid.2017.02.019
41. Tezer H, Sucakli IA, Sayli TR, Celikel E, Yakut I, Kara A, et al. Crimean-Congo hemorrhagic fever in children. J Clin Virol. 2010;48:184–6. https://doi.org/10.1016/j.jcv.2010.04.001
42. Gayretli Aydin ZG, Yesilbas O, Reis GP, Guven B. The first pediatric case of hemophagocytic lymphohistiocytosis secondary to Crimean-Congo hemorrhagic fever successfully treated with therapeutic plasma exchange accompanying ribavirin and intravenous immunoglobulin. J Clin Apher. 2021;36:780–4. https://doi.org/10.1002/jca.21915
43. Oygar PD, Gürlevik SL, Sağ E, İlbay S, Aksu T, Demir OO, et al. Changing disease course of Crimean-Congo hemorrhagic fever in children, Turkey. Emerg Infect Dis. 2023;29:268–77. https://doi.org/10.3201/eid2902.220976
44. Pan H, Wang G, Guan E, Song L, Song A, Liu X, et al. Treatment outcomes and prognostic factors for non-malignancy associated secondary hemophagocytic lymphohistiocytosis in children. BMC Pediatr. 2020;20:288. https://doi.org/10.1186/s12887-020-02178-7
45. Álvarez-Rodríguez B, Tiede C, Hoste ACR, Surtees RA, Trinh CH, Slack GS, et al. Characterization and applications of a Crimean-Congo hemorrhagic fever virus nucleoprotein-specific Affimer: inhibitory effects in viral replication and development of colorimetric diagnostic tests. PLoS Negl Trop Dis. 2020;14:e0008364. https://doi.org/10.1371/journal.pntd.0008364
46. Ergonul O, Celikbas A, Baykam N, Eren S, Dokuzoguz B. Analysis of risk-factors among patients with Crimean-Congo hemorrhagic fever virus infection: severity criteria revisited. Clin Microbiol Infect. 2006;12:551–4. https://doi.org/10.1111/j.1469-0691.2006.01445.x
47. Bakır M, Gözel MG, Köksal I, Aşık Z, Günal Ö, Yılmaz H, et al. Validation of a severity grading score (SGS) system for predicting the course of disease and mortality in patients with Crimean-Congo hemorrhagic fever (CCHF). Eur J Clin Microbiol Infect Dis. 2015;34:325–30. https://doi.org/10.1007/s10096-014-2238-0
48. Cevik MA, Erbay A, Bodur H, Eren SS, Akinci E, Sener K, et al. Viral load as a predictor of outcome in Crimean-Congo hemorrhagic fever. Clin Infect Dis. 2007;45:e96–100. https://doi.org/10.1086/521244
49. Duh D, Saksida A, Petrovec M, Ahmeti S, Dedushaj I, Panning M, et al. Viral load as predictor of Crimean-Congo hemorrhagic fever outcome. Emerg Infect Dis. 2007;13:1769–72. https://doi.org/10.3201/eid1311.070222
50. Ahmed A, Tahir MJ, Siddiqi AR, Dujaili J. Potential of Crimean-Congo hemorrhagic fever outbreak during Eid al-Adha Islamic festival and COVID-19 pandemic in Pakistan. J Med Virol. 2021;93:182–3. https://doi.org/10.1002/jmv.26285

Address for correspondence: Maria G. Frank, University of Colorado Anschutz Medical Campus—Internal Medicine, 12401 E 17th Ave, Mailstop F-782, Aurora, CO 80045-2559, USA; email: maria.frank@dhha.org, maria.frank@cuanschutz.edu

Crimean-Congo Hemorrhagic Fever Virus for Clinicians—Diagnosis, Clinical Management, and Therapeutics

Maria G. Frank, Gretchen Weaver, Vanessa Raabe;[1] State of the Clinical Science Working Group of the National Emerging Pathogens Training and Education Center's Special Pathogens Research Network[2]

Medscape CME Activity

In support of improving patient care, this activity has been planned and implemented by Medscape, LLC and Emerging Infectious Diseases. Medscape, LLC is jointly accredited with commendation by the Accreditation Council for Continuing Medical Education (ACCME), the Accreditation Council for Pharmacy Education (ACPE), and the American Nurses Credentialing Center (ANCC), to provide continuing education for the healthcare team.

Medscape, LLC designates this Journal-based CME activity for a maximum of 1.00 ***AMA PRA Category 1 Credit(s)™***. Physicians should claim only the credit commensurate with the extent of their participation in the activity.

Successful completion of this CME activity, which includes participation in the evaluation component, enables the participant to earn up to 1.0 MOC points in the American Board of Internal Medicine's (ABIM) Maintenance of Certification (MOC) program. Participants will earn MOC points equivalent to the amount of CME credits claimed for the activity. It is the CME activity provider's responsibility to submit participant completion information to ACCME for the purpose of granting ABIM MOC credit.

All other clinicians completing this activity will be issued a certificate of participation. To participate in this journal CME activity: (1) review the learning objectives and author disclosures; (2) study the education content; (3) take the post-test with a 75% minimum passing score and complete the evaluation at https://www.medscape.org/qna/processor/71556?showStandAlone=true&src=prt_jcme_eid_mscpedu; and (4) view/print certificate. For CME questions, see page 1066.

NOTE: It is Medscape's policy to avoid the use of brand names in accredited activities. However, in an effort to be as clear as possible, the use of brand names should not be viewed as a promotion of any brand or as an endorsement by Medscape of specific products.

Release date: April 18, 2024; Expiration date: April 18, 2025

Learning Objectives

Upon completion of this activity, participants will be able to:

1. Evaluate diagnostic tools in cases of suspected Crimean-Congo hemorrhagic fever (CCHF)
2. Analyze characteristics of laboratory tests for CCHF virus
3. Assess the current statuws of vaccinations to protect against CCHF
4. Evaluate treatment options for CCHF

CME Editor

Amy J. Guinn, BA, MA, Technical Writer/Editor, Emerging Infectious Diseases. *Disclosure: Amy J. Guinn, BA, MA, has no relevant financial relationships.*

CME Author

Charles P. Vega, MD, Health Sciences Clinical Professor of Family Medicine, University of California, Irvine School of Medicine, Irvine, California. *Disclosure: Charles P. Vega, MD, has the following relevant financial relationships: served as a consultant or advisor for Boehringer Ingelheim; GlaxoSmithKline.*

Authors

Maria G. Frank, MD; Gretchen Weaver, MPH; Vanessa Raabe, MD, MSc.

Author affiliations: Denver Health and Hospital Authority, Denver, Colorado, USA (M.G. Frank); University of Colorado School of Medicine, Denver (M.G. Frank); University of Massachusetts Chan Medical School, Worchester, Massachusetts, USA (G. Weaver); New York University Grossman School of Medicine, New York, New York, USA (V. Raabe)

DOI: https://doi.org/10.3201/eid3005.231648

[1]Current affiliation: Pfizer Inc., New York, New York, USA. These materials reflect only the personal views of the author and may not reflect the views of her employer.

[2]Members of this group are listed at the end of this article.

Crimean-Congo hemorrhagic fever virus (CCHFV) is the most geographically widespread tickborne viral infection worldwide and has a fatality rate of up to 62%. Despite its widespread range and high fatality rate, no vaccines or treatments are currently approved by regulatory agencies in the United States or Europe. Supportive treatment remains the standard of care, but the use of antiviral medications developed for other viral infections have been considered. We reviewed published literature to summarize the main aspects of CCHFV infection in humans. We provide an overview of diagnostic testing and management and medical countermeasures, including investigational vaccines and limited therapeutics. CCHFV continues to pose a public health threat because of its wide geographic distribution, potential to spread to new regions, propensity for genetic variability, potential for severe and fatal illness, and limited medical countermeasures for prophylaxis and treatment. Clinicians should become familiar with available diagnostic and management tools for CCHFV infections in humans.

Approximately 10,000–15,000 cases of human Crimean-Congo hemorrhagic fever (CCHF) occur annually worldwide (*1*–*3*). However, more definitive case numbers are difficult to ascertain because up to 88% of infections are thought to be subclinical (*1*–*3*), unrecognized, or occurring in locations with limited disease surveillance or laboratory testing capability (*4*,*5*). CCHF virus (CCHFV) causes a spectrum of human clinical manifestations, ranging from asymptomatic infection to a severe hemorrhagic fever marked by shock and multiorgan failure (Figure). During CCHF outbreaks, the case-fatality rate ranges from 5% to 30% (*1*), and some published case series have reported fatality rates up to 62% (*6*). Disease caused by CCHFV infection is limited to humans, but asymptomatic transient viremia lasting up to 15 days has been documented in livestock and wild animals (*7*). Severe or fatal disease correlates with an exuberant proinflammatory immune response leading to vascular dysfunction, disseminated intravascular coagulation, multiorgan failure, and shock (*8*). Although the detection of IgM (usually present as early as day 4–5 of illness) and IgG (usually detectable after days 7–9 of illness) correlates with declining viremia, fatal cases of CCHF often mount no or very late immune responses (*9*). However, the antibody response to CCHFV does not correlate with disease outcome or protection from vaccines. That feature of CCHF, combined with a paucity of available animal models (*10*), makes vaccine and treatment research challenging. The US Food and Drug Administration (FDA) has not approved any vaccines or treatments for CCHF. Ribavirin is commonly used for treatment but clinical evidence regarding its benefit is mixed. Another antiviral medication, favipiravir, shows promise in animal models but has rarely been used in human CCHF management. Vaccine candidates are mostly in preclinical development, and few have advanced to human clinical trials to date.

This third article in a 3-part series summarizing the main aspects of CCHF is intended to provide clinicians with an overview of diagnostic testing, management, and medical countermeasures for CCHF. The first article focuses on the virology, pathogenesis, and pathology of CCHF (*11*) and the second on epidemiology, clinical features, and prevention and control of CCHF (*12*).

Methods

For this paper, we conducted a focused review of National Center for Biotechnology's MeSH (Medical Subject Headings, https://www.ncbi.nlm.nih.gov/mesh) and PubMed (https://pubmed.ncbi.nlm.nih.gov) search strings customized for CCHF and CCHFV. We focused our review on the past 10 years and on human data, when available. We included older relevant data and animal data where appropriate. We conducted title, abstract, and full text reviews of relevant manuscripts, reviews, and book chapters. We also completed bibliography scans on review articles and meta-analyses.

Diagnostic Testing

The nonspecific CCHF characteristics make a high index of suspicion, on the basis of epidemiologic history, clinical signs and symptoms, and initial laboratory findings, key for early diagnosis and initiation of aggressive treatment. Delays in diagnosis and hospitalization are common and have occurred in up to 68% of patients in Turkey and led to increased mortality rates when compared with patients whose infections are diagnosed early (*13*).

Although many laboratory assays have been developed for diagnosing CCHF, the availability and Biosafety Level (BSL) requirements for safe specimen handling vary widely between countries. Sweden, Switzerland, France, Germany, Italy, and the United Kingdom recommend BSL-4 for CCHFV diagnostic assays (*14*). Conversely, the United States, South Africa, Kazakhstan, Slovenia, and Georgia allow diagnostic tests to be performed in BSL-3 laboratories, and Bulgaria, Turkey, and Serbia recommend BSL-2 laboratories (*15*). For most testing modalities, other than viral culture, viral

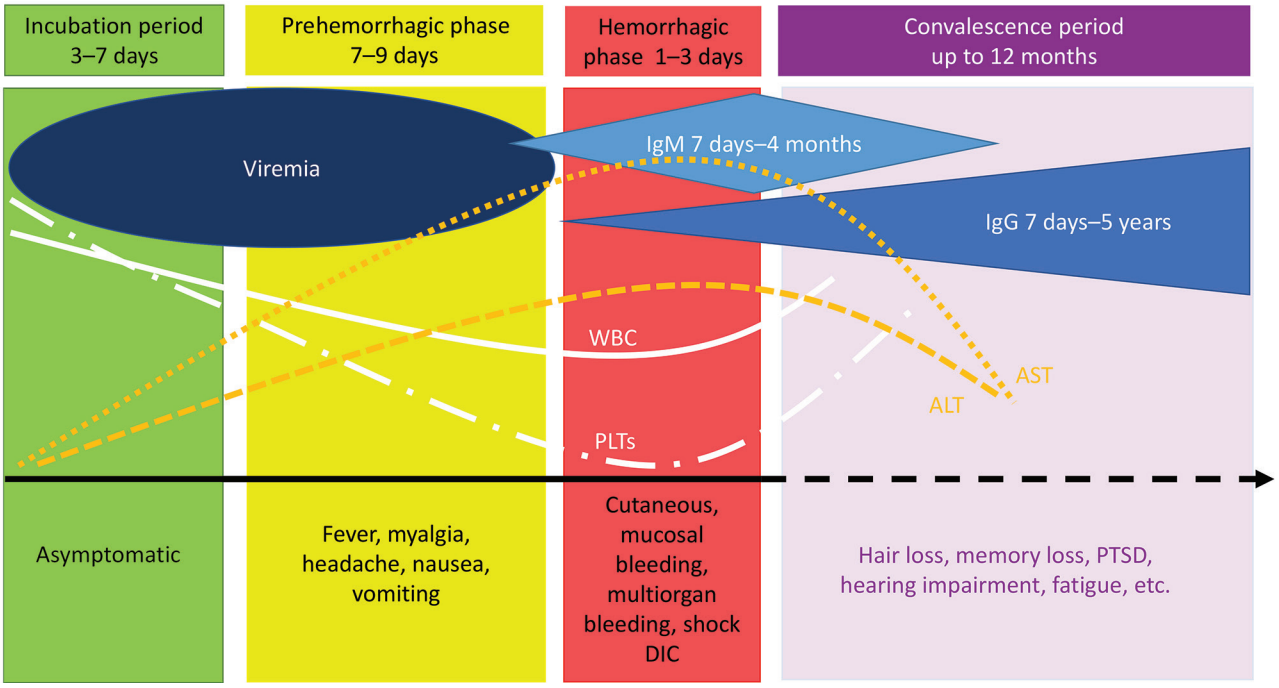

Figure. Overview of Crimean-Congo hemorrhagic fever virus symptom onset, clinical course, and diagnostic testing timeframes. ALT, alanine aminotransferase; AST, aspartate aminotransferase; DIC disseminated intravascular coagulation; PLTs, platelets; PTSD, post-traumatic stress disorder; WBCs, white blood cells.

inactivation of the sample can be performed to downgrade the BSL requirement (*16*,*17*).

Diagnosis can be obtained either by viral detection or identification of an immune response against CCHFV (Table), and test selection is guided by clinical phase. Although most viral detection tests, either viral culture, nucleic acid amplification tests, or viral antigen detection assays, will have greater sensitivity than immunoassays for diagnosis during the prehemorrhagic or early hemorrhagic phases, serologic testing is reserved for a delayed diagnosis or beyond day 5 after symptom onset (*17*) (Table; Figure). If a negative antibody test is obtained during the second week of illness in a patient suspected to have CCHF, a direct viral assay might be warranted for diagnostic clarification (*17*). Undetectable IgM and IgG in CCHF patients with fatal outcomes have been described (*9*). Whether those patients succumbed to CCHF because of failure to mount an antibody response, a rapidly progressive clinical course with fatal outcome before day 7, or formation of immune complexes that made antibodies undetectable is unclear (*9*).

Direct viral detection tests are useful during viremic stages of CCHF. Viral cultures using cell lines or intracerebral inoculation of suckling mice can detect a wide diversity of CCHFV strains; however, viral cultures are time-consuming, and results can take several days. Another challenge is the paucity of BSL-3 and BSL-4 laboratories able to safely perform viral cultures in endemic areas (*17*). Nucleic acid amplification tests, such as reverse transcription PCR (RT-PCR), can be useful for diagnosis until up to days 10–12 of illness. Assays can be run in inactivated samples in BSL-2 and BSL-3 facilities, but correct inactivation methods need to be selected for compatibility with the chosen diagnostic test (*15*,*16*). Some of those assays are designed as multiplex assays instead of CCHFV-specific and provide breadth to rule out other viral hemorrhagic fevers (*17*). Assays capable to detecting viral load also are available (*17*). However, accuracy of those tests varies and is affected by the match between the PCR primers used and the viral strain because of the wide genetic diversity of CCHFV (*17*). Accuracy can be improved by using real-time RT-PCR (rRT-PCR) or a combination of rRT-PCR and conventional RT-PCR or rRT-PCR and nested RT-PCR (*17*). Combining assays can increase accuracy to 80% from 66% of reference samples when using conventional RT-PCR alone and from 46% when using nested RT-PCR alone (*17*).

Viral antigen detection tests, such as ELISA for serum or immunohistochemistry for tissue from biopsies or autopsy samples, also can be used early in the disease. Those assays require a lower level

of laboratory sophistication, can be done on inactivated samples, and offer timely results; however, assay sensitivity decreases as antibodies become detectable. IgM can be detectable as early as 4–5 days and usually by 7–9 days after symptom onset, peaks within 2–3 weeks, and declines to an almost undetectable level by month 4 from symptom onset (*9*,*16*,*17*). IgG typically becomes detectable 1–2 days after IgM (usually 7–9 days after illness onset), peaking in some patients between weeks 2–3 and between 2–5 months in some other patients. IgG remains detectable for at least 3 years (*9*,*16*,*17*). Neutralizing antibodies, although not routinely tested in the clinical setting, often can be detected by day 10 with variable titers (*9*).

CCHF diagnosis can be confirmed not only by the direct viral identification methods described, but also by evidence of a serologic response consistent with acute infection. CCHFV serologic testing is typically recommended 5–7 days after symptom onset; ELISA and immunofluorescence assays are the most common (*16*) (Figure). ELISA results are considered consistent with acute infection if either CCHFV IgM is detected or a 4-fold increase in CCHFV IgG titers occurs between serial blood samples. Some CCHFV antibody assays are known to cross-react with Nairobi sheep disease serogroup, which also causes human disease in some CCHF endemic areas, and with Hazara virus, a member of the CCHFV group with no documented human disease (*18*). Several ELISA kits are commercially available for research but not for clinical diagnostic testing, and their sensitivity and specificity are also susceptible to CCHFV genetic variability (*16*). However, some of those assays have sensitivities >80% and specificities close to 100% (*17*). One commercially available immunofluorescence assay demonstrated a sensitivity of 93.9% for IgM and 86% for IgG and 100% specificity for both (*17*) (Table). No commercial rapid CCHF diagnostic tests are available for clinical use (*16*,*17*,*19*).

In the United States, testing of clinical specimens for CCHFV at designated reference laboratories should be arranged by consulting with respective local public health authorities and coordinating with the Centers for Disease Control and Prevention.

Table. Advantages and disadvantages of various diagnostic tests for CCHFV*

Test selection	Timing	Advantages	Disadvantages
Viral detection†			
Viral culture‡	Early after symptom onset	Detects a wide diversity of CCHFV strains	Requires BSL-3 or BSL-4 laboratory, which are not readily available in endemic areas. Requires several days to yield a result.
NAAT, RT-PCR	≤10–12 days after symptom onset	If samples are inactivated, then NAAT can be run in BSL-2 or BSL-3 facilities. Several multiplex assays available, and some can quantify viral load.	Variable sensitivity depending on match between primers and infecting strain. Sensitivity and specificity can vary by geographic region. Better sensitivity (80%) when PCR combinations used, e.g., rRT-PCR and conventional PCR or rRT-PCR and nested PCR (*17*).
Viral antigen detection			
ELISA	≤5–9 days after symptom onset	Timely results. Viral inactivation can be performed. Requires less laboratory specialization.	Decreased sensitivity after CCHFV antibodies are detectable.
Immunohistochemistry	≤5–9 days after symptom onset	Can assist in retrospective diagnosis for fatal cases.	Requires biopsy or necropsy samples.
Immune response, serology			
IgM ELISA§ or IFA¶	Detectable 7–9 days after symptom onset; peak 2–3 weeks; declines to low levels by month 4	ELISA sensitivity 87.8%, specificity 98.9. IFA sensitivity 93.9%, specificity 100% (*17*).	Commercially available kits for research but not for clinical laboratories; variable geographic sensitivity; IgM might not be detectable in fatal cases
IgG ELISA§, IFA¶, or Luminex xMAP	Detectable 1–2 d after IgM, peaks 2 wks–5 mo; detectable for ≤3 y	ELISA sensitivity 80.4%, specificity 100%. IFA sensitivity 86.1% specificity 100% (*17*).	Commercial ELISA and IFA kits available for research but not for clinical laboratories; variable geographic sensitivity; IgM might not be detectable in fatal cases
Neutralizing antibodies#	≥10 days after illness onset	Can be performed in BSL-2 facilities	Takes several days to perform. Not routinely used for diagnostic purposes.

*BSL, Biosafety Level; CCHFV, Crimean-Congo hemorrhagic fever virus; RT-PCR, reverse transcription PCR; rRT-PCR, real-time RT-PCR; Ddx, differential diagnoses; IFA: immunofluorescence assays; Nabs, neutralizing antibodies.
†Recommended when patient is viremic. Could be performed as cell culture or intracerebral inoculation of mice.
‡RT-PCR could be real-time, conventional, nested or a combination
§VectroCrimea-CHF (Vector-Best, https://en.vector-best.ru).
¶Crimean Congo Fever Mosaic 2 (Euroimmun, https://www.euroimmun.com).
#Pseudoplaque or plaque reduction neutralization tests for CCHFV viral-like particles.

CCHFV is a notifiable communicable disease in the United States and Europe and is considered a category A priority pathogen by the National Institute of Allergy and Infectious Diseases (NIAID; https://www.niaid.nih.gov/research/emerging-infectious-diseases-pathogens). Thus, clinicians should coordinate with public health authorities for collecting and shipping clinical samples and should follow requirements by the US Department of Transportation Hazardous Materials Regulations, 49 CFR 171–180 (https://www.ecfr.gov/current/title-49/subtitle-B/chapter-I/subchapter-C), and the International Air Transport Association Dangerous Goods Regulations (https://www.iata.org/en/publications/dgr).

Medical Countermeasures

No FDA-approved medications or vaccines are available to prevent or treat CCHF, nor are any approved by the European Medicines Agency. In this section, we describe evidence for off-label use of existing medications and upcoming investigational countermeasures that are in development and have been assessed for prophylactic or therapeutic effects on CCHFV infection in humans or animal models. The first article in this series should serve as a reference on virologic features when reviewing medical countermeasures and vaccine sections (*11*).

Preexposure Prophylaxis and CCHF Vaccines

A single vaccine is available to prevent CCHF in humans, produced by BulBio-NCIPD Limited (https://wwww.bulbio.com), but its licensure is limited to Bulgaria. This vaccine originally was developed in the former Soviet Union in 1970 and has been used in at-risk populations in Bulgaria, primarily military and medical personnel, since 1974 (*20*). The vaccine consists of chloroform and heat inactivated CCHFV strain V42/81 isolated from suckling mouse brain tissue (*20*). The vaccine series is administered in 2 intramuscular doses 30 days apart, a 3rd dose at 1 year, and subsequent booster doses every 5 years (*20*). The vaccine has been shown to elicit CCHFV IgG but with low viral neutralization activity and T-cell responses to the CCHFV nucleoprotein (*21*). No vaccine effectiveness data are available. A 4-fold decrease in CCHFV diagnoses in Bulgaria was demonstrated in the 21 years after introduction of that vaccine; however, the degree to which the decrease is attributable to vaccination versus other measures remains unclear (*20*).

Aside from the inactivated vaccine available in Bulgaria, only 1 vaccine candidate, an inactivated vaccine derived from cell culture, has advanced to human clinical trials (https://www.ClinicalTrials.gov, no. NCT03020771). Although a phase 1 trial has been completed, no results were available by early 2023. Several other vaccine candidates are in preclinical development. Those vaccines primarily target the CCHFV glycoprotein, nucleoprotein, or both, including DNA-based (*22*–*29*), RNA-based (*30*,*31*), protein subunit–based (*32*–*34*), viral replicon particle–based platforms (*35*–*38*), and recombinant viral vector–based platforms that use bovine herpesvirus type 4, human adenovirus 5, modified vaccinia Ankara, and vesicular stomatitis virus (*39*–*44*). Vaccine-induced protection might be elicited by vaccines containing either the CCHFV glycoprotein or nucleoprotein in preclinical studies, but not consistently across vaccine platforms expressing the same antigen (Appendix 1 Table, https://wwwnc.cdc.gov/EID/article/30/5/23-1648-App1.pdf).

The World Health Organization has identified development of CCHF vaccines as a priority (*45*) but faces multiple challenges, including the high degree of genetic diversity between CCHFV strains, the need for high biocontainment laboratories to perform challenge studies, and the limited animal models in which CCHF disease can be replicated. Animal models amenable to vaccine studies were not available until lethal CCHF disease models in mice with deficits in type 1 interferon signaling pathways (STAT1−/− and IFNAR−/− mice) were identified in 2010 (*46*,*47*). Recently developed models of CCHF disease in humanized mice, in cynomolgus macaques (*Macaca fascicularis*), and among immunocompetent mice using a mouse-adapted CCHFV variant provide additional options for future CCHF vaccine studies (*48*–*50*). The lack of immune correlates of protection against CCHFV additionally poses a challenge for vaccine development. Neither CCHFV antibody titers nor neutralizing antibody titers correlate with vaccine-induced protection against disease or survival in animal models (*9*,*10*,*25*,*26*,*32*,*43*). However, recent data from a novel repRNA vaccine expressing CCHFV nucleoprotein suggest that a single dose of this vaccine could induce robust and protective immunity in mice (*30*). Some studies suggest that both humoral and cellular immune responses might be required for full protection against CCHF disease and death (*30*,*42*).

Postexposure Prophylaxis

Ribavirin (1-β-D-ribofuranosyl-1,2,4-triazole-3-carboxamide) is a purine nucleoside analog that acts against a wide range of viruses (Appendix 2 [https://wwwnc.cdc.gov/EID/article/30/5/23-1648-App2.pdf] references

51,52). Ribavirin has multiple potential mechanisms of antiviral activity and in vitro antiviral activity against CCHFV (Appendix 2 references *51,52*). The effectiveness of oral ribavirin prophylaxis for preventing CCHF is unknown, but it has been used as postexposure prophylaxis among healthcare workers with known CCHFV exposures (Appendix 2 references *53*–*56*). The optimal dosing and duration of postexposure prophylaxis is unclear; postexposure ribavirin regimens reported to date for CCHFV include total doses ranging from 1,200 to 4,000 mg daily and doses administered from 2 to 4 times daily for 5–14 days, with or without a loading dose (*21*) (Appendix 2 references *53*–*57*). CCHFV seroconversion has been reported among healthcare workers who were administered postexposure ribavirin prophylaxis after sustaining breaches in personal protective equipment while managing CCHF patients (Appendix 2 references *54,58*). Mild symptoms in those healthcare workers initially were attributed to side effects from ribavirin (Appendix 2 references *54,58*). Ribavirin frequently causes side effects, including fatigue, gastrointestinal symptoms, headache, hemolytic anemia, and laboratory abnormalities (Appendix 2 references *54,55*). Ribavirin is contraindicated during pregnancy and has an FDA category X rating because of potential embryotoxic and teratogenic effects (Appendix 2 reference *59*).

Antiviral Drug Treatments

Ribavirin

In addition to postexposure prophylaxis, ribavirin has been used to treat CCHF. Ribavirin reduces CCHFV viral loads in murine models (Appendix 2 references *60,61*). However, similar viremia reductions have not been observed among infected humans treated with ribavirin compared with untreated control patients (Appendix 2 references *62,63*).

Evidence from human studies of ribavirin for CCHF treatment mainly consists of case series, case-control studies that use historical controls, and retrospective analyses, but few randomized clinical trials have been conducted, and meta-analyses identified potential for bias in multiple studies (Appendix 2 references *64*–*67*). In addition to variable study design, comparison of ribavirin effectiveness across studies is challenging because study outcomes could be influenced by other heterogeneous factors, such as differences in the administration route (oral vs. intravenous) and dosing of ribavirin, timing of ribavirin initiation, co-administration of other potential disease-modifying medications, severity of patients analyzed, and variation in predominant CCHFV strains in different geographic regions.

A prospective, randomized clinical trial of oral ribavirin for CCHF treatment conducted in Turkey compared ribavirin with supportive therapy alone (Appendix 2 reference *68*). In that study, patients were administered 30 mg/kg ribavirin as a loading dose, then 15 mg/kg every 6 hours for 4 days, after which they received 7.5 mg/kg every 8 hours for 6 days. The researchers observed no substantial differences in death, hospitalization duration, time to normalization of transaminases, or percentage of patients requiring platelet transfusions (Appendix 2 reference *68*). Several meta-analyses reveal mixed results for effects of ribavirin on CCHF, ranging from no clear survival benefit to a 1.7-fold reduction in mortality rates among CCHF patients treated with ribavirin compared with those not receiving ribavirin (Appendix 2 reference *64*–*67*).

Favipiravir

Favipiravir (6-fluoro-3-hydroxy-2-pyrazinecarboxamide) is a pyrazine analog that inhibits RNA polymerase activity in a wide variety of viruses. In vitro studies suggest that premature chain termination induced by favipiravir exceeds that of ribavirin for CCHFV and demonstrate synergistic antiviral effects when ribavirin and favipiravir are combined (Appendix 2 references *69*,*70*).

Favipiravir is not licensed for use in the United States but is licensed for treatment of novel influenza A in Japan. Early favipiravir treatment for CCHFV infection reduces viral loads and clinical signs in both murine and macaque CCHF models, but prolonged viral detection and occasional late-onset CCHF disease were observed in mice (Appendix 2 references *60*,*71*). In lethal CCHFV challenge mouse models, treatment with favipiravir enhanced disease survival, even when initiated as late as 6 days postinfection (Appendix 2 references *60*,*70*). Only 1 case of human CCHF treatment with favipiravir has been described: a patient hospitalized with CCHFV and SARS-CoV-2 co-infection was treated with 1,600 mg favipiravir twice daily on day 1, then 600 mg twice daily for 4 days; the patient subsequently recovered (Appendix 2 reference *72*). Favipiravir induces teratogenicity in animal models and should be avoided in pregnant and lactating women, if possible. Additional adverse effects include the potential for gastrointestinal distress (e.g., nausea, vomiting, or diarrhea), increased bilirubin levels, transaminitis, QTc prolongation, and hyperuricemia (Appendix 2 reference *73*).

Other Treatments

Supportive therapy remains the mainstay of CCHF treatment. Such therapy includes fluid replacement, management of electrolyte disturbances, blood product replacement for critically low levels and coagulopathy (e.g., fresh frozen plasma, packed red blood cells, or platelets), treatment of secondary infections, and external support for organ dysfunction (e.g., hemodialysis, mechanical ventilation) when necessary (Appendix 2 references *74*–*77*). Aspirin and nonsteroidal antiinflammatory drugs should be avoided because of the potential inhibition of platelet aggregation or agglutination.

Therapeutic plasma exchange and plasmapheresis have been used to treat CCHF, but the clinical benefits of those measures remain unclear because data are limited to individual case reports or small case series (Appendix 2 references *78*–*81*). In patients with CCHF-related hemophagocytic lymphohistiocytosis, use of intravenous immunoglobulin or high dose steroids, in addition to blood product transfusions, has been reported (Appendix 2 references *82*,*83*). In a study of 35 CCHF patients in Iran, high dose methylprednisolone (10 mg/kg for 3 days, followed by 5 mg/kg for 2 days) administered with ribavirin to patients with platelet counts <50,000/mL resulted in higher platelet and leukocyte counts and decreased need for transfusions compared with ribavirin alone, but no difference in deaths was observed (Appendix 2 reference *84*). In 1 retrospective study, fewer deaths were observed among patients with severe CCHF who received both corticosteroids and ribavirin therapy compared with those treated with ribavirin alone, but no statistically significant decrease in deaths was observed among patients with mild or moderate CCHF treated with this combination (Appendix 2 reference *85*). In 1 meta-analysis, an additional decrease in deaths was observed for corticosteroids in addition to ribavirin compared with ribavirin alone (Appendix 2 reference *65*).

Hyperimmune immunotherapy for CCHF using pooled serum or plasma harvested from CCHF survivors or CCHF vaccine recipients has been reported, but its effectiveness is unknown because its use has only been reported in small case series (Appendix 2 references *86*–*88*). Hyperimmune serum for CCHF treatment is not approved by either the FDA or the European Medicines Agency. Monoclonal antibodies for CCHF are in preclinical development and show improved survival among mouse models, but the degree of protection conferred by some monoclonal antibodies varied depending on the infecting CCHFV strain (Appendix 2 references *89*,*90*).

Conclusion

CCHFV poses a continued public health threat given its wide geographic distribution, potential to spread to new regions, propensity for genetic variability, and potential for severe and fatal illness. Although infection control measures can be effective in reducing the risk for CCHFV transmission within community and healthcare settings, those measures require correct and consistent application. An urgent need exists for new CCHF diagnostic tests, prophylaxes, and treatments. The current lack of licensed effective therapeutic and prophylactic drugs, gaps in our understanding of CCHFV pathogenesis and immunology, and slow progression in development of CCHF medical countermeasures are in part related to the dearth of animal models and high level of biosafety precautions needed to safely work with CCHFV.

In conclusion, to promptly diagnose CCHF, clinicians should have a high index of suspicion, collect a comprehensive travel and epidemiologic history, and perform a thorough clinical evaluation. Evidence to demonstrate human benefit from off-label use of ribavirin and favipiravir is disparate. Because few medical countermeasures are available for prophylaxis and treatment, supportive care remains the treatment standard for CCHF disease management. New CCHF diagnostic tests, prophylaxis, and treatments are urgently needed. Given its wide range and potential for severe outcomes, clinicians should become familiar with available diagnostic and management tools for CCHFV infections in humans.

Members of the State of the Clinical Science Working Group of the National Emerging Pathogens Training and Education Center's Special Pathogens Research Network: Richard T. Davey, Jr., Noreen A. Hynes, Mark G. Kortepeter, Nahid Bhadelia, Kerry Dierberg, Aneesh K. Mehta, Corri B. Levine, Peter C. Iwen, Denis A. Bente, Justin Chan, and Adam Beitscher.

Acknowledgments

We thank Nahid Bhadelia, Kerry Dierberg, and Mark G. Kortepeter for completing a previous version of this manuscript.

Research reported in this publication was supported by the Department of Health and Human Services Office of the Assistant Secretary for Preparedness and Response.

About the Author

Dr. Frank is a hospitalist and medical director of Denver Health Hospital Authority's Biocontainment Unit and a professor of medicine at the University of Colorado, School of Medicine, Denver, CO, USA. Her research interests include medical management of special pathogens and involvement of general internists in disaster response.

References

1. Ergonual O, Whitehouse CA, eds. Crimean-Congo hemorrhagic fever: a global perspective. Dordrecht (The Netherlands): Springer; 2007.
2. Mishra AK, Hellert J, Freitas N, Guardado-Calvo P, Haouz A, Fels JM, et al. Structural basis of synergistic neutralization of Crimean-Congo hemorrhagic fever virus by human antibodies. Science. 2022;375:104–9. https://doi.org/10.1126/science.abl6502
3. World Health Organization. Introduction to Crimean Congo haemorrhagic fever: managing infectious hazards [cited 2023 Jul 1]. https://cdn.who.int/media/docs/default-source/documents/health-topics/crimean-congo-haemorrhaigc-fever/introduction-to-crimean-congo-haemorrhagic-fever.pdf
4. Al-Abri SS, Abaidani IA, Fazlalipour M, Mostafavi E, Leblebicioglu H, Pshenichnaya N, et al. Current status of Crimean-Congo haemorrhagic fever in the World Health Organization Eastern Mediterranean Region: issues, challenges, and future directions. Int J Infect Dis. 2017;58:82–9. https://doi.org/10.1016/j.ijid.2017.02.018
5. Hawman DW, Feldmann H. Recent advances in understanding Crimean-Congo hemorrhagic fever virus. F1000 Res. 2018;7:1715. https://doi.org/10.12688/f1000research.16189.1
6. Khan AS, Maupin GO, Rollin PE, Noor AM, Shurie HHM, Shalabi AGA, et al. An outbreak of Crimean-Congo hemorrhagic fever in the United Arab Emirates, 1994–1995. Am J Trop Med Hyg. 1997;57:519–25. https://doi.org/10.4269/ajtmh.1997.57.519
7. Nurettin C, Engin B, Sukru T, Munir A, Zati V, Aykut O. The seroprevalence of Crimean-Congo hemorrhagic fever in wild and domestic animals: an epidemiological update for domestic animals and first seroevidence in wild animals from Turkiye. Vet Sci. 2022;9:462. https://doi.org/10.3390/vetsci9090462
8. Saksida A, Duh D, Wraber B, Dedushaj I, Ahmeti S, Avsic-Zupanc T. Interacting roles of immune mechanisms and viral load in the pathogenesis of Crimean-Congo hemorrhagic fever. Clin Vaccine Immunol. 2010;17:1086–93. https://doi.org/10.1128/CVI.00530-09
9. Rodriguez SE, Hawman DW, Sorvillo TE, O'Neal TJ, Bird BH, Rodriguez LL, et al. Immunobiology of Crimean-Congo hemorrhagic fever. Antiviral Res. 2022;199:105244. https://doi.org/10.1016/j.antiviral.2022.105244
10. Garrison AR, Smith DR, Golden JW. Animal models for Crimean-Congo hemorrhagic fever human disease. Viruses. 2019;11:590. https://doi.org/10.3390/v11070590
11. Frank MG, Weaver G, Raabe V; State of the Clinical Science Working Group of the National Emerging pathogens Training and Education Center's Special Pathogens Research Network. Crimean-Congo hemorrhagic fever virus for clinicians—virology, pathogenesis, and pathology. Emerg Infect Dis. 2024;30:847–853. https://doi.org/10.3201/eid3005.231646
12. Frank MG, Weaver G, Raabe V; State of the Clinical Science Working Group of the National Emerging pathogens Training and Education Center's Special Pathogens Research Network. Crimean-Congo hemorrhagic fever virus for clinicians—epidemiology, clinical manifestations, and prevention. Emerg Infect Dis. 2024;30:854-863. https://doi.org/10.3201/eid3005.231647
13. Tasdelen Fisgin N, Doganci L, Tanyel E, Tulek N. Initial high rate of misdiagnosis in Crimean Congo haemorrhagic fever patients in an endemic region of Turkey. Epidemiol Infect. 2010;138:139–44. https://doi.org/10.1017/S0950268809990318
14. Fletcher TE, Gulzhan A, Ahmeti S, Al-Abri SS, Asik Z, Atilla A, et al. Infection prevention and control practice for Crimean-Congo hemorrhagic fever—a multi-center cross-sectional survey in Eurasia. PLoS One. 2017;12:e0182315. https://doi.org/10.1371/journal.pone.0182315
15. Weidmann M, Avsic-Zupanc T, Bino S, Bouloy M, Burt F, Chinikar S, et al. Biosafety standards for working with Crimean-Congo hemorrhagic fever virus. J Gen Virol. 2016;97:2799–808. https://doi.org/10.1099/jgv.0.000610
16. Emmerich P, von Possel R, Deschermeier C, Ahmeti S, Berisha L, Halili B, et al. Comparison of diagnostic performances of ten different immunoassays detecting anti-CCHFV IgM and IgG antibodies from acute to subsided phases of Crimean-Congo hemorrhagic fever. PLoS Negl Trop Dis. 2021;15:e0009280. https://doi.org/10.1371/journal.pntd.0009280
17. Raabe VN. Diagnostic testing for Crimean-Congo hemorrhagic fever. J Clin Microbiol. 2020;58:e01580-19. https://doi.org/10.1128/JCM.01580-19
18. Suda Y, Chamberlain J, Dowall SD, Saijo M, Horimoto T, Hewson R, et al. The development of a novel diagnostic assay that utilizes a pseudotyped vesicular stomatitis virus for the detection of neutralizing activity against Crimean-Congo hemorrhagic fever virus. Jpn J Infect Dis. 2018;71:205–8. https://doi.org/10.7883/yoken.JJID.2017.354
19. Mattiuzzo G, Bentley EM, Page M. The role of reference materials in the research and development of diagnostic tools and treatments for haemorrhagic fever viruses. Viruses. 2019;11:781. https://doi.org/10.3390/v11090781
20. Papa A, Papadimitriou E, Christova I. The Bulgarian vaccine Crimean-Congo haemorrhagic fever virus strain. Scand J Infect Dis. 2011;43:225–9. https://doi.org/10.3109/00365548.2010.540036
21. Mousavi-Jazi M, Karlberg H, Papa A, Christova I, Mirazimi A. Healthy individuals' immune response to the Bulgarian Crimean-Congo hemorrhagic fever virus vaccine. Vaccine. 2012;30:6225–9. https://doi.org/10.1016/j.vaccine.2012.08.003
22. Spik K, Shurtleff A, McElroy AK, Guttieri MC, Hooper JW, SchmalJohn C. Immunogenicity of combination DNA vaccines for Rift Valley fever virus, tick-borne encephalitis virus, Hantaan virus, and Crimean Congo hemorrhagic fever virus. Vaccine. 2006;24:4657–66. https://doi.org/10.1016/j.vaccine.2005.08.034
23. Garrison AR, Shoemaker CJ, Golden JW, Fitzpatrick CJ, Suschak JJ, Richards MJ, et al. A DNA vaccine for Crimean-Congo hemorrhagic fever protects against disease and death in two lethal mouse models. PLoS Negl Trop Dis. 2017;11:e0005908. https://doi.org/10.1371/journal.pntd.0005908
24. Aligholipour Farzani T, Hanifehnezhad A, Földes K, Ergünay K, Yilmaz E, Hashim Mohamed Ali H, et al. Co-delivery effect of CD24 on the immunogenicity and lethal challenge protection of a DNA vector expressing

nucleocapsid protein of Crimean Congo hemorrhagic fever virus. Viruses. 2019;11:75. https://doi.org/10.3390/v11010075
25. Hinkula J, Devignot S, Åkerström S, Karlberg H, Wattrang E, Bereczky S, et al. Immunization with DNA plasmids coding for Crimean-Congo hemorrhagic fever virus capsid and envelope proteins and/or virus-like particles induces protection and survival in challenged mice. J Virol. 2017;91:e02076-16. https://doi.org/10.1128/JVI.02076-16
26. Suschak JJ, Golden JW, Fitzpatrick CJ, Shoemaker CJ, Badger CV, Schmaljohn CS, et al. A CCHFV DNA vaccine protects against heterologous challenge and establishes GP38 as immunorelevant in mice. NPJ Vaccines. 2021;6:31. https://doi.org/10.1038/s41541-021-00293-9
27. Hawman DW, Meade-White K, Leventhal S, Appelberg S, Ahlén G, Nikouyan N, et al. Accelerated DNA vaccine regimen provides protection against Crimean-Congo hemorrhagic fever virus challenge in a macaque model. Mol Ther. 2023;31:387–97. https://doi.org/10.1016/j.ymthe.2022.09.016
28. Hawman DW, Ahlén G, Appelberg KS, Meade-White K, Hanley PW, Scott D, et al. A DNA-based vaccine protects against Crimean-Congo haemorrhagic fever virus disease in a cynomolgus macaque model. Nat Microbiol. 2020;6:187–95. https://doi.org/10.1038/s41564-020-00815-6
29. Hu YL, Zhang LQ, Liu XQ, Ye W, Zhao YX, Zhang L, et al. Construction and evaluation of DNA vaccine encoding Crimean Congo hemorrhagic fever virus nucleocapsid protein, glycoprotein N-terminal and C-terminal fused with LAMP1. Front Cell Infect Microbiol. 2023;13:1121163. https://doi.org/10.3389/fcimb.2023.1121163
30. Leventhal SS, Meade-White K, Rao D, Haddock E, Leung J, Scott D, et al. Replicating RNA vaccination elicits an unexpected immune response that efficiently protects mice against lethal Crimean-Congo hemorrhagic fever virus challenge. EBioMedicine. 2022;82:104188. https://doi.org/10.1016/j.ebiom.2022.104188
31. Appelberg S, John L, Pardi N, Végvári Á, Bereczky S, Ahlén G, et al. Nucleoside-modified mRNA vaccines protect IFNAR$^{-/-}$ mice against Crimean-Congo hemorrhagic fever virus infection. J Virol. 2022;96:e0156821. https://doi.org/10.1128/jvi.01568-21
32. Kortekaas J, Vloet RP, McAuley AJ, Shen X, Bosch BJ, de Vries L, et al. Crimean-Congo Hemorrhagic fever virus subunit vaccines induce high levels of neutralizing antibodies but no protection in STAT1 knockout mice. Vector Borne Zoonotic Dis. 2015;15:759–64. https://doi.org/10.1089/vbz.2015.1855
33. Wang Q, Wang S, Shi Z, Li Z, Zhao Y, Feng N, et al. GEM-PA–based subunit vaccines of Crimean Congo hemorrhagic fever induces systemic immune responses in mice. Viruses. 2022;14:1664. https://doi.org/10.3390/v14081664
34. Ghiasi SM, Salmanian AH, Chinikar S, Zakeri S. Mice orally immunized with a transgenic plant expressing the glycoprotein of Crimean-Congo hemorrhagic fever virus. Clin Vaccine Immunol. 2011;18:2031–7. https://doi.org/10.1128/CVI.05352-11
35. Scholte FEM, Spengler JR, Welch SR, Harmon JR, Coleman-McCray JD, Freitas BT, et al. Single-dose replicon particle vaccine provides complete protection against Crimean-Congo hemorrhagic fever virus in mice. Emerg Microbes Infect. 2019;8:575–8. https://doi.org/10.1080/22221751.2019.1601030
36. Spengler JR, Welch SR, Scholte FEM, Coleman-McCray JD, Harmon JR, Nichol ST, et al. Heterologous protection against Crimean-Congo hemorrhagic fever in mice after a single dose of replicon particle vaccine. Antiviral Res. 2019;170:104573. https://doi.org/10.1016/j.antiviral.2019.104573
37. Tipih T, Heise M, Burt FJ. Immunogenicity of a DNA-based Sindbis replicon expressing Crimean-Congo hemorrhagic fever virus nucleoprotein. Vaccines (Basel). 2021;9:1491. https://doi.org/10.3390/vaccines9121491
38. Spengler JR, Welch SR, Scholte FEM, Rodriguez SE, Harmon JR, Coleman-McCray JD, et al. Viral replicon particles protect IFNAR$^{-/-}$ mice against lethal Crimean-Congo hemorrhagic fever virus challenge three days after vaccination. Antiviral Res. 2021;191:105090. https://doi.org/10.1016/j.antiviral.2021.105090
39. Aligholipour Farzani T, Földes K, Hanifehnezhad A, Yener Ilce B, Bilge Dagalp S, Amirzadeh Khiabani N, et al. Bovine herpesvirus type 4 (BoHV-4) vector delivering nucleocapsid protein of Crimean-Congo hemorrhagic fever virus induces comparable protective immunity against lethal challenge in IFNα/β/γR−/− mice models. Viruses. 2019;11:237. https://doi.org/10.3390/v11030237
40. Zivcec M, Safronetz D, Scott DP, Robertson S, Feldmann H. Nucleocapsid protein-based vaccine provides protection in mice against lethal Crimean-Congo hemorrhagic fever virus challenge. PLoS Negl Trop Dis. 2018;12:e0006628. https://doi.org/10.1371/journal.pntd.0006628
41. Buttigieg KR, Dowall SD, Findlay-Wilson S, Miloszewska A, Rayner E, Hewson R, et al. A novel vaccine against Crimean-Congo haemorrhagic fever protects 100% of animals against lethal challenge in a mouse model. PLoS One. 2014;9:e91516. https://doi.org/10.1371/journal.pone.0091516
42. Dowall SD, Graham VA, Rayner E, Hunter L, Watson R, Taylor I, et al. Protective effects of a modified vaccinia Ankara-based vaccine candidate against Crimean-Congo haemorrhagic fever virus require both cellular and humoral responses. PLoS One. 2016;11:e0156637. https://doi.org/10.1371/journal.pone.0156637
43. Dowall SD, Buttigieg KR, Findlay-Wilson SJ, Rayner E, Pearson G, Miloszewska A, et al. A Crimean-Congo hemorrhagic fever (CCHF) viral vaccine expressing nucleoprotein is immunogenic but fails to confer protection against lethal disease. Hum Vaccin Immunother. 2016;12:519–27. https://doi.org/10.1080/21645515.2015.1078045
44. Rodriguez SE, Cross RW, Fenton KA, Bente DA, Mire CE, Geisbert TW. Vesicular stomatitis virus-based vaccine protects mice against Crimean-Congo hemorrhagic fever. Sci Rep. 2019;9:7755. https://doi.org/10.1038/s41598-019-44210-6
45. Mehand MS, Al-Shorbaji F, Millett P, Murgue B. The WHO R&D Blueprint: 2018 review of emerging infectious diseases requiring urgent research and development efforts. Antiviral Res. 2018;159:63–7. https://doi.org/10.1016/j.antiviral.2018.09.009
46. Bente DA, Alimonti JB, Shieh WJ, Camus G, Ströher U, Zaki S, et al. Pathogenesis and immune response of Crimean-Congo hemorrhagic fever virus in a STAT-1 knockout mouse model. J Virol. 2010;84:11089–100. https://doi.org/10.1128/JVI.01383-10
47. Bereczky S, Lindegren G, Karlberg H, Akerström S, Klingström J, Mirazimi A. Crimean-Congo hemorrhagic fever virus infection is lethal for adult type I interferon receptor-knockout mice. J Gen Virol. 2010;91:1473–7. https://doi.org/10.1099/vir.0.019034-0

48. Spengler JR, Kelly Keating M, McElroy AK, Zivcec M, Coleman-McCray JD, Harmon JR, et al. Crimean-Congo hemorrhagic fever in humanized mice reveals glial cells as primary targets of neurological infection. J Infect Dis. 2017;216:1386–97. https://doi.org/10.1093/infdis/jix215
49. Haddock E, Feldmann F, Hawman DW, Zivcec M, Hanley PW, Saturday G, et al. A cynomolgus macaque model for Crimean-Congo haemorrhagic fever. Nat Microbiol. 2018;3:556–62. https://doi.org/10.1038/s41564-018-0141-7
50. Oimomi M, Ohkawa J, Saeki S, Baba S. The frequency of C5 + cholinesterase in the normal Japanese population. Clin Chim Acta. 1988;175:349–50. https://doi.org/10.1016/0009-8981(88)90113-1

Address for correspondence: Maria G. Frank, University of Colorado Anschutz Medical Campus, Internal Medicine, 12401 E 17th Ave, Mailstop F-782, Aurora, CO 80045-2559, USA; email: maria.frank@dhha.org or maria.frank@cuanschutz.edu

Case Series of Jamestown Canyon Virus Infections with Neurologic Outcomes, Canada, 2011–2016

Vanessa Meier-Stephenson, Michael A. Drebot, Kristina Dimitrova, Melanie DiQuinzio, Kevin Fonseca, David Forrest, Todd Hatchette, Muhammad Morshed, Glenn Patriquin, Guillaume Poliquin, Lynora Saxinger, Bouchra Serhir, Raymond Tellier, Christian Therrien, Linda Vrbova, Heidi Wood

Jamestown Canyon virus (JCV) is a mosquitoborne orthobunyavirus in the California serogroup that circulates throughout Canada and the United States. Most JCV exposures result in asymptomatic infection or a mild febrile illness, but JCV can also cause neurologic diseases, such as meningitis and encephalitis. We describe a case series of confirmed JCV-mediated neuroinvasive disease among persons from the provinces of British Columbia, Alberta, Quebec, and Nova Scotia, Canada, during 2011–2016. We highlight the case definitions, epidemiology, unique features and clinical manifestations, disease seasonality, and outcomes for those cases. Two of the patients (from Quebec and Nova Scotia) might have acquired JCV infections during travel to the northeastern region of the United States. This case series collectively demonstrates JCV's wide distribution and indicates the need for increased awareness of JCV as the underlying cause of meningitis/meningoencephalitis during mosquito season.

Jamestown Canyon virus (JCV) is a mosquitoborne arbovirus belonging to the California serogroup (CSG) viruses (genus *Orthobunyavirus*, family Peribunyaviridae). JCV was first isolated from pooled *Culiseta inornata* mosquitoes in 1961 in Jamestown Canyon, Colorado, USA (*1*). JCV transmission occurs through bites during blood meal acquisition by *Aedes*, *Culesita*, *or Anopheles* mosquitoes, which have wide geographic ranges across North America (*1*–*3*). Despite the existence of JCV in mosquito and mammal hosts, the first human cases of JCV-associated illness were not recognized until 1980 (*4*–*8*). In North America, the primary amplifying host is thought to be white-tailed deer; however, serologic evidence of JCV has been documented in various domestic and nondomestic animals, including dogs, sheep, mink, cows, horses, foxes, polar bears, elk, and deer (*9*,*10*). In addition, JCV can pass transovarially within the mosquito, which can result in infections early during the mosquito season in May and June; those cases have been documented in different provinces in Canada (*11*; M.A. Drebot, unpub. data).

Human cases of JCV infection are uncommon and have been sporadic. The first JCV infection in Canada was identified in 1981 in an Ontario resident (*8*), and, over the subsequent 4 decades, 1–90 probable and confirmed cases of JCV infection in Canada have been documented each year (*2*,*12*–*15*; M.A. Drebot, unpub. data). In the United States, an average of 16 neuroinvasive JCV cases have been reported each year since 2011 to the Centers for Disease Control and Prevention (CDC) (*16*,*17*). However, JCV infections are likely underdiagnosed and underreported because of asymptomatic or mild manifestations observed in most infected persons (*18*–*22*).

Whereas most exposures to JCV are asymptomatic, clinical manifestations can range from a mild febrile illness to neuroinvasive disease (*23*–*25*). We describe 5 cases of JCV neurologic infections that were reported in the provinces of British Columbia, Alberta, Quebec, and Nova Scotia in Canada during 2011–2016.

Author affiliations: University of Alberta, Edmonton, Alberta, Canada (V. Meier-Stephenson, L. Saxinger); Public Health Agency of Canada, Winnipeg, Manitoba, Canada (M.A. Drebot, K. Dimitrova, G. Poliquin, L. Vrbova, H. Wood); Dalhousie University, Halifax, Nova Scotia, Canada (M. DiQuinzio, T. Hatchette, G. Patriquin); Alberta Precision Labs, Calgary, Alberta, Canada (K. Fonseca); University of British Columbia, Nanaimo, British Columbia, Canada (D. Forrest); British Columbia Centre for Disease Control, Vancouver, British Columbia, Canada (M. Morshed); Institut National de Santé Publique du Québec, Québec City, Quebec, Canada (B. Serhir, C. Therrien); McGill University Health Centre, Montreal, Quebec, Canada (R. Tellier)

DOI: https://doi.org/10.3201/eid3005.221258

Methods

Clinical Data and Ethics Statement

We obtained all clinical data through chart review after patient consent within their respective institutions. The Health Canada and Public Health Agency Research Ethics Board provided approval for this research.

California Serogroup Virus Serology

We screened serum samples for snowshoe hare virus (SSHV) and JCV virus antibodies by using CDC-based or in-house IgM capture ELISAs, as previously described (*26*). We used plaque reduction neutralization tests (PRNTs) to confirm JCV infections and CSG virus exposures (*25*,*27*). We considered the titration endpoint to be the highest dilution of a patient's serum that inhibited >90% of plaque formation relative to virus controls and a serum titer of ≥1:20 to be positive. We used endpoint titrations to discriminate cross-reactivity between related CSG viruses.

Case Definitions

A confirmed case of JCV infection is defined by the Public Health Agency of Canada as clinical illness occurring when and where transmission is likely and laboratory identification of either JCV nucleic acid in blood or cerebrospinal fluid (CSF), a JCV-specific PRNT with ≥4-fold increase in titer between paired acute and convalescent serum samples (ideally collected ≥2 weeks apart), or the presence of JCV IgM in a CSF sample and a PRNT titer of ≥1:20 in a serum sample (Appendix, https://wwwnc.cdc.gov/EID/article/30/5/22-1258-App1.pdf) (*2*). A probable case is defined as clinical illness accompanied by the presence of JCV-specific IgM and a PRNT titer of ≥1:20 in 1 serum sample. The definitions are similar to those in the CDC guidelines (*28*).

Cases

Case 1

On June 23, 2013, a previously healthy 66-year-old man from the Nanaimo region, British Columbia, was admitted to a hospital because of a 2-day history of fever, fatigue, and cough and subsequent vomiting and diarrhea. He was confused at admission and had a Glasgow coma scale score of 11, but his condition deteriorated, requiring transfer to the intensive care unit for worsening encephalopathy and respiratory distress that ultimately required intubation. A computed tomography (CT) scan of his head revealed no abnormalities, and a lumbar puncture was performed; CSF had 50×10^9 leukocytes/L (85% lymphocytes), 3 mmol/L glucose (reference range 2.2–3.9 mmol/L), and 1.45 g/L protein (reference range 0.2–0.45 g/L) (Table). The patient had recurrent myoclonus and possible tonic-clonic seizures; an electroencephalogram showed generalized slowing with bifrontal spike and slow discharges but no clear electrographic seizure activity. Magnetic resonance imaging (MRI) of the brain showed nonspecific white matter hyperintensities and changes consistent with inflammation and was atypical for ischemic injury.

Serum and CSF samples were negative for cryptococcal antigen, and bacterial and fungal culture results were also negative. In CSF samples, results of PCR testing for herpes simplex virus (HSV) and varicella zoster virus and reverse transcription PCR for enteroviruses were negative. Serum samples were negative for *Borrelia*, *Bartonella*, *Leptospira*, *Mycoplasma, Francisella*, *Coxiella burnetii*, *Toxoplasma*, HIV, West Nile virus (WNV), hepatitis viruses, measles, and parvovirus. PRNTs for JCV IgM had positive titers of 1:40 on June 23 and 1:80 on June 30. Further testing documented that both serum and CSF samples had JCV-specific neutralizing antibodies (Table).

Six months later, the patient reported ongoing issues with coordination and balance. He also noted continuing problems with concentration, short term memory, and depression and was consequently unable to resume work.

Cases 2

An otherwise healthy 48-year-old man from Alberta, manifested bilateral retroorbital and temporal pain in late September 2011. He also had left-sided arm and leg parasthesias lasting ≈5 minutes. Exposures before onset of symptoms included travel to Cadomin and Wabamun in Alberta (Figure). He also traveled to his vacation home in Las Vegas, Nevada, USA, where his headache became persistently severe the next day, and vomiting, a stumbling gait, and a spinning sensation developed. He sought medical care but was presumed to have influenza and was discharged. He displayed confusion and unusual behavior, such as calling his wife but not speaking, over the next 4 days. He returned to Alberta, where he was found to be dazed and walking oddly with evident confusion and had several episodes of short-term memory loss. His retroorbital headache and paraesthesia of his right thigh were still present. He was taken to an emergency department (ED). After unremarkable results for CT head scan and symptom improvement were observed, he was again discharged. He was unreachable for a period

Table. CSF and serologic characteristics of patient samples in case series of Jamestown Canyon virus infections with neurologic outcomes, Canada, 2011–2016*

Case no.	Province	Date	Age, y/sex	CSF parameters†	JCV IgM, blood	PRNT titer, acute serum	PRNT titer, convalescent serum	IgM or PRNT titer, CSF
1	BC	Jun 2013	66/M	50×10^9 leukocytes/L, 85% lymphocytes; 1.45 g/L protein; 3.0 mmol/L glucose	+, Jun 23; +, Jun 30	JCV, 1:40, Jun 23; JCV, 1:80, Jun 30; no SSHV reported	NA	JCV, + IgM, 1:10 PRNT, Jun 26; SSHV, – IgM/PRNT
2	AB	Sep 2011	48/M	246×10^9 leukocytes/L, 1% neutrophils, 98% lymphocytes; 1.73 g/L protein; 4.0 mmol/L glucose	+, Sep 27	JCV, 0, Sep 27; SSHV, 0; Sep 27	JCV, >1:80, Oct 4; SSHV, 0; Oct 4	JCV, + IgM, Sep 26
3	AB	Sep 2013	68/M	321×10^9 leukocytes/L, 52% neutrophils, 36% lymphocytes; 0.54 g/L protein; 4.7 mmol/L glucose	+, Sep 26	JCV, 0, Sep 26; SSHV, 0; Sep 26	JCV, 1:40, Nov 5; SSHV, 0; Nov 5	NA
4	QC	Aug 2011	53/M	5×10^9 leukocytes/L, 0.10 g/L protein, 5.3 mmol/L glucose	+, Aug 26; +, Sep 19; +, Sep 30	JCV, 1:640, Aug 26; SSHV, 1:160; Aug 26	JCV, 1:2,560, Sep 19; SSHV, 1:640; Sep 19; JCV, 1:640, Sep 30; SSHV, 1:160, Sept 30	JCV, + IgM, – PRNT, Aug 26; JCV,+ IgM, 1:16 PRNT, Sep 6
5	NS	Jun 2016	70/M	41×10^9 leukocytes/L, 100% lymphocytes; 0.67 g/L protein; 3.2 mmol/L glucose	+, JCV; +, SSHV	JCV, 1:320, Jul 29; SSHV, 1:40; Jul 29	JCV, 1:1,280, Aug 11; SSHV, 1:80, Aug 11	JCV, + IgM, 1:4 PRNT, Jul 27; SSHV, – IgM/PRNT

*AB, Alberta; BC, British Columbia; CSF, cerebrospinal fluid; JCV, Jamestown Canyon virus; NA, not applicable; NS, Nova Scotia; PRNT, plaque reduction neutralization test; QC, Quebec; SSHV, Snowshoe Hare virus; +, positive; –, negative.
†Reference ranges for CSF: leukocyte count, $0–5 \times 10^9$ cells/L; protein, 0.2–0.45 g/L; glucose, 2.2–3.9 mmol/L.

the next day and unable to speak when he answered his phone. He was found in his vehicle on the side of the road, pulled over and vomiting, and he indicated that he had a headache. In the ED, a repeat CT head scan showed a vague 5-mm low-density focus within the right parietal lobe, but no other acute changes were observed. His peripheral complete blood cell count, electrolytes, and renal and liver function measurements were all within reference ranges. CSF revealed 246×10^9 leukocytes/L (98% lymphocytes), 4 mmol/L glucose, and 1.73 g/L protein. Bacterial culture results were negative. CSF was negative for enterovirus/parechovirus, varicella virus, and HSV. He was discharged after 3 days with a plan for a follow-up MRI as an outpatient. While at work the next day, he became uncommunicative and had a headache and right-sided paraesthesias and was hospitalized. His neurologic exam revealed depressed mental status and poor concentration. He had asymmetric reflexes (left side reflexes were greater than the right), spastic tone, and downgoing plantar reflexes. Bloodwork and CSF results were essentially unchanged. He had an electroencephalogram, which showed frontal intermittent rhythmic delta activity; an MRI showed multiple nonspecific hyperintensities in the right frontal cortex and right splenium of the corpus callosum.

Acute and convalescent serum samples were positive for JCV IgM, and a convalescent PRNT had a titer >1:80. In February 2012, a repeat lumbar puncture was performed; CSF was positive for JCV IgM. The patient made a full recovery without any further sequelae.

Case 3

A 65-year-old man with a history of Merkel cell cancer, parotidectomy, well-controlled type 2 diabetes, and hypertension manifested acute onset of a dull, unilateral frontal headache during mid-September 2013 in Alberta. Two weeks before onset of symptoms, the patient had been golfing and camping in Three Hills, Alberta, and recalled having received several mosquito bites (Figure). Chills and sweats accompanied by several episodes of vomiting developed 2 days after headache onset. He sought care at an ED 4 days later because of a persistent headache and fever of 38.2°C. A preliminary examination, including bloodwork for temporal arteritis, was negative. Later that evening, he became progressively confused with fluctuating arousal. A CT head scan showed no intracranial pathology, and normal sinuses were observed. CSF showed pleocytosis; 320.6×10^9 leukocytes/L (52% neutrophils, 36% lymphocytes) was observed. High levels of polymorphonuclear cells but no organisms were seen after Gram staining. Glucose level was 4.7 mmol/L; protein was 0.54 g/L. Peripheral blood showed a leukocyte count of 14.6×10^9 cells/L (12.4×10^9 neutrophils/L); hemoglobin, platelets, electrolytes, and renal function

Figure. Regions of potential virus exposure in case series of Jamestown Canyon virus infections with neurologic outcomes, Canada, 2011–2016. Red stars indicate regions reported by each symptomatic patient with JCV infection across Canada (yellow area) and northeastern United States (gray area). Numbers indicate the number of case-patients residing in specific provinces of Canada. Some case-patients reported >1 potential exposure sites. Image was adapted from Wikipedia Commons (https://commons.wikimedia.org). AB, Alberta; BC, British Columbia; MB, Manitoba; ME, Maine; NB, New Brunswick; NH, New Hampshire; NJ, New Jersey; NL, Newfoundland and Labrador; NS, Nova Scotia; NT, Northwest Territories; NU, Nunavut; ON, Ontario; PA, Pennsylvania; PE, Prince Edward Island; QC, Quebec; SK, Saskatchewan; YT, Yukon.

measurements were within reference ranges. The peripheral glucose level was 12.6 mmol/L, C-reactive protein was 9.0 mg/L, and erythrocyte sedimentation rate was 34 mm/h. Serum samples were negative for HIV, WNV, Lyme disease bacteria, and cytomegalovirus; a nasopharyngeal swab test was negative for respiratory viruses; and CSF was negative for HSV, varicella zoster virus, and enterovirus/parechovirus. All blood and CSF samples had negative bacterial and fungal cultures. Arbovirus serologies (including JCV and SSHV) revealed the presence of JCV IgM in both acute and convalescent serum samples and a 4-fold diagnostic increase in virus-specific neutralizing antibody titers by PRNT (Table) (2). PRNT results were negative for SSHV. The patient began manifesting postencephalitic fatigue and possible seizure-like episodes; subsequently, normal pressure hydrocephalus developed, requiring a ventriculoperitoneal shunt.

Case 4

On August 20, 2011, an otherwise healthy 53-year-old man from Montreal, Quebec, sought care because of a 2-day history of fever, fatigue, left-sided neck swelling and pain, and a pruritic rash on his lower back, buttocks, and genitalia. His leukocyte count was slightly elevated at 12.2 x 10^9 cells/L. His throat was swabbed, and testing later showed a negative result for *Streptococcus*, but he had been given penicillin and antiinflammatory agents at discharge from the ED. He returned to the ED on August 24 because of ongoing fevers, a worsening rash, and 48 hours of increasing shortness of breath, headache, sore throat, and conjunctivitis; he was subsequently admitted. He reported a camping trip in Maine and New Hampshire, USA, during July 31–August 12 but did not recall having any insect bites or contact with ill persons. Bloodwork at admission showed 11.1 × 10^9 leukocytes/L, 81 × 10^9 platelets/L, and renal

and liver function measurements within reference ranges. Within 24 hours of admission, he became confused, and worsening hypotension and dyspnea developed, requiring intubation and vasopressors. He also had pulmonary edema, pericardial effusion, a new right bundle branch block, and an evolving maculopapular rash on the limbs (including palmoplantar rash) and trunk. A lumbar puncture was performed on August 26, and CSF showed 5×10^9 leukocytes/L (1×10^9 lymphocytes/L), 5.3 mmol/L glucose, and 0.10 g/L protein. Results of blood, CSF, urine, and sputum sample cultures were all negative, including for syphilis. Acute and convalescent serum samples tested negative for *Rickettsia*, *Borrelia*, WNV, Powassan virus, western equine encephalitis virus, and eastern equine encephalitis virus; *Anaplasma phagocytophilum* serology results were positive (indirect immunofluorescence assay titer 1:256), which remained the same throughout the course of illness, suggesting prior exposure.

Serum and CSF samples were positive for JCV IgM by using ELISA; serum samples showed a 4-fold increase (1:640 to 1:2,560) in PRNT titers, then a subsequent decline to 1:640 (Table). Seroconversion of neutralizing antibodies in paired CSF samples was observed by using PRNT, and JCV was distinguished from an SSHV infection by the 4-fold difference in PRNT titer between the 2 viruses (Table).

The patient had confusion and hypoactive delirium throughout his hospitalization. He was discharged on September 21 but continued to have short-term memory loss, expressive aphasia, and some muscle pain. Six months later, his expressive aphasia persisted, but the other symptoms had dissipated.

Case 5

In mid-June 2016, an otherwise healthy 70-year-old man with psoriasis (no immunotherapies) sought care at an ED in Nova Scotia after a fall; he had a 3–4-day history of a frontal headache, episodic dizziness, and nausea with vomiting. Approximately 2.5 weeks before ED admission, the patient had traveled in the United States for 10 days, visiting New Hampshire, Pennsylvania, and New Jersey. At admission, he was somnolent and febrile (38.6°C) and had a blanching macular rash on his trunk and petechiae on the dorsa of his feet. His speech was slow, and he had impaired concentration, but no nuchal rigidity was present; the remaining neurologic exam was unremarkable. Empiric treatment was initiated with ceftriaxone, ampicillin, vancomycin, and acyclovir. CT and MRI head scans did not demonstrate abnormalities.

Bloodwork showed mild anemia and leukopenia (2.5×10^9 leukocytes/L; nadir 0.5×10^9 leukocytes/L) and thrombocytopenia (73×10^9 platelets/L; nadir 12×10^9 platelets/L); he recovered spontaneously from those conditions within 2 weeks. The patient had hepatic inflammation; alanine aminotransferase level was 74 U/L (peaking at 147 U/L), aspartate aminotransferase was 151 U/L (peaking at 860 U/L), and lactate dehydrogenase was 573 U/L (peaking at >2,500 U/L). Ferritin was elevated at 88,933 μg/L, and creatinine phosphokinase was high at 3,454 U/L.

A lumbar puncture was performed several days after symptom manifestation; CSF had a leukocyte count of 41×10^9 cells/L (100% lymphocytes), glucose level of 3.2 mmol/L, and elevated protein level of 0.67 g/L. CSF and blood cultures were negative. Serologic tests and confirmatory diagnostics for HIV, parvovirus B19, Lyme disease, WNV, and Powassan virus were negative. Acute serum samples were positive for JCV IgM, which was confirmed with a PRNT titer of 1:320; convalescent serum samples showed a 4-fold increase in titer to 1:1,280. CSF was also positive for JCV (PRNT titer of 1:4) (Table).

The patient defervesced by day 2 but reported diffuse myalgias, although his headache was improving. His hospitalization was further complicated by a pulmonary embolism from which he recovered. After 5 weeks of rehabilitation and resolution of his symptoms, the patient was discharged. Upon follow-up, he was found to have made a full recovery.

Discussion

We describe 5 cases of JCV-associated neurologic disease in patients from British Columbia, Alberta, Quebec, and Nova Scotia in Canada during 2011–2016 and indicate the regions of all potential exposures for each of those cases (Figure). JCV has been shown to circulate across Canada and the United States in various studies (*2*,*7*–*13*,*16*,*20*,*21*,*27*; M.A. Drebot, unpub. data). JCV was first identified as an emerging mosquitoborne pathogen in the early 1980s in both Canada and the United States (*8*). However, of the 23 cases of CSG virus infections identified in Canada during 1978–1989, only 3 were caused by JCV; 18 were caused by SSHV, and 2 had undetermined causes (M.A. Drebot, unpub. data). When CSG virus testing resumed in Canada in 2005, most CSG virus infections were shown to be caused by JCV (*2*), a trend that continues and indicates the emergence of JCV as the primary CSG virus causing infection in Canada (*13*). Although SSHV cases continue to be identified, JCV exposure rates, resulting in both mild and severe illness, appear to have increased. Whether this increase is because of

greater JCV circulation, enhanced diagnostic procedures, or other factors warrants further study.

A literature review of encephalitis in Canada highlighted the number of encephalitis cases without a known etiology, suggesting the possibility of a higher prevalence of arbovirus infections than previously thought (*29*). In the appropriate setting, arboviruses, including CSG viruses, should be added to the differential diagnosis of a patient manifesting encephalitis during the mosquito season.

JCV infections in humans can occur throughout the mosquito season and typically display a bimodal pattern. Infections in late spring (May/June) support the concept of transovarial maintenance and the possibility of vertically-infected mosquitoes transmitting virus early during the mosquito season (*30*,*31*). A second peak of infections typically occurs during the late summer and fall months. Case-patients from British Columbia and Nova Scotia had infections that correlated with JCV exposures in late spring (June), whereas the remaining 3 case-patients in this series had exposures during the summer/fall months. Cases of CSG virus infections early during the mosquito season have been documented in Canada; a total of 9 cases of SSHV and JCV infections were identified in the months of May and June during 1978–1989 (*11*; M.A. Drebot, unpub. data). The bimodal peak of arboviral disease likely reflects both transovarial transmission and natural cycling of specific mosquito species that transmit CSG viruses at different times during the mosquito season (*20*,*32*). Because of the various mosquito species responsible for transmitting JCV, exposure can occur throughout the mosquito season (*33*,*34*).

The incubation period for JCV infection is ≈3–14 days. Therefore, the case-patients from Quebec (case 4) and Nova Scotia (case 5) might have been exposed during travel in the northeastern United States. Although no JCV cases had been documented in Maine or New Hampshire at the time of the 2011 case (case 4), subsequent cases were identified in New Hampshire in 2013 and Maine in 2017 (*16*). According to his date of return to Montreal, symptom onset, and the JCV incubation period, case-patient 4 might have been exposed at his residence or during his camping trip in the United States. Case-patient 5 had possible exposures in multiple locations in quick succession in 2016 before seeking care at a Nova Scotia hospital, including wooded areas of New Hampshire, Pennsylvania, and New Jersey, USA; he could have conceivably been infected in any of those US states or in his home province. One case of neuroinvasive JCV infection occurred in New Hampshire in 2013; although no autochthonous neuroinvasive cases of JCV had been previously identified in Nova Scotia, a high (≈21%) JCV seroprevalence existed in the province (*27*).

Unlike some of the other CSG serogroup viruses, such as SSHV and La Crosse virus (LACV), most symptomatic JCV infections have been identified in adults (*2*,*4*,*20*,*35*). Clinically, JCV infections can be asymptomatic, self-limited febrile illnesses, or cause meningitis/encephalitis syndromes (*1*,*4*,*24*,*25*,*35*–*37*). An upper respiratory prodrome has occasionally been reported (*4*,*32*,*35*). During neuroinvasive disease, CSF typically shows lymphocyte predominance and variable protein and glucose levels; however, our small case series showed considerable variation in CSF profiles (Table).

As indicated in the case definitions, the time and place for virus transmission alludes to evidence that JCV-specific IgM might persist for several months or even years in the serum from patients exposed to CSG viruses (*15*; M.A. Drebot, unpub. data). Persistence of virus-specific IgM in serum samples has been noted for other arboviruses, such as WNV (*38*). As a result, lingering IgM might confound identification of current CSG virus infections when positive serology is documented by using only acute phase serum samples. We observed the presence of JCV IgM in CSF from case-patient 2 several months after symptom onset, a finding previously documented for some WNV patients (*39*).

A diagnostic 4-fold rise in titers for paired acute and convalescent serum samples is typically informative for confirming new or repeat exposures, particularly given the possibility of persistent IgM. CSF from case-patients 1, 2, 4, and 5 had positive JCV IgM or PRNT titers; case-patients 2–5 had a clear 4-fold increase in JSV PRNT titers in convalescent serum samples. Case-patient 1 of the series had repeat serologic tests 1week after collecting the acute sample, which showed an increased titer but was not considered a convalescent sample (which would ideally be taken at 2–4 weeks, but according to the CDC definition, it should be minimum of 8 days later).

For case-patient 4 (Quebec), JCV infection was confirmed through the positive IgM ELISA results, noted seroconversion and diagnostic increases in JCV-specific antibodies obtained by PRNT in both paired serum and CSF, and increase in serum antibodies, even with concomitant *A. phagocytophilum* and SSHV seropositivity. Cross reactions in PRNT and particularly ELISA can occur between SSHV and JCV; however, the IgM increase in serum samples, seroconversion in CSF, and ≥4-fold differences between JCV and SSHV PRNT titers in acute and

convalescent serum samples provide strong evidence of JCV exposure. It is possible that *A. phagocytophilum* seropositivity reflects either a previous infection or co-infection, because anaplasmosis is a known emerging infection in many regions within Canada, including Quebec (*40*–*42*).

A limitation of this work is the lack of testing for LACV, a CSG virus that has diagnostic similarities and cross-reactivity to other CSG members (*35*). Testing for LACV was not part of the initial arbovirus testing panels because previous serologic screening studies for this virus had been negative among collections of CSG virus–positive serum samples (M.A. Drebot, unpub. data), despite the geographic range of *Aedes triseriatus* mosquitoes, the primary LACV vector, in southern Canada. Future inclusion of LACV testing in the diagnostic algorithms for suspected CSG virus exposures in Canada is warranted given possible expansion and increased prevalence of the virus.

In conclusion, we describe 5 cases of JCV infection that occurred in Canada early during the mosquito season, highlighting the potential for acquisition of this virus throughout the entire mosquito season. The JCV case-patients from British Columbia and Alberta provide further evidence of JCV exposure risk across Canada. The case-patients from Nova Scotia and Quebec, who had a travel history, indicate that JCV needs to be recognized as a possible cause of neuroinvasive disease for travelers in the United States as well as in Canada.

About the Author

Dr. Meier-Stephenson is an infectious disease physician and assistant professor in the Department of Medicine, Division of Infectious Diseases, University of Alberta, Edmonton, Alberta, Canada. Her primary research interests focus on viral hepatitis and other pathogenic human viruses.

References

1. Peters CJ. California encephalitis, hantavirus pulmonary syndrome, and bunyavirid hemorrhagic fevers. In: Mandell GL, Bennett JE, Dolin R, editors. Mandell, Douglas, and Bennett's principles and practice of infectious diseases, 7th ed. Philadelphia: Churchill Livingstone Elsevier; 2010. p. 2289–93.
2. Drebot MA. Emerging mosquito-borne bunyaviruses in Canada. Can Commun Dis Rep. 2015;41:117–23. https://doi.org/10.14745/ccdr.v41i06a01
3. Piantadosi A, Kanjilal S. Diagnostic approach for arboviral infections in the United States. J Clin Microbiol. 2020;58:e01926-19. https://doi.org/10.1128/JCM.01926-19
4. Alatoom A, Payne D. An overview of arboviruses and bunyaviruses. Lab Med. 2009;40:237–40. https://doi.org/10.1309/LMPX9OEOAOPPBCJH
5. Grimstad PR, Calisher CH, Harroff RN, Wentworth BB. Jamestown Canyon virus (California serogroup) is the etiologic agent of widespread infection in Michigan humans. Am J Trop Med Hyg. 1986;35:376–86. https://doi.org/10.4269/ajtmh.1986.35.376
6. Grimstad PR, Shabino CL, Calisher CH, Waldman RJ. A case of encephalitis in a human associated with a serologic rise to Jamestown Canyon virus. Am J Trop Med Hyg. 1982;31:1238–44. https://doi.org/10.4269/ajtmh.1982.31.1238
7. Artsob H. Arbovirus activity in Canada. In: Calisher CH, editor. Hemorrhagic fever with renal syndrome, tick- and mosquito-borne viruses. Arch Virol. Supplementum. Vienna: Springer-Verlag; 1990. p. 249–258.
8. Deibel R, Srihongse S, Grayson MA, Grimstad PR, Mahdy MS, Artsob H, et al. Jamestown Canyon virus: the etiologic agent of an emerging human disease? Prog Clin Biol Res. 1983;123:313–25.
9. Goff G, Whitney H, Drebot MA. Roles of host species, geographic separation, and isolation in the seroprevalence of Jamestown Canyon and snowshoe hare viruses in Newfoundland. Appl Environ Microbiol. 2012;78:6734–40. https://doi.org/10.1128/AEM.01351-12
10. Rocheleau JP, Michel P, Lindsay LR, Drebot M, Dibernardo A, Ogden NH, et al. Risk factors associated with seropositivity to California serogroup viruses in humans and pet dogs, Quebec, Canada. Epidemiol Infect. 2018;146:1167–76. https://doi.org/10.1017/S0950268818001000
11. Artsob H. Distribution of California serogroup viruses and virus infections in Canada. Prog Clin Biol Res. 1983;123:277–90.
12. Public Health Agency of Canada. West Nile virus and other mosquito-borne diseases surveillance report: annual edition (2018) [cited 2022 Aug 8]. https://www.canada.ca/en/public-health/services/publications/diseases-conditions/west-nile-virus-other-mosquito-borne-diseases-surveillance-annual-report-2018.html
13. Public Health Agency of Canada. Mosquito-borne diseases surveillance report: annual edition (2019-preliminary) [cited 2022 Aug 8]. https://publications.gc.ca/site/eng/9.903748/publication.html
14. Government of Canada. West Nile virus and other mosquito-borne diseases surveillance in Canada [cited 2022 Aug 8]. https://www.canada.ca/en/public-health/services/diseases/west-nile-virus/west-nile-virus-other-mosquito-borne-disease.html
15. Makowski K, Dimitrova K, Andonova M, Drebot M. An overview of California serogroup virus diagnostics and surveillance in Canada in 2008. In: Abstracts of the 26th International Congress of Chemotherapy and Infection; Toronto, Ontario, Canada; 2009 Jun 18–21. Abstract 53. Int J Antimicrob Agents. 2009:34:S19. https://doi.org/10.1016/S0924-8579(09)70200-6
16. Centers for Disease Control and Prevention. Jamestown Canyon virus: data and maps. 2021 [cited 2022 Aug 8]. https://www.cdc.gov/jamestown-canyon/statistics/data-and-maps.html
17. Soto RA, Hughes ML, Staples JE, Lindsey NP. West Nile virus and other domestic nationally notifiable arboviral diseases—United States, 2020. MMWR Morb Mortal Wkly Rep. 2022;71:628–32. https://doi.org/10.15585/mmwr.mm7118a3
18. Kinsella CM, Paras ML, Smole S, Mehta S, Ganesh V, Chen LH, et al. Jamestown Canyon virus in Massachusetts: clinical case series and vector screening. Emerg Microbes Infect. 2020;9:903–12. https://doi.org/10.1080/22221751.2020.1756697
19. Matkovic E, Hoang Johnson DK, Staples JE, Mora-Pinzon MC, Elbadawi LI, Osborn RA, et al. Enhanced arboviral surveillance to increase detection of Jamestown Canyon

virus infections, Wisconsin, 2011–2016. Am J Trop Med Hyg. 2019;100:445–51. https://doi.org/10.4269/ajtmh.18-0575
20. Pastula DM, Hoang Johnson DK, White JL, Dupuis AP 2nd, Fischer M, Staples JE. Jamestown Canyon virus disease in the United States—2000–2013. Am J Trop Med Hyg. 2015;93:384–9. https://doi.org/10.4269/ajtmh.15-0196
21. Vahey GM, Mathis S, Martin SW, Gould CV, Staples JE, Lindsey NP. West Nile virus and other domestic nationally notifiable arboviral diseases—United States, 2019. MMWR Morb Mortal Wkly Rep. 2021;70:1069–74. https://doi.org/10.15585/mmwr.mm7032a1
22. Curren EJ, Lehman J, Kolsin J, Walker WL, Martin SW, Staples JE, et al. West Nile virus and other nationally notifiable arboviral diseases—United States, 2017. MMWR Morb Mortal Wkly Rep. 2018;67:1137–42. https://doi.org/10.15585/mmwr.mm6741a1
23. Drebot MA, Dimitrova K, Andonova M, Turner S, Serhir B, Couillard M, et al. A laboratory confirmed case of Jamestown Canyon virus encephalitis in a Quebec resident with travel history to Maine and New Hampshire. In: Abstracts of the 61st Annual Meeting of the American Society of Tropical Medicine and Hygiene; Atlanta, GA, USA; 2012 Nov 11–15. Abstract 924. Arlington (VA): American Society of Tropical Medicine and Hygiene; 2012.
24. Evans AB, Winkler CW, Peterson KE. Differences in neuropathogenesis of encephalitic California serogroup viruses. Emerg Infect Dis. 2019;25:728–38. https://doi.org/10.3201/eid2504.181016
25. Vosoughi R, Walkty A, Drebot MA, Kadkhoda K. Jamestown Canyon virus meningoencephalitis mimicking migraine with aura in a resident of Manitoba. CMAJ. 2018;190:E262–4. https://doi.org/10.1503/cmaj.170940
26. Martin DA, Muth DA, Brown T, Johnson AJ, Karabatsos N, Roehrig JT. Standardization of immunoglobulin M capture enzyme-linked immunosorbent assays for routine diagnosis of arboviral infections. J Clin Microbiol. 2000; 38:1823–6. https://doi.org/10.1128/JCM.38.5.1823-1826.2000
27. Patriquin G, Drebot M, Cole T, Lindsay R, Schleihauf E, Johnston BL, et al. High seroprevalence of Jamestown Canyon virus among deer and humans, Nova Scotia, Canada. Emerg Infect Dis. 2018;24:118–21. https://doi.org/10.3201/eid2401.170484
28. Centers for Disease Control and Prevention. Arboviral diseases, neuroinvasive and non-neuroinvasive, 2015 case definition [cited 2022 Aug 8]. https://ndc.services.cdc.gov/case-definitions/arboviral-diseases-neuroinvasive-and-non-neuroinvasive-2015
29. Kulkarni MA, Lecocq AC, Artsob H, Drebot MA, Ogden NH. Epidemiology and aetiology of encephalitis in Canada, 1994–2008: a case for undiagnosed arboviral agents? Epidemiol Infect. 2013;141:2243–55. https://doi.org/10.1017/S095026881200252X
30. Lequime S, Paul RE, Lambrechts L. Determinants of arbovirus vertical transmission in mosquitoes. PLoS Pathog. 2016; 12:e1005548. https://doi.org/10.1371/journal.ppat.1005548
31. Bergren NA, Kading RC. The ecological significance and implications of transovarial transmission among the vector-borne bunyaviruses: a review. Insects. 2018;9:173. https://doi.org/10.3390/insects9040173
32. Grimstad PR. California group virus disease. In: Monath TP, editor. The arboviruses: epidemiology and ecology, 1st ed. Boca Raton (FL): CRC Press; 1988. p. 99–136.
33. Andreadis TG, Anderson JF, Armstrong PM, Main AJ. Isolations of Jamestown Canyon virus (Bunyaviridae: Orthobunyavirus) from field-collected mosquitoes (Diptera: Culicidae) in Connecticut, USA: a ten-year analysis, 1997–2006. Vector Borne Zoonotic Dis. 2008;8:175–88. https://doi.org/10.1089/vbz.2007.0169
34. Anderson JF, Main AJ, Armstrong PM, Andreadis TG, Ferrandino FJ. Arboviruses in North Dakota, 2003–2006. Am J Trop Med Hyg. 2015;92:377–93. https://doi.org/10.4269/ajtmh.14-0291
35. Rust RS, Thompson WH, Matthews CG, Beaty BJ, Chun RW. La Crosse and other forms of California encephalitis. J Child Neurol. 1999;14:1–14. https://doi.org/10.1177/088307389901400101
36. Centers for Disease Control and Prevention. Human Jamestown Canyon virus infection—Montana, 2009. MMWR Morb Mortal Wkly Rep. 2011;60:652–5.
37. Webster D, Dimitrova K, Holloway K, Makowski K, Safronetz D, Drebot MA. California serogroup virus infection associated with encephalitis and cognitive decline, Canada, 2015. Emerg Infect Dis. 2017;23:1423–4. https://doi.org/10.3201/eid2308.170239
38. Roehrig JT, Nash D, Maldin B, Labowitz A, Martin DA, Lanciotti RS, et al. Persistence of virus-reactive serum immunoglobulin m antibody in confirmed West Nile virus encephalitis cases. Emerg Infect Dis. 2003;9:376–9. https://doi.org/10.3201/eid0903.020531
39. Kapoor H, Signs K, Somsel P, Downes FP, Clark PA, Massey JP. Persistence of West Nile virus (WNV) IgM antibodies in cerebrospinal fluid from patients with CNS disease. J Clin Virol. 2004;31:289–91. https://doi.org/10.1016/j.jcv.2004.05.017
40. Campeau L, Roy V, Petit G, Baron G, Blouin J, Carignan A. Identification of an unusual cluster of human granulocytic anaplasmosis in the Estrie region, Québec, Canada in 2021. Can Commun Dis Rep. 2022;48:188–95. https://doi.org/10.14745/ccdr.v48i05a02
41. Parkins MD, Church DL, Jiang XY, Gregson DB. Human granulocytic anaplasmosis: first reported case in Canada. Can J Infect Dis Med Microbiol. 2009;20:124173.e100–2. https://doi.org/10.1155/2009/124173
42. Uminski K, Kadkhoda K, Houston BL, Lopez A, MacKenzie LJ, Lindsay R, et al. Anaplasmosis: an emerging tick-borne disease of importance in Canada. IDCases. 2018;14:e00472. https://doi.org/10.1016/j.idcr.2018.e00472

Address for correspondence: Vanessa Meier-Stephenson, Department of Medicine, Division of Infectious Diseases, University of Alberta, 1-124P CSB, 11350 83 Ave NW, Edmonton, AB T6G 2G3, Canada; email: meierste@ualberta.ca

Coccidioidomycosis-Related Hospital Visits, Texas, USA, 2016–2021

Heather Mayfield, Vanora Davila, Elena Penedo

We analyzed hospital discharge records of patients with coccidioidomycosis-related codes from the International Classification of Diseases, 10th revision, Clinical Modification, to estimate the prevalence of hospital visits associated with the disease in Texas, USA. Using Texas Health Care Information Collection data for 2016–2021, we investigated the demographic characteristics and geographic distribution of the affected population, assessed prevalence of hospital visits for coccidioidomycosis, and examined how prevalence varied by demographic and geographic factors. In Texas, 709 coccidioidomycosis-related inpatient and outpatient hospital visits occurred in 2021; prevalence was 3.17 cases per 100,000 total hospital visits in 2020. Geographic location, patient sex, and race/ethnicity were associated with increases in coccidioidomycosis-related hospital visits; male, non-Hispanic Black, and Hispanic patients had the highest prevalence of coccidioidomycosis compared with other groups. Increased surveillance and healthcare provider education and outreach are needed to ensure timely and accurate diagnosis and treatment of coccidioidomycosis in Texas and elsewhere.

Coccidioidomycosis, also known as Valley fever, is a fungal disease caused by soil-dwelling *Coccidioides* spp., which include *C. immitis* and *C. posadasii* (*1*,*2*). Coccidioidomycosis is considered a nationally notifiable disease in the United States, but only 26 US states have mandatory reporting requirements at the state level, which has led to incomplete surveillance data across the country (*1*–*3*). Since Centers for Disease Control and Prevention (CDC) reporting began in 1998, the number of Valley fever cases has mostly increased. The steepest increase in the number of cases occurred during 2009–2011, followed by a decrease during 2012–2014 (*4*); prevalence has continued to increase again since 2015 (*4*). Valley fever incidence in Texas, a state where coccidioidomycosis is not reportable, is unknown, but historical and contemporary scientific evidence defines West Texas as a coccidioidomycosis-endemic area (*3*,*5*). In addition, recent climate models suggest that the coccidioidomycosis-endemic region is expanding as temperatures increase and precipitation patterns shift, which might have an indirect effect on the dynamics of this disease in the United States (*6*). Approximately 40% of *Coccidioides* infections are symptomatic, yet not all patients seek medical treatment (*1*,*2*). Symptoms of coccidioidomycosis include cough, fever, and shortness of breath, which might resemble other respiratory illnesses and might be clinically indistinguishable from community-acquired pneumonia (*1*). Coccidioidomycosis can result in life-threatening severe pulmonary or disseminated disease, particularly in groups at high risk, and can also result in chronic illness (*1*–*3*). Surveillance data from Arizona and California, as well as previous research, suggests that demographic factors, such as age, sex, race/ethnicity, and occupation, play a role in a person's risk for infection and disease complications (*1*–*4*,*7*,*8*). Testing practices vary substantially across states, but overall testing is underused, leading to delayed diagnosis and inadequate treatment (*1*,*2*).

Although Texas is estimated to be within the geographic range of *C. posadasii*, surveillance data are limited (*3*). We assessed differences in hospital use by patients who had a coccidioidomycosis diagnosis according to demographic and geographic factors. We used data on inpatient hospitalizations and outpatient surgical and radiological procedures from Texas hospitals and ambulatory surgery centers.

Methods

Data Source

We obtained study data from inpatient and outpatient public-use data files for January 1, 2016–December 31,

Author affiliation: Texas Department of State Health Services, Austin, Texas, USA

DOI: https://doi.org/10.3201/eid3005.231624

2021, from the Texas Health Care Information Collection (THCIC), Texas Department of State Health Services Center for Health Statistics (*9*,*10*). Institutional review board approval was not necessary to analyze THCIC files. THCIC data include claims for medical services received at hospitals during admission (inpatient) and services received at hospitals without admission (outpatient) from all state-licensed hospitals and ambulatory surgical centers in Texas, except those that are statutorily exempt. Exempt facilities were those located in small counties with populations <35,000 or those located in a county with a population >35,000 but with <100 licensed hospital beds and not in an area designated as urban by the United States Census Bureau. Other exempt facilities were hospitals that did not seek insurance payment or government reimbursement. THCIC public-use data files represent hospital encounters, where 1 encounter contains the final discharge and all related claims information for a deidentified patient, which prevents differentiation between repeat visits. Because public-use data files were used for the analysis, patients could not be identified and deduplicated from the study, which might result in an overrepresentation of persons with severe disease who required multiple visits over time. In this study, hospital visits reflected all inpatient hospitalizations and outpatient surgical and radiologic procedures, as well as ambulatory surgery center visits.

Study Population

To identify the study population, we used codes from the International Classification of Diseases, 10th Revision, Clinical Modification (ICD-10-CM), related to coccidioidomycosis and used all available diagnostic codes within the patient records, including principal and other diagnosis fields (Table 1). We restricted the analytic sample according to the patient's US state of residence in the record and included only patients with a residence in Texas in our analysis (Figure 1). We identified the exposure status of each patient by using the patient's county of residence described in the record and the estimated *Coccidioides* spp.–endemic range. We determined the 96 Texas counties estimated to be within the Valley fever–endemic region by using CDC Valley fever maps spatially overlaid on a county map of Texas (Figure 2) (*5*). We designated any county that fell within the CDC's estimated area as a Valley fever region.

Analysis

We compiled descriptive statistics of all coccidioidomycosis-related hospital visits, including demographic counts and percentages and geographic areas according to discharge year and inpatient/outpatient hospital visits. We also compiled select clinical diagnostic characteristics of the analytic sample as counts and percentages according to hospital visit type (inpatient/outpatient). We calculated prevalence of coccidioidomycosis-related hospital visits as the number of coccidioidomycosis visits per 100,000 hospital visits for any cause and included annual and stratified prevalence according to disease-endemic region status for each year. We conducted a negative binomial regression analysis to calculate prevalence ratios of coccidioidomycosis-related hospital visits for demographic and geographic groups and to calculate 95% CIs. We chose negative binomial regression analysis for all demographic and geographic variables because the data were overdispersed. We added an offset variable calculated as the log of the total hospital visits for any cause to the model to account for the underlying population differences. We included the demographic variables sex and race/ethnicity in the model after determining they were a good fit by using the likelihood ratio test. We included non-Hispanic White, female, and the non–Valley fever–endemic region as reference groups. We conducted all analyses by using SAS version 9.4 software (SAS Institute, https://www.sas.com).

Results

Of the 3,276 hospital visits representing all inpatient hospitalizations, outpatient surgical and radiologic procedures, and ambulatory surgery center visits for coccidioidomycosis among Texas residents, the percentages of visits were highest among patients who were 46–64 years of age (40.8%), male (56.3%), and Hispanic (47.5%) (Table 2). In 2021, a total of 709 coccidioidomycosis-related hospital visits occurred in Texas (Table 2). Although the 96-county Valley fever region in Texas only accounts for ≈24.0% of the state's population, those counties had 63.4% of coccidioidomycosis-related hospital visits (Table 2).

Table 1. ICD-10-DM codes used for coccidioidomycosis diagnosis*

Definition	Codes
Coccidioidomycosis	B38
Acute pulmonary coccidioidomycosis	B38.0
Chronic pulmonary coccidioidomycosis	B38.1
Pulmonary coccidioidomycosis, unspecified	B38.2
Cutaneous coccidioidomycosis	B38.3
Coccidioidomycosis meningitis	B38.4
Disseminated coccidioidomycosis	B38.7
Other forms of coccidioidomycosis	B38.8, B38.89
Prostatic coccidioidomycosis	B38.81

*ICD-10-CM, International Classification of Diseases, 10th Revision, Clinical Modification.

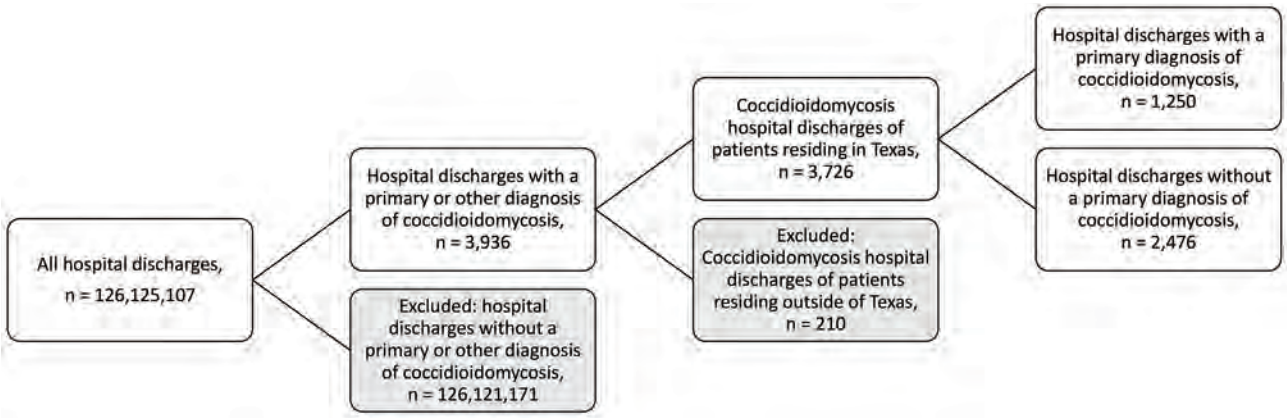

Figure 1. Inclusion and exclusion criteria for study of coccidioidomycosis-related hospital visits, Texas, USA, 2016–2021. Analytic study of patient medical records was conducted to assess prevalence of inpatient and outpatient hospital visits by persons with a coccidioidomycosis diagnosis in Texas. Codes from the International Classification of Diseases, 10th revision, Clinical Modification, were used for diagnoses and included codes B38, B38.0, B38.1, B38.2, B38.3, B38.4, B38.7, B38.8, B38.81, B38.89, and B38.9. Shaded boxes indicate numbers of excluded discharge records and reasons for exclusion from the study. Final analytic study sample was categorized into 2 groups according to clinical diagnostic characteristics.

Inpatient hospital encounters constituted the largest (56.7%) percentage of coccidioidomycosis-related visits (Table 3). The percentage of hospital visits where coccidioidomycosis was the principal diagnosis was only 33.5% (Table 3). When stratified by visit type, only 19.8% of hospital visits that coded as inpatient resulted in a principal coccidioidomycosis diagnosis compared with 51.6% of hospital visits coded as outpatient (Table 3). For inpatient hospital visits where coccidioidomycosis was not the principal diagnosis, many of the diagnosis codes were related to symptoms of severe coccidioidomycosis

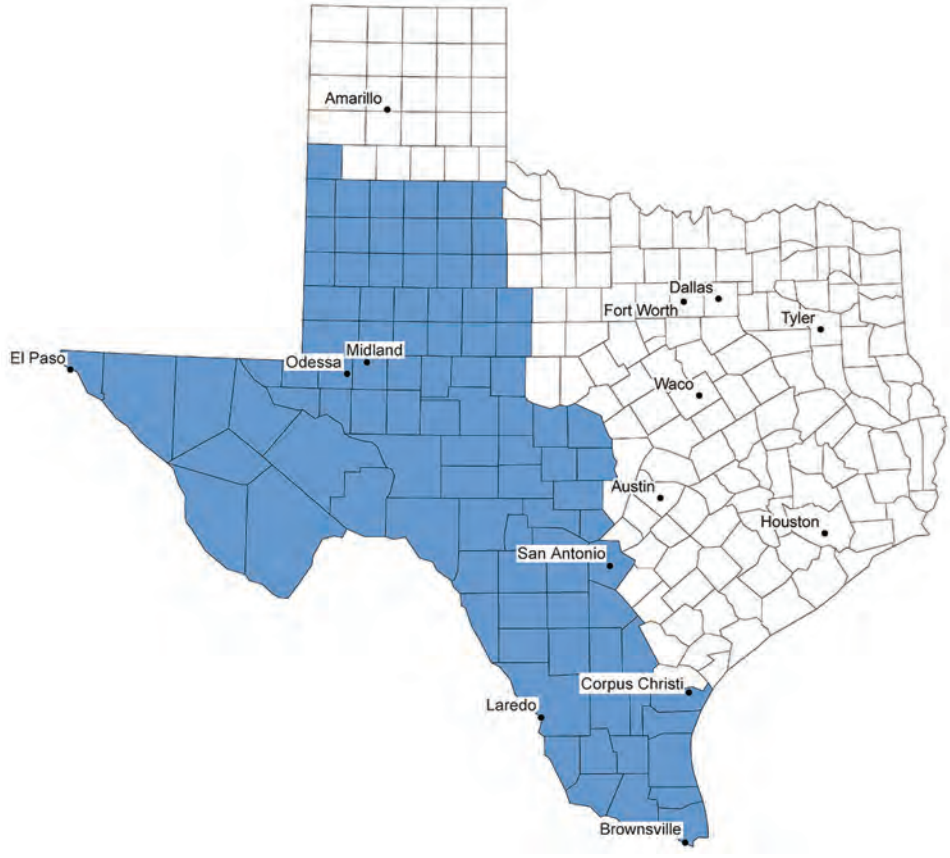

Figure 2. Estimated endemic region of *Coccidioides* spp. fungi in study of coccidioidomycosis-related hospital visits, Texas, USA, 2016–2021. Valley fever region, an estimated 96-county area of Texas determined by using Centers for Disease Control and Prevention Valley fever maps (*5*) spatially overlaid on a Texas county map. Any county that fell within the estimated area was designated as a Valley fever region (blue shading).

infection, including sepsis, pneumonia, and respiratory failure. When assessing the principal diagnosis codes for outpatient hospital visits where coccidioidomycosis was not the primary diagnosis, most were related to abnormal diagnostic findings in the lungs or to mild symptoms, such as cough, throat pain, headaches, and abnormal breathing.

Prevalence of coccidioidomycosis-related hospital visits was highest in 2020 at 3.17 cases/100,000 hospital visits for any cause and lowest in 2018 at 2.73 cases/100,000 hospital visits for any cause (Figure 3). Prevalence for the estimated Valley fever–endemic region was ≈6–8 times higher than that for the nonendemic region (Figure 3). Although prevalence in the Valley fever–endemic region has decreased since 2016, coccidioidomycosis prevalence in the nonendemic region has steadily increased year to year, starting at 1.15 cases/100,000 hospital visits for any cause in 2016 to 1.65 cases/100,000 hospital visits for any cause in 2021 (Figure 3).

Negative binomial regression analysis suggested that Valley fever region status, patient sex, and race/ethnicity were associated with increased hospital visits for coccidioidomycosis (Table 4). The prevalence ratio (PR) for coccidioidomycosis in men was ≈3 times higher (PR 2.81 [95% CI 2.43–3.25]) than in women. Patients who were non-Hispanic Black (PR 1.51 [95% CI 1.24–1.84]) or Hispanic (PR 1.25 [95% CI 1.05–1.48]) had higher PRs for coccidioidomycosis than those who were non-Hispanic White (Table 4).

Discussion

The lack of surveillance in Texas has led to incomplete knowledge and understanding of the dynamics of coccidioidomycosis. Without surveillance, the burden of disease can only be estimated through indirect metrics. Although the number of coccidioidomycosis-related hospital visits have increased over time, prevalence of visits varied year to year. Those differences might be from fluctuations in the population's health-seeking behaviors throughout Texas, such as the decline in all-cause inpatient and outpatient hospital visits during the COVID-19 pandemic (*11*) and changes in disease reporting practices and might not be reflective of a change in disease dynamics. However, the observed numbers of hospital visits are likely an underestimate of the true number of coccidioidomycosis cases in Texas because misdiagnosis by physicians, underreporting of cases, and low awareness of coccidioidomycosis might be influenced by geographic location and other patient sociodemographic factors. In addition, only 40% of infections are symptomatic and most symptoms might be indistinguishable from common respiratory illnesses; subsequently, many patients with mild cases or symptoms might not seek medical care (*1*,*2*). The prevalence of coccidioidomycosis in counties outside of the Valley

Table 2. Patient demographics according to year in study of coccidioidomycosis-related hospital visits, Texas, USA, 2016–2021*

	Year						
Demographics	2016	2017	2018	2019	2020	2021	Total patients
No. patients	634	582	571	640	590	709	3,726 (100.0)
Age group, y							
0–17	27	18	26	10	19	27	127 (3.4)
18–44	192	169	157	179	191	189	1,077 (28.9)
46–64	275	244	237	255	233	278	1,522 (40.8)
65–74	86	111	108	127	91	133	656 (17.6)
≥75	54	40	43	69	56	82	344 (9.2)
Patient sex							
M	358	363	312	340	335	389	2,097 (56.3)
F	202	150	208	227	202	239	1,228 (33.0)
Unknown	74	69	51	73	53	81	401 (10.7)
Race/ethnicity							
Hispanic	323	301	267	272	252	354	1,769 (47.5)
Non-Hispanic Black	75	65	60	69	79	93	441 (11.8)
Non-Hispanic other†	31	49	51	41	37	41	250 (6.7)
Non-Hispanic White	205	165	193	258	222	221	1,264 (33.9)
Unknown	0	2	0	0	0	0	2 (0.1)
Valley fever region status‡							
Valley fever region	449	388	359	391	360	416	2,363 (63.4)
Non–Valley fever region	185	194	203	238	227	288	1,335 (35.8)
Unknown	0	0	9	11	3	5	28 (0.8)

*Values are no. (%). International Classification of Diseases, 10th Revision, Clinical Modification, codes were used to determine a coccidioidomycosis diagnosis and included codes B38, B38.0, B38.1, B38.2, B38.3, B38.4, B38.7, B38.8, B38.81, B38.89, and B38.9.
†Non-Hispanic other category includes American Indian/Eskimo/Aleut, Asian or Pacific Islander, and other. If a hospital had <10 patients of 1 race, that race was categorized as other, and ethnicity of those patients was suppressed.
‡The 96-county area of Texas estimated to be coccidioidomycosis-endemic was determined by using Centers for Disease Control and Prevention Valley fever maps spatially overlaid on a Texas county map. Any county that fell within the estimated area was designated as a Valley fever region.

Table 3. Demographics of inpatients and outpatients with coccidioidomycosis in study of coccidioidomycosis-related hospital visits, Texas, USA, 2016–2021*

Demographics	No. inpatients	No. outpatients	Total no. (%)
No. patients	2,114	1,612	3,726 (100.0)
Primary coccidioidomycosis diagnosis			
Yes	418	832	1,250 (33.5)
No	1,696	780	2,476 (66.5)
Age group, y			
0–17	58	69	127 (3.4)
18–44	633	444	1,077 (28.9)
46–64	865	657	1,522 (40.9)
65–74	359	297	656 (17.6)
≥75	199	145	344 (9.2)
Patient sex			
M	1,156	941	2,097 (56.3)
F	607	621	1,228 (33.0)
Unknown	351	50	401 (10.8)
Race/ethnicity†			
Hispanic	1,073	696	1,769 (47.5)
Non-Hispanic Black	204	237	441 (11.8)
Non-Hispanic other‡	129	121	250 (6.7)
Non-Hispanic White	708	556	1,264 (33.9)
Geographic region§			
Valley fever region¶	1,395	968	2,363 (63.4)
Non–Valley fever region	700	635	1,335 (35.8)

*International Classification of Diseases, 10th Revision, Clinical Modification, codes were used to determine a coccidioidomycosis diagnosis and included codes B38, B38.0, B38.1, B38.2, B38.3, B38.4, B38.7, B38.8, B38.81, B38.89, B38.9.
†Unknown race/ethnicity category was suppressed because the Texas Health Care Information Collection rules dictate any value <10 must be suppressed.
‡Non-Hispanic other category also includes American Indian/Eskimo/Aleut, Asian or Pacific Islander, and other. If a hospital has <10 patients of 1 race, that race is changed to other, and the ethnicity of patients of that race is suppressed.
§Unknown geographic region category was suppressed because the Texas Health Care Information Collection rules dictate any value <10 must be suppressed.
¶The 96-county area of Texas estimated to be coccidioidomycosis-endemic was determined by using Centers for Disease Control and Prevention Valley fever maps spatially overlaid on a Texas county map. Any county that fell within the estimated area was designated as a Valley fever region.

fever region in Texas have been increasing each year, which highlights the need for increased clinician awareness of the disease throughout the state.

Hospital encounters where the principal recorded diagnosis was coccidioidomycosis-related differed substantially between inpatient and outpatient visits, which might have been partly because of different diagnostic practices or medical coding differences for inpatient versus outpatient facilities (*12*). However, patients seeking inpatient care tended to have principal diagnosis codes for conditions related to severe coccidioidomycosis, whereas patients

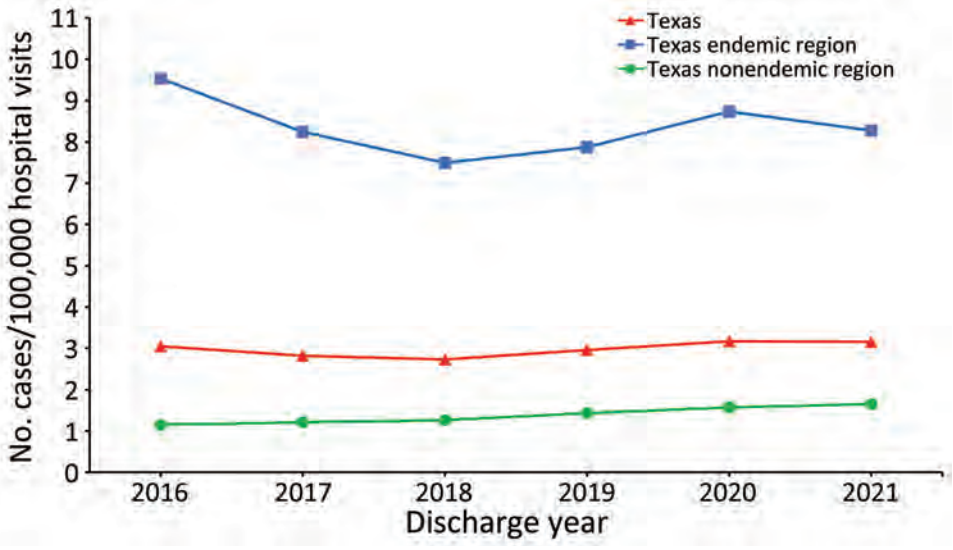

Figure 3. Annual prevalence of inpatient and outpatient hospital visits in study of coccidioidomycosis-related hospital visits, Texas, USA, 2016–2021. Codes from the International Classification of Diseases, 10th Revision, Clinical Modification, were used for diagnoses and included codes B38, B38.0, B38.1, B38.2, B38.3, B38.4, B38.7, B38.8, B38.81, B38.89, and B38.9. Prevalence, defined as the number of Valley fever cases per 100,000 inpatient and outpatient hospital visits for any cause, is indicated statewide by geographic region for each year. Estimated Valley fever–endemic region is a 96-county area of Texas determined by using Centers for Disease Control and Prevention Valley fever maps (*5*) spatially overlaid on a Texas county map. Any county that fell within the estimated area was designated as a Valley fever region.

seeking outpatient care had principal diagnostic codes related to mild coccidioidal syndromic symptoms. Therefore, principal diagnostic codes for inpatient and outpatient settings might have reflected differences in disease severity between the 2 patient populations (*12*,*13*).

National surveillance data for coccidioidomycosis include only the 26 mandatory reporting states, and most cases are from Arizona and California, where coccidioidomycosis has increased since 2000 (*4*). National data from CDC only include data during 1998–2019 and show that case counts have fluctuated through the years (*4*). Additional data from California indicate that case counts decreased from 9,000 in 2019 to 7,000–8,000 during 2020–2022 (*14*). In Arizona, new cases increased from 10,358 cases in 2019 to >11,400 cases each in both 2020 and 2021 but then declined to 9,515 cases in 2022 (*15*). Compared with national trends in new cases, Texas displays similar oscillating patterns in hospital visits related to coccidioidomycosis. We found a significant association between coccidioidomycosis-related hospital visits and patient sex or race/ethnicity ($p \leq 0.01$). Consistent with national surveillance data and previous research, most coccidioidomycosis-related hospital visits in Texas were by male patients who had a higher coccidioidomycosis prevalence than female patients. In Texas, coccidioidomycosis-related hospital visit counts were highest among Hispanic persons, which might reflect the proportion of Hispanic persons residing in the Valley fever–endemic region. According to data from the Texas Demographic Center's population projections, the percentage of Hispanic persons within the Valley fever–endemic region is ≈68% versus 30% within the nonendemic region (*16*). The increased percentage of Hispanic persons in the Valley fever–endemic region likely contributes to the higher coccidioidomycosis-related hospital visit counts in this group overall. Those findings differ from national surveillance data and previous research that show the number of cases is highest in non-Hispanic White persons but varies between states. Prevalence of coccidioidomycosis-related hospital visits was highest in non-Hispanic Black persons compared with other race/ethnicity groups, which aligns with previous research that suggests non-Hispanic Black persons are at increased risk for infection and severe disease.

Although only 96 counties make up the estimated Valley fever–endemic region within Texas, this area might continue to expand because of shifts in climate-related factors, such as increased temperatures and shifts in precipitation patterns throughout the state that create a more suitable climate for *Coccidioides*. As the Valley fever–endemic region expands in Texas, increased surveillance by public health authorities and increased disease awareness by physicians and healthcare professionals will be critical for monitoring disease spread to susceptible populations and for addressing the health needs of the Texas population.

Table 4. Patient demographics and prevalence ratios for coccidioidomycosis-related hospital visits, Texas, USA, 2016–2021*

Demographics	PR (95% CI)	p value
Patient sex		
F	Referent	NA
M	2.81 (2.43–3.25)	<0.01
Race/ethnicity		
Non-Hispanic White	Referent	NA
Non-Hispanic Black	1.51 (1.24–1.84)	<0.01
Non-Hispanic other†	0.97 (0.78–1.19)	0.74
Hispanic	1.25 (1.05–1.48)	0.01
Geographic region		
Non–Valley fever region	Referent	NA
Valley fever region‡	5.79 (5.03–6.66)	<0.01

*International Classification of Diseases, 10th Revision, Clinical Modification, codes were used to determine a coccidioidomycosis diagnosis and included codes B38, B38.0, B38.1, B38.2, B38.3, B38.4, B38.7, B38.8, B38.81, B38.89, B38.9. p values ≤0.01 were considered significant. NA, not applicable; PR, prevalence ratio.
†Non-Hispanic other category also includes American Indian/Eskimo/Aleut, Asian or Pacific Islander, and other. If a hospital has <10 patients of 1 race, that race is changed to other, and the ethnicity of patients of that race is suppressed.
‡The 96-county area of Texas estimated to be coccidioidomycosis-endemic was determined by using Centers for Disease Control and Prevention Valley fever maps spatially overlaid on a Texas county map. Any county that fell within the estimated area was designated as a Valley fever region.

Although coccidioidomycosis is not a reportable disease in Texas, a substantial disease burden is likely affecting the population, as seen by the number of hospital visits for the disease across the state. In addition, we found that certain groups have higher prevalence, which creates health differences within the Texas population and might lead to worse health outcomes for those groups. Coccidioidomycosis is a serious public health concern; the disease can be difficult to prevent, diagnose, and treat. Disease awareness among local public health officials, physicians, healthcare professionals, and the public is critical to ensure persons seek care when infected and healthcare providers can correctly identify and manage the condition. We assessed exposure according to the patient's county of residence, but this method might not be a true reflection of where patients were exposed or where they might seek medical care. Therefore, healthcare providers across Texas need to be aware of coccidioidomycosis and the geographic range of *Coccidioides* fungi and inquire about work and travel to determine potential exposures to *Coccidioides* during patient intake.

Our findings indicate that increased testing for coccidioidomycosis should be performed in Texas for patients with pneumonia of unknown cause to pre-

vent delayed diagnosis and ensure prompt disease management and treatment, especially for patients who live in or have traveled to the 96-county disease-endemic area. Because coccidioidomycosis infections can manifest as common respiratory illnesses, clinicians should consider coccidioidomycosis testing in addition to bacteria and virus testing as part of regular diagnostic practices for patients manifesting symptoms consistent with coccidioidomycosis. CDC has developed a clinical testing algorithm for coccidioidomycosis to aid clinicians in diagnosing patients who manifest nonspecific respiratory symptoms similar to community-acquired pneumonia (*17*).

The first limitation of our study is that THCIC suppression rules dictate that gender is suppressed for any patient with a diagnosis code determined to be of a sensitive nature (e.g., drug or alcohol-related or HIV diagnosis). The suppression rule affected ≈401 (≈10%) records in the analytic study sample, which might have affected the final analysis results, including prevalence ratios. Second, race and ethnicity are required to be reported to THCIC by law, but those variables are not generally collected by hospitals and might be subjectively captured in the record by medical staff. Because of the subjective nature of the race and ethnicity data, patients might have been miscategorized by hospital staff, potentially affecting final analyses. Third, county of residence is not collected by hospitals; instead, Federal Information Processing Standards codes are assigned to counties by the Texas Department of State Health Services according to patients' postal (ZIP) codes, which might be inaccurate for codes that cross county lines and lead to an inaccurate exposure classification in the patient record. Fourth, because the study used public-use data files for inpatient and outpatient records, patients could not be identified and deduplicated from the study sample, which might have resulted in outcome overestimation. Fifth, the nature of medical discharge data might also lead to substantial miscoding or undercoding by medical billing staff, resulting in a potential underestimation of coccidioidomycosis in this study. Finally, the lack of coccidioidomycosis surveillance in Texas might have led to underreporting and underdiagnosis by physicians because of decreased awareness, furthering potential underestimation of case numbers in this study.

In conclusion, coccidioidomycosis-related hospital visits were highest in the estimated Valley fever region of Texas, but ≈33% of visits were in counties located in the non–Valley fever–endemic region, highlighting the need for increased awareness of the disease across the state. Monitoring trends in inpatient and outpatient hospital visits for coccidioidomycosis in medical discharge data and other available data streams will be critical to identify potential new areas of disease endemicity. Monitoring additional data sources for coccidioidomycosis cases in Texas can help close the surveillance gap in the state and increase understanding of disease dynamics. As the Valley fever–endemic region expands, increased surveillance and healthcare provider education and outreach concerning the disease will be needed to ensure timely and accurate diagnosis and treatment.

About the Author

Ms. Mayfield is a public health research scientist at the Center for Health Statistics in the Texas Department of State Health Services. Her primary research interests focus on mental health, vaccine-preventable diseases, and fungal disease epidemiology.

References

1. Williams SL, Chiller T. Update on the epidemiology, diagnosis, and treatment of coccidioidomycosis. J Fungi (Basel). 2022;8:666. https://doi.org/10.3390/jof8070666
2. McCotter OZ, Benedict K, Engelthaler DM, Komatsu K, Lucas KD, Mohle-Boetani JC, et al. Update on the epidemiology of coccidioidomycosis in the United States. Med Mycol. 2019;57:S30–40. https://doi.org/10.1093/mmy/myy095
3. Gorris ME, Ardon-Dryer K, Campuzano A, Castañón-Olivares LR, Gill TE, Greene A, et al. Advocating for coccidioidomycosis to be a reportable disease nationwide in the United States and encouraging disease surveillance across North and South America. J Fungi (Basel). 2023;9:83. https://doi.org/10.3390/jof9010083
4. Centers for Disease Control and Prevention. Valley fever (coccidioidomycosis) statistics. July 18, 2022 [cited 2023 Jun 7]. https://www.cdc.gov/fungal/diseases/coccidioidomycosis/statistics.html
5. Centers for Disease Control and Prevention. Valley fever maps. February 22, 2021 [cited 2023 Jun 7]. https://www.cdc.gov/fungal/diseases/coccidioidomycosis/maps.html
6. Gorris ME, Treseder KK, Zender CS, Randerson JT. Expansion of coccidioidomycosis endemic regions in the United States in response to climate change. Geohealth. 2019;3:308–27. https://doi.org/10.1029/2019GH000209
7. Peterson C, Chu V, Lovelace J, Almekdash MH, Lacy M. Coccidioidomycosis cases at a regional referral center, West Texas, USA, 2013–2019. Emerg Infect Dis. 2022;28:848–51. https://doi.org/10.3201/eid2804.211912
8. Centers for Disease Control and Prevention, National Institute for Occupational Safety and Health. Valley fever (coccidioidomycosis). November 7, 2022 [cited 2023 Jun 7]. https://www.cdc.gov/niosh/topics/valleyfever/risk.html
9. Texas Hospital Inpatient Discharge Public Use Data File, 2016–2021. Texas Department of State Health Services, Center for Health Statistics, Austin, Texas.
10. Texas Outpatient Public Use Data File, 2016–2021. Texas Department of State Health Services, Center for Health Statistics, Austin, Texas.

11. Kazakova SV, Baggs J, Parra G, Yusuf H, Romano SD, Ko JY, et al. Declines in the utilization of hospital-based care during COVID-19 pandemic. J Hosp Med. 2022;17:984–9. https://doi.org/10.1002/jhm.12955
12. Pu J, Donovan FM, Ellingson K, Leroy G, Stone J, Bedrick E, et al. Clinician practice patterns that result in the diagnosis of coccidioidomycosis before or during hospitalization. Clin Infect Dis. 2021;73:e1587–93. https://doi.org/10.1093/cid/ciaa739
13. Gudo ES, Pinto G, Weyer J, le Roux C, Mandlaze A, José AF, et al. Serological evidence of rift valley fever virus among acute febrile patients in Southern Mozambique during and after the 2013 heavy rainfall and flooding: implication for the management of febrile illness. Virol J. 2016;13:96. https://doi.org/10.1186/s12985-016-0542-2
14. California Department of Public Health. Valley fever in California dashboard [cited 2024 Feb 22]. https://www.cdph.ca.gov/Programs/CID/DCDC/Pages/ValleyFeverDashboard.aspx
15. Arizona Department of Health Services. Valley fever [cited 2024 Feb 22]. http://www.azdhs.gov/preparedness/epidemiology-disease-control/valley-fever/index.php
16. Texas Demographic Center. Texas population projections program, 2018 [cited 2024 Feb 22]. https://demographics.texas.gov/Projections/2018/#pageContent
17. Centers for Disease Control and Prevention. Community-acquired pneumonia (CAP): clinical testing algorithm for coccidioidomycosis. November 27, 2023 [cited 2024 Mar 4]. https://www.cdc.gov/fungal/diseases/coccidioidomycosis/diagnosticalgorithms/index.html

Address for correspondence: Heather Mayfield, Texas Department of State Health Services, Center for Health Statistics, 1100 W 49th St, Austin, TX 78756, USA; email: heather.mayfield@dshs.texas.gov

Congenital Syphilis Prevention Challenges, Pacific Coast of Colombia, 2018–2022

Jose F. Fuertes-Bucheli,[1] Diana P. Buenaventura-Alegría,[1] Adriana M. Rivas-Mina, Robinson Pacheco-López

High incidences of congenital syphilis have been reported in areas along the Pacific coast of Colombia. In this retrospective study, conducted during 2018–2022 at a public hospital in Buenaventura, Colombia, we analyzed data from 3,378 pregnant women. The opportunity to prevent congenital syphilis was missed in 53.1% of mothers because of the lack of syphilis screening. Characteristics of higher maternal social vulnerability and late access to prenatal care decreased the probability of having ≥1 syphilis screening test, thereby increasing the probability of having newborns with congenital syphilis. In addition, the opportunity to prevent congenital syphilis was missed in 41.5% of patients with syphilis because of the lack of treatment, which also increased the probability of having newborns with congenital syphilis. We demonstrate the urgent need to improve screening and treatment capabilities for maternal syphilis, particularly among pregnant women who are more socially vulnerable.

Congenital syphilis is an infectious disease that is transmitted from a mother with syphilis to the fetus during pregnancy or childbirth and is caused by the bacterium *Treponema pallidum* (*1*). Globally, congenital syphilis is an infectious disease of high interest for public health but is occasionally neglected and requires collaborative actions for its control (*2*,*3*). In the Americas, congenital syphilis incidence has increased from 0.38/1,000 live births in 2009 to 0.61/1,000 live births in 2020 (*4*). This concerning trend underscores the importance of addressing this disease, which constitutes a major global cause of fetal loss, stillbirths, neonatal death, and congenital infection (*1*,*5*,*6*).

Comprehensive interventions involving diverse stakeholders in the healthcare system and community are crucial to preventing and controlling maternal and congenital syphilis, and those align with the third of the Sustainable Development Goals adopted by the United Nations Member States (*2*,*7*). Strategies used in local programs and shared globally include promoting condom use, ensuring timely access to antenatal care, early gestational syphilis detection through prompt point-of-care screening, and treating infections in a timely manner (*8*). Education on sexual and reproductive health, along with implementing epidemiologic surveillance, are also part of those efforts to prevent and control maternal and congenital syphilis (*9*). However, identifying and prioritizing populations for the specific reinforcement of those strategies in low- to middle-resource contexts is imperative.

In Colombia, a substantial increase in maternal syphilis prevalence was observed during 2017–2021; prevalence rose from 7.8 to 16.2 cases/1,000 newborns (live births and stillbirths). In 2021, maternal syphilis prevalence in Buenaventura alone was 45.8 cases/1,000 newborns, and congenital syphilis incidence also exceeded the national incidence (7.2 vs. 3.2 cases/1,000 newborns) (*10*), leading to the reporting of an epidemic in that area (*11*). Previous studies have aimed to assess the reason for this; a study conducted by Cruz et al. (*11*) in the same area found that only 8% of pregnant women received adequate treatment. Another study in South America revealed that congenital syphilis incidence is elevated in newborns of young Afro-American women who have lower educational attainment and women lacking prenatal care (*12*), elements that could be indicative of social vulnerability (*13*,*14*).

Author affiliations: Universidad Icesi, Cali, Colombia (J.F. Fuertes-Bucheli, R. Pacheco-López); Centro Internacional de Entrenamiento e Investigaciones Médicas–CIDEIM, Cali (J.F. Fuertes-Bucheli); Hospital Distrital Luis Ablanque de la Plata, Buenaventura, Colombia (D.P. Buenaventura-Alegría); Universidad Libre, Cali (D.P. Buenaventura-Alegría, A.M. Rivas-Mina)

DOI: https://doi.org/10.3201/eid3005.231273

[1]These first authors contributed equally to this article.

We sought to identify the characteristics (sociodemographic factors, obstetric history, and level of syphilis screening and treatment) of pregnant women enrolled in a prenatal care program (PCP) on the Pacific coast of Colombia associated with having newborns with congenital syphilis and the lack of maternal syphilis screening. In addition, we explored the characteristics of mothers with syphilis associated with having newborns with congenital syphilis.

Methods

Design

We conducted an analytical retrospective cohort study during January 2018–December 2022 in Buenaventura, Colombia. We used records of pregnant women enrolled in a PCP of a public hospital.

Study Area

Buenaventura is the main city on the Pacific coast of Colombia. The most recent population census in 2018 reported 258,445 inhabitants in the city, of whom 86.7% identify as Afro-Colombian (*15*). In contrast, at the national level, Afro-Colombians make up only 9.34% of Colombia's total population and are predominantly concentrated along the Pacific and Caribbean coasts of the country (*16*). Afro-Colombians face elevated levels of multidimensional poverty, marked by disparities in occupation type, educational attainment, school dropout rates, literacy, and access to healthcare services (*16*).

Study Population

We included records of pregnant women of all ages who accessed a PCP in the main referral public hospital in Buenaventura (*11*) and whose babies were born in that hospital, with or without congenital syphilis. We excluded records of persons with multiple pregnancies and records with duplicate or incomplete data.

Variables and Definitions

Sociodemographic variables were age; ethnicity (Afro-Colombian or others); rural or urban area of residence; educational level, basic or lower (completed secondary school or lower) or postsecondary (technical, university, or higher); socioeconomic level, on the basis of a 1–6 scale (low-low, low, low-middle, middle, middle-high, and high) approximating the hierarchical socioeconomic difference from poverty to wealth in Colombia (*17*); marital status: single or with partner (de facto marriage or married); position as head of household (a person, whether single or married, who bears responsibility for providing financial or social support to their dependents); and the type of health coverage (*18*). We regarded the lowest categories within the outlined sociodemographic factors as characteristics of higher maternal social vulnerability factors. Other variables consisted of past pregnancy history (number of pregnancies, spontaneous abortions, and stillbirths); the gestational trimester in which prenatal care access was obtained; and whether syphilis screening had been performed and, if it was diagnosed, whether there had been a lack of treatment, defined as the lack of ≥1 dose of benzathine penicillin G (BPG) ≥30 days before delivery (*9*,*19*).

We applied the operational definitions of maternal and congenital syphilis according to the clinical practice guide issued by the Ministry of Health and Social Protection of Colombia (*9*). A patient with detected maternal syphilis was any mother with a diagnosis of syphilis during prenatal care, with or without clinical signs, who had a positive rapid point-of-care treponemal test accompanied by a reactive nontreponemal test at any dilution and who had not received adequate treatment or had an untreated reinfection (*9*).

A newborn with congenital syphilis was any live birth or stillbirth that met ≥1 of the following criteria: newborns of a mother with untreated syphilis or inadequate treatment (without ≥1 dose of BPG ≥30 days before delivery) to prevent congenital syphilis (*9*,*19*,*20*), regardless of the result of the nontreponemal test of the newborn; any newborn with nontreponemal test titers 4 times higher than the mother's titers at the time of delivery, which is equivalent to 2 dilutions above the maternal titer; any newborn of a pregnant person whose syphilis was diagnosed during that pregnancy and with ≥1 clinical manifestations suggestive of congenital syphilis on physical examination, along with paraclinical tests suggestive of the infection; or any newborn with demonstrated *T. pallidum* in laboratory tests (*9*).

Data Sources

The hospital PCP provided the database, which included sociodemographic information, gestational age at the start of prenatal care, and obstetric history, as well as screening and treatment data for syphilis. Moreover, the database indicated whether the newborn was classified as a congenital syphilis case-patient. However, the database lacked details on the clinical stage of maternal syphilis and further details of the newborn, and although it reported the reactive or nonreactive result of the nontreponemal test for syphilis, it did not include the result in dilutions.

Statistical Analysis

We organized the data in Excel 365 (Microsoft, https://www.microsoft.com) and conducted analyses using Stata 14.0 (StataCorp LLC, https://www.stata.com). We conducted an exploratory analysis of the database to identify outliers or missing data. We reported categorical variables as frequencies and percentages and continuous variables as medians and interquartile ranges (IQRs). We determined the annual percentage of congenital syphilis cases by dividing the number of newborns with the infection by the total number of newborns for each year and multiplying by 100.

To identify maternal factors associated with having newborns with congenital syphilis, we compared pregnant women whose newborns had congenital syphilis with those whose newborns did not. Furthermore, to assess factors associated with the lack of maternal syphilis screening, we compared pregnant women who had ≥1 rapid point-of-care treponemal test through the PCP with those who did not. For those 2 objectives, we used 2 × 2 tables and calculated crude odds ratios with their respective 95% CIs. We assessed statistical significance using χ^2 and Mann-Whitney U tests as appropriate. We conducted multivariable analyses through multiple logistic regression, and each initial or saturated model included variables with $p \leq 0.25$ in the bivariate analysis, following the approach of Hosmer et al. (*21*), along with other variables considered to reflect social vulnerabilities. We selected the most parsimonious model by using the likelihood ratio test.

We conducted a subanalysis to identify factors in mothers with syphilis associated with having newborns with congenital syphilis. We compared patients with detected maternal syphilis during PCP and who had newborns with congenital syphilis to those who did not. We assessed the probability of having newborns with congenital syphilis using the relative risk (RR) as a measure of association. We determined RRs and corresponding 95% CIs through bivariate analysis. This research was conducted following the Declaration of Helsinki and was approved by the Human Research Ethics Committee of the Universidad Libre under protocol #010.

Results

General Description

During the study period, 5,172 admissions of pregnant women to the PCP were identified. Among those, we excluded 1,589 (30.7%) duplicate records and 205 (4.0%) records with insufficient information. In total, we analyzed 3,378 records. The median age was 24 (IQR 20–29) years, 98.5% were Afro-Colombian, 95.6% were from urban areas, 94.9% were at a basic or lower educational level, 93.8% were at the lowest socioeconomic level, 100% had subsidized health insurance, 78.7% were heads of households, and 19.1% had single marital status.

The median gestational age at initiation of the PCP was 12.3 (IQR 8.6–18.7) weeks, but 53.3% accessed the PCP in the first trimester of pregnancy. In total, 63.3% (2,139) women had ≥1 syphilis screening test; 270 had a positive rapid point-of-care treponemal test. Of those 270 patients, 86.7% (234) were considered cases with reactive nontreponemal tests, 11.1% (30) did not undergo the nontreponemal test, and 2.2% (6) had a nonreactive nontreponemal test. Finally, 96 mothers with newborns with congenital syphilis were reported.

The percentage of pregnant women screened for syphilis improved over time, increasing from <10% in 2018 to nearly 90% in 2022 (Figure 1). The number of participants entering the PCP each year varied; the lowest number was in 2020 and the highest was in 2022. The percentage of newborns with congenital syphilis per year decreased from 3.1% in 2018 to 1.8% in 2022 but increased during the interim years, 2019 and 2020 (Figure 1).

Factors Associated with Having Newborns with Congenital Syphilis

Of all pregnant women enrolled in the PCP, 53.1% who had newborns with congenital syphilis were not screened in the PCP. In the bivariate analysis, not having been screened through the PCP was associated with the probability of having newborns with congenital syphilis (adjusted odds ratio [aOR] 1.99, 95% CI 1.32–3.00; p = 0.001) (Table 1).

Factors Associated with the Lack of Syphilis Screening

In the bivariate analysis, age of ≤18 years or ≥35 years, basic or lower education, low socioeconomic status, single marital status, and accessing the PCP in the second or third trimester of gestation were associated with a lack of syphilis screening (Table 2). On the other hand, Afro-Colombian ethnicity and obstetric history were identified as protective factors.

Multivariate analysis revealed that independent factors associated with the lack of screening during the PCP were basic or lower educational level (aOR 2.22), lowest socioeconomic status (aOR 3.06), occupation as head of household (aOR 1.21), single marital status (aOR 2.02), and accessing the PCP in the second or third trimester of pregnancy

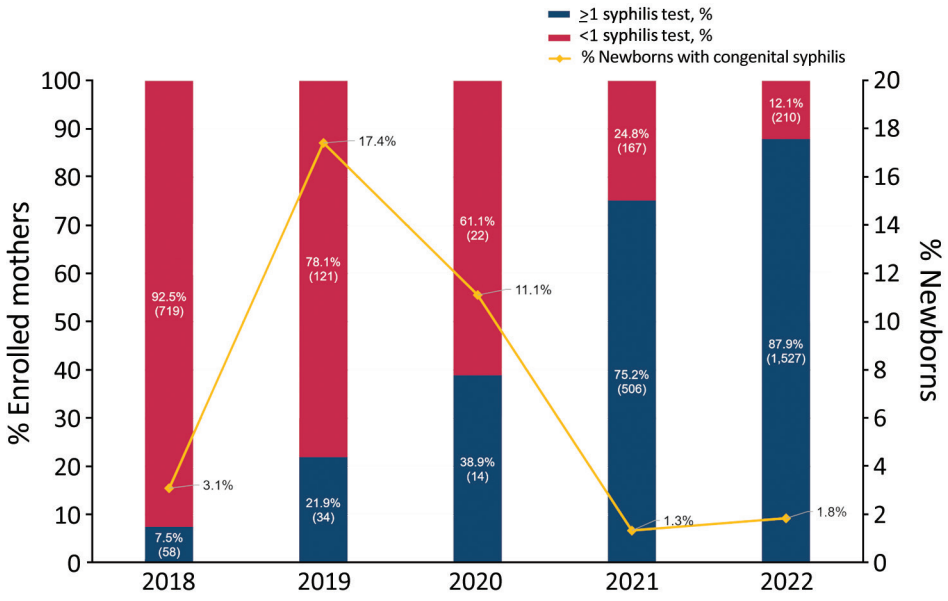

Figure 1. Syphilis screening and percentage of newborns with congenital syphilis by year of mothers' entry into the prenatal care program at a public hospital, Buenaventura, Colombia, 2018–2022. Maternal syphilis screening has improved progressively over the years, though the number of mothers who participated in the prenatal care program dropped in 2020. In addition, variability was observed in the percentage of newborns with congenital syphilis, which decreased from 3.1% to 1.8% in the evaluated period, although the percentage increased slightly from 2021 to 2022. Scales for the y-axes differ substantially to underscore patterns but do not permit direct comparisons.

(aOR 1.23) (Figure 2). Conversely, having had ≥3 previous pregnancies (aOR 0.69) and being of Afro-Colombian ethnicity (aOR 0.12) were identified as protective factors.

Factors of Mothers with Syphilis Associated with Having Newborns with Congenital Syphilis

In 234 pregnant patients, syphilis was detected during prenatal care; 41 had newborns with congenital syphilis. Of those 41 patients, 41.5% did not receive ≥1 dose of BPG ≥30 days before delivery, which was associated with a 4.31-fold increase in the probability of having newborns with the infection (Table 3).

Discussion

In this study conducted in pregnant women enrolled in a PCP on the Pacific coast of Colombia, we observed that the opportunity to prevent congenital syphilis was missed in 53.1% of pregnant women because of the lack of maternal screening. We found that the lack of screening through the PCP significantly increased the probability of having newborns with congenital syphilis, and the independent factors associated with not having had ≥1 screening test through the PCP included characteristics of higher maternal social vulnerability and the late access to the PCP. In addition, we observed that the opportunity to prevent congenital syphilis was missed in 41.5% of pregnant women with syphilis because of the lack of treatment with ≥1 dose of BPG ≥30 days before delivery, which increased the probability of having newborns with syphilis.

In the Americas, the prevalence of maternal syphilis and the incidence of congenital syphilis has increased substantially in recent years (*22*,*23*). In our study, we noted a progressive increase in the number of pregnant persons screened for syphilis during 2018–2022. However, the congenital syphilis case-patient ratio and trend could have been influenced by variability in access to the PCP during the years assessed, lack of screening, and potential surveillance biases. For example, screening in women with more risk factors might have increased in 2019, and underreporting also could have occurred, particularly in 2020. Nevertheless, the improvement in screening could indicate progress in syphilis surveillance and control in this area, possibly attributable to the implementation of the EMTCT Plus initiative (*24*) and Colombia's Resolution 3280 of 2018 (*25*). This resolution established mandatory point-of-care screening using a rapid treponemal test for all pregnant women in each trimester of pregnancy and included administering BPG in case of a positive result (*25*). Although the merits of this screening approach have been debated, implementing point-of-care treponemal tests in low-income settings has been reported to increase the detection and treatment rates of syphilis (*26*). Therefore, that practice could be beneficial in the specific context of the studied region, although additional efforts are still needed to achieve the goal of 95% screening for syphilis in pregnant women. In addition, the defined criteria for congenital syphilis case-patients in Colombia are noteworthy and potentially advantageous (*1*,*9*). That definition could enable patients who might be overlooked using alternative

criteria to be identified and treated (*27*). Nevertheless, future studies must be meticulous in evaluating the benefits and risks associated with these approaches, considering the diverse regional contexts (*27*).

Timely prenatal care is crucial for healthy pregnancy outcomes and early syphilis diagnosis (*28*), but certain sociodemographic factors might hinder healthcare professionals from getting to know patients, identifying their vulnerability factors, and providing comprehensive care (*29*,*30*). Independent factors that contributed to the lack of screening included basic or lower level of education, low socioeconomic status, serving as head of household, single marital status, and accessing prenatal care in the second or third trimester of pregnancy. Similar findings on socioeconomic level, prenatal care access, and compliance with screening were reported in the United States (*20*,*31*). In Colombia, late entry into prenatal care was associated with a low socioeconomic stratum (*32*), and a study in China found that single mothers (aOR 1.95) and women who had inadequate prenatal care (aOR 3.61) were at increased risk of having infants with congenital syphilis (*30*).

Table 1. Bivariate analysis of factors associated with having newborns with congenital syphilis in mothers who entered in a prenatal care program of a public hospital in Buenaventura, Colombia, 2018–2022*

Characteristic	Newborn with congenital syphilis	Newborn without congenital syphilis	Crude OR (95% CI)	p value
Age group, y				
≤18				
Yes	19 (19.8)	592 (18.0)	1.12 (0.63–1.89)	0.659
No	77 (80.2)	2,690 (82.0)	Referent	
19–34				
Yes	72 (75.0)	2,403 (73.2)	1.09 (0.68–1.83)	0.697
No	24 (25.0)	879 (26.8)	Referent	
≥35				
Yes	5 (5.2)	287 (8.7)	0.57 (0.18–1.40)	0.224†
No	91 (94.8)	2,995 (91.3)	Referent	
Educational level				
Basic or lower‡	92 (95.8)	3,115 (94.9)	1.23 (0.45–4.67)	0.684
Postsecondary	4 (4.2)	167 (5.1)	Referent	
Socioeconomic stratum§				
1 (low-low)	94 (97.9)	3,075 (93.7)	3.16 (0.84–26.68)	0.090†
2 (low)	2 (2.1)	207 (6.3)	Referent	
Residential area				
Rural	1 (1.0)	148 (4.5)	0.22 (0.01–1.29)	0.102†
Urban	95 (99.0)	3,134 (95.5)	Referent	
Ethnicity				
Afro-Colombian	92 (95.8)	3,234 (98.5)	0.34 (0.12–1.33)	0.033†
Other	4 (4.2)	48 (1.5)	Referent	
Occupation				
Head of household¶	77 (80.2)	2,580 (78.6)	1.1 (0.65–1.94)	0.706
Other	19 (19.8)	702 (21.4)	Referent	
Marital status				
Single	24 (25.0)	621 (18.9)	1.42 (0.85–2.31)	0.135†
With partner#	72 (75.0)	2,661 (81.1)	Referent	
History of ≥3 pregnancies				
Yes	33 (34.4)	1,024 (31.2)	1.15 (0.73–1.80)	0.508
No	63 (65.6)	2,258 (68.8)	Referent	
History of spontaneous abortions				
Yes	23 (24.0)	655 (20.0)	1.26 (0.75–2.1)	0.334
No	73 (76.0)	2,627 (80.0)	Referent	
History of stillbirths				
Yes	3 (3.1)	89 (2.7)	1.16 (0.23–3.60)	0.806
No	93 (96.9)	3,193 (97.3)	Referent	
Trimester of access to PCP				
Second or third	50 (52.1)	1,526 (46.5)	1.25 (0.81–1.92)	0.279
First	46 (47.9)	1,756 (53.5)	Referent	
≥1 syphilis screening test				
No	51 (53.1)	1,188 (36.2)	1.99 (1.30–3.07)	<0.001†
Yes	45 (46.9)	2,094 (63.8)	Referent	

*Values are no. (%) except as indicated. PCP, prenatal care program.
†Indicates variables with a p value of ≤0.25 included in the logistic regression.
‡Basic or lower: completed secondary school or lower; post-secondary: technical, technologist, university, or higher.
§Socioeconomic stratum scale in Colombia: 1 to 6, with 1 being the lowest level.
¶Person, whether single or married, who bears the ongoing responsibility for providing financial or social support to their minor newborns or other dependents.
#De facto marriage or married.

Table 2. Factors associated with having ≥1 screening test for syphilis in a prenatal care program of a public hospital, Buenaventura, Colombia, 2018–2022*

Characteristic	≥1 syphilis screening test		Crude OR (95% CI)	p value
	No	Yes		
Age group, y				
≤18				
Yes	258 (20.8)	353 (16.5)	1.33 (1.11–1.60)	0.001†
No	981 (79.2)	1,786 (83.5)	Referent	
19–34				
Yes	897 (72.4)	1,578 (73.8)	0.93 (0.79–1.09)	0.383
No	342 (27.6)	561 (26.2)	Referent	
≥35				
Yes	84 (6.8)	208 (9.7)	0.67 (0.51–0.88)	0.003†
No	1,155 (93.2)	1,931 (90.3)	Referent	
Educational level‡				
Basic or lower	1,198 (96.7)	2,009 (93.9)	1.89 (1.31–2.77)	<0.001†
Postsecondary	41 (3.3)	130 (6.1)	Referent	
Socioeconomical stratum§				
1: low-low	1,205 (97.3)	1,964 (91.8)	3.16 (2.16–4.74)	<0.001†
2: low	34 (2.7)	175 (8.2)	Referent	
Residential area				
Rural	52 (4.2)	97 (4.5)	0.92 (0.64–1.31)	0.644
Urban	1,187 (95.8)	2,042 (95.5)	Referent	
Ethnicity				
Afro-Colombian	1,197 (96.6)	2,129 (99.5)	0.13 (0.06–0.27)	<0.001†
Other	42 (3.4)	10 (0.5)	Referent	
Occupation				
Head of household¶	987 (79.7)	1,670 (78.1)	1.09 (0.92–1.31)	0.278#
Other	252 (20.3)	469 (21.9)	Referent	
Marital status				
Single	326 (26.3)	319 (14.9)	2.04 (1.71–2.43)	<0.001†
With partner**	913 (73.7)	1,820 (85.1)	Referent	
History of ≥3 pregnancies				
Yes	321 (25.9)	736 (34.4)	0.67 (0.57–0.78)	<0.001†
No	918 (74.1)	1,403 (65.6)	Referent	
History of spontaneous abortions				
Yes	201 (16.2)	477 (22.3)	0.67 (0.56–0.81)	<0.001†
No	1,038 (83.8)	1,662 (77.7)	Referent	
History of stillbirths				
Yes	23 (1.9)	69 (3.2)	0.57 (0.34–0.93)	0.018†
No	1,216 (98.1)	2,070 (96.8)	Referent	
Trimester of access to PCP				
Second or third	625 (50.4)	951 (44.5)	1.27 (1.10–1.47)	<0.001†
First	614 (49.6)	1,188 (55.5)	Referent	

*Values are no. (%) except as indicated. PCP, prenatal care program.
†Indicates variables with a p value of ≤0.25 included in the logistic regression.
‡Basic or lower: completed secondary school or lower; postsecondary: technical, university, or higher.
§Socioeconomic stratum scale in Colombia: 1 to 6, with 1 being the lowest level.
¶Person, whether single or married, who bears the ongoing responsibility for providing financial or social support to their dependents.
#Was included in the multivariate analysis for the importance in Colombian social context.
**De facto marriage or married.

Several studies have reported that patients' financial difficulties act as barriers to timely diagnosis of maternal syphilis (*33*,*34*). Those barriers can affect the ability of pregnant women to effectively access healthcare services despite being insured under the public healthcare system (*35*), especially when residing in rural areas within a fragmented healthcare system. Factors such as transportation could play a major role in late access or even lack of access (*18*,*36*), as evidenced in our study, where the population residing in rural areas was very low. Geographic barriers should be assessed in future studies on this region of Colombia.

Socioeconomic status, geographic barriers, low educational level, poor community or family social support, and the specific characteristics of the healthcare system in Colombia can result in limited contact with healthcare personnel and limited information (*37*), which leads to low awareness about the importance of timely prenatal care and detecting diseases such as syphilis early (*11*,*18*,*27*,*33*,*35*–*38*). Therefore, developing healthcare strategies and policies that ensure prompt and effective access to healthcare in the complex context of social determinants of health is imperative (*38*). Those strategies are especially crucial when most of the area's residents exhibit

vulnerable characteristics, and identifying population groups that are most socially vulnerable becomes essential to prioritize effective prevention and control strategies (*31*,*38*–*40*).

On the other hand, we identified factors that did not decrease the probability of receiving ≥1 maternal syphilis screening, such as a history of ≥3 pregnancies and Afro-Colombian ethnicity, which is likely related to improvements in healthcare personnel's identification of high-risk pregnancies (*41*,*42*) and the predominance of Afro-Colombian ethnicity in the area. Those findings, combined with progressive improvements in the percentage of screened pregnant persons suggest that previously identified gaps in healthcare providers' knowledge have gradually been addressed (*11*,*42*).

However, we observed that 41.5% of pregnant women with detected syphilis and with newborns with congenital syphilis did not receive ≥1 dose of BPG ≥30 days before delivery. That finding is particularly concerning because in the event of a positive result on the point-of-care treponemal test, administering a dose of BPG immediately is mandatory if the medical history has ruled out BPG allergy (*9*,*25*). A key factor to consider is delayed access to prenatal care, which can lead to late diagnosis and treatment and result in a missed opportunity to prevent congenital syphilis. In addition, although an allergy to penicillin might cause the physician to desensitize the patient to penicillin before initiating treatment (with possible loss of follow-up), true penicillin allergy is extremely rare (*43*), so this allergy is unlikely to result in a missed opportunity to prevent congenital syphilis. Hence, future studies are needed to identify the reasons behind those missed opportunities (*20*).

The missed opportunity to prevent congenital syphilis with BPG administration might be explained in part by documented deficiencies in healthcare professionals' understanding of the appropriate approach to maternal syphilis (*11*,*42*). Of note, similar missed opportunities have been reported in other settings; a report from the United States found lack of adequate maternal treatment despite timely diagnosis was responsible for 30.7% of missed prevention opportunities (*44*), and in 2022, missed prevention opportunities because of inadequate treatment ranged from 15.7% to 54.5% in various regions of the United States (*20*). Those findings underscore

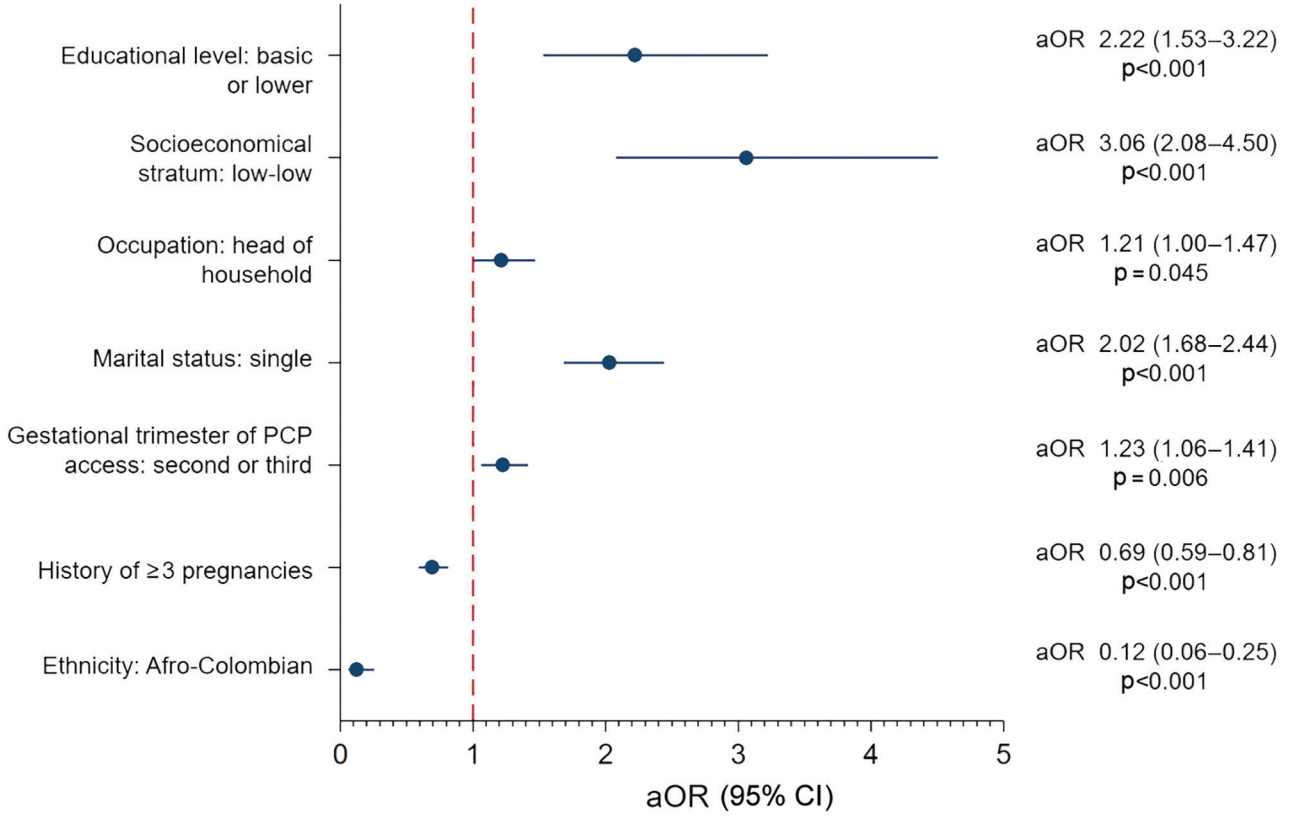

Figure 2. Multivariate analysis of factors associated with the lack of ≥1 maternal syphilis screening test in prenatal care program, Buenaventura, Colombia, 2018–2022. Vertical red dashed line indicates the nonassociation reference point. aOR, adjusted odds ratio; PCP, prenatal care program.

Table 3. Analysis of maternal factors associated with having a newborn with congenital syphilis in pregnant women with syphilis at a public hospital, Buenaventura, Colombia, 2018–2022*

Characteristic	Newborn with congenital syphilis	Newborn without congenital syphilis	RR (95% CI)	p value
Age group, y				
≤18				
Yes	9 (22.0)	35 (18.1)	1.21 (0.62–2.35)	0.570
No	32 (78.0)	158 (81.9)	Referent	
19–34				
Yes	30 (73.2)	146 (75.6)	0.89 (0.48–1.67)	0.738
No	11 (26.8)	47 (24.4)	Referent	
≥35 y				
Yes	2 (4.9)	12 (6.2)	0.80 (0.21–2.99)	0.742
No	39 (95.1)	181 (93.8)	Referent	
Educational level†				
Basic or lower	40 (97.6)	185 (95.9)	1.60 (0.24–10.37)	0.605
Postsecondary	1 (2.4)	8 (4.1)	Referent	
Socioeconomical stratum‡				
1: low-low	41 (100)	184 (95.3)	NA (NA)	0.158
2: low	0	9 (4.7)	Referent	
Residential area				
Rural	0	7 (3.6)	NA (NA)	0.215
Urban	41 (100)	186 (96.4)	Referent	
Ethnicity				
Afro-Colombian	41 (100)	193 (100)	NA (NA)	NA
Other	0	0	Referent	
Occupation				
Head of household§	33 (80.5)	155 (80.3)	1.00 (0.50–2.03)	0.979
Other	8 (19.5)	38 (19.7)	Referent	
Marital status				
Single	11 (26.8)	46 (23.8)	1.13 (0.61–2.12)	0.684
With partner¶	30 (73.2)	147 (76.2)	Referent	
History of ≥3 pregnancies				
Yes	11 (26.8)	76 (39.4)	0.61 (0.32–1.17)	0.131
No	30 (73.2)	117 (60.6)	Referent	
History of spontaneous abortions				
Yes	9 (22.0)	40 (20.7)	1.06 (0.54–2.07)	0.860
No	32 (78.0)	153 (79.3)	Referent	
History of stillbirths				
Yes	1 (2.4)	8 (4.1)	0.62 (0.09–4.05)	0.605
No	40 (97.6)	185 (95.9)	Referent	
Trimester of access to PCP				
Second or third	22 (53.7)	87 (45.1)	1.32 (0.76–2.31)	0.317
First	19 (46.3)	106 (54.9)	Referent	
Lack of syphilis treatment#				
Yes	17 (41.5)	16 (8.3)	4.31 (2.62–7.12)	<0.001
No	24 (58.5)	177 (91.7)	Referent	

*Values are no. (%) except as indicated. BPG, benzathine penicillin G; PCP, prenatal care program; RR, relative risk.
†Basic or lower: completed secondary school or lower; postsecondary: technical, university, or higher.
‡Socioeconomic stratum scale in Colombia: 1 to 6, with 1 being the lowest level.
§Person, whether single or married, who bears the ongoing responsibility for providing financial or social support to their dependents.
¶De facto marriage or married.
#Lack of ≥1 dose of BPG ≥30 d before delivery.

the need for additional research and interventions to ensure the effective treatment of maternal syphilis, given the proven efficacy of BPG (*8*,*27*) and the heightened risk for congenital syphilis when BPG is omitted (*30*). Furthermore, the observation that 58.5% of mothers with diagnosed syphilis and newborns with congenital syphilis had received ≥1 dose of BPG raises concerns about the adequacy of treatment administered (*9*,*20*,*45*), and potential reinfections (*46*). Consequently, ensuring treatment of sex contacts and tailoring treatment with a penicillin-based regimen initiated ≥30 days before delivery, with dosing and spacing appropriate for the stage of maternal syphilis, are imperative (*9*,*20*,*45*).

Despite the small sample size and the predominance of participants with characteristics of social vulnerability, this study contributes valuable information to the literature on congenital syphilis. Furthermore, because of the variability in gestational age at entry into the PCP, the results might exhibit bias. However, consistent with other studies, late entry to the PCP was identified as a factor that affected the prevention and control of congenital syphilis (*30*,*31*,*44*). Therefore, we recommend interpreting our findings

with caution; future research with larger sample sizes would achieve a more comprehensive understanding of the topic.

Overall, we observed a concerning 53.1% missed opportunity in congenital syphilis prevention because of the lack of maternal screening and a 41.5% missed opportunity because of the lack of maternal treatment. Maternal social vulnerability factors, such as basic or low educational level, low socioeconomic status, being head of the family, single marital status, and late access to prenatal care, increased the probability of not having maternal syphilis screening and having newborns with congenital syphilis. In addition, not having ≥1 dose of BPG ≥30 days before delivery, despite being a case-patient with syphilis detected at the PCP, increased the probability of having newborns with syphilis. Therefore, we recommend implementing a comprehensive multidisciplinary approach to identify and address those social vulnerability factors. Furthermore, we suggest intensifying efforts to ensure maternal syphilis is detected in a timely manner and treated adequately to mitigate elevated congenital syphilis incidence on the Pacific coast of Colombia.

About the Author

Dr. Fuertes-Bucheli is a medical doctor, member of the Microbiology and Public Health Research Group at Universidad Icesi, and works at CIDEIM, Cali, Colombia. He is passionate about the control and prevention of infectious diseases. Ms. Buenaventura-Alegría is an epidemiologist and coordinator of the Department of Sexual and Reproductive Health at the Hospital Luis Ablanque de la Plata, Buenaventura. Her interests include the control and prevention of sexually transmitted diseases and public health.

References

1. Sankaran D, Partridge E, Lakshminrusimha S. Congenital syphilis—an illustrative review. Children (Basel). 2023;10:1310. https://doi.org/10.3390/children10081310
2. World Health Organization. Ending the neglect to attain the sustainable development goals: a rationale for continued investment in tackling neglected tropical diseases 2021–2030 [cited 2023 Nov 15]. https://iris.who.int/handle/10665/363155
3. Penner J, Hernstadt H, Burns JE, Randell P, Lyall H. Stop, think SCORTCH: rethinking the traditional 'TORCH' screen in an era of re-emerging syphilis. Arch Dis Child. 2021;106:117–24.
4. Pan American Health Organization. Epidemiological review of syphilis in the Americas, December 2021 [cited 2023 Nov 17]. https://iris.paho.org/handle/10665.2/56085
5. Wijesooriya NS, Rochat RW, Kamb ML, Turlapati P, Temmerman M, Broutet N, et al. Global burden of maternal and congenital syphilis in 2008 and 2012: a health systems modelling study. Lancet Glob Health. 2016;4:e525–33. https://doi.org/10.1016/S2214-109X(16)30135-8
6. Korenromp EL, Rowley J, Alonso M, Mello MB, Wijesooriya NS, Mahiané SG, et al. Global burden of maternal and congenital syphilis and associated adverse birth outcomes—estimates for 2016 and progress since 2012. PLoS One. 2019;14:e0211720. https://doi.org/10.1371/journal.pone.0211720
7. World Health Organization. WHO guideline on syphilis screening and treatment for pregnant women [cited 2023 Nov 15]. https://iris.who.int/handle/10665/259003
8. Lin JS, Eder ML, Bean SI. Screening for syphilis infection in pregnant women: updated evidence report and systematic review for the US Preventive Services Task Force. JAMA. 2018;320:918–25. https://doi.org/10.1001/jama.2018.7769
9. Ministerio de Salud y Protección Social, Fondo de Población de las Naciones Unidas. Evidence-based clinical practice guidelines for the comprehensive care of gestational and congenital syphilis GPC-2014–41 [in Spanish]. 2014 [cited 2023 Nov 15]. https://www.acin.org/images/guias/GPC_GuiaComple_SIFILIS_impresion_n.pdf
10. Instituto Nacional de Salud de Colombia. Report on Gestational Syphilis and Congenital Syphilis Event 2021 [in Spanish]. 2021 [cited 2023 Nov 15]. https://www.ins.gov.co/buscador-eventos/Informesdeevento/SIFILIS%20INFORME%20FINAL%202021.pdf
11. Cruz AR, Castrillón MA, Minotta AY, Rubiano LC, Castaño MC, Salazar JC. Gestational and congenital syphilis epidemic in the Colombian Pacific Coast. Sex Transm Dis. 2013;40:813–8. https://doi.org/10.1097/OLQ.0000000000000020
12. Heringer AL S, Kawa H, Fonseca SC, Brignol SMS, Zarpellon LA, Reis AC. Inequalities in the trend of congenital syphilis in the municipality of Niterói, Brazil, 2007–2016 [in Portuguese]. Rev Panam Salud Publica. 2020;44:e8.
13. Mah JC, Penwarden JL, Pott H, Theou O, Andrew MK. Social vulnerability indices: a scoping review. BMC Public Health. 2023;23:1253. https://doi.org/10.1186/s12889-023-16097-6
14. de Souza CDF, Machado MF, Correia DS, do Carmo RF, Cuevas LE, Santos VS. Spatiotemporal clustering, social vulnerability and risk of congenital syphilis in northeast Brazil: an ecological study. Trans R Soc Trop Med Hyg. 2020;114:657–65. https://doi.org/10.1093/trstmh/traa034
15. Departamento Administrativo Nacional de Estadística de Colombia. National Population and Housing Census 2018 [in Spanish] [cited 2023 Nov 15]. https://sitios.dane.gov.co/cnpv/app/views/informacion/perfiles/76109_infografia.pdf
16. Departamento Administrativo Nacional de Estadística de Colombia. Black, Afro-Colombian, Raizal, and Palenquera population [in Spanish] [cited 2023 Nov 15]. https://www.dane.gov.co/files/investigaciones/boletines/grupos-etnicos/presentacion-grupos-etnicos-poblacion-NARP-2019.pdf
17. Departamento Administrativo Nacional de Estadística de Colombia. Socioeconomic stratification [in Spanish] [cited 2023 Nov 15]. https://www.dane.gov.co/index.php/servicios-al-ciudadano/servicios-informacion/estratificacion-socioeconomica#preguntas-frecuentes
18. Guerrero R, Gallego AI, Becerril-Montekio V, Vásquez J. The health system of Colombia [in Spanish]. Salud Publica Mex. 2011;53(Suppl 2):s144–55.
19. World Health Organization. Global guidance on criteria and processes for validation: elimination of mother-to-child transmission of HIV, syphilis and hepatitis B virus [cited 2023 Nov 20]. https://iris.who.int/handle/10665/349550
20. McDonald R, O'Callaghan K, Torrone E, Barbee L, Grey J, Jackson D, et al. Vital signs: missed opportunities for

preventing congenital syphilis—United States, 2022. MMWR Morb Mortal Wkly Rep. 2023;72:1269–74. https://doi.org/10.15585/mmwr.mm7246e1
21. Hosmer DW, Lemeshow S, Sturdivant RX. Applied logistic regression. Hoboken (NJ): John Wiley & Sons, Inc.; 2013.
22. Ospina-Joaqui WL, Usma-Duque CA, Gálvez-Castaño YA, Gulloso-Pedrozo L, Giraldo-Ospina B. Behavior of gestational and congenital syphilis in Colombia between 2014–2021. Ecological analysis, geo-referenced at the departmental level [in Spanish]. Ginecol Obstet Mex. 2023;91:147–54.
23. Nunes PS, Zara ALSA, Rocha DFNC, Marinho TA, Mandacarú PMP, Turchi MD. Syphilis in pregnancy and congenital syphilis and their relationship with Family Health Strategy coverage, Goiás, Brazil, 2007–2014: an ecological study. [in Portuguese]. Epidemiol Serv Saude. 2018;27:e2018127.
24. Pan American Health Organization. EMTCT Plus. Framework for elimination of mother-to-child transmission of HIV, syphilis, hepatitis B, and Chagas [cited 2023 Nov 15]. https://iris.paho.org/handle/10665.2/34306
25. Ministerio de Salud y Protección Social de Colombia. Resolution number 3280 of 2018 [in Spanish] [cited 2023 Nov 15]. https://www.minsalud.gov.co/sites/rid/Lists/BibliotecaDigital/RIDE/DE/DIJ/resolucion-3280-de-2018.pdf
26. Brandenburger D, Ambrosino E. The impact of antenatal syphilis point of care testing on pregnancy outcomes: a systematic review. PLoS One. 2021;16:e0247649. https://doi.org/10.1371/journal.pone.0247649
27. Moseley P, Bamford A, Eisen S, Lyall H, Kingston M, Thorne C, et al. Resurgence of congenital syphilis: new strategies against an old foe. Lancet Infect Dis. 2024;24:e24–35.
28. Hawkes SJ, Gomez GB, Broutet N. Early antenatal care: does it make a difference to outcomes of pregnancy associated with syphilis? A systematic review and meta-analysis. PLoS One. 2013;8:e56713. https://doi.org/10.1371/journal.pone.0056713
29. Slutsker JS, Hennessy RR, Schillinger JA. Factors contributing to congenital syphilis cases—New York City, 2010–2016. MMWR Morb Mortal Wkly Rep. 2018;67:1088–93. https://doi.org/10.15585/mmwr.mm6739a3
30. Qin JB, Feng TJ, Yang TB, Hong FC, Lan LN, Zhang CL, et al. Synthesized prevention and control of one decade for mother-to-child transmission of syphilis and determinants associated with congenital syphilis and adverse pregnancy outcomes in Shenzhen, South China. Eur J Clin Microbiol Infect Dis. 2014;33:2183–98. https://doi.org/10.1007/s10096-014-2186-8
31. Rowe CR, Newberry DM, Jnah AJ. Congenital syphilis: a discussion of epidemiology, diagnosis, management, and nurses' role in early identification and treatment. Adv Neonatal Care. 2018;18:438–45. https://doi.org/10.1097/ANC.0000000000000534
32. Cáceres-Manrique F M, Ruiz-Rodríguez M. Prevalence of late initiation of prenatal care. Association with the socioeconomic level of the pregnant woman. Cross-sectional study. Bucaramanga, Colombia, 2014–2015 [in Spanish]. Rev Colomb Obstet Ginecol. 2018;69:22–31.
33. Zhang Y, Guy R, Camara H, Applegate TL, Wiseman V, Treloar C, et al. Barriers and facilitators to HIV and syphilis rapid diagnostic testing in antenatal care settings in low-income and middle-income countries: a systematic review. BMJ Glob Health. 2022;7:e009408. https://doi.org/10.1136/bmjgh-2022-009408
34. Moreno PKG, Garzón LEM, Montes RP, Olaya RA, López RP. Factors and temporo-spatial behavior of the gestational syphilis in Cali, Colombia, 2012–2016 [in Spanish]. Rev Inv UNW. 2021;10:18–34.
35. Kozhimannil KB, Hardeman RR, Henning-Smith C. Maternity care access, quality, and outcomes: a systems-level perspective on research, clinical, and policy needs. Semin Perinatol. 2017;41:367–74. https://doi.org/10.1053/j.semperi.2017.07.005
36. Osorio AM, Tovar LM, Rathmann K. Individual and local level factors and antenatal care use in Colombia: a multilevel analysis. Cad Saude Publica. 2014;30:1079–92. https://doi.org/10.1590/0102-311X00073513
37. Viveros A, Valdés P, Gallego A, Freire M. Level of knowledge of syphilis in adolescents of two educational institutions of the Buenaventura district [in Spanish]. ACCB. 2021;1:10–20.
38. Chan EYL, Smullin C, Clavijo S, Papp-Green M, Park E, Nelson M, et al. A qualitative assessment of structural barriers to prenatal care and congenital syphilis prevention in Kern County, California. PLoS One. 2021;16:e0249419. https://doi.org/10.1371/journal.pone.0249419
39. DiOrio D, Kroeger K, Ross A. Social vulnerability in congenital syphilis case mothers: qualitative assessment of cases in Indiana, 2014 to 2016. Sex Transm Dis. 2018;45:447–51. https://doi.org/10.1097/OLQ.0000000000000783
40. Wagman JA, Park E, Giarratano GP, Buekens PM, Harville EW. Understanding perinatal patient's health preferences and patient-provider relationships to prevent congenital syphilis in California and Louisiana. BMC Pregnancy Childbirth. 2022;22:555. https://doi.org/10.1186/s12884-022-04883-w
41. Fajardo Ruiz V, Sebastián Torres-Gómez J, Montaño García J, Marcela Collazos Malagon Y, Rojas Quintero K, María Merchán-Galvis Á. Clinical characterization of pregnant women with high-risk pregnancy in a reference hospital in Cauca [in Spanish]. Interdiscip J Epidemiol Pub Health. 2021;4:8569.
42. Garcés JP, Rubiano LC, Orobio Y, Castaño M, Benavides E, Cruz A. Educating health workers is key in congenital syphilis elimination in Colombia [in Spanish]. Biomedica. 2017;37:416–24. https://doi.org/10.7705/biomedica.v37i3.3397
43. DesBiens M, Scalia P, Ravikumar S, Glick A, Newton H, Erinne O, et al. A closer look at penicillin allergy history: systematic review and meta-analysis of tolerance to drug challenge. Am J Med. 2020;133:452–462.e4. https://doi.org/10.1016/j.amjmed.2019.09.017
44. Kimball A, Torrone E, Miele K, Bachmann L, Thorpe P, Weinstock H, et al. Missed opportunities for prevention of congenital syphilis—United States, 2018. MMWR Morb Mortal Wkly Rep. 2020;69:661–5. https://doi.org/10.15585/mmwr.mm6922a1
45. Workowski KA, Bachmann LH, Chan PA, Johnston CM, Muzny CA, Park I, et al. Sexually transmitted infections treatment guidelines, 2021. MMWR Recomm Rep. 2021;70:1–187. https://doi.org/10.15585/mmwr.rr7004a1
46. Matthias J, Sanon R, Bowen VB, Spencer EC, Peterman TA. Syphilitic reinfections during the same pregnancy—Florida, 2018. Sex Transm Dis. 2021;48:e52–5. https://doi.org/10.1097/OLQ.0000000000001298

Address for correspondence: Robinson Pacheco-López, Universidad Icesi, 18th St. No. 122-135, Cali, Valle del Cauca, Colombia; email: robinson.pachecol@unilibre.edu.co

Epidemiology of SARS-CoV-2 in Kakuma Refugee Camp Complex, Kenya, 2020–2021[1]

Maurice Ope, Raymond Musyoka, John Kiogora, Jesse Wambugu, Elizabeth Hunsperger, Gideon O. Emukule, Peninah Munyua, Bonaventure Juma, Elizabeth Simiyu, Levan Gagnidze, John Burton, Rachel B. Eidex

Understanding SARS-CoV-2 infection in populations at increased risk for poor health is critical to reducing disease. We describe the epidemiology of SARS-CoV-2 infection in Kakuma Refugee Camp Complex, Kenya. We performed descriptive analyses of SARS-CoV-2 infection in the camp and surrounding community during March 16, 2020–December 31, 2021. We identified cases in accordance with national guidelines.We estimated fatality ratios and attack rates over time using locally weighted scatterplot smoothing for refugees, host community members, and national population. Of the 18,864 SARS-CoV-2 tests performed, 1,024 were positive, collected from 664 refugees and 360 host community members. Attack rates were 325.0/100,000 population (CFR 2.9%) for refugees,150.2/100,000 population (CFR 1.11%) for community, and 628.8/100,000 population (CFR 1.83%) nationwide. During 2020–2021, refugees experienced a lower attack rate but higher CFR than the national population, underscoring the need to prioritize SARS-CoV-2 mitigation measures, including vaccination.

In late 2019, a cluster of pneumonia cases caused by a novel coronavirus later named SARS-CoV-2 was identified in Wuhan, China (*1*). The virus spread rapidly in China and globally; the World Health Organization (WHO) declared a pandemic on March 11, 2020 (*2*). The disease caused by SARS-CoV-2 was designated by WHO as COVID-19. Some COVID-19 patients develop severe disease requiring hospitalization in intensive care unit; the risk for severe disease was associated with increasing age, socioeconomic status and underlying conditions (*3*). To contain the pandemic, many countries restricted international travel, implemented social distancing, and encouraged the use of face masks and frequent handwashing and sanitizing (*1*).

The United Nations High Commissioner for Refugees (UNHCR) estimates that as of December 2020, there were 20 million refugees and 4.1 million asylum seekers globally, most of whom were living in low- and middle-income countries, usually with weak health systems and poor capacity to manage severe COVID-19 (*4*). As of December 2021, Kenya hosted 540,068 refugees in urban and camp settings (*5*). The number of refugees into Kenya increased steadily during 2019–2021 (*5*). During the COVID-19 pandemic, the Kakuma Refugee Camp Complex (KRCC) was home to ≈40% of refugees in Kenya. To prevent the introduction and spread of the virus in refugee camps, UNHCR-Kenya and the government of Kenya implemented mitigation measures, including restriction of movement into and out of the camps.

Refugees are at an increased risk for poor health outcomes (*4*) for several reasons: difficulties in access to linguistically and culturally appropriate health related information (*6*); inadequate nutrition, partly because dependence on food rations (*7*); and poor access to adequate health services, including testing for SARS-CoV-2 and management of COVID-19. They

Author affiliations: Centers for Disease Control and Prevention, Nairobi, Kenya (M. Ope, R. Musyoka, E. Hunsperger, G.O. Emukule, P. Munyua, B. Juma, R.B. Eidex); International Rescue Committee, Nairobi (J. Kiogora); United Nations High Commissioner for Refugees, Kakuma, Kenya (J. Wambugu); International Rescue Committee, Kakuma (E. Simiyu); International Organization for Migration, Nairobi (L. Gagnidze); United Nations High Commissioner for Refugees, Nairobi (J. Burton)

DOI: http://doi.org/10.3201/eid3005.231042

[1]Preliminary results from this study were presented at the 2022 North American Refugee Health Conference, June 23–25, 2022, Cleveland, Ohio, USA.

often live in remote locations in crowded shelters with poor access to water, sanitation, and hygiene facilities, thus making implementation and enforcement of COVID-19 mitigation measures such as social distancing, handwashing, isolation, and quarantine challenging (*2*). Moreover, some essential services offered to refugees, such as food distribution and refugee registration, repatriation, and resettlement, cause refugees to congregate, increasing the likelihood of SARS-CoV-2 transmission. In addition, humanitarian workers providing services to refugees may travel from urban areas with a high prevalence of SARS-CoV-2 to the refugee camps and may transmit disease into refugee settings.

The epidemiology of SARS-CoV-2 infection in refugee camps is not well described. Given the unique setting and vulnerabilities of this population, it may also be different from the host community, national, or even global epidemiology. Understanding the epidemiology of SARS-CoV-2 infection in refugee populations may lead to targeted interventions and messaging, which can be different from the messaging and interventions designed for the general population. We sought to describe the epidemiology of SARS-CoV-2 infection in the KRCC during the pandemic and compare it with the national situation.

Kenya Ministry of Health reviewed this project and determined that it was a nonresearch programmatic activity to inform public health prevention strategies and did not require local Institutional Review Board approval. This activity was reviewed by CDC and was conducted consistent with applicable federal law and CDC policy (e.g., 45 C.F.R. part 46.102(l)(2), 21 C.F.R. part 56; 42 U.S.C. §241(d); 5 U.S.C. §552a; 44 U.S.C. §3501 et seq.).

Methods

Study Site and Population

Turkana West subcounty is located in Turkana County in northwestern Kenya. It shares international boundaries with Uganda to the west and South Sudan to the northwest and is ≈600 km from Nairobi (*8*). It hosts Kakuma refugee camp and Kalobeyei integrated settlement, which comprise the current KRCC. Kakuma refugee camp was established in 1992 as a single camp; it is divided into 4 sections (Kakuma 1, 2, 3 and 4). In 2016, the population of Kakuma refugee camp had exceeded its maximum capacity, prompting the establishment of Kalobeyei integrated settlement to provide additional accommodation for refugees. In this new settlement, located 25 km away from Kakuma refugee camp, refugees are integrated into host communities (*9*). The host community mainly consists of pastoralists who live throughout Turkana West subcounty; they are able to mix with refugees and can access health services within the refugee camps (*9*) (Appendix Figure, https://wwwnc.cdc.gov/EID/article/30/5/23-1042-App1.pdf).

During March 1, 2020–December 31, 2021, KRCC hosted 196,050–219,901 refugees and asylum seekers, most of whom were from South Sudan, Democratic Republic of the Congo, Burundi, Ethiopia, and Sudan (*5*). For this analysis, we used the population at the midpoint in time, February 2021, as our denominator; it was 204,309 (*5*). At the same time, an estimated 239,627 host community members were living in Turkana West subcounty. The main UNHCR healthcare implementing partner is the International Rescue Committee (IRC).

Testing for SARS-CoV-2

Since March 11, 2020, when WHO declared COVID-19 a pandemic, patients meeting the definition of a suspected case of COVID-19 and their close contacts were prioritized for testing for SARS-CoV-2 (*10*,*11*). Specimens for SARS-CoV-2 testing were collected from the patient's upper and lower respiratory system in accordance with guidelines from Kenya Ministry of Health (*10*). In May 2020, as we learned that presymptomatic persons could spread the virus (*12*), UNHCR recommended expanded testing to include refugees and humanitarian workers each time they traveled in or out of the camp. Beginning in April 2021, testing was required for refugees on voluntary repatriation to their country of origin and for those being prepared for any surgical procedure. Of note, the case definition of COVID-19 changed over time; fever and history of travel were required initially, and later, persons with other symptoms of COVID-19 but no history of travel met the definition of a suspected case and were eligible for testing. Those changes were consistent with WHO guidelines and were officially communicated by the Kenya Ministry of Health through official notifications and published on the Ministry of Health website (*10*,*11*). SARS-CoV-2 infections were identified following national guidelines and a confirmed SARS-CoV-2 case was anyone with laboratory confirmation of SARS-CoV-2 infection either by real-time reverse transcription PCR (real time RT-PCR), GeneXpert SARS-CoV-2 rapid real-time RT-PCR (GeneXpert; Cephid, https://www.cepheid.com), or antigen rapid diagnostic testing (Ag RDT), irrespective of clinical signs or symptoms (*11*). A COVID-19 case-patient was any symptomatic person who tested positive for SARS-CoV-2.

Severe acute respiratory illness (SARI) and influenza-like illness (ILI) surveillance was established in Kakuma refugee camp in 2007. Samples from persons meeting the SARI/ILI case definitions were tested for influenza viruses, respiratory syncytial virus, human metapneumovirus, and parainfluenza virus. The case definitions for SARI and ILI are described elsewhere (*13*). Effective March 16, 2020, specimens were also tested prospectively for SARS-CoV-2 using real-time RT-PCR at the US Centers for Disease Control and Prevention (CDC)–supported Kenya Medical Research Institute (KEMRI) laboratory in Nairobi. Over time, the testing algorithm for SARS-CoV-2 was modified as the testing capacity was expanded from centralized real-time RT-PCR testing in Nairobi to additional laboratories performing real-time RT-PCR, GeneXpert, and Ag RDT testing (Figure 1). In KRCC, Ag RDT testing was available in April 2021 and GeneXpert testing in June 2021. To ensure timely isolation of COVID-19 cases, SARI and ILI cases in which there was a strong clinical suspicion of COVID-19 were tested using Ag RDT at the IRC laboratory. Persons experiencing symptoms, under quarantine, or being prepared for surgery were also tested using Ag RDT. During April–June 2021, the International Organization for Migration (IOM) laboratory tested refugees on resettlement and humanitarian workers using real time RT-PCR; thereafter, either GeneXpert or real time RT-PCR was used. AMPATH tested specimens from Turkana West Subcounty beginning in May 2021 and Lancet laboratories beginning in June 2021, using real-time RT-PCR whenever it was not feasible to test the specimens either at IRC or CDC-supported KEMRI laboratories.

Study Design

We conducted a descriptive analysis of routinely collected data from March 2020–December 31, 2021, on demographics, SARS-CoV-2 testing results, and clinical outcomes of COVID-19 in KRCC. We used multiple sources of SARS-CoV-2 infection data for Turkana West subcounty and KRCC, each with its own limitations.

National SARS-CoV-2 Testing Repository

On June 16, 2020, the Kenya Ministry of Health established a national repository for SARS-CoV-2 testing at the National Public Health Laboratory (NPHL). All laboratories accredited to perform SARS-CoV-2 testing were required to submit all test results to the national SARS-CoV-2 testing repository through a secure web link. This dataset included all persons tested for SARS-CoV-2 using Ag RDT, GeneXpert, and real-time RT-PCR. For the purposes of our analysis, the national SARS-CoV-2 testing repository data was limited to Turkana West subcounty.

National Line List of SARS-CoV-2–Positive Cases

Upon the detection of the first case of SARS-CoV-2 in Kenya on March 14, 2020, the national Public Health Emergency Operation Center (PHEOC) maintained a line list of all laboratory-confirmed cases. This list was regularly updated for symptomatic cases with outcome of illness.

Line List of Positive Cases in the Refugee Camp

Upon the detection of the first SARS-CoV-2 infection in the camp, UNHCR and IRC maintained a line list of laboratory-confirmed SARS-CoV-2 cases. For symptomatic cases, this list was regularly updated with outcome of illness.

Data Management

We primarily used data from the national SARS-CoV-2 testing repository, line list of SARS-CoV-2 positive cases maintained by IRC, and the national

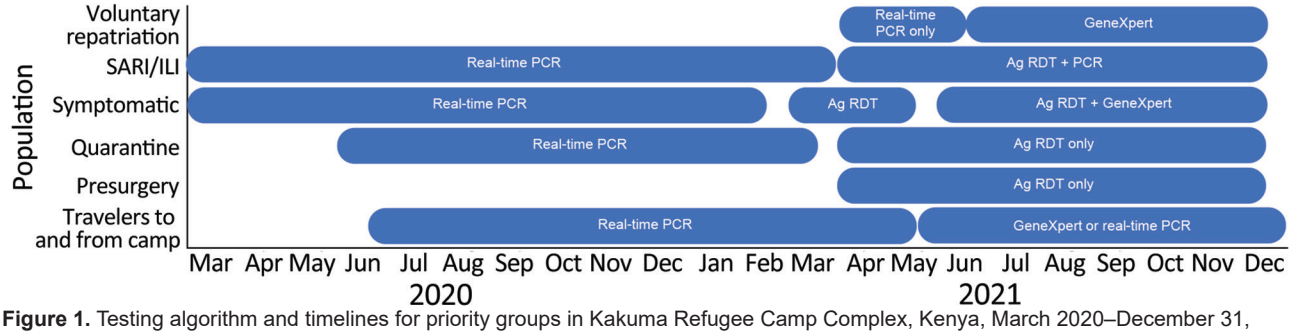

Figure 1. Testing algorithm and timelines for priority groups in Kakuma Refugee Camp Complex, Kenya, March 2020–December 31, 2021. Voluntary repatriation was halted in 2020 because of the pandemic and resumed in April 2021. Symptomatic persons were initially tested for SARS-CoV-2 using real-time PCR; starting April 2021, they were tested used only Ag RDT; starting in June 2021, positive samples were confirmed using GeneXpert (Cephid, https://www.cepheid.com). Persons with SARI/ILI were initially tested using real-time PCR; starting April 2021, they were tested using both Ag RDT and real-time PCR. Ag RDT, antigen rapid diagnostic testing; ILI, influenza-like illness; SARI, severe acute respiratory illness.

Table. Data sources used for analysis of SARS-CoV-2 infection, Kakuma Refugee Camp Complex, Kenya, 2020–2021*

Data source	Refugees	Host	Kenya
National SARS-CoV-2 testing repository	SARS-CoV-2 testing rate	SARS-CoV-2 testing rate	SARS-CoV-2 testing rate
National line list of positive cases	NA	COVID-19 attack rate and case-fatality ratio	COVID-19 attack rate and case-fatality ratio
UNHCR/IRC line list of positive cases from the refugee camp	COVID-19 attack rate and case-fatality ratio	NA	NA
Source of population size	Population statistics from UNHCR	2019 National Housing and Population Census	2019 National Housing and Population Census

*IRC, International Rescue Committee; NA, not applicable; UNHCR, United Nations High Commissioner for Refugees.

PHEOC. We restricted the analysis to KRCC and calculated SARS-CoV-2 testing rates, SARS-CoV-2 infection attack rates, and COVID-19 case-fatality ratios (Table).

We defined refugees as persons living in KRCC or who were noted as a refugee in the database and host community members as nonrefugees who lived in Turkana West subcounty and were not employed as humanitarian workers. We excluded humanitarian workers from this analysis because it was unclear how many were working in the camp during the pandemic. Moreover, the workers traveled several times in and out of the camp as part of their work, thus requiring testing multiple times, unlike refugees and host community members, who moved in and out of the camps much less frequently.

We performed statistical analysis using SAS software version 9.4 (SAS Institute Inc., https://www.sas.com) and plotted graphs using R version 4.1.1 (The R Foundation for Statistical Computing, https://www.r-project.org). We estimated attack rates with their associated 95% CIs for refugees and the host community using population statistics from UNHCR (*14*) and the 2019 national population census (*15*). We estimated attack and testing rates over time using locally weighted scatterplot smoothing, a localized weighted regression with a span of 20% of the nearest point and heavier weighting of closer points. To avoid negative attack rates due to the effect of smoothing caused by values closer to zero, we fitted them on a log scale and then applied exponentiation to get results on the original scale.

Results

The first positive SARS-CoV-2 case from KRCC was detected on May 22, 2020, in a refugee camp 2 months after the first case of SARS-CoV-2 was reported in Kenya. This case-patient was tested because he had traveled from Nairobi to the camp. By December 31, 2021, a total of 1,024 SARS-CoV-2 infection cases were reported in KRCC; among those, 664 (63.4%) were refugees and 360 (36.6%) members of the host community. The median patient age was 25 (1–102) years; 498 (51.0%) patients were male. Nationally, a total of 297,155 SARS-CoV-2 cases were reported as of December 31, 2021.

During March 2020–December 31, 2021, a total of 23 COVID-19 deaths were reported in KRCC and 5,442 nationally. The overall CFRs were 2.25% (95% CI 1.29%–3.20%) for KRCC and 1.83% (95% CI 1.78%–1.87%) for Kenya. Of the 23 deaths in KRCC, 19 deaths (CFR 2.86%, 95% CI 1.52%–4.20%) were reported among refugees, and 4 deaths (CFR 1.11%, 95% CI 0.00%–2.33%) among the host community.

During the same period, a total of 18,864 SARS-CoV-2 tests from Turkana West subcounty were performed. Weekly variation in the testing rates during the pandemic (Figure 2) resulted in part from challenges

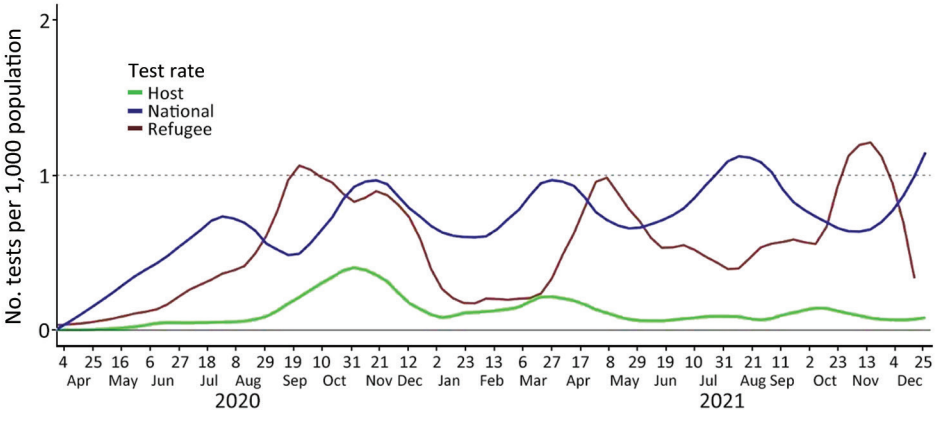

Figure 2. Weekly COVID-19 SARS-CoV-2 testing rates per 1,000 population for the general population and among host and refugee populations in Kakuma Refugee Camp Complex, Kenya, March 16, 2020–December 31, 2021.

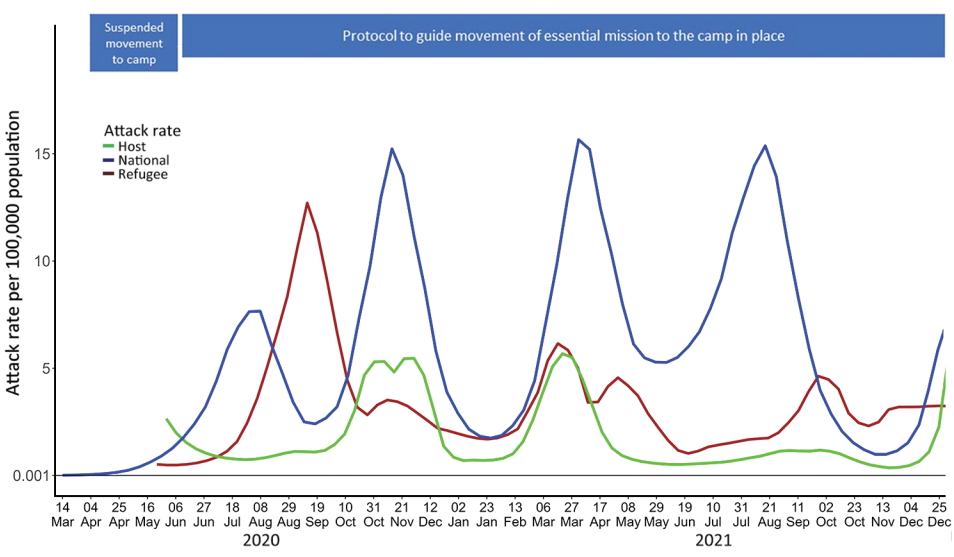

Figure 3. Weekly SARS-CoV-2 infection attack rates per 100,000 population for the general population and among host and refugee populations in Kakuma Refugee Camp Complex, Kenya, March 16, 2020–December 31, 2021.

in obtaining supplies for specimen collection and testing; hence, it is likely that many SARS-CoV-2 infection cases were missed and not reported. The testing rate for SARS-CoV-2 was lower than the WHO recommended minimum weekly testing rate of 1/1,000 population, among all 3 populations in our analysis: refugees (10,689 tests; 0.52/1,000 population), host community members (2,635 tests; 0.11/1,000 population), and nationally (3,260,483 tests; 0.69/1,000 population).

The overall SARS-CoV-2 infection attack rates per 100,000 persons was 325.0 (95% CI 300.1–349.9) among refugees, 150.2 (95% CI 134.5–165.9) in the host community, and 628.8 (95% CI 626.6–631.1) nationally. The COVID-19 pandemic in Kenya occurred in waves. Nationally, there were 5 waves: June–August 2020, September–December 2020, February–May 2021, May–September 2021, and November–December 2021 (Figure 3). Similarly, refugee and host communities experienced waves of infections. The highest attack rate among refugees and host community members during the first wave, and the subsequent waves were of a lesser magnitude than the previous waves. The third national wave coincided with an increase in attack rate among refugees and host community. In contrast, during the fourth national wave there was no increase in attack rate among refugees and host community members.

Discussion

This analysis found that refugees were severely negatively affected by COVID-19 during the pandemic. Refugees experienced a lower attack rate but a higher CFR than the population of Kenya as a whole. The low attack rate among refugees compared with national rates is similar to findings in Jordan's refugee camps (*16*), which may suggest that refugees were not responsible for the continued spread of SARS-CoV-2 but instead were affected by external SARS-CoV-2 transmission. We noted that the pandemic occurred when the Kenya government had given a nonnegotiable ultimatum for closure of refugee camps that was not enforced at the time (*17*); stigmatization, increased restriction, or crackdowns on refugees were possible if they were thought to be responsible for driving infection. At the beginning of the pandemic there were fears of catastrophic effects of COVID-19 among refugee settings because those populations were already vulnerable (*18*). We found a higher CFR among refugees compared to national rates. The low testing rate among host community members may partly explain a lower attack rate, whereas the lower CFR observed among host community members could be a consequence of poor documentation of deaths among this population in Turkana West subcounty.

We cannot fully explain why the refugees experienced a higher CFR than the host and national populations. One possible reason is that, unlike in the host and Kenya populations, all deaths among refugees were meticulously investigated to determine if the cause of death was COVID-19. This process included collection and testing of nasopharyngeal swabs from deceased refugees at both community and health facility levels, potentially inflating the CFR. In addition, contributing factors such as malnutrition, other diseases, or poor health status could put refugees at higher risk for severe disease and death. Unfortunately, that information was not available for analysis.

Measures put in place to either delay introduction of the virus into the camps or contain transmission within Kenya had positive effects and some unintended consequences. In April 2020, the government of Kenya imposed restriction on movement of persons from SARS-CoV-2–infected areas and a lockdown in urban areas (*19*,*20*). Similarly, UNHCR restricted movement into and out of the camps to delay introducing the virus in the refugee camps to enhance pandemic control. Whereas the national lockdown and restriction of movement from SARS-CoV-2–infected areas were imposed with good intentions, they may have had unintended consequences on refugees. Refugees who were living on daily wages in urban settings experienced job losses that caused them to migrate from urban settings with high SARS-CoV-2 attack rates to the camps, introducing SARS-CoV-2 into the camps, as happened with the first case in KRCC.

After the introduction of the virus to the camp, the first wave among refugees had very high attack rates at a time when the testing rates were very low. The high attack rates were partly caused by inability to significantly reduce contact with many undiagnosed case-patients living with other refugees in crowded shelters. At that time, the estimated population of refugees in the camp was 196,120 in an expected capacity of <100,000 (*5*). Also, because most of the cases reported were asymptomatic at that time, there was inadequate information among refugees on SARS-CoV-2. Poor adherence to COVID-19 mitigation measures among refugees was not uncommon, which may partly explain the high attack rates reported. In contrast, the attack rate among host community members was low during the first wave, possibly because it was a sparsely populated rural population, which reduced the risk for transmission.

Although we did not test for the SARS-CoV-2 variants circulating in the refugee camps, it is likely that that the variants that were predominant nationally were also circulating in the refugee camp. The third national wave commenced in January 2021 when the more transmissible Alpha variant B.1.1.7 was detected in Kenya (*21*); during that time, there was a similar increase in attack rate among refugees and host community members. The Delta variant B.1.617.2 was detected in Kenya in March 2021, cocirculating with the Alpha variant (*22*). The Delta variant took over as the predominant variant during the fourth national wave. It is unclear why, during the period when the Delta variant was predominant in Kenya, the attack rate increased nationally but not among refugees.

We also found that testing was low for refugees nearly throughout the pandemic; some SARS-CoV-2 infections were undetected and thus the reported attack rates are likely an underestimate. The introduction of Ag RDTs and GeneXpert testing in the camp led to improvement in testing rate of refugees, although it did not reach the minimum test per population rate recommended by WHO. The improved testing capacity came late in the pandemic, when it was no longer tenable to perform contact tracing for all confirmed cases. The low testing rate among refugees in KRCC is consistent with findings among other refugee populations (*23*).

The first limitation of this descriptive analysis is that we relied on routine data collected by different entities which had gaps, and hence, we had to cross-check with other datasets to have a complete dataset for analysis. To do that, we had to make assumptions because of the unique deficiencies in each dataset: the national SARS-CoV-2 testing repository was established after SARS-CoV-2 cases were detected in the camp; the repository was not routinely checked for errors; multiple tests for the same person were captured even if they were done almost at the same time; and manual transfer of data using Microsoft Excel spreadsheets from the testing laboratory to the national SARS-CoV-2 repository could have led to some errors. In addition, we were unable to identify persons who had multiple tests performed during the same infection or those with prolonged shedding of the virus. Prolonged detection of viral RNA does not indicate infectiousness (*24*). In our analysis, we reported those infections as separate, thus overestimating the attack rates for refugees and for host and national populations. Those deficiencies likely led to reporting bias. Second, the reported positive cases were based on multiple testing platforms such as RT-PCR, GeneXpert, and Ag RDT, which had different sensitivities and specificities. Ag RDT, for example, had a low sensitivity, potentially resulting in false negatives and resulting in an underestimate of the reported attack rates. Third, since we are comparing attack rates, it would have been better if we adjusted for the varying testing rates among the populations; however, this adjustment was not possible because host and refugee populations were a subset of the national database.

In conclusion, KRCC did not escape the COVID-19 pandemic. Refugees experienced a reported lower attack rate but a higher CFR compared with the national rates. It is unclear if the high CFR among refugees was a result of poor utilization of health services, poor access to healthcare by severe cases,

low testing rate, or a general predisposition to ill health because of malnutrition or co-infection with other pathogens.

Testing is an essential component in controlling the pandemic to ensure early isolation, contact tracing, and case management. To provide evidence on the need for behavior change to mitigate the spread of SARS-CoV-2, a robust testing system is critical. Therefore, to prepare for the next pandemic, it is essential to strengthen laboratory capacity that would serve not only refugees but also rural communities hosting the refugees.

The challenges with reliable SARS-CoV-2 data from this refugee population also emphasizes the need for improved integration of migrant populations into national data systems to better understand differences in disease transmission during outbreaks and pandemics. Our findings underscore the need to prioritize COVID-19 mitigation measures, including vaccination for refugees.

Acknowledgments

We thank IRC, who provided care for the refugees, and UNHCR for providing oversight. We thank all the laboratory technicians who performed SARS-CoV-2 testing at IOM, AMPATH, Lancet, and IRC and the CDC-supported KEMRI laboratories.

About the Author

Dr. Ope is a medical epidemiologist and public health advisor with the US Centers for Disease Control and Prevention in Nairobi, Kenya. His main interests are in migration health, infectious diseases and outbreak prevention and control.

References

1. Ji H, Tong H, Wang J, Yan D, Liao Z, Kong Y. The effectiveness of travel restriction measures in alleviating the COVID-19 epidemic: evidence from Shenzhen, China. Environ Geochem Health. 2022; 44:3115–32.
2. Saifee J, Franco-Paredes C, Lowenstein SR. Refugee health during COVID-19 and future pandemics. Curr Trop Med Rep. 2021;8:1–4. https://doi.org/10.1007/s40475-021-00245-2
3. Reis ECD, Rodrigues P, Jesus TR, de Freitas Monteiro EL, Virtuoso Junior JS, Bianchi L. Risk of hospitalization and mortality due to COVID-19 in people with obesity: an analysis of data from a Brazilian state. PLoS One. 2022;17:e0263723. https://doi.org/10.1371/journal.pone.0263723
4. World Health Organization. Tuberculosis prevention and care among refugees and other populations in humanitarian settings: an interagency field guide. 2022 [cited 2022 March 22]. https://www.who.int/publications/i/item/9789240042087
5. United Nations High Commissioner for Refugees. Kenya operations statistics. Kenya statistics package: statistical summary of refugees and asylum seekers in Kenya. 2021 [cited 2022 Feb 17]. https://www.unhcr.org/ke/wp-content/uploads/sites/2/2022/01/Kenya-Statistics-Package-31-December-2021.pdf
6. Matlin SA, Karadag O, Brando CR, Góis P, Karabey S, Khan MMH, et al. COVID-19: marking the gaps in migrant and refugee health in some massive migration areas. Int J Environ Res Public Health. 2021;18:12639. https://doi.org/10.3390/ijerph182312639
7. Ververs M, Muriithi JW, Burton A, Burton JW, Lawi AO. Scurvy outbreak among South Sudanese adolescents and young men—Kakuma Refugee Camp, Kenya, 2017–2018. MMWR Morb Mortal Wkly Rep. 2019;68:72–5. https://doi.org/10.15585/mmwr.mm6803a4
8. Bolon I, Mason J, O'Keeffe P, Haeberli P, Adan HA, Karenzi JM, et al. One Health education in Kakuma refugee camp (Kenya): from a MOOC to projects on real world challenges. One Health. 2020;10:100158. https://doi.org/10.1016/j.onehlt.2020.100158
9. Kisera N, Luxemburger C, Tornieporth N, Otieno G, Inda J. A descriptive cross-sectional study of cholera at Kakuma and Kalobeyei refugee camps, Kenya in 2018. Pan Afr Med J. 2020;37:197. https://doi.org/10.11604/pamj.2020.37.197.24798
10. Republic of Kenya Ministry of Health. Case definition. In: Guidelines on case management of COVID-19 in Kenya. Nairobi: The Ministry; 2021. p. 3–4.
11. Republic of Kenya Ministry of Health. Case definition for novel coronavirus disease (COVID-19). Nairobi, Kenya [cited 2022 Mar 18]. https://www.health.go.ke/wp-content/uploads/2020/04/COVID-19-Case-Definition-25-March-2020.pdf
12. He X, Lau EHY, Wu P, Deng X, Wang J, Hao X, et al. Temporal dynamics in viral shedding and transmissibility of COVID-19. Nat Med. 2020;26:672–5. https://doi.org/10.1038/s41591-020-0869-5
13. Ahmed JA, Katz MA, Auko E, Njenga MK, Weinberg M, Kapella BK, et al. Epidemiology of respiratory viral infections in two long-term refugee camps in Kenya, 2007–2010. BMC Infect Dis. 2012;12:7. https://doi.org/10.1186/1471-2334-12-7
14. Kenya UNHCR. Kenya operation statistics 2022 [cited 2022 Mar 22]. https://www.unhcr.org/ke/wp-content/uploads/sites/2/2020/08/Kenya-Statistics-Package-28-February-2021.pdf
15. Kenya National Bureau of Statistics. 2019 Kenya population and housing census volume III: distribution of population by age and sex. 2022 [cited 2022 Mar 25]. https://www.knbs.or.ke/?wpdmpro=2019-kenya-population-and-housing-census-volume-iii-distribution-of-population-by-age-sex-and-administrative-units
16. Altare C, Kostandova N, OKeeffe J, Hayek H, Fawad M, Musa Khalifa A, et al. COVID-19 epidemiology and changes in health service utilization in Azraq and Zaatari refugee camps in Jordan: a retrospective cohort study. PLoS Med. 2022;19:e1003993. https://doi.org/10.1371/journal.pmed.1003993
17. Africa.com. A roadmap for the closure of Kenya's largest refugee camps. 2021 [cited 2022 Jul 5]. https://www.africa.com/a-roadmap-for-the-closure-of-kenyas-largest-refugee-camps
18. Ismail MB, Osman M, Rafei R, Dabboussi F, Hamze M. COVID-19 and refugee camps. Travel Med Infect Dis. 2021;42:102083. https://doi.org/10.1016/j.tmaid.2021.102083
19. Government of Kenya. The Public Health Act (CAP 242). The public health (COVID-19 restriction of movement of persons

and related measures) rules 2020. Legal notice number 50. In: Kenya Gazette, editor. Nairobi: Government Printer; 2020 [cited 2022 Feb 15]. http://kenyalaw.org/kl/fileadmin/pdfdownloads/LegalNotices/2020/LN50_2020.pdf
20. Government of Kenya. The Public Health Act (CAP 242). The public health (COVID-19 restriction of movement of persons and related measures) rules 2020. Legal notice number 51. In: Kenya Gazette, editor. Nairobi: Government Printer; 2020 [cited 2022 Feb 15]. https://kenyalaw.org/kl/fileadmin/pdfdownloads/LegalNotices/2020/LN51_2020.pdf
21. Wilkinson E, Giovanetti M, Tegally H, San JE, Lessells R, Cuadros D, et al. A year of genomic surveillance reveals how the SARS-CoV-2 pandemic unfolded in Africa. Science. 2021;374:423–31. https://doi.org/10.1126/science.abj4336
22. Nasimiyu C, Matoke-Muhia D, Rono GK, Osoro E, Obado DO, Mwangi JM, et al. Imported SARS-COV-2 variants of concern drove spread of infections across Kenya during the second year of the pandemic. COVID. 2022;2:586–98
23. Manirambona E, Wilkins L, Lucero-Prisno III DE. COVID-19 and its threat to refugees in Africa. Health Promot Perspect. 2021;11:263–6. https://doi.org/10.34172/hpp.2021.33
24. Fotouhi F, Salehi-Vaziri M, Farahmand B, Mostafavi E, Pouriayevali MH, Jalali T, et al. Prolonged viral shedding and antibody persistence in patients with COVID-19. Microbes Infect. 2021;23:104810. https://doi.org/10.1016/j.micinf.2021.104810

Address for correspondence: Maurice O. Ope, CDC Kenya—Africa Field Program, PO Box 621 Village Market, Nairobi, Kenya; email: ybf8@cdc.gov

Identifying Contact Time Required for Secondary Transmission of *Clostridioides difficile* Infections by Using Real-Time Locating System

Min Hyung Kim, Jaewoong Kim, Heejin Ra, Sooyeon Jeong, Yoon Soo Park, Dongju Won, Hyukmin Lee,[1] Heejung Kim[1]

Considering patient room shortages and prevalence of other communicable diseases, reassessing the isolation of patients with *Clostridioides difficile* infection (CDI) is imperative. We conducted a retrospective study to investigate the secondary CDI transmission rate in a hospital in South Korea, where patients with CDI were not isolated. Using data from a real-time locating system and electronic medical records, we investigated patients who had both direct and indirect contact with CDI index patients. The primary outcome was secondary CDI transmission, identified by whole-genome sequencing. Among 909 direct and 2,711 indirect contact cases, 2 instances of secondary transmission were observed (2 [0.05%] of 3,620 cases), 1 transmission via direct contact and 1 via environmental sources. A low level of direct contact (113 minutes) was required for secondary CDI transmission. Our findings support the adoption of exhaustive standard preventive measures, including environmental decontamination, rather than contact isolation of CDI patients in nonoutbreak settings.

Mitigating the incidence of *Clostridioides difficile* infections (CDIs), particularly those acquired in healthcare settings, has received increased attention because of the notable prevalence of this contagion (*1*,*2*). Although the incidence of hospital-acquired CDI has declined because effective infection control measures have been used (*3*), the effectiveness of specific interventions used to curb disease transmission remains unclear (*4*–*6*). The efficacy of contact isolation for symptomatic patients has been questioned because recent reports have highlighted the transmission of *C. difficile* by asymptomatic carriers (*4*). Considering patient room shortages in resource-limited settings and the endemicity of other pathogens, such as carbapenemase-producing Enterobacterales and coronaviruses causing COVID-19 (*7*,*8*), isolating symptomatic patients with CDI requires revaluation. Acquiring data on the secondary transmission rate of CDI is crucial and should emphasize comprehensive patient contact histories, regardless of specific points of contact.

Real-time locating system (RTLS) technology is well suited for acquiring data on secondary CDI transmission rates; the system can be leveraged to precisely quantify human-to-human interactions irrespective of the number of contacts (*9*–*11*). RTLS involves radio-frequency identification and a wireless network tracking system, which calculates the distance and duration of human-to-human interaction by analyzing the signal from a radio-frequency identification tag worn by users (*12*). Although concerns regarding privacy and cost–benefit persist, accumulating evidence supports the validity of using RTLS technology in hospital settings (*9*,*10*,*13*).

Since its inception, Yongin Severance Hospital in South Korea has been equipped with RTLS, which can provide epidemiologic data for patient contact time and distance with high sensitivity. We aimed to determine the real-world CDI transmission rate by using RTLS, focusing on the contact time required for infection transmission in susceptible patients within this hospital.

Methods

Ethics Statement

This study was approved by the Institutional Review Board of the Yonsei University Health System

Author affiliations: Hallym University Dongtan Sacred Heart Hospital, Hwasieong, South Korea (M.H. Kim); Yonsei University College of Medicine, Seoul, South Korea (J. Kim, D. Won, H. Lee); Yonsei University Yongin Severance Hospital, Yongin, South Korea (H. Ra, S. Jeong, Y.S. Park, H. Kim)

DOI: https://doi.org/10.3201/eid3005.231588

[1]These authors contributed equally to this article.

Clinical Trial Centre, and the study protocol adhered to the tenets of the Declaration of Helsinki (approval no. 9–2022–0209; approved on February 24, 2023). Because this was a retrospective study, the Institutional Review Board waived the requirement for written informed consent from the study participants.

Study Design and Participants

We conducted a retrospective cohort study involving hospitalized patients who had direct or indirect contact with index patients who had a CDI diagnosis during September–December 2021. The study concluded on July 29, 2022, when information from the last enrolled patient was acquired. CDI was diagnosed by using PCR, which detected the *C. difficile* toxin B gene, and by identifying *C. difficile* in fecal culture samples obtained from patients experiencing diarrhea (Appendix 1, https://wwwnc.cdc.gov/EID/article/30/5/23-1588-App1.pdf). Diarrhea was defined as new-onset bowel movements >3 times per day. Yongin Severance Hospital is a university-affiliated hospital that has 560 beds; 46.7% (86/184) of rooms have 4–5 beds. Patients in the same room shared toilets, except in the intensive care unit, where most patient beds were isolated, eliminating the need for shared toilets. After discharge, the rooms were cleaned with nonsporicidal disinfectants. Although patients with CDI were not placed under specific contact isolation, the hospital used enhanced standard infection control measures throughout the hospital because of the COVID-19 pandemic, which included encouraging regular handwashing with soap and water and mask use. CDI index patients were not isolated as a contact precaution during hospitalization; their baseline characteristics were recorded (Appendix 1 Table 1).

We tracked CDI contact cases by using 3 different methods. First, we investigated patients who came in direct contact with CDI index patients by using RTLS. We considered patients within a 1-meter radius of index patient to have had direct contact, regardless of the duration. Second, we collected data for patients who came in indirect contact with CDI index patients via healthcare personnel. We used RTLS to identify contact cases where patients interacted with healthcare personnel who had attended to an index patient for >24 hours. We assumed the disease could be potentially transmitted through healthcare workers' hands or through fomites, such as blood pressure cuffs. We systematically calculated contact duration for the entire hospitalization period, irrespective of the presumed contagiousness of the index patient. We adopted this approach to ensure the comprehensive inclusion of patients susceptible to transmission during the asymptomatic phase of the index patient. Third, we identified CDI cases arising from indirect contact through environmental contaminants. We enrolled patients who were hospitalized in the same rooms as index patients within 3 months after the index patient's discharge. The patients were followed up until their last outpatient visit or hospitalization. We tracked diarrhea symptoms and obtained results for *C. difficile* toxin B gene PCR and for the fecal *C. difficile* culture tests from electronic medical records.

The primary outcome was secondary CDI transmission, identified by whole-genome sequencing. We performed PCR ribotyping for all *C. difficile* isolates obtained from the patients with a CDI diagnosis. Among the designated contacts, we sequenced whole genomes of paired *C. difficile* samples from patients harboring identical ribotypes. We determined person-to-person transmission by examining the genetic relatedness of isolates to reveal consistent core genome sequence types and substantial allelic homogeneity. We excluded index patients with a history of CDI within 3 months before the study period, contact case-patients with a history of diarrhea but without laboratory tests to confirm CDI, and contact case-patients who had a short follow-up period of <7 days.

PCR Ribotyping

We performed PCR ribotyping by using the primers CD1–CD1445 (*14*,*15*). We compared PCR ribotyping patterns with those of known standard *C. difficile* strains (VPI10463, UK078, 48489ATCC9689, ATCC43598, and ATCC70057). We considered ribotype patterns with ≥1 band difference to be different ribotypes.

Whole-Genome Sequencing

We generated sequencing libraries for *C. difficile* genomic DNA by using Twist Library Preparation EF 2.0 Kit and Twist UDI Primers (Twist Bioscience, https://www.twistbioscience.com) according to the manufacturer's instructions. We extracted genomic DNA by using the chemagic 360 extraction instrument and chemagic DNA Tissue Kit (both PerkinElmer, https://www.perkinelmer.com). We assessed the quantity of DNA in the libraries by using Qubit 3.0 and the Qubit dsDNA HS Assay Kit (ThermoFisher Scientific, https://www.thermofisher.com) and assessed quality by using the 4200 TapeStation and DNA1000 ScreenTape (Agilent, https://www.agilent.com). We used the quantified final library products for cluster generation and performed next-generation

sequencing on an Illumina NovaSeq 6000 sequencer system (Illumina, https://www.illumina.com) in 300-bp paired-end format according to the Illumina paired-end sequencing protocol. We performed de novo assembly of sequences by using Unicycler version 0.4.8 (https://github.com/rrwick/Unicycler) and analyzed core genomic multilocus sequence typing by using EnteroBase (https://enterobase.warwick.ac.uk).

Among isolate pairs with the same ribotype, 2 pairs of identical core genomic sequence types had allelic differences of 9 and 13. We distinguished between secondary and nonsecondary transmission according to the distribution of allelic differences among pairs of identical ribotypes (104 [interquartile range 27–1,709] differences). The probability of genetic homogeneity was statistically significant for the same core genomic sequence types with allelic differences ≤13 (p = 0.010).

Table 1. Baseline characteristics of patients in study identifying contact time required for secondary transmission of *Clostridioides difficile* infections by using real-time locating system in South Korea*

Characteristics	All patients	Patients with subsequent CDI			Patients without subsequent CDI	p value‡
		Secondary transmission	Nonsecondary transmission	p value†		
Total no. patients	2,520	2	56	NA	2,462	NA
Mean age, y (SD)	60.4 (19.8)	81.5 (2.1)	73.4 (11.6)	<0.001	60.06 (19.80)	0.091
Sex						
M	1,343 (53.3)	2 (100.0)	31 (55.4)	>0.99	1,310 (53.2)	NA
F	1,177 (46.7)	NA	NA	NA	NA	NA
Prior hospitalization	381 (15.1)	0	18 (32.1)	>0.99	263 (14.7)	0.153
Recent antimicrobials	1,686 (66.9)	2 (100.0)	54 (96.4)	>0.99	1,630 (66.2)	0.047
Underlying conditions						
Diabetes mellitus	765 (30.4)	1 (50.0)	25 (44.6)	0.881	739 (30.0)	0.600
COPD	91 (3.6)	0	6 (10.7)	>0.99	85 (3.5)	0.926
Chronic heart failure	617 (24.5)	1 (50.0)	28 (50.0)	>0.99	588 (23.9)	0.876
Hypertension	1,131 (44.9)	1 (50.0)	36 (64.3)	0.683	1,094 (44.4)	0.521
Chronic kidney disease	341 (13.5)	0	18 (32.1)	>0.99	323 (13.1)	0.633
Malignancy	640 (25.4)	1 (50.0)	21 (37.5)	0.723	618 (25.1)	0.905
IBD	1 (0.0)	0	0	NA	1 (0.0)	NA
CVA	279 (11.1)	0	11 (19.6)	>0.99	268 (10.9)	NA
HSCT	104 (4.1)	0	8 (14.3)	>0.99	96 (3.9)	0.821
Median CCI score (IQR)	2 (0–3)	2.5 (2.25–2.75)	4 (2–6)	0.447	2 (0–4)	0.387
No. days before index patient treatment, median (IQR)	1 (0–2)	1.5 (1.25–1.75)	1 (0–2)	>0.99	1 (0–2)	NA
Laboratory tests						
Blood leukocyte count >15,000/μL	244 (11.2)	0	12 (22.2)	>0.99	232 (10.9)	0.710
Median CRP, mg/L (IQR)	3.9 (0.6–34.7)	53.3 (44–62.6)	42.9 (16.3–93.2)	0.794	4.8 (0.7–40.4)	0.209
Mean albumin, g/dL (SD)	3.05 (0.54)	3.15 (0.35)	3.10 (0.55)	0.890	2.96 (0.55)	NA
Clinical conditions						
Ileostomy	29 (1.2)	0	1 (1.8)	>0.99	28 (1.1)	NA
Enteral tube insertion	325 (12.9)	2 (100.0)	21 (37.5)	>0.99	302 (12.3)	0.201
No. contact cases§	3,620	2	124		3,494	
Group 1¶	909 (25.1)	1 (50.0)	43 (34.7)	>0.99	865 (24.7)	0.516
Room sharing#	181 (19.9)	0	11 (25.6)	>0.99	170 (19.7)	NA
Contact during diarrhea episode**	316 (34.8)	0	13 (30.2)	>0.99	303 (35.0)	NA
Group 2††	421 (11.6)	0	11 (8.9)	>0.99	410 (11.7)	NA
Group 3‡‡	2,290 (63.3)	1 (50.0)	70 (56.5)	>0.99	2,219 (63.5)	NA
Median contact time, min (IQR)	4,320 (131.5–8,640)	7,976.5 (4,044.75–11,908.25)	4,320 (133.25–10,080.0)	0.465	4,320 (132–8,640)	NA
No. deaths	162 (6.4)	0	11 (19.6)	>0.99	151 (6.1)	NA

*Values are no. (%) except as indicated. CCI, Charlson comorbidity index; CDI, *Clostridioides difficile* infection; COPD, chronic obstructive pulmonary disease; CRP, C-reactive protein; CVA, cerebrovascular accident; HSCT, hematopoietic stem cell transplantation; IBD, inflammatory bowel disease; IQR, interquartile range; NA, not applicable.
†A univariate logistic regression was used to compute p values, comparing secondary transmission with nonsecondary transmission.
‡A generalized linear mixed model was used to compute p values after adjusting for variables exhibiting statistical significance in the univariate analysis; the model was used to elucidate the odds of subsequent CDI occurrence. The odds ratios and 95% CIs for each variable are shown in Appendix 1 Table 2 (https://wwwnc.cdc.gov/EID/article/30/5/23-1588-App1.pdf).
§Because 744 patients experienced >2 episodes of contact with separate index patients, a disparity emerged between the number of contact cases and the number of contact patients.
¶Group 1 included patients who had direct contact with index patients.
#Co-hospitalization in the same bedroom with the index patient for >24 hours.
**Contact with index patient who had diarrhea.
††Group 2 included patients who had indirect contact with index patients via healthcare personnel.
‡‡Group 3 included patients who had indirect contact with index patients via the environment.

Table 2. Patients manifesting secondary transmission in study identifying contact time required for secondary transmission of *Clostridioides difficile* infections by using real-time locating system conducted in South Korea*

Patient age, y	CCI score	Reason for hospitalization	Ribotype	Contact during diarrhea episode†	Contact time, min	Contact type‡	Indwelling devices
81	3	Pneumonia	RT018	No	113	Group 1	Enteral tube, pleural effusion drainage
83	2	Pneumonia	RT018	NA	15,840	Group 3	Enteral tube

*CCI, Charlson comorbidity index; NA, not applicable; RT018, ribotype 018.
†Contact history during manifestation of diarrhea in the index patient.
‡Group 1 included patients who had direct contact with index patients. Group 3 included patients who had indirect contact with index patients via the environment.

Contact Tracing with Real-Time Locating System

The hospital used RTLS sensors designed to detect signals within a 2-meter radius in bedrooms and within a 10-meter radius in open spaces throughout the facility. Hospital staff and inpatients were required to always wear the RTLS tags. The tags emitted signals every 1–3 seconds, confirming the presence of the person in a specific room. The distance between persons was calculated through a tag-to-tag signal interaction. When 2 persons were at a particular distance from each other, the contact time between them was counted, enabling data collection for the cumulative contact time between the 2 persons.

Statistical Analysis

We used a generalized linear mixed model and a logit link function to model CDI occurrence. The fixed effects in the model encompassed various factors, including age, prior hospitalization, recent antimicrobial use, the elapsed time before treatment of the CDI index patient, comorbidities (diabetes mellitus, chronic obstructive pulmonary disease, congestive heart failure, hypertension, chronic kidney disease, malignancy, inflammatory bowel disease, cerebrovascular accident, and hematopoietic stem cell transplantation), Charlson comorbidity index scores, categorized leukocyte counts, serum levels of C-reactive protein and albumin, presence of ileostomy, insertion of enteral tube, and contact type. In addition, the model incorporated random intercepts for time and an unstructured covariance matrix. For the generalized linear mixed model, only variables demonstrating an effect on CDI occurrence were selected as fixed effects from baseline data. We conducted a univariate logistic regression to determine the influence of each variable on secondary transmission within the group that developed subsequent CDI. For analysis of categorical variables, we used frequencies and percentages for descriptions; for continuous variables, we used means and SDs. We performed statistical analyses and created graphs by using both SPSS Statistics 26.0 (IBM Corp, https://www.ibm.com) and R version 4.2.2 (The R Project for Statistical Computing, https://www.r-project.org). We conducted all statistical tests with a significance level set at 0.05.

Results

Patient Characteristics

Adherence to wearing the RTLS tags was 91.3% (interquartile range 90.5%–92.6%) during the study. We identified 4,196 contact cases for 26 index patients, of which 490 were excluded because of short follow-up periods and 86 were excluded because of a lack of laboratory results, despite a history of diarrhea. A disparity emerged between the number of contact cases and number of contact patients because 744 contact patients experienced >2 episodes of contact with separate index patients. Consequently, we defined instances of contact as contact cases and persons who experienced contact episodes as patients. Among the remaining 3,620 contact cases (comprising 2,520 patients), 2,587 (71.5%) cases were followed up for >30 days. The number of contact cases attributed to direct contact was 909/3,620 (25.1%); 2,711 contact cases resulted from indirect contact occurring either through healthcare personnel (421/3,620 [11.6%]) or through environmental exposure (2,290/3,620 [63.3%]) (Appendix 1 Figure 1). Within the subset of 909 direct contact cases, 181 (19.9%) instances involved patients who shared a bedroom with an index patient for >24 hours; 728 (80.1%) contact cases involved diverse encounters, such as during radiologic exams, rehabilitation, physiotherapy, or brief encounters occurring within the confines of the same bedroom. Furthermore, 316 (34.8%) direct contact cases were identified when the index patients exhibited symptoms of diarrhea, whereas 593 (65.2%) contact cases were identified during an index patient's asymptomatic phase (Table 1).

The mean age (±SD) of the 2,520 contact patients was 60.37 (±19.76) years; 53.3% (1,343) were men and 46.7% (1,177) women. We identified a history of hospitalization in 15.1% and recent antimicrobial use in 66.9% of all contact patients. Among contact patients, 4.1% (104) received hematopoietic stem cell transplantation, whereas 25.4% (640) had a history of malignancies. Only 1 patient with a history of inflammatory bowel disease was included in the study. All index patients underwent treatment for

CDI, which was initiated ≈1 day after identifying the infection. The median contact time was 4,320 (interquartile range 131.5–8,640) minutes. Among the 2,520 patients that had follow-up, CDI was diagnosed in 58 patients. Recent antimicrobial use was greater (96.4%) for patients with a subsequent CDI diagnosis than for those without a subsequent CDI diagnosis (66.2%; p = 0.047) (Table 1; Appendix 1 Table 2). We identified ribotypes of *C. difficile* isolates from index patients and from contact patients who had a subsequent CDI diagnosis (Appendix 1 Figure 2). Ribotype 014/016 had the highest (23.1%) prevalence, whereas ribotype 018 had a lower (8.9%) prevalence than previously described (*16*).

Identifying Secondary Transmission of *C. difficile* Infection

Of 126 contact cases involving 58 patients with a subsequent CDI diagnosis, 13 contact cases (11 patients) had the same *C. difficile* ribotype as their index patient. Two patients had secondary transmission of *C. difficile*; each was associated with a distinct index patient. One secondary transmission occurred through direct contact, whereas the other occurred via exposure to environmental sources (2 of 3,620 cases; 0.05% incidence rate). The mean age of patients with secondary transmission (81.50 ±2.12 years) was greater than that of patients with nonsecondary transmission (73.38 ±11.58 years; p<0.001) (Table 1).

The patient who had secondary *C. difficile* transmission through direct contact with an index patient did not cohabit in the same room. The contact duration was 113 minutes and occurred during the asymptomatic phase of the index patient. The patient with indirect environmental contact was hospitalized 36 days after discharge of the index patient; the contact time was 11 days (Table 2). Neither patient had a hospitalization history; however, they both had a history of recent antimicrobial use and insertion of an enteral tube. Ribotype 018 was associated with both instances of secondary transmission (Tables 1, 2). We defined the secondary transmission rate as the ratio of the cumulative number of secondary transmissions to the total number of contact cases per unit of contact time (Appendix 1 Figure 3). The rapid decrease in transmission rate after the initial surge (1 of 948 cases; 0.001% at 113 minutes), followed by a plateau was attributed to the brief contact time necessary for secondary transmission (Appendix 1 Figure 3).

Discussion

Our findings demonstrate a low contribution of patient contact to CDI transmission. However, we found that a low level of direct contact time was required for secondary transmission of CDI. In-hospital transmission rates observed in previous studies have varied according to the surveillance methods used (*17*–*19*). Most studies have focused on finding the sources of hospital-acquired CDI, which has led to analyses of only confirmed cases, and susceptible patients at risk of contracting the infection have not been extensively evaluated. A precise rate estimation can be made by using the correct choice of susceptible patients in the denominator. In this study, the transmission rate estimations were made by using RTLS. The comprehensive detection capability of RTLS in contact tracing was exemplified by the substantial percentage of contact cases identified beyond shared bedrooms (Table 1). The overall CDI transmission rate (0.05%) observed in this study was lower than that identified in a prospective study conducted at a tertiary hospital in Switzerland (*17*). That study used stringent standard precautions instead of patient isolation, and the subsequent secondary transmission was investigated among patients who had contact with CDI patients. The number of secondary transmission cases in that study, even without including cases of asymptomatic transmission, was comparable to the number in our study. Nevertheless, RTLS identified both direct and indirect contact cases, which have been previously overlooked. In addition, contact cases in our study were distinguished from contact patients; some patients had multiple episodes of contact, mirroring real-world dynamics.

The duration of person-to-person contact required for CDI transmission in our study was as brief as 113 minutes. Infection dose of *C. difficile* is known to be low in a laboratory setting, but those results have not yet been supported in vivo (*20*,*21*). This study investigated the association between contact time and secondary transmission of CDI. A low contact time required for CDI transmission might help explain the absence of differences in CDI incidence rates for genetically related and genetically distant strains, despite the use of contact precautions, as previously described (*18*). Short infection periods for multiple *C. difficile* spreaders have been reported, emphasizing that organism density is more crucial for transmitting the disease than longer contact time (*22*). Patients can spread spores, which can be taken up by susceptible patients within hours, depending on organism density. Therefore, once a patient starts showing symptoms, intervention would be considered delayed. Furthermore, multiple CDI cases identified in this study were categorized as asymptomatic transmission, which is a subject of concern (*4*,*6*,*23*). Because of

adherence to augmented standard precautions in our hospital throughout the study period and considering the role of indirect contact through environmental CDI transmission (*24*), it might be more pragmatic to adopt exhaustive standard preventive measures rather than opting for contact isolation of symptomatic patients with CDI. A comprehensive strategy should encompass additional preventive measures, such as careful excrement management and environmental decontamination.

The overall incidence of CDI in the study institution was ≈19.6 cases/10,000 patient-days in 2021, signifying a notable increase compared with 5.9 cases/10,000 patient-days reported in tertiary hospitals within South Korea during 2020–2021 (*25*). This study was conducted in an environment marked by substantial transitions from long-term care facilities, resulting in a high incidence of imported cases, which contributed to the elevated overall incidence rate. Despite the high CDI incidence in this study compared with previous research, the effect of secondary transmission via direct or indirect contact on CDI incidence was found to be low. Consequently, factors contributing to disease occurrence that are distinct from CDI patient contact warrant investigation. Previous studies have highlighted the significance of prudent antimicrobial use to diminish spontaneous sporulation of toxigenic *C. difficile* (*26*–*30*). Therefore, this precautionary measure should be prioritized, particularly in a setting where a high percentage of patients might experience dysbiosis because of immobility.

The first limitation of our study is that we could have underestimated the secondary transmission rate by not accounting for asymptomatic carriers who could potentially harbor *Clostridioides* spores. However, the optimal timing for collecting rectal swab samples to detect secondary transmission in low-risk patients remains uncertain (*31*). Therefore, the best approach for ascertaining the secondary transmission rate involves estimation of identified symptomatic patients. Second, RTLS serves as a surrogate metric for contact identification; however, RTLS performance evaluation was precluded in this study because of challenges in identifying a suitable counterpart. Nevertheless, RTLS is characterized by its high sensitivity (*32*) and proves advantageous for investigating CDIs when the mode of transmission remains incompletely elucidated (*5*,*18*). Our findings retain importance by revealing only 2 instances of secondary transmission after a comprehensive investigation. Third, this study was conducted in an environment where highly contagious strains, such as ribotype 027 and ribotype 018, were infrequently identified. Of note, both instances of secondary transmission observed in this study were linked to ribotype 018, which is well known for its multidrug resistance and transmission capabilities (*33*,*34*). We acknowledge that different study outcomes might vary according to the predominant ribotypes, emphasizing the importance of incorporating ribotyping results in outbreak investigations. Fourth, the timely identification of CDI cases by following hospital policy and immediate treatment of CDI-confirmed patients could have contributed to the low transmission incidence observed in this study. We recommend exercising caution in extrapolating our results to other environments.

In conclusion, our study showed a low incidence of secondary CDI transmission within a short period of direct contact. Thus, our findings support prioritizing the comprehensive use of standard preventive measures in healthcare facilities, including environmental decontamination, as a more viable approach to prevent *C. difficile* infection than relying on symptom-based contact isolation of patients in non-outbreak settings.

Raw data supporting the conclusions of this study are included in Appendix 2 (https://wwwnc.cdc.gov/EID/article/30/5/23-1588-App2.xlsx).

Acknowledgments

We thank the medical illustration and design team within the Medical Research Support Services for their excellent support for illustrations, all of the nursing staff as well as the physicians for their support of this project, and all of the patients who participated in this study.

This study was supported by a faculty research grant from Yonsei University College of Medicine (grant no. 6-2022-0088).

About the Author

Dr. Kim is as an assistant professor at Hallym University College of Medicine in South Korea. Her research interests focus on infection control and prevention.

References

1. Sahrmann JM, Olsen MA, Stwalley D, Yu H, Dubberke ER. Costs attributable to *Clostridioides difficile* infection based on the setting of onset. Clin Infect Dis. 2023;76:809–15. https://doi.org/10.1093/cid/ciac841
2. Lessa FC, Mu Y, Bamberg WM, Beldavs ZG, Dumyati GK, Dunn JR, et al. Burden of *Clostridium difficile* infection in the United States. N Engl J Med. 2015;372:825–34. https://doi.org/10.1056/NEJMoa1408913

3. Guh AY, Mu Y, Winston LG, Johnston H, Olson D, Farley MM, et al.; Emerging Infections Program Clostridioides difficile Infection Working Group. Trends in U.S. burden of *Clostridioides difficile* infection and outcomes. N Engl J Med. 2020;382:1320–30. https://doi.org/10.1056/NEJMoa1910215
4. Durovic A, Widmer AF, Tschudin-Sutter S. New insights into transmission of *Clostridium difficile* infection—narrative review. Clin Microbiol Infect. 2018;24:483–92. https://doi.org/10.1016/j.cmi.2018.01.027
5. Zhou Y, Zhou W, Xiao T, Chen Y, Lv T, Wang Y, et al. Comparative genomic and transmission analysis of *Clostridioides difficile* between environmental, animal, and clinical sources in China. Emerg Microbes Infect. 2021; 10:2244–55. https://doi.org/10.1080/22221751. 2021.2005453
6. Durham DP, Olsen MA, Dubberke ER, Galvani AP, Townsend JP. Quantifying transmission of *Clostridium difficile* within and outside healthcare settings. Emerg Infect Dis. 2016;22:608–16. https://doi.org/10.3201/eid2204.150455
7. Her M. Repurposing and reshaping of hospitals during the COVID-19 outbreak in South Korea. One Health. 2020;10:100137. https://doi.org/10.1016/j.onehlt.2020.100137
8. Jeong H, Hyun J, Lee YK. Epidemiological characteristics of carbapenemase-producing Enterobacteriaceae outbreaks in the Republic of Korea between 2017 and 2022. Osong Public Health Res Perspect. 2023;14:312–20. https://doi.org/10.24171/j.phrp.2023.0069
9. Patel B, Vilendrer S, Kling SMR, Brown I, Ribeira R, Eisenberg M, et al. Using a real-time locating system to evaluate the impact of telemedicine in an emergency department during COVID-19: observational study. J Med Internet Res. 2021;23:e29240. https://doi.org/10.2196/29240
10. Ho HJ, Zhang ZX, Huang Z, Aung AH, Lim W-Y, Chow A. Use of a real-time locating system for contact tracing of health care workers during the COVID-19 pandemic at an infectious disease center in Singapore: validation study. J Med Internet Res. 2020;22:e19437. https://doi.org/10.2196/19437
11. Huang Z, Guo H, Lee Y-M, Ho EC, Ang H, Chow A. Performance of digital contact tracing tools for COVID-19 response in Singapore: cross-sectional study. JMIR Mhealth Uhealth. 2020;8:e23148. https://doi.org/10.2196/23148
12. Camacho-Cogollo JE, Bonet I, Iadanza E. RFID technology in health care. In: Iadanza E, editor. Clinical engineering handbook, 2nd ed. London: Elsevier/Academic Press; 2020. p. 33–41.
13. Overmann KM, Wu DTY, Xu CT, Bindhu SS, Barrick L. Real-time locating systems to improve healthcare delivery: a systematic review. J Am Med Inform Assoc. 2021;28:1308–17. https://doi.org/10.1093/jamia/ocab026
14. O'Neill GL, Ogunsola FT, Brazier JS, Duerden BI. Modification of a PCR ribotyping method for application as a routine typing scheme for *Clostridium difficile*. Anaerobe. 1996;2:205–9. https://doi.org/10.1006/anae.1996.0028
15. Stubbs SL, Brazier JS, O'Neill GL, Duerden BI. PCR targeted to the 16S-23S rRNA gene intergenic spacer region of *Clostridium difficile* and construction of a library consisting of 116 different PCR ribotypes. J Clin Microbiol. 1999;37:461–3. https://doi.org/10.1128/JCM.37.2.461-463.1999
16. Byun J-H, Kim H, Kim JL, Kim D, Jeong SH, Shin JH, et al. A nationwide study of molecular epidemiology and antimicrobial susceptibility of *Clostridioides difficile* in South Korea. Anaerobe. 2019;60:102106. https://doi.org/10.1016/j.anaerobe.2019.102106
17. Widmer AF, Frei R, Erb S, Stranden A, Kuijper EJ, Knetsch CW, et al. Transmissibility of *Clostridium difficile* without contact isolation: results from a prospective observational study with 451 patients. Clin Infect Dis. 2017;64:393–400. https://doi.org/10.1093/cid/ciw758
18. Eyre DW, Cule ML, Wilson DJ, Griffiths D, Vaughan A, O'Connor L, et al. Diverse sources of *C. difficile* infection identified on whole-genome sequencing. N Engl J Med. 2013;369:1195–205. https://doi.org/10.1056/NEJMoa1216064
19. Barbut F, Gariazzo B, Bonné L, Lalande V, Burghoffer B, Luiuz R, et al. Clinical features of *Clostridium difficile*-associated infections and molecular characterization of strains: results of a retrospective study, 2000–2004. Infect Control Hosp Epidemiol. 2007;28:131–9. https://doi.org/10.1086/511794
20. Otter JA, French GL. Survival of nosocomial bacteria and spores on surfaces and inactivation by hydrogen peroxide vapor. J Clin Microbiol. 2009;47:205–7. https://doi.org/10.1128/JCM.02004-08
21. Humphreys PN. Testing standards for sporicides. J Hosp Infect. 2011;77:193–8. https://doi.org/10.1016/j.jhin.2010.08.011
22. Kumar N, Miyajima F, He M, Roberts P, Swale A, Ellison L, et al. Genome-based infection tracking reveals dynamics of *Clostridium difficile* transmission and disease recurrence. Clin Infect Dis. 2016;62:746–52. https://doi.org/10.1093/cid/civ1031
23. Curry SR, Muto CA, Schlackman JL, Pasculle AW, Shutt KA, Marsh JW, et al. Use of multilocus variable number of tandem repeats analysis genotyping to determine the role of asymptomatic carriers in *Clostridium difficile* transmission. Clin Infect Dis. 2013;57:1094–102. https://doi.org/10.1093/cid/cit475
24. McFarland LV, Mulligan ME, Kwok RY, Stamm WE. Nosocomial acquisition of *Clostridium difficile* infection. N Engl J Med. 1989;320:204–10. https://doi.org/10.1056/NEJM198901263200402
25. Kim S-H, Wi YM. Current strategy and perspective view for preventing *Clostridioides difficile* infection in acute care facilities. Korean J Healthc Assoc Infect Control Prev. 2021;26:70–82. https://doi.org/10.14192/kjicp.2021.26.2.70
26. Shim JK, Johnson S, Samore MH, Bliss DZ, Gerding DN. Primary symptomless colonisation by *Clostridium difficile* and decreased risk of subsequent diarrhoea. Lancet. 1998; 351:633–6. https://doi.org/10.1016/S0140-6736(97)08062-8
27. Chang JY, Antonopoulos DA, Kalra A, Tonelli A, Khalife WT, Schmidt TM, et al. Decreased diversity of the fecal microbiome in recurrent *Clostridium difficile*-associated diarrhea. J Infect Dis. 2008;197:435–8. https://doi.org/10.1086/525047
28. Johnson S. Recurrent *Clostridium difficile* infection: a review of risk factors, treatments, and outcomes. J Infect. 2009;58:403–10. https://doi.org/10.1016/j.jinf.2009.03.010
29. Starr JM, Campbell A, Renshaw E, Poxton IR, Gibson GJ. Spatio-temporal stochastic modelling of *Clostridium difficile*. J Hosp Infect. 2009;71:49–56. https://doi.org/10.1016/j.jhin.2008.09.013
30. Kyne L, Warny M, Qamar A, Kelly CP. Association between antibody response to toxin A and protection against recurrent *Clostridium difficile* diarrhoea. Lancet. 2001;357:189–93. https://doi.org/10.1016/S0140-6736(00)03592-3
31. Jazmati N, Kirpal E, Piepenbrock E, Stelzer Y, Vehreschild MJGT, Seifert H. Evaluation of the use of rectal swabs for laboratory diagnosis of *Clostridium difficile* infection. J Clin Microbiol. 2018;56:e00426-18. https://doi.org/10.1128/JCM.00426-18
32. Koenig KR, Pasupathy KS, Hellmich TR, Hawthorne HJ, Karalius VP, Sir M, et al. Measuring sensitivity and precision

of real-time location systems (RTLS): definition, protocol and demonstration for clinical relevance. J Med Syst. 2021;45:15. https://doi.org/10.1007/s10916-020-01606-6

33. Spigaglia P, Barbanti F, Dionisi AM, Mastrantonio P. *Clostridium difficile* isolates resistant to fluoroquinolones in Italy: emergence of PCR ribotype 018. J Clin Microbiol. 2010;48:2892–6. https://doi.org/10.1128/JCM.02482-09
34. Baldan R, Trovato A, Bianchini V, Biancardi A, Cichero P, Mazzotti M, et al. *Clostridium difficile* PCR ribotype 018, a successful epidemic genotype. J Clin Microbiol. 2015;53:2575–80. https://doi.org/10.1128/JCM.00533-15

Address for correspondence: Heejung Kim, Department of Laboratory Medicine, Yongin Severance Hospital, Yonsei University School of Medicine, 363 Dongbaekjukjeon-daero, Giheung-gu, Yongin-si, Gyeonggi-do 16995, South Korea; email: hjkim12@yuhs.ac

Mpox Diagnosis, Behavioral Risk Modification, and Vaccination Uptake among Gay, Bisexual, and Other Men Who Have Sex with Men, United Kingdom, 2022

Dana Ogaz, Qudsia Enayat, Jack R.G. Brown, Dawn Phillips, Ruth Wilkie, Danielle Jayes, David Reid, Gwenda Hughes, Catherine H. Mercer, John Saunders, Hamish Mohammed; UK Health Security Agency Sexual Health Liaison Group[1]

During the 2022 multicountry mpox outbreak, the United Kingdom identified cases beginning in May. UK cases increased in June, peaked in July, then rapidly declined after September 2022. Public health responses included community-supported messaging and targeted mpox vaccination among eligible gay, bisexual, and other men who have sex with men (GBMSM). Using data from an online survey of GBMSM during November–December 2022, we examined self-reported mpox diagnoses, behavioral risk modification, and mpox vaccination offer and uptake. Among 1,333 participants, only 35 (2.6%) ever tested mpox-positive, but 707 (53%) reported behavior modification to avoid mpox. Among vaccine-eligible GBMSM, uptake was 69% (95% CI 65%–72%; 601/875) and was 92% (95% CI 89%–94%; 601/655) among those offered vaccine. GBMSM self-identifying as bisexual, reporting lower educational qualifications, or identifying as unemployed were less likely to be vaccinated. Equitable offer and provision of mpox vaccine are needed to minimize the risk for future outbreaks and mpox-related health inequalities.

On July 23, 2022, the World Health Organization (WHO) declared a Public Health Emergency of International Concern for the global mpox (formerly known as monkeypox) outbreak (*1*). By late March 2023, more than 85,000 confirmed mpox cases had been reported across 110 countries (*2*). Monkeypox virus, the cause of mpox, can be transmitted through close, personal contact with an infected person, including during sex (*1*). The mpox outbreak that began in 2022 was international, predominantly transmitted through sexual networks, and disproportionately affected gay, bisexual, and other men who have sex with men (GBMSM) (*1*,*3*–*6*).

Mpox was detected in the United Kingdom in May 2022, but community transmission was estimated to have started the previous month (*3*,*5*). UK case numbers peaked in July 2022 and reached >3,500 cases across the country by the end of 2022. The UK Health Security Agency (UKHSA) enacted measures to curb rising incidence, including raising public health awareness, advising a 21-day self-isolation period for persons with an mpox diagnosis, undertaking comprehensive contact-tracing of recent close sexual contacts, and recommending a targeted vaccination campaign using the modified vaccinia Ankara vaccine (*7*). UKHSA closely worked with community-based organizations to inform public health messaging to raise awareness and reduce the risk for mpox (*8*–*10*). An expert consensus panel that included UKHSA and national and community sexual health organizations

Author affiliations: UK Health Security Agency, London, UK (D. Ogaz, Q. Enayat, D. Phillips, R. Wilkie, D. Jayes, G. Hughes, J. Saunders, H. Mohammed); The National Institute for Health and Care Research Health Protection Research Unit in Blood Borne and Sexually Transmitted Infections at University College London in partnership with the UK Health Security Agency, London, UK (D. Ogaz, J.R.G. Brown, D. Reid, G. Hughes, C.H. Mercer, J. Saunders, H. Mohammed); University College London, London, UK (D. Reid, C.H. Mercer, J. Saunders); London School of Hygiene & Tropical Medicine, London, UK (G. Hughes)

DOI: https://doi.org/10.3201/eid3005.230676

[1]Members of this group are listed at the end of this article.

estimated that 111,000 persons would be eligible for mpox vaccination in the United Kingdom, including 103,000 GBMSM and 8,000 healthcare and outreach workers (*11*). The vaccination campaign began in June 2022 and provided 70,837 first doses and 31,827 second doses by the end of May 2023 (*12*). UK case numbers rapidly subsided by the end of September 2022, and few cases were reported in 2023 (*13*).

Vaccine delivery was initially targeted to sexual health services (SHS) in London because 69% of cases through September 2022 were among residents of the city (*11*). National guidance recommended GBMSM at highest risk for mpox could be identified among persons seeking care at SHS by using similar markers of risk used to identify persons eligible for HIV preexposure prophylaxis (PrEP), irrespective of HIV status (*7*,*14*). Vaccine eligibility criteria included a history of multiple recent sexual partners, group sex, or attending sex-on-premises venues, or a diagnosis of a bacterial sexually transmitted infection (STI). Initially, first doses were offered to eligible SHS clients as a subcutaneous injection (*7*,*15*). Later, fractional dosing via intradermal administration also was pilot tested and rolled out to maximize the coverage of the available vaccine supply (*16*). Observational, real-world studies reported 78%–86% vaccine effectiveness in preventing symptomatic mpox (*17*,*18*).

In response to the UK mpox outbreak, UKHSA rapidly deployed the Reducing inequalities in Sexual Health (RiiSH)-Mpox survey during November 24–December 19, 2022. RiiSH-Mpox was designed to assess the effects of the mpox outbreak on the health, well-being, sexual behavior, and SHS use among a community sample of GBMSM in the United Kingdom. We used RiiSH-Mpox survey data to examine self-reported mpox diagnosis history, behavioral risk modification, and uptake of mpox vaccination among GBMSM in the United Kingdom.

Methods

Data Collection and Study Design

The RiiSH-Mpox survey was adapted from an established methodology used to deliver a series of cross-sectional surveys conducted during 2017 and later used during periods before and after COVID-19–related social restrictions in the United Kingdom (*19*,*20*). The RiiSH-Mpox survey included all previous questions on SHS use and sexual risk behavior but incorporated a novel module that was developed with community stakeholders and asked about mpox diagnosis, vaccination uptake, and behavioral risk modification in response to the outbreak. The UKHSA Research and Ethics Governance Group provided ethics approval for this study (reference no. R&D 524), and all methods were performed in accordance with guidelines and regulations set by that group. Online consent was obtained from all participants, and no incentive was offered to participate.

Setting and Sampling

As in previous rounds of RiiSH surveys, RiiSH-Mpox recruited participants via advertisements on social networking sites, including Facebook (https://www.facebook.com), Instagram (https://www.instagram.com), and Twitter (https://www.twitter.com), as well as on Grindr (https://www.grindr.com), a geospatial networking (dating) application. The survey was conducted during November 24–December 19, 2022.

Persons included in the analyses were ≥16 years of age, UK residents, and self-identifying as men (cisgender or transgender), transgender women, or gender-diverse persons assigned male at birth. Included persons also reported having had sex with a cisgender or transgender man or with a gender-diverse person assigned male at birth since November 2021.

Data Analysis

Mpox Testing and Diagnosis History

We calculated the percentage of persons reporting an mpox diagnosis history (i.e., positive mpox test) anytime through survey completion and used the Clopper-Pearson interval to calculate 95% CIs. As a sensitivity analysis and to quantify potentially undiagnosed infections, we calculated the percentage of persons reporting a diagnosis history, those with self-perceived mpox in absence of a positive mpox test, and those with self-reported testing history.

We used the Pearson χ^2 test to assess differences in sociodemographic, clinical, and behavioral characteristics. Because so few participants had a diagnosis history, we did not conduct regression analyses.

Mpox Vaccination Uptake

We defined vaccination uptake as receipt of ≥1 mpox vaccine doses. We assessed report of vaccine offer (i.e., "Have you been offered a vaccine for monkeypox?") among participants who reported no vaccine uptake. We calculated the percentage and 95% CI of uptake among participants offered an mpox vaccine and in all participants. We also assessed vaccine willingness for participants reporting they would likely or definitely take an mpox vaccine if offered and among participants who were not offered the vaccine.

Vaccination Uptake among Vaccine Eligible Participants

We examined uptake among participants assumed to be eligible for mpox vaccination on the basis of equivalent or proxy criteria outlined in national vaccination guidance (*14*). Using survey responses, we defined vaccine eligibility as the report of any of the following since August 2022: ≥10 physical male sex partners; meeting any physical male sex partner at a sex on premises venue, sex party, or cruising grounds (hereafter, public sex environment [PSE]); a positive STI test; or, in the past year, report of PrEP use (as a proxy for persons at higher risk for acquiring mpox) or use of recreational drugs associated with chemsex (i.e., crystal methamphetamine, mephedrone, or gamma-hydroxybutyrate/gamma-butyrolactone). As a sensitivity analysis to consider a less conservative measure of having multiple partnerships, we used a lower threshold of ≥5 physical male sex partners since August 2022, instead of ≥10, to define eligibility.

Factors Associated with Mpox Vaccination

We assessed factors associated with mpox vaccination by using the Pearson χ^2 test and binary logistic regression. We included sociodemographic variables that had a significant bivariate association with vaccination in multivariable regression models and sequentially assessed associations of clinical and behavioral characteristics with mpox vaccination. We selected age group and ethnicity a priori for inclusion in multivariable modeling. We also conducted a sensitivity analysis to examine sociodemographic factors associated with mpox vaccination among vaccine-eligible participants to assess potential uptake inequalities among that group.

We used the following sociodemographic characteristics in our analyses: age group, ethnicity, gender, sexual orientation, country of birth, nation of residence in the United Kingdom (England, Scotland, Wales, or Northern Ireland), education level, employment, household composition (living alone or not), relationship status (single or in a relationship), and report of a comfortable financial situation from the top 2 quartiles (e.g., a response of "I am comfortable" or "I am very comfortable" from the question "How would you best describe your current financial situation?"). We also used clinical characteristics in our multivariable analyses, including HIV status and uptake of ≥1 vaccine doses for hepatitis A virus (HAV), hepatitis B virus (HBV), or human papillomavirus (HPV). We defined behavioral risk modification as the report of any of the following beginning in May 2022: fewer sexual partners; reduced visits to sex on premises venues or PSE; or avoiding any sex, condomless anal sex, skin-to-skin contact, or visiting clubs or crowds. Last, we used the following sexual risk behaviors in our analyses: number and meeting place of male physical sex partners since August 2022, a positive STI test since August 2022, and report of PrEP or recreational drug use associated with chemsex during the previous year. Lookback intervals for sexual risk behaviors varied because the survey aimed to align timeframes used in prior RiiSH surveys or with timeframes from the start of the mpox outbreak in May 2022.

Because some subgroups had small participant numbers, we dichotomized some groups for analyses. Those groups included ethnicity, which we dichotomized to White and all other ethnic groups (non-White); gender, which we dichotomized to cisgender male and all other gender identity groups; and sexual orientation, which we dichotomized to gay or homosexual and bisexual, which included participants identifying as bisexual, straight, or "another way."

We collected survey data via the Snap Surveys platform (https://www.snapsurveys.com). We managed data and conducted analyses by using Stata version 15.0 (StataCorp LLC, https://www.stata.com). We considered $p<0.05$ statistically significant.

Results

Among 1,435 GBMSM that engaged with the RiiSH-Mpox survey, 93% (1,333) met eligibility criteria (Figure). Missing data were limited (<3% item nonresponse) because most survey questions were compulsory. Median age among participants was 45 (range 16–78, interquartile range [IQR] 35–55) years (Table 1; Appendix Table 1, https://wwwnc.cdc.gov/EID/aticle/30/5/23-0676-App1.pdf). Most participants self-identified as cisgender male (99%), gay or homosexual (89%), of White ethnicity (92%), residents of England (86%), and employed (81%). Nearly half (48%) of participants reported a comfortable financial situation, 63% had degree-level qualifications, and 15% were living with HIV (Appendix Tables 1, 2). Most (58%) participants were recruited from Facebook, 24% were recruited from Grindr and 15% from Twitter. Among all participants, 53% (707/1,333) reported behavioral modification to avoid getting mpox, most (72% [510/707]) of whom reported reducing the number of physical male sex partners as a prevention measure (Table 2).

Mpox Diagnosis History

Among all 1,333 participants, 35 (2.6% [95% CI 1.8%–3.6%]) reported an mpox diagnosis history (i.e., mpox test positivity) (Table 1; Appendix Table 1, Figure 1). An additional 17 participants reported self-perceived

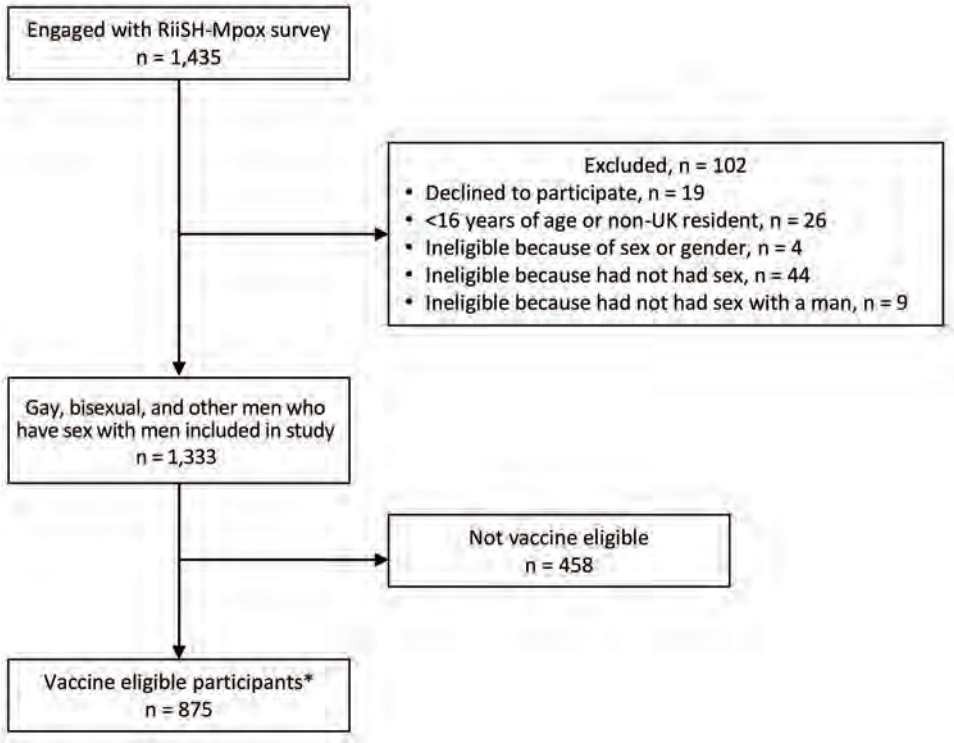

Figure. Flowchart of selection criteria in a survey of mpox diagnosis, behavioral risk modification, and vaccination uptake among gay, bisexual, and other men who have sex with men, United Kingdom, 2022. *Participants were eligible for mpox vaccination if they self-reported any of the following: meeting recent male physical sex partners at sex on premises venues, sex parties, or public sex environment (i.e., cruising grounds) since August 2022; ≥10 recent male physical sex partners since August 2022; recreational drug use associated with chemsex (e.g., crystal methamphetamine, mephedrone, or gamma-hydroxybutyrate/gamma-butyrolactone) in the past year; recent positive sexually-transmitted infection test since August 2022; or current HIV preexposure prophylaxis use since December 2021. RiiSH-Mpox, Reducing inequalities in Sexual Health Mpox survey.

mpox, including 3 who were never tested and 14 who were tested before survey completion, for a total of 52 participants (3.9% [95% CI 2.9%–5.1%]) reporting either mpox test positivity or self-perceived mpox (Appendix Table 3, Figure 1).

Compared with 1,298 participants without an mpox diagnosis history (i.e., no mpox test positivity), the 35 participants who had an mpox-positive test result were more likely to be ≥35 years of age (91% vs. 76%; p = 0.031), born outside the United Kingdom (37% vs. 16%; p = 0.001), in a comfortable financial situation (66% vs. 48%; p = 0.034), and living with HIV (37% vs. 15%; p≤0.001) (Table 1; Appendix Table 1). Participants with an mpox diagnosis via testing also reported higher levels of SHS clinic engagement in the past year, recent STI test positivity, and sexual risk behaviors such as meeting partners at sex on premises venue, sex party, or PSE (Table 1; Appendix Table 1). Persons with and without an mpox diagnosis history reported similar proportions of outbreak-related behavior modification since May 2022 (49% vs. 53%; p = 0.592); those results were similar to findings on the sensitivity analysis (Appendix Table 3).

Mpox Vaccination Uptake among All Participants

More than half (58%, 771/1,333) of participants were offered an mpox vaccination, and 692 received vaccination. Vaccination uptake was 52% (95% CI 49%–55%) for all participants and 90% (95% CI 87%–92%) for those who were offered a vaccine (Table 3; Appendix Table 2). Of participants reporting receiving vaccination, only 41% (288/692) had received a second dose. Of participants who were offered a vaccine but were not vaccinated, 48% (26/54) reported they decided not to get vaccinated (Appendix Figure 2). Among all participants who had not been offered the mpox vaccine, 75% (421/559) were willing to be vaccinated (Table 3; Appendix Figure 2).

Mpox Vaccination Uptake among Vaccine-Eligible Participants

Among GBMSM considered vaccine eligible (66%; n = 875), 75% (n = 655) were offered a vaccine and 601 received vaccination (Table 3; Appendix Table 2, Figure 2). Vaccination uptake was 69% (95% CI 65%–72%) for all eligible participants and 92% (95% CI 89%–94%) for those who were offered a vaccine. Second doses were reported by 41% (252/601) of eligible GBMSM vaccinated; 25% (220/875) of eligible participants were not offered an mpox vaccine, but 77% (168/218) indicated vaccine willingness (Appendix Figure 2). In sensitivity analyses using a lower threshold for multiple partners (≥5) to assume vaccine eligibility, we noted a similar level of vaccine uptake (Appendix Table 5).

Factors Associated with Vaccination

We found evidence of bivariate association with mpox vaccination by age group, sexual orientation, educational qualifications, employment, and financial situation. In adjusted models, bisexual men were less likely to report mpox vaccination (32% vs. 54% of gay or homosexual men; adjusted odds ratio [aOR] 0.43, 95% CI 0.29–0.62), as were participants with below

Table 1. Sociodemographic and clinical characteristics of participants in a survey of mpox diagnosis, behavioral risk modification, and vaccination uptake among gay, bisexual, and other men who have sex with men, United Kingdom, 2022*

Characteristics	RiiSH-Mpox participants, no. (%)	Mpox diagnosis history, no. (%)	No mpox diagnosis history, no. (%)	p value
Total	1,333 (100)	35 (100)	1,298 (100)	
Recruitment site				
Facebook	769 (58)	28 (80)	741 (57)	
Grindr	316 (24)	5 (14)	311 (24)	
Twitter	198 (15)	2 (6)	196 (15)	
Instagram	18 (1)	0	18 (1)	
Other	32 (2)	0	32 (2)	0.099
Sociodemographic characteristics				
Median age, y (range; IQR)	45 (16–78; 35–55)	42 (25–58; 38–47)	45 (16–78; 35–55)	
Binary age group, y				
<35	319 (24)	3 (9)	316 (24)	
≥35	1,014 (76)	32 (91)	982 (76)	0.031
Gender identity, sex at birth				
Cisgender male	1,314 (99)	30 (86)	1,193 (92)	
Other gender identity group	19 (1)	0	19 (1)	0.376
Sexual orientation				
Gay or homosexual	1,187 (89)	32 (91)	1,155 (89)	
Bisexual†	146 (11)	3 (9)	143 (11)	0.648
Ethnicity				
White	1,223 (92)	45 (87)	1,178 (92)	
Non-White	110 (8)	5 (14)	105 (8)	0.189
Country of birth				
United Kingdom	1,113 (83)	22 (63)	1,091 (84)	
Outside the United Kingdom	220 (17)	13 (37)	207 (16)	0.001
Nation of residence				
England	1,148 (86)	34 (97)	1,114 (86)	
Scotland, Wales, or Northern Ireland	185 (14)	1 (3)	184 (14)	0.056
Educational level				
Below degree level	495 (37)	7 (20)	488 (38)	
Degree level or higher	838 (63)	28 (80)	810 (62)	0.033
Clinical and behavioral characteristics				
HIV status				
Negative or unknown	1,131 (85)	22 (63)	1,109 (85)	
Living with HIV	202 (15)	13 (37)	189 (15)	0.001
STI tested in past year				
N	405 (30)	1 (3)	404 (31)	
Y	928 (70)	34 (97)	894 (69)	<0.001
Recreational drug use associated with chemsex in past year‡				
N	1,222 (92)	27 (77)	1,195 (92)	
Y	111 (8)	8 (23)	103 (8)	0.002
Number of recent male physical sexual partners since August 2022				
0	100 (8)	1 (3)	99 (8)	
1	180 (14)	2 (6)	178 (14)	
2–4	389 (29)	9 (26)	380 (29)	
5–9	280 (21)	6 (17)	274 (21)	
≥10	384 (29)	17 (49)	367 (28)	0.094
Met recent male physical sex partners in sex on premises venue, sex party, or PSE since August 2022				
N	888 (67)	17 (49)	871 (67)	
Y	445 (33)	18 (51)	427 (33)	0.022
Behavior modification to avoid getting mpox since May 2022§				
N	626 (47)	18 (51)	608 (47)	
Y	707 (53)	17 (49)	690 (53)	0.592

*Participants with self-reported mpox test positivity. Those without mpox test positivity (i.e., no diagnosis history) include those without a known positive test (n = 67) and those without a test history (n = 1,231). Percentages may not sum to 100 due to rounding. PSE, public sex environment (i.e., cruising grounds); RiiSH-Mpox, Reducing inequalities in Sexual Health Mpox survey; STI, sexually transmitted infection.
†Includes those identifying as bisexual, straight, or another orientation.
‡Includes crystal methamphetamine, mephedrone, or gamma-hydroxybutyrate/gamma-butyrolactone.
§Behavior modification includes self-report of any of the following from May 2022: fewer sexual partners, reduced visits to sex on premises venues or PSE (i.e., cruising grounds), and avoiding: all sex, condomless anal sex, skin-to-skin contact, or visiting clubs or crowds.

Table 2. Behavior modification measures and other precautions reported among participants in a survey of mpox diagnosis, behavioral risk modification, and vaccination uptake among gay, bisexual, and other men who have sex with men, United Kingdom, 2022*

Behavior modification measure†	No. participants	% All participants, n = 1,333	% Reporting any modification measures, n = 707
Self-report of ≥1 behavior modification measure since May 2022 to avoid getting mpox	707	53	100
I've chosen fewer sexual partners	510	38	72
I've reduced visits to or avoided sex-on-premises venues such as saunas and backrooms	351	26	50
I've avoided sex	206	15	29
I've reduced visits to or avoided cruising grounds	185	14	26
I've avoided nightclubs or other crowded spaces	138	10	20
I've avoided condomless sex	106	8	15
I've avoided skin-to-skin contact	69	5	10
None of the above behavior modification measures reported	626	47	NA
Other precautions reported since May 2022§			
I've asked potential sex partners if they've had a monkeypox vaccination	187	14	NA
I've washed my hands more regularly	129	10	NA
I've asked potential partners if they've had mpox symptoms	124	9	NA
I've asked sexual partners for contact details for contact tracing	22	2	NA

*Behavior modifications were derived from the question, "Since the start of the UK monkeypox outbreak in May 2022, have you done any of the following in order to avoid getting monkeypox?" NA, not applicable.
†Participants could select ≥1 behavioral modification measure listed; responses are not mutually exclusive.
§Shown for information not included as behavioral modification measures in analysis; responses are not mutually exclusive.

degree-level education qualifications (40% vs. 59% in degree-level or higher; aOR 0.50, 95% CI 0.39–0.63), and unemployed participants (37% vs. 55% of employed participants; aOR 0.59, 95% CI 0.43–0.80) (Appendix Table 2). Participants reporting relationship status as single were more likely to be vaccinated (54% vs. 50% of those in a relationship; aOR 1.27, 95% CI 1.01–1.60). We found no evidence of independent association to age, but we noted the lowest levels of vaccination among persons 16–24 years of age (30% vs. 58% among persons 45–54 years of age; aOR 0.47, 95% CI 0.25–0.87). Persons 16–24 years of age comprised only 5% of mpox vaccinated participants. After adjusting for sociodemographic characteristics, the greatest predictors of mpox vaccination were reporting a positive STI test since August 2022 (aOR 4.09, 95% CI: 2.69–6.22); having an HAV, HBV, or HPV vaccination history (aOR 5.27, 95% CI: 3.72–7.47); reporting a higher (≥10 vs. 1) number of physical sex partners since August 2022 (aOR 7.73, 95% CI 5.06–11.8); and reporting PrEP use since December 2021 (aOR 7.09, 95% CI 5.49–9.15). Among mpox vaccinated GBMSM, 87% (601/692) met proxy mpox vaccination eligibility. Participants who met mpox vaccination eligibility were 8 times more likely to have been vaccinated than those who did not meet eligibility (aOR 8.38, 95% CI 6.35–11.1).

In sensitivity analyses examining sociodemographic factors associated with mpox vaccination among vaccine-eligible participants, we found mpox vaccine uptake was less likely among bisexual than gay or homosexual men (aOR 0.49, 95% CI 0.30–0.79), participants with lower educational qualifications (aOR 0.46, 95% CI 0.34–0.63), and unemployed (aOR 0.63, 95% CI 0.42–0.95) (Appendix Tables 2, 4). Those findings were consistent with our analyses of those groups among all participants.

Discussion

In this large, online survey of GBMSM in the United Kingdom conducted shortly after the 2022 mpox outbreak began, 53% of participants reported adopting a risk modification measure, 75% of eligible participants had been mpox vaccinated, and participants offered a vaccine had very high uptake. Most (87%) participants who were vaccinated met proxy eligibility criteria. Among all 1,333 participants, vaccine uptake was associated with higher levels of sexual risk, suggesting fidelity to targeted vaccination set out by national guidelines during rapid vaccine rollout across the United Kingdom in June 2022. Demographic and behavioral characteristics among participants with mpox-positive tests broadly reflected those described in enhanced surveillance of confirmed cases undertaken by UKHSA (*11*). Among participants who tested mpox-positive, 37% were living with HIV, consistent with high mpox case reporting (*21*–*23*), and 58% vaccine uptake among that group exceeded participant estimates but was subject to small sample size.

We found UK mpox vaccine uptake was similar to levels reported in British Columbia among all (51%) and eligible (66%) transgender persons and GBMSM at sexual health clinics shortly after vaccination implementation (*24*). Although changes to sexual behavior were reported among GBMSM in the United Kingdom during COVID-19 restrictions (*19*,*20*,*25*),

limited evidence on behavioral modification in response to the 2022 mpox outbreak is available. Our findings support other evidence of behavioral modification among GBMSM during the mpox outbreak; UK surveillance data show a concurrent, but temporary, decline in lymphogranuloma venereum and *Shigella* species, infections that primarily circulate in the dense, interconnected sexual networks that are also associated with monkeypox transmission (*11*,*26*).

In our study, participants with lower educational qualifications and those without employment reported lower vaccine uptake, differences that we also found in sensitivity analyses restricted to vaccine-eligible participants. Those findings mirrored COVID-19 vaccine uptake inequalities identified in the previous RiiSH survey; during that survey period (December 2021), COVID-19 vaccination was widely accessible in the United Kingdom (*27*). We found bisexual and straight-identifying participants also were less likely to report mpox vaccination, consistent with findings in a smaller cross-sectional study exploring mpox vaccination uptake (*24*). The effects and epidemiology of mpox in bisexual and heterosexual-identifying MSM are unknown. However, a previous systematic review reported lower SHS engagement despite high sexual risk among heterosexual-identifying men who have sex with men (*28*), suggesting a need for tailored vaccination promotion efforts for those groups during mpox resurgence or endemicity, or for other STI outbreaks.

National guidance for targeting mpox vaccination recommended using markers of historical sexual risk associated with STI and HIV incidence (*29*,*30*). Most mpox vaccinated GBMSM met proxy eligibility criteria; however, 31% of those considered vaccine eligible did not report mpox vaccination, most (220/274) of whom did not receive a vaccine offer. That finding could reflect SHS access barriers because only 38% of vaccine-eligible participants who were not offered a vaccine had visited an SHS since August 2022. However, that group might have less regular engagement with SHS (*31*,*32*). Vaccine provision and service-level constraints resulting from increased mpox infection control measures and service reconfigurations that included online triage could have limited face-to-face vaccine offers and subsequent uptake (*33*,*34*).

To ensure respondent anonymity, the survey did not collect any data that would indicate the region of participant residence; vaccination offer and uptake might have been lower in regions of England that did not experience large outbreaks or where local services did not provide vaccination. Participant-level barriers to vaccination, such as low perceived mpox risk, might also have limited vaccine uptake among eligible participants, especially when mpox incidence fell sharply across the United Kingdom after the July 2022 peak.

Only 41% of mpox-vaccinated participants reported having received a second dose by the survey period, despite availability beginning in September 2022; that finding is similar to uptake reported nationally through May 2023 (*12*). Further exploration of low vaccine course completion is needed, especially because little data exist on the length of protection conferred by a single mpox vaccine dose or complete vaccination (*35*). Although rapid, first-dose vaccination was recommended for outbreak control after favorable efficacy studies (*17*), since September 2022, UKHSA and the Joint Committee on Vaccination and Immunization have recommended 2 mpox vaccine doses for eligible groups (*15*,*36*,*37*).

The RiiSH-Mpox survey was part of a series of repeat, cross-sectional surveys that use consistent

Table 3. Mpox vaccine offer and uptake among participants in a survey of mpox diagnosis, behavioral risk modification, and vaccination uptake among gay, bisexual, and other men who have sex with men, United Kingdom, 2022*

	Mpox vaccine offered and vaccinated, no. (%)				Mpox vaccination uptake, % (95% CI)	
Eligibility group	Total offered vaccine	Offered, vaccinated	Offered, not vaccinated	Not offered, not vaccinated	Among those offered vaccine†	All participants‡
Eligible, n = 875	655 (75)	601 (69)	54 (6)§	220 (25)¶	92 (89–94)	69 (65–72)
Not eligible, n = 458	116 (25)	91 (20)	25 (5)	342 (75)	78 (70–86)	20 (16–24)
All participants, n = 1,333	771 (58)	692 (52)	79 (6)#	562 (42)**	90 (88–92)	52 (49–55)

*Participants were eligible for mpox vaccination if they self-reported any of the following: meeting recent male physical sex partners at sex on premises venues, sex parties, or public sex environment (i.e., cruising grounds) since August 2022; ≥10 recent male physical sex partners since August 2022; recreational drug use associated with chemsex in the past year; recent positive STI test since August 2022; or current HIV PrEP use since December 2021. Percentages may not total 100 due to rounding. PrEP, pre-exposure prophylaxis; SHS, sexual health service, STI, sexually transmitted infection.
†Percentage (%) reporting uptake of ≥1 mpox vaccine dose among those offered an mpox vaccine [(a/(a+b)) × 100%].
‡Percentage (%) reporting uptake of ≥1 mpox vaccine dose among all groups [(a/(a+b+c)) × 100%].
§Among participants who were eligible for mpox vaccine eligible and offered a vaccine, but not vaccinated (n = 54), 28 (52%) were waiting to get vaccinated, 26 (48%) decided not to get vaccinated.
¶Among those eligible and not offered, 38% (83/220) had visited an SHS since August 2022 and 57% (126/220) had visited an SHS in the past year.
#Among all participants offered an mpox vaccine, but not vaccinated (n = 79), 42 (53%) were waiting to get vaccinated, 37 (47%) decided not to get vaccinated.
**Among participants not offered an mpox vaccine, 20% (111/562) had visited an SHS since August 2022 and 32% (182/562) had visited an SHS in the past year.

methodology and provide key behavioral insights to supplement routine national surveillance data for STIs and HIV. This study provides a timely examination of mpox in a community sample of GBMSM and contextualizes interpretation of the trends in the UK mpox outbreak. However, because of its cross-sectional design, our study is subject to key limitations. First, we cannot determine the time of vaccination in relation to most reported sexual risk behaviors comprising eligibility. Moreover, given the report of behavioral risk modification resulting from the mpox outbreak, vaccine eligibility could be underestimated, and behavior could have changed after vaccine uptake. Second, although observational studies of GBMSM in the United Kingdom and other high-income countries have reported a high mpox vaccine willingness (*38*–*40*), uptake estimates might be subject to sampling and social desirability bias and primarily representative of GBMSM using social media or Grindr. Third, information about survey impressions and click-through rates were not available, limiting insight into survey reach and engagement. Fourth, given higher educational attainment and employment, RiiSH-Mpox participants might represent a more health-literate sample relative to national probability survey estimates in GBMSM (*41*). Prior RiiSH cross-sectional samples reported near universal uptake of complete COVID-19 vaccination (*27*). Thus, although RiiSH-Mpox participants might not be representative of all GBMSM in the United Kingdom, our study sample likely represents key groups targeted for mpox vaccination and vaccination for other sexually transmissible pathogens, such as hepatitis A. Finally, small subgroup sizes across ethnicity and gender identity indicators limit assessment of inequalities in vaccine uptake.

Although high vaccine uptake in eligible GBMSM and adoption of risk modification measures likely led to the reduction of mpox incidence in the United Kingdom in July 2022, the degree of contribution of each measure is unknown. Before and during the reactive vaccine program, timely vaccine resource information distributed and amplified by community-based organizations for GBMSM and other at-risk groups likely contributed to the sharp drop in mpox incidence by the end of 2022 (*9*,*42*). Vaccination implementation across freely accessible and confidential SHS systems across the United Kingdom might have contributed to high uptake.

In conclusion, the use of key behavioral proxies guided mpox vaccination eligibility for GBMSM and aided vaccination implementation for those at risk for mpox in the United Kingdom. Future targeted vaccination rollout should consider rapid, yet equitable provision strategies and engage underserved populations via local outreach and community groups to maximize outreach and vaccine uptake and minimize mpox-related stigma (*43*). Uptake barriers for groups already described to have unmet sexual health needs, such as sexual minority groups and persons with lower social and financial capital (*19*), must be understood to minimize exacerbation of vaccine uptake inequalities. Moreover, because SHS reconfigurations continue, often led by online service expansion, effective vaccination offer and provision strategies for persons using online SHS warrant exploration. Optimizing SHS and outreach-led mpox vaccine offer, as part of a package of preventive interventions for persons with unmet needs, should be considered to maximize the benefit of each sexual health contact. To reduce the likelihood of future mpox outbreaks, given threats of resurgence, provision of first mpox vaccine doses and completion of the vaccination course among those receiving a first dose must be urgently prioritized.

This article was preprinted at https://doi.org/10.1101/2023.05.11.23289797

Additional members of the UK Health Security Agency Sexual Health Liaison Group who contributed to the review and update of the survey instrument, analysis plan, and interpretation of findings: Katy Sinka, Helen Fifer, Hannah Charles, Helen Corkin, Norah O'Brien, and Kate Folkard.

Acknowledgments

We thank all the participants who took part in this study. We acknowledge members of the National Institute for Health and Care Research Health Protection Research Unit (NIHR HPRU) in Blood Borne and Sexually Transmitted Infections (BBSTI) Steering Committee for research support in partnership with the UKHSA Health Security Agency: Caroline Sabin, John Saunders, Catherine H. Mercer, Hamish Mohammed (previously Gwenda Hughes), Greta Rait, Ruth Simmons, William Rosenberg, Tamyo Mbisa, Rosalind Raine, Sema Mandal, Rosamund Yu, Samreen Ijaz, Fabiana Lorencatto, Rachel Hunter, Kirsty Foster and Mamooma Tahir. We also thank Takudzwa Mukiwa and Will Nutland for their review of the mpox module in the RiiSH-Mpox survey that was used for this research.

About the Author

Ms. Ogaz is an epidemiologist at the UK Health Security Agency. Her work focuses on STI and HIV surveillance and prevention, program delivery, and sexual health service improvement.

References

1. Ghebreyesus TA; World Health Organization. Why the monkeypox outbreak constitutes a public health emergency of international concern. BMJ. 2022;378:o1978. https://doi.org/10.1136/bmj.o1978
2. Centers for Disease Control and Prevention. 2022–2023 mpox outbreak global map [cited 2023 Mar 24]. https://www.cdc.gov/poxvirus/mpox/response/2022/world-map.html
3. The UK Health Security Agency (UKHSA). UK strategy for mpox control, 2022 to 2023 [cited 2023 Mar 24]. https://www.gov.uk/government/publications/mpox-monkeypox-control-uk-strategy-2022-to-2023/uk-strategy-for-mpox-control-2022-to-2023
4. Iñigo Martínez J, Gil Montalbán E, Jiménez Bueno S, Martín Martínez F, Nieto Juliá A, Sánchez Díaz J, et al. Monkeypox outbreak predominantly affecting men who have sex with men, Madrid, Spain, 26 April to 16 June 2022. Euro Surveill. 2022;27:2200471. https://doi.org/10.2807/1560-7917.ES.2022.27.27.2200471
5. Vivancos R, Anderson C, Blomquist P, Balasegaram S, Bell A, Bishop L, et al.; UKHSA Monkeypox Incident Management team; Monkeypox Incident Management Team. Community transmission of monkeypox in the United Kingdom, April to May 2022. Euro Surveill. 2022;27:2200422. https://doi.org/10.2807/1560-7917.ES.2022.27.22.2200422
6. Allan-Blitz L-T, Gandhi M, Adamson P, Park I, Bolan G, Klausner JD. A position statement on mpox as a sexually transmitted disease. Clin Infect Dis. 2023;76:1508–12. https://doi.org/10.1093/cid/ciac960
7. The UK Health Security Agency. Mpox (monkeypox) outbreak vaccination strategy [cited 2023 Mar 24]. https://www.gov.uk/guidance/monkeypox-outbreak-vaccination-strategy
8. The UK Health Security Agency. Mpox and sexual health: outreach and engagement fund [cited 2023 Apr 24]. https://www.gov.uk/government/publications/mpox-and-sexual-health-outreach-and-engagement-fund
9. Terrence Higgins Trust. Mpox (monkeypox) in the UK [cited 2023 Apr 24]. https://www.tht.org.uk/hiv-and-sexual-health/sexual-health/mpox-monkeypox-uk
10. The Love Tank. The love tank [cited 2023 Apr 24]. http://thelovetank.info
11. The UK Health Security Agency (UKHSA). Investigation into monkeypox outbreak in England: technical briefing 8 [cited 2023 Mar 24]. https://www.gov.uk/government/publications/monkeypox-outbreak-technical-briefings/investigation-into-monkeypox-outbreak-in-england-technical-briefing-8
12. National Health Service England. Vaccinations for mpox: MVA vaccinations 4 May 2023 [cited 2023 May 10]. https://www.england.nhs.uk/statistics/statistical-work-areas/vaccinations-for-mpox
13. The UK Health Security Agency. Mpox (monkeypox) outbreak: epidemiological overview, 4 May 2023. [cited 2023 May 10]. https://www.gov.uk/government/publications/monkeypox-outbreak-epidemiological-overview
14. The UK Health Security Agency. Smallpox and monkeypox: the green book, chapter 29 [cited 2023 Feb 15]. https://assets.publishing.service.gov.uk/government/uploads/system/uploads/attachment_data/file/1106454/Green-Book-chapter-29_Smallpox-and-monkeypox_26September2022.pdf
15. The UK Health Security Agency. People still eligible for mpox vaccine urged to come forward [cited 2023 Mar 24]. https://www.gov.uk/government/news/people-still-eligible-for-mpox-vaccine-urged-to-come-forward
16. The UK Health Security Agency. Monkeypox vaccines to be piloted in smaller but equally effective doses [cited 2023 May 10]. https://www.gov.uk/government/news/monkeypox-vaccines-to-be-piloted-in-smaller-but-equally-effective-doses
17. Bertran M, Andrews N, Davison C, Dugbazah B, Boateng J, Lunt R, et al. Effectiveness of one dose of MVA-BN smallpox vaccine against mpox in England using the case-coverage method: an observational study. Lancet Infect Dis. 2023;12:828–35. https://doi.org/10.1016/S1473-3099(23)00057-9
18. Wolff Sagy Y, Zucker R, Hammerman A, Markovits H, Arieh NG, Abu Ahmad W, et al. Real-world effectiveness of a single dose of mpox vaccine in males. Nat Med. 2023;29:748–52. https://doi.org/10.1038/s41591-023-02229-3
19. Brown JR, Reid D, Howarth AR, Mohammed H, Saunders J, Pulford CV, et al. Changes in STI and HIV testing and testing need among men who have sex with men during the UK's COVID-19 pandemic response. Sex Transm Infect. 2022; 99:226–38. https://doi.org/10.1136/sextrans-2022-055429
20. Howarth AR, Saunders J, Reid D, Kelly I, Wayal S, Weatherburn P, et al. 'Stay at home …': exploring the impact of the COVID-19 public health response on sexual behaviour and health service use among men who have sex with men: findings from a large online survey in the UK. Sex Transm Infect. 2022;98:346–52. https://doi.org/10.1136/sextrans-2021-055039
21. Curran KG, Eberly K, Russell OO, Snyder RE, Phillips EK, Tang EC, et al.; Monkeypox, HIV, and STI Team. HIV and sexually transmitted infections among persons with monkeypox—eight U.S. jurisdictions, May 17–July 22, 2022. MMWR Morb Mortal Wkly Rep. 2022;71:1141–7. https://doi.org/10.15585/mmwr.mm7136a1
22. Tarín-Vicente EJ, Alemany A, Agud-Dios M, Ubals M, Suñer C, Antón A, et al. Clinical presentation and virological assessment of confirmed human monkeypox virus cases in Spain: a prospective observational cohort study. Lancet. 2022;400:661–9. https://doi.org/10.1016/S0140-6736(22)01436-2
23. O'Shea J, Daskalakis D, Brooks JT. The emergence of mpox as an HIV-related opportunistic infection. Lancet. 2023;401:1264. https://doi.org/10.1016/S0140-6736(23)00395-1
24. Gilbert M, Ablona A, Chang HJ, Grennan T, Irvine MA, Sarai Racey C, et al. Uptake of mpox vaccination among transgender people and gay, bisexual and other men who have sex with men among sexually-transmitted infection clinic clients in Vancouver, British Columbia. Vaccine. 2023; 41:2485–94. https://doi.org/10.1016/j.vaccine.2023.02.075
25. Nadarzynski T, Nutland W, Samba P, Bayley J, Witzel TC. The impact of first UK-wide lockdown (March–June 2020) on sexual behaviors in men and gender diverse people who have sex with men during the COVID-19 pandemic: a cross-sectional survey. Arch Sex Behav. 2023;52:617–27. https://doi.org/10.1007/s10508-022-02458-6
26. Thorley K, Charles H, Greig DR, Prochazka M, Mason LCE, Baker KS, et al. Emergence of extensively drug-resistant and multidrug-resistant *Shigella flexneri* serotype 2a associated with sexual transmission among gay, bisexual, and other men who have sex with men, in England: a descriptive epidemiological study. Lancet Infect Dis. 2023;23:22–6. https://doi.org/10.1016/S1473-3099(22)00807-6
27. Ogaz D, Allen H, Reid D, Brown JRG, Howarth AR, Pulford CV, et al. COVID-19 infection and vaccination uptake in men and gender-diverse people who have sex with men in the UK: analyses of a large, online community cross-sectional survey (RiiSH-COVID) undertaken

November–December 2021. BMC Public Health. 2023;23:829. https://doi.org/10.1186/s12889-023-15779-5
28. Curtis T, Bennett K, Mcdonagh L, Field N, Mercer C. P532 The sexual behaviour and health of heterosexual-identifying men who have sex with men: a systematic review. Sexually Transmitted Infections. 2019;95:A242-A. https://doi.org/10.1136/sextrans-2019-sti.610
29. Desai S, Burns F, Schembri G, Williams D, Sullivan A, McOwan A, et al. Sexual behaviours and sexually transmitted infection outcomes in a cohort of HIV-negative men who have sex with men attending sexual health clinics in England. Int J STD AIDS. 2018;29:1407–16. https://doi.org/10.1177/0956462418789333
30. Mitchell HD, Desai S, Mohammed H, Ong KJ, Furegato M, Hall V, et al. Preparing for PrEP: estimating the size of the population eligible for HIV pre-exposure prophylaxis among men who have sex with men in England. Sex Transm Infect. 2019;95:484–7. https://doi.org/10.1136/sextrans-2019-054009
31. O'Halloran C, Owen G, Croxford S, Sims LB, Gill ON, Nutland W, et al. Current experiences of accessing and using HIV pre-exposure prophylaxis (PrEP) in the United Kingdom: a cross-sectional online survey, May to July 2019. Euro Surveill. 2019;24:1900693. https://doi.org/10.2807/1560-7917.ES.2019.24.48.1900693
32. Ogaz D, Logan L, Curtis TJ, McDonagh L, Guerra L, Bradshaw D, et al. PrEP use and unmet PrEP-need among men who have sex with men in London prior to the implementation of a national PrEP programme, a cross-sectional study from June to August 2019. BMC Public Health. 2022;22:1105. https://doi.org/10.1186/s12889-022-13425-0
33. Wise J. Monkeypox: UK to run out of vaccine doses by next week. BMJ. 2022;378:o2053. https://doi.org/10.1136/bmj.o2053
34. Heskin J, Dickinson M, Brown N, Girometti N, Feeney M, Hardie J, et al. Rapid reconfiguration of sexual health services in response to UK autochthonous transmission of mpox (monkeypox). Sex Transm Infect. 2023;99:81–4.
35. Jamard S, Handala L, Faussat C, Vincent N, Stefic K, Gaudy-Graffin C, et al. Resurgence of symptomatic Mpox among vaccinated patients: first clues from a new-onset local cluster. Infect Dis Now. 2023;53:104714. https://doi.org/10.1016/j.idnow.2023.104714
36. Department of Health and Social Care. JCVI statement on vaccine dose prioritisation in response to the monkeypox outbreak [cited 2023 Apr 1]. https://www.gov.uk/government/publications/monkeypox-outbreak-jcvi-statement-on-vaccine-dose-prioritisation-september-2022/jcvi-statement-on-vaccine-dose-prioritisation-in-response-to-the-monkeypox-outbreak#updated-advice-september-2022
37. Department of Health and Social Care. JCVI statement on mpox vaccination as a routine programme [cited 2023 Nov 11]. https://www.gov.uk/government/publications/mpox-vaccination-programme-jcvi-advice-10-november/jcvi-statement-on-mpox-vaccination-as-a-routine-programme
38. Paparini S, Whitacre R, Smuk M, Thornhill J, Mwendera C, Strachan S, et al. Public understanding and awareness of and response to monkeypox virus outbreak: A cross-sectional survey of the most affected communities in the United Kingdom during the 2022 public health emergency. HIV Med. 2023;24:544–57. https://doi.org/10.1111/hiv.13430
39. Dukers-Muijrers NHTM, Evers Y, Widdershoven V, Davidovich U, Adam PCG, Op de Coul ELM, et al. Mpox vaccination willingness, determinants, and communication needs in gay, bisexual, and other men who have sex with men, in the context of limited vaccine availability in the Netherlands (Dutch Mpox-survey). Front Public Health. 2023;10:1058807. https://doi.org/10.3389/fpubh.2022.1058807
40. MacGibbon J, Cornelisse V, Smith AKJ, Broady TR, Hammoud MA, Bavinton BR, et al. Mpox (monkeypox) knowledge, concern, willingness to change behaviour, and seek vaccination: results of a national cross-sectional survey. Sex Health. 2023;20:403–10. https://doi.org/10.1071/SH23047
41. Mercer CH, Prah P, Field N, Tanton C, Macdowall W, Clifton S, et al. The health and well-being of men who have sex with men (MSM) in Britain: evidence from the third National Survey of Sexual Attitudes and Lifestyles (Natsal-3). BMC Public Health. 2016;16:525. https://doi.org/10.1186/s12889-016-3149-z
42. Queer Health. Everything we know about MPOX (monkeypox) so far [cited 2023 Apr 20]. https://www.queerhealth.info/projects/monkeypox
43. Logie CH. What can we learn from HIV, COVID-19 and mpox stigma to guide stigma-informed pandemic preparedness? J Int AIDS Soc. 2022;25:e26042. https://doi.org/10.1002/jia2.26042

Address for correspondence: Dana Ogaz, UK Health Security Agency, Blood Safety, Hepatitis, Sexually Transmitted Infections (STIs) and HIV Division, 61 Colindale Ave, London NW9 5EQ, UK; email: dana.ogaz@ukhsa.gov.uk

Analysis of Suspected Measles Cases with Discrepant Measles-Specific IgM and rRT-PCR Test Results, Japan

Yumani Kuba,[1] Minoru Nidaira, Noriyuki Maeshiro, Katsuhiro Komase, Hajime Kamiya, Hisako Kyan

We investigated clinically suspected measles cases that had discrepant real-time reverse transcription PCR (rRT-PCR) and measles-specific IgM test results to determine diagnoses. We performed rRT-PCR and measles-specific IgM testing on samples from 541 suspected measles cases. Of the 24 IgM-positive and rRT-PCR–negative cases, 20 were among children who received a measles-containing vaccine within the previous 6 months; most had low IgG relative avidity indexes (RAIs). The other 4 cases were among adults who had an unknown previous measles history, unknown vaccination status, and high RAIs. We detected viral nucleic acid for viruses other than measles in 15 (62.5%) of the 24 cases with discrepant rRT-PCR and IgM test results. Measles vaccination, measles history, and contact history should be considered in suspected measles cases with discrepant rRT-PCR and IgM test results. If in doubt, measles IgG avidity and PCR testing for other febrile exanthematous viruses can help confirm or refute the diagnosis.

Measles is a highly contagious febrile exanthematous disease caused by the measles virus. The measles virus spreads via airborne and droplet transmission and can cause severe complications, such as pneumonia, acute encephalitis, and sometimes death (*1*). Vaccination with 2 doses of measles-containing vaccine (MCV) is the best way to protect against measles virus infection and achieving and maintaining a high level of immunity in a population can prevent the spread of the virus (*2*).

In March 2015, the World Health Organization Western Pacific Regional Office verified Japan as a country having achieved measles elimination (*3*). However, although measles frequency has decreased since the achievement of elimination (*4*), outbreaks initiated by measles-susceptible persons traveling to or from measles-endemic countries still occur (*5*–*7*). Therefore, enhanced measles surveillance has been ongoing in Japan since achieving elimination status.

Samples from clinically suspected measles cases are required to undergo laboratory testing. Although ELISA detection of specific measles virus IgM in serum is the standard diagnostic method for measles (*8*), detection of measles virus RNA in clinical specimens via real-time reverse transcription PCR (rRT-PCR) is considered the most reliable diagnostic test during the first few days after rash onset (*9*). In Japan, recommendations call for taking 3 specimens (throat swab, and blood and urine samples) from patients with clinically suspected measles and performing rRT-PCR testing to detect measles viral RNA in addition to measles-specific IgM testing (*10*). Samples collected from 3 days before the onset of the fever or rash symptoms to 1 week after the onset of the rash are appropriate for rRT-PCR testing (*10*).

In Okinawa Prefecture, Japan, no confirmed measles case had been reported since 2014, then a prefecture-wide measles outbreak occurred during March–May 2018 (*7*). Samples were collected from all persons suspected of having measles and were subjected rRT-PCR and IgM testing at the Okinawa Prefectural Institute of Environment and Health (OPIEH). For most cases, laboratory testing confirmed the diagnosis, but for some cases, rRT-PCR and IgM test results were inconsistent, IgM-positive and rRT-PCR–negative results. Because the public health response

Author affiliations: Okinawa Prefectural Institute of Health and Environment, Okinawa, Japan (Y. Kuba, M. Nidaira, N. Maeshiro, H. Kyan); National Institute of Infectious Diseases, Tokyo, Japan (K. Komase, H. Kamiya)

DOI: https://doi.org/10.3201/eid3005.231757

[1]Current affiliation: Center for Emergency Preparedness and Response, National Institute of Infectious Diseases, Tokyo, Japan

differs depending on whether measles is confirmed, we conducted additional laboratory testing in conjunction with collecting additional patient epidemiologic information to make an accurate diagnosis of measles in cases with discrepant IgM and rRT-PCR results.

Material and Methods

All specimens collected from persons with suspected measles in Okinawa during the 2018 outbreak underwent rRT-PCR testing to confirm the diagnosis. IgM testing was also performed for all cases with serum samples. If the specimen collection period was appropriate, the rRT-PCR–positive result was defined as a confirmed measles case regardless of the measles-specific IgM test result. An rRT-PCR–negative and IgM-negative or IgM-equivocal result was also defined as a non–measles case. For cases with rRT-PCR–negative and IgM-positive results, we could not determine a diagnosis because of the inconsistency of the 2 test results. For those cases, we collected demographic information, including vaccination and exposure histories, to evaluate the test discrepancies. Furthermore, we conducted measles IgG avidity testing by using serum samples and an rRT-PCR or conventional PCR by using throat swab, serum, and urine samples to detect other viruses that cause fever and exanthemata. We chose target viruses that cause febrile exanthematous illnesses and can cause cross-reactions with the measles-specific IgM tests on the basis of reports from previous studies (*11*). Target viruses included rubella virus, human herpesvirus 6 (HHV-6), human herpesvirus 7 (HHV-7), parvovirus B19 (B19), Epstein-Barr virus (EBV), cytomegalovirus (CMV), human parechovirus (HPeV), enterovirus, and adenovirus. This study was approved by the ethics committee of the Okinawa Prefectural Institute of Health and Environment (approval no. 694-2).

Data Collection

Under the Infectious Disease Control Law in Japan (*12*), all 6 public health centers in Okinawa Prefecture are required to collect information on suspected measles cases, including demographic characteristics, symptoms, onset date, vaccination history, and outcomes. Those data were sent to the OPIEH and used for the analysis.

Specimen Collection and Pretreatment

Physicians collected throat swab, whole blood, and urine samples from persons with suspected measles and local public health center staff delivered samples to the OPIEH under refrigerated conditions. OPIEH performed measles-specific rRT-PCR testing by extracting viral nucleic acid from 140 μL of each specimen by using the QIAmp Viral RNA Mini Kit (QIAGEN, https://www.qiagen.com). Staff isolated serum from blood and tested serum for measles-specific IgM and IgG and by using IgG avidity tests.

Measles-Specific rRT-PCR

We performed rRT-PCR as reported previously (*7*). We used MVN1139F (5′-TGGCATCTGAACTCGGTATCAC-3′) and MVN1213R (5′-TGTCCTCAGTAGTATGCATTGCAA-3′) primers and an MVNP1163P probe (5′-FAM-CCGAGGATGCAAGGCTTGTTTCAGA-TAMRA-3′) targeting the nucleocapsid (N) gene of measles virus (*13*).

Measles-Specific IgM

We tested serum samples for measles-specific IgM by using the Measles IgM-EIA (Denka Seiken, Ltd., https://denka-seiken.com), an IgM capture assay. We interpreted test results in accordance with the manufacturer's definition: positive, >1.2 relative unit (RU); equivocal, 0.8–1.2 RU; and negative, <0.8 RU.

Measles-Specific IgG and IgG Avidity Tests

We used the Anti-Measles Virus ELISA (IgG) (EUROIMMUN, https://www.euroimmun.com) to detect measles-specific IgG. We interpreted results in accordance with the manufacturer's definitions: positive, ≥275 IU/L; borderline, ≥200 to <275 IU/L; and negative, <200 IU/L.

We measured measles-specific IgG avidity by using the Anti-Measles Virus IgG Avidity ELISA Kit (EUROIMMUN). We calculated the relative avidity index (RAI) for each sample according to the manufacturer's instructions: RAI <40% indicated low avidity antibodies, RAI 40%–60% equivocal, and RAI >60% indicated high avidity antibodies. IgG avidity test results can help distinguish recent primary infection, characterized by a low RAI, from past infection, characterized by a high RAI (*14*,*15*).

Febrile Exanthematous Virus Detection

For rRT-PCR–negative but IgM-positive samples, we extracted viral nucleic acid and used PCR and rRT-PCR to test for 9 different viruses: rubella virus, HHV-6, HHV-7, B19, EBV, CMV, HPeV, enterovirus, and adenovirus (*16*–*24*). Those viruses are known to cause febrile exanthemata and to cross-react with measles-specific IgM (*11*). Previous reports showing that the QIAmp VIral RNA Mini Kit (QIAGEN) effectively isolates viral DNA (*25*,*26*). Thus, we used that kit to extract viral nucleic acid for detecting DNA

and RNA viruses using various primers and probes (Appendix Table 1, https://wwwnc.cdc.gov/EID/article/30/5/23-1757-App1.pdf). We used Ex Taq DNA Polymerase (TaKaRa Bio, Inc., http://www.takara-bio.com) for PCR testing to detect EBV and CMV under the following conditions: 10 minutes at 95°C, followed by 10 cycles for 30 seconds at 95°C, 30 seconds at 70–61°C with a 1°C decrease in temperature per cycle, and 1 minute at 72°C, followed by 35 cycles for 30 seconds at 95°C, 30 seconds at 60°C, and 30 seconds at 60°C. Finally, we performed an additional extension step for 5 minutes at 72°C. We performed the PCR test to detect adenovirus under the following conditions: 3 min at 94°C, followed by 40 cycles for 30 seconds at 94°C, 60 seconds at 50°C, 2 minutes at 72°C, and 5 minutes at 72°C. We performed the rRT-PCR test by using 4 × TaqMan Fast Virus 1-step Master Mix (Thermo Fisher Scientific, https://www.thermofisher.com) under the following conditions: 5 minutes at 50°C, 20 seconds at 95°C, followed by 40 cycles of 15 seconds at 95°C and 1 minute at 60°C. We validated the sensitivity of the test by confirming that serially diluted virus-positive control RNA or DNA was detectable up to ≈5–50 copies per reaction. We included a negative control (no viral genome) and a positive control (viral RNA or DNA) in each test.

Results

We conducted rRT-PCR testing on samples from 578 persons with suspected measles, of which samples from 541 (93.6%) persons also underwent serologic testing (Figure 1). Of those 541 suspected cases, 93 (17.2%) were diagnosed as measles on the basis of rRT-PCR using specimens collected within 7 days of symptom onset. Among the other 448 (82.8%) specimens, 424 were collected during the appropriate period and were classified as non–measles cases on the basis of rRT-PCR and IgM test results. However, 24 of the 448 rRT-PCR–negative cases tested positive for measles-specific IgM, resulting in discrepant rRT-PCR and IgM test results (Figure 1). For those 24 cases, we collected vaccination history and epidemiologic information, such as history of contact with confirmed cases or viral transmission to others, to support the diagnosis. Furthermore, we performed additional measles IgG, IgG avidity, and detection of other febrile exanthematous viruses to support the diagnoses.

We collected characteristics of the 24 patients with discrepant laboratory test results (Table 1). Of those patients, 19 (79.2%) were infants <1 year of age, 1 (4.2%) was child 4 years of age, and 4 (16.7%) were adults >20 years of age. All 20 children had a history

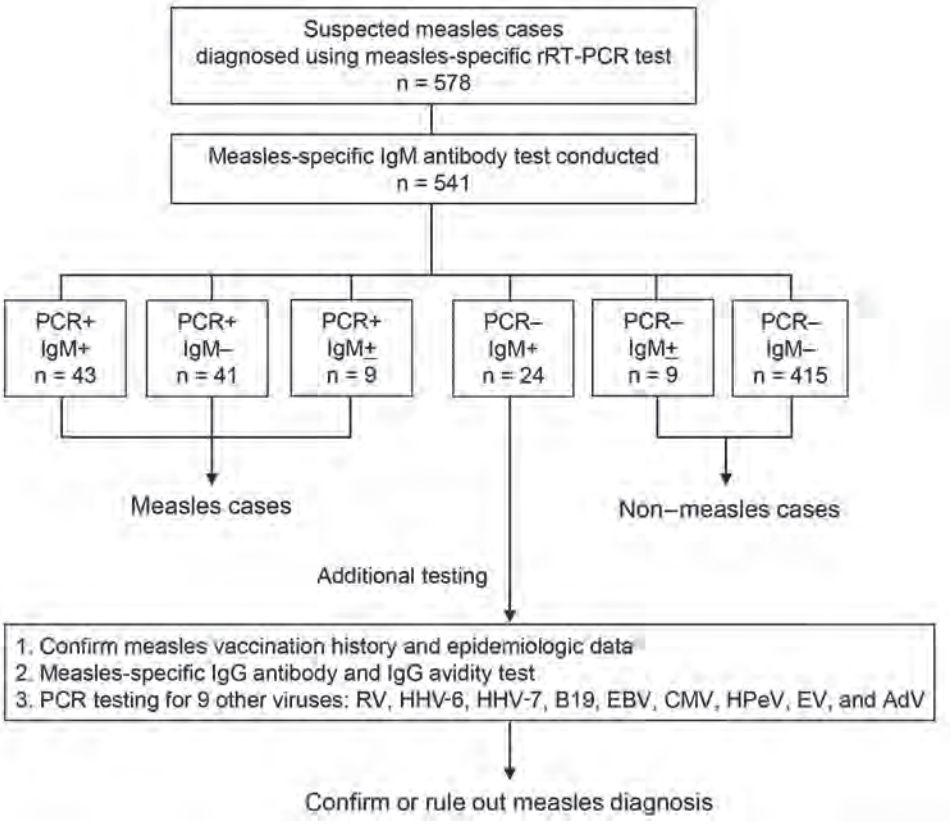

Figure 1. Flow diagram for analysis of suspected measles cases with discrepant measles-specific IgM and rRT-PCR test results, Japan. AdV, adenovirus; B19, parvovirus B19; CMV, cytomegalovirus; EBV, Epstein-Barr virus; EV, enterovirus; HHV-6, human herpesvirus 6; HHV-7, human herpesvirus 7; HPeV, human parechovirus; rRT-PCR, real-time reverse transcription PCR; RV, rubella virus; + positive, –, negative; ±, equivocal.

of receiving a dose of MCV within 6 months before specimen collection, and 17 (85%) were vaccinated within 60 days before specimen collection. The vaccination histories of the 4 adult patients were unknown. Of note, 12 infants 6–11 months of age received MCV because the Okinawa prefectural government made infants in that age range eligible for MCV vaccination as an emergency response to measles outbreak (*7*). None of the patients with inconsistent test results had epidemiologic links to laboratory-confirmed measles cases. Moreover, we observed no secondary measles cases associated with those cases. Specimens were collected within 10 days after the fever onset, and the median measles-specific IgM result was 2.32 (range 1.23–6.83) RU (Table 2).

We measured measles-specific IgG titer and conducted measles IgG avidity testing on samples from the 24 persons with measles-specific IgM-positive and rRT-PCR–negative results. We used results from those tests to distinguish between a recent primary infection and previous contact with either wild-type measles virus or vaccination as the cause of positive measles-specific IgM results. Among the 20 children, 16 had positive measles-specific IgG results (range 396.7 to >5,000 IU/L). The 4 (cases 1, 2, 5, and 9) children who had negative measles-specific IgG results had their first MCV vaccination within 2 weeks before specimen collection (Table 2). Although all 4 adult cases had positive measles-specific IgG results, a 45-year-old patient (case 24) had a relatively low IgG titer (518.7 IU/L) compared with the other 3 adults (≥4,000 IU/L) who were all in their 20s (Table 2).

Among the 20 children, 17 had a low RAI, and 3 children (cases 18–20) had equivocal or high RAIs. The median interval from vaccination to specimen collection was 25 (range 4–136) days. The RAIs of the 20 children who had received 1 dose of MCV vaccine correlated with the number of days since vaccination ($R^2 = 0.6877$) and tended to increase over time after vaccination (Appendix Figure 1). All 4 adult cases had high RAIs.

We detected viral nucleic acid other than measles virus in 15 cases, 13 in children and 2 in adults. Viruses detected from the children's samples were HHV-6 (n = 8), CMV (n = 7), HPeV (n = 3), and EBV (n = 1). Among the adults, HHV-7 was identified in throat swab samples, and B19 was identified in a throat swab and serum sample. Multiple pathogens were detected in samples from 4 children and 1 adult. We noted no difference in the distribution of measles-specific IgM values between cases with and without viruses other than the measles virus detected (p = 0.318 by Mann–Whitney U test) (Figure 2).

Table 1. Characteristics of 24 suspected measles cases with discrepant measles-specific IgM and rRT-PCR test results, Japan*

Characteristics	Value
Sex	
M	13 (54.2)
F	11 (45.8)
Age	
6–11 mo	12 (50.0)
1 y	7 (29.2)
4 y	1 (4.2)
>19 y	4 (16.7)
Fever, temperature ≥37.5°C†	20 (83.3)
Rash	23 (95.8)
No. doses of measles vaccine‡	
1	20 (83.3)
2	0 (0)
Unknown§	4 (16.7)
Median time from vaccination to specimen collection, d (range)	25 (4–136)
Time from illness onset to specimen collection, d	
Median (range)	3 (0–10)
<4	14 (58.3)
≥4	10 (41.7)
No epidemiologic link to confirmed measles case	24 (100)

*Values are no. (%) except as indicated. rRT-PCR, real-time reverse transcription PCR.
†The other 4 cases also had reported fever, but details of body temperature were unknown.
‡In Japan, the measles-rubella vaccine is used for routine vaccination and has the following schedule: first dose at 1 year of age, second dose at 5–7 years of age. During the 2018 measles outbreak in Okinawa, Japan, 12 infants 6–11 months of age were vaccinated as part of the outbreak response before routine vaccination.
§Four adult cases had no details of vaccination history. Among those cases, 1 patient recalled receiving 2 doses of the measles vaccine but did not have a vaccination record.

Discussion

Even after the declaration of measles elimination in 2015, measles outbreaks initiated by imported measles cases have occurred in Japan (*5*–*7*). Thus, accurate diagnosis of measles and continuous surveillance are required to maintain measles elimination status. In Japan, both the rRT-PCR and ELISA measles-specific IgM tests are recommended to confirm measles (*27*). Although rRT-PCR is the most reliable test to diagnose measles, its optimal time for specimen collection is limited to within 7 days after the symptom onset. Furthermore, measles-like symptoms can be caused by other viruses, such as rubella virus, B19, HHV-6, enterovirus, adenovirus, dengue fever, coxsackievirus, and several bacterial and rickettsia diseases (*11*,*28*). Consequently, unless a patient has had close contact with a confirmed measles case or measles is prevalent in the community, physicians might find it difficult to suspect measles only on the basis of symptoms and specimen collection at the optimal period could easily be missed. Therefore, a measles-specific ELISA IgM test is required to complement the short window for accurate diagnosis by rRT-PCR. The ELISA IgM test has a longer appropriate specimen

collection period and is the reference standard for confirmation and surveillance of measles worldwide (*8*).

Results of rRT-PCR and ELISA measles-specific IgM usually agree, but diagnosis can be difficult for

Table 2. Characteristics and laboratory results for 24 suspected measles cases with discrepant measles-specific IgM and rRT-PCR test results, Japan*

Case no.	Age/ sex	No. measles vaccine doses	Fever, °C	Rash	Time to specimen collection, d		IgM/ IgG†	% RAI, avidity‡	Other febrile exanthematous viruses detected on PCR			Results§	Measles virus infection
					After vaccine	After fever onset			Throat swab	Serum	Urine		
1	6 mo/M	1	39.5	Y	4	3	1.37/ND	ND, L	HHV-6	HHV-6	ND	CX or MCV	N
2	1 y/F	1	40.0	Y	6	0	1.56/ND	ND, L	CMV	ND	ND	CX or MCV	N
3	1 y/M	1	40.0	Y	18	2	4.71/ 984.9	16.6, L	HHV-6	HHV-6	ND	MCV	N
4	4 y/F	1	+	N	26	1	1.78/ 2,286	35.9, L	EBV, HHV-6, CMV	ND	CMV	MCV	N
5	10 mo/M	1	37.9	Y	11	1	1.74/ 149.2	39.6, L	CMV	ND	CMV	CX or MCV	N
6	9 mo/M	1	38.0	Y	16	0	3.96/ 1,200	21.7, L	HHV-6, CMV	ND	ND	MCV	N
7	11 mo/F	1	Y	Y	21	1	6.83/ 1,242	24.6, L	CMV	ND	CMV	MCV	N
8	6 mo/M	1	38.7	Y	16	0	5.54/ 1,224	15.6, L	CMV	HHV-6, CMV	HPeV, CMV	MCV	N
9	7 mo/F	1	39.0	Y	12	2	2.74/ 14.4	17.3, L	ND	ND	ND	MCV	N
10	9 mo/M	1	38.3	Y	24	0	2.53/ 1,037	14.0, L	ND	ND	ND	MCV	N
11	7 mo/M	1	38.2	Y	42	0	2.50/ 2,112	17.5, L	ND	HPeV	ND	MCV	N
12	11 mo/M	1	39.1	Y	58	1	2.39/ 1,033	18.4, L	ND	ND	ND	MCV	N
13	1 y/F	1	39.3	Y	47	6	1.23/ 1,606	27.9, L	ND	CMV	CMV	MCV	N
14	7 mo/F	1	38.0	Y	25	4	2.15/ 396.7	12.3, L	ND	ND	ND	MCV	N
15	6 mo/F	1	38.9	Y	18	10	4.56/ 1,118	17.8, L	ND	ND	ND	MCV	N
16	1 y/M	1	Y	Y	33	5	1.42/ 1,047	28.1, L	HHV-6, HPeV	HHV-6	ND	MCV	N
17	10 mo/F	1	39.4	Y	41	4	1.37/ 4,440	25.5, L	HHV-6	HHV-6	HHV-6	MCV	N
18	1 y/M	1	40.4	Y	61	6	3.82/ 1,825	47.9, E	ND	ND	ND	MCV	N
19	1 y/F	1	39.0	Y	88	3	1.45/ >5,000	50.6, E	ND	ND	ND	MCV	N
20	1 y/F	1	40.6	Y	136	10	2.25/ 2,076	76.1, H	ND	HHV-6	ND	MCV or CX	N
21	24 y/F	Unk	38.8	Y	Unk	2	2.55/ >5,000	79.7, H	HHV-7	ND	ND	RI or CX	Y or N
22	21 y/M	2	38.0	Y	Unk	5	2.05/ >5,000	88.4, H	ND	ND	ND	RI	Y
23	29 y/M	Unk	Y	Y	Unk	5	3.89/ 4,228	91.7, H	ND	ND	ND	RI	Y
24	45 y/M	Unk	39.1	Y	Unk	5	1.29/ 518.7	91.0, H	HHV-7, B19	B19	ND	RI or CX	Y or N

*B19, human parvovirus B19; CMV, cytomegalovirus; CX, cross-reaction; E, equivocal; EBV, Epstein-Barr virus; H, high; HHV-6, human herpesvirus 6; HHV-7, human herpesvirus 7; HPeV, human parechovirus; L, low; MCV, measles-containing vaccine; ND, not detected; RAI, relative avidity index; RI, reinfection; Unk, unknown.
†IgM values indicate RU; IgG values indicate IU/L.
‡IgG avidity test results can help distinguish recent primary infection (characterized by a low RAI) from past infection (characterized by a high RAI). RAI <40% indicated low-avidity antibodies, RAI 40%–60% equivocal, and RAI >60% indicated high-avidity antibodies.
§MCV indicates that an increased IgM titer might be influenced by vaccination with a measles-containing vaccine; CX indicates a cross-reaction of a febrile exanthematous virus infection other than the measles virus, respectively.

discrepant results, especially in cases of rRT-PCR–negative and IgM-positive results. We analyzed samples from 24 patients with suspected measles whose samples previously tested rRT-PCR–negative and IgM-positive during a 2018 outbreak in Okinawa Prefecture, Japan. To understand the cause of the discrepancy, we performed 2 additional tests on those patient samples, IgG avidity test and detection of viral nucleic acid other than measles virus.

Measles-specific IgG avidity test results can provide useful information to distinguish between a recent infection or recent MCV vaccination, which are characterized by a low RAI, and past infection or past MCV vaccination, which are characterized by a high RAI (*15*,*29*). Among 20 suspected cases in children, 17 had low RAIs and 3 children (cases 18–20) showed equivocal or high RAIs. All 4 adult cases had high RAIs. The cases with low RAIs can be explained by recent MCV vaccination. Our results showed that in children who had received 1 dose of MCV, the RAI was correlated with the number of days after vaccination, consistent with results of a previous study (*15*). Suspected cases in children with equivocal or high RAIs had longer intervals between vaccination and sample collection compared with cases with low RAIs. One of the children (case 20) who had the longest interval between vaccination and sample collection tested positive for HHV-6 in a serum sample. Therefore, false-positive measles IgM could have been related to either an earlier MCV or an HHV-6 infection causing cross-reactivity, and we concluded that a measles infection was highly unlikely.

Four children (cases 1, 2, 5, and 9) had low RAIs and low measles-specific IgG antibody levels (<275 IU/L). All the samples from those cases were collected within 2 weeks after vaccination with MCV, which is before the body had time to produce a robust antibody response. We detected other viral pathogens in some specimens. In those cases, cross-reactivity with other viruses could have caused a false-positive measles IgM result. Although we could not establish the exact cause of the low RAIs with low IgG, those results ruled out a diagnosis of measles.

Four adult cases (cases 21–24) had high IgG titers and high RAIs shortly after the onset of the disease. Those results match previous studies that confirmed measles cases with either vaccination or natural infection show a low or undetectable IgM titer, a high RAI, and a high IgG titer in the early period after illness onset (*30*). Among the 4 adult cases, we detected febrile exanthematous viruses other than measles from the acute phase specimens of 2 cases (cases 21 and 24).

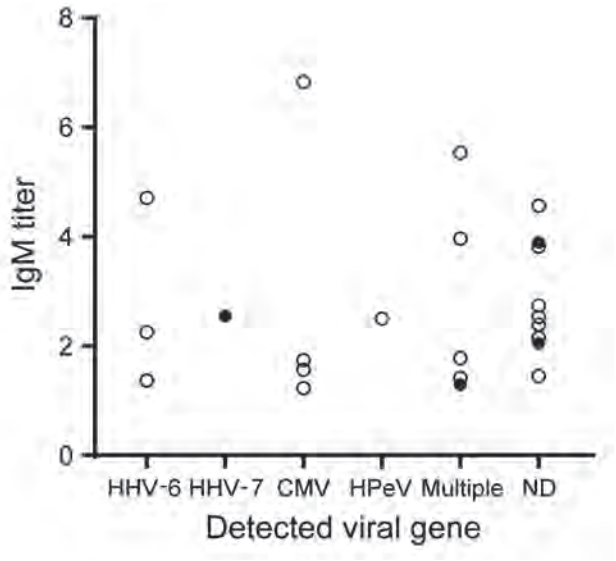

Figure 2. Measles-specific antibody titers and febrile exanthematous viral gene detection results in an analysis of suspected measles cases with discrepant measles-specific IgM and rRT-PCR test results, Japan. Figure represents 24 cases with measles-specific IgM-positive and rRT-PCR–negative results. White circles represent cases in children <1 year to 4 years of age with ≥1 doses of measles-containing vaccine; black circles represent cases in adults with unknown vaccination history. CMV, cytomegalovirus; HHV-6, human herpesvirus 6; HHV-7, human herpesvirus 7; HPeV, human parechovirus; multiple, multiple pathogens were detected; ND, not detected.

The subtle increase of measles IgM titer for those cases was possibly caused by a cross-reaction with other viruses rather than measles infection. Completely ruling out measles on the basis of results of avidity testing and tests for other pathogens is difficult when the measles vaccination and previous measles disease history are unknown. Therefore, when in doubt, clinicians should treat indeterminate cases as positive in terms of the public health response.

Vaccine-associated measles cases can be detected using rRT-PCR if symptoms occur within 2 weeks after vaccination and specimens are collected within 7 days from symptom onset (*7*). One limitation of this study is that rRT-PCR possibly did not detect the vaccine strain because most children with an elevated measles-specific IgM titer had not received MCV within the past 2 weeks. However, even though the vaccine strain was not detected, taking the RAI result and immunization date information into consideration, we can infer that the symptoms were caused by the vaccine strain. Another limitation of this study is that we only conducted nucleic acid testing for a few viral pathogens that cause febrile exanthemata; thus, the symptoms might have been attributable to other viruses or bacteria that

cause similar symptoms. Next-generation sequencing could help to identify the causal pathogen of febrile exanthemata. In addition, results of this study indicate a complete measles diagnosis would require additional testing, such as paired IgG and neutralizing antibody tests. However, collecting convalescent serum samples and conducting neutralizing antibody tests would require more time and would not be suitable when rapid determination of measles cases is needed in an outbreak setting. Therefore, we measured IgG levels as part of the avidity test instead of performing paired IgG testing.

During outbreaks, field staff are extremely busy investigating the source of infection and close contacts. Accurately identifying measles cases is vital for a rapid and accurate outbreak response and maintaining measles elimination status in Japan. Therefore, for suspected measles cases, collecting specimens at the appropriate time and collecting accurate vaccination and past infection history are crucial. When a definitive diagnosis still cannot be made, conducting IgG avidity testing and testing for febrile exanthematous pathogens other than measles virus can help clarify the diagnosis.

In conclusion, 2 diagnostic tests, rRT-PCR and measles-specific IgM, are used in Japan to maintain measles elimination status. Because 2 tests are conducted, test results sometimes differ, making definitive diagnosis difficult. Our results indicate that conducting measles IgG avidity testing and PCR testing for other febrile exanthematous viruses and collecting a detailed history of measles vaccination and measles history can reduce the difficulty of making a final diagnosis in most cases with discrepant rRT-PCR and IgM results.

Acknowledgments

The authors thank all staff at public health centers, hospitals, municipality offices, and Okinawa prefectural government office, who vigorously worked to control and end this measles outbreak and contributed to data and specimen collections.

This work was partly supported by the Research Program on Emerging and Re-emerging Infectious Diseases from the Japan Agency for Medical Research and Development (grant nos. JP21fk0108086 and JP22fk0108628).

About the Author

Ms. Kuba is a researcher at the National Institute of Infectious Diseases in Tokyo, Japan. Her main research interest is developing new diagnostic methods for viral infections of public health importance.

References

1. Moss WJ. Measles. Lancet. 2017;390:2490–502. https://doi.org/10.1016/S0140-6736(17)31463-0
2. World Health Organization. Global measles and rubella strategic plan 2012–2020 [cited 2023 Dec 2]. https://www.who.int/publications/i/item/9789241503396
3. World Health Organization. Brunei Darussalam, Cambodia, Japan verified as achieving measles elimination [cited 2023 Dec 2]. https://www.who.int/westernpacific/news/item/27-03-2015-brunei-darussalam-cambodia-japan-verified-as-achieving-measles-elimination
4. National Institute of Infection Diseases. Measles in Japan, as of February 2020. Infect Agents Surveill Rep. 2020;41:53–5.
5. Watanabe A, Kobayashi Y, Shimada T, Yahata Y, Kobayashi A, Kanai M, et al. Exposure to H1 genotype measles virus at an international airport in Japan on 31 July 2016 results in a measles outbreak. Western Pac Surveill Response J. 2017;8:37–9. https://doi.org/10.5365/wpsar.2016.7.4.007
6. Komabayashi K, Seto J, Tanaka S, Suzuki Y, Ikeda T, Onuki N, et al. The largest measles outbreak, including 38 modified measles and 22 typical measles cases in its elimination era in Yamagata, Japan, 2017. Jpn J Infect Dis. 2018;71:413–8. https://doi.org/10.7883/yoken.JJID.2018.083
7. Kuba Y, Kyan H, Iha Y, Kato T, Oyama M, Miyahira M, et al. Emergent measles-containing vaccination recommendation for aged 6–11 months and detection of vaccine-associated measles during a large measles outbreak in Okinawa, Japan, in 2018. Vaccine. 2020;38:2361–7. https://doi.org/10.1016/j.vaccine.2020.01.067
8. Hübschen JM, Bork SM, Brown KE, Mankertz A, Santibanez S, Ben Mamou M, et al. Challenges of measles and rubella laboratory diagnostic in the era of elimination. Clin Microbiol Infect. 2017;23:511–5. https://doi.org/10.1016/j.cmi.2017.04.009
9. Michel Y, Saloum K, Tournier C, Quinet B, Lassel L, Pérignon A, et al. Rapid molecular diagnosis of measles virus infection in an epidemic setting. J Med Virol. 2013;85:723–30. https://doi.org/10.1002/jmv.23515
10. National Institute of Infection Diseases. The manual for detecting measles virus, version 4 [in Japanese] [cited 2023 Nov 15]. https://www.niid.go.jp/niid/images/lab-manual/Measles20221003.pdf
11. World Health Organization. Manual for the laboratory diagnosis of measles and rubella virus infection, 2nd edition [cited 2023 Dec 3]. https://www.who.int/publications/i/item/WHO-IVB-07.01
12. Government of Japan. Act no. 114: Act on prevention of infectious diseases and medical care for patients with infectious diseases [in Japanese] [cited 2024 Apr 3]. https://elaws.e-gov.go.jp/document?lawid=410AC0000000114
13. Hummel KB, Lowe L, Bellini WJ, Rota PA. Development of quantitative gene-specific real-time RT-PCR assays for the detection of measles virus in clinical specimens. J Virol Methods. 2006;132:166–73. https://doi.org/10.1016/j.jviromet.2005.10.006
14. Hamkar R, Mahmoodi M, Nategh R, Jelyani KN, Eslami MB, Mohktari-Azad T. Distinguishing between primary measles infection and vaccine failure reinfection by IgG avidity assay. East Mediterr Health J. 2006;12:775–82.
15. Mercader S, Garcia P, Bellini WJ. Measles virus IgG avidity assay for use in classification of measles vaccine failure in measles elimination settings. Clin Vaccine Immunol. 2012;19:1810–7. https://doi.org/10.1128/CVI.00406-12
16. Okamoto K, Fujii K, Komase K. Development of a novel TaqMan real-time PCR assay for detecting rubella virus

RNA. J Virol Methods. 2010;168:267–71. https://doi.org/10.1016/j.jviromet.2010.05.016
17. Verstrepen WA, Kuhn S, Kockx MM, Van De Vyvere ME, Mertens AH. Rapid detection of enterovirus RNA in cerebrospinal fluid specimens with a novel single-tube real-time reverse transcription-PCR assay. J Clin Microbiol. 2001;39:4093–6. https://doi.org/10.1128/JCM.39.11.4093-4096.2001
18. Benschop K, Molenkamp R, van der Ham A, Wolthers K, Beld M. Rapid detection of human parechoviruses in clinical samples by real-time PCR. J Clin Virol. 2008;41:69–74. https://doi.org/10.1016/j.jcv.2007.10.004
19. Locatelli G, Santoro F, Veglia F, Gobbi A, Lusso P, Malnati MS. Real-time quantitative PCR for human herpesvirus 6 DNA. J Clin Microbiol. 2000;38:4042–8. https://doi.org/10.1128/JCM.38.11.4042-4048.2000
20. Ogawa H, Suzutani T, Baba Y, Koyano S, Nozawa N, Ishibashi K, et al. Etiology of severe sensorineural hearing loss in children: independent impact of congenital cytomegalovirus infection and GJB2 mutations. J Infect Dis. 2007;195:782–8. https://doi.org/10.1086/511981
21. Fernandez C, Boutolleau D, Manichanh C, Mangeney N, Agut H, Gautheret-Dejean A. Quantitation of HHV-7 genome by real-time polymerase chain reaction assay using MGB probe technology. J Virol Methods. 2002;106:11–6. https://doi.org/10.1016/S0166-0934(02)00131-3
22. Takao S, Shigemoto N, Shimazu Y, Tanizawa Y, Fukuda S, Matsuo T. Detection of exanthematic viruses using a TaqMan real-time PCR assay panel in patients with clinically diagnosed or suspected measles. Jpn J Infect Dis. 2012;65:444–8. https://doi.org/10.7883/yoken.65.444
23. Tanaka T, Kogawa K, Sasa H, Nonoyama S, Furuya K, Sato K. Rapid and simultaneous detection of 6 types of human herpes virus (herpes simplex virus, varicella-zoster virus, Epstein-Barr virus, cytomegalovirus, human herpes virus 6A/B, and human herpes virus 7) by multiplex PCR assay. Biomed Res. 2009;30:279–85. https://doi.org/10.2220/biomedres.30.279
24. Miura-Ochiai R, Shimada Y, Konno T, Yamazaki S, Aoki K, Ohno S, et al. Quantitative detection and rapid identification of human adenoviruses. J Clin Microbiol. 2007;45:958–67. https://doi.org/10.1128/JCM.01603-06
25. Klenner J, Kohl C, Dabrowski PW, Nitsche A. Comparing viral metagenomic extraction methods. Curr Issues Mol Biol. 2017;24:59–70. https://doi.org/10.21775/cimb.024.059
26. Zhang D, Lou X, Yan H, Pan J, Mao H, Tang H, et al. Metagenomic analysis of viral nucleic acid extraction methods in respiratory clinical samples. BMC Genomics. 2018;19:773. https://doi.org/10.1186/s12864-018-5152-5
27. Ministry of Health, Labour and Welfare. Guidelines for the prevention of specific infectious diseases: measles [in Japanese] [cited 2023 Dec 2]. https://www.mhlw.go.jp/content/001110643.pdf
28. Davidkin I, Valle M, Peltola H, Hovi T, Paunio M, Roivainen M, et al. Etiology of measles- and rubella-like illnesses in measles, mumps, and rubella-vaccinated children. J Infect Dis. 1998;178:1567–70. https://doi.org/10.1086/314513
29. Sowers SB, Rota JS, Hickman CJ, Mercader S, Redd S, McNall RJ, et al. High concentrations of measles neutralizing antibodies and high-avidity measles IgG accurately identify measles reinfection cases. Clin Vaccine Immunol. 2016;23:707–16. https://doi.org/10.1128/CVI.00268-16
30. Atrasheuskaya AV, Blatun EM, Neverov AA, Kameneva SN, Maksimov NL, Karpov IA, et al. Measles in Minsk, Belarus, 2001–2003: clinical, virological and serological parameters. J Clin Virol. 2005;34:179–85. https://doi.org/10.1016/j.jcv.2004.11.024

Address for correspondence: Yumani Kuba, Center for Emergency Preparedness and Response, National Institute of Infectious Diseases, 4-7-1 Gakuen, Musashimurayama-shi, Tokyo 208-0011, Japan; email: yumakuba@niid.go.jp

Kinetics of Hepatitis E Virus Infections in Asymptomatic Persons

Ricarda Plümers, Jens Dreier, Cornelius Knabbe, Eike Steinmann, Daniel Todt, Tanja Vollmer

To determine the kinetics of hepatitis E virus (HEV) in asymptomatic persons and to evaluate viral load doubling time and half-life, we retrospectively tested samples retained from 32 HEV RNA-positive asymptomatic blood donors in Germany. Close-meshed monitoring of viral load and seroconversion in intervals of ≈4 days provided more information about the kinetics of asymptomatic HEV infections. We determined that a typical median infection began with PCR-detectable viremia at 36 days and a maximum viral load of 2.0×10^4 IU/mL. Viremia doubled in 2.4 days and had a half-life of 1.6 days. HEV IgM started to rise on about day 33 and peaked on day 36; IgG started to rise on about day 32 and peaked on day 53. Although HEV IgG titers remained stable, IgM titers became undetectable in 40% of donors. Knowledge of the dynamics of HEV viremia is useful for assessing the risk for transfusion-transmitted hepatitis E.

Hepatitis E virus (HEV; family *Hepeviridae*), is a single-stranded positive-sense RNA virus with 3 open reading frames (*1*). Members of the HEV species *Paslahepevirus balayani* have been assigned to 8 genotypes, of which genotypes HEV-1 through HEV-4 are particularly relevant for human infection (*1*,*2*). Although infections with HEV-1 and HEV-2 are endemic to tropical countries and are transmitted by the oral–fecal route, HEV-3 and HEV-4 are transmitted zoonotically and infections are mainly found in Europe, North and South America, and Asia (*3*).

The dynamics of HEV infections are diverse among the cases described in the literature, which almost exclusively describe progression in symptomatic persons. Knowledge of progression of asymptomatic infection is limited, partly because asymptomatic infections are normally not detected. However, detection of HEV infection has increased in recent years, after analytical testing of blood donations for HEV became a focus of attention to improve the safety of blood transfusions. Systematic blood donor screening offers the possibility of identifying a large number of asymptomatic cases. Since 2004, transfusion-transmitted HEV infections have been repeatedly reported and pose a high risk for symptomatic or even chronic progression, particularly in immunosuppressed patients (*4*–*6*).

HEV infections in otherwise healthy persons are usually asymptomatic and self-limiting (*7*). However, according to the World Health Organization, using estimates from 2015 data, HEV is a leading cause for acute viral hepatitis in 20 million persons annually, including 3.3 million with symptomatic cases and 44,000 HEV-related deaths (*8*). Collecting data on the progression of viral load over the course of acute infection is difficult. The onset of symptoms coincides with the peak of viremia, and the first phase of infection cannot be analyzed (*9*). In addition, a large proportion of infections are not investigated because of the absence of symptoms. If HEV infection is identified by chance, such as during screening as part of quality assurance of blood products after donation, the donor is suspended from donation (*10*). For that reason, the data on HEV antibody detection are denser, and data on viremia are lacking, especially for persons with asymptomatic infections.

Several factors can be used to consider the course of infection progression, including the maximum viral load and when it is reached, depending on the time of infection or onset of signs/symptoms. Furthermore, the time it takes for the viral load to double before reaching the maximum load and the half-life of the viral load after that point can provide information about the nature of the infection. Comparable data have been collected (e.g., for hepatitis A [HAV], B [HBV], and C [HCV] viruses) from healthy blood donors or symptomatic patients (*11*–*14*).

Author affiliations: Herz- und Diabeteszentrum Nordrhein-Westfalen, Bad Oeynhausen, Germany (R. Plümers, J. Dreier, C. Knabbe, T. Vollmer); German Centre for Infection Research, Bochum (E. Steinmann); Ruhr University Bochum, Germany (E. Steinmann, D. Todt); European Virus Bioinformatics Center, Jena, Germany (D. Todt)

DOI: https://doi.org/10.3201/eid3005.231764

An incubation period of 2–9 weeks is assumed for HEV infections (*15*). HEV is detectable in blood samples for ≈4 weeks and in fecal samples for 6 weeks by screening with nucleic acid amplification testing (NAT) (*16*). Studies of the serologic status of HEV-infected rhesus monkeys and patients with acute hepatitis E have shown increased HEV IgG and IgM titers 3–4 weeks after HEV RNA detection-based confirmation of infection. Although HEV IgM is detectable for only a few months, HEV IgG remains for years (*17*–*19*).

We performed voluntary HEV RNA NAT of routinely collected blood donation samples retained over years and collected before 2019, when HEV screening of blood products became mandatory (*20*). Because of the retrospective nature of the analysis, donors were not excluded from donating in the interim. In addition, only a few days elapsed between each donation, resulting in dense data on viral load progression. HEV RNA–positive donors underwent serologic status follow-up, sometimes over several weeks. The data from our study provide detailed insight into the dynamics of HEV infection in asymptomatic persons as well as evaluation of viral load doubling time and half-life during the infection in this cohort.

Material and Methods

Blood Donors and HEV RNA screening

We retrospectively screened samples for HEV RNA, using blood collected for donation before mandatory HEV NAT screening was initiated. All donors denied having an acute illness and stated that they had no known risk factor for a viral infection.

We conducted the screening for HEV RNA in master pools of 96 samples (200 µL/donor) by using the Chemagic viral DNA/RNA reagent kit for RNA extraction (PerkinElmer Chemagen Technologies, https://www.revvity.com) and the RealStar HEV-RT-PCR Kit (Altona Diagnostic Technologies, https://altona-diagnostics.com) for amplification (95% limit of detection [LOD] 4.7 IU/mL, 95% CI 3.6 –7.6 IU/mL; 95% LOD of 451 IU/mL for a single donation in a 96-sample mini pool), as described previously (*21*). Alternatively, we extracted and amplified HEV RNA by using the AltoStar AM16 and the AltoStar HEV RNA RT-PCR Kit (Altona Diagnostic Technologies) (95% LOD 3.41 IU/mL, 95% CI 2.28–6.4 IU/mL; 95% LOD of 327 IU/mL for a single donation in a 96-sample minipool).

We quantified the viral load by using the AltoStar HEV RNA RT-PCR Kit on the Biorad CFX96 DeepWell system (Bio-Rad Laboratories, https://www.bio-rad.com). We quantified the viral load in reference to internal kit standards, calibrated against World Health Organization International Standard (PEI code 6329/10).

Calculation of Generation Time

Assuming exponential growth, we determined the doubling times and the half-lives between 2 data points to be comparable to the calculation of the kinetics of the hepatitis A virus (*11*), based on the formula

$$n = \log(2) \times \log\left(\frac{N_t}{N_0}\right)$$

N_0 corresponds to the viral load at the beginning of the period, N_t to the viral load after the considered time t, and n to the number of doublings. We used division to calculate the number of doublings per day.

For each person, we determined and graphically displayed the median of the virus doubling time and the half-life. To exclude that the parameters at the beginning and end of phases differ compared with the core region of the course, we considered 2 intervals for calculation. The first interval includes the calculations between all data points (first, last, and peak; whole course). The second interval includes only the core region (excluding first, last, and peak; trimmed course). Considering the doubling time and half-life, we appended the courses of viral loads from 7 donors, for whom other kinetic data had been previously published (*21*).

Serologic Testing

We traced seroconversion of HEV RNA-positive blood donors, evaluating HEV IgM and IgG titers by using HEV ELISA Kits (Wantai, https://www.sanbio.nl) according to manufacturer instructions. We determined the semiquantitative evaluation of titers as the signal to cutoff ratio (S/CO).

We visualized the data by using GraphPad Prism 9.0 software (GraphPad Software, https://www.graphpad.com). All calculations were also performed by using GraphPad Prism 9.

Results

We analyzed progression of HEV viremia in 32 HEV RNA-positive persons. On average, there were 4 days (interquartile range [IQR] 3–7 days) between donations. Analysis and quantification of the viral load and determination of the serostatus in all subsequent samples from the corresponding persons provided deeper insight into the course of HEV infection in terms of doubling time and clearance (half-life) of the virus, as well as seroconversion.

On average, HEV viremia reached maximum viral load after 22 days (IQR 10–27 days) (Figure 1).

The highest viral load was detected at the initial positive donation for 3 persons. Note that the maximum viral load for those persons was reached before the measurement period. The longest period until detection of the maximum was 64 days. An HEV RNA–negative donation marking the end of the infection was recorded for 28 donors on day 39 (IQR 25–56 days, total range 9–154 days). The last positive donation for those donors was at a median of 36 days (IQR 19–49 days, total range 5–83 days) after the first HEV RNA–positive donation (Figure 1, panel A).

HEV IgM was detected in 28 persons on average at day 33 (IQR 25–40 days, total range 7–108 days) initially and reached the maximum S/CO at day 36 (IQR 28–54 days, total range 14–115 days). HEV IgM detectability disappeared for 13 persons at a median of 85 days (IQR 59–108 days, total range 42–265 days). HEV IgG was detected in 31 persons on average at day 32 (IQR 24–39 days, total range 9–108 days) initially and reached the maximum S/CO at day 53 (IQR 32–72 days, total range 17–108 days) (Figure 1, panel B). For 3 persons, HEV IgM could not be detected at any time. For 1 person, no seroconversion was detected because the last donation analyzed corresponded to day 26 after initial detection of HEV RNA.

Over time, decline of the proportion of RNA positive-persons and increased proportion of persons positive for HEV IgM and IgG was recorded as expected. Of note, during the rise of the curves, the proportions did not differ significantly between

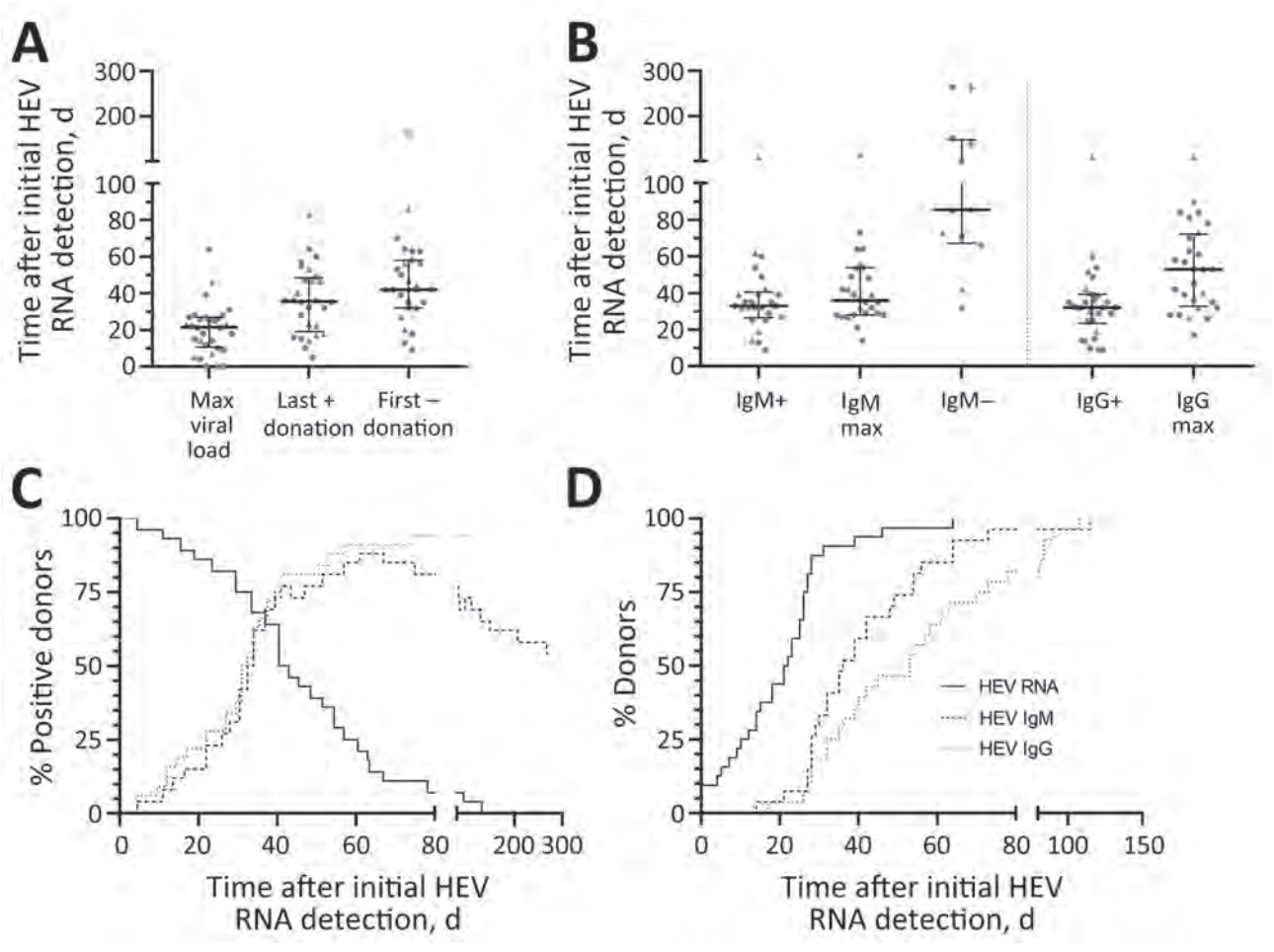

Figure 1. Progression of HEV infection in asymptomatic persons determined from retrospectively tested blood samples, Germany. A) Days at which the maximum viral load was reached as well as the time points of last HEV RNA–positive and the first HEV RNA–negative donation. B) Serostatus for HEV IgM and HEV IgG revealing the time points of primary HEV IgM or IgG detection, maximum ratio signal to cutoff, and loss of detectability of HEV IgM. In panels A and B, data points indicate each person; error bars indicate medians with interquartile ranges; circles indicate donors who donated HEV-negative blood before first detection of HEV RNA; and triangles indicate persons who did not donate HEV-negative blood before first detection of HEV RNA. C) percentages of persons who were positive for the markers HEV RNA, HEV IgM, and HEV IgG. D) Progression curves for the percentages of persons in whom the maximum of those markers was exceeded, depending on the time since initial HEV RNA detection. HEV, hepatitis E virus; max, maximum; +, positive; –, negative.

persons positive for HEV IgM or for HEV IgG, indicating simultaneous production onset of antibodies of both classes. However, the decline of the percentage of HEV IgM–positive persons again represents the loss of IgM titer for some (Figure 1, panel C).

When comparing the proportions of persons for whom HEV RNA viral load, HEV IgM, and IgG S/CO maximums were exceeded, we observed that maximum viral load was reached earlier than maximum HEV IgM and IgG S/CO. The proportion of persons for whom maximum HEV IgG S/CO was attained is always lower than the proportion for whom maximum HEV IgM S/CO was attained during the observed period, indicating an earlier peak in HEV IgM than IgG titers (Figure 1, panel D).

In addition to determining the time course of infection markers, we quantified viral load for several follow-up samples to identify the maximum viral load and development of the viral load during infection, leading to our analysis of the correlation between the maximum viral load and duration of HEV RNA positivity as well as the calculation of the doubling time and the half-life of the viral load (Figure 2). The average maximum viral load amounted to 2.0×10^4 IU/mL (IQR 2.0×10^3–1.5×10^5 IU/mL, total range 2.3×10^2–1.1×10^7 IU/mL) (Figure 2, panel A). The overlayed development of the viral load in the time course for all persons (Figure 2, panel B) demonstrates an approximated exponential increase and decrease of viral load. Based on these data, plotting of the maximum viral load against the duration of the infection showed a weak correlation, with a coefficient of $r = 0.5642$ at a significance level of $p = 0.0018$ (Figure 2, panel C).

In addition to the kinetics we observed (n = 32) and with regard only to the doubling time and half-life, we included in our calculation data collected from asymptomatic blood donors published before (n = 7), which have not yet been examined for those parameters (*21*). We differentiated between the median doubling time per person in the whole course and in the trimmed course (excluding values corresponding to the first or last HEV RNA–positive sample or the maximum viral load). The calculation in the rising phase of the viral load revealed an average doubling time of 2.8 days (IQR 2.0–3.3 days, total range 0.9–5.0 days; n = 33) during the whole course and of 2.4 days (IQR 1.7–3.7 days, total range 0.6–4.8 days; n = 21) during the trimmed course. The calculations for the declining phase of the viral load resulted in an average half-life of 1.8 days (IQR 1.2–2.2 days, total range 0.9–4.4 days; n = 32) during the whole course and of 1.6 days (IQR 0.8–2.2 days, total range 0.7–3.3 days; n = 14) during the trimmed course (Figure 2, panel D).

Discussion

The course progression of a viral infection is usually difficult to follow because viremia often proceeds unobserved before symptom onset. For HEV, a large proportion of infections are additionally assumed to be asymptomatic and self-limiting (*22*), which is reflected in the discrepancy between the number of reported cases and the high HEV IgG seroprevalence in the general population (*23*). The introduction of standard screening of blood donors in some countries in Europe has enabled early detection of viremia (*10*). However, doing so gives rise to a second problem with analyzing viral kinetics, because affected donors are excluded from further donations for months, so no progression statistics can be applied. Symptomatic patients are also rarely suitable for analysis of viremia in the second half of infection because treatments (e.g., ribavirin) inherently affect the course progression (*24*,*25*).

Because our studied data represent asymptomatic infected persons retrospectively identified from retained samples stored over years, closely meshed follow-up samples are available for viral load, and those data provide a unique opportunity to gain understanding of kinetics in asymptomatic blood donors. Blood donations from asymptomatic donors pose a risk for development of transfusion-transmitted severe and chronic hepatitis E in immunosuppressed patients and recipients of solid organ transplants (*5*).

In the overall evaluation of our results, we mainly discuss median values that were calculated. It should be noted that infection characteristics differed greatly among individual donors. In that context, case–control studies might be appropriate for assessing differences among donors in terms of kinetics shift in context with secondary factors (e.g., patient age, virus genotype). Of note, to evaluate the effect of specific mutations on doubling time and maximum viral load possibly correlating with severity of infection, as has been shown for hepatitis B virus infections, our data provide necessary baseline information for infection courses (*14*).

Several serologic studies of kinetics during HEV infection have been published and state detection of HEV RNA in blood over 4 weeks, which is comparable to the 36 days (or 5 weeks) of viremia that we detected (*16*–*18*). Although both HEV IgM and IgG have been described as appearing ≈2 weeks after first detection of HEV RNA during acute hepatitis E, we observed

a much longer period of 32 (IgM) and 33 (IgG) days, although similar simultaneous onset of both immunoglobulins was confirmed (*17*,*18*,*26*). We were able to display a fast increase in HEV IgM S/CO reflected by the reaching of maximum HEV IgM S/CO at day 36, followed by a slow decrease leading to titers below the LOD in around one third of the donors at a median of day 85. Meanwhile, HEV IgG S/CO increased more slowly but stayed detectable at a high level in all persons. Those kinetics are in line with the general expectations for the course of the serologic response during a self-limiting infection (*27*,*28*).

The data presented here on the viremic course of asymptomatic persons have been published only to a

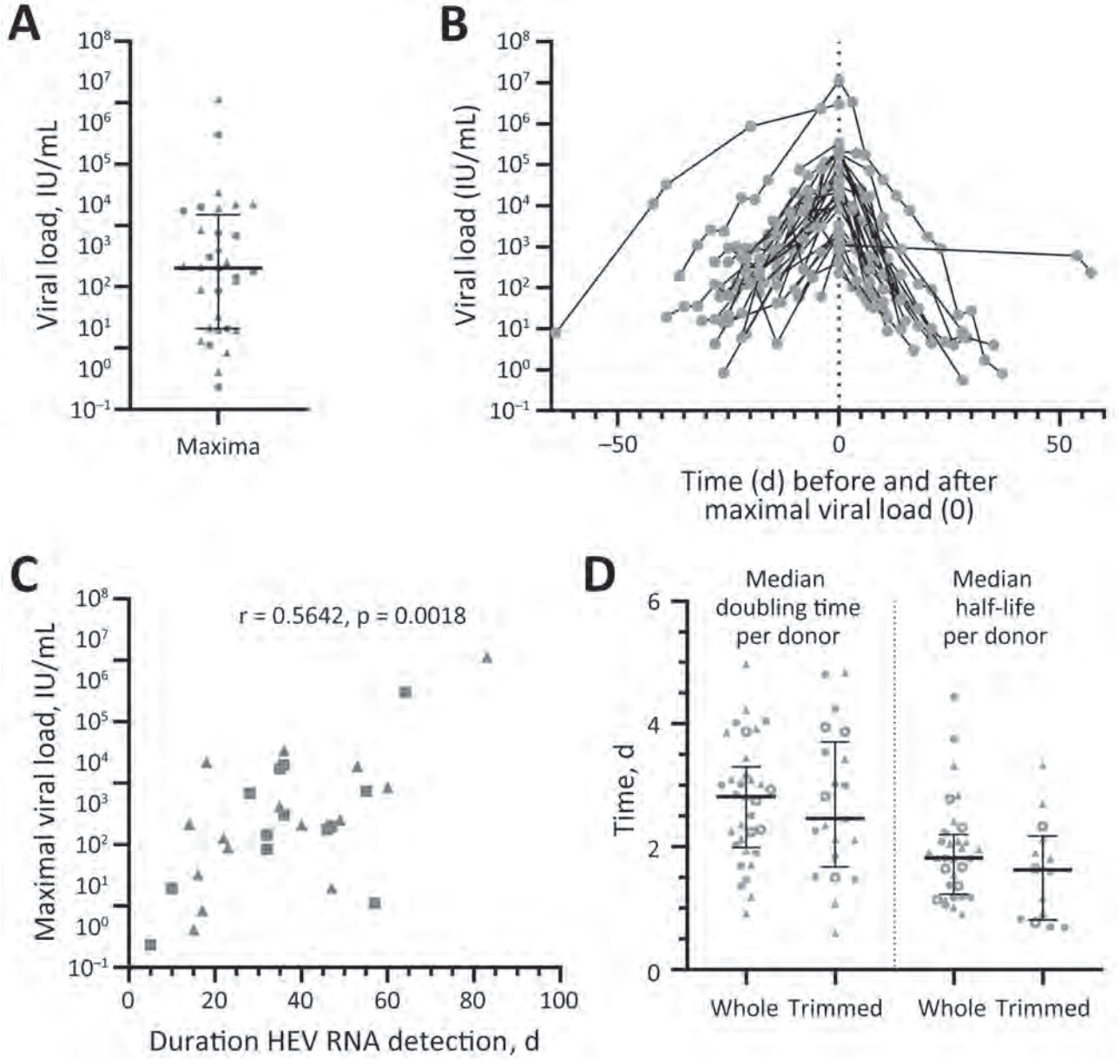

Figure 2. Hepatitis E virus (HEV) viral load in asymptomatic persons determined from retrospectively tested blood samples, Germany. A) Maximum viral load for each person (n = 32). B) Viral loads during the infection have been overlayed for all persons depending on the timepoint when the maximum viral load (set as day 0) was reached. C) Spearman coefficient r calculated for the correlation of the maximum viral load and the duration of HEV RNA detection in the blood for persons with confirmed end of infection by HEV RNA–negative donation (n = 28). D) Doubling time was determined in the rising phase of the viral load, whereas the half-life was determined in the declining phase for the whole or a trimmed course. Data points indicate each person; error bars indicate medians with interquartile ranges; circles indicate donors who donated HEV-negative blood before first detection of HEV RNA (n = 14); and triangles indicate persons who did not donate HEV-negative blood before first detection of HEV RNA (n = 18). Data points calculated from data extracted from Vollmer et al. are displayed as open circles (n = 7) (*21*). HEV, hepatitis E virus.

limited extent because of the restrictions mentioned above. A previous study of ours, with data from 10 asymptomatic persons, provided insight into the viremic kinetics and reported a median maximum viral load of 1.88×10^4 IU/mL reached at day 23 and a total interval of HEV RNA positivity of 28 days (*21*), which is in line with the maximum viral load of 2.0×10^4 IU/mL reached at day 22 and a total period of 36 days of RNA positivity that we report. Therefore, we considered it reasonable to include the data from that study when calculating the doubling time and half-life of HEV viral loads.

A comparison of data from asymptomatic persons with viremia characteristics of patients after solid organ transplantation published by Pas et al. resulted in a striking discrepancy (*29*). First, the discrepancy is reflected in the fact that, in the Pas et al. study, the median time between detection of HEV RNA and detection of HEV IgG was 124 days, whereas in our study that period was only 33 days. Second, in that study, chronic hepatitis E developed in 11 of 12 organ recipients with a median duration of 16 months, whereas, among the asymptomatic donors in our study, chronic hepatitis E developed in none (>3 months viremia) with a median infection period of 36 days. Consequently, the kinetics of acute and chronic hepatitis E need to be differentiated.

When considering the doubling time and half-life of viral load during HEV viremia, comparative data (e.g., from symptomatic patients) are missing. Our calculations resulted, depending on the analysis window considered, in a doubling time of 2.8–2.4 days and a half-life of 1.8–1.6 days. The values in the whole or the trimmed core intervals were similar, indicating uniform growth and fall of the viral load. Therefore, we did not take complex calculations for different phase into account as has been done for HBV, for example (*30*). HEV infections are closely related to HAV infections in terms of not only the route of transmission and the self-limiting character but also the signs/symptoms (*15*,*31*). A higher maximum viral load of 2.6×10^7 IU/mL, a longer infection duration of 106 days, and a doubling time of 17.5 hours for asymptomatic HAV positive blood donors have been published (*11*). A comparably low doubling time of 13.8 hours has been demonstrated in HCV-infected liver transplant recipients (*13*). For HBV-infected persons, a doubling time of 2.5–3.7 days and a half-life of 1.6–3.7 days has been reported, which is more similar to the HEV kinetics (*12*,*14*). At the same time, a stable maximum viral load for HBV of 10^8–$10^{9.5}$ IU/mL has been detected in this context and was interpreted as the viral load associated with the infection of nearly all hepatocytes (*12*,*30*). The median maximum HEV viral load that we detected is a few logs lower and fluctuated between donors, not accounting for infection of all hepatocytes.

In conclusion, our data provide insight into the kinetics of asymptomatic HEV infection. Although key characteristics (e.g., humoral immune response, maximum viral load, and duration of viremia) confirmed results of previous studies, doubling time and half-life of the viral load were additionally determined. Comparison with the course of infection in organ transplant recipients as well as patients with other viral liver infections revealed characteristic deviations, highlighting that HEV infection in healthy persons is less extensive and leads to fewer health impairments and that risk factors such as immunosuppression influence the infection. Our data provide a baseline for evaluating self-limiting HEV infection. With the addition of secondary factors such as age or immune status, it can be determined which factors influence the kinetics of the infection and represent a risk to, for example, recipients of transfusion-transmitted hepatitis E.

Acknowledgments

We thank Birgit Drawe for her excellent technical assistance and Philip Saunders for his linguistic advice.

D.T. was supported by the German Federal Ministry of Education and Research (project VirBio, grant no. 01KI2106). E.S. and T.V. were supported by the German Federal Ministry of Education and Research (project HepEDiaSeq, FKZ 01EK2106A).

About the Author

Dr. Plümers is working at Herz- und Diabeteszentrum Nordrhein-Westfalen as a postdoctoral research fellow with a focus on HEV infections in transfusion medicine.

References

1. Cao D, Meng XJ. Molecular biology and replication of hepatitis E virus. Emerg Microbes Infect. 2012;1:e17. https://doi.org/10.1038/emi.2012.7
2. Purdy MA, Harrison TJ, Jameel S, Meng XJ, Okamoto H, Van der Poel WHM, et al.; Ictv Report Consortium. ICTV virus taxonomy profile: Hepeviridae. J Gen Virol. 2017;98:2645–6. https://doi.org/10.1099/jgv.0.000940
3. Horvatits T, Varwig-Janssen D, Schulze Zur Wiesch J, Lübke R, Reucher S, Frerk S, et al. No link between male infertility and HEV genotype 3 infection. Gut. 2020;69:1150–1. https://doi.org/10.1136/gutjnl-2019-319027
4. Cheung CKM, Wong SH, Law AWH, Law MF. Transfusion-transmitted hepatitis E: What we know so far? World J Gastroenterol. 2022;28:47–75. https://doi.org/10.3748/wjg.v28.i1.47

5. Westhölter D, Hiller J, Denzer U, Polywka S, Ayuk F, Rybczynski M, et al. HEV-positive blood donations represent a relevant infection risk for immunosuppressed recipients. J Hepatol. 2018;69:36–42. https://doi.org/10.1016/j.jhep.2018.02.031
6. Harvala H, Hewitt PE, Reynolds C, Pearson C, Haywood B, Tettmar KI, et al. Hepatitis E virus in blood donors in England, 2016 to 2017: from selective to universal screening. Euro Surveill. 2019;24:1800386. https://doi.org/10.2807/1560-7917.ES.2019.24.10.1800386
7. Aggarwal R, Jameel S. Hepatitis E. Hepatology. 2011;54:2218–26. https://doi.org/10.1002/hep.24674
8. World Health Organization (WHO). Hepatitis E [cited 2023 Jul 26]. https://www.who.int/news-room/fact-sheets/detail/hepatitis-e
9. Pérez-Gracia MT, Suay B, Mateos-Lindemann ML. Hepatitis E: an emerging disease. Infect Genet Evol. 2014;22:40–59. https://doi.org/10.1016/j.meegid.2014.01.002
10. Federal Ministry of Justice. Announcement on the authorisation of medicinal products—defence against drug risks - order to test blood donors to prevent the transmission of hepatitis E virus through blood components for transfusion and stem cell preparations for haematopoietic reconstitution [in German] [cited 2023 Jul 26]. https://www.bundesanzeiger.de/pub/publication/8ziFMqlkUHaYCwHxuin?0
11. Schoch S, Wälti M, Schemmerer M, Alexander R, Keiner B, Kralicek C, et al. Hepatitis A virus incidence rates and biomarker dynamics for plasma donors, United States. Emerg Infect Dis. 2021;27:2718–824. https://doi.org/10.3201/eid2711.204642
12. Whalley SA, Murray JM, Brown D, Webster GJM, Emery VC, Dusheiko GM, et al. Kinetics of acute hepatitis B virus infection in humans. J Exp Med. 2001;193:847–54. https://doi.org/10.1084/jem.193.7.847
13. Garcia-Retortillo M, Forns X, Feliu A, Moitinho E, Costa J, Navasa M, et al. Hepatitis C virus kinetics during and immediately after liver transplantation. Hepatology. 2002;35:680–7. https://doi.org/10.1053/jhep.2002.31773
14. Yoshikawa A, Gotanda Y, Itabashi M, Minegishi K, Kanemitsu K, Nishioka K. Hepatitis B NAT virus-positive blood donors in the early and late stages of HBV infection: analyses of the window period and kinetics of HBV DNA. Vox Sang. 2005;88:77–86. https://doi.org/10.1111/j.1423-0410.2005.00602.x
15. Velavan TP, Pallerla SR, Johne R, Todt D, Steinmann E, Schemmerer M, et al. Hepatitis E: An update on One Health and clinical medicine. Liver Int. 2021;41:1462–73. https://doi.org/10.1111/liv.14912
16. Huang S, Zhang X, Jiang H, Yan Q, Ai X, Wang Y, et al. Profile of acute infectious markers in sporadic hepatitis E. PLoS One. 2010;5:e13560. https://doi.org/10.1371/journal.pone.0013560
17. Zhang J, Ge SX, Huang GY, Li SW, He ZQ, Wang YB, et al. Evaluation of antibody-based and nucleic acid-based assays for diagnosis of hepatitis E virus infection in a rhesus monkey model. J Med Virol. 2003;71:518–26. https://doi.org/10.1002/jmv.10523
18. Clayson ET, Myint KSA, Snitbhan R, Vaughn DW, Innis BL, Chan L, et al. Viremia, fecal shedding, and IgM and IgG responses in patients with hepatitis E. J Infect Dis. 1995;172:927–33. https://doi.org/10.1093/infdis/172.4.927
19. Hoofnagle JH, Nelson KE, Purcell RH. Hepatitis E. N Engl J Med. 2012;367:1237–44. https://doi.org/10.1056/NEJMra1204512
20. Vollmer T, Diekmann J, Johne R, Eberhardt M, Knabbe C, Dreier J. Novel approach for detection of hepatitis E virus infection in German blood donors. J Clin Microbiol. 2012;50:2708–13. https://doi.org/10.1128/JCM.01119-12
21. Vollmer T, Diekmann J, Eberhardt M, Knabbe C, Dreier J. Hepatitis E in blood donors: investigation of the natural course of asymptomatic infection, Germany, 2011. Euro Surveill. 2016;21:30332. https://doi.org/10.2807/1560-7917.ES.2016.21.35.30332
22. Pischke S, Behrendt P, Bock CT, Jilg W, Manns MP, Wedemeyer H. Hepatitis E in Germany—an under-reported infectious disease. Dtsch Arztebl Int. 2014;111:577–83.
23. Faber M, Willrich N, Schemmerer M, Rauh C, Kuhnert R, Stark K, et al. Hepatitis E virus seroprevalence, seroincidence and seroreversion in the German adult population. J Viral Hepat. 2018;25:752–8. https://doi.org/10.1111/jvh.12868
24. Ambrosioni J, Mamin A, Hadengue A, Bernimoulin M, Samii K, Landelle C, et al. Long-term hepatitis E viral load kinetics in an immunocompromised patient treated with ribavirin. Clin Microbiol Infect. 2014;20:O718–20. https://doi.org/10.1111/1469-0691.12576
25. Lhomme S, Kamar N, Nicot F, Ducos J, Bismuth M, Garrigue V, et al. Mutation in the hepatitis E virus polymerase and outcome of ribavirin therapy. Antimicrob Agents Chemother. 2015;60:1608–14. https://doi.org/10.1128/AAC.02496-15
26. Hofmann AF. Chemistry and enterohepatic circulation of bile acids. Hepatology. 1984;4(Suppl):4S–14S. https://doi.org/10.1002/hep.1840040803
27. Miller JFAP. Cellular basis of the immune response. Acta Endocrinol Suppl (Copenh). 1975;194(Supplement):55–76.
28. Perelson AS, Goldstein B, Rocklin S. Optimal strategies in immunology III. The IgM-IgG switch. J Math Biol. 1980;10:209–56. https://doi.org/10.1007/BF00276984
29. Pas SD, de Man RA, Mulders C, Balk AHMM, van Hal PTW, Weimar W, et al. Hepatitis E virus infection among solid organ transplant recipients, the Netherlands. Emerg Infect Dis. 2012;18:869–72. https://doi.org/10.3201/eid1805.111712
30. Tsiang M, Rooney JF, Toole JJ, Gibbs CS. Biphasic clearance kinetics of hepatitis B virus from patients during adefovir dipivoxil therapy. Hepatology. 1999;29:1863–9. https://doi.org/10.1002/hep.510290626
31. Naoumov NV. Hepatitis A and E. Medicine (Baltimore). 2007;35:35–8. https://doi.org/10.1053/j.mpmed.2006.10.004

Address for correspondence: Ricarda Plümers, Heart and Diabetes Center North Rhine-Westphalia, Institute for Laboratory and Transfusion Medicine, Gergstr. 11 Bad Oeynhausen 32545, Germany; email: rpluemers@hdz-nrw.de

Cross-Sectional Study of Q Fever Seroprevalence among Blood Donors, Israel, 2021

Nesrin Ghanem-Zoubi,[1] Yafit Atiya-Nasagi,[1] Evgeniy Stoyanov, Moran Szwarcwort, Basel Darawsha, Mical Paul, Eilat Shinar

We evaluated Q fever prevalence in blood donors and assessed the epidemiologic features of the disease in Israel in 2021. We tested serum samples for *Coxeilla burnetii* phase I and II IgG using immunofluorescent assay, defining a result of ≥200 as seropositive. We compared geographic and demographic data. We included 1,473 participants; 188 (12.7%) were seropositive. The calculated sex- and age-adjusted national seroprevalence was 13.9% (95% CI 12.2%–15.7%). Male sex and age were independently associated with seropositivity (odds ratio [OR] 1.6, 95% CI 1.1–2.2; p = 0.005 for male sex; OR 1.2, 95% CI 1.01–1.03; p<0.001 for age). Residence in the coastal plain was independently associated with seropositivity for Q fever (OR 1.6, 95% CI 1.2–2.3; p<0.001); residence in rural and farming regions was not. Q fever is highly prevalent in Israel. The unexpected spatial distribution in the nonrural coastal plain suggests an unrecognized mode of transmission.

Q fever, caused by infection with the bacterium *Coxeilla burnetii*, is an endemic disease in Israel. In 2021, a total of 341 cases of Q fever were reported to the Epidemiology Division, Ministry of Health (*1*), representing an estimated incidence of 3.6/100,000 population. For comparison, the highest incidence of Q fever in recent years in the European Union was reported from Spain, reaching 0.7/100,000 population in 2019 (*2*). Despite the longstanding endemicity of Q fever in Israel, little is known about the actual epidemiology, geographic distribution, and groups at highest risk for the disease (*3*–*6*). Ministry of Health data are based on passive notifications, relying on reporting by the treating physician and laboratory staff where the diagnostic test suggestive of Q fever was performed. This reporting system is known to be highly affected by the awareness and motivation of medical staff (both physicians and laboratory workers). Almost half of acute Q fever cases are asymptomatic (*7*), but infections can progress years later to the more severe, chronic form of the disease. Thus, the actual population incidence of Q fever, including events missed by the passive surveillance system, has not been documented in Israel. In this study, we evaluated the prevalence of Q fever in adult healthy volunteer blood donors in Israel and assessed the epidemiologic features of the disease.

Methods

Study Design and Setting

We conducted a cross-sectional nationwide prevalence study using blood samples collected during January 1–October 8, 2021. Samples were collected by Magen David Adom (MDA) National Blood Service. Blood donations were performed in locations across the country. Samples were collected and stored from donors who signed an informed consent agreeing to participate in the study. Participants completed an obligatory donor health questionnaire that included their demographic details and health status. The study was performed in line with the principles of the Declaration of Helsinki. The study was approved by the ethics committees of Rambam Health Care Campus and MDA's research committee. Informed consent was obtained from all individual participants included in the study.

Author affiliations: Rambam Health Care Campus, Haifa, Israel (N. Ghanem-Zoubi, M. Szwarcwort, M. Paul); The Ruth and Bruce Rappaport Faculty of Medicine, Technion-Israel Institute of Technology, Haifa (N. Ghanem-Zoubi, B. Darawsha, M. Paul); Israel Institute for Biological Research, Ness-Ziona, Israel (Y. Atiya-Nasagi); Magen David Adom National Blood Services, Ramat Gan, Israel (E. Stoyanov, E. Shinar)

DOI: https://doi.org/10.3201/eid3005.230645

[1]These authors contributed equally to this article.

Participants

Participants were male and nonpregnant female adult blood donors ≥18 years of age (pregnant women are excluded from blood donation) who completed the donor health questionnaire and signed the MDA consent form for use of blood donations in research. Samples for this study were selected randomly from the full sample pool (≈1,000 donations/day) by donation site from all districts in Israel. To achieve a study group representative of the whole population, we enriched the final study set with samples taken from female donors and from Arab-populated locations; however, sample selection was performed randomly from the respective sample pools.

Study Flow and Data Collection

We centrifuged specimens obtained from blood donors, saved serum samples at 4°C, and transferred samples to the reference laboratory for antibody testing. We kept samples anonymous and did not convey results to the blood donors.

We collected demographic data on date of donation, date and country of birth, sex, and location of residence. We extracted data on the residence localities' sociodemographic characteristics from the Israeli Central Bureau of Statistics (CBS) website. Those data consisted of population size, ethnicity of population, and socioeconomic index cluster (categorized as 1–10 on the basis of multiple social and economic variables). We defined Arab localities as localities in which >80% of the population were Arab. Localities were classified by socioeconomic cluster as low (1–3), middle (4–7), or high (8–10) status. Rural localities were defined as those with <5,000 inhabitants.

Microbiological Methods

We performed screening for presence of phase I and phase II *C. burnetii* IgG by using an in-house indirect immunofluorescence assay at the National Central Laboratory for Rickettsiosis in the Israel Institute for Biologic Research. We performed the test by using antigens of phase I Ohio strain and phase II Nine Mile strain of *Coxiella burnetii*. This test has been used clinically for many years as the standard for Q fever diagnosis in Israel. The test was externally validated upon its introduction and continues to be under periodic internal and external quality assurance control programs. Results were reported as borderline if positive in a titer of 100 and seropositive with antibody titers of phase I or phase II IgG ≥200.

Seroprevalence Spatial Distribution

We calculated Q fever seroprevalence rate by locality, natural region, and subdistrict and district level. Israel is divided into districts and subdistricts on the basis of administrative considerations and into natural regions on the basis of regional geographic features. We used the natural regions to divide the country into 4 areas: the coastal plain and the inner regions of the north, center, and south. We created prevalence choropleth maps according to district, subdistrict, and natural region classification. We created maps using ArcGIS Desktop software (Esri, https://www.esri.com) to display spatial prevalence data.

Statistical Methods

We expressed seroprevalence rates as an overall rate and in geographic and demographic groups. We calculated the sex- and age-adjusted seroprevalence to estimate national Q fever prevalence in adults >18 years of age using the sex and age distribution of the population of Israel according to 2019 CBS data. We used the χ^2 test to assess the association between available epidemiologic characteristics and seropositivity for Q fever. We used binary logistic regression for multivariate analysis. We included variables with $p<0.05$ in bivariate analysis in the binary regression. All statistical tests were 2-tailed.

The sample size needed for prevalence estimation was calculated targeting a 95% CI and assuming a Q fever prevalence in Israel of 4% (on the basis of previous studies from Q fever–endemic developed countries that reported a prevalence range of 3%–5%). We targeted a precision of 1%. The sample size needed was calculated to be 1,476.

Results

During January 1–October 8, 2021, samples were collected from 1,600 blood donors; we tested 1,473 samples with complete epidemiologic data. Of those, 188 (12.7%) samples were positive for *C. burnetii* antibodies. Phase II IgG ≥200 was detected in 187 participants; concomitant phase I IgG ≥200 was detected in 57 (30%) of those participants' samples. Only 1 sample was found with positive phase I IgG and negative phase II IgG (Table 1).

The mean age of the participants was 36.6 ± 13.9 years; 859 (58.3%) were men and 614 (41.7%) women. The sex- and age-adjusted prevalence rate was 13.9% (95% CI 12.2%–15.7%).

The seroprevalence of Q fever was higher among men (14.9% [128/859]) than women (9.8% [60/614]) (Table 2). In addition, seroprevalence increased with age, reaching a rate of 17.4% (52/299) among participants >50 years of age. Participants living in rural locations had seropositivity of 10.6% (51/480). Seroprevalence rates were similar in Arab and Jewish

Table 1. Q fever antibody results in cross-sectional study of Q fever seroprevalence among blood donors, Israel, 2021

	No. (%) participants				
Antibody	Negative	Borderline, = 100	Positive, ≥200	200–800	≥1,600
Phase II IgG	1,152 (78.2)	134 (9)	187 (12.6)	158 (10.7)	29 (1.9)
Phase I IgG	1,374 (93.2)	41 (2.7)	58 (3.9)	56 (3.8)	2 (0.1)

localities and in low, middle, and high socioeconomic status localities.

Seropositive cases were widely distributed across all parts of the country. Prevalence rates varied among regions; rates were highest in the coastal plain (15.9% [100/629]) and lowest in the noncoastal central region (8.8% [37/419]) (Figure; Appendix Table 1, https://wwwnc.cdc.gov/EID/article/30/5/23-0645-App1.pdf).

In bivariate comparison, older age, male sex, and residence in the coastal plain were more prevalent in the seropositive group than the seronegative one (Table 3). Residence in a rural area was less prevalent in the seropositive group but did reach statistical significance. In multivariate logistic regression analysis, variables that were independently associated with Q fever seropositivity were age (odds ratio [OR] 1.2, 95% CI 1.01–1.03; p<0.001), male sex (OR 1.6, 95% CI 1.1–2.2; p = 0.005), and residence in the coastal plain (OR 1.6, 95% CI 1.2–2.3; p<0.001).

Discussion

We found high Q fever seroprevalence at an estimated rate of 13.9% among healthy adults in Israel, with wide geographic distribution. Seropositive status was independently associated with male sex, older age, and residence in the coastal plain.

National seroprevalence studies of Q fever from the past 2 decades have been conducted in several countries. In the United States (*8*), the Netherlands (before the large outbreak in 2007) (*9*), and Chile (*10*), prevalence was ≈3%. Higher prevalence rates were reported from Australia (5.6%) (*11*), French Guiana (9.6%) (*12*), and Northern Ireland (12.8%) (*13*). Smaller studies from other countries demonstrated a broad range of Q fever prevalence: 6.9% in Bhutan (*14*), 6.9% in Reunion Islands (*15*), 24.2% in Jordan (*16*), and 52.7% in Cyprus (*17*). Those studies used different testing methods and different cutoff titers to define seropositivity, which could have contributed to differences in reported prevalence rates.

In this study, we used a relatively high cutoff titer to define seropositivity, which could have led to an underestimation of seroprevalence rate. For example, if we had used a cutoff of 100 instead of 200 to define seropositivity, the crude overall prevalence rate would have increased from 12.7% to 21.8%. Nevertheless, the high seroprevalence rate we found seems to correlate with reported ongoing and increasing incidence of the disease, as reflected in clinical reports in the national surveillance (*1*) (Appendix Figure). The increase in incidence observed in recent years had been preceded by several outbreaks reported in different areas (*18*–*20*).

Increasing age and male sex as risk factors for Q fever have been reported in various countries in both clinical and epidemiological studies (*8*,*11*,*21*,*22*); possible explanations have been related to increased exposure from living in endemic places and certain occupational exposures. We did

Table 2. Crude prevalence of anti-*Coxiella burnetti* IgG in cohort groups in cross-sectional study of Q fever seroprevalence among blood donors, Israel, 2021

Parameter	No. participants	No. seropositive (%)
Overall	1,473	188 (12.7)
Sex		
M	859	128 (14.9)
F	614	60 (9.8)
Age group, y		
18–30 y	550	50 (9.0)
31–50 y	502	85 (16.9)
>50 y	299	52 (17.4)
Geographic factors		
Born in Israel	1,205	153 (12.7)
Living in Jewish locality	1,310	167 (12.7)
Living in Arab locality	157	21 (13.4)
Rural	372	38 (10.2)
Urban	1,095	150 (13.7)
Socioeconomic status of residence localities		
Low	328	39 (11.9)
Middle	714	94 (13.2)
High	416	54 (13.0)

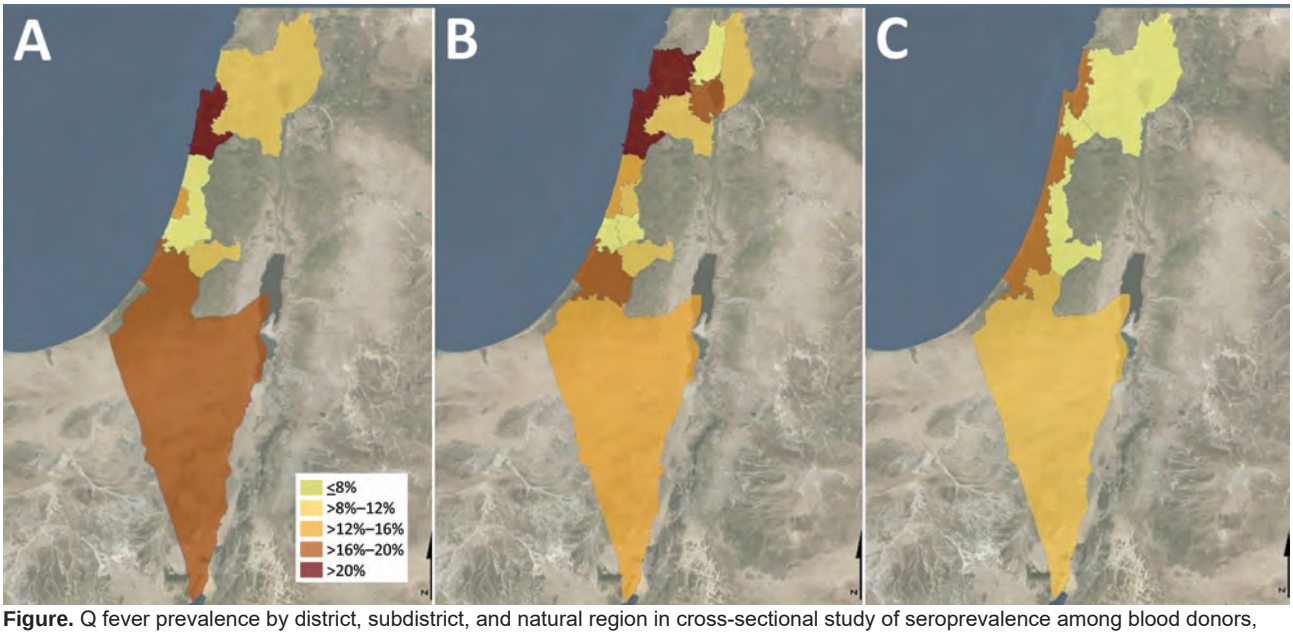

Figure. Q fever prevalence by district, subdistrict, and natural region in cross-sectional study of seroprevalence among blood donors, Israel, 2021. Spatial distribution of Q fever seroprevalence uses different geographic classifications. A) Seroprevalence rates by district; the highest rate was in Haifa district. B) Seroprevalence rates by subdistrict; the highest rate was in Hadera subdistrict. C) Seroprevalence rates by 4 natural region clusters; the highest rate was in the coastal plain area.

not have occupational data for participants in this study, but previous local reports have frequently mentioned that animal exposure does not seem to be a risk factor (*23*–*25*). Similarly, residence in a rural area was not associated with Q fever seroprevalence in our study, contrary to previous reports (*11*,*15*,*17*,*26*). Yet, the significance of male sex as a risk factor might be related to exposure factors that should be further investigated.

Residence in the coastal plain was significantly associated with Q fever prevalence in our study. Of note, the coastal plain region in Israel contains more urban and highly populated localities than other regions, whereas livestock farms are more prevalent in noncoastal areas, mainly in the south and north (*27*). For example, the subdistrict with the highest seroprevalence rate in our study was Hadera (26%); only 7.2% of sheep farms and 4.2% of cattle farms in Israel are located in that subdistrict (*27*). Wind can carry sporelike forms of *C. burnetii* to distances of up to 18 km, as documented in previous studies (*28*,*29*). The short 17-km distance of Hadera subdistrict from the eastern border (an area for which data are missing) should be taken into consideration in further studies. However, those factors alone cannot explain the unique spatial pattern of prevalence depicted in our study; in those circumstances, we would have expected a decreasing gradient of prevalence in which the highest rates would be observed in rural and inner noncoastal regions. Our spatial prevalence data point to an unknown mode of transmission of the disease that seems to play a major role in current epidemiology in Israel. The possibility of an unrecognized animal

Table 3. Risk factors for Q fever seropositivity and results of univariate and multivariate analyses in cross-sectional study of Q fever seroprevalence among blood donors, Israel, 2021*

Parameter	All participants, N = 1,473	Seropositive, n = 188	Seronegative, n = 1,285	Univariate analysis p value	Multivariate analysis	
					Odds ratio (95% CI)	p value
Mean age ±SD, y	36.6 ±13.9	41.1 ±13.3	35.9 ±13.9	<0.001	1.2 (1.01–1.03)	<0.001
Male sex	859 (58.3)	128 (68.1)	731 (56.9)	0.004	1.6 (1.1–2.2)	0.005
Born in Israel	1,211 (82.9)	153 (81.3)	1,058 (83)	0.677		
Living in Jewish locality	1,310 (89.3)	167 (88.8)	1,143 (89.4)	0.824		
Rural locality	372 (25.4)	38 (20.2)	334 (26.1)	0.082		
Socioeconomic status of residence localities				0.683		
Low	328 (22.5)	39 (20.9)	289 (22.7)			
Moderate	714 (49.0)	94 (50.3)	620 (48.8)			
High	416 (28.5)	54 (28.9)	362 (28.5)			
Living in coastal plain	629 (42.9)	100 (53.2)	529 (41.4)	0.002	1.6 (1.2–2.3)	<0.001

*Values are no. (%) except as indicated.
†<5,000 population.

that might be a reservoir for the bacterium in the urban environment should be investigated. Special attention should be paid to stray cats and wild boars, particularly because wild boars have become a frequent observation inside Haifa, the largest city in the northern coastal plain. In addition, rivers and streams could theoretically play a role in the transmission of the bacterium from the inner areas of the country to the coastal plain; in 1 study, *C. burnetii* was detected in contaminated river water (*30*).

Compared with brucellosis, another endemic zoonotic disease in Israel, in which most cases occur among Arabs (*31*), in this study, Q fever seems to affect Arab and Jewish locations at similar rates. The transmission mode of brucellosis is clearly associated with consumption of unpasteurized dairy products and direct contact with infected sheep (*32*). The fact that sheep herds, which are most likely the common source of both diseases, are found mostly inside or in close proximity to Arab locations (*27*) supports a different transmission mode of Q fever.

The first limitation of our study is the epidemiologic differences between healthy blood donors and the general population. We did not include persons <18 years of age, pregnant women, and persons who were not qualified to donate blood because of responses on the donor health questionnaire or results of physical tests performed before donation (i.e., blood pressure, heart rate, hemoglobin levels). For estimating national prevalence, we adjusted our results to age and sex distribution of the general population. Still, underrepresentation of Arab population in our cohort was prominent and might have missed prevalence ethnic differences. Another limitation is the absence of data on individual risk factors such as occupation and animal exposure. As mentioned previously, those data were not found to be associated with clinical illness in reports from Israel (*23*) but should be further studied prospectively.

In conclusion, our study presents key data on the epidemiology of Q fever in Israel, demonstrating high seroprevalence throughout the country, with predominance in the coastal plain for unknown reasons and no association with rural areas or livestock farms. Future studies should further investigate environmental factors that seem to play a major role in the transmission of this endemic disease. Improving our knowledge of disease transmission is critical in planning prevention programs for this highly endemic disease with significant consequences for public health.

Acknowledgments

We thank Faris Jahshan for the advice and assistance in map creation. We thank Sharon Eliyahu and Michal Bitan for administrative and technical assistance. We also thank Dina Gohaman, Yafa Afrimov, and Ayala Itzik for the laboratory technical work.

All authors contributed to the study conception and design. Material preparation, data collection and analysis were performed by N.G.-Z. and M.P. The first draft of the manuscript was written by N.G.-Z. and all authors commented on previous versions of the manuscript. All authors read and approved the final manuscript.

About the Author

Dr. Ghanem-Zoubi is an infectious diseases and internal medicine specialist and the deputy director of the Infectious Diseases Institute, Rambam Health Care Campus, Haifa, Israel. Her primary research interest in recent years is infective endocarditis and zoonoses, including brucellosis and Q fever.

References:

1. Israeli Ministry of Health. Epidemiological weekly report [cited 2022 Nov 16]. https://www.gov.il/he/Departments/DynamicCollectors/weekly-epidemiological-report
2. European Food Safety Authority and European Centre for Disease Control and Prevention. The European Union summary report on trends and sources of zoonoses, zoonotic agents and food–borne outbreaks in 2014. EFSA Journal. 2015;13:4329.
3. Ergas D, Keysari A, Edelstein V, Sthoeger ZM. Acute Q fever in Israel: clinical and laboratory study of 100 hospitalized patients. Isr Med Assoc J. 2006;8:337–41.
4. Reisfeld S, Mhamed SH, Stein M, Chowers M. Acute Q fever in Israel: clinical and demographic data 2006–2016. Open Forum Infect Dis. 2017;4(suppl_1):S124.
5. Siegman-Igra Y, Kaufman O, Keysary A, Rzotkiewicz S, Shalit I. Q fever endocarditis in Israel and a worldwide review. Scand J Infect Dis. 1997;29:41–9. https://doi.org/10.3109/00365549709008663
6. Bishara J, Pitlik S, Yagupsky P, Hershkovitz D. Comparative incidence of acute Q fever in two ethnic groups in Israel. Eur J Clin Microbiol Infect Dis. 2004;23:224–5. https://doi.org/10.1007/s10096-003-1095-z
7. Raoult D, Marrie T. Q fever. Clin Infect Dis. 1995;20:489–95, quiz 496. https://doi.org/10.1093/clinids/20.3.489
8. Anderson AD, Kruszon-Moran D, Loftis AD, McQuillan G, Nicholson WL, Priestley RA, et al. Seroprevalence of Q fever in the United States, 2003–2004. Am J Trop Med Hyg. 2009;81:691–4. https://doi.org/10.4269/ajtmh.2009.09-0168
9. Schimmer B, Notermans DW, Harms MG, Reimerink JHJ, Bakker J, Schneeberger P, et al. Low seroprevalence of Q fever in The Netherlands prior to a series of large outbreaks. Epidemiol Infect. 2012;140:27–35. https://doi.org/10.1017/S0950268811000136
10. Tapia T, Olivares MF, Stenos J, Iglesias R, Díaz N, Vergara N, et al. National seroprevalence of coxiella burnetii in Chile, 2016–2017. Pathogens. 2021;10:531. https://doi.org/10.3390/pathogens10050531

11. Gidding HF, Peng CQ, Graves S, Massey PD, Nguyen C, Stenos J, et al. Q fever seroprevalence in Australia suggests one in twenty people have been exposed. Epidemiol Infect. 2020;148:1–5. https://doi.org/10.1017/S0950268820000084
12. Bailly S, Hozé N, Bisser S, Zhu-Soubise A, Fritzell C, Fernandes-Pellerin S, et al. Transmission dynamics of Q fever in French Guiana: a population-based cross-sectional study. Lancet Reg Health Am. 2022;16:100385.
13. McCaughey C, McKenna J, McKenna C, Coyle PV, O'Neill HJ, Wyatt DE, et al. Human seroprevalence to Coxiella burnetii (Q fever) in Northern Ireland. Zoonoses Public Health. 2008;55:189–94. https://doi.org/10.1111/j.1863-2378.2008.01109.x
14. Tshokey T, Stenos J, Durrheim DN, Eastwood K, Nguyen C, Graves SR. Seroprevalence of rickettsial infections and Q fever in Bhutan. PLoS Negl Trop Dis. 2017;11:e0006107. https://doi.org/10.1371/journal.pntd.0006107
15. Jaubert J, Naze F, Camuset G, Larrieu S, Pascalis H, Guernier V, et al. Seroprevalence of *Coxiella burnetii* (Q fever) exposure in humans on Reunion Island. Open Forum Infect Dis. 2019;6:ofz227. https://doi.org/10.1093/ofid/ofz227
16. Obaidat MM, Malania L, Imnadze P, Roess AA, Bani Salman AE, Arner RJ. Seroprevalence and risk factors for *Coxiella burnetii* in Jordan. Am J Trop Med Hyg. 2019;101:40–4. https://doi.org/10.4269/ajtmh.19-0049
17. Psaroulaki A, Hadjichristodoulou C, Loukaides F, Soteriades E, Konstantinidis A, Papastergiou P, et al. Epidemiological study of Q fever in humans, ruminant animals, and ticks in Cyprus using a geographical information system. Eur J Clin Microbiol Infect Dis. 2006;25:576–86. https://doi.org/10.1007/s10096-006-0170-7
18. Amitai Z, Bromberg M, Bernstein M, Raveh D, Keysary A, David D, et al. A large Q fever outbreak in an urban school in central Israel. Clin Infect Dis. 2010;50:1433–8. https://doi.org/10.1086/652442
19. Steiner HA, Raveh D, Rudensky B, Paz E, Jerassi Z, Schlesinger Y, et al. Outbreak of Q fever among kitchen employees in an urban hospital. Eur J Clin Microbiol Infect Dis. 2001;20:898–900. https://doi.org/10.1007/s10096-001-0641-9
20. Oren I, Kraoz Z, Hadani Y, Kassis I, Zaltzman-Bershadsky N, Finkelstein R. An outbreak of Q fever in an urban area in Israel. Eur J Clin Microbiol Infect Dis. 2005;24:338–41. https://doi.org/10.1007/s10096-005-1324-8
21. Kampschreur LM, Dekker S, Hagenaars JCJP, Lestrade PJ, Renders NHM, de Jager-Leclercq MGL, et al. Identification of risk factors for chronic Q fever, the Netherlands. Emerg Infect Dis. 2012;18:563–70. https://doi.org/10.3201/eid1804.111478
22. Melenotte C, Protopopescu C, Million M, Edouard S, Carrieri MP, Eldin C, et al. Clinical features and complications of *Coxiella burnetii* infections from the French National Reference Center for Q Fever. JAMA Netw Open. 2018;1:e181580. https://doi.org/10.1001/jamanetworkopen.2018.1580
23. Finn T, Babushkin F, Geller K, Alexander H, Paikin S, Lellouche J, et al. Epidemiological, clinical and laboratory features of acute Q fever in a cohort of hospitalized patients in a regional hospital, Israel, 2012–2018. PLoS Negl Trop Dis. 2021;15:e0009573. https://doi.org/10.1371/journal.pntd.0009573
24. Ghanem-Zoubi N, Paul M, Szwarcwort M, Agmon Y, Kerner A. Screening for Q fever in patients undergoing transcatheter aortic valve implantation, Israel, June 2018–May 2020. Emerg Infect Dis. 2021;27:2205–7. https://doi.org/10.3201/eid2708.204963
25. Ghanem-Zoubi N, Karram T, Kagna O, Merhav G, Keidar Z, Paul M. Q fever vertebral osteomyelitis among adults: a case series and literature review. Infect Dis (Lond). 2021;53:231–40 https://doi.org/10.1080/23744235.2020.1871508
26. Pijnacker R, Reimerink J, Smit LAM, van Gageldonk-Lafeber AB, Zock JP, Borlée F, et al. Remarkable spatial variation in the seroprevalence of *Coxiella burnetii* after a large Q fever epidemic. BMC Infect Dis. 2017;17:725. https://doi.org/10.1186/s12879-017-2813-y
27. Israelli Central Bureau of Statistics. Data from the Agricultural Census 2017 [cited 2023 Feb 13]. https://www.cbs.gov.il/en/publications/Pages/2021/Data-from-Agricultural-Census-2017.aspx
28. Nusinovici S, Hoch T, Brahim ML, Joly A, Beaudeau F. The effect of wind on *Coxiella burnetii* transmission between cattle herds: a mechanistic approach. Transbound Emerg Dis. 2017;64:585–92. https://doi.org/10.1111/tbed.12423
29. Clark NJ, Soares Magalhães RJ. Airborne geographical dispersal of Q fever from livestock holdings to human communities: a systematic review and critical appraisal of evidence. BMC Infect Dis. 2018;18:218. https://doi.org/10.1186/s12879-018-3135-4
30. D'Ugo E, Sdanganelli M, Grasso C, Magurano F, Marcheggiani S, Boots B, et al. Detection of *Coxiella burnetii* in urban river water. Vector Borne Zoonotic Dis. 2017;17:514–6. https://doi.org/10.1089/vbz.2017.2107
31. Ghanem-Zoubi N, Pessah Eljay S, Anis E, Paul M. Re-emergence of human brucellosis in Israel. Isr Med Assoc J. 2019;21:10–2.
32. Dabaja-Younis H, Atarieh M, Paul M, Nasrallah E, Geffen Y, Kassis I, et al. Predictive factors for focal disease in human brucellosis, an observational cohort study. Eur J Clin Microbiol Infect Dis. 2023;42:221–6. https://doi.org/10.1007/s10096-022-04541-1

Address for correspondence: Nesrin Ghanem-Zoubi, Infectious Diseases Institute, Rambam Health Care Campus, Ha-Aliya 8 St, Haifa 3109601, Israel; email: n_ghanem@rambam.health.gov.il

COVID-19 Vaccination Site Accessibility, United States, December 11, 2020–March 29, 2022

Randy Yee, David Carranza, Christine Kim, James Phillip Trinidad, James L. Tobias, Roma Bhatkoti, Sachiko Kuwabara

During December 11, 2020–March 29, 2022, the US government delivered ≈700 million doses of COVID-19 vaccine to vaccination sites, resulting in vaccination of ≈75% of US adults during that period. We evaluated accessibility of vaccination sites. Sites were accessible by walking within 15 minutes by 46.6% of persons, 30 minutes by 74.8%, 45 minutes by 82.8%, and 60 minutes by 86.7%. When limited to populations in counties with high social vulnerability, accessibility by walking was 55.3%, 81.1%, 86.7%, and 89.4%, respectively. By driving, lowest accessibility was 96.5% at 15 minutes. For urban/rural categories, the 15-minute walking accessibility between noncore and large central metropolitan areas ranged from 27.2% to 65.1%; driving accessibility was 79.9% to 99.5%. By 30 minutes driving accessibility for all urban/rural categories was >95.9%. Walking time variations across jurisdictions and between urban/rural areas indicate that potential gains could have been made by improving walkability or making transportation more readily available.

On December 11, 2020, the US Food and Drug Administration (FDA) authorized the first COVID-19 vaccine for emergency use for persons ≥16 years of age (*1*). Although during the initial period of limited supply the vaccine was allocated to at-risk older adults and certain essential workers, by the end of spring 2021 vaccine eligibility gradually expanded to all adults (*2*). On September 22, 2021, the Pfizer-BioNTech (https://www.pfizer.com) COVID-19 vaccine emergency use authorization was amended to allow a single booster dose for elderly adults and adults with underlying medical conditions. By November 19, 2021, a booster dose was recommended for all adults (*1*), and on March 29, 2022, emergency use authorization allowed for a second booster dose (*3*). By March 29, 2022, the percentage of adults who had completed the primary COVID-19 vaccination series was 75.4%, and 48.2% had received a booster dose (*4*).

A major structural barrier of the US COVID-19 vaccination campaign is vaccine accessibility. The Assistant Secretary for Planning and Evaluation, Office of Health Policy, found that major barriers to vaccine coverage were transportation-related costs, opportunity costs, and inadequate functional proximity to the vaccines (*5*). The US Centers for Disease Control and Prevention (CDC) has provided recommendations to jurisdictions with regard to the planning of convenient COVID-19 vaccination sites, including use of gap analysis to spatially assess optimal locations for additional sites, especially those with populations of homebound persons or persons living in remote places (*6*,*7*).

Another major theme of the vaccination campaign has been equity of access. The CDC COVID-19 Response Health Equity Strategy has outlined tangible activities for ensuring equity in the nationwide distribution and administration of COVID-19 vaccines through data-driven approaches such as expanding vaccine data collection, reporting, and analyses (*8*). Organizations such as the Office for Civil Rights also have highlighted accessibility challenges and the need for federally assisted healthcare providers to ensure fair and equitable access to vaccines and boosters, citing laws such as Title VI of the Civil Rights Act of 1964 and Section 1557 of the Affordable Care Act (*9*). The White House has repeatedly confirmed its commitment to ensuring equitable access to COVID-19 vaccines (*10*–*12*).

Author affiliations: Centers for Disease Control and Prevention, Atlanta, Georgia, USA (R. Yee, D. Carranza, C. Kim, J.L. Tobias, R. Bhakoti, S. Kuwabara); US Department of Health and Human Services Coordination Operations and Response Element, Washington, DC (J.P. Trinidad)

DOI: https://doi.org/10.3201/eid3005.230357

Geographic information systems have proven valuable for evaluating functional proximity of populations to vaccination sites; geospatial analyses use dynamic travel time estimation methods for vaccine modeling and planning increasing during the COVID-19 pandemic (*13*–*21*). For example, Whitehead et al. calculated travel times between Aotearoa, the New Zealand census-derived Statistical Area 1 level, to all potential vaccine delivery sites with a road network and origin/destination analysis (J. Whitehead et al., unpub. data, https://www.medrxiv.org/content/10.1101/2021.08.26.21262647v1). In a nationwide study in England, Duffy et al. measured accessibility from statistical and administrative neighborhood centroids to COVID-19 vaccination sites by using the closest travel time routes and the most likely transport mode in each area: by car, by public transport, or on foot (*20*). Another study conducted in Kenya used a cost–distance algorithm based on walking and motorized modes to generate a gridded travel time surface at the 1 × 1–km spatial resolution level together with a population density layer from WorldPop (https://www.worldpop.org) to determine accessibility of population to vaccination centers (*21*). A Bayesian conditional autoregressive model was then used to identify inequalities in accessibility and to predict vaccination coverage rates (*21*).

Knowledge of the functional proximity to vaccine sites for different populations is essential for effective planning and for ensuring equity of health

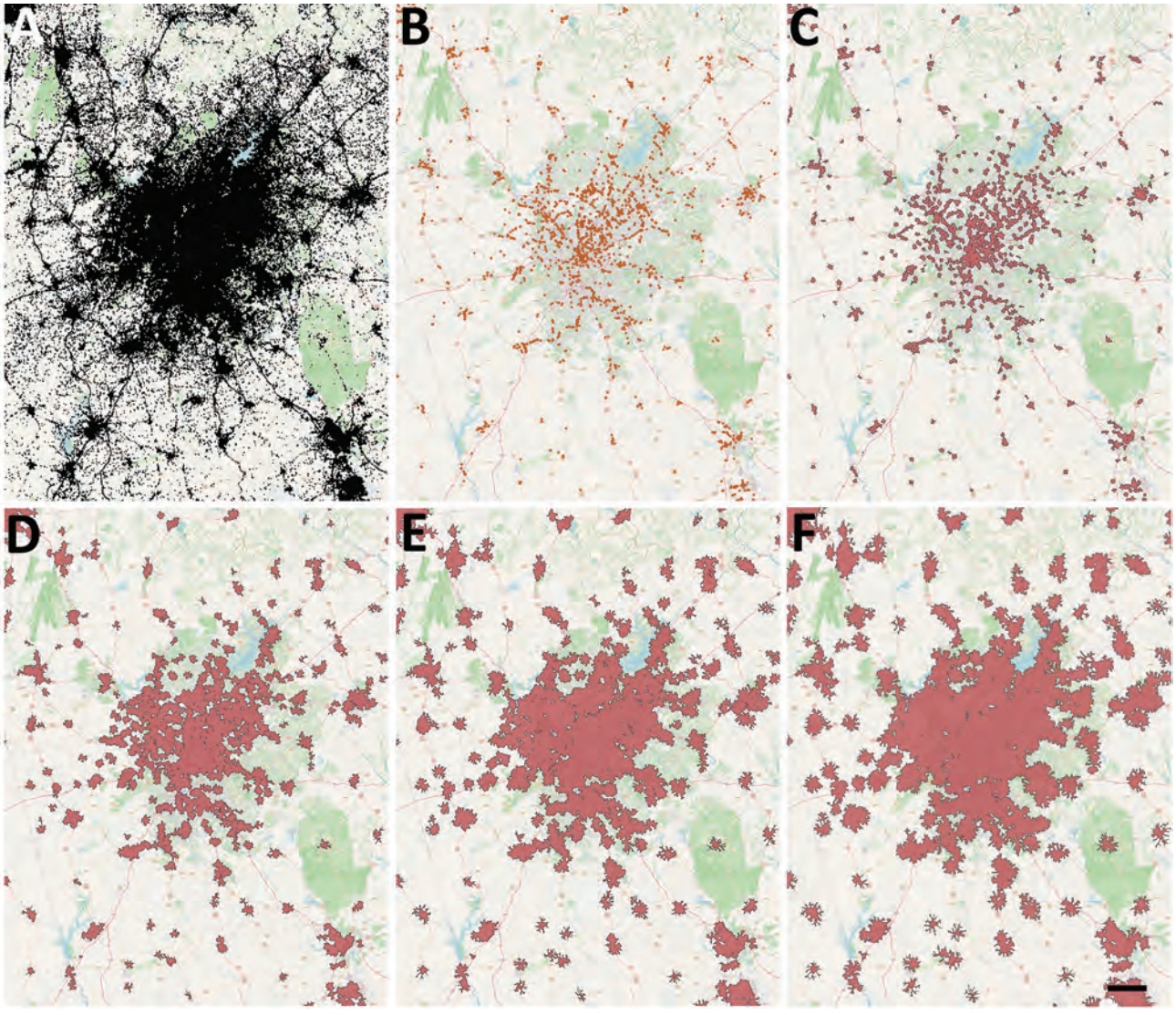

Figure 1. COVID-19 vaccination site accessibility, Atlanta metropolitan area, Georgia, USA, December 11, 2020–March 29, 2022. A) Adult population density; B) COVID-19 providers; C) COVID-19 vaccination site accessible by 15-minute walk; D) 30-minute walk; E) 45-minute walk; F) 60-minute walk. Scale bar indicates 20 km.

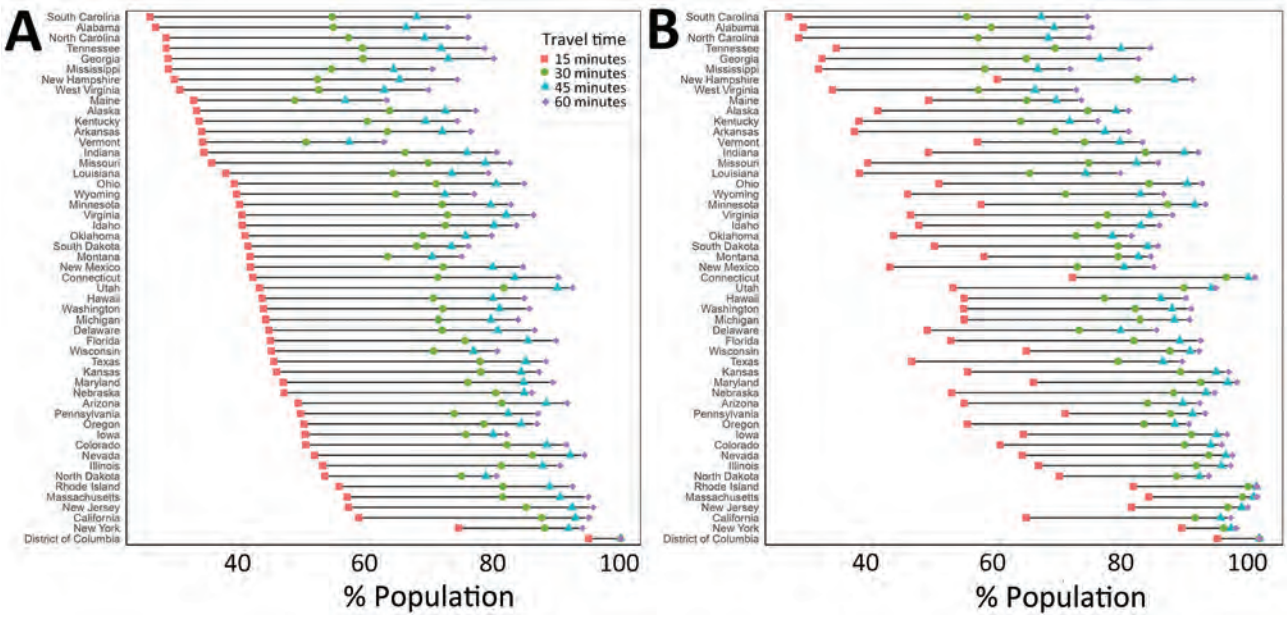

Figure 2. Adult COVID-19 vaccination site accessibility according to walking time in 15-minute intervals, by state, United States, December 11, 2020–March 29, 2022. A) Overall accessibility; B) accessibility for areas with high scores on the Centers for Disease Control and Prevention/Agency for Toxic Substances and Disease Registry Social Vulnerability Index.

resource access in public health emergencies. With our retrospective study, we evaluated accessibility of COVID-19 vaccine sites nationally by walking and driving travel times at the jurisdiction, community social vulnerability, and urban/rural levels.

The study was approved by the CDC National Center for Health Statistics. CDC investigators did not interact with human subjects or have access to identifiable data or specimens.

Methods

To obtain a list of active provider sites, we queried the official platform for US COVID-19 vaccine distribution, the Tiberius system (https://www.cdc.gov/vaccines/programs/tiberius/index.html). We defined an active provider site as any provider site from December 11, 2020 (with FDA authorization for emergency use of the first COVID-19 vaccine, Pfizer-BioNTech) through March 29, 2022 (with FDA authorization of a second booster dose for older and immunocompromised persons) that at any point reported any inventory in the preceding 7 days, received a shipment in the preceding 28 days, or administered ≥1 dose of adult COVID-19 vaccine during the preceding 28 days (*1*,*3*). Sites must have been a provider of one of the approved or authorized adult COVID-19 vaccines in the United States during the study period: Pfizer-BioNTech, Moderna (https://www.modernatx.com), and Janssen (https://www.jnj.com). To avoid potentially overestimating provider site accessibility for the general population, we excluded sites serving institutionalized or long-term resident populations (e.g., prisons, detention facilities, and nursing homes) or military personnel (e.g., Department of Defense provider sites).

We grouped provider sites into 1 of 5 self-reported categories: community health, hospital, medical practice, pharmacy, and unknown/other (Appendix Figure 1, https://wwwnc.cdc.gov/EID/article/30/5/23-0357-App1.pdf). Community health providers were reported as public health, tribal health, or commercial vaccination service sites. The hospital category included only those reporting as hospital providers. Medical practice providers were reported as doctor's offices or practices, health centers, urgent care, or Indian Health Service. Pharmacy sites were reported as retail pharmacy or other pharmacy sites. Sites categorized as unknown/other were either reported as home health, other, or no selection.

To calculate isochrones (areas from which a site can be reached within a specific travel time) for each provider site we used OpenRouteService (https://openrouteservice.org), an open-source global spatial routing service. We obtained the latest OpenStreetMaps road data for the United States (https://planet.openstreetmap.org) from Geofabrik (http://www.geofabrik.de). We deployed OpenRouteService locally on Docker, a containerization platform for creating and running applications, and accessed it through Quantum GIS (http://www.qgis.org) via

the OpenRouteService Tools plugin (*22*,*23*). We generated isochrones around each site for walking and driving with the time thresholds of 15, 30, 45, and 60 minutes. We calculated walking and driving travel speeds by using the OpenRouteService algorithm, which is described in their documentation. For the underlying US adult population raster layer, we obtained 2019 US population estimates for female/male ≥15-year age bands constrained to built settlements from WorldPop and aggregated the data in Python (*24*,*25*). We then calculated site accessibility by overlaying the isochrone contours on top of the population layer and using zonal statistics in Quantum GIS to determine the population residing within the isochrones (Figure 1).

We evaluated accessibilities for US adults living at different community social vulnerability levels and urbanicity by using the CDC/Agency for Toxic Substances and Disease Registry Social Vulnerability Index (SVI), a composite index based on 15 US Census variables grouped by socioeconomic status, household composition and disability, minority status and language, and housing and transportation (*26*). The most recent SVI was released in 2018, and the range was 0–1, with 1 representing the highest vulnerability (*26*). High SVI was defined as an overall SVI >0.5 and was used as a filter for the population residing in those areas.

The National Center for Health Statistics Urban-Rural Classification Scheme for 2013 classified counties into 1 of 6 categories: large central metropolitan, large fringe metropolitan, medium metropolitan, small metropolitan, micropolitan, and noncore (core urban population <10,000) (*27*). We aggregated the adult population for each of these urban/rural areas and calculated accessibilities by using the same isochrones generated previously.

Results

The total number of active provider sites for the study period was 131,951. There were 57,064 pharmacy sites, 35,728 medical practice sites, 10,606 community

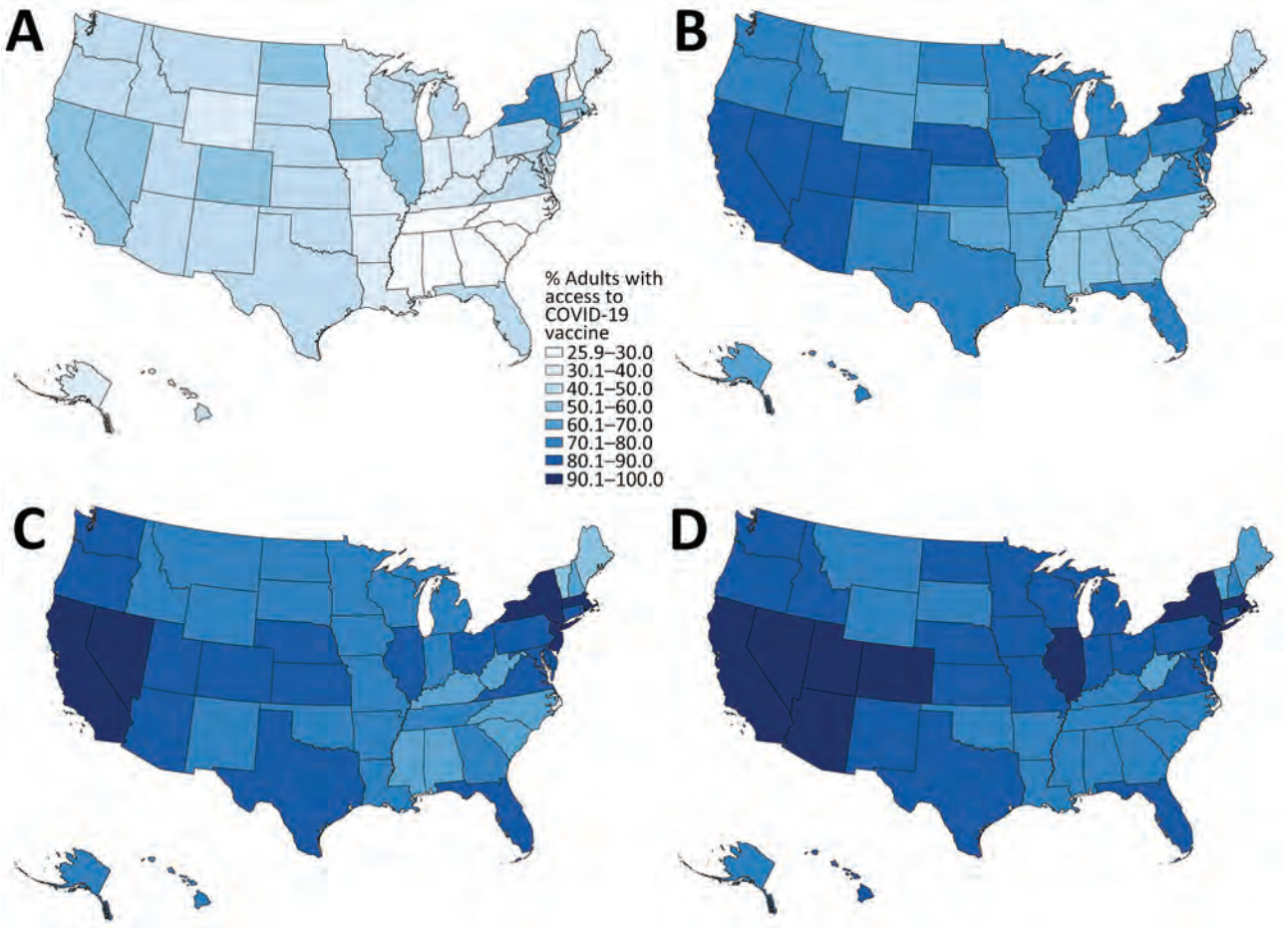

Figure 3. Walking accessibility for COVID-19 vaccination sites, by state, United States, December 11, 2020–March 29, 2022: A) 15 minutes; B) 30 minutes; C) 45 minutes; D) 60 minutes.

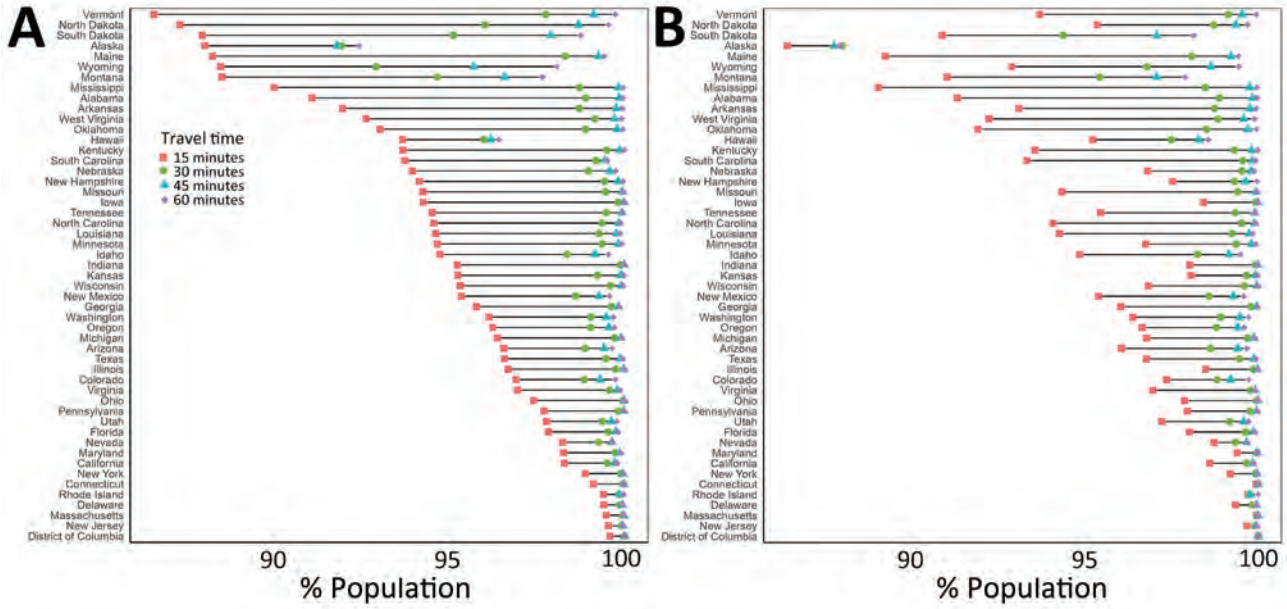

Figure 4. Adult COVID-19 vaccination site accessibility according to driving time in 15-minute intervals, by state, United States, December 11, 2020–March 29, 2022. A) Overall accessibility; B) accessibility for areas with high scores on the Centers for Disease Control and Prevention/Agency for Toxic Substances and Disease Registry Social Vulnerability Index.

health sites, 5,222 hospitals, and 23,331 unknown or other provider site type (Appendix Figure 2).

National walking accessibilities (the proportion of the population within the stated travel time areas) were found to be 46.6% within 15 minutes, 74.8% within 30, 82.8% within 45 minutes, and 86.7% within 60 minutes. The national driving accessibilities for those times were 96.5%, 99.4%, 99.7%, and 99.8%, respectively (Figures 2–5).

When we limited the population to persons residing in high SVI areas, sites were accessible within a 15-minute walk for 55.3% of the population, 30-minute walk for 81.1%, 45-minute walk for 86.7%, and 60-minute walk for 89.4%; accessibilities for those same times by driving were 97.0%, 99.5%, 99.8%, and 99.9%, respectively (Figures 2, 4). Overall, accessibility was greater in high-SVI areas than in the entire area.

Accessibility tended to improve with increasing urbanicity of the location of provider sites. The noncore walking accessibilities ranged from 15 minutes (27.2%) to 60 minutes (52.7%), and accessibilities for large central metropolitan areas ranged from 65.1% to 97.7%. Driving accessibility ranges were 79.9%–99.0% for noncore and 99.5%–99.9% for large central metropolitan areas (Figure 6).

Discussion

With this study, we estimated a range of accessibilities to COVID-19 vaccination sites for US adults: 46.6% of US adults were within a 15-minute walk to a COVID-19 vaccine provider site, which increased to 86.7% for a 60-minute walk. Accessibility increased further, to 96.5%, for a 15-minute drive. Although access tended to be greater than or equal for high-SVI areas compared with the entire jurisdiction, jurisdictional and urban/rural variations suggest potential inequalities with regard to access. Although we do not attempt to say what the accessibility target should be for each area, future public health campaigns should factor these perspectives into planning.

Given that driving has the potential to greatly increase accessibility, making motorized transportation more readily available to areas in which walking times are high should be considered. Despite rural counties having more households with cars, large numbers of zero-car ownership households depend on underfunded public transportation systems (*28*,*29*). Vaccine transportation programs such as MyTurn (https://myturn.ca.gov) and those offered by rideshare services such as Uber and Lyft were initiated as part of the response, but whether they are situated for maximum effect could be a topic for another study (*30*,*31*). Conversely, another perspective worth investigating is strategic placement of vaccination sites, such as mobile clinics or temporary vaccination sites for walking.

Our analysis considers only 2 travel modalities: walking and driving. We acknowledge that those modalities might not be suitable or preferred by everyone. For example, the average travel time for a person

requiring use of a wheelchair may be greater than the walking speeds calculated by using the OpenRoute Service algorithm. Public transportation, another common mode of travel, can vary according to traffic conditions and whether dedicated travel lanes are available. Nonetheless, walking and driving should give a reasonable range with regard to accessibility of the vaccine.

Among potential limitations of the provider list, not all vaccine provider sites are equally accessible to the public. Provider sites may have policies that restricted access to specific groups of persons or hours of operation that may have excluded persons. Some sites may not be accessible at all because our selection criteria capture sites that are not intended for vaccine administration, such as distribution hubs. Our study assessed only accessibility of static sites and did not consider mobile vaccination clinics or services that provide in-home vaccination. Our study reports the cumulative list of active provider sites, including sites that were not active during the entire period, such as mass vaccination sites operational only during the early months of the vaccination campaign. Site inactivation is a relevant consideration; a recent study has shown how closures can result in heavy losses of access resulting from increased driving travel times in the more rural parts of the country (*32*). Furthermore, our analysis did not account for characteristics of the provider vaccine supply, such as availability of specific vaccines or vaccine stockouts during the study period. The criteria for being an active provider depend on accurate data. The Tiberius platform data are frequently updated, and provider data can be updated days or even weeks later. Although the provider list was pulled well after the close of the study period, those delays could still shift the number of providers flagged as active, depending on the time of data export.

Another limitation is that our analysis evaluated only proximity to a vaccine provider site via established road networks. OpenStreetMaps is an open-sourced project, and although the project is regularly updated by independent contributors, there may be network gaps such as informal roads or hidden back roads. In addition, connecting isochrone endpoints

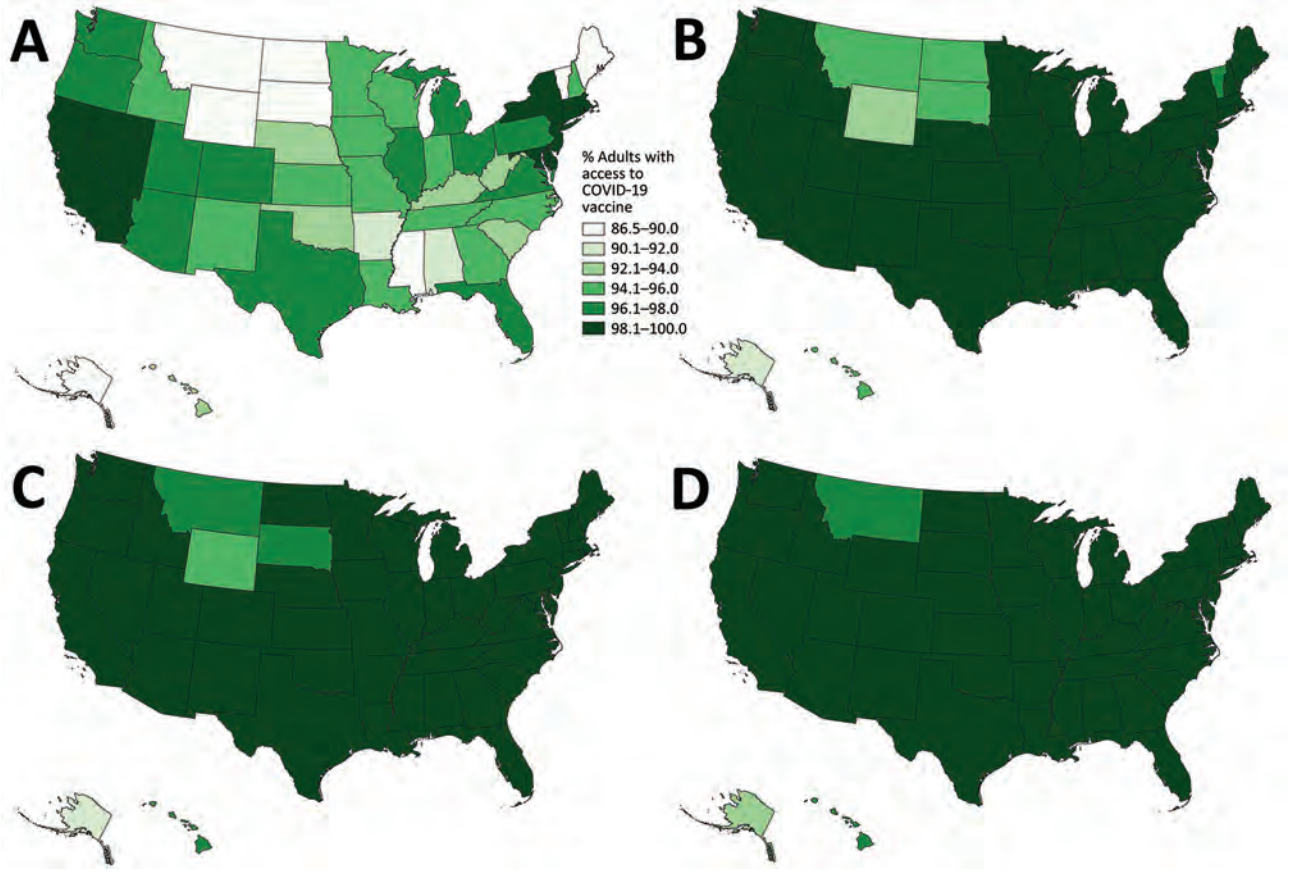

Figure 5. Driving accessibility for COVID-19 vaccination site, by state, United States, December 11, 2020–March 29, 2022: A) 15 minutes; B) 30 minutes; C) 45 minutes; D) 60 minutes.

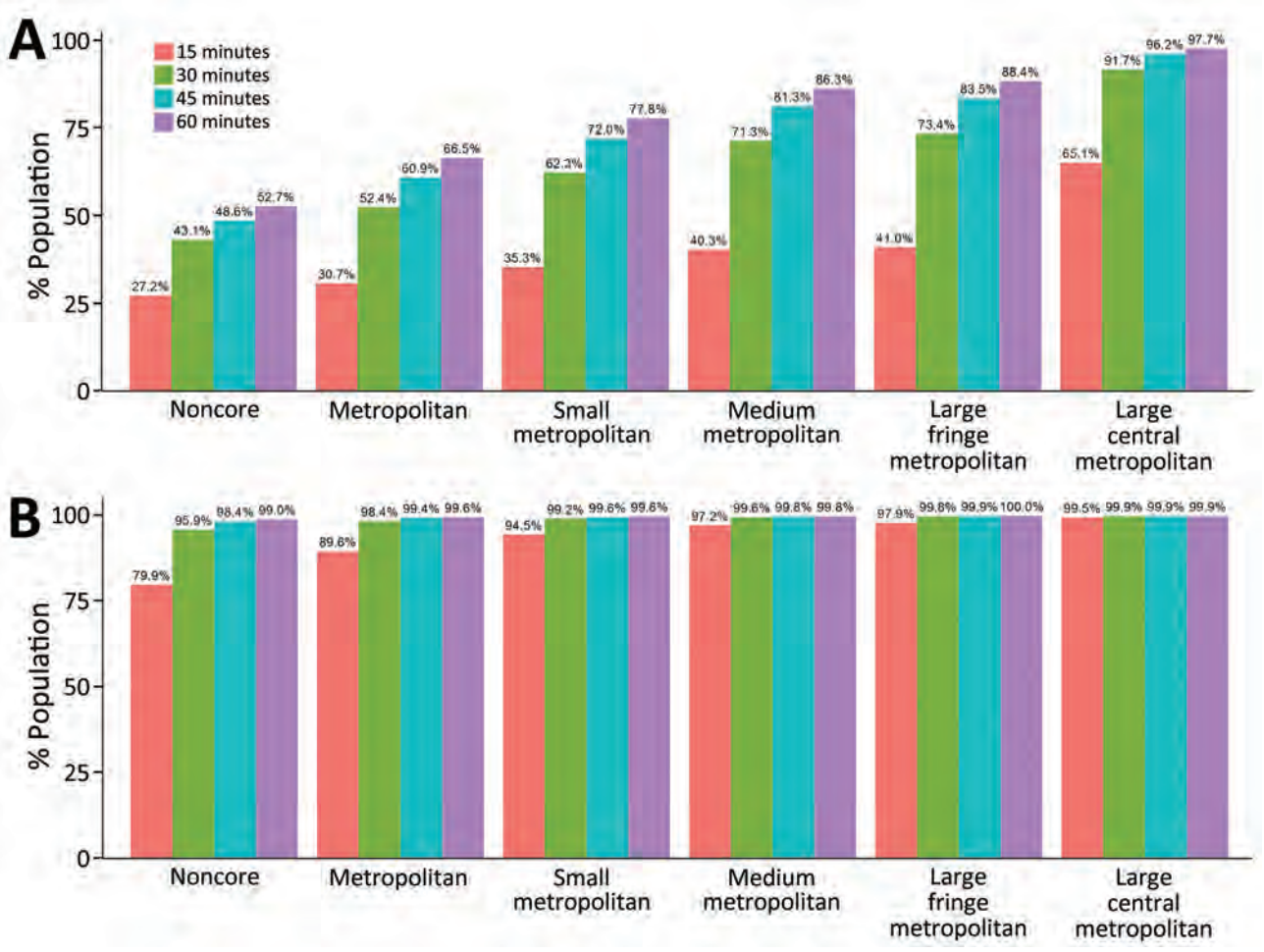

Figure 6. Adult COVID-19 vaccination site accessibility by 2013 Centers for Disease Control and Prevention Urban-Rural Classification, United States, December 11, 2020–March 29, 2022. A) Walking accessibility; B) driving accessibility.

on road networks can produce minor differences in the polygon contours, depending on the method used. Numerous resources compare results between different routing services (*33*).

One more limitation was timeliness of the geospatial data sources. Worldpop estimates were produced in 2019; the CDC/Agency for Toxic Substances and Disease Registry SVI in 2018; and the National Center for Health Statistics Urban/Rural Classification Scheme in 2013 (*24*,*26*,*27*). Furthermore, we used population estimates for persons ≥15 years of age to approximate those eligible for the vaccine within the study period as well as those able to drive. Those estimates may overestimate the driving accessibility for some jurisdictions because driving age does not start at age 15 for all states. Because the estimates were produced in 2019, at the time of our analysis, the entire estimated population would be a few years older (more persons ≥15 years of age), better estimating the driving population during the study. Researchers using our methods should consider the timeliness of their data sources and should either contact the data providers directly or use estimation methods if data sources are out of date. Despite those limitations, we assert the value of our methods and results for vaccine planning purposes.

Our article addresses only the issue of physical access, but accessibility itself is a multifaceted concept. For example, Levesque et al. developed a framework with 5 dimensions of accessibility: approachability, acceptability, availability and accommodation, affordability, and appropriateness (*34*). Although we have explored some aspects of availability and accommodation, future work could focus on evaluating accessibility along these other dimensions.

In conclusion, the initial US COVID-19 vaccination campaign was a monumental logistical undertaking resulting in deliveries of ≈700 million doses to fully vaccinate ≈75% of US adults by the end of the study period. Despite that achievement, our analysis

has identified potential areas for improvement at the national, jurisdiction, and urban/rural levels. Our findings highlight the value of evaluating accessibility at different levels for vaccine planning.

US COVID-19 data can be accessed via the CDC COVID Data Tracker (https://covid.cdc.gov/covid-data-tracker/#datatracker-home). Map data copyrighted OpenStreetMap contributors are available from https://www.openstreetmap.org. No chatbot or artificial intelligence tool was used for any portion of this work.

Acknowledgments

We acknowledge the 62 participating jurisdictions, 21 federal retail pharmacy program partners, and federal entities (Indian Health Services, Health Resources and Services Administration, US Department of Defense, Veterans Health Administration, US Department of State); the CDC COVID-19 Emergency Response Vaccine Task Force, Countermeasures Acceleration Group; and the US Department of Health and Human Services Coordination Operations and Response Element team.

R.Y. and D.C. wrote the main manuscript text, including the figures. All authors reviewed the manuscript.

About the Author

Mr. Yee is a data scientist with the CDC Center for Global Health Division of Global HIV & TB. His research interests include data analytics, mathematical modeling, and capacity building.

References

1. Food and Drug Association. Pfizer-BioNTech COVID-19 vaccine [cited 2022 Oct 31]. https://www.fda.gov/emergency-preparedness-and-response/coronavirus-disease-2019-covid-19/pfizer-biontech-covid-19-vaccines
2. US Department of Health and Human Services. COVID-19 vaccines [cited 2022 Oct 31]. https://www.hhs.gov/coronavirus/covid-19-vaccines/index.html
3. Food and Drug Association. COVID-19 vaccines [cited 2022 Oct 30]. https://www.fda.gov/emergency-preparedness-and-response/coronavirus-disease-2019-covid-19/covid-19-vaccines
4. Centers for Disease Control and Prevention. COVID-19 vaccinations in the United States, jurisdiction [cited 2022 Oct 30]. https://data.cdc.gov/Vaccinations/COVID-19-Vaccinations-in-the-United-States-Jurisdi/unsk-b7fc
5. Office of the Assistant Secretary for Planning and Evaluation. Overview of barriers and facilitators in covid-19 vaccine outreach [cited 2022 Oct 31]. https://aspe.hhs.gov/reports/covid-19-vaccine-outreach
6. Centers for Disease Control and Prevention. Ensuring equitable COVID-19 vaccine access for older adults and people with disabilities [cited 2022 Aug 23]. https://www.cdc.gov/vaccines/covid-19/clinical-considerations/older-adults-and-disability/access.html
7. Centers for Disease Control and Prevention. What to consider when planning COVID-19 vaccination sites [cited 2022 Oct 31]. https://www.cdc.gov/vaccines/covid-19/planning/index.html
8. Centers for Disease Control and Prevention. Health equity [cited 2022 Oct 31]. https://www.cdc.gov/coronavirus/2019-ncov/community/health-equity/cdc-strategy.html
9. US Department of Health and Human Services. Guidance on federal legal standards prohibiting race, color and national origin discrimination in COVID-19 vaccination programs [cited 2022 Oct 31]. https://www.hhs.gov/civil-rights/for-providers/civil-rights-covid19/guidance-federal-legal-standards-covid-19-vaccination-programs/index.html
10. The White House. American Rescue Plan [cited 2022 Oct 30]. https://www.whitehouse.gov/american-rescue-plan
11. The White House. COVID-19 [cited 2022 Oct 30]. https://www.whitehouse.gov/priorities/covid-19
12. The White House. National COVID-19 Preparedness Plan [cited 2022 Oct 30]. https://www.whitehouse.gov/covidplan
13. Lovett A, Haynes R, Sünnenberg G, Gale S. Car travel time and accessibility by bus to general practitioner services: a study using patient registers and GIS. Soc Sci Med. 2002;55:97–111. https://doi.org/10.1016/S0277-9536(01)00212-X
14. Todd A, Copeland A, Husband A, Kasim A, Bambra C. Access all areas? An area-level analysis of accessibility to general practice and community pharmacy services in England by urbanity and social deprivation. BMJ Open. 2015;5:e007328. https://doi.org/10.1136/bmjopen-2014-007328
15. Fletcher-Lartey SM, Caprarelli G. Application of GIS technology in public health: successes and challenges. Parasitology. 2016;143:401–15. https://doi.org/10.1017/S0031182015001869
16. Wigley AS, Tejedor-Garavito N, Alegana V, Carioli A, Ruktanonchai CW, Pezzulo C, et al. Measuring the availability and geographical accessibility of maternal health services across sub-Saharan Africa. BMC Med. 2020;18:237. https://doi.org/10.1186/s12916-020-01707-6
17. Sahar L, Douangchai Wills VL, Liu KK, Kazerooni EA, Dyer DS, Smith RA. Using geospatial analysis to evaluate access to lung cancer screening in the United States. Chest. 2021;159:833–44. https://doi.org/10.1016/j.chest.2020.08.2081
18. Whitehead J, Scott N, Carr PA, Lawrenson R. Will access to COVID-19 vaccine in Aotearoa be equitable for priority populations? N Z Med J. 2021;134:25–35.
19. Mollalo A, Mohammadi A, Mavaddati S, Kiani B. Spatial analysis of COVID-19 vaccination: a scoping review. Int J Environ Res Public Health. 2021;18:12024. https://doi.org/10.3390/ijerph182212024
20. Duffy C, Newing A, Górska J. Evaluating the geographical accessibility and equity of COVID-19 vaccination sites in England. Vaccines (Basel). 2021;10:50. https://doi.org/10.3390/vaccines10010050
21. Muchiri SK, Muthee R, Kiarie H, Sitienei J, Agweyu A, Atkinson PM, et al. Unmet need for COVID-19 vaccination coverage in Kenya. Vaccine. 2022;40:2011–9. https://doi.org/10.1016/j.vaccine.2022.02.035
22. Merkel D. Docker: lightweight linux containers for consistent development and deployment [cited 2022 Oct 30]. https://www.seltzer.com/margo/teaching/CS508.19/papers/merkel14.pdf

23. Nolde N. ORS Tools QGIS plugin [cited 2022 Oct 30]. https://github.com/GIScience/orstools-qgis-plugin
24. WorldPop. Open spatial demographic data and research [cited 2022 Oct 30]. https://www.worldpop.org
25. Python Software Foundation. The Python language reference [cited 2022 Oct 30]. https://docs.python.org/3/reference/index.html.
26. Agency for Toxic Substances and Disease Registry. CDC/ATSDR Social Vulnerability Index [cited 2022 Oct 30]. https://www.atsdr.cdc.gov/placeandhealth/svi/index.html
27. Ingram DD, Franco SF. NCHS Urban-Rural Classification Scheme for Counties. National Center for Health Statistics. Vital Health Stat 2. 2014:1–73.
28. Pucher J, Renne JL. Urban-rural differences in mobility and mode choice: evidence from the 2001 NHTS [cited 2022 Oct 30]. https://vtc.rutgers.edu/wp-content/uploads/2014/04/Articles.Urban-Rural_differences.pdf
29. US Department of Agriculture. Rural transportation at a glance [cited 2022 Oct 30]. https://www.ers.usda.gov/publications/pub-details/?pubid=42594
30. Lyft. Millions of people can't get to their vaccine. Let's pick them up [cited 2022 Oct 31]. https://lyft.com/vaccine-access
31. Uber. Rides for vaccines [cited 2022 Oct 31]. https://www.uber.com/us/en/impact/rides-for-vaccines
32. McCarthy S, Moore D, Smedley WA, Crowley BM, Stephens SW, Griffin RL, et al. Impact of rural hospital closures on health-care access. J Surg Res. 2021;258:170–8. https://doi.org/10.1016/j.jss.2020.08.055
33. Riccardo. Comparing isochrone APIs: an insight into different providers [cited 2022 Oct 30]. https://digital-geography.com/comparing-isochrone-apis-an-insight-into-different-providers
34. Levesque JF, Harris MF, Russell G. Patient-centred access to health care: conceptualising access at the interface of health systems and populations. Int J Equity Health. 2013;12:18. https://doi.org/10.1186/1475-9276-12-18

Address for correspondence: Randy Yee, Centers for Disease Control and Prevention, 1600 Clifton Rd NE, Mailstop H21-6, Atlanta, GA 30329-4018, USA; email: pcx5@cdc.gov

SARS-CoV-2 Transmission in Alberta, British Columbia, and Ontario, Canada, January 2020–January 2022

Aubrey D. Kehoe,[1] Arshpreet Kaur Mallhi,[1] Charles R. Barton,[2] Hunter M. Martin,[2] Christopher M. Turner,[2] Xinyi Hua, Kin On Kwok, Gerardo Chowell, Isaac Chun-Hai Fung

We estimated COVID-19 transmission potential and case burden by variant type in Alberta, British Columbia, and Ontario, Canada, during January 23, 2020–January 27, 2022; we also estimated the effectiveness of public health interventions to reduce transmission. We estimated time-varying reproduction number (R_t) over 7-day sliding windows and nonoverlapping time-windows determined by timing of policy changes. We calculated incidence rate ratios (IRRs) for each variant and compared rates to determine differences in burden among provinces. R_t corresponding with emergence of the Delta variant increased in all 3 provinces; British Columbia had the largest increase, 43.85% (95% credible interval [CrI] 40.71%–46.84%). Across the study period, IRR was highest for Omicron (8.74 [95% CrI 8.71–8.77]) and burden highest in Alberta (IRR 1.80 [95% CrI 1.79–1.81]). Initiating public health interventions was associated with lower R_t and relaxing restrictions and emergence of new variants associated with increases in R_t.

Emergence of SARS-CoV-2 in 2019 resulted in the COVID-19 pandemic (*1*). Since then, the virus has mutated into multiple variants. Each variant differed in transmissibility and severity of health outcomes, leading to differences in incident case and death counts in different regions (*2*,*3*). COVID-19 transmission rates vary depending on multiple factors, including public health policies and characteristics of emerging variants. Interventions such as working from home, school closures, face mask mandates, and vaccination were implemented as efforts to control the pandemic.

Various studies have evaluated the effectiveness of pandemic interventions in Canada (*4*–*7*). Indoor mask mandates were found to be associated with weekly decreases of 22% in case counts (*4*). Physical distancing was found to effectively mitigate COVID-19 spread in Ontario (*5*). The mitigating effect of stay-at-home policies on COVID-19 spread in Toronto was also reported (*7*). Most of the previous studies conducted on populations in Canada have evaluated COVID-19 preventive measures in a single city or province or evaluated only 1 or 2 preventive measures. Limited research has been conducted comparing the additive mitigating effects of prevention and control measures among major provinces in Canada. With the exception of a few studies focused mainly on COVID-19 vaccine effectiveness, little research has examined the effects of initiating public health interventions or the emergence of new variants on COVID-19 transmission potential and disease burden in Canada (*8*,*9*). Moreover, differences in time-varying reproduction number (R_t) and incidence rate ratio (IRR) associated with specific SARS-CoV-2 variants have yet to be explored among populations in Canada. A 2020 study calculated IRR to compare disease burden across 3 provinces (*10*); however, variant-specific comparisons have yet to be explored.

We addressed 2 of those research questions in this study. First, we investigated transmission potential

Author affiliations: Georgia Southern University Jiann-Ping Hsu College of Public Health, Statesboro, Georgia, USA (A.D. Kehoe, A.K. Mallhi, C.R. Barton, H.M. Martin, C.M. Turner, X. Hua, I.C.-H. Fung); Chinese University of Hong Kong JC School of Public Health and Primary Care, Hong Kong (K.O. Kwok); Georgia State University School of Public Health, Atlanta, Georgia, USA (G. Chowell)

DOI: https://doi.org/10.3201/eid3005.230482

[1]These first authors contributed equally to this article.

[2]These second authors contributed equally to this article..

and case burden associated with wild-type, Alpha, Delta, and Omicron SARS-CoV-2 variants in Alberta, British Columbia, and Ontario. Second, we investigated the effectiveness of public health interventions to reduce SARS-CoV-2 transmission potential in those 3 provinces. The Georgia Southern University institutional review board determined that this project (H20364) did not involve human subjects under the G8 exemption category of Code of Federal Regulations Title 45, Part 46.

Methods

Data Acquisition

We downloaded and analyzed publicly available COVID-19 case data from Ontario, British Columbia, and Alberta. Data from Ontario, which is divided into 6 subprovincial public health regional areas—Central, East, North-East, North-West, Toronto, and West—came from 1,033,294 cases reported during January 23, 2020–January 27, 2022 (Appendix Table 1, https://wwwnc.cdc.gov/EID/article/30/5/23-0482-App1.pdf) (*11*,*12*). Data from British Columbia, which is divided into 5 subprovincial regional health authorities—Fraser, Interior, Northern, Vancouver Coastal, and Vancouver Island—came from 320,540 cases reported during January 29, 2020–January 27, 2022 (Appendix Table 2) (*13*,*14*). Data from Alberta, which is divided into 5 subprovincial health services zones—Calgary, Central, Edmonton, North, and South—came from 487,045 cases during March 6, 2020–January 27, 2022 (Appendix Table 3) (*15*,*16*).

We obtained information from the government of Canada, the Canadian Institute for Health Information, and the Upper Canada District School Board websites on COVID-19 policies, including descriptions and dates of implementation and relaxation (Appendix Table 4) (*17*–*19*). In addition to the policy timepoints, we recorded dates of incidence spikes because of Delta and Omicron variants, chosen to represent the beginning of the time period when emergence of the variant resulted in increases in case counts and R_t (Appendix Table 4). Through this analysis, we aimed to examine the effect on R_t of mitigation policies and emergence of highly transmissible variants. We used the Government of Canada website (*20*) as the source for data on COVID-19 variants, including weekly percentages for each identified variant among all cases for which samples were sequenced. Percentages represented the weekly distribution of confirmed cases by variant. We multiplied daily case counts by weekly variant percentages to estimate daily cases attributed to each variant (Appendix).

Statistical Analysis

We presented epidemic curves of weekly incident case count by province according to age group, sex, and public health district and $\log_{10}$-transformed monthly cumulative case counts in maps at the subprovincial level. Basic reproduction number (R_0) is the average number of secondary cases of an infectious disease infected by the primary case-patient in a totally susceptible population (*21*). R_t, which is the expected number of new cases attributed to 1 infected person, changes over time because of public health interventions and the changing proportion of the population with immunity against the infection. An R_t >1 indicates epidemic growth, whereas R_t <1 indicates epidemic decline (*22*).

We used the R package EpiEstim (The R Project for Statistical Computing, https://cran.r-project.org/web/packages/EpiEstim/index.html) to estimate R_t from incident COVID-19 case counts in Ontario, British Columbia, and Alberta. R_t is estimated by calculating the ratio between the number of incident cases at time t and the total infectiousness of all infected persons at that same time (*23*,*24*). We specified a mean serial interval (SI) distribution of 4.60 d (SD *5.55 d) for the analysis (25*). We generated 2 forms of R_t: a 7-day sliding-window R_t and a policy change R_t over nonoverlapping time-windows. The 7-day sliding-window R_t estimate is an average of daily R_t estimates over a sliding-window time period comprising the current day and the 6 immediately previous days; therefore, each daily R_t estimate is included in 7 different estimates. The policy change R_t is an average of daily R_t estimates over a nonoverlapping time-window in which each daily R_t is included in only 1 estimate. We conducted a sensitivity analysis of provincial-level R_t estimates that incorporated uncertainty associated with underreporting of infections. We calculated R_t using estimated infection counts assuming averages from one sensitivity analysis using a multiplier of 4 (*26*) and another using a multiplier of 11 (*27*) infected persons reported as case-patients.

To calculate incidence rates, we divided cumulative case counts by observed person-time data and multiplied by 100,000. Person-time observed was the product of the estimated population size in 2021 (*28*) and the number of days observed by province, variant, or both. We stratified incidence rates over the entire study period and IRR by sex, age, and variant for each province (Appendix). We analyzed data using R version 4.2.2 (https://cran.r-project.org/bin/windows/base/old/4.2.2).

Results

Descriptive Statistics and R_t by Province

Ontario

Ontario experienced 3 major pandemic waves during our study period; more substantial case burdens occurred in metropolitan areas. The first surge, which peaked in December 2020, was attributed to wild-type virus; the second surge, peaking in April 2021, was mainly from Alpha; and the third, peaking in December 2021, was mainly from Omicron (Figure 1; Appendix Figures 1, 2). Unlike British Columbia and Alberta, Ontario did not experience a surge because of Delta; when the Delta variant became the dominant strain in June 2021, the daily incident case count remained stable and Delta did not cause any major surges during June–December 2021, after which the Omicron variant became dominant (Figure 1). Corresponding to the sustained transmission presented in the epidemic curves, R_t was >1 during August–September 2020, February–April 2021, July–August 2021, and November–December 2021. Except for February and March 2020, R_t was not >2. Sensitivity analysis using estimated infection counts generated similar R_t trends but with a wider 95% credible interval (CrI) that included 1 throughout much of the study period time frame (Appendix Figure 3).

The policy change R_t fluctuated throughout the study period with implementation of policies and emergence of new variants (Figure 1; Table 1). Before policies were implemented, a median R_t of 1.64 (95% CrI 1.52–1.76) was observed. Initiating school closures in March 2020 (policy A), recommendation of face coverings (policy B), partial school reopening after Christmas/New Year holiday break (policy E), school closures in April 2021 (policy F), and required vaccination for government workers (policy H) were associated with decreased median R_t, whereas relaxation of policies such as phased school reopening (policy

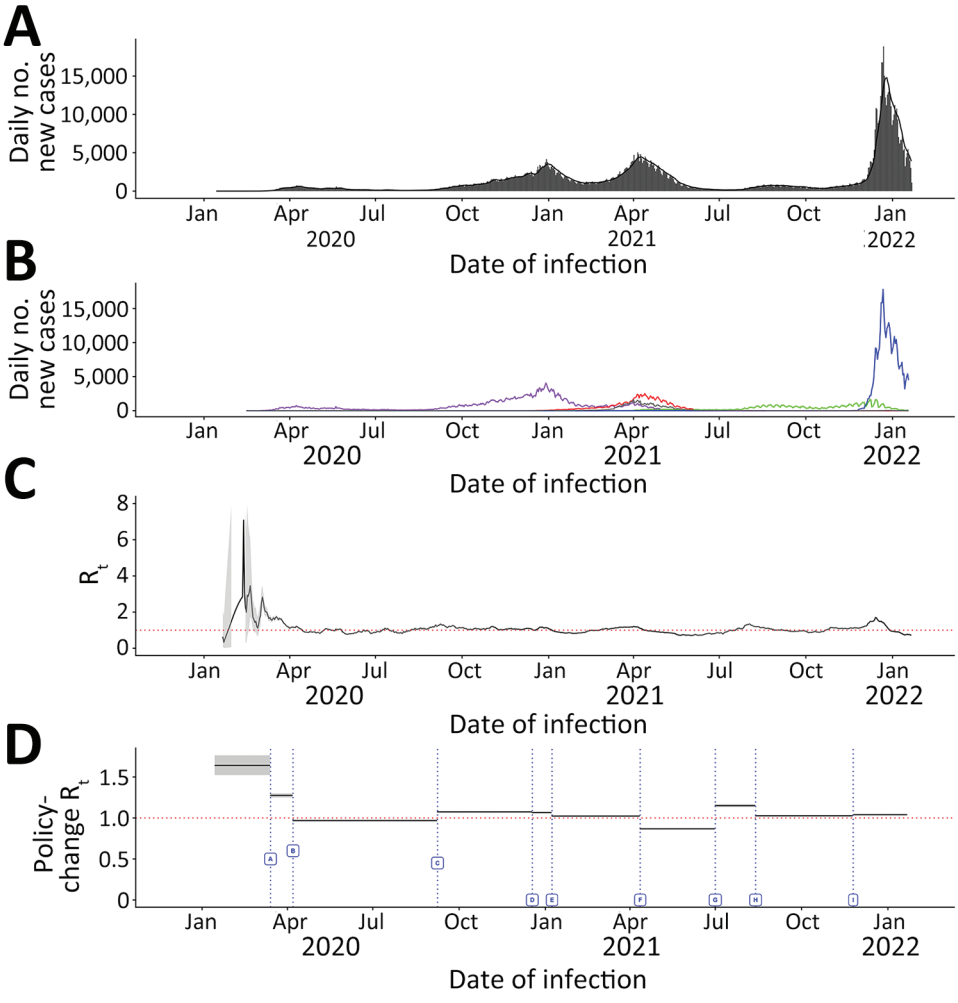

Figure. Daily incident COVID-19 case count and 7-day moving average Rt, by date of infection and policy-change Rt or new variants by initiation dates, Ontario, Canada, January 23, 2020–January 27, 2022. Dates are assumed infection dates (i.e., report date minus 9 days); red dotted lines in panels C and D indicate Rt = 1. A, B) Incident case count by date of infection for all variants combined (A) and by variant type (B). Colors indicate COVID-19 variants: purple, wild-type; red, Alpha; green, Delta; blue, Omicron; and gray, other variants. C) Seven-day moving average Rt by date of infection. D) Policy-change Rt. Policy changes or detection of new variations by dates of initiation: A, school closure (March 14, 2020); B, recommendation for use of face masks (April 7, 2020); C, phased school reopening (September 8, 2020); D, priority populations vaccination rollout (December 18, 2020); E, partial school reopening (January 8, 2021); F, school closure (April 12, 2021); G, increase in cases because of Delta COVID-19 variant (July 1, 2021); H, requirement of vaccination for federal workers (August 13, 2021); I, increase in cases because of the Omicron COVID-19 variant (November 25, 2021).

Table 1. Estimates for median R_t and percentage change in R_t after implementation of policies and the emergence of COVID-19 variant in 3 provinces of Canada (Ontario, British Columbia, and Alberta) during January 23, 2020–January 27, 2022*

Policy/variant	Median R_t (95% credible interval)	% Change (95% credible interval)
Ontario		
Policy label/emergent variant†		
Before A	1.641 (1.523–1.764)	Not applicable
A→B	1.275 (1.249–1.301)	−22.426 (−28.083 to −16.190)
B→C	0.968 (0.958–0.979)	−24.008 (−25.597 to −22.302)
C→D	1.075 (1.069–1.081)	10.964 (9.753–12.243)
D→E	1.066 (1.058–1.074)	−0.828 (−1.733–0.131)
E→F	1.023 (1.019–1.028)	−4.021 (−4.854 to −3.145)
F→G	0.867 (0.862–0.872)	−15.232 (−15.841 to −14.556)
G→H	1.150 (1.130–1.170)	32.629 (30.223–35.067)
H→I	1.027 (1.019–1.035)	−10.789 (−12.515 to −9.077)
After I	1.040 (1.036–1.043)	1.296 (0.440–2.094)
British Columbia		
Policy label/emergent variant†		
Before A	1.641 (1.505–1.784)	Not applicable
A→B	0.945 (0.889–1.004)	−42.558 (−48.205 to −35.902)
B→C	1.069 (1.043–1.096)	13.263 (5.929–21.413)
C→D	1.042 (1.032–1.052)	−2.577 (−5.004–0.087)
D→E	1.007 (0.989–1.026)	−3.333 (−5.309 to −1.139)
E→F	1.036 (1.028–1.044)	2.802 (0.796–4.972)
F→G	0.862 (0.852–0.873)	−16.787 (−17.974 to −15.455)
G→H	1.240 (1.218–1.262)	43.849 (40.706–46.835)
H→I	0.984 (0.976–0.992)	−20.725 (−22.297 to −19.154)
After I	1.075 (1.069–1.082)	9.364 (8.235–10.445)
Alberta		
Policy label/emergent variant†		
Before A	1.815 (1.614–2.031)	Not applicable
A→B	1.187 (1.130–1.245)	−34.710 (−42.227 to −25.800)
B→C	1.021 (1.004–1.038)	−13.898 (−17.841 to −9.344)
C→D	1.056 (1.049–1.063)	3.467 (1.733–5.358)
D→E	0.945 (0.932–0.958)	−10.522 (−11.882 to −9.013)
E→F	1.049 (1.040–1.057)	10.925 (9.174–12.810)
F→G	0.906 (0.898–0.913)	−13.657 (−14.622 to −12.595)
G→H	1.270 (1.246–1.294)	40.273 (37.563–42.923)
H→I	0.989 (0.982–0.995)	−22.172 (−23.655 to −20.689)
After I	1.101 (1.095–1.106)	11.385 (10.452–12.280)

*Calculations performed by using the instantaneous reproduction number method as implemented in the R package EpiEstim (The R Foundation for Statistical Computing, https://www.r-project.org). The analysis used a γ-distributed serial interval (mean 4.60 days; SD 5.55 days; $\alpha = 0.05$). R_t, time-varying reproduction number.
†The labels are defined in the text and in the captions of Figures 1–3.

C) were associated with increased median R_t. Emergence of Delta (denoted by G) and Omicron variants (denoted by I) were associated with increased median R_t. Implementation of vaccination rollout for priority populations (policy D) was not associated with any change in median R_t. In Ontario, the most significant increase in R_t, 32.63% (95% CrI 30.22%–35.07%), was observed after the Delta variant emerged. In contrast, the greatest decrease in R_t, −24.01% (95% CrI −25.60% to −22.30%), was observed after the face covering recommendation took effect. The lowest median R_t, 0.87 (95% CrI, 0.86–0.87), during the study period was observed after school closures in April 2021.

British Columbia

British Columbia experienced 4 major pandemic waves during our study period with greater case burden in metropolitan areas. The first surge, peaking in November 2020, was attributed to wild-type virus; the second, peaking in April 2021, mainly to Alpha; the third, peaking in September 2021, to Delta; and the fourth, peaking in December 2021, to Omicron (Figure 2; Appendix Figures 4, 5). The case counts during the Omicron surge in early December 2021 were substantially higher than during preceding months. During July–November 2020, July–August 2021, and December 2021, British Columbia experienced elevated R_t values of 1–2 (Appendix Figure 6).

As in Ontario, the median policy change R_t in British Columbia fluctuated as policies were implemented or rescinded and with emergence of new variants (Figure 2; Table 1). From the early cases to the day before school closure in March 2020, a median R_t of 1.64 (95% CrI 1.51–1.78) similar to R_t in Ontario was observed. In British Columbia, initiating school closures in March 2020 and April 2021, rollout of vaccination for priority populations and required vaccination for government workers were policies associated with decreased median

R_t. In contrast, phased school reopening was associated with increased R_t. In contrast to Ontario and Alberta, in British Columbia initiating recommendation of face coverings was associated with slightly increased R_t, and partial school reopening after the holiday break did not substantially affect R_t. Delta and Omicron emergence led to increased R_t. As for Ontario, British Columbia also experienced the greatest increase in R_t, 43.85% (95% CrI 40.71%–46.84%) after Delta emerged. The greatest decrease in R_t, −42.56% (95% CrI −48.21% to −35.90%), was observed after school closures in March 2020. The lowest median R_t, 0.86 (95% CrI 0.85–0.87) was achieved after school closures in April 2021.

Alberta

Similar to British Columbia, Alberta experienced 4 major pandemic waves with greater case burden in metropolitan areas. The first surge, peaking in November 2020, was attributed to wild-type virus; the second, peaking in April 2021, mainly to Alpha; the third, peaking in September 2021, to Delta; and the fourth, peaking in January 2022, to Omicron (Figure 3; Appendix Figures 7, 8). As in other provinces, Omicron led to the highest R_t in Alberta during the study period. During September–December 2020, March–May 2021, July–September 2021, and January 2022, Alberta experienced rising transmission rates peaking with R_t values of 1–2 (Appendix Figure 9).

Fluctuations in median policy change R_t in Alberta followed a trend similar to those observed in Ontario and British Columbia (Figure 3; Table 1). In Alberta, at the beginning of the study period, median R_t was 1.82 (95% CrI 1.61–2.03), higher than

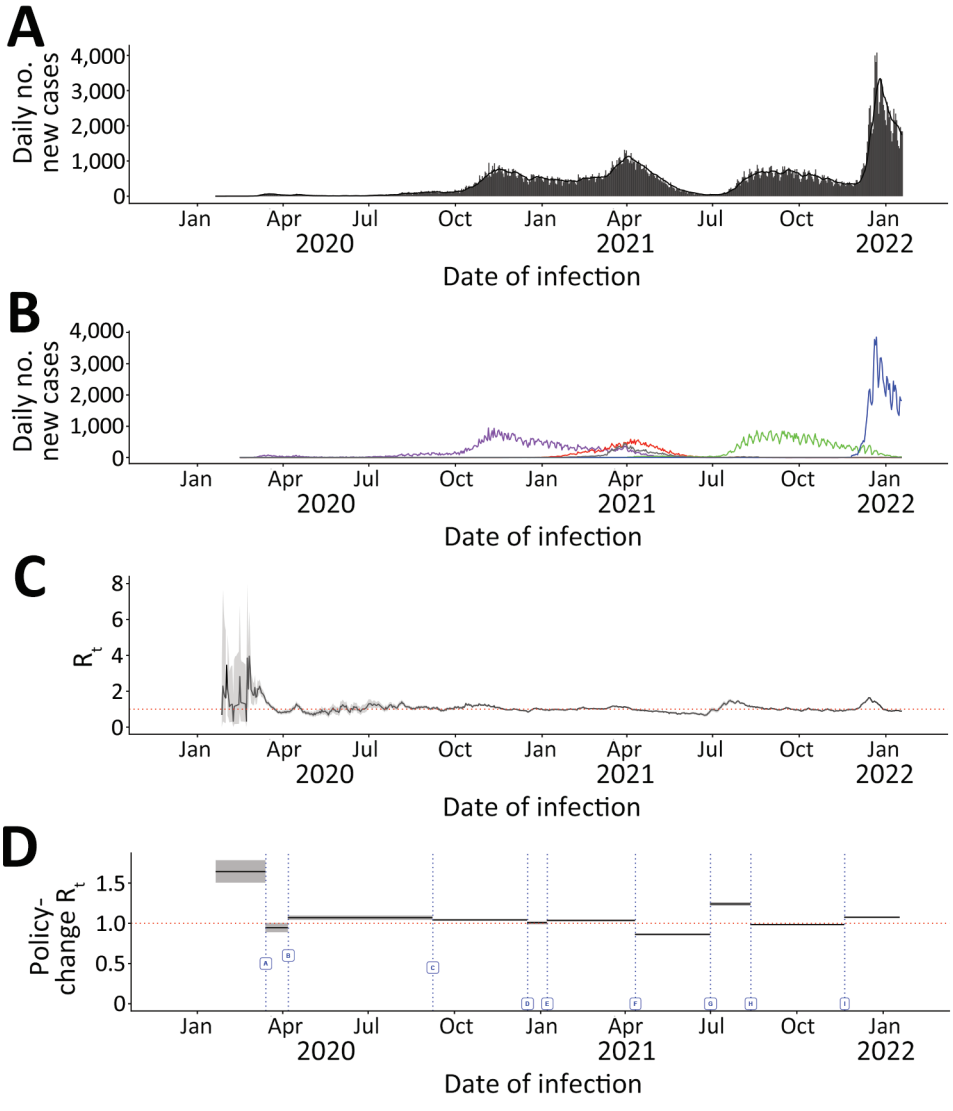

Figure 2. Daily incident COVID-19 case count and 7-day moving average Rt, by date of infection and policy-change Rt or new variants by initiation dates, British Columbia, Canada, January 23, 2020–January 27, 2022. Dates are assumed infection dates (i.e., report date minus 9 days); red dotted lines in panels C and D indicate Rt = 1. A, B) Incident case count by date of infection for all variants combined (A) and by variant type (B). Colors indicate COVID-19 variants: purple, wild-type; red, Alpha; green, Delta; blue, Omicron; and gray, other variants. C) Sevenday moving average Rt by date of infection. D) Policy-change Rt. Policy changes or detection of new variants by dates of initiation: A, school closure (March 14, 2020); B, recommendation for use of face masks (April 7, 2020); C, phased school reopening (September 8, 2020); D, priority populations vaccination rollout (December 18, 2020); E, partial school reopening (January 8, 2021); F, school closure (April 12, 2021); G, increase in cases because of Delta COVID-19 variant (July 1, 2021); H, requirement of vaccination for federal workers (August 13, 2021); I, increase in cases because of the Omicron COVID-19 variant (November 21, 2021).

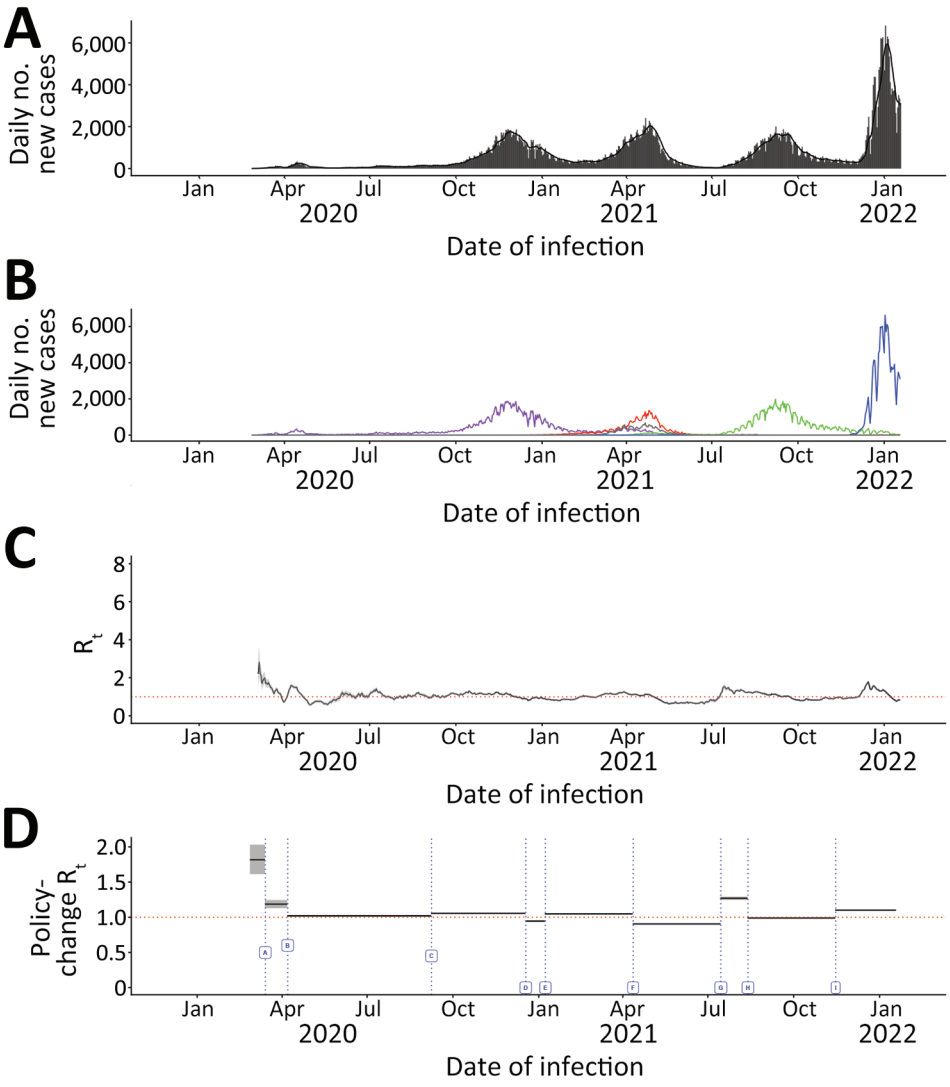

Figure 3. Daily incident COVID-19 case count and 7-day moving average Rt, by date of infection and policy-change Rt or new variants by initiation dates, Alberta, Canada, January 23, 2020–January 27, 2022. Dates are assumed infection dates (i.e., report date minus 9 days); red dotted lines in panels C and D indicate Rt = 1. A, B) Incident case count by date of infection for all variants combined (A) and by variant type (B). Colors indicate COVID-19 variants: purple, wildtype; red, Alpha; green, Delta; blue, Omicron; and gray, other variants. C) Seven-day moving average Rt by date of infection.D) Policy-change Rt. Policy changes or detection of new variants by dates of initiation: A, school closure (March 14, 2020); B, recommendation for use of face masks (April 7, 2020); C, phased school reopening (September 8, 2020); D, priority populations vaccination rollout (December 18, 2020); E, partial school reopening (January 8, 2021); F, school closure (April 12, 2021); G, increase in cases because of Delta COVID-19 variant (July 15, 2021); H, requirement of vaccination for federal workers (August 13, 2021); I, increase in cases because of the Omicron COVID-19 variant (November 15, 2021).

the initial R_t in Ontario and British Columbia. Initiating school closures in March 2020 and April 2021, recommendation of face coverings, rollout of vaccination for priority populations, and required vaccination for government workers were policies associated with decreased median R_t; policies that relaxed those interventions, such as phased school reopening and partial school reopening after holiday break were associated with increased median R_t. Emergence of Delta and Omicron variants also increased R_t. As in other provinces, the greatest increase in R_t, 40.27% (95% CrI 37.56%–42.92%), was observed after emergence of Delta, whereas the most significant decrease in R_t, −34.71% (95% CrI −42.23% to −25.80%), was observed after school closures in March 2020. Similar to other provinces, the lowest median R_t, 0.91 (95% CrI 0.90, 0.91), was observed after school closure in April 2021.

R_t by Variant

We calculated median 7-day sliding-window R_t by variant for Ontario (Figure 4), British Columbia (Figure 5), and Alberta (Figure 6). We note that each time a new variant emerged in each province, R_t was >1: R_t was 2–3 for wild-type, 1–2 for Alpha, ≈2 for Delta, and ≈3 for Omicron. Soon after this initial increase, R_t would decrease to ≈1. Before wild-type, Alpha, and Delta variants were overtaken by other variants, R_t would drop to <1.

IRR at the Provincial Level

We calculated the number of cases per 100,000 person-days for each variant stratified by province and for each province stratified by variant (Table 2). We observed that overall, incidence rate for Omicron was 8.742 (95% CI 8.710–8.774) times that for wild-type, which we used as referent, whereas rates were <0.7

times those for wild-type for Delta (0.692 [95% CI 0.689–0.695]) and Alpha (0.370 [95% CI 0.368–0.372]). When stratified by province, variants followed similar trends, with Omicron having a higher incidence rate and Alpha and Delta lower incidence rates than wild-type, except in British Columbia, where the incidence rate for Delta was higher than for wild-type: IRR 1.126 (95% CI 1.116–1.137). When stratified by variant, with British Columbia as the referent, Alberta had the highest IRR for all variants: wild-type, 1.927 (95% CI 1.912–1.943); Alpha, 1.734 (95% CI 1.711–1.757); Delta, 1.664 (95% CI 1.649–1.678); and Omicron, 1.827 (95% CI 1.801–1.832). Next highest IRRs were for Ontario for all variants except Delta, for which the IRR was 0.519 (95% CI 0.514, 0.524). For all variants combined, with British Columbia as the referent, Alberta (1.799 [95% CI 1.790, 1.807]) had a higher IRR than Ontario (1.117 [95% CI 1.112, 1.121]) (Appendix Tables 8, 9).

Discussion

We found that daily incident case count and R_t fluctuations during the study period followed trends consistent across the 3 provinces (Figures 1–3). COVID-19 case count was highest in Ontario, followed by Alberta and British Columbia (Table 2). All 3 provinces experienced surges in case counts and increased R_t after Delta and Omicron variants emerged. Nationwide interventions included school closures, face mask recommendations, and rollout of vaccination for priority populations. Our results showed that these interventions were associated with lowered R_t, which in turn decreased COVID-19 burden. Across the 3 provinces, the school closure policy in April 2021 (policy F) corresponded with the lowest R_t during the study period; that decrease underscores the fact that social distancing, in addition to other interventions, can play a substantial role in mitigating spread. However, school closure alone was insufficient to miti-

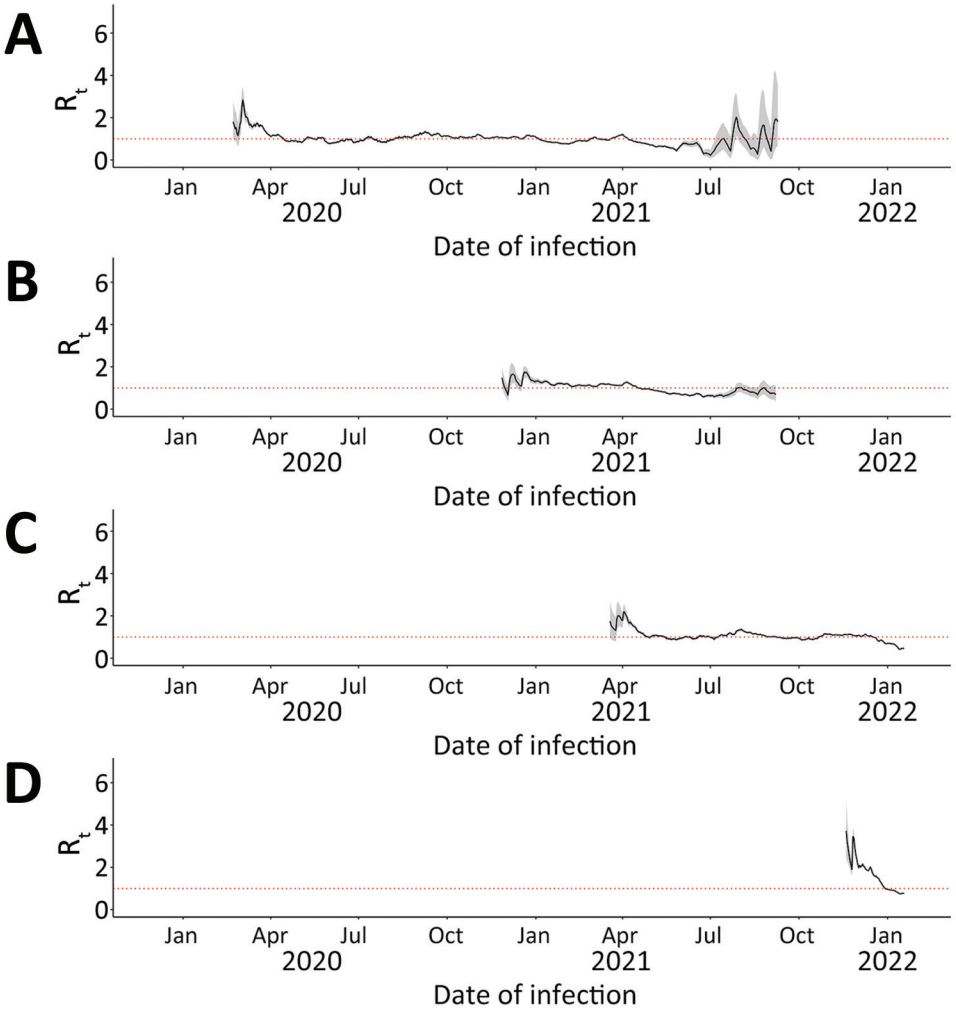

Figure 4. Seven-day sliding-window R_t by COVID-19 variant in Ontario, Canada, January 23, 2020–January 27, 2022. A) Wild-type; B) Alpha; C) Delta; D) Omicron. We estimated infection dates by subtracting 9 days from report dates. Red dotted lines indicate $R_t = 1$.

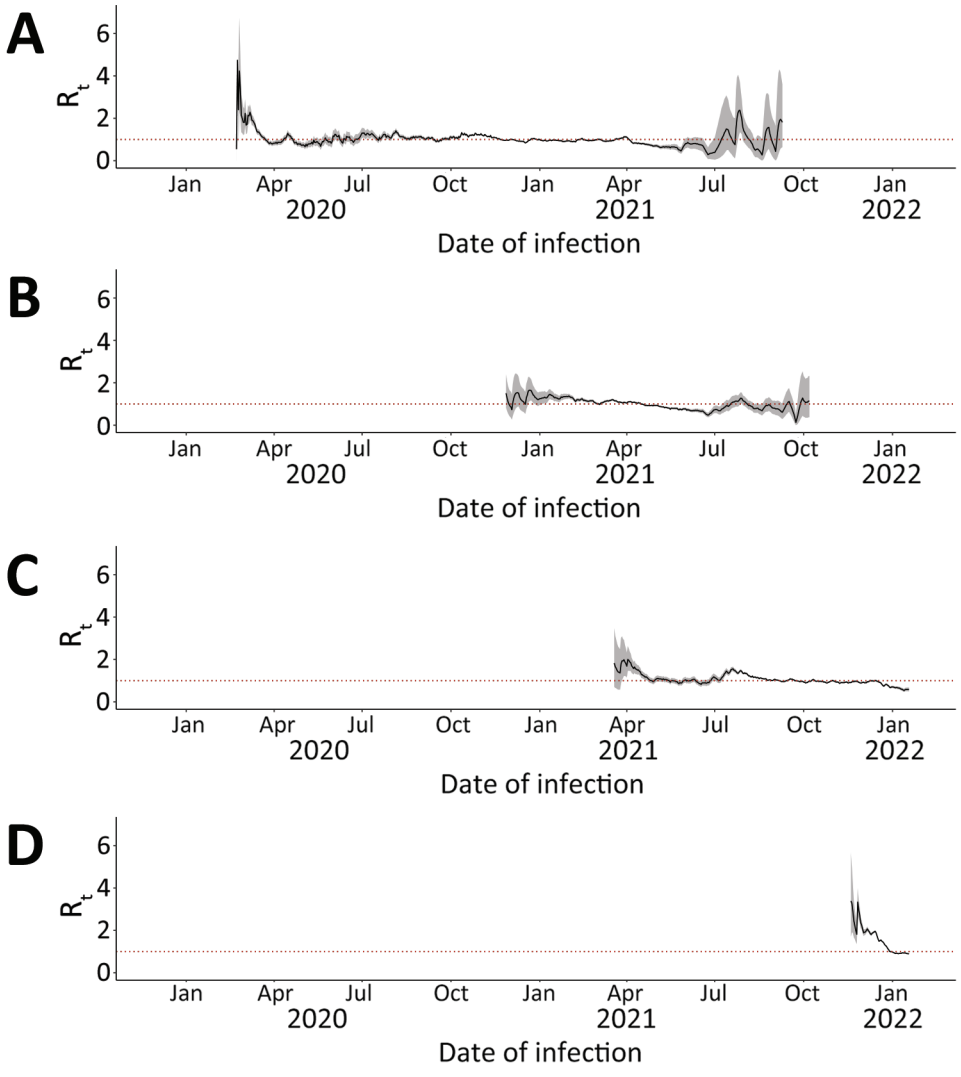

Figure 5. Seven-day sliding-window R_t by COVID-19 variant in British Columbia, Canada, January 23, 2020–January 27, 2022. A) Wild-type; B) Alpha; C) Delta; D) Omicron. We estimated infection dates by subtracting 9 days from report dates. Red dotted lines indicate $R_t = 1$.

gate transmission (*29*,*30*). Our results were consistent with previous studies that suggested mandating face masks (*4*,*31*), physical distancing (*5*), shelters in place (*32*), and school closures (*33*) have been powerful tools for controlling the pandemic. Our study confirms the critical role of high compliance by affected populations towards nonpharmaceutical interventions and other recommended measures for pandemic control before vaccines became available (*34*). Even after vaccine availability, emergence of new variants led to surges with R_t >1. Exhausting the numbers of susceptible persons during case surges led to declines in R_t.

Policy effectiveness was influenced by variant prevalence at any given time. In agreement with previous studies (*35*–*37*), our study showed that most cases in July–December 2021 were attributed to the Delta variant and in December 2021–January 2022 to the Omicron variant. R_t increased in all 3 provinces after emergence of Delta (label G). However, despite having the highest Delta case count, for persons in Ontario, risk of contracting Delta was least across the 3 provinces (Table 2). Also, in contrast with the other 2 provinces, emergence of Omicron did not substantially affect the policy change R_t in Ontario. Although Ontario, with its larger population, accounted for more than half of all cases across the 3 provinces, Alberta had the highest total IRR, indicating that residents had the highest risk for COVID-19 among the 3 provinces despite enacting similar mitigation policies. Attitudes and behaviors toward COVID-19 preventive measures could explain the higher total IRR in Alberta. For example, according to 1 study, during the COVID-19 pandemic, Alberta had the highest percentage of antivaccination posts (i.e., tweets) in Canada on the social media site Twitter (now X; https://twitter.com) (*38*).

After school closures in March 2020, British Columbia was the only one of the 3 provinces that experienced

a drastic decrease in the policy change R_t, from 1.64 to 0.95 (Table 1). After the World Health Organization pandemic declaration on March 11, 2020, British Columbia was the first province to implement stringent public health responses and declare an outbreak (*39*). Also, among the 3 provinces, the highest Oxford Stringency Index score, a measure of adoption of government-recommended policies, was observed in British Columbia both before and after the outbreak declaration (*39*).

The high incidence rate for Omicron compared with wild-type could be attributed to the high contagiousness of Omicron and its ability to evade naturally acquired immunity against previous strains (*40*,*41*). The lower-than-expected IRR for Alpha might be attributable to the long duration when the variant was prevalent but not the dominant strain; higher person-time under observation for Alpha could have accounted for the lower incidence rate.

Among limitations in our study, the original data lacked information on date of infection; to account for that missing information, following a simple acceptable method (*42*), we estimated the approximate date of infection by subtracting 9 days (sum of the median delay in reporting and the mean incubation period) from the report date. Second, we assumed the same case-detection rate across provinces. However, if this assumption did not hold, our case burden findings would be skewed. Third, for policy change R_t, we used dates of specific major policy changes as cutoff points for each time period. In addition, because >1 nonpharmaceutical intervention could be in effect during the same period, we could not attribute changes in R_t solely to a single policy change. Fourth, we could not adjust our results to account for differences in levels of policy compliance because those data were not accessible to us. Fifth, potential variation in the availability of COVID-19 testing across the study period and among provinces could affect the daily incident case count reported and thus affect R_t estimates. Sixth, we a priori defined an SI distribution for estimating R_t. Therefore, we could not

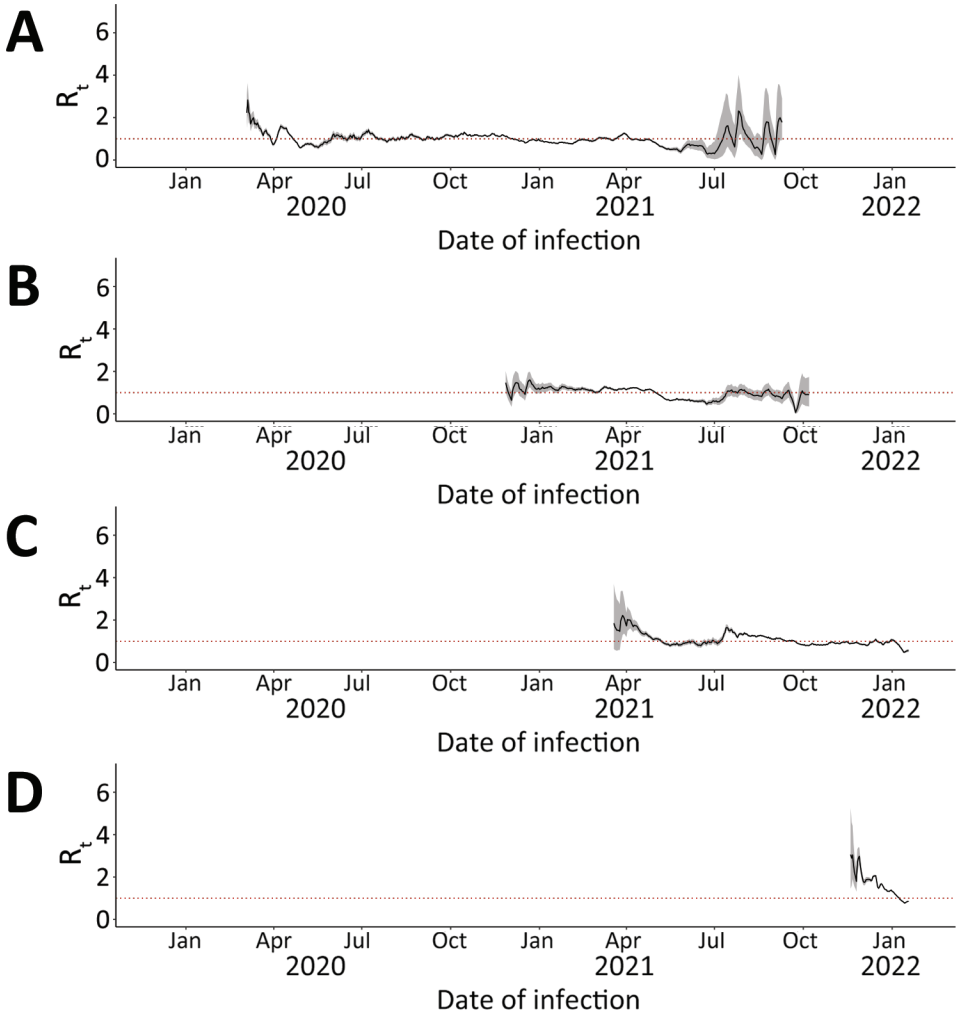

Figure 6. 7-day sliding-window R_t by COVID-19 variant in Alberta, Canada, January 23, 2020–January 27, 2022. A) Wild-type; B) Alpha; C) Delta; D) Omicron. We estimated infection dates by subtracting 9 days from report dates. Red dotted lines indicate $R_t = 1$.

Table 2. Number of days observed, cumulative case count, cumulative case count per 100,000 person-days, and incidence rate ratio between variants by province, and between provinces by variant in 3 provinces of Canada (Ontario, British Columbia, and Alberta) during January 23, 2020–January 27, 2022*

Category	Alberta	British Columbia	Ontario	Overall
Population size, 2021	4,262,635	5,000,879	14,223,942	23,487,456
No. days observed				
Variant				
Wild-type	562	573	572	Not applicable
Alpha	602	602	602	Not applicable
Delta	460	460	460	Not applicable
Omicron	68	68	68	Not applicable
Cumulative case count				
Variant				
Wild-type	146,910	91,170	337,299	575,379
Alpha	54,621	36,951	133,162	224,734
Delta	116,902	82,441	121,710	321,053
Omicron	141,661	91,491	366,495	599,646
Total (%)	460,094 (26.74)	302,053 (17.55)	958,666 (55.71)	1,720,812 (100)
Cumulative case count per 100,000 person-days				
Variant				
Wild-type	6.13	3.18	4.15	4.29
Alpha	2.13	1.23	1.56	1.59
Delta	5.96	3.58	1.86	2.97
Omicron	48.87	26.90	37.89	37.54
Total	6.38	3.45	3.96	4.31
IRR between variant by province				
Variant				
Wild-type (95% CI)	Referent	Referent	Referent	Referent
Alpha (95% CI)	0.347 (0.344–0.351)†	0.386 (0.381–0.390)†	0.375 (0.373–0.378)†	0.370 (0.368–0.372)†
Delta (95% CI)	0.972 (0.965–0.980)†	1.126 (1.116–1.137)†	0.449 (0.446–0.452)†	0.692 (0.689–0.695)†
Omicron (95% CI)	7.969 (7.911–8.028)†	8.456 (8.379–8.534)†	9.140 (9.097–9.183)†	8.742 (8.710–8.774)†
IRR between province by variant				
Variant				
Wild-type (95% CI)	1.927 (1.912–1.943)†	Referent	1.303 (1.294–1.313)†	Not applicable
Alpha (95% CI)	1.734 (1.711–1.757)†	Referent	1.267 (1.252–1.282)†	Not applicable
Delta (95% CI)	1.664 (1.649–1.678)†	Referent	0.519 (0.514–0.524)†	Not applicable
Omicron (95% CI)	1.827 (1.801–1.832)†	Referent	1.408 (1.398–1.419)†	Not applicable
Overall (95% CI)	1.799 (1.790–1.807)†	Referent	1.117 (1.112–1.121)†	Not applicable

*IRR, incidence rate ratio.
†p<0.0001.

assess changes in SI because we lacked information on infector-infectee pairs. SI for SARS-CoV-2 could have been shortened over time by use of nonpharmaceutical interventions (*43*). We also did not assess the possibility of variant-specific SI distribution. Seventh, case count data reflected only the subset of SARS-CoV-2 infections testing positive, because many asymptomatic or mildly symptomatic infected persons were never tested. We attempted to demonstrate the effects of that uncertainty in our 7-day sliding-window R_t estimates through sensitivity analysis (Appendix Figures 3, 6, and 9). Eighth, lacking population data by public health district, we could not calculate incidence rates by district, which limited the scope of our analysis. Ninth, calculations of provincial variant incidence rates might have been influenced by the subjectively chosen length of duration for variant surges, which we based on the number of days from the index to the last reported cases for each variant in each province. Tenth, ecologic fallacy is possible in a study such as ours using aggregated data; association does not demonstrate causality.

In conclusion, we observed substantial fluctuations in R_t for COVID-19 across 3 provinces in Canada during January 2020–January 2022. Our findings showed that initiating pandemic policies, such as recommendations for face coverings, school closures, and rollout of vaccination for priority populations, were associated with decreases in R_t. Conversely, relaxing mask mandates and reopening schools were associated with increases in R_t, especially in conjunction with emergence of new SARS-CoV-2 variants. As mutated variants continue to emerge, public health authorities must remain vigilant to adapt mitigation, testing, and treatment strategies.

About the Author

Mx. Kehoe is a DrPH student in epidemiology at the Georgia Southern University Jiann-Ping Hsu College of Public Health with research interests in infectious disease modeling, behavioral impacts on infectious disease transmission, and the intersection of social justice and mental health epidemiology. Dr. Mallhi earned her DrPH in epidemiology from the Georgia Southern University

Jiann-Ping Hsu College of Public Health in December 2023. Her research interests include chronic disease epidemiology and women's health.

References

1. Khan M, Adil SF, Alkhathlan HZ, Tahir MN, Saif S, Khan M, et al. COVID-19: a global challenge with old history, epidemiology and progress so far. Molecules. 2020;26:39. https://doi.org/10.3390/molecules26010039
2. Centers for Disease Control and Prevention. SARS-COV-2 variant classifications and definitions [cited 2022 May 3]. https://www.cdc.gov/coronavirus/2019-ncov/variants/variant-classifications.html
3. Sah P, Vilches TN, Moghadas SM, Fitzpatrick MC, Singer BH, Hotez PJ, et al. Accelerated vaccine rollout is imperative to mitigate highly transmissible COVID-19 variants. EClinicalMedicine. 2021;35:100865. https://doi.org/10.1016/j.eclinm.2021.100865
4. Karaivanov A, Lu SE, Shigeoka H, Chen C, Pamplona S. Face masks, public policies and slowing the spread of COVID-19: evidence from Canada. J Health Econ. 2021;78:102475. https://doi.org/10.1016/j.jhealeco.2021.102475
5. Tuite AR, Greer AL, De Keninck S, Fisman DN. Risk for COVID-19 resurgence related to duration and effectiveness of physical distancing in Ontario, Canada. Ann Intern Med. 2020;173:675–8. https://doi.org/10.7326/M20-2945
6. Tuite AR, Fisman DN, Greer AL. Mathematical modelling of COVID-19 transmission and mitigation strategies in the population of Ontario, Canada. CMAJ. 2020;192:E497–505. https://doi.org/10.1503/cmaj.200476
7. Yuan P, Li J, Aruffo E, Gatov E, Li Q, Zheng T, et al. Efficacy of a "stay-at-home" policy on SARS-CoV-2 transmission in Toronto, Canada: a mathematical modelling study. CMAJ Open. 2022;10:E367–78. https://doi.org/10.9778/cmajo.20200242
8. Adeyinka DA, Neudorf C, Camillo CA, Marks WN, Muhajarine N. COVID-19 vaccination and public health countermeasures on variants of concern in Canada: evidence from a spatial hierarchical cluster analysis. JMIR Public Health Surveill. 2022;8:e31968. https://doi.org/10.2196/31968
9. Périnet S, Cadieux G, Mercure SA, Drouin M, Allard R. Analysis of COVID-19 risk following a ring vaccination intervention to address SARS-CoV-2 alpha variant transmission in Montreal, Canada. JAMA Netw Open. 2022;5:e2147042. https://doi.org/10.1001/jamanetworkopen.2021.47042
10. Fung IC-H, Hung YW, Ofori SK, Muniz-Rodriguez K, Lai P-Y, Chowell G. SARS-CoV-2 transmission in Alberta, British Columbia, and Ontario, Canada, December 25, 2019, to December 1, 2020. Disaster Med Public Health Prep. 2021;16:1–10.
11. Government of Ontario. Confirmed positive cases of COVID-19 in Ontario [cited 2022 Jan 28]. https://data.ontario.ca/dataset/confirmed-positive-cases-of-covid-19-in-ontario
12. Ontario Health. Annual business plan 2022/23 [cited 2023 Feb 6]. https://www.ontariohealth.ca/sites/ontariohealth/files/2022-05/OHBusinessPlan22_23.pdf
13. British Columbia Centre for Disease Control. Archived BC COVID-19 data [cited 2022 Jan 28]. http://www.bccdc.ca/health-info/diseases-conditions/covid-19/archived-b-c-covid-19-data
14. Government of British Columbia. Regional health authorities [cited 2022 Sep 10]. https://www2.gov.bc.ca/gov/content/health/about-bc-s-health-care-system/partners/health-authorities/regional-health-authorities
15. Government of Alberta. COVID-19 Alberta statistics 2020 [cited 2022 Jan 28]. https://web.archive.org/web/20220128231728/https://www.alberta.ca/stats/covid-19-alberta-statistics.htm
16. Alberta Health Services. AHS map and zone overview. 2020–21: report to the community [cited 2022 Sep 10]. https://www.albertahealthservices.ca/assets/about/publications/ahs-ar-2021/zones.html
17. Government of Canada, Department of Justice, Electronic Communication. Government of Canada's response to COVID-19 [cited 2022 May 2]. https://www.justice.gc.ca/eng/csj-sjc/covid.html#shr-pg0
18. Canadian Institute of Health Information. Canadian COVID-19 intervention timeline [cited 2022 May 2]. https://www.cihi.ca/en/covid-19-intervention-timeline-in-canada
19. Upper Canada District School Board. 2021–2022 school year calendar [cited 2022 May 18]. https://web.archive.org/web/20220518125851/https://www.ucdsb.on.ca/for_families/school_year_calendar
20. Government of Canada. COVID-19 epidemiology update [cited 2022 May 2]. https://health-infobase.canada.ca/covid-19/epidemiological-summary-covid-19-cases.html
21. Guerra FM, Bolotin S, Lim G, Heffernan J, Deeks SL, Li Y, et al. The basic reproduction number (R_0) of measles: a systematic review. Lancet Infect Dis. 2017;17:e420–8. https://doi.org/10.1016/S1473-3099(17)30307-9
22. Ogwara CA, Mallhi AK, Hua X, Muniz-Rodriguez K, Schwind JS, Zhou X, et al. Spatially refined time-varying reproduction numbers of COVID-19 by health district in Georgia, USA, March–December 2020. Epidemiologia (Basel). 2021;2:179–97. https://doi.org/10.3390/epidemiologia2020014
23. Cori A, Ferguson NM, Fraser C, Cauchemez S. A new framework and software to estimate time-varying reproduction numbers during epidemics. Am J Epidemiol. 2013;178:1505–12. https://doi.org/10.1093/aje/kwt133
24. Thompson RN, Stockwin JE, van Gaalen RD, Polonsky JA, Kamvar ZN, Demarsh PA, et al. Improved inference of time-varying reproduction numbers during infectious disease outbreaks. Epidemics. 2019;29:100356. https://doi.org/10.1016/j.epidem.2019.100356
25. You C, Deng Y, Hu W, Sun J, Lin Q, Zhou F, et al. Estimation of the time-varying reproduction number of COVID-19 outbreak in China. Int J Hyg Environ Health. 2020;228:113555. https://doi.org/10.1016/j.ijheh.2020.113555
26. Centers for Disease Control and Prevention. Estimated COVID-19 burden [cited 2022 Aug 28]. https://stacks.cdc.gov/view/cdc/117147
27. Centers for Disease Control and Prevention. COVID-19 pandemic planning scenarios [cited 2022 Aug 28]. https://www.cdc.gov/coronavirus/2019-ncov/hcp/planning-scenarios.html
28. Statistics Canada. Census profile, 2021 census of population [cited 2022 June 25]. https://www12.statcan.gc.ca/census-recensement/2021/dp-pd/prof/index.cfm
29. Esposito S, Principi N. School closure during the coronavirus disease 2019 (COVID-19) pandemic: an effective intervention at the global level? JAMA Pediatr. 2020;174:921–2. https://doi.org/10.1001/jamapediatrics.2020.1892
30. Lee B, Raszka WV Jr. COVID-19 transmission and children: the child is not to blame. Pediatrics. 2020;146:e2020004879. https://doi.org/10.1542/peds.2020-004879
31. Ueki H, Furusawa Y, Iwatsuki-Horimoto K, Imai M, Kabata H, Nishimura H, et al. Effectiveness of face masks in preventing airborne transmission of SARS-CoV-2. MSphere. 2020;5:e00637-20. https://doi.org/10.1128/mSphere.00637-20

32. Feyman Y, Bor J, Raifman J, Griffith KN. Effectiveness of COVID-19 shelter-in-place orders varied by state. PLoS One. 2020;15:e0245008. https://doi.org/10.1371/journal.pone.0245008
33. Abdollahi E, Haworth-Brockman M, Keynan Y, Langley JM, Moghadas SM. Simulating the effect of school closure during COVID-19 outbreaks in Ontario, Canada. BMC Med. 2020;18:230. https://doi.org/10.1186/s12916-020-01705-8
34. Kwok KO, Li KK, Tang A, Tsoi MTF, Chan EYY, Tang JWT, et al. Psychobehavioral responses and likelihood of receiving COVID-19 vaccines during the pandemic, Hong Kong. Emerg Infect Dis. 2021;27:1802–10. https://doi.org/10.3201/eid2707.210054
35. Mohapatra RK, Tiwari R, Sarangi AK, Sharma SK, Khandia R, Saikumar G, et al. Twin combination of Omicron and Delta variant triggering a tsunami wave of ever high surges in COVID–19 cases: a challenging global threat with a special focus on Indian sub–continent. J Med Virol. 2022;94:1761–5. https://doi.org/10.1002/jmv.27585
36. Klompas M, Karan A. Preventing SARS-CoV-2 transmission in health care settings in the context of the Omicron variant. JAMA. 2022;327:619–20. https://doi.org/10.1001/jama.2022.0262
37. Wee LE, Ko KK-K, Conceicao EP, Sim JX-Y, Rahman NA, Tan SY-L, et al. Linking sporadic hospital clusters during a community surge of the severe acute respiratory coronavirus virus 2 (SARS-CoV-2) B. 1.617. 2 Delta variant: the utility of whole-genome sequencing. Infect Control Hosp Epidemiol. 2023;44:1014–8.
38. To QG, To KG, Huynh VN, Nguyen NT, Ngo DT, Alley S, et al. Anti-vaccination attitude trends during the COVID-19 pandemic: a machine learning-based analysis of tweets. Digit Health. 2023;9:20552076231158033. https://doi.org/10.1177/20552076231158033
39. McCoy LG, Smith J, Anchuri K, Berry I, Pineda J, Harish V, et al.; COVID-19 Canada Open Data Working Group: Non-Pharmaceutical Interventions. Characterizing early Canadian federal, provincial, territorial and municipal nonpharmaceutical interventions in response to COVID-19: a descriptive analysis. CMAJ Open. 2020;8:E545–53. https://doi.org/10.9778/cmajo.20200100
40. Okpeku M. Possibility of COVID-19 eradication with evolution of a new Omicron variant. Infect Dis Poverty. 2022;11:30. https://doi.org/10.1186/s40249-022-00951-7
41. Pulliam JRC, van Schalkwyk C, Govender N, von Gottberg A, Cohen C, Groome MJ, et al. Increased risk of SARS-CoV-2 reinfection associated with emergence of Omicron in South Africa. Science. 2022;376:eabn4947. https://doi.org/10.1126/science.abn4947
42. Gostic KM, McGough L, Baskerville EB, Abbott S, Joshi K, Tedijanto C, et al. Practical considerations for measuring the effective reproductive number, Rt. PLOS Comput Biol. 2020;16:e1008409. https://doi.org/10.1371/journal.pcbi.1008409
43. Ali ST, Wang L, Lau EHY, Xu X-K, Du Z, Wu Y, et al. Serial interval of SARS-CoV-2 was shortened over time by nonpharmaceutical interventions. Science. 2020;369:1106–9. https://doi.org/10.1126/science.abc9004

Address for correspondence: Isaac Chun-Hai Fung, PO Box 7989, Department of Biostatistics, Epidemiology and Environmental Health Sciences, Jiann-Ping Hsu College of Public Health, Georgia Southern University, Statesboro, GA 30460, USA; email: cfung@georgiasouthern.edu

Economic Burden of Acute Gastroenteritis among Members of Integrated Healthcare Delivery System, United States, 2014–2016

John F. Dickerson, Suzanne B. Salas, Judy Donald, Holly C. Groom, Mi H. Lee, Claire P. Mattison, Aron J. Hall, Mark A. Schmidt

We conducted a large surveillance study among members of an integrated healthcare delivery system in Pacific Northwest of the United States to estimate medical costs attributable to medically attended acute gastroenteritis (MAAGE) on the day care was sought and during 30-day follow-up. We used multivariable regression to compare costs of MAAGE and non-MAAGE cases matched on age, gender, and index time. Differences accounted for confounders, including race, ethnicity, and history of chronic underlying conditions. Analyses included 73,140 MAAGE episodes from adults and 18,617 from children who were Kaiser Permanente Northwest members during 2014–2016. Total costs were higher for MAAGE cases relative to non-MAAGE comparators as were costs on the day care was sought and costs during follow-up. Costs of MAAGE are substantial relative to the cost of usual-care medical services, and much of the burden accrues during short-term follow-up.

Medically attended acute gastroenteritis (MAAGE) is a substantial driver of health services use by patients, accounting for >10 million outpatient encounters and 1 million hospitalizations each year (*1*,*2*). Initial MAAGE encounters in primary care and urgent need departments impart an immediate burden on healthcare systems (*3*). In addition, MAAGE-related hospitalizations may persist for multiple days, and patients may return for additional MAAGE services if symptoms worsen or fail to abate. Determining the financial impact of MAAGE on health systems and their members would provide important information about the potential value of interventions targeting acute gastroenteritis (AGE).

Several studies in Europe and the United States have evaluated the costs of AGE and of MAAGE, with a focus on the costs attributable to the onset and duration of an MAAGE episode. Researchers in Belgium estimated that MAAGE episodes accounted for direct costs of €112 million ($126 million in 2017 US dollars) in Belgium annually (*4*), and researchers in Switzerland estimated that healthcare costs resulting from AGE in combination with campylobacteriosis amounted to €29–45 million ($33–51 million in 2017 US dollars) in Switzerland annually (*5*). A study estimating the impact of MAAGE among a managed care population in the United States estimated a substantial annual burden of MAAGE episodes to health systems of $3.88 billion and demonstrated that the costs attributed to AGE increased ≈26% during 2006–2011 (*6*). However, those prior studies did not include subsequent, short-term costs attributable to AGE through exacerbation of underlying conditions or illnesses or services for lingering symptoms or sequelae. As has been recently shown (*7*), much of the burden associated with an AGE episode could be experienced during the short-term follow-up period. Given the high prevalence of MAAGE encounters and the acute need for medical resources to treat AGE episodes, additional data on short-term costs would help to more comprehensively quantify the economic costs of MAAGE encounters and assess potential economic benefits of prevention of or early intervention in AGE episodes.

We evaluated the economic burden of MAAGE on a fully integrated healthcare delivery system serving members residing in the Pacific Northwest of the United States. As part of a large surveillance study

Author affiliations: Center for Health Research, Kaiser Permanente Northwest, Portland, Oregon, USA (J.F. Dickerson, S.B. Salas, J. Donald, H.C. Groom, M.H. Lee, M.A. Schmidt); Cherokee Nation Assurance, Arlington, Virginia, USA (C.P. Mattison); Centers for Disease Control and Prevention, Atlanta, Georgia, USA (C.P. Mattison, A.J. Hall)

DOI: http://doi.org/10.3201/eid3005.230356

of AGE, we quantified initial medical expenditures at the time care was sought, as well as all ongoing short-term medical costs during a 30-day follow-up period (*8*). We used data from electronic health records (EHR) of health system members identified with MAAGE and of matched members without MAAGE who had a health system visit (either outpatient, emergency, or telephone encounters) during the same time period, with the aim of estimating both the same-day and incremental 30-day health care expenditures associated with MAAGE. We evaluated health care expenditures separately for children and adults and further stratified analyses by age among both children (0–4 years and 5–17 years) and adults (18–64 years and ≥65 years).

Methods

Data Source

We used EHR data from Kaiser Permanente Northwest (KPNW), a fully integrated health care delivery system serving ≈616,000 medical members located primarily in Oregon and southwest Washington. Those data, stored in the research data warehouse at the KPNW Center for Health Research in Oregon contained information on diagnoses, physical findings, tests, procedures, medications, insurance enrollment, claims, state mortality records, and census-derived neighborhood characteristics. Medical care costs for all expenses except for pharmacy dispensing were estimated using the standardized relative resource cost algorithm (*9*); pharmacy retail costs were obtained from internal health plan data. Algorithm cost estimate outcomes for healthcare utilization approximate those using Medicare fee schedules, and internal pharmacy cost estimates are similar to retail prices within the local community. Cost estimates represent the total costs to the health system. The Institutional Review Board at Kaiser Permanente Northwest approved the study.

Study Design and Population

The parent study was designed to estimate all-age, population-based incidence rates of norovirus and other pathogens that contribute to AGE in the United States by using an integrated healthcare delivery system as a surveillance platform (*8*). Using a subset of these data, we conducted a retrospective cohort study of all MAAGE cases identified through the surveillance program along with a comparable group of KPNW medical members who were free from MAAGE for at least 3 months before any non-MAAGE index medical encounter within the health system.

Cases

All MAAGE case-patients who sought care during April 1, 2014–September 30, 2016, within the health system were identified using an EHR-based automated extraction program searching for MAAGE-related encounters as identified through codes from the International Classification of Diseases (ICD), 9th Revision (ICD-9) or 10th Revision (ICD-10) and standardized variables from the EHR (*8*). Case-patients could be included more than once if they had separate, distinct episodes of MAAGE separated by >30 days. Episodes of MAAGE represented a continuous illness and could include multiple MAAGE-related encounters. Inclusion and exclusion criteria were minimal at the case-identification stage of the project: patients had to be medical members at the time of the encounter, which served as their index visit; have an ICD-9 or ICD-10 diagnosis related to AGE at an outpatient, urgent care, emergency department, or inpatient encounter; or have a chief complaint of AGE at a telephone encounter (video telehealth visits were uncommon in the health system during this time period). The only patients excluded were those who opted out of research studies during insurance registration (≈0.2% of the KPNW population).

Comparators

We selected comparators retrospectively and matched them to MAAGE cases at a 1:1 ratio. As with study cases, comparators had to be current medical members at the time of an index healthcare encounter and were excluded if they had opted out of research. We also required comparators to have no indication of MAAGE in the 3 months before their index encounter. We chose to require comparators to have an index encounter rather than selecting from the general population to minimize the risk of bias from barriers to health services access. It is important to note, however, that the comparison of MAAGE in these analyses is specific to a similar health services–seeking population rather than to the general population. Any non–MAAGE-related visit within the medical system qualified as an index visit. For adults ≥18 years of age at their index encounter, comparators were matched to cases based on gender, age (±2.5 years), and the timing of the index visit (±3 months). We used the same criteria for children but with closer matching on age: children ≤2 years were matched on month of age, and children >2 years were matched on year of age. A single healthcare encounter for each comparator was selected randomly from eligible encounters, which was used as their index encounter, and we matched without replacement.

Study Outcomes and Control Variables

Study outcomes were all-cause health system costs on the day of and for 30 days after the index encounter, as well as the sum total of costs over these 2 specified times. We also examined separately the total outpatient and pharmacy costs associated with each index encounter and the 30 days after.

We selected control variables that were the most likely observable confounders between MAAGE categorization and health services use: indicators of a history of cancer or diabetes, and diseases of the blood, heart, immune system, kidney, liver, lung, metabolism, or brain. Although we expected lower prevalence among children, we selected the same confounding variables in analyses of both adults and children. We also included self-reported race and ethnicity, as available in the EHR.

Statistical Analyses

We conducted statistical analyses by using SAS software version 9.4 (SAS Institute, Inc., https://www.sas.com). We conducted separate analyses for adults (≥18 years of age) and children (≤17 years of age). We performed additional analyses, including analyzing data by smaller age subsets (0–4 years, 5–17 years, 18–64 years, and ≥65 years). We compared baseline characteristics between cases and comparators by using χ^2 tests for categorical variables and *t*-tests for continuous variables.

We modeled outcomes by using general linear models with a gamma distribution and a log link. Cost data are typically nonnormal and highly skewed, and those models can well accommodate these types of data. All comparisons accounted for the matching structure of the data and potential clustering within persons (for cases with >1 MAAGE episode). We calculated and presented adjusted mean differences (AMDs), which are model-based estimates of the mean difference between cases and comparators (MAAGE–comparator), adjusting for the likely confounders included in regression models. We calculated quasi-likelihood modifications to the Akaike Information Criteria (QICs) as model goodness of fit statistics (*10,11*).

Our primary analyses included all cases and matched comparators. Because we anticipated outliers in the data, we conducted sensitivity analyses to identify and exclude overly influential outliers (*12*) to determine their influence on our primary analyses. All tests of statistical inference used a 2-sided $\alpha = 0.05$.

Results

Adults

We compiled the baseline characteristics of adult MAAGE cases and matched comparators (Table 1). The mean age of adult cases was 51.6 years (SD ±19.4) and the mean age of adult comparators was 50.8 years (SD ±19.4). The adult study sample was approximately two thirds female and one third male; 63.7% of case-patients and 63.6% of comparators were female. There were significant differences between

Table 1. Demographic characteristics and underlying conditions among adult medically attended acute gastroenteritis case-patients and age- and gender-matched comparators in an integrated health system in the Pacific Northwest of the United States, April 1, 2014–September 30, 2016*

EHR-derived measures	Case-patients, n = 31,865†	Comparators, n = 34,265	p value‡
Age, y, mean (±SD)	51.6 (19.4)	50.8 (19.4)	<0.0001
Sex, %			
F	63.7	63.6	NA
M	36.3	36.4	NA
Race/ethnicity, %			
Hispanic	7.1	6.7	<0.001
Non-Hispanic White	82.4	81.3	<0.001
Non-Hispanic other race	8.9	9.9	<0.001
Unknown	1.6	2.1	<0.001
Comorbidity, %§			
Blood disease	4.3	2.9	<0.0001
Cancer	5.0	4.7	0.277
Diabetes	14.4	11.2	<0.0001
Heart disease	18.2	15.0	<0.0001
Immune disease	4.3	3.0	<0.0001
Kidney disease	10.6	8.5	<0.0001
Liver disease	2.1	1.3	<0.0001
Lung disease	13.0	9.7	<0.0001
Metabolic disease	21.7	17.7	<0.0001
Neurologic disease	10.2	7.7	<0.0001

*All participants were Kaiser Permanente Northwest medical members, ≥18 y of age, with ≥1 encounter at the time of the study. EHR, electronic health records; NA, not applicable.
†Corresponds to 36,117 episodes; 2,758 MAAGE cases are comparators at some time in the study.
‡Paired t-test or χ^2 test.
§Percentage with diagnosis codes from the International Classification of Diseases, 9th Revision or 10th Revision, in the 12 mo before index encounter date.

Table 2. Demographic characteristics and underlying conditions among pediatric medically attended acute gastroenteritis case-patients and age- and gender-matched comparators in an integrated health system in the Pacific Northwest of the United States, April 1, 2014–September 30, 2016*

EHR-derived measures	MAAGE cases, n = 8,558†	Comparators, N = 8,580	p value‡
Mean age, y (±SD)	6.0 (5.2)	6.3 (5.3)	<0.001
Sex, %			
F	47.0	47.1	NA
M	53.0	52.9	NA
Race/ethnicity, %			
Hispanic	18.0	11.7	<0.001
Non-Hispanic White	63.5	70.2	<0.001
Non-Hispanic other race	15.0	14.3	<0.001
Unknown	3.5	3.8	<0.001
Comorbidity, %§			
Blood disease	0.7	0.6	0.384
Cancer	0.2	0.3	0.547
Diabetes	0.4	0.5	0.651
Heart disease	1.4	1.5	0.524
Immune disease	0.4	0.3	0.047
Kidney disease	0.4	0.4	0.800
Liver disease	0.02	0.03	0.655
Lung disease	8.1	6.6	<0.001
Metabolic disease	0.7	0.8	0.528
Neurologic disease	1.8	2.0	0.317

*All participants were Kaiser Permanente Northwest medical members, <18 y of age, with ≥1 encounter at the time of the study. EHR, electronic health records; NA, not applicable
†Corresponds to 9,203 episodes; 834 MAAGE cases were comparators at some time in the study
‡Paired *t*-test or χ^2 test.
§Percentage with diagnosis codes from the International Classification of Diseases, 9th Revision or 10th Revision, in the 12 mo before index encounter date.

adult cases and comparators in race and ethnicity and in almost all underlying conditions, except cancer; case-patients were somewhat more likely than comparators to be Hispanic or non-Hispanic White and having higher rates of all underlying conditions.

Regression analyses of costs among adults (Appendix Table 1, https://wwwnc.cdc.gov/eid/article/30/5/23-0356-App1.pdf) revealed that costs were higher for MAAGE cases than comparators both on the day of their index encounter (AMD = $140; p<0.001) as well as during the 30-day follow-up period (AMD = $296; p<0.001). Accordingly, cases had higher total costs than comparators (AMD = $451; p<0.001). Category-specific costs were higher for cases than comparators in both the outpatient (AMD = $111; p<0.001) and pharmaceutical (AMD = $262; p<0.001) categories.

Differences between adult case-patients and comparators were consistently significantly higher in both the younger (18–64 years) and older (≥65 years) age groups. Comparing case-patients to comparators among older adults (≥65 years), total costs were higher (AMD = $599; p<0.001), both at the index date (AMD = $84; p = 0.004) and during the 30-day follow-up (AMD = $526; p<0.001). We also found that outpatient costs were higher (AMD = $114; p<0.001) as were pharmacy costs (AMD = $280; p<0.001), among cases involving older patients as compared with their comparator counterparts.

Comparing cases to comparators among younger adults, we found that total costs were higher (AMD = $361; p<0.001), both at the index date (AMD = $152; p<0.001) and during the 30-day follow-up (AMD = $196; p<0.001). We also found that outpatient costs were higher (AMD = $106; p<0.001), as were pharmacy costs (AMD = $235; p<0.001), among the younger cases as compared with the comparator patients. Sensitivity analyses identified 2 overly influential outliers in the total cost model and 2 overly influential outliers in the pharmacy cost model. In neither case did removal of those observations substantively change the results; p values remained the same, and the coefficients reduced by 0.8% in the total cost model and 0.3% in the pharmacy cost model.

Children

We compiled baseline characteristics for child MAAGE cases and matched comparators (Table 2). The mean age of child case-patient s was 6.0 years (SD ±5.2) and the mean age of child comparators was 6.3 years (SD ±5.3). Forty-seven percent of case-patients and 47.1% of comparators were female; 53% of case-patient s and 52.9% of comparators were male. There were significant differences between child case-patients and comparators in race and ethnicity. Child case-patients were more likely to be Hispanic or non-White than comparators. Child case-patients were also more likely than comparators to have lung disease, although there were no significant differences in other underlying conditions.

Regression analyses of costs among children (Appendix Table 2) showed, as for adults, costs were higher for case-patients than for comparators both on the day of the index encounter (AMD = $42; p = 0.001) and during the 30-day follow-up (AMD = $105; p = 0.002), resulting in higher total costs (AMD = $141; p<0.001). Category-specific costs were also higher for case-patients compared with comparators in both the outpatient (AMD = $35; p<0.001) and pharmaceutical (AMD = $40; p = 0.002) categories.

For older children (5–17 years of age), all measured costs were significantly higher for case-patients than comparators. However, for younger children (0–4 years of age), there were no significant differences in total, same-day, or follow-up costs between case-patients and comparators. Among younger children, differences in costs between case-patients and comparators were significantly higher for outpatient costs and pharmacy costs (outpatient AMD = $29; pharmacy AMD = $24; p<0.001 for both). Comparing cases to comparators among older children, total costs were higher (AMD = $358; p<0.001), both at the index date (AMD = $133; p = 0.004) and during the 30-day follow-up (AMD = $214; p<0.001). We also found that outpatient costs were higher (AMD = $47; p<0.001), as were pharmacy costs (AMD = $92; p<0.001), among the older child case-patients compared with their comparator counterparts.

Sensitivity analyses identified 5 overly influential outliers in the total cost model and 4 overly influential outliers in the pharmacy cost model. Removal of those observations did not substantively change the results: p values remained subjectively the same, and coefficients increased by 0.1% in the total cost model and by 11.2% in the pharmacy cost model.

Discussion

Our data show that medical care expenditures were significantly higher among adult and child healthcare delivery service members identified with MAAGE relative to usual-care medical services among similar healthcare delivery service members, both on the date of an index medical visit and for 30 days following the visit, after controlling for observable differences. This pattern was consistent across total, pharmacy, and outpatient expenditures for all patients ≥5 years of age (total costs did not differ for children 0–4 years of age). Among the cost components contributing to total costs, the magnitude of the difference was largest for pharmacy costs. We also found that follow-up costs were consistently higher than costs accrued on the day of the index encounter. These data fill in gaps in knowledge about the short-term costs of MAAGE among adults and children, particularly in the days following an initial medical encounter. Our findings substantially inform the study of resource burden by incorporating the subsequent, short-term follow-up costs related to a MAAGE episode, which is often omitted in calculating the overall economic burden of MAAGE, thereby underestimating the true burden of MAAGE episodes.

Higher short-term costs associated with MAAGE relative to usual-care medical services may be partly attributable to ongoing pharmacologic intervention, as suggested by differences in pharmacy-related costs. In addition, exacerbation of underlying conditions and illnesses could contribute to the observed differences in cost between those with MAAGE and other patients.

Among adults, incremental total costs associated with MAAGE relative to usual-care medical services were almost twice as high among those ≥65 years of age compared with those 18–64 years of age. When considered as a group, children 0–17 years of age who were identified with MAAGE had higher total costs compared with similar children without MAAGE; however, there were no statistically significant differences in total costs among young children (0–4 years of age). This observation could be because older children may be using medical care less frequently and an episode of AGE would warrant an independent encounter. Conversely, younger children may be using services more frequently and AGE symptoms could be addressed as part of another regular visit.

This study leveraged a large sample of members of an integrated care delivery system and used matched comparators to estimate the associated costs of MAAGE, controlling for likely confounders and measuring MAAGE-related costs in the 30 days following the initial date of presentation. However, among the study's limitations is that unobserved (and thus uncontrolled) differences between MAAGE case-patients and comparators could have confounded cost estimates, and we observed significant differences between groups after matching. This limitation is inherent to observational studies; however, we controlled for important, observable confounders. Despite matching and the direct control of these observable confounders, biases from unobserved confounders (e.g., income or education levels) likely persist in our estimates. An additional limitation of the study is that findings may not be generalizable beyond the region served by KPNW or to nonintegrated health systems. Although there are similarities across Kaiser Permanente regions, regional differences in member populations and practice patterns limit our

ability to generalize to other areas served by Kaiser Permanente. Our findings benefit from the complete capture of health services through the integrated care delivery system, but future research is needed to see if the patterns and magnitude of the economic burden associated with MAAGE vary across healthcare system types, regions, and important patient factors. The data used in our study are 6–8 years old and may not represent current costs. Our analyses adjust to a common year and primarily focus on relative costs between groups, which, although prone to influence from differential changes in costs of medical services over time, are less influenced by general medical-care inflation.

In conclusion, in a large surveillance cohort, we found significantly increased, incremental cost associated with MAAGE-related services relative to usual-care medical services. We noted this increased cost for both adults and for children ≥5 years of age, and those higher costs persisted during the 30-day follow-up period from initial encounters. These findings suggest opportunities to prevent or intervene in the short-term period following a new MAAGE episode to mitigate costs, especially in adults ≥65 years of age.

Acknowledgments

We acknowledge the contributions of the MAAGE study recruiters (Peggy Cook, Michelle Depew, Camille Friason, Ann Macfarlane, Joanne Price, Judy Sanseri, and Sarah Vertress), as well as Elizabeth Esterberg and Kevin Moua for assisting with data collection, management, and analysis.

The Kaiser Permanente Center for Health Research received institutional research funding for the MAAGE project from the CDC Foundation and through investigator-initiated research grants from Takeda Vaccines, Inc. (IISR-2015-101015 and IISR-2017-101938). Takeda had no role in study design, data collection and analysis, decision to publish, or preparation of the manuscript. The Centers for Disease Control and Prevention received no funding from Takeda. J.F.D. receives funding from Janssen Pharmaceuticals, Pfizer, and Novartis. M.A.S. receives funding from Gilead, Janssen Pharmaceuticals, and Pfizer.

About the Author

Dr. Dickerson is an investigator at the Kaiser Permanente Center for Health Research located in Portland, Oregon. Dr. Dickerson's primary research interests are in health economics and methods to model mechanisms of bias in observational and controlled studies.

References

1. Burke RM, Mattison CP, Pindyck T, Dahl RM, Rudd J, Bi D, et al. Burden of norovirus in the United States, as estimated based on administrative data: updates for medically attended illness and mortality, 2001-2015. Clin Infect Dis. 2021;73:e1–8. https://doi.org/10.1093/cid/ciaa438
2. Schmidt MA, Groom HC, Rawlings AM, Mattison CP, Salas SB, Burke RM, et al. Incidence, etiology, and healthcare utilization for acute gastroenteritis in the community, United States. Emerg Infect Dis. 2022;28:2234–42. https://doi.org/10.3201/eid2811.220247
3. Burke RM, Mattison CP, Marsh Z, Shioda K, Donald J, Salas SB, et al. Norovirus and other viral causes of medically attended acute gastroenteritis across the age spectrum: results from the medically attended acute gastroenteritis study in the United States. Clin Infect Dis. 2021;73:e913–20. https://doi.org/10.1093/cid/ciab033
4. Papadopoulos T, Klamer S, Jacquinet S, Catry B, Litzroth A, Mortgat L, et al. The health and economic impact of acute gastroenteritis in Belgium, 2010–2014. Epidemiol Infect. 2019;147:e146. https://doi.org/10.1017/S095026881900044X
5. Schmutz C, Mäusezahl D, Bless PJ, Hatz C, Schwenkglenks M, Urbinello D. Estimating healthcare costs of acute gastroenteritis and human campylobacteriosis in Switzerland. Epidemiol Infect. 2017;145:627–41. https://doi.org/10.1017/S0950268816001618
6. Karve S, Krishnarajah G, Korsnes JS, Cassidy A, Candrilli SD. Burden of acute gastroenteritis, norovirus and rotavirus in a managed care population. Hum Vaccin Immunother. 2014;10:1544–56. https://doi.org/10.4161/hv.28704
7. Moon RC, Bleak TC, Rosenthal NA, Couturier B, Hemmert R, Timbrook TT, et al. Epidemiology and economic burden of acute infectious gastroenteritis among adults treated in outpatient settings in US health systems. Am J Gastroenterol. 2023;118:1069–79. https://doi.org/10.14309/ajg.0000000000002186
8. Schmidt MA, Groom HC, Naleway AL, Biggs C, Salas SB, Shioda K, et al. A model for rapid, active surveillance for medically-attended acute gastroenteritis within an integrated health care delivery system. PLoS One. 2018;13:e0201805. https://doi.org/10.1371/journal.pone.0201805
9. O'Keeffe-Rosetti MC, Hornbrook MC, Fishman PA, Ritzwoller DP, Keast EM, Staab J, et al. A standardized relative resource cost model for medical care: application to cancer control programs. J Natl Cancer Inst Monogr. 2013;2013:106–16. https://doi.org/10.1093/jncimonographs/lgt002
10. Pan W. Akaike's information criterion in generalized estimating equations. Biometrics. 2001;57:120–5. https://doi.org/10.1111/j.0006-341X.2001.00120.x
11. Akaike H. Information theory and an extension of the maximum likelihood principle. In: Parzen E, Tanabe K, Kitagawa G, eds. Selected papers of Hirotugu Akaike. Springer Series in Statistics. New York: Springer; 1998. https://doi.org/10.1007/978-1-4612-1694-0_15
12. Weichle T, Hynes DM, Durazo-Arvizu R, Tarlov E, Zhang Q. Impact of alternative approaches to assess outlying and influential observations on health care costs. Springerplus. 2013;2:614. https://doi.org/10.1186/2193-1801-2-614

Address for correspondence: Holly Groom, Center for Health Research, Kaiser Permanente Northwest, 3800 N Interstate Ave, Portland, OR 97227, USA; email: holly.c.groom@kpchr.org

Antimicrobial Resistance as Risk Factor for Recurrent Bacteremia after *Staphylococcus aureus*, *Escherichia coli*, or *Klebsiella* spp. Community-Onset Bacteremia

Salam Abbara, Didier Guillemot, David R.M. Smith, Salma El Oualydy, Maeva Kos, Cécile Poret, Stéphane Breant, Christian Brun-Buisson, Laurence Watier

We investigated links between antimicrobial resistance in community-onset bacteremia and 1-year bacteremia recurrence by using the clinical data warehouse of Europe's largest university hospital group in France. We included adult patients hospitalized with an incident community-onset *Staphylococcus aureus*, *Escherichia coli*, or *Klebsiella* spp. bacteremia during 2017–2019. We assessed risk factors of 1-year recurrence using Fine–Gray regression models. Of the 3,617 patients included, 291 (8.0%) had ≥1 recurrence episode. Third-generation cephalosporin (3GC)-resistance was significantly associated with increased recurrence risk after incident *Klebsiella* spp. (hazard ratio 3.91 [95% CI 2.32–6.59]) or *E. coli* (hazard ratio 2.35 [95% CI 1.50–3.68]) bacteremia. Methicillin resistance in *S. aureus* bacteremia had no effect on recurrence risk. Although several underlying conditions and infection sources increased recurrence risk, 3GC-resistant *Klebsiella* spp. was associated with the greatest increase. These results demonstrate a new facet to illness induced by 3GC-resistant *Klebsiella spp.* and *E. coli* in the community setting.

Author affiliations: Institut National de la Santé et de la Recherche Médicale, Montigny–Le-Bretonneux, France (S. Abbara, D. Guillemot, C. Brun-Buisson, L. Watier); Versailles Saint Quentin en Yvelines University, Montigny–Le-Bretonneux (S. Abbara, D. Guillemot, C. Brun-Buisson, L. Watier); Institut Pasteur, Paris, France (S. Abbara, D. Guillemot, C. Brun-Buisson, L. Watier); Paris–Cité University, Paris (S. Abbara, D. Guillemot, C. Brun-Buisson, L. Watier); Paris–Saclay University, Le Kremlin–Bicêtre, France (D. Guillemot); Assistance Publique–Hôpitaux de Paris, Paris (D. Guillemot, C. Poret, S. Breant); University of Oxford, Oxford, UK (D.R.M. Smith); Plateforme de Données de Santé, Paris (S. El Oualydy, M. Kos)

DOI: https://doi.org/10.3201/eid3005.231555

Antimicrobial resistance (AMR) is a major global health issue, associated with an estimated 4.95 million deaths worldwide in 2019 (*1*,*2*). Although the effects of AMR on clinical and economic outcomes have been studied extensively, relatively little is known about the effects of AMR on infection recurrence, a significant event that results in substantial illness, death, and healthcare costs (*3*). Recurrence is of particular concern among bacteremia patients, who are often fragile and have underlying conditions, because bacteremia is associated with high rates of death and AMR (*4*). AMR in bacteremia is associated with greater infection severity, higher risk for treatment failure, and longer length of hospital stay, all of which may affect risk for recurrence (*5*–*7*).

Few studies have investigated AMR as a potential risk factor for recurrent bacteremia, and all have been limited to recurrence of infection attributable to the same bacterium that caused initial infection (*8*–*13*). Conversely, the few studies not targeting a specific bacterial species or patient population (e.g., those with underlying conditions) and studying risk factors associated with recurrence within 1 year did not consider AMR as a potential risk factor (*14*–*16*). However, when studying the link between AMR and recurrence, it is important to consider the prolonged microbial imbalance that broad-spectrum antibiotic exposure (i.e., standard bacteremia treatment) can induce on the host microbiome. This imbalance includes ensuing effects on host susceptibility to colonization and infection (*17*) and effects on selection and duration of carriage of antibiotic-resistant bacteria, which, for instance, can exceed 1 year for extended-spectrum β-lactamase (ESBL)–producing Enterobacteriaceae (*18*). AMR in an initial bacteremia episode may thus increase risk for

recurrence attributable not only to the same bacterium that caused the initial infection but to any bacterium, whether acquired in the community or hospital. As such, studying bacteremia recurrence across all bacterial species and sources of infection seems clinically relevant. Moreover, it is particularly important to focus on community-onset infections, given the increasing spread of ESBL-producing Enterobacteriaceae in community settings globally (*19*).

In this study, we investigated the effect of AMR in incident community-onset bacteremia on the probability of bacteremia recurrence within 1 year. We restricted incident bacteremia episodes to infections caused by *S. aureus*, *E. coli*, and *Klebsiella* spp., 3 leading pathogens responsible for community-onset bacteremia, and to their leading forms of AMR of major public health concern: methicillin resistance for *S. aureus* and third-generation cephalosporin (3GC) resistance for *E. coli* and *Klebsiella* spp., the major mechanism of which is ESBL production (*20*).

Material and Methods

Setting

This observational study used routinely collected data extracted retrospectively from the clinical data warehouse of the Assistance Publique–Hôpitaux de Paris (AP-HP) (https://www.aphp.fr). AP-HP is the largest university hospital group in Europe, with 39 hospitals mainly located in the Greater Paris area and totaling 1.5 million hospitalizations per year (10% of all hospitalizations in France). We focused on 14 AP-HP hospitals with acute care activity, covering ≈22% of all short stays in Île-de-France, the largest region in France. The construction of the database and the included variables have been previously described (*4*). Available data include medical-administrative data describing patient characteristics and hospital stays, as well as microbiological data including infection etiology and antibiotic-susceptibility results. We obtained approval for data collection from the Scientific and Ethical Committee of the Assistance Publique–Hôpitaux de Paris on March 28, 2019. The AP-HP clinical data warehouse initiative ensures that patient information and informed consent regarding the different approved studies are in accordance with European regulations on data protection and authorization number 1980120 from the French Data Protection Authority.

Study Population

The study population included all patients ≥18 years of age who were hospitalized with a first clinically important episode of community-onset, monomicrobial bacteremia attributable to *S. aureus*, *E. coli*, or *Klebsiella* spp. in 14 AP-HP university hospitals during January 1, 2017–December 31, 2019. We categorized bacteremia episodes as community-onset if first positive blood culture was collected within 48 hours of admission; otherwise, we categorized the bacteremia as hospital-acquired. We identified incident stays by excluding stays by patients with any history of bacteremia within the previous 12 months, regardless of microbial etiology and location of onset (i.e., whether community-onset or hospital-acquired). We excluded stays ending with death. To avoid including early relapses, we defined recurrence as any clinically important episode of bacteremia (whatever the species, wherever the onset) occurring 7–365 days after hospital discharge from the incident episode (*21*). We identified bacteremia episodes by using microbiologic results (i.e., positive blood cultures) and defined them as previously described (*4*). For statistical analysis, we considered 2 main patient groups: those with recurrence and those without.

Data Collected

For each patient, data collected were sex, age, and date of death (if applicable). For each incident stay, data collected were dates of admission and discharge; hospital care pathways (e.g., surgery, admission to intensive care unit [ICU], and presence of a septic shock); codes from the International Classification of Diseases, 10th Revision (ICD-10), for underlying conditions; and microbiologic results (e.g., types and dates of microbiologic samples drawn, bacterial species isolated, and antibiotic-susceptibility results). Bacterial antibiotic susceptibilities were determined by the laboratories of participating hospitals by using clinical breakpoints from Comité de l'Antibiogramme de la Société Francaise de Microbiologie–European Committee on Antimicrobial Susceptibility Testing (*22*) and the qualitative susceptibility categories of susceptible, standard dosing regimen (S), susceptible, increased exposure (I), and resistant (R). For antibiotics of interest, we considered strains reported as I to be resistant. When available, empirical therapy data were collected 24 hours before and after the collection date of the first positive blood culture. For each recurrent stay, we collected only dates of hospital admission and discharge and microbiologic results.

Variables Studied

Patient variables included sex, age group, Charlson comorbidity index (calculated by using comorbidity-associated ICD-10 codes), and comorbidities (i.e.,

underlying conditions) defined with ICD-10 codes. For each incident stay, other variables considered include patient length of stay (LOS) with bacteremia (the number of days in hospital from the first positive blood culture to the end of the stay), surgery, ICU admission, presence of septic shock, identified bacterial species (*S. aureus*, *E. coli*, or *Klebsiella* spp.), antibiotic susceptibility results, and infection sources (defined according to ICD-10 codes, as previously described) (*4*). Because the effect of resistance may differ according to bacterial species, we considered a 6-class bacteria resistance composite variable (methicillin-susceptible *S. aureus* [MSSA] and methicillin-resistant *S. aureus* [MRSA], 3GC-susceptible and resistant *E. coli*, and 3GC-susceptible and resistant *Klebsiella* spp.) We considered empirical therapy appropriate if ≥1 antibiotic administered within 24 hours of drawing the first positive blood culture was effective in vitro on the isolated bacteria.

Statistical Analysis

We described all included patient and hospital stay characteristics according to the presence or absence of recurrence. We also briefly described first recurrent bacteremia and their etiologies. We used Fine–Gray regression models to identify risk factors for recurrence within 1 year after an incident stay, considering death as a competing event. We calculated subdistribution hazard ratios (HRs) by using Gray's test of the subdistribution function for univariate analyses and Fine–Gray regression models for multivariable analyses. HRs represent the relative change in the instantaneous rate of the occurrence of recurrence in patients who are recurrence-free or who have experienced death, considering patients who have died as nonexposed to recurrence (*23*). The direction of HRs also describes the direction of the effect of covariates on the probability of recurrence occurring over time (incidence) (*23*). We considered variables that had a p value ≤0.20 in univariate analyses in the multivariable models. We selected variables in the multivariable models by using both backward and forward stepwise methods, and we used a 2-tailed p value <0.05 to define statistical significance. We assessed proportional hazards assumptions in Fine–Gray regressions. We forced the variables age and sex in the multivariable model because they usually are associated with bacterial infections. To confirm results and because the effect of resistance may differ according to bacterial species, we conducted an analysis stratified by bacteria. To assess whether empirical treatment is a confounding factor, we performed an additional analysis considering only patients with information on the adequacy of empirical treatment. For comparability purposes, we estimated a multivariable logistic regression model, considering the same covariates as in the final Fine–Gray regression model. Adjusted odds ratios calculated in the logistic regression model quantify associations between included variables and the odds of bacteremia recurrence, without considering death as a competing event. Finally, to ensure that the type of recurrence, to the same species or to a different species, was not a confounding factor, we estimated a specific Fine–Gray regression model and a multivariable logistic regression model in each of the 2 subgroups, following the same methodology as for the overall sample.

We used HiveQL (https://hive.apache.org), Python 3 (https://www.python.org), PySpark 2.4.3 (https://spark.apache.org/docs/2.4.3), and R 4.0.0 (The R Foundation for Statistical Computing, https://cran.r-project.org) to perform the statistical analyses, and we used the survival R package to compute Fine–Gray regression models (*24*). This study follows the Strengthening the Reporting of Observational Studies in Epidemiology reporting guideline (*25*).

Results

During 2017–2019, we identified 4,400 patients hospitalized with a community-onset bacteremia attributable to *S. aureus*, *E. coli*, or *Klebsiella* spp. We retained their first hospital stay with bacteremia. Of those first stays, 6.9% (n = 304) were excluded because of history of bacteremia within the previous 12 months (Figure 1). Among the remaining 4,096 patients, 11.7% (n = 479) died during their hospital stay and were excluded. In total, we included in the study 3,617 patients with incident hospital stays with community-onset bacteremia attributable to *S. aureus*, *E. coli*, or *Klebsiella* spp. Of those, 8.0% (n = 291) sought treatment for ≥1 recurrent bacteremia during the following year.

Descriptive Analyses

Incident Stays

Patients with recurrence were more often male than patients without recurrence (56.7% male vs. 47.9% female; p = 0.004) and were more likely to be <80 years of age (81.8% <80 vs. 73.4% ≥80; age distribution p = 0.0005) (Table 1). Patients with recurrence also had more underlying conditions (27% had a null Charlson comorbidity index vs. 44% of those without recurrence) and were almost twice as likely as their counterparts to have cancer (37.6% vs. 19.5%; p<0.0001), renal disease (22.3% vs. 13.6%; p = 0.002), or liver disease (13.8% vs. 7.5%; p = 0.0007).

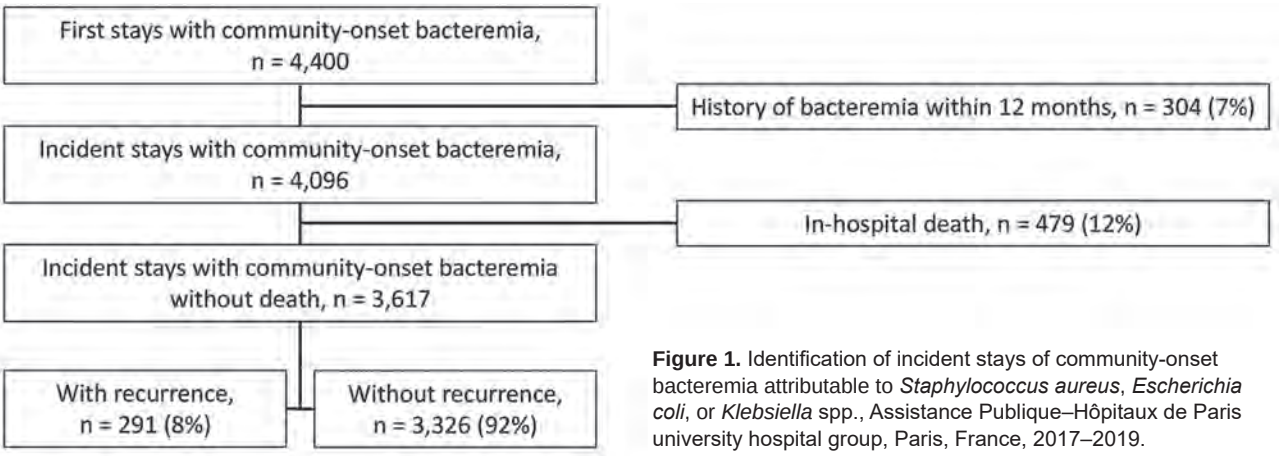

Figure 1. Identification of incident stays of community-onset bacteremia attributable to *Staphylococcus aureus*, *Escherichia coli*, or *Klebsiella* spp., Assistance Publique–Hôpitaux de Paris university hospital group, Paris, France, 2017–2019.

We observed no statistical difference (p>0.05) between patients with and without recurrence in terms of incident stay characteristics, including LOS with bacteremia (median 7–8 days), rates of surgery, ICU admission, and occurrence of septic shock. However, we observed significant differences regarding the infection source, isolated bacteria, and rates of AMR (p<0.0001 for all). Compared with patients that did not have recurrence, recurrence was more often associated with bacteremia without an identified infection source (24.1% vs. 14.0%) or associated with a digestive (12.1% vs. 9.5%) or device-related infection (7.8% vs. 4.4%) and less often with urinary-source bacteremia (26.2% vs. 35.7%). Moreover, recurrences were more often associated with incident infections attributable to 3GC-resistant *E. coli* (13.1% vs 7.6%), 3GC-susceptible (13.1% vs. 9.3%) or resistant (7.2% vs. 1.9%) *Klebsiella* spp.

Recurrent Stays

Patients with recurrence had an average of 2.3 (range 2–8 stays) hospital stays with bacteremia over the study period, including their incident stay. First recurrent stays occurred within a median of 80 days (first quartile–third quartile 30.0–175.0 after the incident stay) and were predominantly community-onset (n = 166/291 [57.0%]); median LOS was 11 days (first quartile–third quartile 6.0–19.0 days). The most identified bacteria in first recurrent stays were *E. coli*, *Klebsiella* spp., polymicrobial infection, *S. aureus*, and *Pseudomonas aeruginosa* (Appendix Table 1, https://wwwnc.cdc.gov/EID/article/30/5/23-1555-App1.pdf). In 47.4% of first recurrent episodes (n = 138/291), the same bacterial species was identified as in the incident stay. This rate was higher for E. coli (n = 92/174 [53%]) than for Klebsiella spp. (n = 25/59 [42%]) or S. aureus (n = 21/58 [36%]). In cases of recurrence attributable to the same species, >80% of isolates had the same resistance phenotype as identified in the incident stay (Appendix Table 2).

Regression Models

Variables not selected for inclusion in the multivariable analysis were heart failure, diabetes, systemic disease, LOS with bacteremia, surgery, ICU admission, and presence of septic shock (Table 2). We did not include Charlson scores in the multivariable model because individual underlying conditions were preferred. In the final model, vascular disease, chronic lung disease, dementia, and presence of paralysis were not retained, and proportional hazards assumptions were validated (p = 0.39).

Underlying Conditions and Infection Sources

Certain infectious sources were associated with increased recurrence risk within 1 year: absence of an identified infection source (HR 2.26 [95% CI 1.60–3.19]), device-related infection (HR 1.93 [95% CI 1.16–3.23]), and digestive tract infection (HR 1.57 [95% CI 1.03–2.38]). Certain underlying conditions also were identified as associated with increased recurrence risk within 1 year: cancer (HR 2.03 [95% CI 1.58–2.62]), renal disease (HR 1.72 [95% CI 1.28–2.31]), and liver disease (HR 1.66 [95% CI 1.17–2.35]) (Table 2).

Antimicrobial Resistance

Isolation of MRSA in incident bacteremia episodes did not affect the incidence of recurrence (HR 0.79 [95% CI 0.29–2.19]; referent MSSA). Conversely, isolation of 3GC-resistant *E. coli* (HR 2.02 [95% CI 1.41–2.91]; referent 3GC-susceptible *E. coli*) or 3GC-resistant *Klebsiella* spp. (HR 2.77 [95% CI 1.60–4.79]; referent 3GC-susceptible *Klebsiella* spp.) were associated with an increased risk for recurrence (Table 3). Cumulative incidence function curves of recurrence

over time (Figure 2) show the differential effect of bacteria-resistance pairs on risk for recurrence, which was highest for 3GC-resistant *Klebsiella* spp. Those results were similar in an analysis stratified by bacterial species (Table 4) and in the multivariable logistic regression model (Appendix Table 3). A sensitivity analysis considering only stays (36%) with information on empirical treatment showed comparable results, with a higher HR for 3GC-resistant *Klebsiella* spp. and no effect of adequacy of empirical treatment on recurrence risk (Appendix Table 4).

Fine–Gray models limited to recurrence to the same or a different species (Appendix Tables 5–7) showed similar HRs for 3GC-resistant *Klebsiella* spp.

Table 1. Characteristics of patients and their incident stays with community-onset bacteremia attributable to *Staphylococcus aureus*, *Escherichia coli*, or *Klebsiella* spp., with and without recurrence, Assistance Publique–Hôpitaux de Paris university hospital group, Paris, France, 2017–2019*

Characteristic	With recurrence, n = 291	Without recurrence, n = 3,326	p value
Patients			
Sex			0.004
M	165 (56.7)	1,594 (47.9)	
F	126 (43.3)	1,732 (52.1)	
Age group, y			0.0005
18–35	10 (3.4)	227 (6.8)	
35–50	34 (11.7)	378 (11.4)	
50–65	84 (28.9)	765 (23.0)	
65–80	110 (37.8)	1,070 (32.2)	
>80	53 (18.2)	886 (26.6)	
Charlson comorbidity index†			<0.0001
0	75 (26.6)	1,389 (44.1)	
1–2	109 (38.7)	1,004 (31.9)	
>2	98 (34.7)	7,59 (24.0)	
Underlying conditions†			
Cancer	106 (37.6)	615 (19.5)	<0.0001
Heart failure	35 (12.4)	423 (13.4)	0.61
Diabetes	63 (22.3)	730 (23.2)	0.79
Vascular disease	23 (8.2)	340 (10.8)	0.18
Renal disease	63 (22.3)	430 (13.6)	0.002
Liver disease	39 (13.8)	237 (7.5)	0.0007
Chronic pulmonary disease	12 (4.3)	189 (6.0)	0.24
Dementia	9 (3.2)	178 (5.7)	0.06
Paralysis (hemiplegia or paraplegia)	4 (1.4)	84 (2.7)	0.21
Systemic disease	5 (1.8)	32 (1.0)	0.30
Incident stays			
Length of stay with bacteremia, days			
Median (first quartile–third quartile)	8.0 (4.0–15.5)	7.0 (3.0–15.0)	
Duration, d			0.30
≤7	139 (47.8)	1,730 (52.0)	
7–14	74 (25.4)	706 (21.2)	
14–30	50 (17.2)	613 (18.4)	
>30	28 (9.0)	277 (8.3)	
Surgery	37 (12.7)	426 (12.8)	0.97
ICU admission	70 (24.1)	718 (21.6)	0.30
Septic shock†	27 (9.6)	279 (8.9)	0.68
Infection source†			<0.0001
None identified	68 (24.1)	442 (14.0)	
Multiple sites	59 (20.9)	747 (23.7)	
Urinary tract	74 (26.2)	1,125 (35.7)	
Lower respiratory tract	14 (5.0)	190 (6.0)	
Digestive tract	34 (12.1)	300 (9.5)	
Device-related	22 (7.8)	137 (4.4)	
Other	11 (3.9)	211 (6.7)	
Bacteria resistance			<0.0001
MSSA	54 (18.6)	737 (22.2)	
MRSA	4 (1.4)	75 (2.2)	
3GC-susceptible *E. coli*	136 (46.7)	1,889 (56.8)	
3GC-resistant *E. coli*	38 (13.05)	253 (7.6)	
3GC-susceptible *Klebsiella* spp.	38 (13.05)	310 (9.3)	
3GC-resistant *Klebsiella* spp.	21 (7.2)	62 (1.9)	

*Values are no. (%) except as indicated. p values calculated by using likelihood ratio tests. 3GC, third-generation cephalosporin; ICU, intensive care unit; MRSA, methicillin-resistant *S. aureus*; MSSA, methicillin-susceptible *S. aureus*.
†Missing data: 9 stays with recurrence, 174 stays without recurrence.

Table 2. Univariable and multivariable analyses of risk factors for bacteremia recurrence at 1 year after an incident stay with community-onset bacteremia attributable to *Staphylococcus aureus*, *Escherichia coli*, or *Klebsiella* spp., Assistance Publique–Hôpitaux de Paris university hospital group, Paris, France, 2017–2019*

	Univariable analyses		Multivariable analyses	
Characteristic	HR (95% CI)	p value	HR (95% CI)	p value
Patients				
Sex; referent male	0.71 (0.57–0.90)	0.004	0.94 (0.73–1.20)	0.59
Age group, y; referent 35–50 y		0.0005		0.075
≥18–35	0.51 (0.25–1.03)		0.66 (0.31–1.38)	
50–65	1.23 (0.82–1.83)		1.15 (0.76–1.74)	
65–80	1.14 (0.78–1.69)		1.13 (0.76–1.69)	
>80	0.68 (0.44–1.05)		0.77 (0.49–1.20)	
Charlson comorbidity index; referent 0		<0.0001		
1–2	1.95 (1.46–2.62)			
>2	2.31 (1.71–3.12)			
Underlying conditions				
Cancer	2.36 (1.86–3.00)	<0.0001	2.03 (1.58–2.62)	<0.0001
Heart failure	0.91 (0.64–1.30)	0.61		
Diabetes	0.96 (0.73–1.27)	0.79		
Vascular disease	0.75 (0.49–1.14)	0.18		
Renal disease	1.60 (1.20–2.13)	0.002	1.72 (1.28–2.31)	0.0007
Liver disease	1.89 (1.35–2.65)	0.0007	1.66 (1.17–2.35)	0.007
Chronic pulmonary disease	0.71 (0.40–1.26)	0.24		
Dementia	0.56 (0.29–1.09)	0.06		
Paralysis (hemiplegia / paraplegia)	0.53 (0.20–1.43)	0.21		
Systemic disease	1.70 (0.70–4.12)	0.30		
Incident stays				
Length of stay with bacteremia; referent 7–14 d		0.30		
≤7	0.78 (0.59–1.03)			
14–30	0.79 (0.55–1.13)			
>30	0.97 (0.63–1.50)			
Surgery	1.01 (0.71–1.42)	0.97		
ICU admission	1.15 (0.89–1.51)	0.30		
Septic shock	1.09 (0.73–1.62)	0.68		
Infection source; referent urinary tract		<0.0001		0.0002
None identified	2.25 (1.62–3.13)		2.26 (1.60–3.19)	
Multiple sites	1.19 (0.85–1.68)		1.22 (0.85–1.75)	
Lower respiratory tract	1.12 (0.63–1.98)		1.26 (0.70–2.26)	
Digestive tract	1.69 (1.13–2.54)		1.57 (1.03–2.38)	
Device-related	2.32 (1.44–3.74)		1.93 (1.16–3.23)	
Other	0.80 (0.43–1.51)		0.98 (0.51–1.75)	
Bacteria resistance; referent MSSA		<0.0001		<0.0001
MRSA	0.74 (0.27–2.04)		0.79 (0.29–2.19)	
3GC-susceptible *E. coli*	0.99 (0.72–1.36)		1.16 (0.81–1.66)	
3GC-resistant *E. coli*	1.99 (1.31–3.01)		2.35 (1.50–3.68)	
3GC-susceptible *Klebsiella* spp.	1.64 (1.09–2.49)		1.41 (0.91–2.21)	
3GC-resistant *Klebsiella* spp.	4.11 (2.48–6.81)		3.91 (2.32–6.59)	

*p values calculated by using Gray's test of the subdistribution function for univariable analyses, and Fine–Gray regression models for multivariable analyses. 3GC, third-generation cephalosporin; HR, subdistribution hazard ratio; ICU, intensive care unit; MRSA, methicillin-resistant *S. aureus*; MSSA, methicillin-susceptible *S. aureus*.

(referent 3GC-susceptible *Klebsiella* spp.). For 3GC-resistant *E. coli*, the HR was slightly higher for recurrence to the same species (2.47 [95% CI 1.54–3.95]), and slightly lower for recurrence to a different species (1.68 [95% CI 0.94–3.01]; referent 3GC-resistant *E. coli*). Stratified analysis by bacteria found comparable results, except for the HR of the association between 3GC-resistant *Klebsiella* spp. and recurrence to the same species, which was slightly lower (2.32 [95% CI 0.96–5.62]), likely attributable to reduced sample size (Appendix Table 8). Multivariate logistic regression models for recurrence to the same and to different species yielded similar associations (Appendix Table 9).

Discussion

In this cohort study, we have shown that 3GC resistance in *Klebsiella* spp. or *E. coli* in community-onset bacteremia significantly increases the probability of all-cause bacteremia recurrence within 1 year, whereas identification of MRSA does not affect risk for recurrence. Our results confirm, in community-onset bacteremia, that certain patient underlying conditions (cancer, liver disease, and renal disease) and infection sources (digestive tract, device-related, and no identified infection source) are important risk factors for bacteremia recurrence. Of all identified risk factors, the isolation of 3GC-resistant *Klebsiella* spp. was associated with the greatest increase in the probability of recurrence over time.

Table 3. Subdistribution HRs for relationship between each bacteria-resistance pair and recurrence of bacteremia at 1 year in final multivariable model, by reference, in study of community-onset bacteremia attributable to *Staphylococcus aureus*, *Escherichia coli*, or *Klebsiella* spp., Assistance Publique–Hôpitaux de Paris university hospital group, Paris, France, 2017–2019*

	HR (95% CI)		
Bacteria resistance	Referent MSSA	Referent 3GC-susceptible *E. coli*	Referent 3GC-susceptible *Klebsiella* spp.
MSSA	Referent	0.86 (0.60–1.23)	0.71 (0.45–1.11)
MRSA	0.79 (0.29–2.19)	0.68 (0.25–1.86)	0.56 (0.20–1.59)
3GC-susceptible *E. coli*	1.16 (0.81–1.66)	Referent	0.82 (0.56–1.20)
3GC-resistant *E. coli*	2.35 (1.50–3.68)	2.02 (1.41–2.91)	1.66 (1.04–2.66)
3GC-susceptible *Klebsiella* spp.	1.41 (0.91–2.21)	1.22 (0.83–1.78)	Referent
3GC-resistant *Klebsiella* spp.	3.91 (2.32–6.59)	3.37 (2.10–5.41)	2.77 (1.60–4.79)

*Results are adjusted on all the variables described in Table 2. 3GC, third-generation cephalosporin; HR, subdistribution hazard ratio; MRSA, methicillin-resistant *S. aureus*; MSSA, methicillin-susceptible *S. aureus*.

Few studies have examined the relationship between AMR and bacteremia recurrence (*8*–*13*). Woudt et al. (*8*) showed an association between the isolation of MRSA or 3GC-resistant Enterobacteriaceae and recurrence of bacteremia attributable to the same species, with crude relative risks of <2. Choi et al. (*9*) found no effect of MRSA on recurrence of *S. aureus* bacteremia over a 7-year study period, after adjustment. One study has focused on the community context and showed crude associations between *E. coli* sequence types 131 or 405, which could be used as a proxy for AMR, and the risk for recurrence (*13*). Our study has shown an effect of 3GC-resistance in community-onset bacteremia attributable to *Klebsiella* spp. or *E. coli* on the probability of recurrence over time, after adjustment for diverse risk factors and while considering death as a competing event.

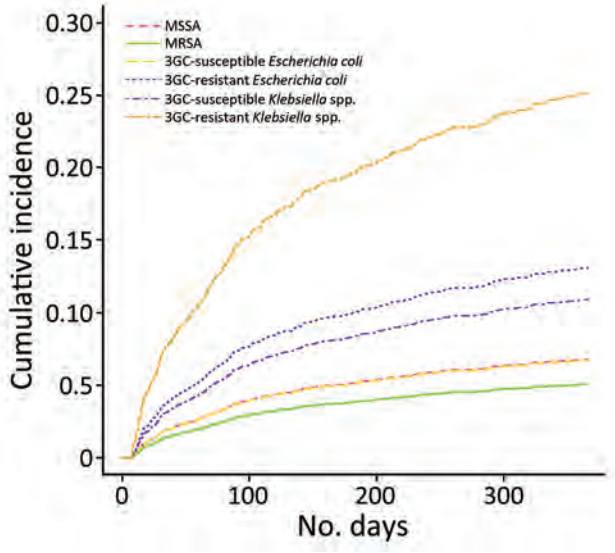

Figure 2. Cumulative incidence function curves showing probability of recurrence over time for each bacteria-resistance pair after community-onset bacteremia attributable to *Staphylococcus aureus*, *Escherichia coli*, or *Klebsiella* spp., Assistance Publique–Hôpitaux de Paris university hospital group, Paris, France, 2017–2019. 3GC, third-generation cephalosporin; ICU, intensive care unit; MRSA, methicillin-resistant *S. aureus*; MSSA, methicillin-susceptible *S. aureus*.

In agreement with Choi et al. (*9*), we found no effect of MRSA on recurrence after adjustment, although our findings are not directly comparable given the community-onset nature of the incident stays and shorter duration of follow-up.

We studied recurrence up to 1 year, accounting for all species and types of bacteremia onset. Although this definition differs from previous works, which focused on recurrence to the same bacterium, we argue that it better captures the potential effect of AMR and ensuing antibiotic exposure on host microbiota and overall susceptibility to infection (*17*). Irrespective of their appropriateness to treat a given bacterium, antibiotics can induce dysbiosis, with repercussions for host immunity, selection of antibiotic-resistant strains, colonization, and infection by antibiotic-susceptible or antibiotic-resistant strains (*17*,*26*–*28*). Given that approximately half the recurrences were attributable to the same species, we conducted sensitivity analyses in the 2 subgroups with recurrence attributable to the same or to a different species. Those analyses showed results consistent with the overall analysis, while suggesting a greater effect of isolating 3GC-resistant *E.coli* during the incident episode on the risk for recurrence attributable to the same species compared with recurrence attributable to a different species. On the other hand, the link between 3GC-resistant *Klebsiella spp.* and the risk for recurrence attributable to the same or a different species was similar. Those results support previous works showing higher rates of illness associated with *Klebsiella spp.* infections compared with *E. coli* infections. Al-Hasan et al. (*29*) showed that isolation of *Klebsiella* spp. was associated with bacteremia recurrence, relative to isolation of *E. coli* and after adjustment. Other work has suggested that patients with ESBL-producing *Klebsiella pneumoniae* bacteremia have higher rates of ICU admission and death compared with patients with ESBL-producing *E. coli* bacteremia (*30*,*31*). Overall, our findings

Table 4. Subdistribution HRs for the relationship between bacteria resistance and recurrence of bacteremia at 1 year in analysis stratified by species in study of community-onset bacteremia attributable to *Staphylococcus aureus*, *Escherichia coli*, or *Klebsiella* spp., Assistance Publique–Hôpitaux de Paris university hospital group, Paris, France, 2017–2019*

	HR (95% CI)		
Bacteria resistance	*S. aureus*	*E. coli*	*Klebsiella* spp.
Susceptible	Referent	Referent	Referent
Resistant	0.82 (0.29–2.31)	2.08 (1.44–3.00)	2.41 (1.35–4.30)

*Results were adjusted on all variables included in the multivariable model. Susceptible category included methicillin-susceptible *S. aureus*, and third-generation cephalosporin-susceptible *E. coli* and *Klebsiella* spp. Resistant category included methicillin-resistant *S. aureus*, and third-generation cephalosporin-resistant *E. coli* and *Klebsiella* spp. HR, subdistribution hazard ratio.

demonstrate a new facet to the disease burden imposed by 3GC resistance in *E. coli* and especially *Klebsiella* spp. infections, the proportions of which are increasing in community settings worldwide (*32*). Our findings support ongoing calls for increased awareness and intervention to limit the spread of antibiotic-resistant *E. coli* and *Klebsiella* spp. in the community. For clinicians in particular, our results highlight the need for increased caution in the follow-up of patients with community-onset bacteremia attributable to 3GC-resistant *Klebsiella* spp. or *E. coli*.

In this study, we have also shown that specific underlying conditions, namely cancer, liver disease, and renal disease, are associated with recurrence, and should thus warrant special attention during patient follow-up. To date, such findings were absent for community-onset bacteremia, and available studies considering certain underlying conditions have shown heterogeneous results (*9*–*12*,*33*,*34*). Furthermore, as previously observed, we underlined that the absence of an infection source or the presence of a digestive or device-related infection source were associated with recurrence (*16*).

Strengths of our study include the large size of our cohort, as well as the richness of the clinical and microbiologic data available, which allowed for the evaluation of potential effects of diverse risk factors. Although the numbers of antibiotic-resistant bacterial isolates in the recurrence group varied, we found statistically significant results for *E. coli* and *Klebsiella* spp. and were able to describe a bacteria-specific effect of resistance on recurrence. Moreover, it is notable that subdistribution HRs calculated with the Fine–Gray regression model were very close to adjusted odds ratios calculated with the multivariable logistic regression model, which supports our results. A close relationship between HRs and ORs values is expected if the event studied has a low probability of occurrence over time (*23*), which is the case in our study, given that the 1-year recurrence rate of bacteremia was 8.0%. This rate was lower than that reported by other studies (9%–12%), which could be explained by the selection of community-onset incident stays (*14*–*16*) or by the fact that recurrent stays were only identified among AP-HP hospitals.

Despite the size of our cohort, this study is not population-based, given that it covers approximately one quarter of all acute care inpatients in Île-de-France. Moreover, it included patients hospitalized in university hospitals, who may have more underlying conditions and exposures to care, affecting the risk for recurrence. To minimize this bias, we adjusted our results on most previously identified risk factors of recurrence, which could be related to patients or their hospital stay and infection characteristics (*14*–*16*). Because data on exposure to care was only available among AP-HP hospitals, we could not study this risk factor and used a commonly accepted definition of community-onset infections as occurring within the first 48 hours of admission (*15*,*16*). Moreover, information on empirical treatment, which could affect recurrence risk, was only available for one third of included cases because of the multiplicity of drug prescription software platforms used across included hospitals (*14*,*16*). Despite this limitation, a sensitivity analysis on patients with information on their empirical treatment showed similar results to the main analysis, thereby supporting our findings.

In conclusion, we have shown that resistance to 3GCs in *Klebsiella* spp. and *E. coli* during incident community-onset bacteremia significantly increases bacteremia recurrence risk over time. This risk was highest for 3GC-resistant *Klebsiella* spp., for which increasing community dissemination represents an urgent public health problem. These findings reveal an important facet to the disease and death induced by antimicrobial-resistant Enterobacteriaceae and inform a need for careful follow-up of patients recovering from bacteremia caused by these bacteria, as well as and a need for interventions to limit their further spread in the community.

Acknowledgments

The authors thank the Health Data Hub staff, which provided essential administrative and technical support

to the study, without which this database could not have been built. Our thanks also go to the AP-HP clinical data warehouse staff (particularly the Innovation and Data team) who implemented the clinical data warehouse and greatly assisted us in selecting our population, building, and qualifying this database. We would like to also thank other AP-HP staff (particularly the Direction of Clinical Research, Innovation, and Relations with Universities and Research organizations, the Clinical Research Unit of Paris Saclay Ouest, and all hospital departments that provided the data), and L'Institut National de la Santé et de la Recherche Médicale staff (particularly the Institut National de la Santé et de la Recherche Transfert, the Department of Legal Affairs, and the Délégation Régionale Paris–Île-de-France Sud).

Data sharing statement: All pseudonymized data collected for the study can be made available on request from the AP-HP clinical data warehouse staff, on the condition that the research project is accepted by the scientific and ethics committee of the AP-HP clinical data warehouse.

S.A. received a doctoral fellowship from the Ecole des Hautes Etudes en Santé Publique (https://www.ehesp.fr). Funding received by S.A. had no role in the design of the study, in the collection, analyses, or interpretation of data, in the writing of the manuscript, or in the decision to publish the results. L.W. received consulting fees from Pfizer, HEVA, and Sanofi for unrelated projects. Other authors report no competing interests.

Author contributions: S.A., D.G., C.B., and L.W. conceptualized and determined the methodology for the study. L.W. was the scientific manager and main supervisor. S.B. ran the requests to identify patients with bacteremia within the AP-HP clinical data warehouse and worked with M.K., S.A., and S.E.O. to qualify the data. M.K., S.A., and S.E.O. verified, qualified, cleaned, and structured the database. During the construction of the database, C.P. supervised the project on the AP-HP clinical data warehouse side. S.A. selected the population for this study within the database, did the analyses, and wrote the first draft of the paper. S.A., C.B., D.R.M.S., and L.W. edited and revised the manuscript until the final version. S.A., L.W., S.E.O., M.K., and S.B. had access to the study data. All authors have seen and approved the final manuscript.

About the Author

Dr. Abbara is an infectious diseases physician and epidemiologist. Her primary research interests are antimicrobial resistance and community-onset infections, with a focus on the contribution of hospital clinical data warehouses.

References

1. Murray CJ, Ikuta KS, Sharara F, Swetschinski L, Robles Aguilar G, Gray A, et al.; Antimicrobial Resistance Collaborators. Global burden of bacterial antimicrobial resistance in 2019: a systematic analysis. Lancet. 2022;399:629–55. PubMed https://doi.org/10.1016/S0140-6736(21)02724-0
2. Cassini A, Högberg LD, Plachouras D, Quattrocchi A, Hoxha A, Simonsen GS, et al.; Burden of AMR Collaborative Group. Attributable deaths and disability-adjusted life-years caused by infections with antibiotic-resistant bacteria in the EU and the European Economic Area in 2015: a population-level modelling analysis. Lancet Infect Dis. 2019;19:56–66. https://doi.org/10.1016/S1473-3099(18)30605-4
3. Founou RC, Founou LL, Essack SY. Clinical and economic impact of antibiotic resistance in developing countries: a systematic review and meta-analysis. PLoS One. 2017;12:e0189621.
4. Abbara S, Guillemot D, El Oualydy S, Kos M, Poret C, Breant S, et al. Antimicrobial resistance and mortality in hospitalized patients with bacteremia in the Greater Paris area from 2016 to 2019. Clin Epidemiol. 2022;14:1547–60. https://doi.org/10.2147/CLEP.S385555
5. Cosgrove SE. The relationship between antimicrobial resistance and patient outcomes: mortality, length of hospital stay, and health care costs. Clin Infect Dis. 2006;42(Suppl 2):S82–9. https://doi.org/10.1086/499406
6. de Kraker MEA, Wolkewitz M, Davey PG, Koller W, Berger J, Nagler J, et al. Burden of antimicrobial resistance in European hospitals: excess mortality and length of hospital stay associated with bloodstream infections due to *Escherichia coli* resistant to third-generation cephalosporins. J Antimicrob Chemother. 2011;66:398–407. https://doi.org/10.1093/jac/dkq412
7. Stewardson AJ, Allignol A, Beyersmann J, Graves N, Schumacher M, Meyer R, et al.; TIMBER Study Group. The health and economic burden of bloodstream infections caused by antimicrobial-susceptible and non-susceptible *Enterobacteriaceae* and *Staphylococcus aureus* in European hospitals, 2010 and 2011: a multicentre retrospective cohort study. Euro Surveill. 2016;21:30319. https://doi.org/10.2807/1560-7917.ES.2016.21.33.30319
8. Woudt SHS, de Greeff SC, Schoffelen AF, Vlek ALM, Bonten MJM, Cohen Stuart JWT, et al.; Infectious Diseases Surveillance Information System–Antimicrobial Resistance (ISIS-AR) Study Group. Antibiotic resistance and the risk of recurrent bacteremia. Clin Infect Dis. 2018;66:1651–7. https://doi.org/10.1093/cid/cix1076
9. Choi SH, Dagher M, Ruffin F, Park LP, Sharma-Kuinkel BK, Souli M, et al. Risk factors for recurrent *Staphylococcus aureus* bacteremia. Clin Infect Dis. 2021;72:1891–9. https://doi.org/10.1093/cid/ciaa801
10. Turett GS, Blum S, Telzak EE. Recurrent pneumococcal bacteremia: risk factors and outcomes. Arch Intern Med. 2001;161:2141–4. https://doi.org/10.1001/archinte.161.17.2141
11. Lee CH, Su LH, Chen FJ, Tang YF, Chien CC, Liu JW. Clinical and microbiologic characteristics of adult patients with recurrent bacteraemia caused by extended-spectrum β-lactamase-producing *Escherichia coli* or *Klebsiella pneumoniae*. Clin Microbiol Infect. 2015;21:1105.e1–8. https://doi.org/10.1016/j.cmi.2015.07.025
12. Harris PNA, Peri AM, Pelecanos AM, Hughes CM, Paterson DL, Ferguson JK. Risk factors for relapse or persistence of bacteraemia caused by *Enterobacter* spp.: a case-control study. Antimicrob Resist Infect Control. 2017;6:14. https://doi.org/10.1186/s13756-017-0177-0

13. Fröding I, Hasan B, Sylvin I, Coorens M, Nauclér P, Giske CG. Extended-spectrum-β-lactamase- and plasmid AmpC-producing *Escherichia coli* causing community-onset bloodstream infection: association of bacterial clones and virulence genes with septic shock, source of infection, and recurrence. Antimicrob Agents Chemother. 2020;64:e02351–19. https://doi.org/10.1128/AAC.02351-19
14. Gradel KO, Jensen US, Schønheyder HC, Østergaard C, Knudsen JD, Wehberg S, et al.; Danish Collaborative Bacteraemia Network (DACOBAN). Impact of appropriate empirical antibiotic treatment on recurrence and mortality in patients with bacteraemia: a population-based cohort study. BMC Infect Dis. 2017;17:122. https://doi.org/10.1186/s12879-017-2233-z
15. Jensen US, Knudsen JD, Wehberg S, Gregson DB, Laupland KB. Risk factors for recurrence and death after bacteraemia: a population-based study. Clin Microbiol Infect. 2011;17:1148–54. https://doi.org/10.1111/j.1469-0691.2011.03587.x
16. Jensen US, Knudsen JD, Østergaard C, Gradel KO, Frimodt-Møller N, Schønheyder HC. Recurrent bacteraemia: a 10-year regional population-based study of clinical and microbiological risk factors. J Infect. 2010;60:191–9. https://doi.org/10.1016/j.jinf.2009.12.007
17. Smith DR, Temime L, Opatowski L. Microbiome-pathogen interactions drive epidemiological dynamics of antibiotic resistance: a modeling study applied to nosocomial pathogen control. eLife. 2021;10:e68764. https://doi.org/10.7554/eLife.68764
18. Titelman E, Hasan CM, Iversen A, Nauclér P, Kais M, Kalin M, et al. Faecal carriage of extended-spectrum β-lactamase-producing Enterobacteriaceae is common 12 months after infection and is related to strain factors. Clin Microbiol Infect. 2014;20:O508–15. https://doi.org/10.1111/1469-0691.12559
19. Bezabih YM, Sabiiti W, Alamneh E, Bezabih A, Peterson GM, Bezabhe WM, et al. The global prevalence and trend of human intestinal carriage of ESBL-producing *Escherichia coli* in the community. J Antimicrob Chemother. 2021;76:22–9. https://doi.org/10.1093/jac/dkaa399
20. Coque TM, Baquero F, Cantón R. Increasing prevalence of ESBL-producing Enterobacteriaceae in Europe. Euro Surveill. 2008;13:19044. https://doi.org/10.2807/ese.13.47.19044-en
21. Gauzit R, Castan B, Bonnet E, Bru JP, Cohen R, Diamantis S, et al. Anti-infectious treatment duration: the SPILF and GPIP French guidelines and recommendations. Infect Dis Now. 2021;51:114–39. https://doi.org/10.1016/j.idnow.2020.12.001
22. Comité de l'Antibiogramme de la Société Francaise de Microbiologie–European Committee on Antimicrobial Susceptibility Testing. Guidelines of the Comité de l'Antibiogramme de la Société Francaise de Microbiologie–European Committee on Antimicrobial Susceptibility Testing [cited 2024 Apr 3]. https://www.sfm-microbiologie.org/casfm
23. Austin PC, Fine JP. Practical recommendations for reporting Fine–Gray model analyses for competing risk data. Stat Med. 2017;36:4391–400. https://doi.org/10.1002/sim.7501
24. Therneau TM. A package for survival analysis in R. 2020 [cited 2024 Apr 3]. https://CRAN.R-project.org/package=survival
25. von Elm E, Altman DG, Egger M, Pocock SJ, Gøtzsche PC, Vandenbroucke JP, et al. The strengthening the reporting of observational studies in epidemiology (STROBE) statement: guidelines for reporting observational studies. Lancet. 2007;370:1453–7.
26. Dethlefsen L, Relman DA. Incomplete recovery and individualized responses of the human distal gut microbiota to repeated antibiotic perturbation. Proc Natl Acad Sci U S A. 2011;108(Suppl 1):4554–61. https://doi.org/10.1073/pnas.1000087107
27. Zhang M, Jiang Z, Li D, Jiang D, Wu Y, Ren H, et al. Oral antibiotic treatment induces skin microbiota dysbiosis and influences wound healing. Microb Ecol. 2015;69:415–21. https://doi.org/10.1007/s00248-014-0504-4
28. Bhalodi AA, van Engelen TSR, Virk HS, Wiersinga WJ. Impact of antimicrobial therapy on the gut microbiome. J Antimicrob Chemother. 2019;74(Suppl 1):i6–15. https://doi.org/10.1093/jac/dky530
29. Al-Hasan MN, Eckel-Passow JE, Baddour LM. Recurrent gram-negative bloodstream infection: a 10-year population-based cohort study. J Infect. 2010;61:28–33. https://doi.org/10.1016/j.jinf.2010.03.028
30. Scheuerman O, Schechner V, Carmeli Y, Gutiérrez-Gutiérrez B, Calbo E, Almirante B, et al.; REIPI/ESGBIS/INCREMENT investigators. Comparison of predictors and mortality between bloodstream infections caused by ESBL-producing *Escherichia coli* and ESBL-producing *Klebsiella pneumoniae.* Infect Control Hosp Epidemiol. 2018;39:660–7. https://doi.org/10.1017/ice.2018.63
31. Burnham JP, Kwon JH, Olsen MA, Babcock HM, Kollef MH. Differences in mortality between infections due to extended-spectrum-beta-lactamase-producing *Klebsiella pneumoniae* and *Escherichia coli.* Infect Control Hosp Epidemiol. 2018;39:1138–9. https://doi.org/10.1017/ice.2018.142
32. Chang D, Sharma L, Dela Cruz CS, Zhang D. Clinical epidemiology, risk factors, and control strategies of *Klebsiella pneumoniae* infection. Front Microbiol. 2021;12:750662. https://doi.org/10.3389/fmicb.2021.750662
33. Albertson J, McDanel JS, Carnahan R, Chrischilles E, Perencevich EN, Goto M, et al. Determination of risk factors for recurrent methicillin-resistant *Staphylococcus aureus* bacteremia in a Veterans Affairs healthcare system population. Infect Control Hosp Epidemiol. 2015;36:543–9. https://doi.org/10.1017/ice.2015.25
34. Sanz-García M, Fernández-Cruz A, Rodríguez-Créixems M, Cercenado E, Marin M, Muñoz P, et al. Recurrent *Escherichia coli* bloodstream infections: epidemiology and risk factors. Medicine (Baltimore). 2009;88:77–82. https://doi.org/10.1097/MD.0b013e31819dd0cf

Address for correspondence: Salam Abbara, Institut Pasteur Paris, 25 rue du Docteur Roux, 75015 Paris, France; email: salam.abbara@gmail.com

Epidemiologic Survey of Crimean-Congo Hemorrhagic Fever Virus in Suids, Spain

Mario Frías, Kerstin Fischer, Sabrina Castro-Scholten, Caroline Bost, David Cano-Terriza, Maria Ángeles Risalde, Pelayo Acevedo, Saúl Jiménez-Ruiz, Balal Sadeghi, Martin H. Groschup, Javier Caballero-Gómez, Ignacio García-Bocanegra

We conducted a cross-sectional study in wild boar and extensively managed Iberian pig populations in a hotspot area of Crimean-Congo hemorrhagic fever virus (CCHFV) in Spain. We tested for antibodies against CCHFV by using 2 ELISAs in parallel. We assessed the presence of CCHFV RNA by means of reverse transcription quantitative PCR protocol, which detects all genotypes. A total of 113 (21.8%) of 518 suids sampled showed antibodies against CCHFV by ELISA. By species, 106 (39.7%) of 267 wild boars and 7 (2.8%) of 251 Iberian pigs analyzed were seropositive. Of the 231 Iberian pigs and 231 wild boars analyzed, none tested positive for CCHFV RNA. These findings indicate high CCHFV exposure in wild boar populations in endemic areas and confirm the susceptibility of extensively reared pigs to CCHFV, even though they may only play a limited role in the enzootic cycle.

Crimean-Congo hemorrhagic fever virus (CCHFV; genus *Orthonairovirus*, family Nairoviridae), is an emerging pathogen mainly transmitted by ticks of the genus *Hyalomma* (*1*,*2*). This arbovirus is the causative agent of Crimean-Congo hemorrhagic fever (CCHF), a severe and lethal zoonotic and hemorrhagic disease in humans (*2*,*3*). In Europe, human cases of CCHF have been traditionally reported only in southeastern countries (*2*,*4*). However, shortly after the virus was detected in Spain (western Europe) in *Hyalomma lusitanicum* ticks collected on red deer (*Cervus elaphus*) in 2010 (*5*), human CCHF clinical cases have been confirmed in western and southwestern Spain since 2013 (*6*–*8*).

Since 2010, endemic circulation of CCHFV has been reported in the Iberian Peninsula in *H. lusitanicum* ticks (*9*,*10*) and red deer, which are the primary host of adult specimens of this tick species (*11*). In this region, red deer populations usually share habitat and natural resources with other susceptible wild ungulate species, such as wild boar (*Sus scrofa*), another important natural host of adult *H. lusitanicum* ticks. This connection, together with the drastic increase of the wild boar population since 1990 in the Iberian Peninsula (*12*), may contribute to the spread and maintenance of the virus in Mediterranean ecosystems.

Few studies have assessed CCHFV circulation in red deer and wild boar (*11*,*13*–*16*). In addition, those 2 wild ungulate species usually cohabit with extensively managed domestic Iberian pigs; direct and indirect contact between those sympatric species are frequent (*17*). Iberian pig is a breed of the domestic pig autochthonous to the Iberian Peninsula; they are usually reared under extensive management conditions and fattened during the Montanera period (October–February) by feeding on acorns within large, fenced areas. Most of the Iberian pig farms (80%) are in southwestern Spain, where circulation of CCHFV is high. The European Food Safety Authority (EFSA) has prioritized surveillance of CCHFV in pigs (*18*); however, data on exposure to CCHFV in pigs are lacking (*19*,*20*).The aim of our study was to analyze the circulation of CCHFV in wild boar and sympatric Iberian domestic pigs in southwestern Spain, a hotspot area of CCHFV, where CCHFV-positive ticks are present (*5*,*21*,*22*) and high seroprevalence has been reported in animal hosts (*11*,*14*).

Author affiliations: Universidad de Córdoba, Córdoba, Spain (M. Frías, S. Castro-Scholten, D. Cano-Terriza, M.Á. Risalde, S. Jiménez-Ruiz, J. Caballero-Gómez, I. García-Bocanegra); CIBERINFEC, ISCIII, Madrid, Spain (M. Frías, D. Cano-Terriza, M.Á. Risalde, J. Caballero-Gómez, I. García-Bocanegra); Friedrich-Loeffler-Institut, Greifswald-Insel Riems, Germany (K. Fischer, C. Bost, B. Sadeghi, M.H. Groschup); Universidad de Castilla La Mancha y Consejo Superior de Investigaciones Científicas (CSIC), Ciudad Real, Spain (P. Acevedo)

DOI: http://doi.org/10.3201/eid3005.240074

Methods

Study Area and Sampling

In this cross-sectional study, we assumed a seroprevalence of 40.6% (*11*) for wild boar and calculated the sample size as 251; we assumed a seroprevalence of 50% (which provides the highest sample size in studies in which seroprevalence is unknown) for a sample of 267 pigs. We calculated those estimates with 95% CI and a desired precision of ±6%. Whenever possible, we sampled 14 Iberian pigs in each farm to detect exposure with a 95% probability, assuming a minimum within-farm seroprevalence of 20%.

We sampled wild boar in 35 hunting states between the hunting seasons 2015–16 and 2020–21 in 5 provinces of southwestern Spain. In addition, we collected blood samples from Iberian pigs from 18 farms managed under extensive production systems during 2017–2019 in the same study area (Figure). We collected blood samples from pigs at the slaughterhouse and from wild boar by puncture of the cavernous sinus of the dura mater (*23*). We obtained serum samples by blood centrifugation at 400 × *g* for 10 minutes and froze them until serologic and molecular analysis. We recorded epidemiologic information, including sex, age, origin, and year of sampling, from sampled animals whenever possible. We estimated age of wild boar on the basis of tooth replacement patterns. We obtained all Iberian pig samples at the end of the Montanera period.

Serologic Methods

We tested for antibodies against CCHFV using 2 different ELISAs, both based on recombinant CCHFV nucleoprotein (N) as described elsewhere (*24*). In brief,

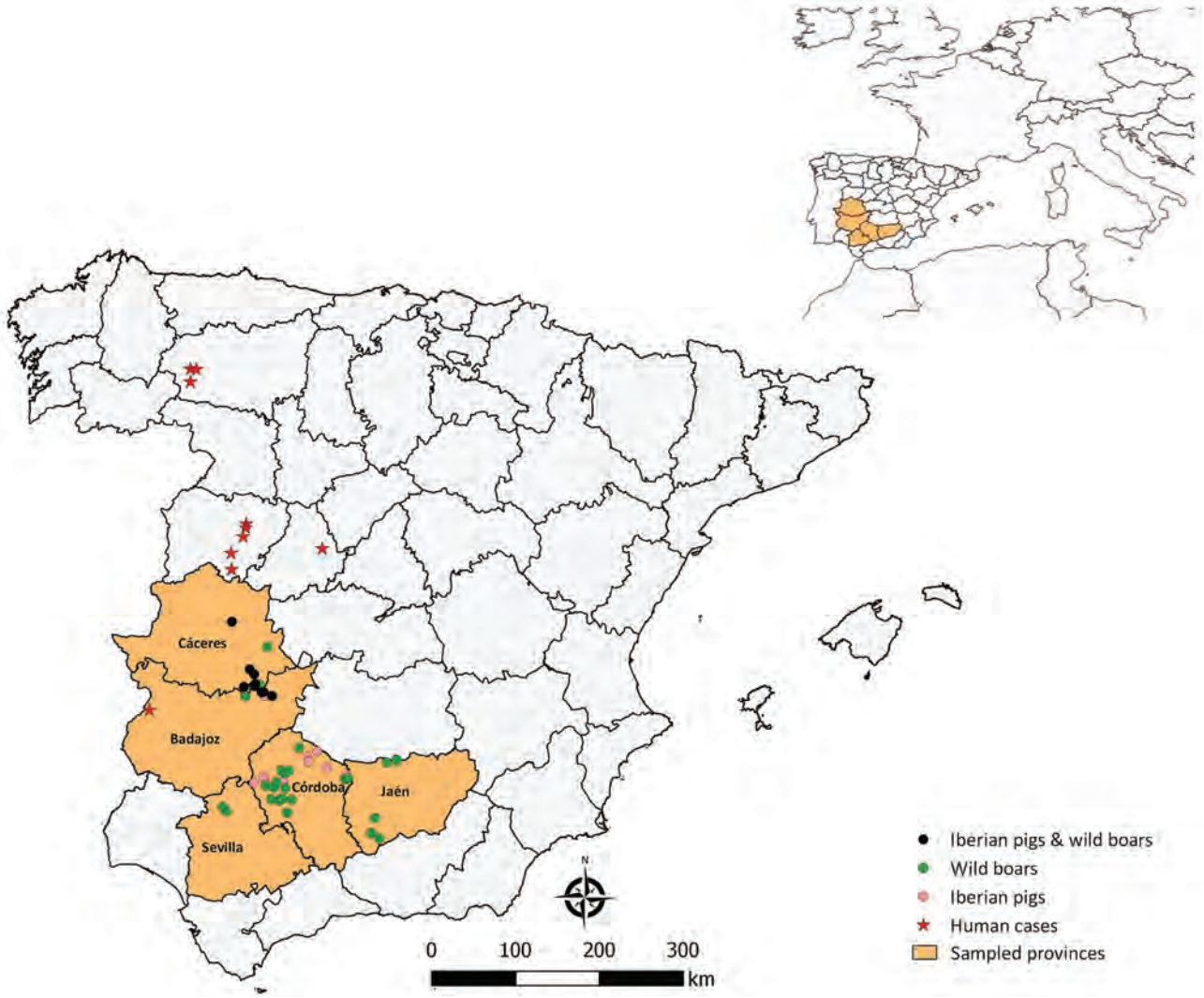

Figure. Spatial distribution of samples and human cases notified from epidemiologic survey of Crimean-Congo hemorrhagic fever virus in suids, Spain. Inset map shows location of survey area in western Europe.

the first test was the CCHF Double Antigen Multispecies ELISA (IDvet Screen, https://www.innovative-diagnostics.com), which is based on the CCHFV IbAr10200 strain N of clade III (GenBank accession no. U88410). This commercial test was validated by analyzing several animal species, including pigs (*25*). The second ELISA was an in-house indirect ELISA based on the CCHFV Kosovo Hoti strain N belonging to clade V (GenBank accession no. DQ133507). For this study, we considered samples seropositive if CCHFV antibodies were detected by both ELISAs (double-reactive).

Molecular Detection

We analyzed a total of 462 serum samples, 231 available from each species, for molecular detection. We extracted RNA from serum samples using the NucleoMag Vet Kit (Macherey-Nagel, https://www.mn-net.com). We assessed the presence of CCHFV RNA by means of QuantiTect Probe RT-PCR Kit (QIAGEN, https://www.qiagen.com) using the multiplex quantitative RT-PCR described elsewhere (*26*), which can amplify a fragment of the short (S) segment of the 6 known CCHFV genotypes.

Statistical Analysis

We calculated seroprevalence and prevalence of active infection by dividing the number of seropositive animals by ELISA and positive animals by quantitative PCR by the total number of animals tested, using 2-sided exact binomial of 95% CI. We initially assessed associations between serologic results and explanatory variables by species using bivariate analysis with the Pearson χ^2 or Fisher exact tests, as appropriate. We selected variables with p values ≤0.10 as potential risk factors. We evaluated collinearity between variables using the Cramer V coefficient, selecting the variable with the highest biologic plausibility if we obtained a correlation coefficient between variables >0.6 and p≤0.05. Finally, we evaluated the influence of the selected explanatory variables on CCHFV seropositivity using a generalized linear mixed model (GLMM), assuming a binomial data distribution and the variable municipality as random effect. We considered the Akaike information criterion score for each model to select the most accurate. Variables with p≤0.05 were statistically significant. We performed all statistical analyses using RStudio (https://github.com/rstudio/rstudio).

Results

Of the 518 suids sampled, 71 animals tested positive exclusively through the commercial ELISA, whereas 7 tested positive solely through the in-house assay (*24*). Of note, a total of 113 of the 518 suids sampled showed antibodies against CCHFV by both ELISAs. Thus, the seroprevalence obtained in the preset study was 21.8% (95% CI 18.4%–25.5%; 113/518). By species, 106 (39.7%, 95% CI 34.0%–45.7%) of the 267 wild boar and 7 (2.8%, 95% CI 0.8%–4.8%) of the 251 Iberian pigs analyzed were seropositive (Table 1). We found significantly higher seroprevalence in wild boar than in pigs (relative risk 14.23, 95% CI 6.7–30.0; p<0.001).

We found antibodies against CCHFV in wild boar in 26 (70.3%) of the 37 hunting estates sampled and in the 5 provinces analyzed; seroprevalence ranged

Table 1. Distribution and seroprevalence of Crimean-Congo hemorrhagic fever in wild boars and extensively raised Iberian pigs, Spain*

	Wild boars			Iberian pigs		
Variable	No. positive/no. analyzed	Seroprevalence, % (95% CI)	p value	No. positive/no. analyzed	Seroprevalence, % (95% CI)	p value
Season						
2015–16	10/20	50.0 (28.8–71.1)	0.8885	NA	NA	
2016–17	16/45	35.5 (22.6–50.2)		NA	NA	
2017–18	27/66	40.9 (29.5–53.0)		1/126	0.8 (0–2.3)	0.0123
2018–19	26/63	41.2 (29.6–53.6)		6/77	7.8 (1.8–13.8)	
2019–20	20/52	38.4 (26.0–52.1)		0/48	0 (0–0)	
2020–21	7/21	33.3 (15.9–55.1)		NA	NA	
Province						
Badajoz	7/32	21.9 (7.6–36.2)	0.0119	0/79	0 (0–0.3)	<0.001
Cáceres	20/45	44.4 (30.5–59.1)		6/46	13.0 (3.3–22.8)	
Córdoba	51/100	51.0 (41.2–60.8)		1/126	0.8 (0–2.3)	
Jaén	13/44	29.5 (17.5–44.1)		NA	NA	
Sevilla	15/46	32.6 (19.1–46.2)		NA	NA	
Age						
Yearling	9/45	20.0 (0–26.1)	<0.001	NA	NA	NA
Subadult	23/70	32.9 (21–38.6)		NA	NA	
Adult	72/147	49.0 (41.0–57.0)		NA	NA	
Sex						
M	41/124	33.1 (25.2–41.7)	0.0435	NA	NA	NA
F	64/139	46.0 (37.8–54.3)		NA	NA	

*NA, not applicable.

from 21.9% in Badajoz to 51.0% in Córdoba (Figure). We detected ≥1 seropositive wild boar in each of the hunting seasons (Table 1). We detected seropositivity in 2 (11.1%) of the 18 pig farms analyzed; within-farm seroprevalence was 5%–70%. We identified seropositive pigs in 2 provinces sampled; seroprevalence ranged from 0.8% (95% CI 0–2.3%) in Córdoba to 7.8% (95% CI 1.8%–13.8%) in Cáceres (Table 1). We sampled 6/7 seropositive pigs in the province of Cáceres, in the same extensively managed pig farm.

The GLMM model identified age and sex as risk factors potentially associated with human exposure to CCHFV in wild boar (Table 2). We found significantly higher seropositivity in adults (49.0%; odds ratio (OR) 3.9, 95% CI 1.6–9.5) than in yearlings (20.0%). Female (46.0%) wild boar showed 2 times (OR 1.89, 95% CI 1.0–3.4) higher risk of exposure to the virus than males. We identified no risk factor in Iberian pigs by GLMM model. None of the 231 Iberian pigs (0.0%, 95% CI 0.0–1.6%) and 231 wild boars (0.0%, 95% CI 0.0–1.6%) analyzed tested positive to CCHFV RNA presence in their serum.

Table 2. Risk factors associated with Crimean-Congo hemorrhagic fever virus seropositivity in wild boar of the Iberian Peninsula, Spain*

Variable	Category	Odds ratio (95% CI)	p value
Age	Yearling	Referent	
	Subadult	2.14 (0.79-5.77)	0.135
	Adult	3.92 (1.61-9.56)	0.003
Sex	M	Referent	
	F	1.89 (1.04-3.42)	0.036

*Analysis by generalized linear mixed model.

Discussion

Despite extensive data on potential CCHFV hosts and their influence in the maintenance and transmission of this virus (*27*), information on the role of suids in the epidemiology of CCHFV worldwide is very limited. As of February 2024, all surveys conducted worldwide in wild boar have been done in Spain, except for 1 in Turkey, where 2.5% of wild boar were exposed to the virus (*28*). The seroprevalence detected in this species in our study (39.7%) is in accordance with the 40.6% obtained in this species in Doñana National Park in southwestern Spain (*13*) and indicates a high exposure of wild boar populations to CCHFV in this region of Spain. In contrast, lower frequencies of seropositivity were found in northeastern Spain, where 3.2% of wild boar showed antibodies against CCHFV (*15*), and eastern Spain, where 15.3% of wild boar had antibodies (*16*). Those spatial differences found in Spain are consistent with the risk gradient of exposure to CCHFV observed in wild boar on the Iberian Peninsula (*14*) and could be associated with certain climatic factors that can condition the density and abundance of the competent vector species throughout Spain. The presence of *Hyalomma* spp. ticks in northeastern Spain had not been described until recently (*29,30*) and in the eastern part of the country was detailed through a study conducted on primary care on bites from these ticks (*31*). In contrast, the presence of *Hyalomma* spp. ticks, including *H. marginatum* and *H. lusitanicum*, has been widely described in southwestern Spain (*9*,*10*,*32*,*33*).

This study provides evidence on the potential role of domestic pigs in the enzootic cycle of CCHFV. As of February 2024, the 2 serosurveys of pigs did not detect antibodies against CCHFV in any of the 25 sampled pigs from India or the 46 sampled in Egypt (*19, 20*). The seroprevalence obtained (2.8%) confirmed the susceptibility of Iberian pigs to CCHFV infection but indicate a low exposure of extensively raised populations to the virus in a hotspot area, thus suggesting a limited role of this species in the enzootic cycle of CCHFV on the Iberian Peninsula. Nonetheless, it is significantly different from the seroprevalence determined in wild boar. Of note, the period that Iberian pigs are extensively managed (October–February) does not coincide with the period of main activity of *Hyalomma* spp. ticks (April–June) (*34*). The pigs are exposed to the vectors for a few months, in contrast to wild boars' exposure throughout their lives, which could explain the differences in seroprevalence between these species. In addition, this finding could be related to potential differences in susceptibility to viral infection between pigs and wild boar. Future experimental studies can clarify this hypothesis.

In the case of wild boar, we found that age and sex were associated with CCHFV exposure (Table 2). Adults were at 3.6 times higher risk of CCHFV exposure than yearlings, which could be associated with the higher probability of tick bites throughout the life of adult wild boar and with the persistence of CCHFV antibodies over time. This finding is in line with those of Cuadrado-Matías et al. (*13*) and with previous studies that linked the age of cattle with greater seropositivity to CCHFV antibodies (*35*–*37*). On the other hand, female wild boar had significantly higher seroprevalence than males. Previous studies found a higher proportion of female than male wild boar infested by ticks, possibly caused by behavioral differences (*37*). Similarly, other studies have found a higher proportion of CCHFV-seropositive female cattle (*38*,*39*). However, statistically significant differences in CCHFV seropositivity between sexes had not previously been found in the limited serosurveys carried out in wild boar. Additional studies in boar species are needed to evaluate the role of age and sex in CCHFV exposure.

We detected seropositivity every year and in all provinces sampled, indicating an endemic and widespread circulation of CCHFV in southwestern Spain. Of note, yearling animals were seropositive in all of the hunting seasons analyzed except 2020–2021. Although maternal antibodies in yearling mammals cannot be ruled out, our findings denote active circulation during the study period. On the other hand, wild boar from Córdoba province had the highest seroprevalence value; 51% of animals tested seropositive to CCHFV, which was higher than in Badajoz province where human cases have been reported (Figure). In Córdoba, the presence of CCHFV has already been demonstrated by the detection of CCHFV RNA in ticks (*21*,*22*), which would indicate that this region has a high circulation of the virus. Those data highlight the need to carry out studies throughout Spain to establish spatial distribution of CCHFV to promote surveillance and control programs in areas identified as hotspots. On the other hand, 6/7 (85.7%) seropositive pigs were sampled in 2018 in the same extensively managed pig farm in Cáceres. That finding indicates a nonhomogeneous spatiotemporal distribution pattern of the virus in this domestic species, which implies a possible role of the Iberian pig as accidental host rather than true host of CCHFV.

Finally, even though the quantitative PCR used in this study has the capacity to detect all the clades of the virus (*26*), we did not find CCHFV RNA in any of the 462 serum specimens tested. This result is consistent with those previously reported in other mammal species (*40*–*42*) and could be explained by the transient short period of viremia described (<7 days) in small mammals, small ruminants, and hares (*43*,*44*). However, we know of no studies evaluating viremia in suids, which would be necessary to establish their role as natural host of CCHFV.

In conclusion, the results obtained in this study suggest an endemic and widespread circulation of the virus in southwestern Spain. Specifically, these findings indicate high CCHFV exposure in wild boar populations in endemic areas. We report CCHFV exposure in domestic pigs, confirming the susceptibility of this species to the virus, although the low seroprevalence found indicates a limited role in the enzootic cycle of CCHFV in the Iberian and Mediterranean ecosystems. Therefore, we recommend the use of biosecurity measures for high-risk activities with this species to limit exposure to this pathogen. This study highlights the need to develop surveillance programs in suids to evaluate spatiotemporal changes in the circulation of CCHFV to prevent infection in humans.

Acknowledgments

We thank Sarah Knapp for excellent technical assistance.

This work has been partially supported by TED2021-132599B-C22 project, funded by MCIN/AEI/10.13039/501100011033 and by the European Union NextGenerationEU/Plan de Recuperación, Transformación y Resiliencia and by CIBER -Consorcio Centro de Investigación Biomédica en Red- (CB 2021), Instituto de Salud Carlos III, Ministerio de Ciencia e Innovación and Unión Europea-NextGenerationEU. S.C.-S. was supported by a Formación de Profesorado Universitario grant from the Spanish Ministry of Universities (FPU19/06026). J.C.-G. is supported by the CIBER Consorcio Centro de Investigación Biomédica en Red- (CB21/13/00083), Instituto de Salud Carlos III, Ministerio de Ciencia e Innovación and Unión Europea-NextGenerationEU. S.J.-R. is supported by a Juan de la Cierva contract (JDC2022-048850-I) funded by the Ministerio de Ciencia e Innovación/AEI/10.13039/501100011033 and the European Union NextGenerationEU/PRTR.

About the Author

Dr. Frías is a postdoctoral researcher at Animal Health and Zoonosis Research Group (GISAZ) at the University of Cordoba and the Clinical Virology and Zoonoses Group at the Maimonides Biomedical Research Institute of Cordoba. His main field of study is zoonotic emerging diseases.

References

1. Bartolini B, Gruber CE, Koopmans M, Avšič T, Bino S, Christova I, et al. Laboratory management of Crimean-Congo haemorrhagic fever virus infections: perspectives from two European networks. Euro Surveill. 2019;24:1800093. https://doi.org/10.2807/1560-7917.ES.2019.24.5.1800093
2. Messina JP, Pigott DM, Golding N, Duda KA, Brownstein JS, Weiss DJ, et al. The global distribution of Crimean-Congo hemorrhagic fever. Trans R Soc Trop Med Hyg. 2015;109:503–13. https://doi.org/10.1093/trstmh/trv050
3. Hawman DW, Feldmann H. Recent advances in understanding Crimean-Congo hemorrhagic fever virus. F1000Res. 2018;7:F1000 Faculty Rev-1715.
4. Papa A, Weber F, Hewson R, Weidmann M, Koksal I, Korukluoglu G, et al. Meeting report: first international conference on Crimean-Congo hemorrhagic fever. Antiviral Res. 2015;120:57–65. https://doi.org/10.1016/j.antiviral.2015.05.005
5. Estrada-Peña A, Palomar AM, Santibáñez P, Sánchez N, Habela MA, Portillo A, et al. Crimean-Congo hemorrhagic fever virus in ticks, Southwestern Europe, 2010. Emerg Infect Dis. 2012;18:179–80. https://doi.org/10.3201/eid1801.111040
6. Negredo A, de la Calle-Prieto F, Palencia-Herrejón E, Mora-Rillo M, Astray-Mochales J, Sánchez-Seco MP, et al.; Crimean Congo Hemorrhagic Fever@Madrid Working Group. Autochthonous Crimean-Congo hemorrhagic fever in Spain. N Engl J Med. 2017;377:154–61. https://doi.org/10.1056/NEJMoa1615162

7. Monsalve Arteaga L, Muñoz Bellido JL, Negredo AI, García Criado J, Vieira Lista MC, Sánchez Serrano JÁ, et al. New circulation of genotype V of Crimean-Congo haemorrhagic fever virus in humans from Spain. PLoS Negl Trop Dis. 2021;15:e0009197. https://doi.org/10.1371/journal.pntd.0009197
8. Negredo A, Sánchez-Arroyo R, Díez-Fuertes F, de Ory F, Budiño MA, Vázquez A, et al. Fatal case of Crimean-Congo hemorrhagic fever caused by reassortant virus, Spain, 2018. Emerg Infect Dis. 2021;27:1211–5. https://doi.org/10.3201/eid2704.203462
9. Ruiz-Fons F, Fernández-de-Mera IG, Acevedo P, Höfle U, Vicente J, de la Fuente J, et al. Ixodid ticks parasitizing Iberian red deer (*Cervus elaphus hispanicus*) and European wild boar (*Sus scrofa*) from Spain: geographical and temporal distribution. Vet Parasitol. 2006;140:133–42. https://doi.org/10.1016/j.vetpar.2006.03.033
10. European Centre for Disease Prevention and Control and European Food Safety Authority. Tick maps. 2023 [cited 2024 Feb 25]. https://ecdc.europa.eu/en/disease-vectors/surveillance-and-disease-data/tick-maps
11. Cuadrado-Matías R, Cardoso B, Sas MA, García-Bocanegra I, Schuster I, González-Barrio D, et al. Red deer reveal spatial risks of Crimean-Congo haemorrhagic fever virus infection. Transbound Emerg Dis. 2022;69:e630–45. https://doi.org/10.1111/tbed.14385
12. Massei G, Kindberg J, Licoppe A, Gačić D, Šprem N, Kamler J, et al. Wild boar populations up, numbers of hunters down? A review of trends and implications for Europe. Pest Manag Sci. 2015;71:492–500. https://doi.org/10.1002/ps.3965
13. Cuadrado-Matías R, Baz-Flores S, Peralbo-Moreno A, Herrero-García G, Risalde MA, Barroso P, et al. Determinants of Crimean-Congo haemorrhagic fever virus exposure dynamics in Mediterranean environments. Transbound Emerg Dis. 2022;69:3571–81. https://doi.org/10.1111/tbed.14720
14. Baz-Flores S, Herraiz C, Peralbo-Moreno A, Barral M, Arnal MC, Balseiro A, et al. Mapping the risk of exposure to Crimean-Congo haemorrhagic fever virus in the Iberian Peninsula using Eurasian wild boar (*Sus scrofa*) as a model. Ticks Tick Borne Dis. 2024;15:102281. https://doi.org/10.1016/j.ttbdis.2023.102281
15. Carrera-Faja L, Cardells J, Pailler-García L, Lizana V, Alfaro-Deval G, Espunyes J, et al. Evidence of prolonged Crimean-Congo hemorrhagic fever virus endemicity by retrospective serosurvey, eastern Spain. Emerg Infect Dis. 2022;28:1031–4. https://doi.org/10.3201/eid2805.212335
16. Espunyes J, Cabezón O, Pailler-García L, Dias-Alves A, Lobato-Bailón L, Marco I, et al. Hotspot of Crimean-Congo hemorrhagic fever virus seropositivity in wildlife, northeastern Spain. Emerg Infect Dis. 2021;27:2480–4. https://doi.org/10.3201/eid2709.211105
17. Triguero-Ocaña R, Laguna E, Jiménez-Ruiz S, Fernández-López J, García-Bocanegra I, Barasona JÁ, et al. The wildlife livestock interface on extensive free-ranging pig farms in central Spain during the "montanera" period. Transbound Emerg Dis. 2021;68:2066–78. https://doi.org/10.1111/tbed.13854
18. Nigsch A; A; European Food Safety Authority. Surveillance plan proposal for early detection of zoonotic pathogens in pigs and poultry. EFSA J. 2023;20:EN-7855. 10.2903/sp.efsa.2023.EN-7855 https://doi.org/10.2903/sp.efsa.2023.EN-7855
19. Darwish MA, Imam IZ, Omar FM, Hoogstraal H. Results of a preliminary seroepidemiological survey for Crimean-Congo hemorrhagic fever virus in Egypt. Acta Virol. 1978;22:77.
20. Mourya DT, Yadav PD, Shete AM, Gurav YK, Raut CG, Jadi RS, et al. Detection, isolation and confirmation of Crimean-Congo hemorrhagic fever virus in human, ticks and animals in Ahmadabad, India, 2010–2011. PLoS Negl Trop Dis. 2012;6:e1653. https://doi.org/10.1371/journal.pntd.0001653
21. Moraga-Fernández A, Ruiz-Fons F, Habela MA, Royo-Hernández L, Calero-Bernal R, Gortazar C, et al. Detection of new Crimean-Congo haemorrhagic fever virus genotypes in ticks feeding on deer and wild boar, Spain. Transbound Emerg Dis. 2021;68:993–1000. https://doi.org/10.1111/tbed.13756
22. Sánchez-Seco MP, Sierra MJ, Estrada-Peña A, Valcárcel F, Molina R, de Arellano ER, et al.; Group for CCHFv Research. Widespread detection of multiple strains of Crimean-Congo hemorrhagic fever virus in ticks, Spain. Emerg Infect Dis. 2021;28:394–402. https://doi.org/10.3201/eid2802.211308
23. Arenas-Montes A, García-Bocanegra I, Paniagua J, Franco JJ, Miró F, Fernández-Morente M, et al. Blood sampling by puncture in the cavernous sinus from hunted wild boar. Eur J Wildl Res. 2013;59:299–303. https://doi.org/10.1007/s10344-013-0701-3
24. Bost C, Castro-Scholten S, Sadeghi B, Cano-Terriza D, Frías Mo, Jiménez-Ruiz S, et al. Approaching the complexity of Crimean-Congo hemorrhagic fever virus serology: a study in swine. J Virol Methods. 2024;326:114915.
25. Sas MA, Comtet L, Donnet F, Mertens M, Vatansever Z, Tordo N, et al. A novel double-antigen sandwich ELISA for the species-independent detection of Crimean-Congo hemorrhagic fever virus-specific antibodies. Antiviral Res. 2018;151:24–6. https://doi.org/10.1016/j.antiviral.2018.01.006
26. Sas MA, Vina-Rodriguez A, Mertens M, Eiden M, Emmerich P, Chaintoutis SC, et al. A one-step multiplex real-time RT-PCR for the universal detection of all currently known CCHFV genotypes. J Virol Methods. 2018;255:38–43. https://doi.org/10.1016/j.jviromet.2018.01.013
27. Spengler JR, Bergeron É, Rollin PE. Seroepidemiological studies of Crimean-Congo hemorrhagic fever virus in domestic and wild animals. PLoS Negl Trop Dis. 2016;10:e0004210. https://doi.org/10.1371/journal.pntd.0004210
28. Nurettin C, Engin B, Sukru T, Munir A, Zati V, Aykut O. The seroprevalence of Crimean-Congo hemorrhagic fever in wild and domestic animals: an epidemiological update for domestic animals and first seroevidence in wild animals from Turkiye. Vet Sci. 2022;9:462. https://doi.org/10.3390/vetsci9090462
29. Castillo-Contreras R, Magen L, Birtles R, Varela-Castro L, Hall JL, Conejero C, et al. Ticks on wild boar in the metropolitan area of Barcelona (Spain) are infected with spotted fever group Rickettsiae. Transbound Emerg Dis. 2022;tbed.14268. https://doi.org/10.1111/tbed.14268
30. Pradera C, Estrada-Peña A. *Hyalomma lusitanicum* (Acari: Ixodidae) como potencial problema de salud pública en el área de Barcelona. Butlletí de la Institució Catalana d'Història Natural. 2022;86:111-116
31. Falcó Garí JV, López-Peña D, de la Torre J, Safont-Adsuara L, Bellido-Blasco J, Jiménez-Peydró R. Incidence of disease-transmitting ticks on the human population in the province of Castellón [in Spanish]. Presented at: XV Environmental Health Congress; May 22–24, 2019; Valencia, Spain. Rev Salud Ambient. 2019;19(Espec. Congr):135.
32. Remesar S, Castro-Scholten S, Cano-Terriza D, Díaz P, Morrondo P, Jiménez-Martín D, et al. Molecular identification of zoonotic *Rickettsia* species in Ixodidae parasitizing wild lagomorphs from Mediterranean ecosystems. Transbound Emerg Dis. 2022;69:e992–1004. https://doi.org/10.1111/tbed.14379

33. Díaz-Cao JM, Adaszek Ł, Dzięgiel B, Paniagua J, Caballero-Gómez J, Winiarczyk S, et al. Prevalence of selected tick-borne pathogens in wild ungulates and ticks in southern Spain. Transbound Emerg Dis. 2022;69:1084–94. https://doi.org/10.1111/tbed.14065
34. Valcárcel F, González J, González MG, Sánchez M, Tercero JM, Elhachimi L, et al. Comparative ecology of *Hyalomma lusitanicum* and *Hyalomma marginatum* Koch, 1844 (Acarina: Ixodidae). Insects. 2020;11:303. https://doi.org/10.3390/insects11050303
35. Adam IA, Mahmoud MA, Aradaib IE. A seroepidemiological survey of Crimean Congo hemorrhagic fever among cattle in North Kordufan State, Sudan. Virol J. 2013;10:178. https://doi.org/10.1186/1743-422X-10-178
36. Phonera MC, Simuunza MC, Kainga H, Ndebe J, Chembensofu M, Chatanga E, et al. Seroprevalence and risk factors of Crimean-Congo hemorrhagic fever in cattle of smallholder farmers in central Malawi. Pathogens. 2021;10:1613. https://doi.org/10.3390/pathogens10121613
37. Ciebiera O, Łopińska A, Gabryś G. Ticks on game animals in the fragmented agricultural landscape of western Poland. Parasitol Res. 2021;120:1781–8. https://doi.org/10.1007/s00436-021-07132-9
38. Atim SA, Ashraf S, Belij-Rammerstorfer S, Ademun AR, Vudriko P, Nakayiki T, et al. Risk factors for Crimean-Congo haemorrhagic fever (CCHF) virus exposure in farming communities in Uganda. J Infect. 2022;85:693–701. https://doi.org/10.1016/j.jinf.2022.09.007
39. Matthews J, Secka A, McVey DS, Dodd KA, Faburay B. Serological prevalence of Crimean-Congo hemorrhagic fever virus infection in small ruminants and cattle in the Gambia. Pathogens. 2023;12:749. https://doi.org/10.3390/pathogens12060749
40. Balinandi S, von Brömssen C, Tumusiime A, Kyondo J, Kwon H, Monteil VM, et al. Serological and molecular study of Crimean-Congo hemorrhagic fever virus in cattle from selected districts in Uganda. J Virol Methods. 2021;290:114075. https://doi.org/10.1016/j.jviromet.2021.114075
41. Bouaicha F, Eisenbarth A, Elati K, Schulz A, Ben Smida B, Bouajila M, et al. Epidemiological investigation of Crimean-Congo haemorrhagic fever virus infection among the one-humped camels (*Camelus dromedarius*) in southern Tunisia. Ticks Tick Borne Dis. 2021;12:101601. https://doi.org/10.1016/j.ttbdis.2020.101601
42. Goletic T, Satrovic L, Softic A, Omeragic J, Goletic S, Soldo DK, et al. Serologic and molecular evidence for circulation of Crimean-Congo hemorrhagic fever virus in ticks and cattle in Bosnia and Herzegovina. Ticks Tick Borne Dis. 2022;13:102004. https://doi.org/10.1016/j.ttbdis.2022.102004
43. Nalca A, Whitehouse CA. Crimean-Congo hemorrhagic fever virus infection among animals. In: Ergonul, O, Whitehouse, CA, editors. Crimean-Congo hemorrhagic fever. Dordrecht (the Netherlands): Springer; 2007. https://doi.org/10.1007/978-1-4020-6106-6_13
44. Spengler JR, Estrada-Peña A, Garrison AR, Schmaljohn C, Spiropoulou CF, Bergeron É, et al. A chronological review of experimental infection studies of the role of wild animals and livestock in the maintenance and transmission of Crimean-Congo hemorrhagic fever virus. Antiviral Res. 2016;135:31–47. https://doi.org/10.1016/j.antiviral.2016.09.013

Address for correspondence: Javier Caballero-Gómez, Clinical Virology and Zoonoses, Maimonides Biomedical Research Institute of Cordoba (IMIBIC), Avenida Menéndez Pidal, s/n. 14004, Córdoba, Spain; email: javiercaballero15@gmail.com

Detection of Recombinant African Swine Fever Virus Strains of p72 Genotypes I and II in Domestic Pigs, Vietnam, 2023

Van Phan Le, Van Tam Nguyen, Tran Bac Le, Nguyen Tuan Anh Mai, Viet Dung Nguyen, Thi Tam Than, Thi Ngoc Ha Lai, Ki Hyun Cho, Seong-Keun Hong, Yeon Hee Kim, Tran Anh Dao Bui, Thi Lan Nguyen, Daesub Song, Aruna Ambagala

African swine fever virus (ASFV) genotype II is endemic to Vietnam. We detected recombinant ASFV genotypes I and II (rASFV I/II) strains in domestic pigs from 6 northern provinces in Vietnam. The introduction of rASFV I/II strains could complicate ongoing ASFV control measures in the region.

African swine fever is a devastating and lethal swine disease that poses a major threat to wild boars and domestic pigs (*1*). The causative agent, African swine fever virus (ASFV), belongs to the Asfaviridae family and has a double-stranded DNA genome with a length of ≈170–190 kb (*2*). The ASFV genome encodes ≥150 proteins. ASFV strains have been classified into 24 genotypes on the basis of the C-terminal sequence of the B646L gene, which encodes the p72 protein (*3*). Recently, a new classification based on the complete protein sequence of p72 was proposed that would classify ASFV strains into 6 genotypes (*4*). ASFV of the p72 genotype II first emerged in China in 2018, then spreading to nearby countries in Asia, including Vietnam, Myanmar, South Korea, Indonesia, the Philippines, Cambodia, India, and Bangladesh. In 2021, China reported the detection of low-virulence genotype I ASFV strains (Pig/HeN/ZZ-P1/2021 and Pig/SD/DY-I/2021) with high genetic similarity to the nonhemadsorbing strains NH/P68, isolated in 1968, and OURT88/3, isolated in 1988, both from Portugal (*5*). Several attenuated, low-virulence p72 isolates of genotype II have also been reported from China (*6*).

In 2023, China reported the emergence of highly virulent recombinant ASFV strains of genotypes I and II (rASFV I/II) from Jiangsu (JS/LG/21) and Henan (HeN/123014/22) Provinces and Inner Mongolia (IM/DQDM/22) that show resistance to immunity induced by HLJ/18–7GD, a 7-gene deleted live-attenuated ASFV genotype II vaccine (*7*). The first outbreak of African swine fever in Vietnam was reported in Hung Yen Province in 2019 (*8*). The responsible virus was later identified as a highly pathogenic p72 genotype II strain that was like the strains circulating in China at that time. Because China announced the discovery of the ASFV p72 genotype I, II, and rASFV I/II strains, we have conducted a rigorous surveillance program focused on the northern provinces of Vietnam to monitor emerging ASFV strains (*9*,*10*).

The Study

In September and October 2023, we collected a total of 26 whole blood samples from pigs suspected to be infected with ASFV from family farms in 6 different northern provinces of Vietnam (Hai Duong, Bac Giang, Hanoi, Phu Tho, Tuyen Quang, and Thai Nguyen) (Appendix Figure 1, https://wwwnc.cdc.gov/EID/article/30/5/23-1775-App1.pdf). We tested the samples by using an ASFV-specific real-time PCR (Median Diagnostics Inc., https://mediandiagnostics.0com), according to the kit instructions. Our results

Author affiliations: Vietnam National University of Agriculture, Hanoi, Vietnam (V.P. Le, N.T.A. Mai, V.D. Nguyen, T.T. Than, T.N.H. Lai, T.A.D. Bui, T.L. Nguyen); Institute of Veterinary Science and Technology, Hanoi (V.T. Nguyen); Chungnam National University, Daejeon, South Korea (T.B. Le); Animal and Plant Quarantine Agency, Gimcheon, South Korea (K.H. Cho, S.-K. Hong, Y.H. Kim); Seoul National University, Seoul, South Korea (D. Song); National Centre for Foreign Animal Disease, Winnipeg, Canada (A. Ambagala).

DOI: https://doi.org/10.3201/eid3005.231775

Table. Characteristics of 6 rASFV I/II isolates obtained from infected swine on family farms that contained p72 sequences of ASFV genotype I, p54 sequences belonging to genotype II, and the CD2v sequence belonging to serotype VIII, according to phylogenetic analysis, northern Vietnam, 2023*

No.	Isolate name	Collection date	Province	Sample type	Cycle threshold
1	VNUA/rASFV/HD1/23	2023 Sep 23	Hai Duong	Whole blood	20.31
2	VNUA/rASFV/BG1/23	2023 Oct 6	Bac Giang	Whole blood	17.25
3	VNUA/rASFV/Hanoi1/23	2023 Oct 11	Hanoi	Whole blood	17.49
4	VNUA/rASFV/PT1/23	2023 Oct 12	Phu Tho	Whole blood	18.41
5	VNUA/rASFV/TQ1/23	2023 Oct 12	Tuyen Quang	Whole blood	20.41
6	VNUA/rASFV/TN1/23	2023 Oct 13	Thai Nguyen	Whole blood	20.42

*ASFV, African swine fever virus; rASFV, recombinant ASFV.

showed that all samples were positive for ASFV; cycle threshold values ranged from 16.58 to 32.13 (data not shown). We then tested the samples by using conventional PCR to amplify the C-terminal region of B646L (p72) and the full-length sequences of the E183L (p54) and EP402R (CD2v) genes, followed by Sanger sequencing (1st BASE, https://base-asia.com) (*11*). We assembled and analyzed the sequences by using Geneious Prime (Geneious, https://www.geneious.com), and we performed the alignment of nucleotide and amino acid sequences by using BioEdit version 7.7.1.0 (https://thalljiscience.github.io/page2.html).

Our phylogenetic analysis using MEGAX (https://www.megasoftware.net) revealed that 6 of the 26 samples contained p72 sequences of genotype I, but the p54 sequence belonged to genotype II, and the CD2v sequence belonged to serotype VIII (Table).

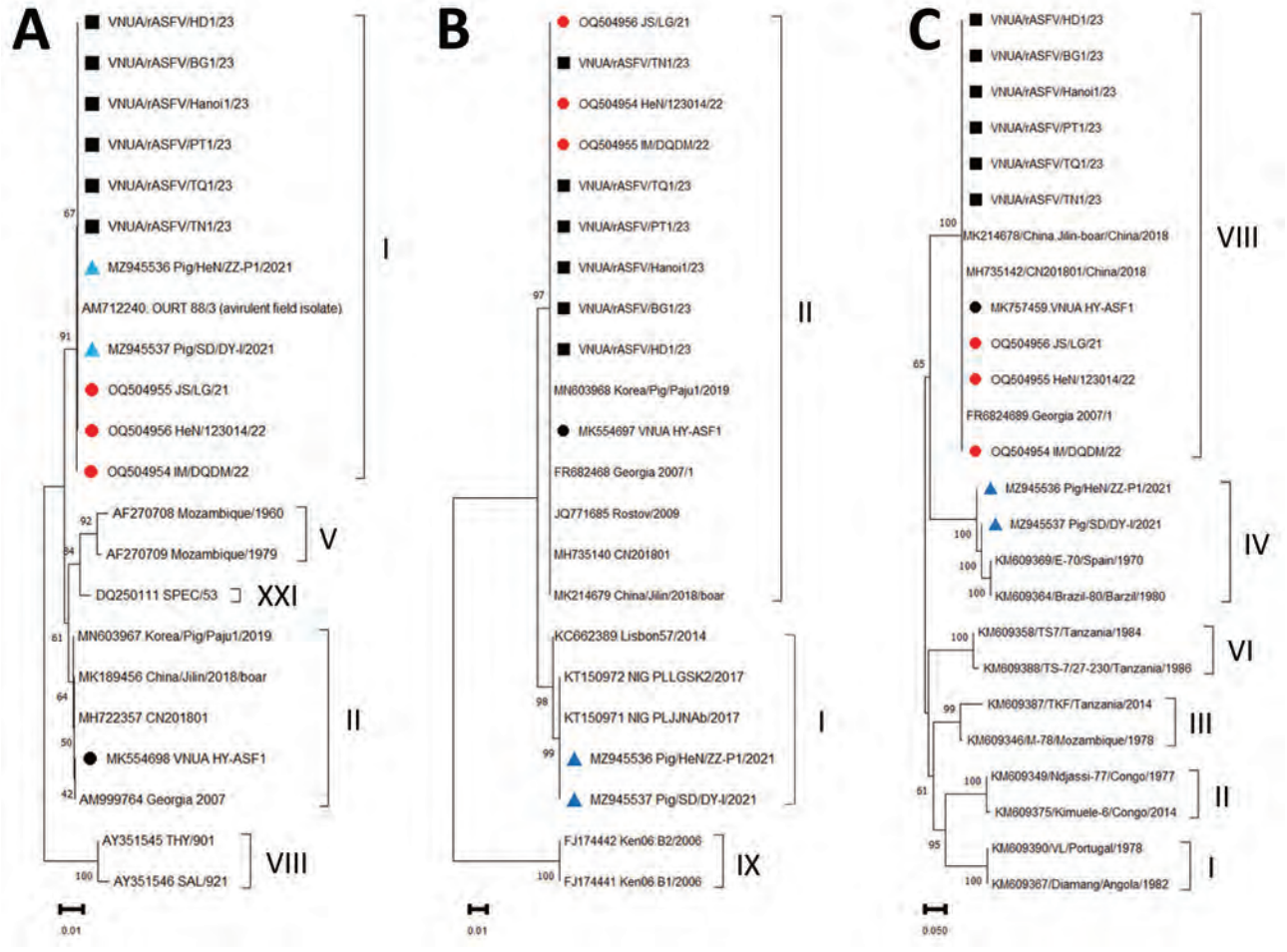

Figure 1. Phylogenetic trees of ASFV, based on the sequences found in the p72 (A), p54 (B), and CD2v (C) regions, Vietnam, 2023. Black squares indicate rASFV I/II strain from Vietnam, red circles indicate rASFV I/II strain from China, black circles indicate first reported ASFV p72 genotype II strain from Vietnam, and blue triangles indicate ASFV p72 genotype I strain from China. Scale bars indicate phylogenetic distance (nucleotide substitutions per site). ASFV, African swine fever virus; rASFV, recombinant ASFV.

No.	Virus strain	CVR pattern
1	VNUA/rASFV/HD1/23	ABNAAAAAAAAAAAAAA----------CBNABNAAAAACBNABNABNABTDBNAFA
2	VNUA/rASFV/BG1/23	ABNAAAAAAAAAAAAAA----------CBNABNAAAAACBNABNABNABTDBNAFA
3	VNUA/rASFV/Hanoi1/23	ABNAAAAAAAAAAAAAA----------CBNABNAAAAACBNABNABNABTDBNAFA
4	VNUA/rASFV/TQ1/23	ABNAAAAAAAAAAAAAA----------CBNABNAAAAACBNABNABNABTDBNAFA
5	VNUA/rASFV/TN1/23	ABNAAAAAAAAAAAAC----------CBNABNAAAAACBNABNABNABTDBNAFA
6	VNUA/rASFV/PT1/23	ABNAAAAAAAAAAAAAAAAAAAAAACBNABNAAAAACBNABNABNABTDBNAFA
7	JS/LG/21 (OQ504956)	ABNAAAAAAAAAAAAC----------CBNABNAAAAACBN-------ABNABTDBNAFA
8	IM/DQDM/22 (OQ504955)	ABNAAAAAAAAAAAAC----------CBNABNAAAAACBNABNABNABTDBNAFA
9	HeN/123014/22 (OQ504954)	ABNAAAAAAAAAAAAC----------CBNABNAAAAACBNABNABNABTDBNAFA
10	HeN/ZZ-P1/2021 (MZ945536)	ABNAAAAAAAAAAAAAAA----------CBNABN----------ABNABTDBNAFA
11	SD/DY-I/2021 (MZ945537)	ABN----------AAAAC----------CBNABNAAAAACBNABNABNABTDBNAFA

Figure 2. Alignment of ASFV CVR signatures between rASFV genotype I/II strains from Vietnam and China, and genotype I strains from China, recovered from domestic swine in Vietnam and China, 2023. Numbers in parentheses are GenBank accession numbers. ASFV, African swine fever virus; rASFV, recombinant ASFV; CVR, central variable region.

This finding was consistent with recent pandemic ASFV genotype II viruses (Figure 1), suggesting that those 6 whole blood samples possibly contained recombinant ASFV p72 viruses of genotypes I and II (rASFV I/II). The p72, p54, and CD2v sequences of the remaining viruses were like the viruses from the ASFV genotype II viruses reported in Vietnam (*8*). We inoculated the 6 whole blood samples onto primary porcine alveolar macrophages obtained from the lungs of 8–10-week-old healthy pigs, and we monitored the cultures daily for 5–7 days for hemadsorption. We obtained ASFV isolates positive for hemadsorption from all 6 samples (Appendix Figure 2).

To gain further insight into the genomes of the 6 rASFV I/II isolates, we amplified 10 additional genes (MGF-505–1R, B119L [9GL], I177L, DP96R [UK], A238L, A137R, MGF 360–12L, I226R, B602L, and IGR [between I73R and I329L]) from all 6 isolates by using previously reported and newly designed primers, and we sequenced by using Sanger sequencing (Appendix Table 1) (*12*–*14*). All of the gene sequences we obtained were deposited into GenBank (accession nos.: p72, OR999183–88; p54, OR999177–82; CD2v, OR999147–52; B119L, OR999135–40; DP96R, OR999153–58; B602L, OR999141–46; I177L, OR999159–64; MGF 505–1R, OR999171–76; A238L, PP464965–70; A137R, PP464971–76; MGF 360–12L, PP464977–82; I226R, PP464983–88; and IGR, OR999165–70). Our genetic analysis showed that all target gene sequences of the 6 Vietnamese rASFV I/II isolates matched at the nucleotide level with the corresponding gene sequences of the 3 rASFV I/II strains (JS/LG/21, HeN/123014/22, and IM/DQDM/22) previously reported in China, with the exception of the central variable region (CVR) (Appendix Table 2). The nucleotide sequences of the CVR region of all 3 rASFV I/II strains from China showed a 96-nucleotide insertion compared with the genotype I strain pig/SD/DY-I/2021 isolated from China. The isolate VNUA/rASFV/TN1/23 from Thai Nguyen Province showed the same 96-nucleotide insertion in the CVR region (Appendix Figure 3, panel A). However, the unique 36-nucleotide deletion observed in the CVR region of the JS/LG/21 strain from China was not detected in any of the rASFV I/II strains from Vietnam (Appendix Figure 3, panel B). Four rASFV I/II isolates from Vietnam (VNUA/rASFV/HD1/23, VNUA/rASFV/BG1/23, VNUA/rASFV/Hanoi1/23, and VNUA/rASFV/TQ1/23) had an additional 12-nucleotide insertion (108 nucleotides in total) in the CVR region. The Vietnam isolate VNUA/rASFV/PT1/23 from Phu Tho Province had an additional 108-nucleotide insertion (204 nucleotides in total) in the CVR region (Appendix Figure 3, panel A). Those differences were reflected in the CVR profile of the viruses (Figure 2).

Conclusions

We report the discovery of 6 rASFV I/II strains from northern Vietnam. To characterize the virus strains, while attempting to sequence the whole genome of the 6 isolates, we rapidly sequenced 13 target genes of these 6 isolates and compared their nucleotide sequences with the corresponding sequences of rASFV I/II strains from China. All sequences, except for the CVR region, matched with the corresponding sequences of rASFV I/II strains from China. The observation of 3 different CVR variants in Vietnam indicates 3 possible independent introductions of rASFV I/II strains into Vietnam. Because ASFV p72 genotype I strains have not been reported in Vietnam, the rASFV I/II strains detected in Vietnam may have originated from China.

Two live-attenuated ASFV vaccines are now licensed in Vietnam. Both vaccines have been proven

to protect young pigs against highly pathogenic ASFV p72 genotype II strains circulating in Vietnam. However, the rASFV I/II strains detected in China appear to be resistant to the live-attenuated ASFV p72 genotype II vaccine candidates (*7*). Therefore, the newly discovered rASFV I/II strains in Vietnam are likely resistant to the immunity induced by the current live ASFV vaccines and could replace the ASFV p72 genotype II strains circulating in the region. This possibility poses a major challenge for disease control and vaccine development and emphasizes the need for increased vigilance in the global control of ASFV.

This work was supported by the Institute of Veterinary Science and Technology (VUSTA), Vietnam, and by grants from the Animal and Plant Quarantine Agency (grant no. I-1543085-2022-24-02), Ministry of Agriculture, Food and Rural Affairs, Republic of Korea, and US Swine Health Information Centre (grant no. 20-085).

About the Author

Dr. Le is a veterinarian and associate professor at the Vietnam National University of Agriculture and conducts research in the field of virology, focusing on viruses of pigs and birds.

References

1. World Organisation for Animal Health. African swine fever. 2023 [cited 2023 Jan 12]. https://www.woah.org/en/disease/african-swine-fever
2. Gallardo C, Mwaengo DM, Macharia JM, Arias M, Taracha EA, Soler A, et al. Enhanced discrimination of African swine fever virus isolates through nucleotide sequencing of the p54, p72, and pB602L (CVR) genes. Virus Genes. 2009;38:85–95. https://doi.org/10.1007/s11262-008-0293-2
3. Bastos ADS, Penrith ML, Crucière C, Edrich JL, Hutchings G, Roger F, et al. Genotyping field strains of African swine fever virus by partial p72 gene characterisation. Arch Virol. 2003;148:693–706. https://doi.org/10.1007/s00705-002-0946-8
4. Spinard E, Dinhobl M, Tesler N, Birtley H, Signore AV, Ambagala A, et al. A re-evaluation of African swine fever genotypes based on p72 sequences reveals the existence of only six distinct p72 groups. Viruses. 2023;15:2246. https://doi.org/10.3390/v15112246
5. Sun E, Huang L, Zhang X, Zhang J, Shen D, Zhang Z, et al. Genotype I African swine fever viruses emerged in domestic pigs in China and caused chronic infection. Emerg Microbes Infect. 2021;10:2183–93. https://doi.org/10.1080/22221751.2021.1999779
6. Zhenzhong W, Chuanxiang Q, Shengqiang G, Jinming L, Yongxin H, Xiaoyue Z, et al. Genetic variation and evolution of attenuated African swine fever virus strain isolated in the field: a review. Virus Res. 2022;319:198874. https://doi.org/10.1016/j.virusres.2022.198874
7. Zhao D, Sun E, Huang L, Ding L, Zhu Y, Zhang J, et al. Highly lethal genotype I and II recombinant African swine fever viruses detected in pigs. Nat Commun. 2023;14:3096. https://doi.org/10.1038/s41467-023-38868-w
8. Le VP, Jeong DG, Yoon SW, Kwon HM, Trinh TBN, Nguyen TL, et al. Outbreak of African swine fever, Vietnam, 2019. Emerg Infect Dis. 2019;25:1433–5. https://doi.org/10.3201/eid2507.190303
9. Nguyen VT, Cho KH, Mai NTA, Park JY, Trinh TBN, Jang MK, et al. Multiple variants of African swine fever virus circulating in Vietnam. Arch Virol. 2022;167:1137–40. https://doi.org/10.1007/s00705-022-05363-4
10. Mai NTA, Dam VP, Cho KH, Nguyen VT, Van Tuyen N, Nguyen TL, et al. Emergence of a novel intergenic region (IGR) IV variant of African swine fever virus genotype II in domestic pigs in Vietnam. Vet Res Commun. 2023;47:1773–6. https://doi.org/10.1007/s11259-022-10068-9
11. Mai NTA, Vu XD, Nguyen TTH, Nguyen VT, Trinh TBN, Kim YJ, et al. Molecular profile of African swine fever virus (ASFV) circulating in Vietnam during 2019–2020 outbreaks. Arch Virol. 2021;166:885–90. https://doi.org/10.1007/s00705-020-04936-5
12. O'Donnell V, Risatti GR, Holinka LG, Krug PW, Carlson J, Velazquez-Salinas L, et al. Simultaneous deletion of the 9GL and UK genes from the African swine fever virus Georgia 2007 isolate offers increased safety and protection against homologous challenge. J Virol. 2016;91:e01760–16. https://doi.org/10.1128/jvi.01760-16
13. O'Donnell V, Holinka LG, Krug PW, Gladue DP, Carlson J, Sanford B, et al. African swine fever virus Georgia 2007 with a deletion of virulence-associated gene 9GL (B119L), when administered at low doses, leads to virus attenuation in swine and induces an effective protection against homologous challenge. J Virol. 2015;89:8556–66. https://doi.org/10.1128/JVI.00969-15
14. Rodriguez JM, Salas ML, Viñuela E. Genes homologous to ubiquitin-conjugating proteins and eukaryotic transcription factor SII in African swine fever virus. Virology. 1992;186:40–52. https://doi.org/10.1016/0042-6822(92)90059-X

Address for correspondence: Van Phan Le, Vietnam National University of Agriculture, Trau Quy, Gia Lam, Hanoi, Vietnam; email: letranphan@vnua.edu.vn

Toxoplasma gondii Infections and Associated Factors in Female Children and Adolescents, Germany

Laura Giese,[1] Frank Seeber,[1] Anton Aebischer, Ronny Kuhnert, Martin Schlaud, Klaus Stark, Hendrik Wilking

In a representative sample of female children and adolescents in Germany, *Toxoplasma gondii* seroprevalence was 6.3% (95% CI 4.7%–8.0%). With each year of life, the chance of being seropositive increased by 1.2, indicating a strong force of infection. Social status and municipality size were found to be associated with seropositivity.

Toxoplasmosis, caused by the protozoan parasite *Toxoplasma gondii,* is the most common parasitic foodborne disease in Germany. The seroprevalence in adults is exceptionally high (50%) compared with other countries (*1*). After infection via either undercooked meat from infected animals (pathway 1) or uptake of infectious oocysts shed by infected cats (pathway 2), *T. gondii* persists lifelong in infected persons, posing a risk for reactivation of latent infections (*2*). The proportion of pathways 1 and 2 leading to infection is largely unknown. We previously argued that in Germany, eating habits like consumption of raw pork products are likely responsible for the high seroprevalence (*1*). Infections in immune-competent persons remain largely asymptomatic or cause only mild, influenza-like symptoms. However, severe disease manifestations can occur, including ocular toxoplasmosis with sequalae, severe and often fatal consequences in immunocompromised persons, and congenital toxoplasmosis (*2*).

Worldwide, the World Health Organization (WHO) considered the burden of disease from toxoplasmosis to be high. Nevertheless, routine disease and pathogen surveillance is inadequate, so the incidence of human infection and parasite occurrence in animals and food is underestimated (*3*). In Germany, *T. gondii* screening during pregnancy to detect and treat primary infection, which could prevent parasite transmission to the unborn, is not covered by the statutory health insurance. Ongoing discussions to reevaluate this policy demand data specifically assessing risk estimates for women of reproductive age.

In adults, age, dietary habits, and region of residence are associated with seroprevalence (*1*). Comparable analyses for children and adolescents are missing but are needed to estimate the public health problem and to suggest countermeasures. To provide such baseline data, this study aimed to estimate seroprevalence and to determine associated factors of *T. gondii* infections in female children and adolescents in Germany. The Hannover Medical School ethics committee approved the study (*4*).

The Study

The second wave of the nationwide German Health Interview and Examination Survey for Children and Adolescents (KiGGS Wave 2) was conducted as a 2-stage sampling survey during 2014–2017 in 167 representative sample points in Germany (*4*). Serum specimens of participants 3–17 years of age were tested for the presence of *T. gondii* IgG using a highly sensitive and specific commercial enzyme linked fluorescence assay (ELFA), as described previously (*1*,*5*).

We determined overall and stratified seroprevalence. We used data from standardized interviews to assess factors associated with seropositivity. On the basis of our previous serosurvey results in adults (*1*), we tested potential associations between seropositivity and vegetarianism, residence (eastern or western Germany), municipality size, and socioeconomic status. We identified minimal adjustment sets for multivariable logistic regression models by using directed acyclic graphs (Appendix, https://wwwnc.cdc.gov/EID/article/30/5/23-1045-App1.pdf). We determined adjusted odds ratios (aOR) for each exposure variable with 95% CIs. We used sampling weights

Author affiliation: Robert Koch Institute, Berlin, Germany

DOI: http://doi.org/10.3201/eid3005.231045

[1]These authors contributed equally to this article.

Table. Stratified weighted seroprevalence of *Toxoplasma gondii* and results of weighted logistic regression analyses of factors potentially associated with seropositivity in female children and adolescents, Germany, 2014–2017*

Characteristics	No. positive/no. total†	Prevalence (95% CI)	Multivariable analysis aOR (95% CI)
Age group, y			
3–6	11/272	3.5 (1.3–5.8)	Referent
7–10	11/339	3.0 (0.8–5.1)	0.8 (0.3–2.3)
11–13	23/363	7.0 (3.5–10.4)	2.0 (0.9–4.9)
14 –17	49/481	11.3 (6.7–15.8)	3.5 (1.6–7.4)
Socioeconomic status‡			
Low	20/211	10.8 (4.7–16.9)	2.7 (1.3–5.9)
Middle	51/868	4.7 (3.1–6.3)	Referent
High	19/325	6.1 (3.1–9.2)	1.5 (0.7–3.0)
Municipality size§			
<5,000	26/308	9.1 (4.4–13.7)	2.6 (1.1–5.7)
5,000 to <20,000	24/411	4.0 (1.9–6.1)	Referent
20,000 to <100,000	23/401	6.4 (2.8–9.9)	1.9 (0.8–4.5)
≥100,000	21/333	6.7 (3.9–9.5)	2.2 (1.1–4.4)
Residence¶			
East	57/954	6.3 (4.3–8.3)	Referent
West	37/499	6.5 (4.0–8.9)	1.1 (0.6–1.8)
Vegetarian			
Yes	7/129	6.4 (4.6–8.2)	1.3 (0.5–3.3)
No	86/1,273	7.4 (1.3–13.5)	Referent
Total	94/1,453	6.3 (4.7–8.0)	

*We tested 5 hypothesized associations toward seropositivity. Minimum adjustment sets were identified based on directed acyclic graphs (Appendix, https://wwwnc.cdc.gov/EID/article/30/5/23-1045-App1.pdf). aOR, adjusted odds ratio.
†Unweighted.
‡Based on the multidimensional socioeconomic index according to Lampert et al. (*4*).
§By number of inhabitants.
¶Western states: Baden-Württemberg, Bavaria, Bremen, Hamburg, Hesse, Lower Saxony, North Rhine-Westfalia, Rhineland-Palatinate, Saarland, Schleswig-Holstein; Eastern states: Berlin, Brandenburg, Mecklenburg-West Pomerania, Saxony, Saxony-Anhalt, Thuringia.

for all statistical analyses accounting for the study design. In addition, we calculated survey weights based on age, sex, residence, nationality, and education to correct for deviations from national population statistics.

We included 1,453 girls and adolescents (mean age 10.3 years) in the analyses. Of those, 1,359 tested negative and 94 tested positive for *T. gondii*–specific IgG. We estimated overall weighted seroprevalence at 6.3% (95% CI 4.7%–8.0%) (Table).

With each year of life, the chance of being seropositive increased significantly, by 1.2 (95% CI 1.1–1.3). When we combined the data from the girls with those of female adults, seroprevalence steadily increased

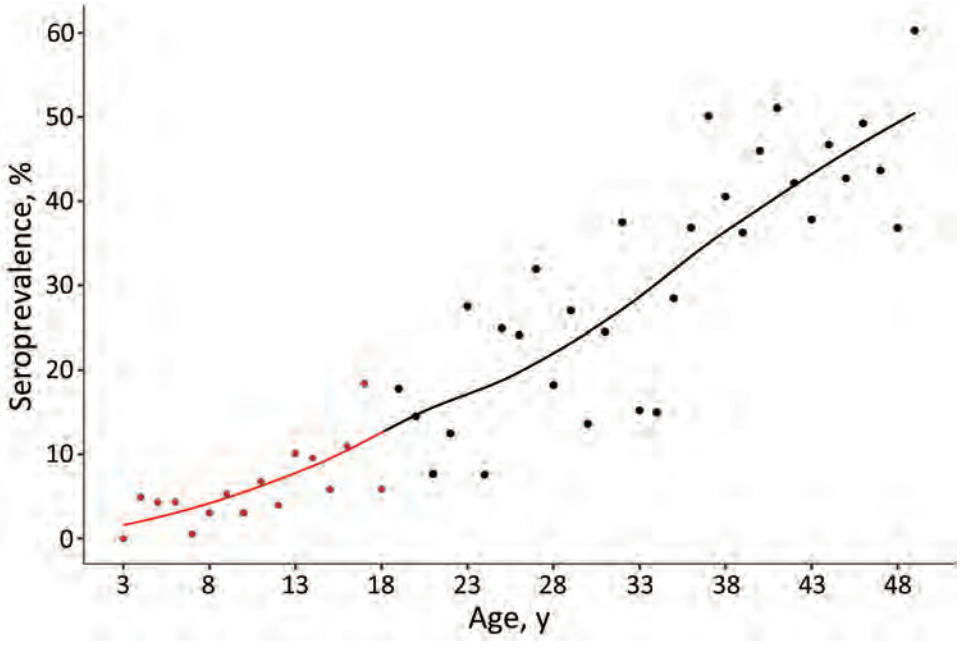

Figure 1. Weighted seroprevalence of *Toxoplasma gondii* infections in female children and adolescents by age, Germany, 2014–2017 (red). For comparison, results of Wilking et al. (*3*), a previous study among adults, were added to the graph (black)

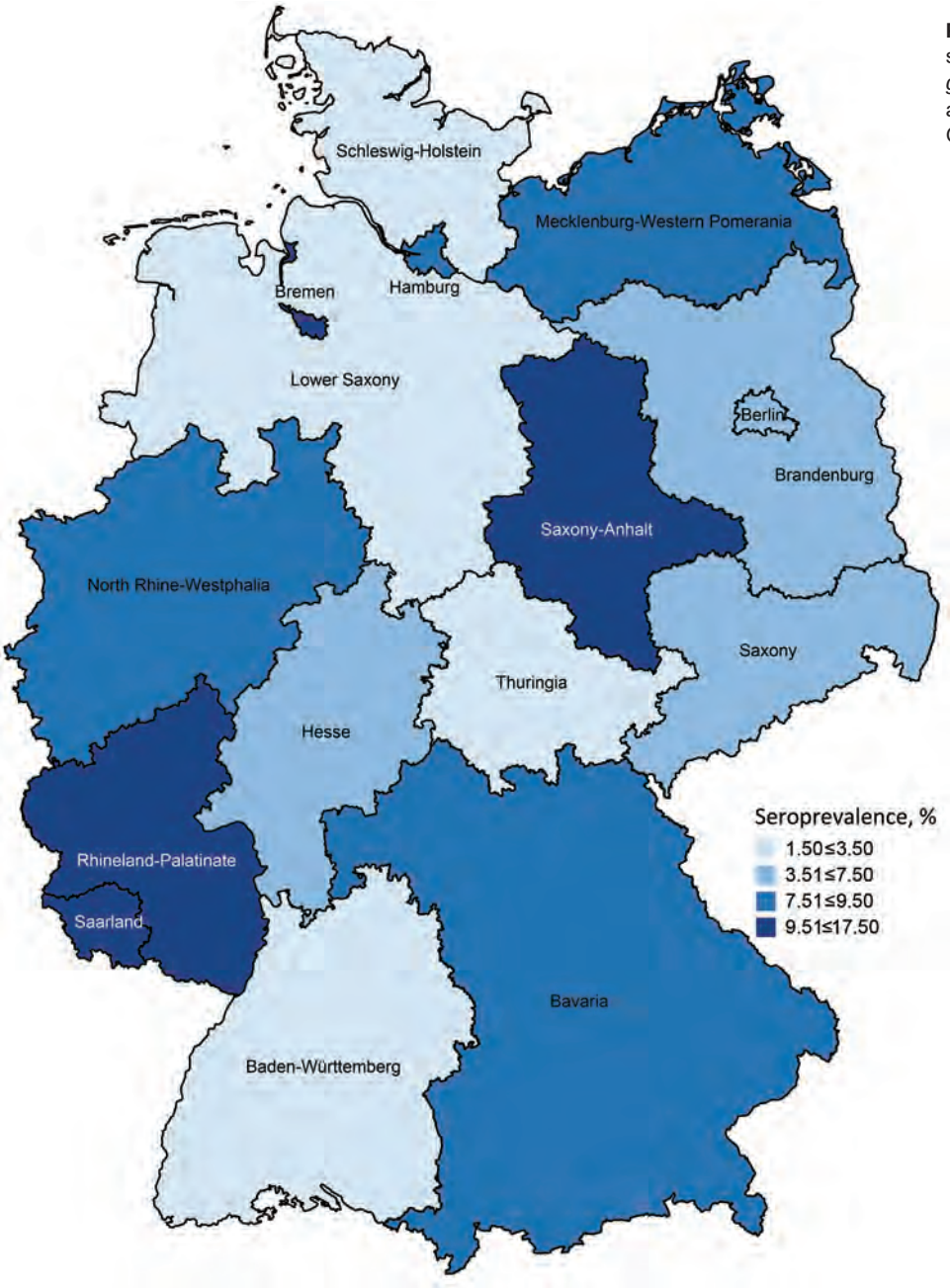

Figure 2. Weighted seroprevalence of *Toxoplasma gondii* infections in female children and adolescents by federal state, Germany, 2014–2017.

with age (Figure 1). This increase is a result of cumulative seropositivity because *T. gondii* infection is persistent and shows little seroreversion.

Girls living in families with low socioeconomic status (SES) showed the highest prevalence (10.8%, 95% CI 4.7%–16.9%). Their chance of being seropositive is 2.7 (95% CI 1.3–5.9) times higher than that of girls with middle SES. Low social status is often found to be associated with various disease risks, which may be a result of lower health literacy and reduced options to avoid health-related risks (*4*).

The seroprevalence among girls living in rural areas (<5,000 inhabitants) was significantly higher than seroprevalence for girls living in small towns (5,000–<20,000 inhabitants) (aOR 2.6, 95% CI 1.1–5.7). Similarly, girls living in urban areas (>100,000 inhabitants) were also 2.2 (95% CI 1.1–4.4) times more likely to be seropositive than those living in small towns. Greater exposure to natural habitats, including sand and soil contaminated due to free-roaming cats (*6*), as well as cats and children using the same limited spaces (e.g., sandboxes) (*7*), might explain the respective higher

risks of infection. We did not observe any regional distribution patterns (e.g., differences between eastern and western Germany) (Figure 2).

Overall, 9.3% of the participants reported being vegetarian; of those, 6.4% (95% CI 4.6%–8.2%) were seropositive (aOR 1.3, 95% CI 0.5–3.3). This result is not significantly different from results for nonvegetarians and is consistent with other studies (*8*–*10*). Diet appeared to have less effect on the risk for infection in children and adolescents than in adults. This finding may indicate that the relevance of the 2 transmission pathways differs significantly between age groups, and more environmentally associated infections occur in children and adolescents. Alternatively, risk factors associated with transmission pathway 1 may have shifted over time, for example, from improvements in the production and preparation of meat. However, more detailed information on the type (raw or undercooked) and quantity of meat consumed would have been beneficial but were not available in our dataset.

Conclusions

Overall, 6 of every 100 girls in Germany become infected with *T. gondii* during the first 18 years of life, corresponding to ≈340,504 total infections in this population group. Internationally comparable studies are limited. Seroprevalence estimates vary worldwide, from <10% to >60% for girls and 10%–80% for adults (*11*,*12*). Toxoplasmosis causes a higher infection pressure for girls and young women in Germany than in countries with similar socioeconomic conditions (*11*,*13*). In the United States, for example, the seroprevalence is significantly lower in age groups 6–11 years (0.9%, 95% CI 0.5%–1.5%) and 12–19 years (3.1%, 95% CI 2.0%–4.6%) (*11*).

Independent risk factors identified in our study were age, low social status, and growing up in rural or urban areas. Those factors have also been associated with seropositivity in children and adolescents in other countries (*12*,*14*). Further risk factors include contact with cats (*12*,*14*,*15*), contact with soil or sand (*8*,*9*,*15*), and consumption of unwashed vegetables (*8*). Growing up on a farm or keeping farm animals was also associated with increased seroconversions (*8*,*10*). Regular handwashing showed protective effects (*9*,*15*).

Our data may be helpful as an empirical basis for prevention guidelines. Implementing screening of pregnant women is one possibility and should be reevaluated using current data. Furthermore, our results indicate that meat consumption does not appear to be a driving force in children and adolescents, which calls for different prevention strategies in this population than in adults (Appendix). However, our serosurvey is cross-sectional and represents the cumulated lifetime risk for infection. Therefore, misclassification of exposures (e.g., participants reported vegetarianism but consumed raw meat earlier in life) and unmeasured confounding is likely. Thus, our data are not appropriate for establishing causal relationships. Future studies should use longitudinal data containing detailed information on exposures and time of infection to disentangle different transmission pathways. The ultimate goal is efficient primary prevention of *T. gondii* infections; the goal requires integrating the fields of veterinary, human, and environmental medicine in a One Health approach.

Acknowledgments

We thank Daniela Heckmann, Petra Gosten-Heinrich, Elisabeth Kamal, Sandra Klein, Gudrun Kliem, Ilka McCormick-Smith, and Elke Radam for expert technical help.

This work was supported by the Robert Koch Institute, Berlin, Germany.

About the Author

Ms. Giese is an epidemiologist at the Robert Koch Institute with strong interest in gastrointestinal infections, zoonoses and tropical infections.

References

1. Wilking H, Thamm M, Stark K, Aebischer T, Seeber F. Prevalence, incidence estimations and risk factors of *Toxoplasma gondii* infection in Germany: a representative, cross-sectional, serological study. Sci Rep. 2016;6:22551. https://doi.org/10.1038/srep22551
2. Pleyer U, Gross U, Schlüter D, Wilking H, Seeber F. Toxoplasmosis in Germany. Dtsch Arztebl Int. 2019; 116:435–44.
3. EFSA Panel on Biological Hazards (BIOHAZ); Koutsoumanis K, Allende A, Alvarez-Ordónez A, Bolton D, Bover-Cid S, Chemaly M, et al. Public health risks associated with food-borne parasites. EFSA J. 2018;16:5495.
4. Lampert T, Hoebel J, Kuntz B, Müters S, Kroll LE. Socioeconomic status and subjective social status measurement in KiGGS Wave 2. J Health Monit. 2018;3:108–25.
5. Murat JB, Dard C, Fricker Hidalgo H, Dardé ML, Brenier-Pinchart MP, Pelloux H. Comparison of the Vidas system and two recent fully automated assays for diagnosis and follow-up of toxoplasmosis in pregnant women and newborns. Clin Vaccine Immunol. 2013;20:1203–12. https://doi.org/10.1128/CVI.00089-13
6. Candela MG, Fanelli A, Carvalho J, Serrano E, Domenech G, Alonso F, et al. Urban landscape and infection risk in free-roaming cats. Zoonoses Public Health. 2022;69:295–311. https://doi.org/10.1111/zph.12919
7. Pacheco-Ortega GA, Chan-Pérez JI, Ortega-Pacheco A, Guzmán-Marín E, Edwards M, Brown MA, et al. Screening of zoonotic parasites in playground sandboxes of public parks

from subtropical Mexico. J Parasitol Res. 2019;2019:7409076. https://doi.org/10.1155/2019/7409076
8. Hofhuis A, van Pelt W, van Duynhoven YTHP, Nijhuis CDM, Mollema L, van der Klis FRM, et al. Decreased prevalence and age-specific risk factors for *Toxoplasma gondii* IgG antibodies in the Netherlands between 1995/1996 and 2006/2007. Epidemiol Infect. 2011;139:530–8. https://doi.org/10.1017/S0950268810001044
9. Sharif M, Daryani A, Barzegar G, Nasrolahei M. A seroepidemiological survey for toxoplasmosis among schoolchildren of Sari, Northern Iran. Trop Biomed. 2010;27:220–5.
10. Nash JQ, Chissel S, Jones J, Warburton F, Verlander NQ. Risk factors for toxoplasmosis in pregnant women in Kent, United Kingdom. Epidemiol Infect. 2005;133:475–83. https://doi.org/10.1017/S0950268804003620
11. Jones JL, Kruszon-Moran D, Elder S, Rivera HN, Press C, Montoya JG, et al. *Toxoplasma gondii* infection in the United States, 2011–2014. Am J Trop Med Hyg. 2018;98:551–7. https://doi.org/10.4269/ajtmh.17-0677
12. Fan CK, Lee LW, Liao CW, Huang YC, Lee YL, Chang YT, et al. *Toxoplasma gondii* infection: relationship between seroprevalence and risk factors among primary schoolchildren in the capital areas of Democratic Republic of São Tomé and Príncipe, West Africa. Parasit Vectors. 2012;5:141. https://doi.org/10.1186/1756-3305-5-141
13. Liassides M, Christodoulou V, Moschandreas J, Karagiannis C, Mitis G, Koliou M, et al. Toxoplasmosis in female high school students, pregnant women, and ruminants in Cyprus. Trans R Soc Trop Med Hyg. 2016;110:359–66. https://doi.org/10.1093/trstmh/trw038
14. Cabral Monica T, Evers F, de Souza Lima Nino B, Pinto-Ferreira F, Breganó JW, Ragassi Urbano M, et al. Socioeconomic factors associated with infection by *Toxoplasma gondii* and *Toxocara canis* in children. Transbound Emerg Dis. 2022;69:1589–95. https://doi.org/10.1111/tbed.14129
15. Wang S, Yao Z, Li H, Li P, Wang D, Zhang H, et al. Seroprevalence and risk factors of *Toxoplasma gondii* infection in primary school children in Henan province, central China. Parasite. 2020;27:23. https://doi.org/10.1051/parasite/2020018

Address for correspondence: Laura Giese, Robert Koch Institute, Department of Infectious Disease Epidemiology, Seestraße 10, 13353 Berlin, Germany; email: giesel@rki.de

Paranannizziopsis spp. Infection in Wild Vipers, Europe

Gaëlle Blanvillain, Fernando Martínez-Freiría, Joseph R. Hoyt, Jeffrey M. Lorch, Albert Martinez-Silvestre

We describe the detection of *Paranannizziopsis* sp. fungus in a wild population of vipers in Europe. Fungal infections were severe, and 1 animal likely died from infection. Surveillance efforts are needed to better understand the threat of this pathogen to snake conservation.

Over the past few decades, fungal pathogens have been implicated in wildlife population declines, posing a substantial challenge to the conservation of many species, including herpetofauna (*1*). In reptiles, most fungal pathogens are within the genera *Nannizziopsis*, *Paranannizziopsis*, and *Ophidiomyces*, members of the order Onygenales (*2*). Of those genera, the most well-documented genus in wild reptiles is *Ophidiomyces*, consisting of the single species *O. ophidiicola*, which is responsible for ophidiomycosis, also called snake fungal disease (SFD) (*3*). Infections with *Paranannizziopsis* spp. fungi, on the other hand, are not well documented, possibly because of wide overlap with ophidiomycosis in how the disease manifests (*4*). Disease associated with *Paranannizziopsis* infection has been described in captive collections in North America (*2*,*5*–*7*) and Australasia (*2*,*8*). In wild populations, *Paranannizziopsis* spp. fungi have only been detected in nonnative free-living panther chameleons (*Furcifer pardalis*) from central Florida, USA (*9*), and in wild snakes in the United States and Canada (*4*). The geographic extent in wild host populations and severity of infection associated with *Paranannizziopsis* spp. fungi is unknown and deserves more thorough evaluation. We report infection with a *Paranannizziopsis* sp. fungus in 2 wild Seoane's vipers (*Vipera seoanei*) from northwestern Spain. Handling of snakes was reviewed and approved by Virginia Tech Institute for Animal Care and Use Committee protocol 20-055. Vipers and tissue samples were collected under permit from Xunta de Galicia, Spain (permit no. EB-015/2021).

Author affiliations: Virginia Polytechnic Institute and State University, Blacksburg, Virginia, USA (G. Blanvillain, J.R. Hoyt); Centro de Investigação em Biodiversidade e Recursos Genéticos da Universidade do Porto, Vairão, Portugal (F. Martínez-Freiría); US Geological Survey, Madison, Wisconsin, USA (J.M. Lorch); Catalonian Reptiles and Amphibians Rescue Center, Masquefa, Spain (A. Martinez-Silvestre)

DOI: https://doi.org/10.3201/eid3005.231317

The Study

On May 14, 2021, two *V. seoanei* vipers, a subadult male (body length 31.7 cm, weight 10.3 g) and an adult female (body length 44.7 cm, weight 61 g), were captured near Zamáns in Vigo, Spain (42.16N, 8.68W; WGS1984). Both animals were in the process of molting and displayed many skin lesions on the head and body. The lesions were particularly abundant for the subadult male, for which the molting process was abnormal (i.e., dysecdysis). The animal was lethargic and appeared moribund. This snake was brought into captivity for supportive care but died the next day. The carcass was placed in ethanol until we performed necropsy and histopathological analyses. The adult female was reproductive, and, after we collected biometric data and skin swab samples, she was immediately released at the place of capture.

We swabbed the ventral and dorsal areas of the snakes in duplicate using a premoistened, sterile polyester-tipped applicator (Puritan, https://www.puritanmedproducts.com) and stored frozen swab samples at −20°C until analysis. We extracted DNA from the samples using PrepMan Ultra Sample Preparation Reagent (ThermoFisher Scientific, https://www.thermofisher.com). In addition, we excised 7 skin lesions (≈2 × 4 mm) from the subadult male at various locations across the body and stored them in 70% ethanol. We extracted DNA using a QIAGEN Blood and Tissue kit (QIAGEN, https://www.qiagen.com) following manufacturer's instructions, which included a lyticase lysis step (200 U for 30 min at 30°C) to degrade fungal cell walls.

We screened extracted DNA from both the swab and tissue samples for the presence of *Paranannizziopsis* spp. and *O. ophidiicola* fungi using real-time PCR. *O. ophidiicola* fungi were not detected in any of the

samples using a quantitative PCR (qPCR) targeting the internal transcribed spacer (ITS) region of the fungus (*10*). Samples from both vipers were qPCR-positive for *Paranannizziopsis* sp. fungus by genus-specific qPCR (*4*). We amplified and sequenced the full-length ITS and a portion of the mitochondrial cytochrome oxidase subunit III (*COX3*) gene (GenBank accession nos. OR353533 and OR351968) of the *Paranannizziopsis* sp. fungus, according to published methods (*4*). We compared sequences from those loci with existing sequences in GenBank using BLASTn (*11*). The ITS sequence most closely matched *P. australasiensis* strains in GenBank: 99.1%–99.6% identity over the ≈500 bp region sequenced for strains UAMH 12461 (OR100710), NWHC 24878–7 (OR100711), UAMH 12464 (OR100712), UAMH 12463 (OR100713), UAMH 10439 (KF477218), and UAMH 11645 (NR_111879). The *COX3* sequence shared 99.9%–100.0% identity (over the ≈670-bp portion sequenced) with sequence data from *P. australasiensis* (strain UAMH 12461 [OR103159], NWHC 24878–7 [OR103160], UAMH 12464 [OR103161], UAMH 12463 [OR103162], UAMH 10439 [OR103163], UAMH 11645 [OR164]), *P. californiensis* (strain UAMH 10693 [OR103165]), and *P. tardicrescens* (strain CBS 142038 [OR103166]) in GenBank. After positive detections for *Paranannizziopsis* sp. fungi from those 2 animals, we also screened additional skin swab samples collected from *V. seoanei* vipers in Spain and Portugal in 2020 and 2021 (n = 37, including 1 with a ventral skin lesion). We did not identify *Paranannizziopsis* spp. fungi in those additional samples, indicating a pathogen prevalence of ≈5% (2 of 39 samples) (Figure 1).

At necropsy, the subadult male viper had variable numbers of multifocal to coalescing, raised, white-gray to dark brown discolored cutaneous lesions, ranging in size from 1 to 6 mm in diameter, along the left side of the mouth and labial scales; the lower jaw; and the central, dorsal, and caudal regions (Figure 2, panel A). We took samples of skin, bone, stomach, liver, kidney, and intestine for histopathological analysis. Tissue sections were stained by hematoxylin and eosin and Grocott-Gomori methenamine silver stains. Microscopically, skin lesions included areas of necrosis with granulocytic inflammation in the superficial to mid-epidermis; we observed slight edema adjacent to the mid-epidermis. Small chronic inflammatory cell aggregates composed of degenerated heterophils mixed with necrotic cellular debris and proteinaceous fluid were observed in these lesions. We detected nonpigmented fungal

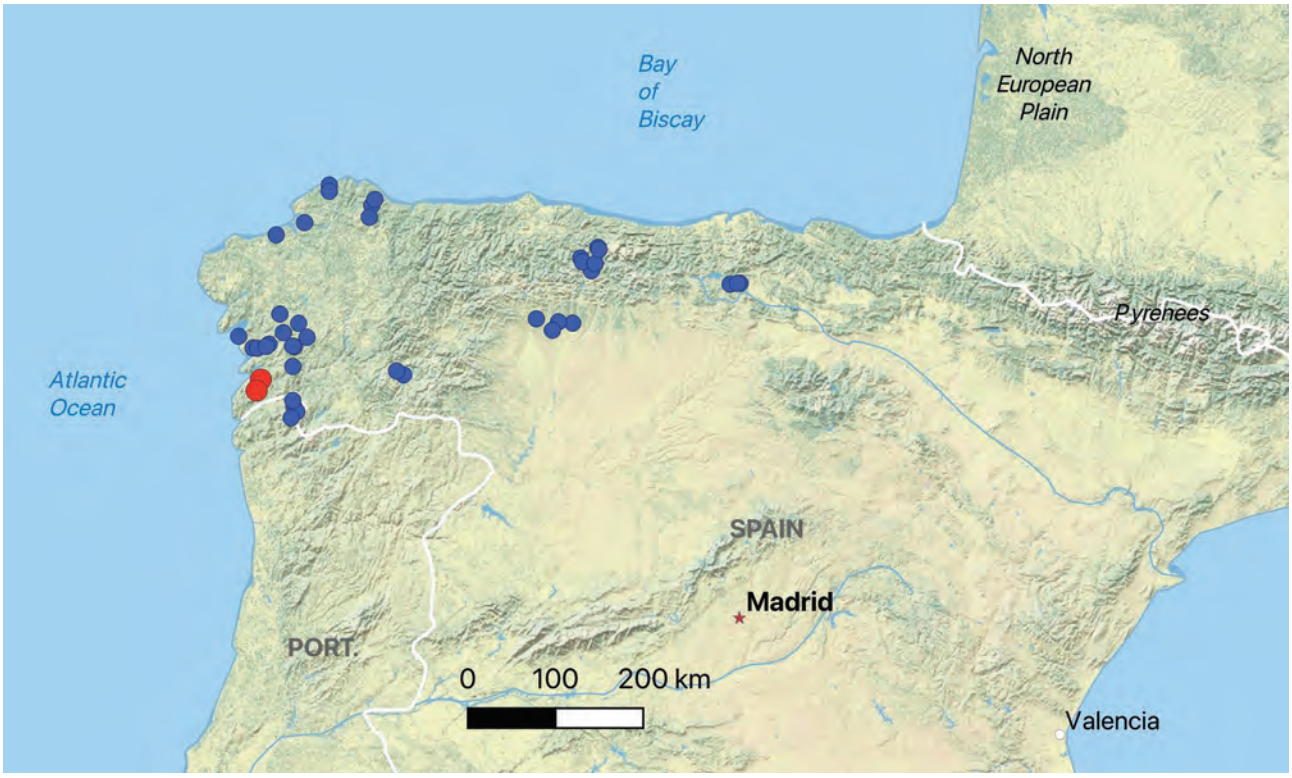

Figure 1. Spatial distribution of Seoane's viper (*Vipera seoanei*) captures and detections of *Paranannizziopsis* sp. fungus in Spain and Portugal. Each dot represents an individual snake capture; overlapping points were slightly jittered for visualization. Blue dots represent snakes that tested negative by real-time PCR, and red dots represent snakes that tested positive by real-time PCR.

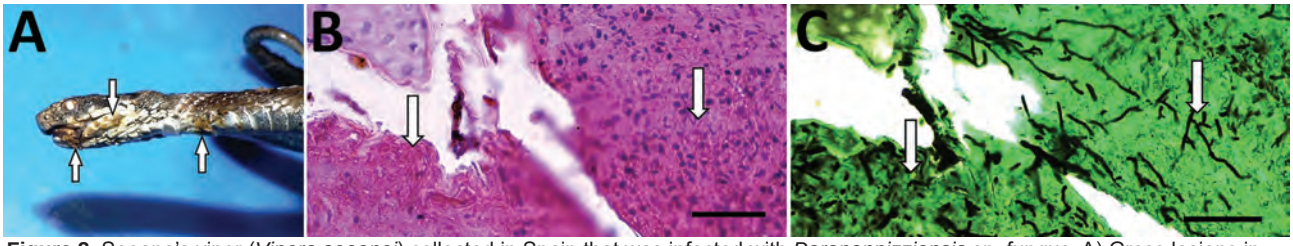

Figure 2. Seoane's viper (*Vipera seoanei*) collected in Spain that was infected with *Paranannizziopsis* sp. fungus. A) Gross lesions in the mouth, on the lower jaw, and on the ventral areas of the body (arrows). B) Lightly stained hyphae (arrows)in section of epidermis stained with hematoxylin and eosin. Scale bar indicates 20 µm. C) Intralesional hyphae (arrows) in section of epidermis stained with the Grocott-Gomori methenamine silver method. Scale bar indicates 20 µm.

hyphae at the epidermal surface and breaching the epidermis under hematoxylin and eosin stain (Figure 2, panel B). We observed structures morphologically compatible with hyphae under Grocott-Gomori methenamine silver stain (Figure 2, panel C). Those hyphae were 1.8–4.9 µm in diameter, were septate, and had parallel walls with irregular dichotomous branching. We did not observe any relevant lesions or fungal elements in the internal tissues and viscera.

Conclusions

The effects of fungal diseases on reptiles have been difficult to evaluate, especially in cryptic species such as snakes. We report detection of a *Paranannizziopsis* sp. fungal infection in a wild population of *V. seoanei* vipers in Spain, and at least 1 viper likely died because of the infection. The pathology and fungal morphology were consistent with *Paranannizziopsis* spp. infections reported elsewhere (*2*,*4*–*7*). Although the strain detected in the snake that died was most similar to *P. australasiensis*, we were unable to identify the strain to a particular species of *Paranannizziopsis* fungus. Additional genetic analyses on the *Paranannizziopsis* sp. fungus detected in Spain might help better resolve its taxonomy.

Whether *Paranannizziopsis* spp. fungi are native to the Iberian Peninsula or whether our detections could represent recent transmission events from captive snakes remains unclear. We did not detect *Paranannizziopsis* spp. fungi in additional snakes sampled from Spain and Portugal, and *O. ophidiicola* fungus has not been detected in the Iberian Peninsula (*11*). Thus, if the pathogen was recently introduced, spread of this fungus to other vulnerable reptile populations is of concern, and further investigation is warranted considering the conservation need for most reptiles worldwide (*12*). *V. seoanei* vipers are a nearly endemic species to the Iberian Peninsula and is restricted to the northern region of the Atlantic climate (*13*). Populations have been severely impacted by habitat loss and fragmentation, and ecological models indicate high vulnerability of this species to climate change (*14*). Western populations, where these 2 infected snakes were found, are at the edge of the species' distribution and are the most genetically diverse and isolated, highlighting their importance for maintaining genetic diversity (*14*,*15*). In light of this factor, detection of a species of *Paranannizziopsis* fungus raises concerns regarding the additive effects of other stressors and disease on the health of this imperiled population, and increased surveillance for this pathogen in wild populations might be warranted.

Acknowledgments

We thank Megan Winzeler for laboratory assistance.

This material is based upon work supported by the NSF GRFP grant no. 480040. Additional funding to G.B. was provided by a Virginia Tech Cunningham fellowship, and a CeZAP (Center for Emerging, Zoonotic, and Arthropod-borne Pathogens) grant as part of the Infectious Diseases Interdisciplinary Graduate Education Program. F.M.-F. is supported by FCT - Fundação para a Ciência e a Tecnologia, Portugal (contract ref. DL57/2016/CP1440/CT0010).

About the Author

Ms. Blanvillain is a PhD candidate in the department of biological sciences at Virginia Tech. Her primary research interest is infectious disease in wildlife, specifically in herpetofauna.

References

1. Fisher MC, Gurr SJ, Cuomo CA, Blehert DS, Jin H, Stukenbrock EH, et al. Threats posed by the fungal kingdom to humans, wildlife, and agriculture. MBio. 2020;11:e00449–20. https://doi.org/10.1128/mBio.00449-20
2. Sigler L, Hambleton S, Paré JA. Molecular characterization of reptile pathogens currently known as members of the *chrysosporium* anamorph of *Nannizziopsis vriesii* complex and relationship with some human-associated isolates. J Clin Microbiol. 2013;51:3338–57. https://doi.org/10.1128/JCM.01465-13
3. Lorch JM, Lankton J, Werner K, Falendysz EA, McCurley K, Blehert DS. Experimental infection of snakes with *Ophidiomyces ophiodiicola* causes pathological changes that

typify snake fungal disease. MBio. 2015;6:e01534–15. https://doi.org/10.1128/mBio.01534-15
4. Lorch JM, Winzeler ME, Lankton JS, Raverty S, Snyman HN, Schwantje H, et al. *Paranannizziopsis* spp. infections in wild snakes and a qPCR assay for detection of the fungus. Front Microbiol. 2023;14:1302586. https://doi.org/10.3389/fmicb.2023.1302586
5. Bertelsen MF, Crawshaw GJ, Sigler L, Smith DA. Fatal cutaneous mycosis in tentacled snakes (*Erpeton tentaculatum*) caused by the *Chrysosporium* anamorph of *Nannizziopsis vriesii*. J Zoo Wildl Med. 2005;36:82–7. https://doi.org/10.1638/04-020
6. Rainwater KL, Wiederhold NP, Sutton DA, Garner MM, Maguire C, Sanders C, et al. Novel *Paranannizziopsis* species in a Wagler's viper (*Tropidolaemus wagleri*), tentacled snakes (*Erpeton tentaculatum*), and a rhinoceros snake (*Rhynchophis boulengeri*) in a zoological collection. Med Mycol. 2019;57:825–32. https://doi.org/10.1093/mmy/myy134
7. Díaz-Delgado J, Marrow JC, Flanagan JP, Bauer KL, Zhang M, Rodrigues-Hoffmann A, et al. Outbreak of *Paranannizziopsis australasiensis* infection in captive African bush vipers (*Atheris squamigera*). J Comp Pathol. 2020;181:97–102. https://doi.org/10.1016/j.jcpa.2020.10.004
8. Masters NJ, Alexander S, Jackson B, Sigler L, Chatterton J, Harvey C, et al. Dermatomycosis caused by *Paranannizziopsis australasiensis* in five tuatara (*Sphenodon punctatus*) and a coastal bearded dragon (*Pogona barbata*) in a zoological collection in New Zealand. N Zealand Vet J. 2016;64:301–7.
9. Claunch NM, Goodman CM, Harman M, Vilchez M, Smit SD, Kluever BM, et al. Dermatomycosis caused by *Paranannizziopsis australasiensis* in non-native panther chameleons (*Furcifer pardalis*) captured in Central Florida, USA. J Wildl Dis. 2023;59:322–31. https://doi.org/10.7589/JWD-D-22-00018
10. Bohuski E, Lorch JM, Griffin KM, Blehert DS. TaqMan real-time polymerase chain reaction for detection of *Ophidiomyces ophiodiicola*, the fungus associated with snake fungal disease. BMC Vet Res. 2015;11:95. https://doi.org/10.1186/s12917-015-0407-8
11. Blanvillain G, Lorch JM, Joudrier N, Bury S, Cuenot T, Franzen M, et al. Contribution of host species and pathogen clade to snake fungal disease hotspots in Europe. Commun Biol. 2024;7,:440. https://doi.org/10.1038/s42003-024-06092-x
12. Cox N, Young BE, Bowles P, Fernandez M, Marin J, Rapacciuolo G, et al. A global reptile assessment highlights shared conservation needs of tetrapods. Nature. 2022; 605:285–90. https://doi.org/10.1038/s41586-022-04664-7
13. Martínez-Freiría F, Brito JC. *Vipera seoanei* (Lataste, 1879). In: Milla AS, Ramos MA, editors. Reptiles [in Spanish]. 2nd ed. Fauna Ibérica, vol. 10. Madrid: Museo Nacional de Ciencias Naturales, CSIC; 2014. p. 942–56.
14. Martínez-Freiría F. Assessing climate change vulnerability for the Iberian viper *Vipera seoanei*. Basic Appl Herpetol. 2015;29:61–80. https://doi.org/10.11160/bah.15001
15. Martínez–Freiría F, Velo–Antón G, Brito JC. Trapped by climate: interglacial refuge and recent population expansion in the endemic Iberian adder *Vipera seoanei*. Divers Distrib. 2015;21:331–44. https://doi.org/10.1111/ddi.12265

Address for correspondence: Gaëlle Blanvillain, Virginia Tech, 1015 Life Science Cir, Steger 352, Blacksburg, VA 24061, USA; email: gaelle.blanvillain@gmail.com or gblanvillain@vt.edu

Protective Efficacy of Lyophilized Vesicular Stomatitis Virus–Based Vaccines in Animal Model

Abd'jeleel Salawudeen, Geoff Soule, Nikesh Tailor, Levi Klassen, Jonathan Audet, Angela Sloan, Yvon Deschambault, David Safronetz

We evaluated the in vitro effects of lyophilization for 2 vesicular stomatitis virus–based vaccines by using 3 stabilizing formulations and demonstrated protective immunity of lyophilized/reconstituted vaccine in guinea pigs. Lyophilization increased stability of the vaccines, but specific vesicular stomatitis virus–based vaccines will each require extensive analysis to optimize stabilizing formulations.

Live recombinant vesicular stomatitis virus (VSV) expressing the Ebola virus (EBOV) glycoprotein (VSVΔG/EBOVGP) was evaluated during 2014–2015 as a vaccine to limit the effects of EBOV disease (*1*). Because of the success and safety of the EBOV vaccine, similar VSV-based vaccines have been proposed for Sudan and Marburg viruses and for other etiologic agents of viral hemorrhagic fever diseases, such as Lassa virus (LASV) (*2*).

Cold chain maintenance for distributing and storing VSV-based vaccines is a logistical challenge, especially when ultralow temperatures (−60°C to −80°C) are required. The challenge is greater in rural areas, particularly in developing countries, where infrastructure and transport systems are often deficient. We evaluated the effects of lyophilization on the in vitro recoverability and in vivo protective efficacy of VSV-based vaccines.

We conducted animal studies in accordance with the Canadian Council of Animal Care guidelines; studies received approval from the Canadian Science Centre for Human and Animal Health's institutional Animal Care and Use Committee. We performed work involving infectious Lassa virus in a Biosafety Level 4 laboratory within the Public Health Agency of Canada. When required, we inactivated materials for subsequent analysis according to approved procedures.

Author affiliations: University of Manitoba, Winnipeg, Manitoba, Canada (A. Salawudeen, D. Safronetz); Public Health Agency of Canada, Winnipeg (G. Soule, N. Tailor, L. Klassen, J. Audet, A. Sloan, Y. Deschambault, D. Safronetz)

DOI: https://doi.org/10.3201/eid3005.231248

The Study

We conducted propagation and titration (50% tissue culture infectious dose [$TCID_{50}$]) of VSVΔG/EBOVGP and VSV-based LASV (VSVΔG/LASVGPC) vaccines by using Vero E6 cells as previously described (*3*). We evaluated 4 excipients as stabilizers: 2.5% lactalbumin hydrolysate (L), 5% sucrose (S), 2.5% trehalose (T), and 0.25% gelatin (G). We prepared 2× concentrations of each solution initially in Hanks' balanced salt solution and then evaluated 3 combinations (LS, LST, or LSTG) (*4*,*5*). The control formulation for lyophilization was Dulbecco modified Eagle medium (DMEM) without additives. We mixed each excipient combination 1:1 with VSVΔG/EBOVGP (stock titer 1.26×10^7 $TCID_{50}$/mL) or VSVΔG/LASVGPC (2.83×10^7 $TCID_{50}$/mL) and dispensed 200 μL of the mixture into 4 mL sterile glass vials (Electron Microscopy Sciences, https://www.emsdiasum.com). We lyophilized the vaccine mixtures by using an automated FreeZone Triad Benchtop Freeze Dryer (Labconco, https://www.labconco.com) according to the manufacturer's specifications (Appendix Table, https://wwwnc.cdc.gov/EID/article/30/5/23-1248-App1.pdf).

We stored the vials at 4°C, 21°C, or 37°C for 1, 7, 30, and 90 days after lyophilization. At those time points, we reconstituted each vaccine/stabilizer combination in triplicate in 200 μL of 0.85% saline for 1 hour at room temperature by using gentle agitation. We then prepared 10-fold serial dilutions in DMEM and determined virus titers by using standard $TCID_{50}$ methodologies, as previously described (*3*). Titrations of formulations conducted immediately before lyophilization indicated that the addition of stabilizers had

Table 1. Infectious titers of lyophilized vaccines after 90 day storage at different temperatures in study of protective efficacy of lyophilized vesicular stomatitis virus–based vaccines in animal model*

Vaccine	Lyophilization medium			
	DMEM	DMEM + LS	DMEM + LS +T	DMEM + LS + T + G
VSVΔG/LASVGPC				
4°C	6.36 (5.49–7.23)	0.25 (–0.62 to 1.12)	1.25 (0.38–2.12)	0.88 (0.005–1.75)
21°C	NC	3.00 (2.06–3.94)	2.88 (1.94–3.82)	1.50 (0.56–2.44)
37°C	NC	NC	NC	NC
VSVΔG/EBOVGP				
4°C	1.57 (0.83–2.31)	0.43 (–0.32 to 1.17)	1.13 (0.39–1.87)	1.55 (0.81–2.29)
21°C	4.50 (4.22–4.78)	2.00 (1.72–2.28)	6.63 (6.35–6.91)	6.25 (5.97–6.53)
37°C	4.38 (4.20–4.56)	4.50 (4.32–4.68)	4.38 (4.20–4.56)	3.75 (3.57–3.93)

*Values are no. (95% CI), representing the $\log_{10}$ decreases in infectious titers (median 50% tissue culture infectious dose) for vaccines that were lyophilized in the presence of various stabilizers, stored at the indicated temperatures for 90 days, and then reconstituted. Comparisons are between 1 and 90 days after lyophilization. DMEM, Dulbecco modified Eagle medium; G, gelatin; LS, lactalbumin hydrolysate and sucrose; NC, not calculated; T, trehalose; VSVΔG/EBOVGP, vesicular stomatitis virus expressing Ebola virus glycoprotein; VSVΔG/LASVGPC, vesicular stomatitis virus expressing Lassa virus glycoprotein.

no adverse effect on vaccine recovery. We performed mean difference calculations to compare $TCID_{50}$ data collected on day 1 and day 90 after lyophilization by using 2-way analysis of variance in GraphPad Prism 10 (Graphpad, https://www.graphpad.com). For the VSVΔG/LASVGPC vaccine, the 3 stabilizer formulations provided consistent levels of virus recovery; we observed little variation after lyophilization/reconstitution and only minor decreases in titers when stored at 4°C (Table 1; Figure 1). The VSVΔG/LASVGPC

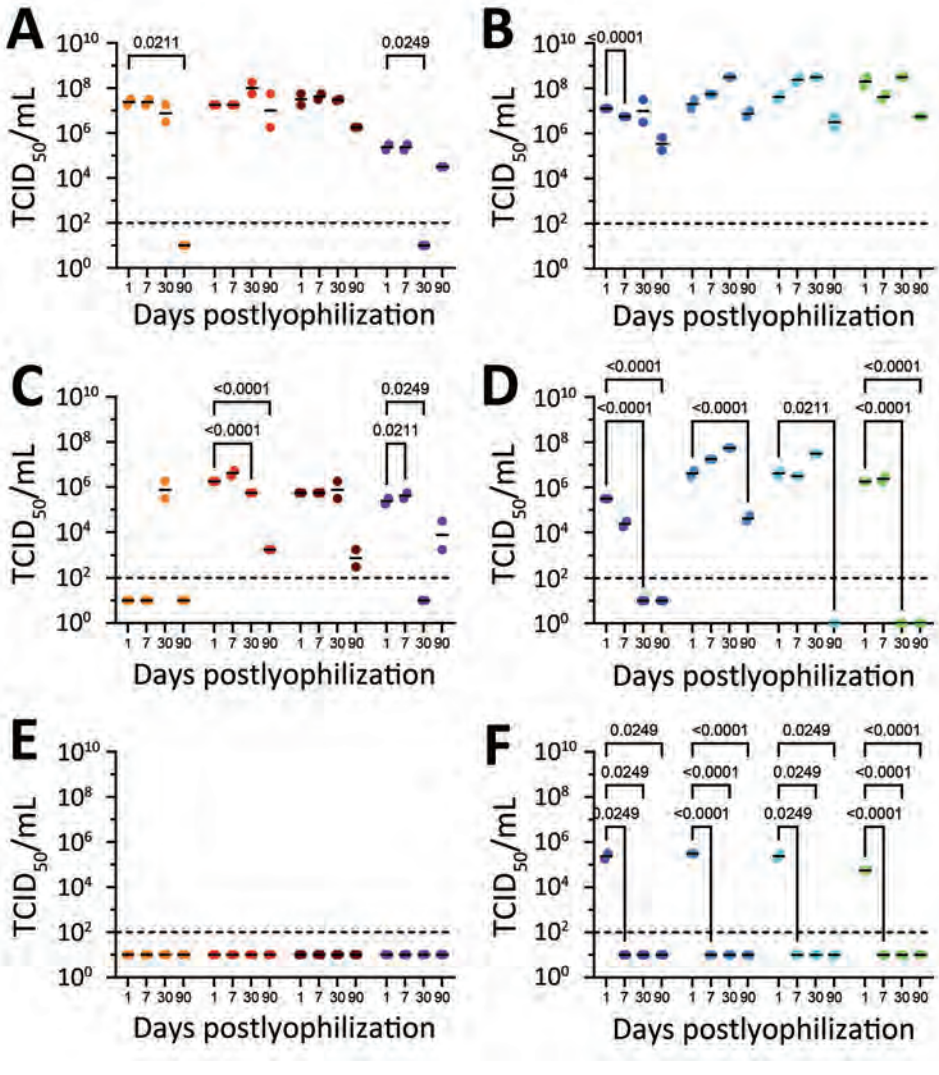

Figure 1. Vaccine recovery after lyophilization in study of protective efficacy of lyophilized vesicular stomatitis virus–based vaccines in animal model. A) VSVΔG/LASVGPC vaccine stored at 4°C; B) VSVΔG/EBOVGP vaccine stored at 4°C; C) VSVΔG/LASVGPC vaccine stored at 21°C; D) VSVΔG/EBOVGP vaccine stored at 21°C; E) VSVΔG/LASVGPC vaccine stored at 21°C; F) VSVΔG/EBOVGP vaccine stored at 21°C. VSVΔG/LASVGPC or VSVΔG/EBOVGP vaccines were lyophilized in DMEM containing no excipients or containing combinations of 5% lactalbumin hydrolysate, 10% sucrose, 5% trehalose, or 0.5% gelatin and stored at different temperatures. At the specified time points, vaccines were resuspended in triplicate in normal saline, titered by using standard tissue culture techniques, and the median $TCID_{50}$ was calculated for each. p values are indicated above brackets. Errors bars are SDs. DMEM, Dulbecco modified Eagle medium; G, gelatin; LS, lactalbumin hydrolysate and sucrose; NC, not calculated; T, trehalose; $TCID_{50}$, 50% tissue culture infectious dose; VSV-Lassa, vesicular stomatitis virus expressing Lassa virus glycoprotein; VSV-Zebov, vesicular stomatitis virus expressing Ebola virus glycoprotein.

construct was stable for ≥90 days. By comparison, the vaccine was not recoverable after >30 days when stored at 4°C without stabilizers (DMEM only). We observed similar patterns of stability for the VSVΔG/LASVGPC vaccine when storage temperatures were increased; albeit, even with the addition of stabilizers, vaccine recovery was immediately impaired by >1 $\log_{10}$ when stored at room temperature (21°C), and no recoverable vaccine was observed when formulations were stored at 37°C. The recovery trends for stabilizer formulations and storage temperature were similar for VSVΔG/EBOVGP and VSVΔG/LASVGPC. However, in general, the VSVΔG/EBOVGP vaccine was more stable than the VSVΔG/LASVGPC vaccine even without stabilizing agents or when stored at increased temperatures (Table 1).

The protective efficacy of VSVΔG/EBOVGP and VSVΔG/LASVGPC vaccines against lethal homologous virus challenge is well established (*6*). To further evaluate lyophilized VSV formulations, we immunized groups of 10 Hartley guinea pigs 1 time with 1×10^6 PFU of either VSVΔG/LASVGPC or lyophilized/reconstituted VSVΔG/LASVGPC (Ly-VSVΔG/LASVGPC) or lyophilized/reconstituted VSVΔG/EBOVGP (Ly-VSVΔG/EBOVGP) via intraperitoneal injection as previously described (*7*). According to in vitro assessments, the lyophilized vaccines contained the LST stabilizer formulation and were stored after lyophilization for 1 week at 4°C. We collected a blood sample from each of the 30 animals at 28 days postimmunization, after which we challenged them with a previously determined lethal dose (10^4 $TCID_{50}$) or 10× the 50% lethal dose of guinea pig–adapted LASV Josiah strain via intraperitoneal inoculation (*8*). We monitored 6 animals per group for disease progression and survival; we euthanized the remaining 4 animals per group on postinfection day 13 to analyze virus titers in tissue samples. The first signs of infection developed on postinfection day 8; increased body temperatures near 40°C occurred in most animals (Figure 2, panel A). Body temperatures in animals immunized with VSVΔG/LASVGPC or Ly-VSVΔG/LASVGPC returned to normal within 2–3 days, whereas body temperatures in animals that received Ly-VSVΔG/EBOVGP remained elevated at 40°C–41°C until death of those animals, which occurred 14–16 days postinfection. We observed weight loss >12% only in Ly-VSVΔG/EBOVGP immunized animals (control group); consistent weight losses occurred during 8–10 days postinfection (Figure 2, panel B). One animal immunized with VSVΔG/LASVGPC experienced an abrupt drop in body weight requiring humane euthanasia on day 13 postinfection. Overall, 100% (6/6) of animals immunized with Ly-VSVΔG/LASVGPC and 83.3% (5/6) immunized with VSVΔG/LASVGPC survived the LASV challenge compared with 16.6% (1/6)

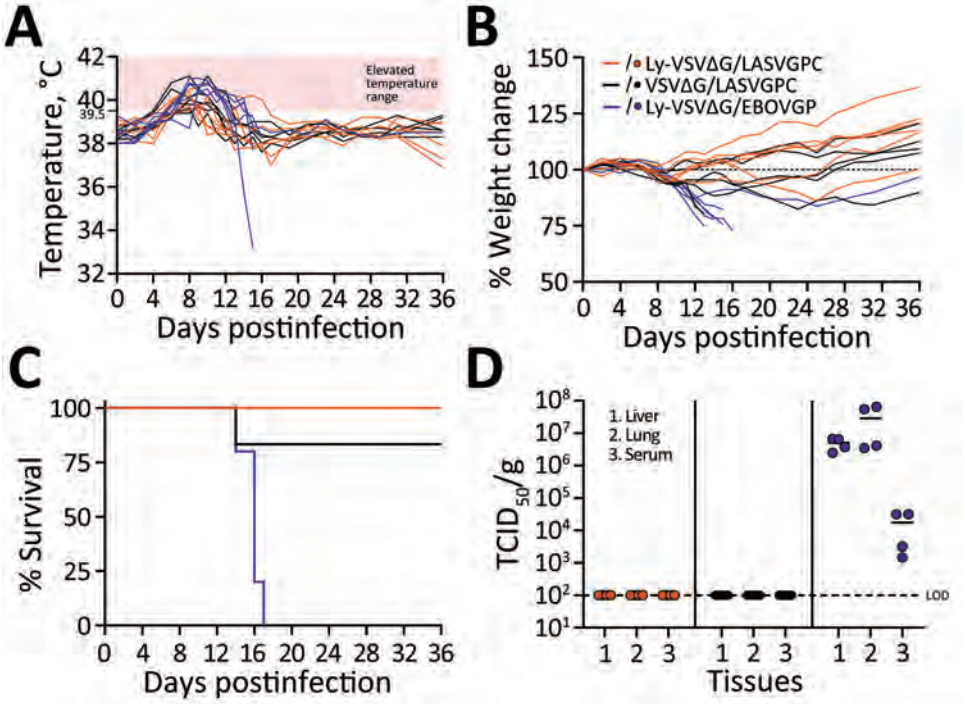

Figure 2. Protective efficacy of lyophilized vesicular stomatitis virus–based vaccines in guinea pig model. A) Body temperatures; B) weight changes; C) survival; D) virus titrations in different tissues. Groups of 10 Hartley guinea pigs each were immunized with VSVΔG/LASVGPC vaccine or lyophilized/reconstituted Ly-VSVΔG/LASVGPC or Ly-VSVΔG/EBOVGP. Ly-VSVΔG/EBOVGP was used as the sham-vaccinated inoculum control group. Animals were challenged 28 days after immunization with a lethal dose of guinea pig–adapted Lassa virus Josiah strain. Disease progression was monitored in 6 animals in each group; the remaining 4 animals per group were euthanized on day 13 postinfection for analysis of infectious Lassa virus in tissues. LOD, limit of detection; Ly-VSVΔG/EBOVGP, lyophilized vesicular stomatitis virus expressing Ebola virus glycoprotein; Ly-VSVΔG/LASVGPC, lyophilized vesicular stomatitis virus expressing Lassa virus glycoprotein; $TCID_{50}$, 50% tissue culture infectious dose; VSVΔG/LASVGPC, vesicular stomatitis virus expressing Lassa virus glycoprotein.

Table 2. Serologic evaluation of Lassa virus antibodies in immunized guinea pigs in study of protective efficacy of lyophilized vesicular stomatitis virus–based vaccines in an animal model*

Animal group, n = 10 each	Median (range)	Average (SEM)	Fold increase†
Preimmunization	1.4 (0.8–3.8)	1.8 (0.4)	NA
Ly-VSVΔG/LASVGPC	100.7 (8–373)	148.6 (44.2)	82
VSVΔG/LASVGPC	160.5 (79–262.8)	172 (17.7)	95
Ly-VSVΔG/EBOVGP	2 (0.7–6.1)	2.4 (0.6)	1.4

*Serum was analyzed for the presence of Lassa glycoprotein-specific antibodies by using an ELISA before challenge with Lassa virus. The standard curve was generated by using human control serum samples; therefore, values should be considered relative and for comparison purposes only. Ly-VSVΔG/EBOVGP, lyophilized vesicular stomatitis virus expressing Ebola virus glycoprotein; Ly-VSVΔG/LASVGPC, lyophilized vesicular stomatitis virus expressing Lassa virus glycoprotein; NA, not applicable; VSVΔG/LASVGPC, vesicular stomatitis virus expressing Lassa virus glycoprotein.
†Fold change of average values from immunized animals compared with randomized preimmunization control specimens.

in the Ly-VSVΔG/EBOVGP control group (Figure 2, panel C). Supporting the survival data, we only found infectious LASV in tissues collected on postinfection day 13 from the Ly-VSVΔG/EBOVGP–immunized control animals (Figure 2, panel D). Although not tested in vivo, the in vitro data supports similar protective responses from lyophilized VSVΔG/LASVGPC stabilized with LST or LS formulations for ≥30 days at 21°C or 90 days at 4°C.

We evaluated vaccine-induced humoral immune responses in serum samples collected immediately before virus challenge (28 days postimmunization) by using LASV and EBOV glycoprotein-specific ELISAs, as previously described (*8*,*9*). Animals immunized with Ly-VSVΔG/EBOVGP vaccine all had EBOV-specific ELISA titers ≥1:6,400. Although those animals were not challenged with EBOV to assess the in vivo protective efficacy of the Ly-VSVΔG/EBOVGP vaccine, their antibody responses were consistent with a predicted protective response on the basis of findings from other studies, including studies using a similar EBOV guinea pig model (*9*,*10*). Instead, we used Ly-VSVΔG/EBOVGP–immunized animals as sham-vaccinated control animals in the lethal LASV challenge experiment to control for nonspecific immunity associated with the LST stabilizer formulation. We monitored LASV-specific responses by using a glycoprotein ELISA developed for use in humans (Zalgen Labs, https://www.zalgen.com), which impedes direct determination of antibody concentrations in guinea pig samples. Nevertheless, we observed >75-fold increases in seroreactivity according to optical densities and average calculated concentrations in animals immunized with the Ly-VSVΔG/LASVGPC or VSVΔG/LASVGPC vaccines compared with preimmunization samples or serum samples collected from animals immunized with Ly-VSVΔG/EBOVGP (Table 2). Furthermore, the similar average values calculated for animals immunized with Ly-VSVΔG/LASVGPC and VSVΔG/LASVGPC indicates the lyophilization process did not appear to deleteriously effect the overall immunogenicity of the VSV-LASV vaccine.

Conclusions

We show that lyophilization can increase stability of VSV-based vaccines, potentially enhancing infrastructure and transport systems in rural areas and developing countries where cold chain management is challenging. Although the 2 VSV-based vaccines evaluated in this study only varied in their glycoproteins, in vitro recoverability efficiencies between them using different stabilizers, particularly gelatin, imply that a universal lyophilization method for all VSV-based vaccines might not be achievable. Therefore, each VSV-based vaccine will require in-depth experimentation to optimize formulations.

This work was funded by the Public Health Agency of Canada and completed in partial fulfillment of A.S.'s MSc degree from the University of Manitoba.

About the Author

Mr. Salawudeen is a graduate student in the Department of Medical Microbiology and Infectious Diseases, University of Manitoba, and a pharmacist. His research interests focus on vaccination strategies, especially prophylactic vaccines for emerging pathogens in sub-Saharan Africa.

References

1. Henao-Restrepo AM, Camacho A, Longini IM, Watson CH, Edmunds WJ, Egger M, et al. Efficacy and effectiveness of an rVSV-vectored vaccine in preventing Ebola virus disease: final results from the Guinea ring vaccination, open-label, cluster-randomised trial (Ebola Ça Suffit!). Lancet. 2017;389:505–18. https://doi.org/10.1016/S0140-6736(16)32621-6
2. Fathi A, Dahlke C, Addo MM. Recombinant vesicular stomatitis virus vector vaccines for WHO blueprint priority pathogens. Hum Vaccin Immunother. 2019;15:2269–85. https://doi.org/10.1080/21645515.2019.1649532
3. Garbutt M, Liebscher R, Wahl-Jensen V, Jones S, Möller P, Wagner R, et al. Properties of replication-competent vesicular stomatitis virus vectors expressing glycoproteins of filoviruses and arenaviruses. J Virol. 2004;78:5458–65. https://doi.org/10.1128/jvi.78.10.5458-5465.2004
4. Kang MS, Jang H, Kim MC, Kim MJ, Joh SJ, Kwon JH, et al. Development of a stabilizer for lyophilization of an

attenuated duck viral hepatitis vaccine. Poult Sci. 2010;89:1167–70. https://doi.org/10.3382/ps.2009-00620
5. Sarkar J, Sreenivasa BP, Singh RP, Dhar P, Bandyopadhyay SK. Comparative efficacy of various chemical stabilizers on the thermostability of a live-attenuated peste des petits ruminants (PPR) vaccine. Vaccine. 2003;21:4728–35. https://doi.org/10.1016/S0264-410X(03)00512-7
6. Liu G, Cao W, Salawudeen A, Zhu W, Emeterio K, Safronetz D, et al. Vesicular stomatitis virus: from agricultural pathogen to vaccine vector. Pathogens. 2021;10:1092. https://doi.org/10.3390/pathogens10091092
7. Stein DR, Sroga P, Warner BM, Deschambault Y, Poliquin G, Safronetz D. Evaluating temperature sensitivity of vesicular stomatitis virus-based vaccines. Emerg Infect Dis. 2019;25:1563–6. https://doi.org/10.3201/eid2508.190281
8. Safronetz D, Rosenke K, Westover JB, Martellaro C, Okumura A, Furuta Y, et al. The broad-spectrum antiviral favipiravir protects guinea pigs from lethal Lassa virus infection post-disease onset. Sci Rep. 2015;5:14775. https://doi.org/10.1038/srep14775
9. Cao W, He S, Liu G, Schulz H, Emeterio K, Chan M, et al. The rVSV-EBOV vaccine provides limited cross-protection against Sudan virus in guinea pigs. NPJ Vaccines. 2023;8:91. https://doi.org/10.1038/s41541-023-00685-z
10. Marzi A, Engelmann F, Feldmann F, Haberthur K, Shupert WL, Brining D, et al. Antibodies are necessary for rVSV/ZEBOV-GP-mediated protection against lethal Ebola virus challenge in nonhuman primates. Proc Natl Acad Sci USA. 2013;110:1893–8. https://doi.org/10.1073/pnas.1209591110

Address for correspondence: David Safronetz, Special Pathogens Program, National Microbiology Laboratory Branch, Public Health Agency of Canada, 1015 Arlington St, Winnipeg, MB R3E 3R2, Canada; email: david.safronetz@phac-aspc.gc.ca

Serogroup B Invasive Meningococcal Disease in Older Adults Identified by Genomic Surveillance, England, 2022–2023

Emily Loud, Stephen A. Clark, David S. Edwards, Elizabeth Knapper, Lynsey Emmett, Shamez Ladhani, Helen Campbell

We report a cluster of serogroup B invasive meningococcal disease identified via genomic surveillance in older adults in England and describe the public health responses. Genomic surveillance is critical for supporting public health investigations and detecting the growing threat of serogroup B *Neisseria meningitidis* infections in older adults.

Cases of invasive meningococcal disease (IMD) have declined in England, from 2,595 in 2000 to 205 in 2022 (*1*). During 2021–2022, a total of 89% of IMD cases occurred in persons <25 years of age, and 87% were caused by *Neisseria meningitidis* capsular group B (MenB) strains (*1*). IMD remains a disease of concern, resulting in high rates of disability; the estimated case-fatality rate was 6% during 2021–2022 (*1*). We describe a MenB cluster in older adults in the East of England region and the local and national public health response. The UK Health Security Agency (UKHSA) designated this investigation as a surveillance activity and, thus, ethics review was not required.

The Study

Case-patient 1 was a 58-year-old woman who experienced a headache and sore throat in early 2023. Her symptoms worsened, she became confused, and she sought care 1 week later at a hospital in East of England, UK (Table). She was intubated, admitted directly to intensive care, and treated with ceftriaxone. *N. meningitidis* was cultured from the patient's blood and cerebrospinal fluid samples. Her case was reported to the local UKHSA team 2 days after hospitalization. Follow-up revealed she had not received any meningococcal vaccinations, nor had she traveled abroad or attended mass gatherings. Two household contacts were given antimicrobial chemoprophylaxis. Case-patient 1 survived.

Case-patient 2 was an 86-year-old woman who experienced abdominal pain, diarrhea, and vomiting in early 2023. She manifested sepsis at the same hospital 2 days after admission of patient 1 and was treated with amoxicillin/clavulanic acid (Table). *N. meningitidis* was cultured from the patient's blood sample, and the local UKHSA health protection team was notified 3 days after hospitalization. She had not previously received any meningococcal vaccinations and reported no recent travel history. One household contact was given antimicrobial chemoprophylaxis. Case-patient 2 survived.

Initial contact tracing did not identify any links between the 2 cases. However, on day 16 after patient 1's symptoms began (Table), the UKHSA's Meningococcal Reference Unit (MRU) identified both *N. meningitidis* isolates as serogroup B, type 4, subtype P1.12-1,16-183. A review of the records revealed that a contact of patient 1 (who had stayed overnight) had a relative outside of the household who had also been admitted to a hospital. After further investigation, that relative was identified as patient 2. It was then ascertained that this close contact of patient 1 was visiting patient 2 regularly but not staying overnight.

In accordance with UK national public health guidance (*2*), the 3 household contacts were provided antimicrobial chemoprophylaxis and information about IMD. Once the link between the 2 cases

Author affiliations: UK Health Security Agency East of England, Harlow, UK (E. Loud, D.S. Edwards, E. Knapper, L. Emmett); UK Health Security Agency Meningococcal Reference Unit, Manchester, UK (S.A. Clark); St. George's University of London, London, UK (S. Ladhani); UK Health Security Agency, London (S. Ladhani, H. Campbell)

DOI: https://doi.org/10.3201/eid3005.231714

was known, an incident management team meeting was convened, involving the health protection team, MRU, local authority public health team, and National Health Service Integrated Care Board members. A decision was made to offer chemoprophylaxis to 3 additional contacts outside of the immediate household. A total of 9 contacts, including the 6 who received prophylaxis and 3 extended family members, were offered the 4CMenB vaccine (Bexsero, https://www.bexsero.com); vaccinations were arranged with each person's general practitioner. The hospital infection prevention control and microbiology teams were also involved in managing the risks to exposed healthcare workers; some of the healthcare team members involved in the intubation of patient 1 were prescribed antimicrobial chemoprophylaxis.

The MRU identified the isolates from cases 1 and 2 as sequence type (ST) 485 (clonal complex 41/44). Core genome multilocus sequence typing revealed that the 2 isolates clustered closely together in a monophyletic group that had only 4 allelic differences (out of 1422 core genes) between them (Figure) (*3*). Genotypic analysis of meningococcal vaccine antigens showed the isolates harbored factor H binding protein peptide variant 4 and Neisserial heparin binding antigen peptide 2, both of which are expected to cross-react with 4CMenB antibodies (*4*). Therefore, the outbreak strain was predicted to be covered by the 4CMenB vaccine.

Recent cases of ST485 infection have occurred in Yorkshire and the Humber, the Midlands, East of England, and London. An analysis of MenB strain distribution revealed an increasing proportion of MenB cases caused by ST485 since 2010; ST485 was the most common ST among MenB cases in England in 2022 (*5*). An earlier case (designated case-patient 0) within the same area of East of England in autumn 2022 was also caused by MenB ST485. Case-patient 0 was a 92-year-old woman who sought care in late 2022 at the emergency department of the same hospital that admitted patients 1 and 2 (4 months before patient 1's symptoms began). She had a 3-day history of diarrhea, vomiting, and confusion and died on the same day that she sought care. Her blood culture test was positive for *N. meningitidis*. She had no household contacts or recent travel history. She shared a general practitioner surgery and postal code district with patient 2, but no known contact occurred between the 2 patients. Core genome multilocus sequence typing analysis of the case 0 isolate showed that it clustered closely with the isolates from cases 1 and 2, suggesting that the ST485 strain had persisted in the local area and later caused IMD in patients 1 and 2.

Conclusions

We identified an unusual cluster of MenB IMD in older adults within a small geographic area (<10 miles across with <20,000 persons) over a 6-month period after an alert from the MRU. Our findings highlight a role for genomic surveillance in supporting standard public health measures and contact tracing processes and enhancing investigations. Furthermore, clinical inquiry and good record keeping during the initial contact tracing process were crucial for identifying the epidemiologic connection between 2 seemingly unrelated cases.

Another unusual feature of this cluster was the patients' ages. In England, a rapid decline in IMD (along with other infectious diseases) was seen during the COVID-19 pandemic. After removing COVID-19 mitigations in July 2021, an increase in MenB was initially observed among teenagers and young adults, which subsequently expanded across all age groups (S. Clark et al., unpub. data, https://doi.org/10.2139/ssrn.3998164). MenB is rare in older adults, but this cluster indicates community transmission of an expanding MenB strain and the ongoing vulnerability of older adults to such strains. Because of increasing vaccination of children and adolescents

Table. Initial timelines for 2 cases of serogroup B invasive meningococcal disease in older adults identified by genomic surveillance, England, 2022–2023*

Day	Case 1	Case 2
0	Symptom onset	NA
5	Admitted to hospital	NA
6	NA	Symptom onset
7	Case was reported to health protection team; 2 contacts were identified for prophylaxis.	Admitted to hospital
10	NA	Case was reported to health protection team; 1 contact was identified for prophylaxis.
16	UKHSA Meningococcal Reference Unit flagged possible link between cases from 2 isolates.	
17	Epidemiologic link was confirmed, cluster declared, and local partners were alerted. Initial incident management team meeting was held, where cluster was risk assessed and cases were reexamined.	
20	Decision was made to offer vaccination to 9 contacts.	
21	Contacts were informed and vaccinations were arranged with primary care personnel.	

*NA, not applicable; UKHSA, UK Health Security Agency.

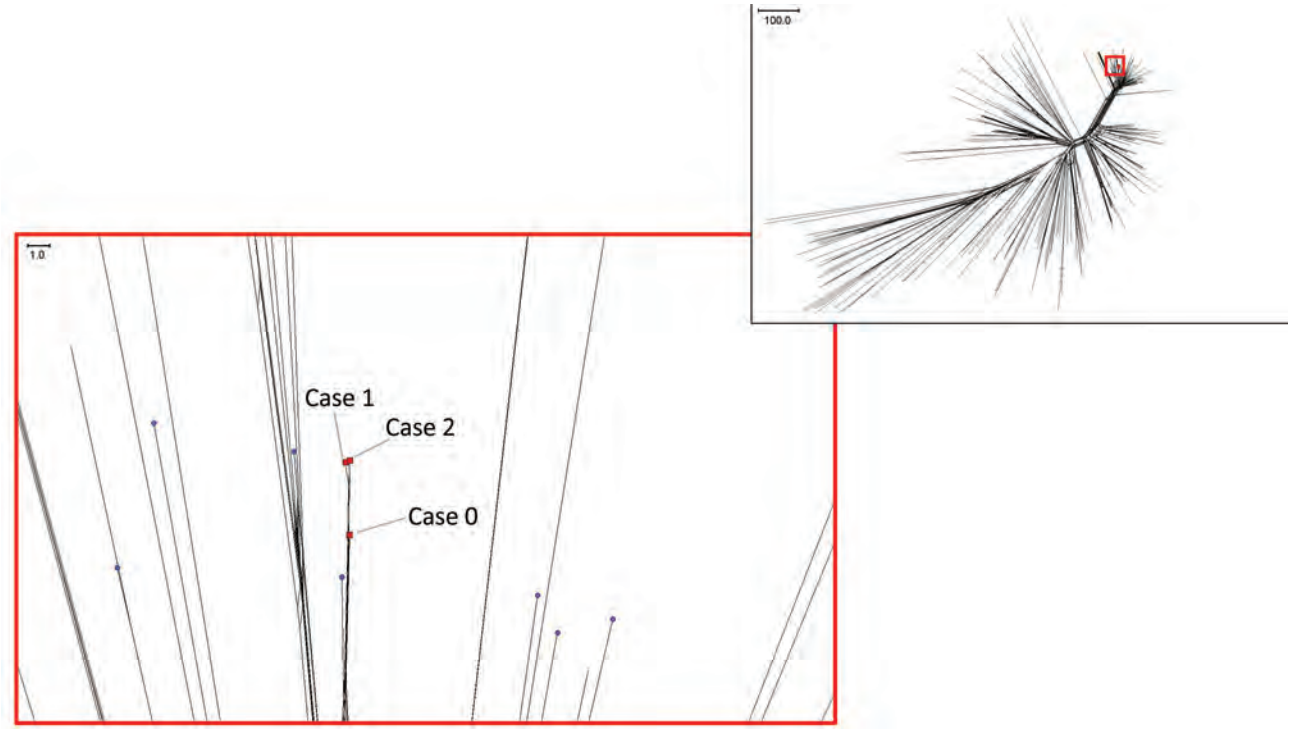

Figure. Phylogenetic analysis of *Neisseria meningitidis* isolates in study of serogroup B invasive meningococcal disease in older adults identified by genomic surveillance, England, 2022–2023. Inset indicates the entire phylogenetic tree generated by using the neighbor-net algorithm. Red box indicates the location of the 3 *N. meningitidis* isolates from East of England within the tree. Core genome sequences were compared for *N. meningitidis* clonal complex 41/44 isolates from England, including the 3 East of England isolates, collected during 2016–2023 (n = 356). Comparisons were made by using the Genome Comparator tool (https://www.pubmlst.org). The 3 *N. meningitidis* isolates from East of England clustered closely together in a monophyletic group. Scale bars indicate nucleotide substitutions per site.

against IMD in the UK (*6*,*7*), the proportion of cases in older adults will likely grow, a shift that has also been observed across Europe and North America (*8*). This shift is concerning because of the comparatively high case-fatality rates within this older age group (*9*).

Unlike many polysaccharide-conjugated meningococcal vaccines, such as MenC/ACWY, currently licensed MenB vaccines are protein based and do not affect carriage and, therefore, do not confer herd immunity (*10*). Protection against MenB can only be derived from individual vaccination, which in the United Kingdom is only offered to infants born since September 1, 2015 (*11*). Consequently, enhanced strain characterization and surveillance is crucial to provide vaccine strain coverage predictions, which inform decisions on MenB vaccine use during outbreak scenarios (*12*).

In conclusion, although an adolescent MenACWY conjugate vaccine program protects all age groups through herd immunity (*13*), no such protection is conferred for MenB, which could lead to a larger proportion of MenB cases in older adults in the longer term. Limited data exists on meningococcal carriage levels and transmission dynamics in older adults (*14*). Effective strategies, such as genomic surveillance, are needed to prevent and control clusters and outbreaks of *N. meningitidis* infections in this unprotected group of older adults.

About the Author

Ms. Loud is a public health registrar based in East of England and worked as part of the regional health protection team and at the screening and immunization department. Her research interests include vaccination strategies and climate change.

References

1. UK Health Security Agency. Invasive meningococcal disease in England: annual laboratory confirmed reports for epidemiological year 2021 to 2022. June 1, 2023 [cited 2023 Dec 15]. https://www.gov.uk/government/publications/meningococcal-disease-laboratory-confirmed-cases-in-england-in-2021-to-2022/invasive-meningococcal-disease-in-england-annual-laboratory-confirmed-reports-for-epidemiological-year-2021-to-2022

2. Public Health England. Meningococcal disease: guidance on public health management. August 6, 2019 [cited 2 023 Dec 15]. https://www.gov.uk/government/publications/meningococcal-disease-guidance-on-public-health-management
3. Bratcher HB, Corton C, Jolley KA, Parkhill J, Maiden MCJ. A gene-by-gene population genomics platform: de novo assembly, annotation and genealogical analysis of 108 representative *Neisseria meningitidis* genomes. BMC Genomics. 2014;15:1138. https://doi.org/10.1186/1471-2164-15-1138
4. Muzzi A, Brozzi A, Serino L, Bodini M, Abad R, Caugant D, et al. Genetic Meningococcal Antigen Typing System (gMATS): a genotyping tool that predicts 4CMenB strain coverage worldwide. Vaccine. 2019;37:991–1000. https://doi.org/10.1016/j.vaccine.2018.12.061
5. Clark S, Lucidarme J, Lekshmi A, Walsh L, Willerton L, Walker A, et al. The expansion of a group B invasive meningococcal ST-485 (ST-41/44 clonal complex) strain in England: 2010–2022. In: Abstracts of the 16th EMGM Congress, European Meningococcal and Haemophilus Disease Society; Dubrovnik, Croatia; 2023 May 29–June 1. Abstract OC43. Croatia: The European Meningococcal and Haemophilus Disease Society; 2023.
6. Parikh SR, Andrews NJ, Beebeejaun K, Campbell H, Ribeiro S, Ward C, et al. Effectiveness and impact of a reduced infant schedule of 4CMenB vaccine against group B meningococcal disease in England: a national observational cohort study. Lancet. 2016;388:2775–82. https://doi.org/10.1016/S0140-6736(16)31921-3
7. Campbell H, Andrews N, Parikh SR, White J, Edelstein M, Bai X, et al. Impact of an adolescent meningococcal ACWY immunisation programme to control a national outbreak of group W meningococcal disease in England: a national surveillance and modelling study. Lancet Child Adolesc Health. 2022;6:96–105. https://doi.org/10.1016/S2352-4642(21)00335-7
8. Guedes S, Bertrand-Gerentes I, Evans K, Coste F, Oster P. Invasive meningococcal disease in older adults in North America and Europe: is this the time for action? A review of the literature. BMC Public Health. 2022;22:380. https://doi.org/10.1186/s12889-022-12795-9
9. Guedes S, Bricout H, Langevin E, Tong S, Bertrand-Gerentes I. Epidemiology of invasive meningococcal disease and sequelae in the United Kingdom during the period 2008 to 2017—a secondary database analysis. BMC Public Health. 2022;22:521. https://doi.org/10.1186/s12889-022-12933-3
10. Borrow R, Taha M-K, Giuliani MM, Pizza M, Banzhoff A, Bekkat-Berkani R. Methods to evaluate serogroup B meningococcal vaccines: from predictions to real-world evidence. J Infect. 2020;81:862–72. https://doi.org/10.1016/j.jinf.2020.07.034
11. Public Health England. MenB vaccination: introduction from September 2015. June 22, 2015 [cited 2023 Dec 15]. https://www.gov.uk/government/publications/menb-vaccination-introduction-from-1-september-2015
12. Clark SA, Lucidarme J, Angel G, Lekshmi A, Morales-Aza B, Willerton L, et al. Outbreak strain characterisation and pharyngeal carriage detection following a protracted group B meningococcal outbreak in adolescents in South-West England. Sci Rep. 2019;9:9990. https://doi.org/10.1038/s41598-019-46483-3
13. Carr JP, MacLennan JM, Plested E, Bratcher HB, Harrison OB, Aley PK, et al.; UKMenCar4 and 'Be on the TEAM' Study Collaborators. Impact of meningococcal ACWY conjugate vaccines on pharyngeal carriage in adolescents: evidence for herd protection from the UK MenACWY programme. Clin Microbiol Infect. 2022;28:1649.e1–e8. https://doi.org/10.1016/j.cmi.2022.07.004
14. Lawler J, Lucidarme J, Parikh S, Smith L, Campbell H, Borrow R, et al. Suspected cluster of *Neisseria meningitidis* W invasive disease in an elderly care home: do new laboratory methods aid public health action? United Kingdom, 2015. Euro Surveill. 2019;24:1900070. https://doi.org/10.2807/1560-7917.ES.2019.24.23.1900070

Address for correspondence: Emily Loud, UK Health Security Agency, The Mildenhall Hub, Sheldrick Way, Mildenhall, Bury St Edmunds, Suffolk IP28 7JX, UK; email: emily.loud@ukhsa.gov.uk

Molecular Epidemiology of Mayaro Virus among Febrile Patients, Roraima State, Brazil, 2018–2021

Julia Forato, Cássio A. Meira, Ingra M. Claro, Mariene R. Amorim, Gabriela F. de Souza, Stefanie P. Muraro, Daniel A. Toledo-Teixeira, Miguel F. Dias, Cátia A. R. Meneses, Rodrigo N. Angerami, Pritesh Lalwani, Scott C. Weaver, Ester C. Sabino, Nuno R. Faria, William M. de Souza,[1] Fabiana Granja,[1] José Luiz Proenca-Modena[1]

We detected Mayaro virus (MAYV) in 3.4% (28/822) of febrile patients tested during 2018–2021 from Roraima State, Brazil. We also isolated MAYV strains and confirmed that these cases were caused by genotype D. Improved surveillance is needed to better determine the burden of MAYV in the Amazon Region.

Mayaro virus (MAYV) is an endemic and neglected mosquitoborne alphavirus that causes acute and chronic debilitating arthritogenic disease in Latin America and the Caribbean (*1*). MAYV infection can cause fever, rash, and arthralgia that can persist for over a year in some patients (2). MAYV is transmitted in its enzootic cycle mainly by sylvatic *Haemagogus janthinomys* mosquitoes among nonhuman primates and other mammals, which can lead to spillover to humans (2). However, some experimental studies suggest that MAYV could establish a human-amplified cycle in urban environments when transmitted by *Aedes aegypti* and *Ae. albopictus* mosquitoes, which could lead to a larger public health threat (*3*,*4*). No specific antiviral drugs or vaccines are available to treat or prevent MAYV infection.

MAYV infections have been reported in Central and South America since the 1950s (*1*,*2*). However, reports of active circulation of MAYV in human populations remain scarce, even in MAYV-endemic areas. We conducted a molecular epidemiology study to investigate the active circulation of MAYV in patients with acute febrile illness during 2018–2021 from the Amazon Region in Roraima State, Brazil.

The Study

During December 2018–December 2021, we collected serum samples from 822 patients with acute febrile illness (up to 10 days from onset of symptoms) seeking care at primary health care units across 11 of the 15 municipalities of Roraima State, North Region, Brazil. We collected patient information, such as age, sex, occupation, sample collection data, date of symptom onset, and symptoms, from medical records. We conducted all procedures in accordance with ethics committee approval from the Federal University of Roraima (approval no. 2.881.239) and the University of Campinas (approval no. 5.625.875).

Next, we extracted RNA from all serum samples and performed real-time reverse transcription PCR (rRT-PCR) to detect RNA of MAYV, chikungunya virus (CHIKV), Zika virus, dengue virus (DENV), and Oropouche virus. We also carried out viral isolation in African green monkey kidney cells (Vero CCL-81) with some positive samples. Then, we performed sequencing by using the nanopore approach (*5*) and conducted maximum-likelihood phylogenetic

Author affiliations: Universidade Estadual de Campinas, Campinas, São Paulo, Brazil (J. Forato, M.R. Amorim, D.A. Toledo-Teixeira, R.N. Angerami, F. Granja, J.L. Proenca-Modena); Laboratório Central de Saúde Pública de Roraima, Boa Vista, Brazil (C.A. Meira, C.A.R. Meneses); University of São Paulo, São Paulo (I.M. Claro, E.C. Sabino, N.R. Faria); Imperial College London, London, UK (I.M. Claro, N.R. Faria); University of Kentucky, Lexington, Kentucky, USA (W.M. de Souza); Global Virus Network, Baltimore, Maryland, USA (W.M. de Souza, S.C. Weaver); Federal University of Roraima, Boa Vista (M.F. Dias, F. Granja); Fiocruz Amazônia, Manaus, Brazil (P. Lalwani); University of Texas Medical Branch, Galveston, Texas, USA (S.C. Weaver); University of Oxford, Oxford, UK (N.R. Faria)

DOI: https://doi.org/10.3201/eid3005.231406

[1]These senior authors contributed equally to this article.

inferences(Appendix,https://wwwnc.cdc.gov/EID/article/30/5/23-1406-App1.pdf).

Of 822 patients tested by rRT-PCR, 190 (23.1%) were positive for ≥1 arbovirus (Appendix Figure 1). We detected MAYV RNA in 28 (3%) patients, including 15 (54%) patients from Boa Vista, the most populous municipality in Roraima State (Appendix Figure 2). Most (19 [68%]) MAYV cases occurred during January–July 2021. Among patients with rRT-PCR–confirmed MAYV, median age was 31 years (interquartile range 26–43 years), and the male-to-female ratio was 1:5. The most common signs and symptoms reported were fever and myalgia, both of which were reported in 23 (82%) MAYV cases. Arthralgia was reported in 6 (21%) and rash in 3 (11%) cases. The median time between symptom onset and sample collection interval was 3 days (interquartile range 1–4 days). Three (11%) of the MAYV cases were in fishermen who had direct contact with wildlife.

Next, we isolated 2 MAYV strains in Vero CCL-81 cells, and we observed cytopathic effects (CPE) ≈30 hours after inoculation. Then, we performed 3 blind passages and confirmed the viral isolation of 2 strains by using rRT-PCR to detect viral RNA in the supernatant of culture cell passages exhibiting CPE. We observed decreased cycle threshold values representing increased viral loads between passages (Appendix Figure 3). In addition, we confirmed MAYV isolates by using immunofluorescent staining (Appendix Figure 4). Subsequently, we used nanopore sequencing to generate the nearly complete coding sequencing of 3 MAYV strains (2 isolates and 1 directly from a clinical sample). We obtained >90% of MAYV genomes with a mean depth of coverage of ≥20-folds per nucleotide. We submitted sequences to GenBank (accession nos. PP339762–PP339764).

The maximum-likelihood phylogenetic analysis showed that the MAYV strains circulating in Roraima

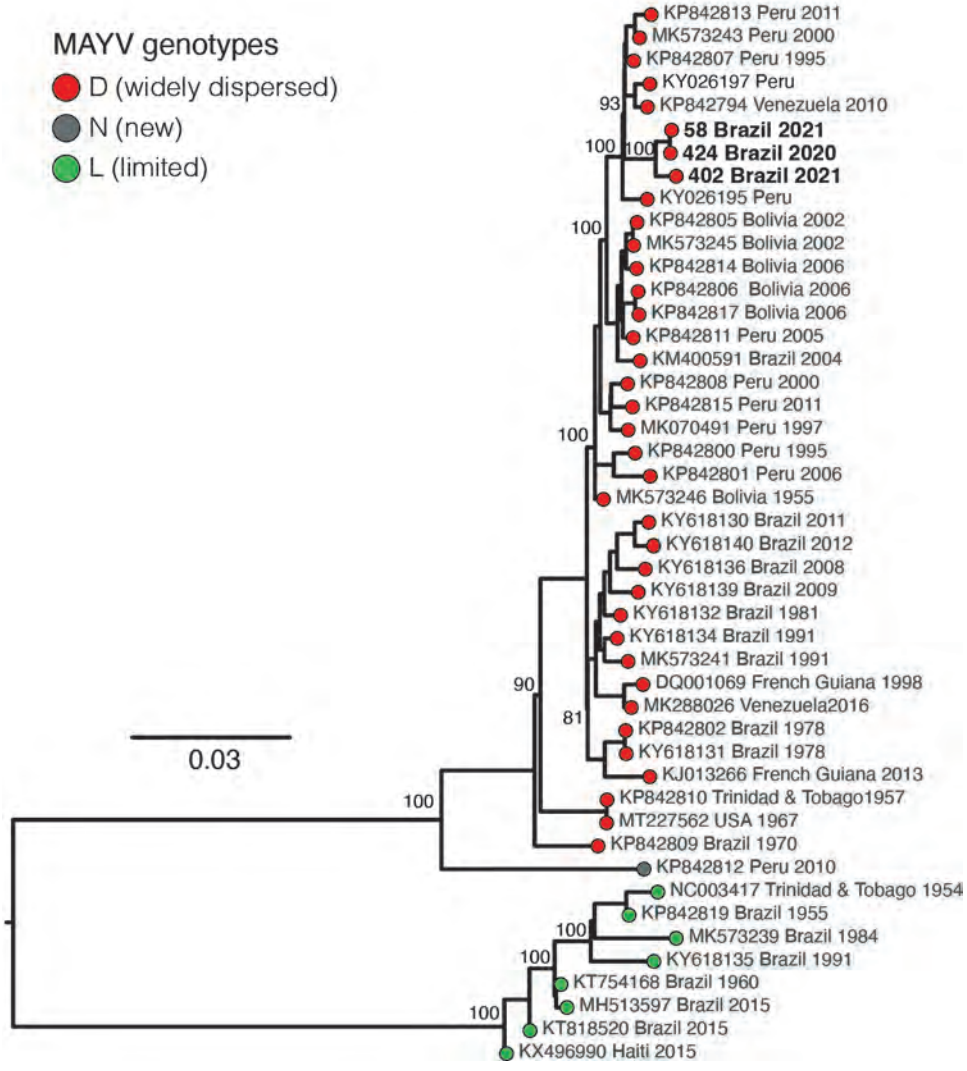

Figure. Maximum-likelihood phylogenetic tree of Mayaro virus, Roraima State, Brazil, 2018–2021. Phylogeny is midpoint rooted for clarity of presentation. Bold text indicates 3 new Mayaro virus genomes. Bootstrap values based on 1,000 replicates are shown on principal nodes. Scale bar indicates the evolutionary distance of substitutions per nucleotide site.

State in 2021 belong to genotype D (widely dispersed) (Figure). We identified no evidence of recombination in MAYV strains from Roraima State. The novel MAYV strains shared 98.6%–98.9% nucleotide sequence identity with other genotype D strains. The new strains formed a distinct and highly supported monophyletic clade (bootstrap support 100%) and clustered with strains sampled in Peru and Venezuela during 1995–2010.

Finally, we also detected CHIKV RNA in 16 (2%) and DENV in 146 (17.8%) patients tested (Appendix Figures 1, 5). This number includes 63 patients with DENV serotype 1 and 89 patients with DENV serotype 2. Of those, we identified 6 (1%) cases with co-detection of DENV-1 and DENV-2. We detected most (13 [81%]) chikungunya cases in patients with febrile illness during January–July 2021, overlapping with the peak of detection for MAYV. Conversely, dengue cases were predominantly confirmed (110 [75.3%]) in patients with fever during July 2019–January 2020. All samples tested were negative for RNA of Zika virus, Oropouche viruses, and DENV serotypes 3 and 4.

Conclusions

This study reports the active MAYV circulation in humans during the concurrent chikungunya and dengue epidemic in Roraima State, Brazil. We found that the MAYV infection cases were caused by genotype D, suggesting that this widespread genotype continued to circulate in the Amazon Region for ≥60 years. In addition, this same genotype has been detected in outbreaks in Venezuela (*6*,*7*), which, like Guyana, shares borders with Brazil through Roraima State.

Arthralgia has been described as a major clinical characteristic of human MAYV infection (*8*). However, only 21% of MAYV-positive patients reported arthralgia in this study. Our data suggest that laboratory diagnosis of MAYV should be considered for patients with febrile illness in MAYV-endemic areas, even in the absence of clinical characteristics typically associated with MAYV infection. We also found that young adults and men account for most of the MAYV infection cases, probably because of occupational exposure (*9*). Persons who work in forest environments (e.g., in mining, logging, and fishing) could be a bridge to facilitate the eventual introduction and establishment of MAYV transmission in urban settings (*7*). Moreover, the implementation of augmented molecular and genomic surveillance in human and urban vector populations (i.e., *Ae. aegypti* and *Ae. albopictus* mosquitoes) will be critical to monitor the potential establishment of MAYV in a human-amplified transmission cycle.

One limitation of our study is that we focused on active MAYV infections by using a molecular approach; however, further serologic studies are needed to determine the fraction of the population previously infected. Serologic studies can shed light on the potential effect of cross-protection between CHIKV and MAYV in the Amazon Region (*10*). Moreover, the higher percentage (76.9%) of samples negative for the arboviruses tested shows that the metagenomic approach could be useful in further studies to determine the landscape of etiologic agents linked with febrile illness in the triple border region (i.e., Brazil, Guyana, and Venezuela). Further, we were unable to determine whether MAYV infections occurred in urban or forest settings, and we have no follow-up information on MAYV cases.

In conclusion, our study identified the active co-circulation of MAYV, DENV, and CHIKV in patients with febrile illness in Roraima State, Brazil. These findings underscore the critical need for continuous laboratory diagnosis for MAYV to determine the prevalence of MAYV in the Amazon Region and the potential changes associated with urbanization.

Acknowledgments

We thank Clarice Arns for her technical support and Rafael Elias Marques for providing the Mayaro and dengue virus isolates.

This study was supported by grants from São Paulo Research Foundation (grant nos. 2016/00194-8, 2020/04558-0, and 2022/10442-0). J.F. was supported by Coordination for the Improvement of Higher Education Personnel scholarships (grant no. 309971/2023-3). W.M.d.S. was supported by a Global Virus Network fellowship, Burroughs Wellcome Fund (grant no. 1022448), and Wellcome Trust–Digital Technology Development award (climate sensitive infectious disease modelling, under grant no. 226075/Z/22/Z). I.M.C. was supported by São Paulo Research Foundation (grant no. 2018/17176-8) and the Bill and Melinda Gates Foundation (grant no. INV-034540). S.C.W. was supported by the National Institutes of Health (grant nos. AI12094, U01AI151801, and AI121452). J.L.P.-M. is supported by Conselho Nacional de Desenvolvimento Científico e Tecnológico (grant no. 305628/2020-8). This project was supported by the Medical Research Council and São Paulo Research Foundation Centre for Arbovirus Discovery, Diagnosis, Genomics and Epidemiology partnership award (grant nos. MR/S0195/1 and FAPESP 2018/14389-0).

About the Author

Ms. Forato is a master's candidate at the Department of Genetics, Evolution, Microbiology, and Immunology at the University of Campinas, São Paulo, Brazil. Her research interests include epidemiologic surveillance of emerging viruses with a focus on arboviruses.

References

1. Caicedo EY, Charniga K, Rueda A, Dorigatti I, Mendez Y, Hamlet A, et al. The epidemiology of Mayaro virus in the Americas: a systematic review and key parameter estimates for o utbreak modelling. PLoS Negl Trop Dis. 2021;15:e0009418. https://doi.org/10.1371/journal.pntd.0009418
2. Hoch AL, Peterson NE, LeDuc JW, Pinheiro FP. An outbreak of Mayaro virus disease in Belterra, Brazil. III. Entomological and ecological studies. Am J Trop Med Hyg. 1981;30:689–98. https://doi.org/10.4269/ajtmh.1981.30.689
3. Fernández D, Yun R, Zhou J, Parise PL, Mosso-González C, Villasante-Tezanos A, et al. Differential susceptibility of *Aedes aegypti* and *Aedes albopictus* mosquitoes to infection by Mayaro virus strains. Am J Trop Med Hyg. 2023;109:115–22. https://doi.org/10.4269/ajtmh.22-0777
4. Weaver SC. Urbanization and geographic expansion of zoonotic arboviral diseases: mechanisms and potential strategies for prevention. Trends Microbiol. 2013;21:360–3. https://doi.org/10.1016/j.tim.2013.03.003
5. Claro IM, Ramundo MS, Coletti TM, da Silva CAM, Valenca IN, Candido DS, et al. Rapid viral metagenomics using SMART-9N amplification and nanopore sequencing. Wellcome Open Res. 2023;6:241. https://doi.org/10.12688/wellcomeopenres.17170.2
6. Auguste AJ, Liria J, Forrester NL, Giambalvo D, Moncada M, Long KC, et al. Evolutionary and ecological characterization of Mayaro virus strains isolated during an outbreak, Venezuela, 2010. Emerg Infect Dis. 2015;21:1742–50. https://doi.org/10.3201/eid2110.141660
7. Guégan JF, Ayouba A, Cappelle J, De Thoisy B. Forests and emerging infectious diseases: unleashing the beast within [cited 2023 Aug 17]. https://iopscience.iop.org/article/10.1088/1748-9326/ab8dd7
8. Halsey ES, Siles C, Guevara C, Vilcarromero S, Jhonston EJ, Ramal C, et al. Mayaro virus infection, Amazon Basin region, Peru, 2010-2013. Emerg Infect Dis. 2013;19:1839–42. https://doi.org/10.3201/eid1911.130777
9. Forshey BM, Guevara C, Laguna-Torres VA, Cespedes M, Vargas J, Gianella A, et al.; NMRCD Febrile Surveillance Working Group. Arboviral etiologies of acute febrile illnesses in western South America, 2000–2007. PLoS Negl Trop Dis. 2010;4:e787. https://doi.org/10.1371/journal.pntd.0000787
10. Fumagalli MJ, de Souza WM, de Castro-Jorge LA, de Carvalho RVH, Castro ÍA, de Almeida LGN, et al. Chikungunya virus exposure partially cross-protects against Mayaro virus infection in mice. J Virol. 2021;95:e0112221. https://doi.org/10.1128/JVI.01122-21

Address for correspondence: Julia Forato, Universidade Estadual de Campinas, Rua Monteiro Lobato, No. 255, 13.083-862, Campinas, São Paulo, Brazil; email: foratojulia@gmail.com

Seasonal Patterns of Mpox Index Cases, Africa, 1970–2021

Camille Besombes, Festus Mbrenga, Ella Gonofio, Christian Malaka, Cedric-Stephane Bationo, Jean Gaudart, Manon Curaudeau, Alexandre Hassanin, Antoine Gessain, Romain Duda, Tamara Giles Vernick, Arnaud Fontanet, Emmanuel Nakouné, Jordi Landier

Across 133 confirmed mpox zoonotic index cases reported during 1970–2021 in Africa, cases occurred year-round near the equator, where climate is consistent. However, in tropical regions of the northern hemisphere under a dry/wet season cycle, cases occurred seasonally. Our findings further support the seasonality of mpox zoonotic transmission risk.

Mpox, caused by monkeypox virus (MPXV), remains a neglected tropical zoonotic disease of forested Central and West Africa (*1*). Mpox epidemiology is poorly understood, and the MPXV animal reservoir remains unknown (*1*). Risk factors for zoonotic infection reportedly include direct or indirect contact with wildlife among subsistence activities in forests (*2*–*4*). Those characteristics may have evolved in West Africa because Nigeria reported sustained interhuman transmission of MPXV clade II in 2017, which led to the emergence of clade IIb and the global outbreak declared in May 2022 (*5*). In Central Africa at the time of our study, however, mpox cases remain typically linked to short chains of interhuman transmission after zoonotic spillover (*1*).

After 1990, reported case numbers increased sharply for Congo Basin/clade I, then a sharp increase in West African/clade II began in 2000 (*1*). The lack of systematic surveillance hinders investigative understanding of long-term temporal trends (*1*) and potential seasonality. Available index case time series suggested seasonal changes in risk and high-risk periods: outbreaks occurred predominantly in September in the Central African Republic (CAR) (*6*), and during June–August in different regions of Democratic Republic of the Congo (DRC) (*7*–*11*). We analyzed potential zoonotic transmission seasonality from reported mpox index cases in Africa during 1970–2021.

The Study

We systematically analyzed peer-reviewed and gray literature reporting mpox (formerly monkeypox) index cases from zoonotic origin in Africa during 1970–2021. We extracted index case geographic localization and occurrence dates for temporal and spatial analysis. We used the PubMed query ("1970"[Date-Publication]: "2021/12/31"[Date-Publication]) AND monkeypox AND Africa (Appendix Figure 1, https://wwwnc.cdc.gov/eid/article/30/5/23-0293-App1.pdf).

We only included index cases defined as the first reported case presumed to result from zoonotic transmission in an epidemiologic outbreak investigation. We excluded cases outside Africa and those related to secondary interhuman transmission. We also excluded cases without PCR, viral isolation or culture, or electron microscopy confirmation; and cases without onset month or geographic localization (Appendix Figure 2).

We defined index sites as locations with ≥1 index case. We extracted remotely sensed meteorologic (precipitation, daytime and nighttime temperature), topographic (altitude and slope), land use–land cover data, and fire occurrence data using a 10-km radius buffer zone around each site (Appendix Table 1).

We conducted unsupervised clustering to regroup sites into climate and seasonality (hereafter climate), landscape, and environment profiles. For climate profiles, we included the average

Author affiliations: Institut Pasteur, Paris, France (C. Besombes, A. Gessain, R. Duda, T. Giles Vernick, A. Fontanet); Institut Pasteur de Bangui, Bangui, Central African Republic (F. Mbrenga, E. Gonofio, C. Malaka, E. Nakouné); Aix Marseille Univ, Marseille, France (C.-S. Bationo, J. Gaudart); Institut de Recherche pour le Développement, Marseille (J. Landier); National Museum of Natural History, Paris (M. Curaudeau, A. Hassanin); Conservatoire National des Arts et métiers, Paris (A. Fontanet)

DOI: http://doi.org/10.3201/eid3005.230293

cumulative rainfall, daytime and nighttime temperature, and fire index values (Appendix Table 1) for each month in a principal component analysis. We performed hierarchical clustering on principal components, including 99% of dataset inertia, by using R version 4.3 (The R Foundation for Statistical Computing, https://www.r-project.org) and FactoMineR package (https://cran.r-project.org/web/packages/FactoMineR/index.html). We grouped sites by maximizing within-group similarity and between-groups difference. Following the same approach, we used variables describing the percentage of each buffer occupied by each land use–land cover class (e.g., evergreen closed forest, cropland) and topographic variables to obtain landscape profiles. Finally, we combined the 2 sets of variables to generate combined environment profiles (Appendix).

Table. Location and case characteristics in a study of seasonal patterns of mpox index cases, Africa, 1970–2021

Variable	No. (%) cases, n = 133
Country	
Cameroon	7 (5.3)
Central African Republic	44 (33)
Democratic Republic of the Congo	58 (44)
Gabon	2 (1.5)
Ivory Coast	1 (0.8)
Liberia	5 (3.8)
Nigeria	3 (2.3)
Republic of Congo	8 (6.0)
Sierra Leone	4 (3.0)
South Sudan	1 (0.8)
Timeframe	
1970–1980	35 (26)
1981–1990	8 (6.0)
1991–2000	5 (3.8)
2001–2010	16 (12)
2011–2021	69 (52)
Strain	
Clade I	115 (86)
Clade II	17 (13)
Unknown	1 (0.8)
Outbreak month	
January	15 (11)
February	20 (15)
March	12 (9.0)
April	6 (4.5)
May	7 (5.3)
June	5 (3.8)
July	3 (2.3)
August	14 (11)
September	16 (12)
October	9 (6.8)
November	14 (11)
December	12 (9.0)
Climate or seasonality profile	
Northern hot, wet-dry	23 (17)
Northern cool, wet-dry	47 (35)
Equatorial cool	44 (33)
Southern hot, wet-dry	14 (11)
Other	5 (3.8)
Landscape profile	
Open forest + river or wetlands	23 (17)
Evergreen closed forest	68 (51)
Deciduous forest, closed or open	26 (20)
Grassland + hills	11 (8.3)
Other	5 (3.8)
Combined environmental profile	
Evergreen closed forest + warm night	80 (60)
Evergreen open forest + high precipitation	10 (7.5)
Southern tropical, grassland + hills	14 (11)
Deciduous forest + hot month of January	24 (18)
Other	5 (3.8)

We used the Kruskall-Wallis test to first compare the distribution of latitudes by month of index case occurrence and then to compare months of occurrence according to site environmental characteristics defined by each profile. Using months as a quantitative variable enabled comparison of periods of the year rather than specific months. Sensitivity analyses determined whether the association remained when restricting the analysis to clade II and to recent (2001–2021) cases (Appendix).

We identified 208 index cases: 145 reported from 53 peer-reviewed articles, 26 from 35 gray literature sources, and 37 from CAR national surveillance data (Appendix Figure 2). After exclusion criteria, we retained 133 index cases from 113 sites; 64% were reported from 2000 onward (Appendix Figure 2). Clade I represented 86% of index cases, and clade II represented 13%. DRC accounted for 44% of index cases, and CAR accounted for 33% (Table).

Index cases occurred at a median latitude of 3.44°N (range: −5.87 to 9.53). Index cases latitudes differed significantly across months ($p = 0.0354$). During January–July (April excluded), index cases mostly occurred <3.44°N, whereas during August–December, most cases occurred >3.44°N (Figure 1).

We excluded 4 index sites at high altitude (>1,000 m) and 1 Sahelian index site because rare mpox occurrence prevented seasonality characterization in those settings. The other 108 sites clustered into 4 climate profiles. The equatorial cool profile had temperatures ≤30°C and day-night amplitude ≤10°C, rainfall across all months, and site latitudes ranging from −4.00° to 4.00°N (Figure 2, panels A, B). The northern cool wet-dry profile had similarly low temperatures and amplitude, a dry season during December–February, and site latitudes in the northern hemisphere. The northern hot wet-dry profile displayed temperatures >30°C during the hottest months, a marked dry season during November–March, and latitude sites in the northern hemisphere. The southern hot wet-dry profile had similarly hot temperatures, a dry season in May–August, and latitude sites in the southern hemisphere (Figure 2, panels A, B). Index cases occurred mostly in the equatorial cool (33%),

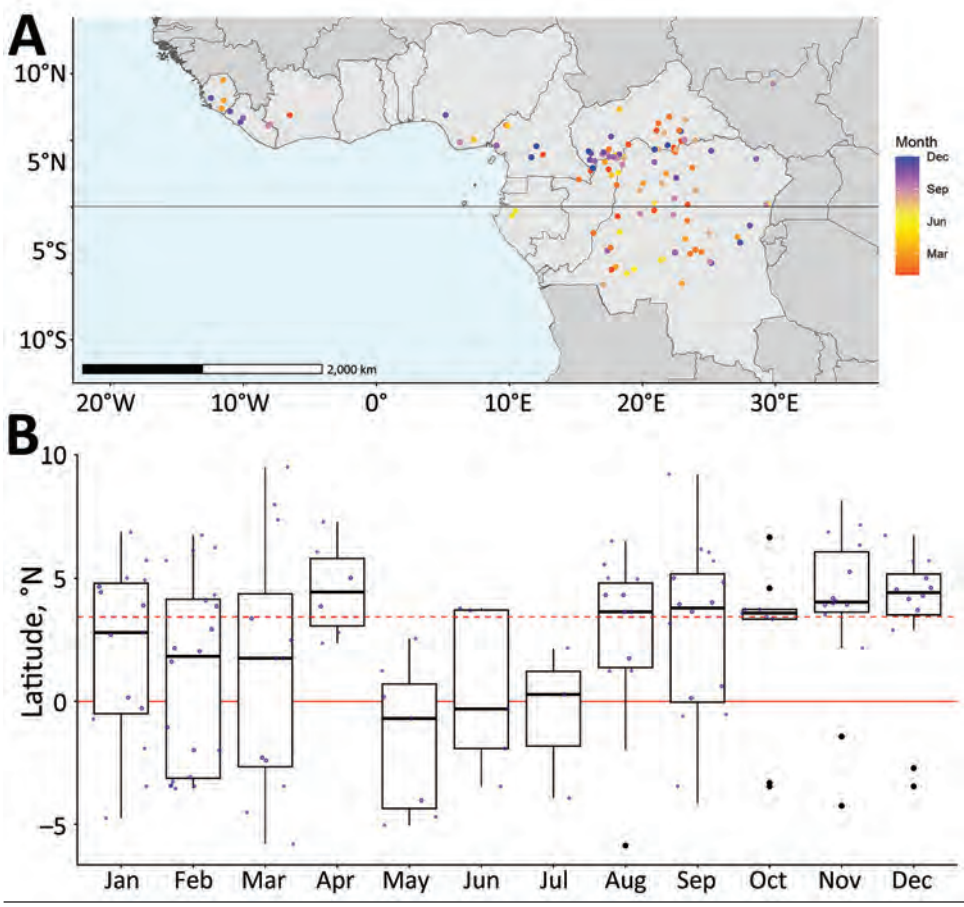

Figure 1. Distribution of cases in study of seasonal patterns of mpox index cases, Africa, 1970–2021. A) Mpox index case sites and month recorded; black horizontal line indicates equator. B) Boxplot of latitude of index case according to month of occurrence. Red dashed line indicates the median latitude of index cases; red solid line indicates the equator (latitude = 0). The thick black line indicates the median latitude, and the box tops and bottom indicate the upper quartile (above) and the lower quartile (below). Whiskers extend from upper quartile to upper quartile+1.5 interquartile range and extend down from lower quartile to lower quartile−1.5 interquartile range. Solid black dots signify outlying observations beyond whiskers range; blue circles identify all other observations.

northern cool wet-dry (35%), and northern hot wet-dry profiles (17%) (Table).

Cases occurred throughout the year in the equatorial cool profile and varied seasonally in the 2 northern wet-dry profiles; cases were nearly absent during April–July (Figure 2, panel C). Seasonality analysis remained inconclusive in the southern hot wet-dry profile, which had low sample size (n = 14). The distribution of index case months was significantly different between climate profiles (p = 0.004). That association persisted in sensitivity analyses (Appendix Tables 2, 3). Landscape and combined environment profiles had poorer association with the month of an index case (Appendix Tables 2, 3, Figures 4, 6, 7).

Conclusions

We showed that the monthly distribution of mpox index cases varied with latitude and was associated with specific climates across the main ecologic mpox niche, excluding high altitude and Sahelian sites. We identified high-risk and low-risk periods across the year in sites located in northern hemisphere climates with alternating dry and wet seasons (>50% of index cases analyzed).

A potential high-risk season occurred during August–March, spanning the last 3 months of the rainy season and all the dry season. That finding suggests complex drivers likely related to human and wildlife ecology. Various seasonal activities can increase human contact with wildlife. During the wet season, human populations settle in forest camps to collect edible caterpillars (*6*), a major source of protein and income (*12*). Hunting and trapping activities, generally conducted year round, intensify during the dry season (*10*). Likewise, dry season slash-and-burn activities tend to drive mammals, notably rodents, toward food resources in neighboring fields, resulting in closer contact with humans.

Multiple obstacles, including access to healthcare, hinder exhaustive mpox reporting from endemic regions. Therefore, this analysis relied on a limited series of well-characterized index cases. Such data and indirect approaches were used extensively to study mpox ecologic niches (*13*) and emerging diseases with similar surveillance gaps (e.g., Ebola virus) (*14*). Our conclusion that MPXV zoonotic transmission risk could be seasonal in regions under a dry-wet season cycle warrants further investigation.

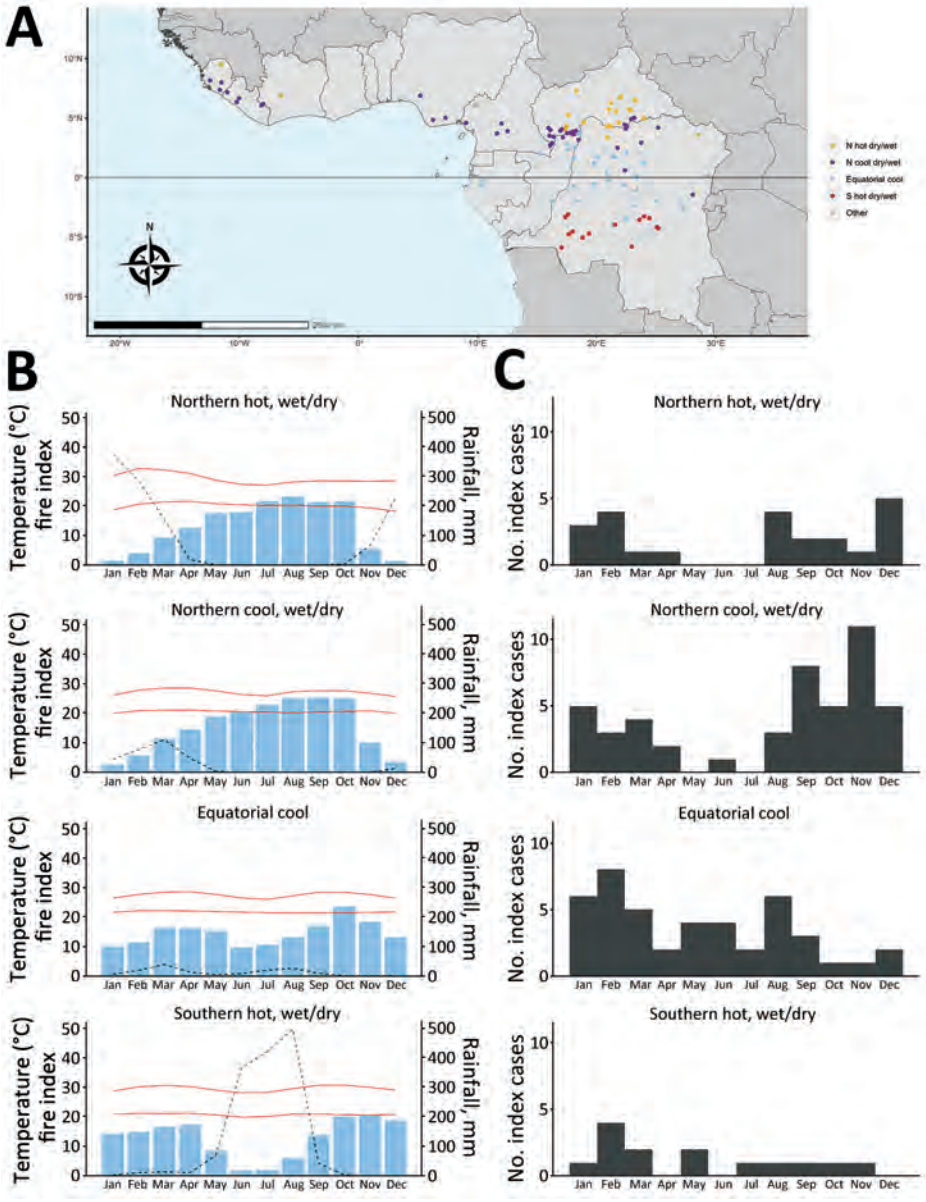

Figure 2. Seasonal distribution of mpox index cases according to the climate profile in Africa, 1970–2021. A) Climate/seasonal profile by site. B) Average monthly rainfall, temperature, and fire index (dotted line) for each climate/seasonal profile. C) Distribution of outbreak index cases by month for each climate/seasonal profile.

Ongoing climate and environmental changes could exacerbate potential underlying seasonal drivers of human MPXV exposure. Determining whether specific seasons or periods bring greater risk for human transmission can improve prevention and surveillance initiatives and contribute to identifying animal reservoirs. For this, a genuine One Health approach is crucial (*15*).

Acknowledgments

Financial support for this study was provided by the French Agence Nationale de Recherche (grant no.: ANR 2019 CE-35), the Projets Transversaux de Recherche (grant no.: PTR 218-19) fund from the Institut Pasteur Paris.

About the Author

Dr. Besombes is an infectious and tropical disease clinician and an epidemiologist, who works as a medical epidemiologist in the Emerging Diseases Epidemiology Unit at Institut Pasteur, Paris, France. Her primary research interests include the understanding of emerging infectious diseases and zoonotic diseases, through One Health and EcoHealth approaches.

References

1. Bunge EM, Hoet B, Chen L, Lienert F, Weidenthaler H, Baer LR, et al. The changing epidemiology of human monkeypox-A potential threat? A systematic review. PLoS Negl Trop Dis. 2022;16:e0010141. https://doi.org/10.1371/journal.pntd.0010141

2. Hutin YJ, Williams RJ, Malfait P, Pebody R, Loparev VN, Ropp SL, et al. Outbreak of human monkeypox, Democratic Republic of Congo, 1996 to 1997. Emerg Infect Dis. 2001;7:434–8. https://doi.org/10.3201/eid0703.017311
3. Patrono LV, Pléh K, Samuni L, Ulrich M, Röthemeier C, Sachse A, et al. Monkeypox virus emergence in wild chimpanzees reveals distinct clinical outcomes and viral diversity. Nat Microbiol. 2020;5:955–65. https://doi.org/10.1038/s41564-020-0706-0
4. Narat V, Alcayna-Stevens L, Rupp S, Giles-Vernick T. Rethinking human-nonhuman primate contact and pathogenic disease spillover. EcoHealth. 2017;14:840–50. https://doi.org/10.1007/s10393-017-1283-4
5. Forni D, Cagliani R, Molteni C, Clerici M, Sironi M. Monkeypox virus: The changing facets of a zoonotic pathogen. Infect Genet Evol. 2022;105:105372. https://doi.org/10.1016/j.meegid.2022.105372
6. Besombes C, Mbrenga F, Schaeffer L, Malaka C, Gonofio E, Landier J, et al. National monkeypox surveillance, Central African Republic, 2001–2021. Emerg Infect Dis. 2022;28:2435–45. https://doi.org/10.3201/eid2812.220897
7. Heymann DL, Szczeniowski M, Esteves K. Re-emergence of monkeypox in Africa: a review of the past six years. Br Med Bull. 1998;54:693–702. https://doi.org/10.1093/oxfordjournals.bmb.a011720
8. Breman JG, Kalisa-Ruti, Steniowski MV, Zanotto E, Gromyko AI, Arita I. Human monkeypox, 1970–79. Bull World Health Organ. 1980;58:165–82.
9. Jezek Z, Grab B, Szczeniowski MV, Paluku KM, Mutombo M. Human monkeypox: secondary attack rates. Bull World Health Organ. 1988;66:465–70.
10. Mandja BM, Brembilla A, Handschumacher P, Bompangue D, Gonzalez JP, Muyembe JJ, et al. Temporal and spatial dynamics of monkeypox in Democratic Republic of Congo, 2000–2015. EcoHealth. 2019;16:476–87. https://doi.org/10.1007/s10393-019-01435-1
11. Ježek Z, Fenner F. Human monkeypox. Basel, Switzerland: S. Karger AG; 1988. https://doi.org/10.1159/isbn.978-3-318-04039-5.
12. Malaisse F, Lognay G. Edible caterpillars from tropical Africa. In: Motte-Florac E, Thomas JMC, eds. "Insects" an oral tradition [in French]. Paris-Louvain: Peeters-SELAF; 2003. pp 279–304.
13. Levine RS, Peterson AT, Yorita KL, Carroll D, Damon IK, Reynolds MG. Ecological niche and geographic distribution of human monkeypox in Africa. PLoS One. 2007;2:e176. https://doi.org/10.1371/journal.pone.0000176
14. Lee-Cruz L, Lenormand M, Cappelle J, Caron A, De Nys H, Peeters M, et al. Mapping of Ebola virus spillover: Suitability and seasonal variability at the landscape scale. PLoS Negl Trop Dis. 2021;15:e0009683. https://doi.org/10.1371/journal.pntd.0009683
15. Mandja BA, Handschumacher P, Bompangue D, Gonzalez JP, Muyembe JJ, Sauleau EA, et al. Environmental drivers of monkeypox transmission in the Democratic Republic of the Congo. EcoHealth. 2022;19:354–64. https://doi.org/10.1007/s10393-022-01610-x

Address for correspondence: Camille Besombes, Institut Pasteur, 211 rue de Vaugirard, Paris 75015, France; email: camille.besombes@sciencespo.fr

Recurrence, Microevolution, and Spatiotemporal Dynamics of *Legionella pneumophila* Sequence Type 1905, Portugal, 2014–2022

Vera Manageiro,[1] Vítor Borges,[1] Raquel Rodrigues, Célia Bettencourt, Cecília Silva, João Paulo Gomes, Paulo Gonçalves

We investigated molecular evolution and spatiotemporal dynamics of atypical *Legionella pneumophila* serogroup 1 sequence type 1905 and determined its long-term persistence and linkage to human disease in dispersed locations, far beyond the large 2014 outbreak epicenter in Portugal. Our finding highlights the need for public health interventions to prevent further disease spread.

Legionella, the causative agent of Legionnaires' disease (LD), is a facultative intracellular gram-negative bacterium that is ubiquitous in freshwater environments. *Legionella* bacteria usually thrive in natural and artificial water sources, such as cooling towers, hot water tanks, and plumbing systems. Humans acquire infection by inhaling bacteria-contaminated droplets, usually generated by water systems or devices (*1*). Although the primary mode of transmission is exposure to contaminated aerosolized water, not all *Legionella* species known to cause disease in humans are exclusively associated with water sources. For example, infection with *L. longbeachae* is associated with exposure to soil and compost-related products (*2*). Although *Legionella* bacteria typically do not spread from person to person, that transmission route has been reported (*3*,*4*).

Incidence of *Legionella* infection in a population is primarily influenced by 3 factors: individual susceptibility, environment, and type of exposure. Outbreaks often occur in healthcare settings (e.g., hospitals or long-term care facilities) because of the presence of persons at increased risk for infection and severe disease (*5*).

One of the world's largest outbreaks of LD (>400 cases and 14 deaths) occurred in the Vila Franca de Xira (VFX) region of Portugal, in 2014 (*6*,*7*). The outbreak was associated with the novel sequence type (ST) 1905 of *L. pneumophila* subspecies *fraseri* serogroup 1 strain (PtVFX/2014), which probably originated from a local industrial cooling tower (*6*,*7*). In-depth genomic analyses showed that PtVFX/2014 possesses a unique and mosaic genomic backbone marked by specific evolutionary and genetic traits (*3*), including a recently identified novel effector with nucleotropism (*8*), that may affect its ability to adapt and persist in diverse environments and cause human disease. The *L. pneumophila* ST1905 strain was also implicated by the strongest evidence to date of person-to-person transmission of LD (*3*,*4*). To our knowledge, *L. pneumophila* ST1905 has not been reported in countries other than Portugal. To elucidate the molecular evolution and spatiotemporal dynamics of *L. pneumophila* serogroup 1 ST1905 during 2014–2022, we investigated the phylogenetic relationship of strains isolated during that period at the National Institute of Health, Portugal, in the context of the National Legionnaires' Disease Surveillance Programme.

The Study

Since the large 2014 LD outbreak, the ST1905 genotype has been identified several times in Portugal. For our study, we analyzed all *L. pneumophila* serogroup 1 ST1905 isolates (6 clinical and 6 environmental) obtained from samples collected in 3 interconnected

Author affiliations: European Centre for Disease Prevention and Control, Stockholm, Sweden (V. Manageiro); National Institute of Health Doutor Ricardo Jorge, Lisbon, Portugal (V. Manageiro, V. Borges, R. Rodrigues, C. Bettencourt, C. Silva, J.P. Gomes, P. Gonçalves); Lusófona University, Lisbon (J.P. Gomes)

DOI: https://doi.org/10.3201/eid3005.231383

[1]These first authors contributed equally to this article.

municipalities in the Lisbon region (Lisbon, Loures, and VFX) in the context of clinical case investigations (outbreaks or as sporadic cases) (Figures 1, 2; Appendix 1, https://wwwnc.cdc.gov/EID/article/30/5/23-1383-App1.xlsx; Appendix 2, https://wwwnc.cdc.gov/EID/article/30/5/23-1383-App2.pdf). We also included 2 culture-negative clinical samples genotyped as ST1905 for analysis of the temporal and geographic distribution of this strain after 2014 (Appendices 1, 2).

Single-nucleotide polymorphism (SNP)–based diversity analysis confirmed that all ST1905 isolates were genetically similar to PtVFX/2014, differing by 3–6 SNPs. Overall, the observed microevolution across the 12 isolates was marked by 10 SNPs (9 nonsynonymous and 1 synonymous mutations), 4 insertion/deletions, and 1 small recombination event (Figure 2). The low number of SNPs during the 8-year period supports the notion that *L. pneumophila* evolves at a very slow rate, resulting in substantial temporal and spatial conservation, as previously reported (*9*,*10*). When compared with PtVFX/2014, all isolates presented a recombination event in an ≈2.5-kb region (contig 8, PtVFX/2014_08985-08995) belonging to the type IVA secretion system, which is associated with the survival of the bacteria in the environment (*11*). Of note, Lpn_PT_E259_y2021, isolated from a sporadic LD case, presented mutational events, including 2 deletions and 1 insertion, not found in any other isolates included in this study. The first deletion encompasses a 45,479-bp segment (contig 8, PtVFX/2014_09080-09280) that includes an ≈37.5-Kb genomic island containing an *lvh/lvr* type IVA secretion system cluster. That cluster was first identified within the *L. pneumophila* species in the PtVFX/2014 strain (PtVFX/2014_09115-09280), possibly because of interspecies transfer from *L. oakridgensis* (*3*). The second deletion spanned 142 bp and occurred in a CRISPR-associated intergenic region (PtVFX/2014_08935/08940). Moreover, we observed a frameshift 25-bp insertion at the PtVFX/2014_13190 locus, coding for a protein with unknown function. That locus seems to be specific for *L. pneumophila* subsp. *fraseri* and is located within a larger genomic region that contains known Dot/Icm substrates (*3*). Although we cannot make

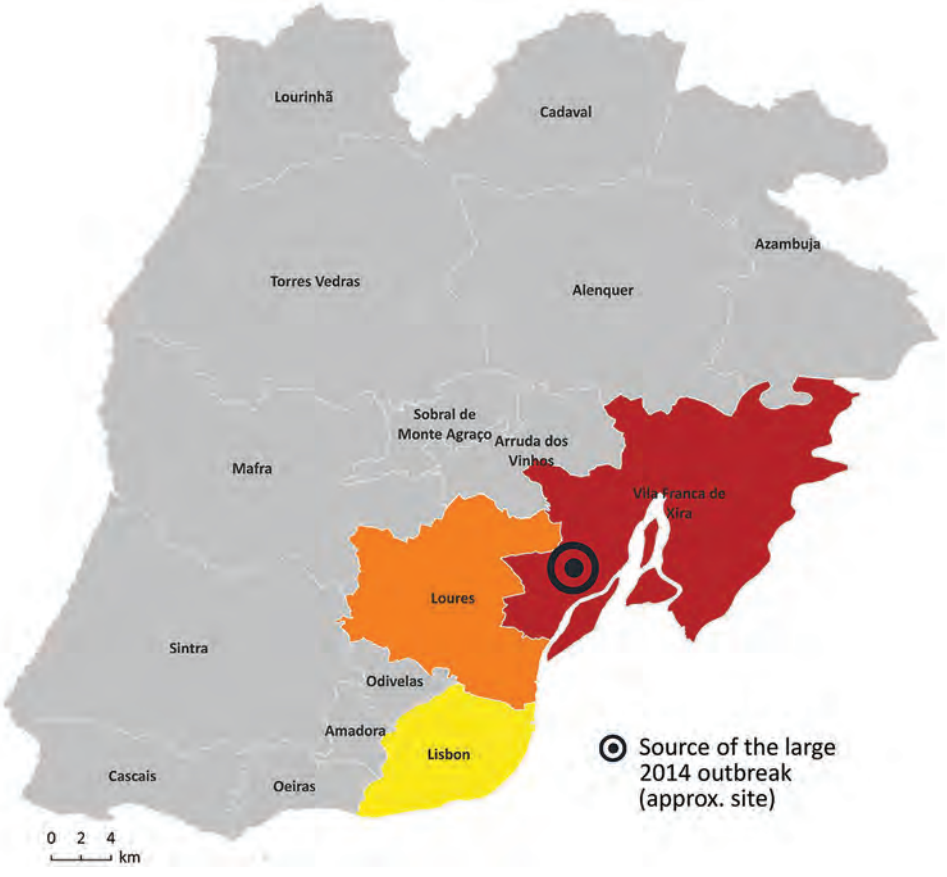

Figure 1. Geographic spread of 12 *Legionella pneumophila* sequence type 1905 isolates by probable municipality of exposure (clinical) or sampling (environmental), Lisbon region, Portugal, 2014–2022. Location of 2014 Legionnaires' disease outbreak is indicated.

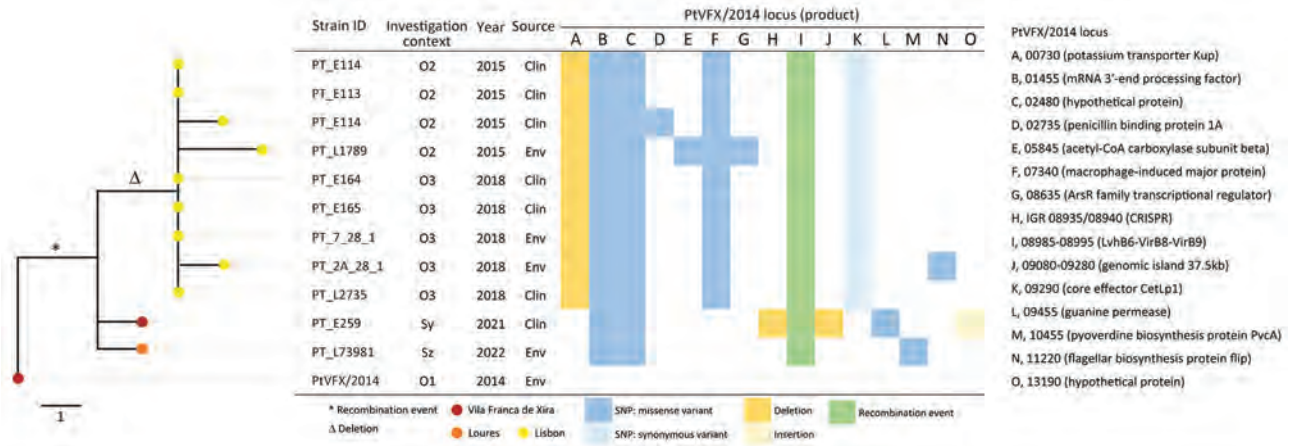

Figure 2. Core SNP-based phylogeny of whole-genome sequencing data from 12 *Legionella pneumophila* isolates obtained from samples collected in 3 interconnected municipalities in the Lisbon region, Portugal. Phylogeny was generated using a maximum-likelihood phylogenetic tree, rooted to the *L. pneumophila* PtVFX/2014 genome sequence (LORH00000000.1) (*2*). The investigation context, year, source, and genetic diversity profile within *L. pneumophila* genomes (SNPs, indels, and recombination event) compared with PtVFX/2014, are shown next to the tree. Clin, clinical; env, environmental; ID, identification; o, outbreak investigation; PtVFX, strain from 2014 Legionnaires' disease outbreak in Vila Franca de Xira, Portugal; SNP, single-nucleotide polymorphism; s, sporadic case investigation.

conclusions about a potential adaptive role of the observed mutations, it has been hypothesized that mutations found exclusively in clinical isolates, as in our study, might reflect human-specific adaptation (*10*). *L. pneumophila* can infect and replicate in human alveolar macrophages, but human-to-human transmission is assumed to be rare; thus, fixation of those mutations into *L. pneumophila* circulating in the human population is unlikely (*10*,*12*). Still, it has been proposed that the recent expansion of *L. pneumophila* in manmade water systems, together with the widespread distribution of specific clones at global scale, aligns with the potential dissemination between humans or from humans to the environment (*13*).

In-depth phylogenetic and microevolutionary analysis showed that ST1905 isolates did not cluster by year of isolation (Figure 2). Still, it is noteworthy that all clinical and environmental isolates associated with a particular location clustered apart, supporting persistence of the strain in that location and linkage between different events in some specific settings. Indeed, in one facility, located in the Lisbon municipality, we observed a genetic and epidemiologic correlation between the isolates collected in the outbreak investigation in 2015 and those from 2018 (Figures 1, 2; Appendix 1). In that facility, when both clinical and environmental isolates collected in the same investigation context were available, they differed by ≤3 SNPs, further supporting their epidemiologic linkage. Local microevolution is expected (*13*) and might contribute to fitness changes, such as increased tolerance to copper (*14*).

Three mutation events (2 SNPs and 1 recombination) were shared by all ST1905 isolates collected after the 2014 outbreak (Figure 2) We retrospectively inspected isolates from the 2014 outbreak for evidence of any of those mutations (*3*) and found that 1 nonsynonymous mutation (in PtVFX/2014_02480, coding for a hypothetical protein) had already been detected in 1 of the 2014 clinical strains (data not shown). That observation provides further evidence that the recurrent ST1905 detections derived from the large bacterial dispersion that occurred in 2014, probably resulting from atypical atmospheric conditions (*6*,*7*,*15*). It also supports the knowledge that *L. pneumophila* outbreaks can be caused by multiple same-strain subpopulations (present simultaneously in a source of infection and diversified over time) or even by different co-existing strains (*9*).

Conclusions

Our results strongly indicate that the atypical *L. pneumophila* sg1 ST1905 strain is potentially persistent in diverse and geographically dispersed environments, far beyond the epicenter of the large 2014 outbreak in Portugal (VFX region). The recurrence of isolated cases or outbreaks in other regions with susceptible populations is thus of public health concern. Moreover, the observed microevolutionary traits and the potential of genetic recombination raise additional uncertainties regarding the evolutionary landscape of the ST1905 strain and its ability to further adapt and persist in the environment and, ultimately, cause human disease. Our study highlights the need for targeted public

health preparedness and control strategies, emphasizing the added value of molecular epidemiology in the surveillance and management of LD.

Acknowledgments

We acknowledge all health professional (in particular clinicians, pathologists, and environmental health technicians) who contribute to the National Legionnaire's Disease Surveillances Programme.

Illumina reads generated in this study were deposited in the European Nucleotide Archive (BioProject accession no. PRJEB65289; run IDs: ERR11862821-ERR11862831) (http://www.ebi.ac.uk/ena/data/view/PRJEB65289).

We report no potential conflict of interest.

About the Author

Dr. Manageiro is a researcher at the Department of Infectious Diseases, National Institute of Health Doutor Ricardo Jorge, Lisbon, Portugal. Her research focuses on gram-negative pathogen antibiotic resistance, with an emphasis on the roles of resistome and mobilome as linkages between human, animal, and environmental reservoirs. Dr. Borges is a researcher at the Department of Infectious Diseases, National Institute of Health Doutor Ricardo Jorge, Lisbon, Portugal. His research focuses on using genomics and transcriptomics to survey and investigate pathogens with effects on public health.

References

1. Iliadi V, Staykova J, Iliadis S, Konstantinidou I, Sivykh P, Romanidou G, et al. *Legionella pneumophila*: the journey from the environment to the blood. J Clin Med. 2022;11:6126. https://doi.org/10.3390/jcm11206126
2. Chambers ST, Slow S, Scott-Thomas A, Murdoch DR. Legionellosis caused by non-*Legionella pneumophila* species, with a focus on *Legionella longbeachae*. Microorganisms. 2021;9:291. https://doi.org/10.3390/microorganisms9020291
3. Borges V, Nunes A, Sampaio DA, Vieira L, Machado J, Simões MJ, et al. *Legionella pneumophila* strain associated with the first evidence of person-to-person transmission of Legionnaires' disease: a unique mosaic genetic backbone. Sci Rep. 2016;6:26261. https://doi.org/10.1038/srep26261
4. Correia AM, Ferreira JS, Borges V, Nunes A, Gomes B, Capucho R, et al. Probable person-to-person transmission of Legionnaires' disease. N Engl J Med. 2016;374:497–8. https://doi.org/10.1056/NEJMc1505356
5. Beauté J, Plachouras D, Sandin S, Giesecke J, Sparén P. Healthcare-associated Legionnaires' disease, Europe, 2008–2017. Emerg Infect Dis. 2020;26:2309–18.
6. Shivaji T, Sousa Pinto C, San-Bento A, Oliveira Serra LA, Valente J, Machado J, et al. A large community outbreak of Legionnaires disease in Vila Franca de Xira, Portugal, October to November 2014. Euro Surveill. 2014;19:20991. https://doi.org/10.2807/1560-7917.ES2014.19.50.20991
7. George F, Shivaji T, Pinto CS, Serra LAO, Valente J, Albuquerque MJ, et al. A large outbreak of Legionnaires' disease in an industrial town in Portugal. Rev Port Saude Publica. 2016;34:199–208. https://doi.org/10.1016/j.rpsp.2016.10.001
8. Monteiro IP, Sousa S, Borges V, Gonçalves P, Gomes JP, Mota LJ, et al. A search for novel *Legionella pneumophila* effector proteins reveals a strain specific nucleotropic effector. Front Cell Infect Microbiol. 2022;12:864626. https://doi.org/10.3389/fcimb.2022.864626
9. David S, Mentasti M, Lai S, Vaghji L, Ready D, Chalker VJ, et al. Spatial structuring of a *Legionella pneumophila* population within the water system of a large occupational building. Microb Genom. 2018;4:e000226. https://doi.org/10.1099/mgen.0.000226
10. Leenheer D, Moreno AB, Paranjape K, Murray S, Jarraud S, Ginevra C, et al. Rapid adaptations of *Legionella pneumophila* to the human host. Microb Genom. 2023;9:mgen000958. https://doi.org/10.1099/mgen.0.000958
11. Qin T, Zhou H, Ren H, Liu W. Distribution of secretion systems in the genus *Legionella* and its correlation with pathogenicity. Front Microbiol. 2017;8:388. https://doi.org/10.3389/fmicb.2017.00388
12. Oliva G, Sahr T, Buchrieser C. The life cycle of *L. pneumophila*: cellular differentiation is linked to virulence and metabolism. Front Cell Infect Microbiol. 2018;8:3. https://doi.org/10.3389/fcimb.2018.00003
13. David S, Rusniok C, Mentasti M, Gomez-Valero L, Harris SR, Lechat P, et al. Multiple major disease-associated clones of *Legionella pneumophila* have emerged recently and independently. Genome Res. 2016;26:1555–64. https://doi.org/10.1101/gr.209536.116
14. Bédard E, Trigui H, Liang J, Doberva M, Paranjape K, Lalancette C, et al. Local adaptation of *Legionella pneumophila* within a hospital hot water system increases tolerance to copper. Appl Environ Microbiol. 2021;87:e00242-21. https://doi.org/10.1128/AEM.00242-21
15. Russo A, Gouveia CM, Soares PMM, Cardoso RM, Mendes MT, Trigo RM. The unprecedented 2014 Legionnaires' disease outbreak in Portugal: atmospheric driving mechanisms. Int J Biometeorol. 2018;62:1167–79. https://doi.org/10.1007/s00484-018-1520-8

Address for correspondence: Paulo Gonçalves, National Reference Laboratory for *Legionella*, Department of Infectious Diseases, National Institute of Health Doutor Ricardo Jorge (INSA), Lisbon, Portugal; email: paulo.goncalves@insa.min-saude.pt

Antigenic Characterization of Novel Human Norovirus GII.4 Variants San Francisco 2017 and Hong Kong 2019

Kentaro Tohma, Michael Landivar, Lauren A. Ford-Siltz, Kelsey A. Pilewski, Joseph A. Kendra, Sandra Niendorf, Gabriel I. Parra

Norovirus is a major cause of acute gastroenteritis; GII.4 is the predominant strain in humans. Recently, 2 new GII.4 variants, Hong Kong 2019 and San Francisco 2017, were reported. Characterization using GII.4 monoclonal antibodies and serum demonstrated different antigenic profiles for the new variants compared with historical variants.

Norovirus is a major cause of acute gastroenteritis (*1*). Over past decades, variants of the predominant genotype, genotype 4 (GII.4), have continuously emerged to escape immunity (*2*–*5*). Since 2012, the Sydney 2012 variant has predominated worldwide (*6*). In 2019, GII.4 noroviruses that did not cluster with any known variants were reported circulating in different countries as early as 2016 (*7*,*8*). Based on phylogenetic clustering and number of mutations on major capsid viral proteins (VP1), the variant was classified GII.4 Hong Kong 2019 (*7*). The new variant caused no large outbreaks and did not eclipse the predominance of Sydney 2012. Another recently reported unique group of GII.4 noroviruses, the San Francisco 2017 variant, was retrospectively detected circulating during 2017–2022 (*9*). Both variants showed multiple mutations on major antigenic sites, including a single amino acid insertion next to the antigenic site A in San Francisco 2017 (*7*,*9*,*10*). We characterize the antigenicity of these 2 new variants using panels of GII.4 mouse monoclonal antibodies (mAbs) and hyperimmune serum developed against historical GII.4 variants (*11*,*12*).

Author affiliations: US Food and Drug Administration Center for Biologics Evaluation and Research, Silver Spring, Maryland, USA (K. Tohma, M. Landivar, L.A. Ford-Siltz, K.A. Pilewski, J.A. Kendra, G.I. Parra); Robert Koch Institute, Berlin, Germany (S. Niendorf)

DOI: https://doi.org/10.3201/eid3005.231694

The Study

To determine the cross-reactivity of the 2 new variants with previously circulating variants, we produced virus-like particles (VLPs) for Hong Kong 2019 (GenBank accession no.: MN400355) and San Francisco 2017 (GenBank accession no. MW506849) viruses. We performed ELISA by using mAbs developed against Sydney 2012 virus (*11*) and the newly developed VLPs. Results demonstrated that the Hong Kong 2019 VLPs bound to most of the mAbs mapping to conserved sites from protruding (P) and shell (S) domains of the VP1, but only bound to 2/25 mAbs that mapped to variable antigenic sites and showed histo-blood group antigen (HBGA) blockade activity (Figure 1, panel A) (*11*). Those results were expected because mutational analyses showed that the Hong Kong 2019 viruses present multiple mutations on variable antigenic sites (Appendix, https://wwwnc.cdc.gov/EID/article/30/5/23-1694-App1.pdf) (*7*). The loss of binding of 3 cross-reactive mAbs that mapped to the P domain could be explained by unique mutations on the conserved sites (Appendix). VLPs from the San Francisco 2017 variant bound to all mAbs mapping to conserved sites of the VP1, but only to 4 mAbs that mapped to variable antigenic sites. Based on previous observations, alanine on positions 356, 359, or both, play a role in binding to mAbs 1C10 and 17A5 (*11*). Thus, alanine on those positions could explain the binding of mAbs to Hong Kong 2019 and San Francisco 2017 VLPs. Other mAbs mapping to the antigenic site G, 26E5 and 29A9, seem to require residues from antigenic site A (*11*). Mutations on antigenic site A in San Francisco 2017 could therefore result in loss of binding of these mAbs

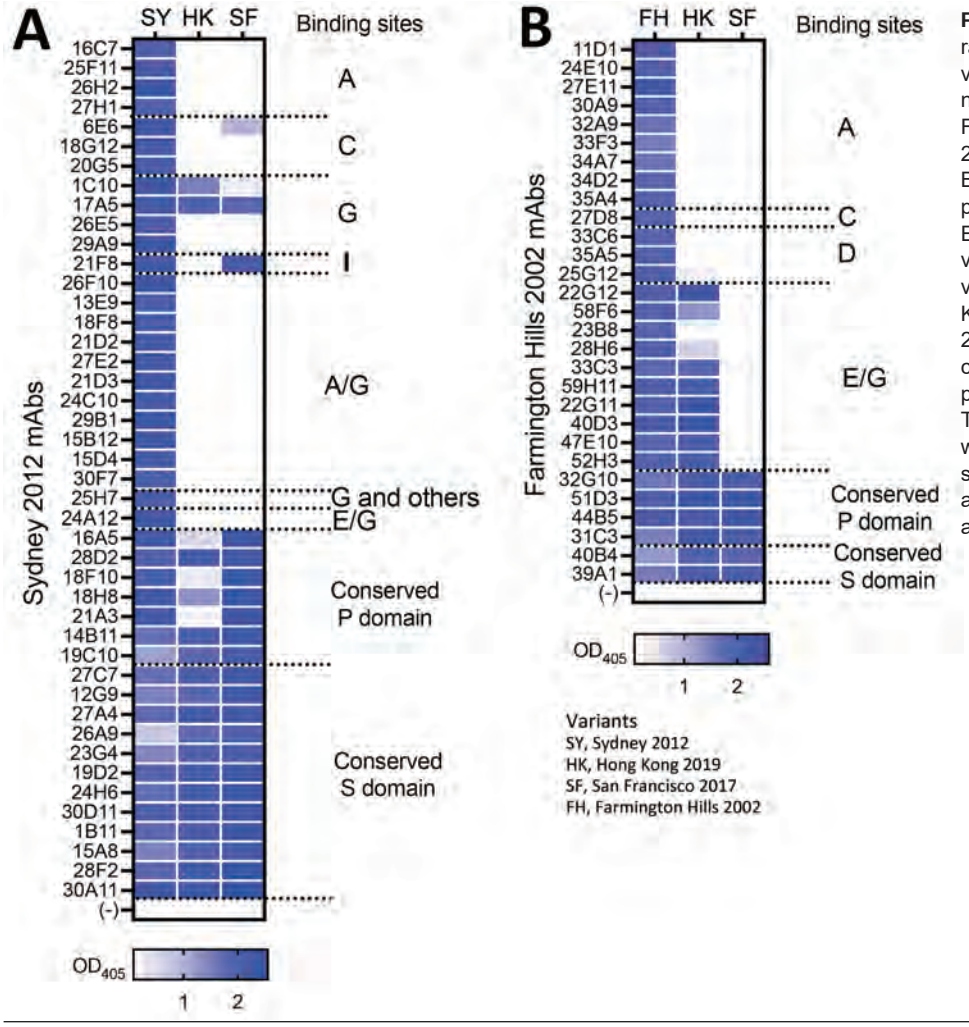

Figure 1. Monoclonal antibodies raised against 2 major GII.4 variants in a study of novel human norovirus GII.4 variants, San Francisco 2017 and Hong Kong 2019. A) Sydney 2012 mAb panel; B) Farmington Hills 2002 mAb panel. The heatmaps indicate ELISA binding strength (OD_{405} values) of individual mAbs against virus-like particles from GII.4 Hong Kong 2019 and San Francisco 2017. Antibodies indicate minimal cross-reactivity between new and previously described variants. The binding sites of the mAbs were characterized in a previous study (*11*). mAbs, monoclonal antibodies; OD_{405}, optical density at 405 nm; P, protruding; S, shell.

regardless of similarity to antigenic site G on the Sydney 2012 variant. The 6E6 mAb, mapping to antigenic site C, was previously reported to cross-react weakly to Farmington Hills 2002 variant (*11*), which has 3 mutations compared with Sydney 2012. The San Francisco 2017 presented 4 mutations compared with Sydney 2012; the Hong Kong 2019 variant had 6 mutations on that site, explaining the differential binding of this mAb. Similarly, sequence differences on antigenic site I could explain the lack of binding of mAb 21F8 to Hong Kong 2019 VLPs.

Because Hong Kong 2019 and San Francisco 2017 present evolutionary convergence and share similar residues on several of the antigenic sites compared with the Farmington Hills 2002 variant (Appendix), we also tested those strains with mAbs developed against this ancestral variant (Figure 1, panel B). Both VLPs showed reactivity with all mAbs binding to conserved epitopes. As expected based on sequence similarity, Hong Kong 2019 showed reactivity only with mAbs mapping on antigenic site E/G. San Francisco 2017 was negative to all mAbs mapping to variable sites, including antigenic site A, which presented only 3 mutations from Farmington Hills 2002 VLPs. Those data indicate that either a small number of changes are sufficient to abrogate binding of all 9 A-mapping mAbs or that the insertion near the antigenic site A has a major influence on the characteristics of this antigenic site.

To further characterize the antigenicity of these new variants, we tested the HBGA blocking activity of serum from mice immunized with VLPs from historical variants (Figure 2, panels A, B) (*12*), including the currently circulating Sydney 2012, the ancestral Farmington Hills 2002, and genetically or phylogenetically related variants: Osaka 2007 for Hong Kong 2019 viruses (*7*), and New Orleans 2009 and Apeldoorn 2007 for San Francisco 2017 viruses (*9*) (Appendix). The Hong Kong 2019 VLPs presented weak cross-blockade reactivity with the serum raised against all 3 viruses (mean 50% effective concentration = 118.5 for Sydney 2012,

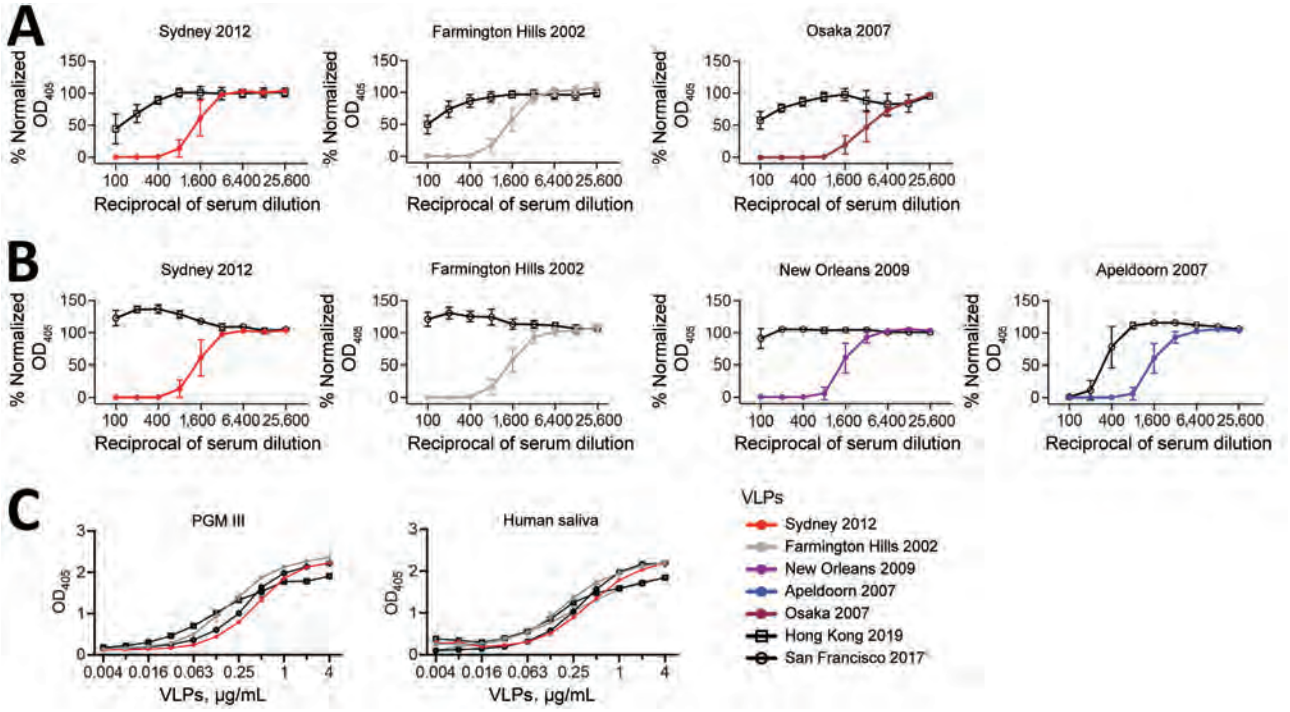

Figure 2. HBGA blockade and binding assays in a study of novel human norovirus GII.4 variants, San Francisco 2017 and Hong Kong 2019. A,B) Line graphs indicating normalized OD_{405} curves of GII.4 variants in HBGA blockade assays using mouse hyperimmune serum raised against currently circulating strains; A) Hong Kong 2019 VLPs against historical strains; B) San Francisco 2017 VLPs against historical strains. Normalized OD_{405} values were calculated by using values from positive and negative (serum only) control wells. C) OD_{405} curves of GII.4 variant VLPs in HGBA binding assays of Hong Kong 2019 and San Francisco 2017 VLPs and PGM III and human saliva, expressing the Lewis^a, Lewis^b, Lewis^y, H type-1, and H type-2 HBGA carbohydrates. PGM III was used as a source of HBGA carbohydrates. Human saliva was collected from a healthy adult volunteer under US Food and Drug Administration, Center for Biologics Evaluation and Research protocol no. CBER IRB 16–069B. HBGA, histo-blood group antigen; OD_{405}, optical density at 405 nm; PGM, porcine gastric mucin; VLP, virus-like particles.

116.9 for Farmington Hills 2002, and 87.6 for Osaka 2007 serum), with >12-fold differences compared with their homologous VLPs (Figure 2, panel A). That result was consistent with data from children with the fewest previous norovirus infections (*10*), supporting minimal cross-reactivity of Hong Kong 2019 to previous variants. In contrast, the San Francisco 2017 VLPs did not show cross-blockade reactivity with any of the serum samples tested from pandemic variants (Figure 2, panel B), including Sydney 2012 and Farmington Hills 2002, that shared similar sequences on the antigenic sites E/G (Sydney 2012) and A (Farmington Hills 2002) (Appendix). The only exception for cross-reactivity was with the serum raised against Apeldoorn 2007, which showed moderate cross-blockade activity with the San Francisco 2017 (50% effective concentration = 309.2, a 5-fold difference compared with homologous VLPs). Of note, GII.4 Apeldoorn 2007 and San Francisco 2017 share the same motif on the antigenic site D (Appendix). Thus, that cross-reactivity might be explained by antibodies mapping on the antigenic site D from Apeldoorn 2007 variant.

Our data indicate that both Hong Kong 2019 and San Francisco 2017 variants present distinct antigenic profiles, yet both viruses have been circulating for ≥7 years without causing large outbreaks globally. Multiple examples of antigenically distinct noroviruses that spread worldwide without causing large outbreaks exist. Minor variants such as Osaka 2007 and Apeldoorn 2007 showed distinct antigenic profiles to variants that circulated before their emergence (*12*). Those variants caused local outbreaks and spread to multiple countries, but none predominated at the global level (*13*). Therefore, changes in antigenicity might not be the only factor determining the epidemic potential of noroviruses. Indeed, specific HBGA binding profiles were associated with emerging noroviruses (*14*,*15*). The new GII.4 variants bound to porcine gastric mucin III and human saliva, as did other current and archival variants (*9*,*10*) (Figure 2, panel C), suggesting that impairment of binding to HBGA did not cause the lower circulation of these viruses.

In conclusion, these 2 new norovirus variants are antigenically distinct from previously circulating variants. Whether these variants will predominate or are examples of the subdued circulation of minor norovirus variants remains to be determined. To prepare for future pandemics, we must delineate the factors that determine the overall fitness and predominance of GII.4 noroviruses, including but not limited to replication kinetics, pathogenicity, HBGA binding spectrum, and epidemiologic confounder.

Acknowledgments

We thank Yamei Gao for her technical support on virus-like particle production.

Financial support for this work was provided by the US Food and Drug Administration intramural funds (program no. Z01 BK 04012 LHV–G.I.P). K.A.P. and M.L. are recipients of a CBER/FDA-sponsored Oak Ridge Institute for Science and Education (ORISE) fellowship.

About the Author

Dr. Tohma is a visiting associate at the Division of Viral Products, Food and Drug Administration, Silver Spring, Maryland, USA. His research interests include viral genetic and antigenic evolution, epidemiology, and norovirus vaccine design.

References

1. Lopman BA, Steele D, Kirkwood CD, Parashar UD. The vast and varied global burden of norovirus: prospects for prevention and control. PLoS Med. 2016;13:e1001999. PubMed https://doi.org/10.1371/journal.pmed.1001999
2. Lindesmith LC, Costantini V, Swanstrom J, Debbink K, Donaldson EF, Vinjé J, et al. Emergence of a norovirus GII.4 strain correlates with changes in evolving blockade epitopes. J Virol. 2013;87:2803–13. https://doi.org/10.1128/JVI.03106-12
3. Lindesmith LC, Donaldson EF, Lobue AD, Cannon JL, Zheng DP, Vinje J, et al. Mechanisms of GII.4 norovirus persistence in human populations. PLoS Med. 2008;5:e31. https://doi.org/10.1371/journal.pmed.0050031
4. Siebenga JJ, Lemey P, Kosakovsky Pond SL, Rambaut A, Vennema H, Koopmans M. Phylodynamic reconstruction reveals norovirus GII.4 epidemic expansions and their molecular determinants. PLoS Pathog. 2010;6:e1000884. https://doi.org/10.1371/journal.ppat.1000884
5. Tohma K, Lepore CJ, Gao Y, Ford-Siltz LA, Parra GI. Population genomics of GII.4 noroviruses reveal complex diversification and new antigenic sites involved in the emergence of pandemic strains. mBio. 2019;10:10. https://doi.org/10.1128/mBio.02202-19
6. Parra GI, Tohma K, Ford-Siltz LA, Eguino P, Kendra JA, Pilewski KA, et al. Minimal antigenic evolution after a decade of norovirus GII.4 Sydney_2012 circulation in humans. J Virol. 2023;97:e0171622. https://doi.org/10.1128/jvi.01716-22
7. Chan MC, Roy S, Bonifacio J, Zhang LY, Chhabra P, Chan JCM, et al.; for NOROPATROL2. Detection of norovirus variant GII.4 Hong Kong in Asia and Europe, 2017–2019. Emerg Infect Dis. 2021;27:289–93. https://doi.org/10.3201/eid2701.203351
8. Chuchaona W, Chansaenroj J, Puenpa J, Khongwichit S, Korkong S, Vongpunsawad S, et al. Human norovirus GII.4 Hong Kong variant shares common ancestry with GII.4 Osaka and emerged in Thailand in 2016. PLoS One. 2021;16:e0256572. https://doi.org/10.1371/journal.pone.0256572
9. Chhabra P, Tully DC, Mans J, Niendorf S, Barclay L, Cannon JL, et al. Emergence of novel norovirus GII.4 variant. Emerg Infect Dis. 2023;30:163–7.
10. Lindesmith LC, Boshier FAT, Brewer-Jensen PD, Roy S, Costantini V, Mallory ML, et al. Immune imprinting drives human norovirus potential for global spread. mBio. 2022;13:e0186122. https://doi.org/10.1128/mbio.01861-22
11. Tohma K, Ford-Siltz LA, Kendra JA, Parra GI. Dynamic immunodominance hierarchy of neutralizing antibody responses to evolving GII.4 noroviruses. Cell Rep.2022;39:110689. https://doi.org/10.1016/j.celrep.2022.110689
12. Kendra JA, Tohma K, Ford-Siltz LA, Lepore CJ, Parra GI. Antigenic cartography reveals complexities of genetic determinants that lead to antigenic differences among pandemic GII.4 noroviruses. Proc Natl Acad Sci U S A. 2021;118:e2015874118. https://doi.org/10.1073/pnas.2015874118
13. Kendra JA, Tohma K, Parra GI. Global and regional circulation trends of norovirus genotypes and recombinants, 1995–2019: a comprehensive review of sequences from public databases. Rev Med Virol. 2022;32:e2354. https://doi.org/10.1002/rmv.2354
14. Shanker S, Choi JM, Sankaran B, Atmar RL, Estes MK, Prasad BV. Structural analysis of histo-blood group antigen binding specificity in a norovirus GII.4 epidemic variant: implications for epochal evolution. J Virol. 2011;85:8635–45. https://doi.org/10.1128/JVI.00848-11
15. Zhang XF, Huang Q, Long Y, Jiang X, Zhang T, Tan M, et al. An outbreak caused by GII.17 norovirus with a wide spectrum of HBGA-associated susceptibility. Sci Rep. 2015;5:17687. https://doi.org/10.1038/srep17687

Address for correspondence: Kentaro Tohma, Center for Biologics Evaluation and Research, US Food and Drug Administration, 10903 New Hampshire Ave, Bldg 52/72, Rm 1376, Silver Spring, MD 20993, USA; email: kentaro.tohma@fda.hhs.gov

Interventional Study of Nonpharmaceutical Measures to Prevent COVID-19 Aboard Cruise Ships

Varvara A. Mouchtouri, Leonidas Kourentis, Lemonia Anagnostopoulos, Michalis Koureas, Maria Kyritsi, Katerina Maria Kontouli, Fani Kalala, Mattheos Speletas, Christos Hadjichristodoulou

Cruise ships carrying COVID-19–vaccinated populations applied near-identical nonpharmaceutical measures during July–November 2021; passenger masking was not applied on 2 ships. Infection risk for masked passengers was 14.58 times lower than for unmasked passengers and 19.61 times lower than in the community. Unmasked passengers' risk was slightly lower than community risk.

In the summer of 2021, several European Union Member States (EUMS) and European Economic Area (EEA) countries gradually lifted COVID-19 public health measures and reopened borders. The easing of restrictions enabled cruise lines to resume operations, applying guidelines published by the EU Healthy Gateways Joint Action, the European Centre for Disease Prevention and Control, and European Maritime Safety Agency. We assessed the effectiveness of nonpharmaceutical measures (NPMs) by comparing COVID-19 incidence rates among EUMS and EEA communities and populations of cruise ships and applying different sets of measures.

The Study

We conducted an ecologic study in which cruise ships in group 1 (passenger and crew populations on 2 cruise ships, ships A and B) and group 2 (passenger and crew populations of 9 cruise ships) carrying vaccinated populations applied identical NPMs apart from face masking in passengers and physical distancing, which group 1 did not apply (*1*) (Table). The cruise ship company provided epidemiologic data and screening and diagnostic results for group 1 (Appendix, https://wwwnc.cdc.gov/EID/article/30/5/23-1364-App1.pdf). Ship captains or doctors reported epidemiologic data and screening and diagnostic results to competent health authorities and EU Healthy Gateways Joint Action (Appendix). Passenger populations changed in every cruise, but ≈6 passengers remained onboard the ship for >1 voyage. COVID-19 imposed severe crew change restrictions, and most crew remained the same during the study; the percentage of crew disembarking likely represented <0.5% of the crew population. We calculated COVID-19 incidence rates for the period of July–November 2021 for groups 1, 2, and 3 (EUMS communities). We obtained epidemiologic data for EUMS communities from the European Centre for Disease Prevention and Control website (*4*).

We calculated incidence rate ratios, standardized incidence ratios (SIRs), and 95% CI using the epiR package in R (*5*). We used Fisher's exact test to determine statistical significance. We considered $p<0.05$ statistically significant. We calculated SIRs for groups 1 and 2 by using epidemiologic COVID-19 data in EUMS and EEA countries during the study period as a reference population to calculate expected number of cases onboard (*4*) (Appendix).

The group 1 health measures protocol was reviewed and agreed upon by the Hellenic Ministry of Health's national COVID-19 taskforce. The study received approval from the University of Thessaly's Research Ethics Committee (protocol no. 103/16.11317 1.2021; decision no. 103/01.12.2021). Written consent for serologic testing was obtained from all crew members.

Author affiliations: European Union Healthy Sailing Project, Larissa, Greece (V.A. Mouchtouri, L. Kourentis, L. Anagnostopoulos, K.M. Kontouli, C. Hadjichristodoulou); European Union Healthy Gateways Joint Action, Larissa (V.A. Mouchtouri, L. Kourentis, L. Anagnostopoulos, C. Hadjichristodoulou); University of Thessaly, Larissa (V.A. Mouchtouri, M. Koureas, M. Kyritsi, F. Kalala, M. Speletas, C. Hadjichristodoulou)

DOI: https://doi.org/10.3201/eid3005.231364

The risk for COVID-19 infection in group 2 (masked passengers of 9 ships) was 14.58 (95% CI 7.799–28.361) times lower than risk for group 1 (unmasked passengers) and 19.61 (95% CI 18.86–34.48) times lower than in group 3 (EUMS community members). Infection risk for unmasked passengers in group 1 was lower than in the community (SIR 0.744, 95% CI 0.512–1.045; p = 0.094) (Appendix).

Conclusions

Our ecologic study demonstrated that COVID-19 infection risk among masked cruise ship passengers was 19.61 times lower than in the community (95% CI 18.86–34.48); the risk for infection among unmasked passengers was lower than in the community but not statistically significant (SIR 0.744, 95% CI 0.512–1.045; p = 0.094). Those findings suggest that NPMs implemented onboard the cruise ships were effective in reducing risk (*1*). Recent vaccination for the circulating variant appeared to contribute to reduced infection risk onboard ships, where vaccination coverage was almost 100%, compared with 66% cumulative vaccine uptake among the EUMS population (*3*). No outbreak occurred during the study period (group 1: median no. cases per voyage 1.00, range 0–15; group 2: median 0 cases per

Table. COVID-19 health measures, laboratory screening, and diagnostic testing for SARS-CoV-2 per comparison population group in interventional study of nonpharmaceutical measures to prevent COVID-19 aboard cruise ships*

Variable	Comparison population groups		
	Group 1: cruise ships A and B sailing in EUMS waters	Group 2: 9 cruise ships sailing in EUMS waters	Group 3: EUMS/EEA community populations
Mask wearing	Unmasked passengers, masked crew†	Masked passengers and crew	Policies varied
Physical distancing‡	N	Y	Policies varied
Daily body temperature measurement for passengers and crew	Y	Y	NA
Pre-embarkation health screening questionnaire for passengers and crew§	Y	Y	NA
Quarantine measures for close contacts of SARS-CoV-2–positive passengers and crew members	Y	Y	Yes
Buffet line allowed in food service areas¶	Y	N	NA
>95% passengers and crew members vaccinated#	Y	Y	Vaccine coverage varied in EUMS
Serologic testing for crew members	Y	N	NA
End of voyage reporting by cruise line to competent authorities for COVID-19 surveillance data	Y	Y	NA
Other NPMs: education and training; restrictions for population density, excursions, and port visit; policy enforcement	Y	Y	Policies varied**
Screening/diagnostic testing for crew members			
All crew members already onboard the cruise ship tested by RADT within 1 wk before resuming operations	Y	Y	NA
Day of embarkation RADT	Y	Y	NA
Routine RADT	Every 7 d	Every 7 d	Varied among EUMS
Screening/diagnostic testing for passengers			
Day of embarkation RADT	Y	Y	NA
RADT before disembarkation	Y	Y	NA
Nonvaccinated (or not fully vaccinated) passengers tested by RADT on day 3 or 4 of cruise††	Y	Y	NA

*See Appendix (https://wwwnc.cdc.gov/EID/article/30/5/23-1364-App1.pdf) for more detailed information about definitions and methods used in the study. EEA, European Economic Area; EUMS, European Union member states; NA, not applicable; NPM, nonpharmaceutical measures; RADT, rapid antigen detection test.
†All passengers wore masks on 1 voyage in which elevated number of cases occurred in cruise ship A.
‡Physical distancing of 1.5 m.
§Information collected included demographic information (name, date/time of itinerary, port of disembarkation, cabin number, contact telephone number for 14 d after disembarkation), health questions regarding the past 14 d (presence of COVID-19 compatible symptoms, close contact of COVID-19 case, and whether person provided care was in close proximity, traveled on conveyance, or shared household with SARS-CoV-2–positive person).
¶Group 1 ships provided meals as sitting service and in a buffet line with strict hand hygiene measures, sneeze-guards, replacement of serving utensils, and food service by crew. Group 2 ships provided meals in a sitting service and not in a buffet line. Both groups applied the same rules about handwashing, maximum number of persons in food service areas, and distancing of tables and chairs.
#Persons were considered fully vaccinated 14 d after the last dose of a COVID-19 vaccine.
**Other measures applied in the community: gathering restrictions with maximum capacities, masking and physical distancing in indoor public spaces (theaters, gyms), hybrid policies for education and workplace settings, and proof of vaccination or negative tests to attend events (*2*).
††During the study period, the cumulative vaccine uptake (%) in the total population in EUMS/EEA (group 3) was ≈66% for the primary course (*3*).

voyage, range 0–4). Of 44 close contacts of SARS-CoV-2–positive persons, 10 tested positive during quarantine, which could be attributed to protective effects of up-to-date vaccination for the circulating SARS-CoV-2 Delta variant. No deaths or severe cases were reported among the 11 cruise ships, despite the highly pathogenic nature of the Delta variant and older average age of cruise passengers.

Experimental studies in confined spaces demonstrated that masking is one of the most effective NPMs to prevent aerosol infection transmission (*6*). However, a systematic review of clinical trials in community settings and healthcare facilities demonstrated that wearing masks in the community likely makes little difference to outcomes compared with not wearing a mask (*7*). Masking in different settings (ships, hospitals, communities) might have different effects, however, the effectiveness of masking measures is likely influenced by how strictly those measures are enforced. During the pandemic, an absence of mask-wearing measures resulted in large outbreaks onboard ships (*8*,*9*). Our study demonstrated reduced COVID-19 incidence rates because of the protective effect of masking onboard ships. We suggest integrating use of high-filtration masks into routine case management, outbreak response measures, and preparedness and contingency planning for future public health emergencies of international concern. Crew members presented a lower infection risk than passengers and community populations, possibly because of mandatory mask use, recent vaccination, the strict enforcement of masking and vaccination policies, and reinforced education on symptoms and reporting requirements.

The first limitation of our study is that direct, individual observation of passenger and crew compliance was impossible in the uncontrolled environments of live cruises. The estimated case underreporting rates applied (1:4) were based on US data (February 2020–September 2021), but our study was implemented in Europe (July–November 2021), so differences could apply (*10*). The practice of 14-day quarantine and monitoring for disembarking passengers was applied only for close contacts of SARS-CoV-2–positive persons, so secondary cases could have been unidentified. We did not collect data on vaccination type, cabin occupancy, shore-based excursions, and onboard activities for the entire study population, so incidence rate differences for those factors could not be tested. Previous research of a COVID-19 cruise outbreak demonstrated that involvement in certain group activities (e.g., shows) and shore-based bus excursions were associated with infection, as well as a consistent dose-response relationship between number of cabinmates and attack rates in which attack rates decreased as passenger occupancy per cabin decreased (*11*,*12*). Alternative exposures, such as preembarkation queuing, social activities, contaminated surface contact, and common area use, deserve attention. Incubating passengers might not have been identified, but daily fever screening and diagnostic testing before boarding, during voyage, and before disembarking enhanced surveillance, reducing the possibility of undetected incubating COVID-19 cases (*1*). Strategies guaranteeing study protocol adherence were unfeasible on active voyages; however, enforcing company protocols and competent authority inspections maintained the intervention's fidelity. Use of buffet lines in group 1 might be a confounder, but both groups applied identical food service occupancy limits; fomite transmission was unlikely given strict hand hygiene measures, replacement of serving utensils, sneeze-guards, and food service by crew. The ship company uniformly applied and enforced clear policies in groups 1 and 2. That uniform application was impossible in group 3 (communities) because implementation policies varied: full or partial; national, regional, or local; mandatory or voluntary; and groups targeted (i.e., at-risk persons, healthcare workers, travelers). Topics for further research include cost-effectiveness of NPMs on cruise ships in the context of pandemics, public health emergencies of international concern or during respiratory illness outbreaks.

In conclusion, our ecologic study demonstrated the safe restart of cruise ship sector operations and indicated that mask use added an extra layer of protection; further studies should be conducted to verify the results. Masking should be considered in future public health emergencies when making decisions regarding NPMs and other measures that could interfere with international traffic and trade.

Acknowledgments

We wish to acknowledge the contribution of the Hellenic Ministry of Health's COVID-19 taskforce, the National Public Health Organization of Greece and the Biomedical Research Foundation, Academy of Athens, for the next-generation sequencing (NGS) analysis of positive samples. Moreover, we thank the ships' medical doctors and all ship officers and crew members for their contributions. We express our sincere thanks to the National Public Health Organization of Greece and to the President of the Biomedical Research Foundation, Academy of Athens, Dimitrios Thanos for the NGS analysis of positive samples.

Part of this research was conducted in the framework of the Healthy Sailing project which received funding from the European Union's Horizon Framework Programme under grant agreement no. 101069764. Moreover, part of this research was conducted in the framework of the EU Healthy Gateways Joint Action, which received funding from the European Union's Health Programme (2014–2020) under grant agreement no. 801493. The cost of laboratory testing (serological tests and rapid antigen detection tests conducted onboard ships) was covered by the cruise lines.

About the Author

Dr. Mouchtouri, an associate professor of hygiene and epidemiology at the University of Thessaly, is scientific manager of the European Union project Healthy Sailing and led the maritime transport work package of the European Union Joint Action Healthy Gateways. Her primary research interests include the prevention and control of cross-border health threats and public health aspects in maritime transport.

References

1. EU Healthy Gateways Joint Action. Advice for restarting cruise ship operations after lifting restrictive measures in response to the COVID-19 pandemic (version 2—April 2021) [cited 2021 Jun 29]. https://www.healthygateways.eu/Novel-coronavirus
2. European Centre for Disease Prevention and Control. Data on country response measures to COVID-19 (archived) [cited 2024 Feb 9]. https://www.ecdc.europa.eu/en/publications-data/download-data-response-measures-covid-19
3. European Centre for Disease Prevention and Control. COVID-19 vaccine tracker [cited 2024 Feb 9]. https://qap.ecdc.europa.eu/public/extensions/COVID-19/vaccine-tracker.html
4. European Centre for Disease Prevention and Control. Data on the daily number of new reported COVID-19 cases and deaths by EU/EEA country [cited 2022 Jul 23]. https://www.ecdc.europa.eu/en/publications-data/data-daily-new-cases-covid-19-eueea-country
5. Stevenson MSE. epiR: tools for the analysis of epidemiological data [cited 2024 Feb 9]. https://CRAN.R-project.org/package=epiR
6. Wang Z, Galea ER, Grandison A, Ewer J, Jia F. A coupled computational fluid dynamics and Wells-Riley model to predict COVID-19 infection probability for passengers on long-distance trains. Saf Sci. 2022;147:105572. https://doi.org/10.1016/j.ssci.2021.105572
7. Jefferson T, Dooley L, Ferroni E, Al-Ansary LA, van Driel ML, Bawazeer GA, et al. Physical interventions to interrupt or reduce the spread of respiratory viruses. Cochrane Database Syst Rev. 2023;1:CD006207. https://doi.org/10.1002/14651858.CD006207.pub6
8. Veenstra T, van Schelven PD, Ten Have YM, Swaan CM, van den Akker WMR. Extensive spread of SARS-CoV-2 Delta variant among vaccinated persons during 7-day river cruise, the Netherlands. Emerg Infect Dis. 2023;29:734–41. https://doi.org/10.3201/eid2904.221433
9. Hatzianastasiou S, Mouchtouri VA, Pavli A, Tseroni M, Sapounas S, Vasileiou C, et al. COVID-19 outbreak on a passenger ship and assessment of response measures, Greece, 2020. Emerg Infect Dis. 2021;27:1927–30. https://doi.org/10.3201/eid2707.210398
10. Centers for Disease Control and Prevention. Estimated COVID-19 burden 2023 [cited 2024 Feb 9]. https://www.cdc.gov/coronavirus/2019-ncov/cases-updates/burden.html
11. World Health Organization. WHO advice for international travel and trade in relation to the outbreak of pneumonia caused by a new coronavirus in China 2020 [cited 2024 Feb 9]. https://www.who.int/news-room/articles-detail/who-advice-for-international-travel-and-trade-in-relation-to-the-outbreak-of-pneumonia-caused-by-a-new-coronavirus-in-china
12. Plucinski MM, Wallace M, Uehara A, Kurbatova EV, Tobolowsky FA, Schneider ZD, et al. Coronavirus disease 2019 (COVID-19) in Americans aboard the Diamond Princess cruise ship. Clin Infect Dis. 2021;72:e448–57. https://doi.org/10.1093/cid/ciaa1180

Address for correspondence: Varvara A. Mouchtouri, Laboratory of Hygiene and Epidemiology, Faculty of Medicine, University of Thessaly, 22 Papakyriazi str, 41222, Larissa, Greece; email: mouchtourib@uth.gr

Novel Variant and Known Mutation in 23S rRNA Gene of *Mycoplasma pneumoniae*, Northern Vietnam, 2023

Dinh-Dung Nguyen,[1] Nhan Thi Ho,[1] Lynn G. Dover, Anh Hang Mai Vo, Ha Thi Thanh Ly, Phuong Mai Doan, Hang Thi Nguyen, Nguyen Thi Thao Luu, An Nhat Pham, Huyen Thi Thanh Tran

Author affiliations: Vinmec Healthcare System, Hanoi, Vietnam (D.-D. Nguyen, N.T. Ho, A.H.M. Vo, H.T.T. Ly, P.M. Doan, H.T. Nguyen, N.T.T. Luu, A.N. Pham, H.T.T. Tran); Northumbria University, Newcastle upon Tyne, UK (L.G. Dover)

DOI: https://doi.org/10.3201/eid3005.231632

During a 2023 outbreak of *Mycoplasma pneumoniae*–associated community-acquired pneumonia among children in northern Vietnam, we analyzed *M. pneumoniae* isolated from nasopharyngeal samples. In almost half (6 of 13) of samples tested, we found known A2063G mutations (macrolide resistance) and a novel C2353T variant on the 23S rRNA gene.

Mycoplasma pneumoniae is a common etiologic agent of community-acquired pneumonia (CAP) among children. Although *M. pneumoniae* infection often causes a mild and self-limiting disease, pneumonia develops in ≈10%–20% of pediatric patients (*1*). First-line therapies for *M. pneumoniae* infection are based on macrolides, a group of antimicrobial drugs widely used in outpatient settings because of their high oral bioavailability. However, overuse and indiscriminate use of macrolides have contributed to the emergence of macrolide-resistant *M. pneumoniae* (MRMP). Point mutations in the V region of the *M. pneumoniae* 23S rRNA gene have been associated with macrolide resistance (*2*). In recent years, prevalence of MRMP has increased and is very high in Asia (13.6%–100%) (*2*–*4*). During spring/summer 2023, hundreds of children with CAP were admitted daily to each of the major hospitals in Hanoi, Vietnam. *M. pneumoniae* has emerged as the major pathogen detected in approximately one third of patients with CAP (5). We analyzed the mutations in the 23S rRNA gene of *M. pneumoniae* isolated from nasopharyngeal samples of pediatric CAP patients during the 2023 outbreak in Vinmec Times City Hospital, Hanoi.

During May 1–July 31, 2024, the real-time PCR Allplex Respiratory Panel 4 detected *M. pneumoniae* in 411 (26.1%) of 1,578 nasopharyngeal samples from children with suspected CAP. Among *M. pneumoniae*–positive samples with a cycle threshold <30, we randomly selected 13 samples from 13 patients for gene sequencing. We amplified the DNA sequence of the 748-bp region (nt 1963–2710) of the 23S rRNA gene containing all known MRMP mutations by using MRMP-F1 (5′-CGTCCCGCTTGAATGGTGTA-3′) and MRMP-R1 (5′-GGCGCTACAACTGGAGCATA-3′). We sequenced the amplicons according to the Sanger sequencing method by using a BigDye Terminator v3.1 Cycle Sequencing Kit and Applied Biosystems 3500 Dx Genetic Analyzer instrument (both Thermo Fisher Scientific, https://www.thermofisher.com). We assembled the generated sequence data and analyzed them for variations by comparing with the reference *M. pneumoniae* strain M129 23S ribosomal RNA gene (GenBank accession no. NR_077056.1), using BLAST (http://blast.ncbi.nlm.nih.gov). We used ClustalW to perform multiple alignments (*6*). Subsequently, we constructed the phylogenetic tree according to the maximum-likelihood method with bootstrap analysis (n = 500) by using MEGA11 software (https://www.megasoftware.net). The 2-dimensional secondary structure of the 23S rRNA gene was predicted by the R2DT tool (RNAcentral) according to an SA_LSU_3D template provided by RiboVision (*7*).

Of the 13 samples, 6 (46.2%) showed single-nucleotide variation from the type strain sequence in the V region of the 23S rRNA gene. A known A2063G mutation was detected in 4 samples, and a novel variant C2353T was found in 2 samples (Figure, panel A).

The known MRMP mutation A2063G is the most prevalent mutation reported to date compared with other infrequent mutations (e.g., A2063T/C, A2064G, A2067G, A1290G, and C2617A) (*2*,*8*). Mutations at site 2063 are also associated with a high level of macrolide resistance (*9*,*10*). The National Institutes of Health databases showed no recorded evidence for the sequences containing the C2353T variant observed in our study (Figure, panel B). We hypothesize that under selection pressure during CAP treatment with macrolides, C2353T mutants have emerged with macrolide resistance. Previous reports have shown that different mutations can lead to different levels of macrolide affinity as well as MIC elevation (*8*). Demonstration of MRMP by culture and MIC is not regularly done in clinical practice; thus, rapid detection of MRMP mutation may provide useful information for guiding antimicrobial drug therapy.

[1]These authors contributed equally to this article.

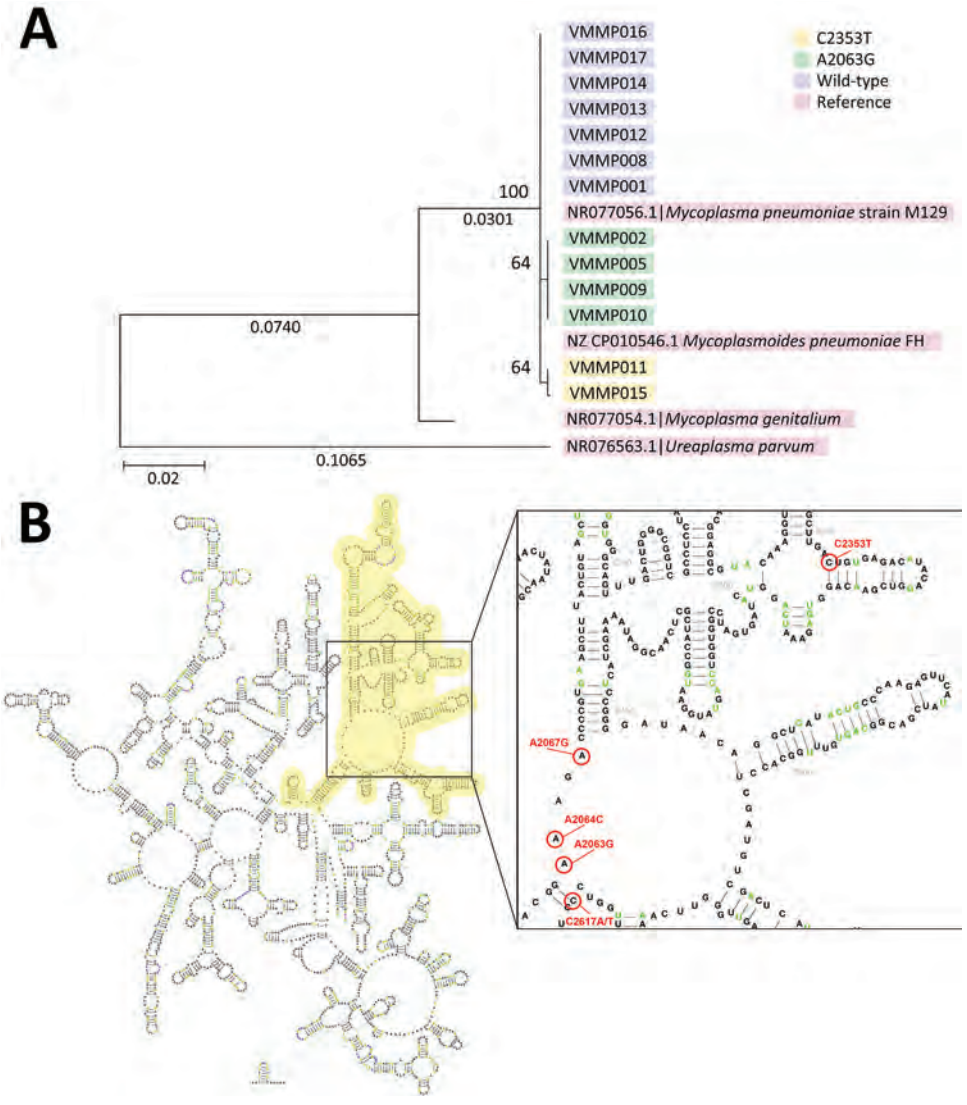

Figure. Phylogenetic tree and location of mutations for *Mycoplasma pneumoniae* strains identified in pediatric patients hospitalized with community-acquired pneumonia, Hanoi, Vietnam, spring/summer 2023. A) Maximum-likelihood phylogenetic analysis of the domain V region of the 23S rRNA gene. B) Predicted RNA secondary structure of 23S rRNA gene constructed with the description of known mutations (A2063G/C/T, A2064G, A2067G, C2617G) and novel variant (C2353T). Yellow highlights indicate the domain V region of 23S rRNA. Scale bar indicates base substitutions per site.

Clinical nonresponse to initial macrolide treatment was experienced by 3 (50%) of the 6 patients with the novel or known mutation and 2 (28.6%) of the 7 without (Table, https://wwwnc.cdc.gov/EID/article/30/5/23-1632-T1.htm; Appendix Table, https://wwwnc.cdc.gov/EID/article/30/5/23-1632-App1.pdf). Other respiratory bacteria were co-detected in approximately two thirds of patients in both groups, which might also affect clinical characteristics.

In summary, we detected the novel C2353T variant and known A2063G mutations in the 23S rRNA gene in nearly half of the pediatric patients with *M. pneumoniae*–associated CAP in Vinmec Times City Hospital during the 2023 outbreak in northern Vietnam. Our findings are consistent with those of other studies regarding the rising prevalence of MRMP in Southeast Asia. Our study findings may indicate circulation of different MRMP variants in Vietnam or emergence of new MRMP variants during the recent *M. pneumoniae*-associated CAP outbreak among children.

About the Author

Dr. Dinh-Dung Nguyen is a molecular genetics specialist at the Medical Genetics Department, Vinmec Hitech Center. His research interests are molecular biology, immunology, and gene-editing technology.

References

1. Krafft C, Christy C. *Mycoplasma* pneumonia in children and adolescents. Pediatr Rev. 2020;41:12–9. https://doi.org/10.1542/pir.2018-0016
2. Cao B, Qu JX, Yin YD, Eldere JV. Overview of antimicrobial options for *Mycoplasma pneumoniae* pneumonia: focus on macrolide resistance. Clin Respir J. 2017;11:419–29. https://doi.org/10.1111/crj.12379

3. Chen YC, Hsu WY, Chang TH. Macrolide-resistant *Mycoplasma pneumoniae* infections in pediatric community-acquired pneumonia. Emerg Infect Dis. 2020;26:1382–91. https://doi.org/10.3201/eid2607.200017
4. Yamazaki T, Kenri T. Epidemiology of *Mycoplasma pneumoniae* infections in Japan and therapeutic strategies for macrolide-resistant *M. pneumoniae*. Front Microbiol. 2016;7:693.https://doi.org/10.3389/fmicb.2016.00693
5. Hieu Vy NT. Children with increased *Mycoplasma* pneumonia, instructions for disease prevention [in Vietnamese] [cited 2023 Jun 26]. https://benhviennhitrung-guong.gov.vn/tre-mac-viem-phoi-do-mycoplasma-gia-tang-huong-dan-phong-benh.html
6. Thompson JD, Higgins DG, Gibson TJ. CLUSTAL W: improving the sensitivity of progressive multiple sequence alignment through sequence weighting, position-specific gap penalties and weight matrix choice. Nucleic Acids Res. 1994;22:4673–80.
7. Sweeney BA, Hoksza D, Nawrocki EP, Ribas CE, Madeira F, Cannone JJ, et al. R2DT is a framework for predicting and visualising RNA secondary structure using templates. Nat Commun. 2021;12:3494. https://doi.org/10.1038/s41467-021-23555-5
8. Kim JH, Kim JY, Yoo CH, Seo WH, Yoo Y, Song DJ, et al. Macrolide resistance and its impacts on *M. pneumoniae* pneumonia in children: comparison of two recent epidemics in Korea. Allergy Asthma Immunol Res. 2017;9:340–6. https://doi.org/10.4168/aair.2017.9.4.340
9. Lucier TS, Heitzman K, Liu SK, Hu PC. Transition mutations in the 23S rRNA of erythromycin-resistant isolates of *Mycoplasma pneumoniae*. Antimicrob Agents Chemother. 1995;39:2770–3. https://doi.org/10.1128/AAC.39.12.2770
10. Matsuoka M, Narita M, Okazaki N, Ohya H, Yamazaki T, Ouchi K, et al. Characterization and molecular analysis of macrolide-resistant *Mycoplasma pneumoniae* clinical isolates obtained in Japan. Antimicrob Agents Chemother. 2004;48:4624–30. https://doi.org/10.1128/AAC.48.12.4624-4630.2004

Address for correspondence: Huyen Thi Thanh Tran, Medical Genetics Department, Vinmec High Tech Center, 458 Minh Khai, Hai Ba Trung Hanoi 100000, Vietnam; email: v.huyenttt47@vinmec.com

Crimean-Congo Hemorrhagic Fever Virus in Ticks Collected from Cattle, Corsica, France, 2023

Paloma Kiwan, Shirley Masse, Geraldine Piorkowski, Nazli Ayhan, Morena Gasparine, Laurence Vial, Remi N. Charrel, Xavier de Lamballerie, Alessandra Falchi

Author affiliations: Unité des Virus Emergents, Aix Marseille Université, Università di Corsica, IRD140, INSERM 207 IRBA, Marseille, France (P. Kiwan, S. Masse, G. Piorkowski, N. Ayhan, M. Gasparine, R.N. Charrel, X. de Lamballerie, A. Falchi); Université de Corse–Institut National de Santé et de la Recherche Médicale, Corte, France (P. Kiwan, S. Masse, G. Piorkowski, N. Ayhan, M. Gasparine, R.N. Charrel, X. de Lamballerie, A. Falchi); Centre National de Référence des Arbovirus, Marseille, France (N. Ayhan, X. de Lamballerie); Université de Montpellier, Montpellier, France (L. Vial)

We report the detection of Crimean-Congo hemorrhagic fever virus (CCHFV) in Corsica, France. We identified CCHFV African genotype I in ticks collected from cattle at 2 different sites in southeastern and central-western Corsica, indicating an established CCHFV circulation. Healthcare professionals and at-risk groups should be alerted to CCHFV circulation in Corsica.

DOI: https://doi.org/10.3201/eid3005.231742

Crimean-Congo hemorrhagic fever (CCHF) is a tickborne disease caused by CCHF virus (CCHFV) (species *Orthonairovirus haemorrhagiae*, genus *Orthonairovirus,* family *Nairoviridae*, order *Bunyavirales*). Endemic in Africa, the Middle East, Asia, and Eastern Europe, CCHF has expanded to Western Europe (*1*). Repeated detection of CCHFV in Spain (*2*) raises questions about its circulation in neighboring countries, such as Portugal, Italy, and France.

In Corsica, a French Mediterranean island, a seroprevalence study of CCHFV conducted in livestock (cattle, goats, and sheep) during 2014–2016 showed an overall seroprevalence of 9.1%, and cattle harbored the highest rates (*3*). A subsequent surveillance study of 8,051 ticks collected from wild (wild boar, deer, and mouflon sheep) and domestic (cattle, horses, sheep) animals during 2016–2020 failed to detect CCHFV or nairovirus RNA (*4*).

Since 2022, we have continued CCHFV surveillance by collecting ticks from cattle at 2 slaughterhouses ≥2 times/month. Cattle originate from a broad

geographic area, and the national ear-tag identification system enables tracing of each animal's origin and farm owner (Figure). We identified ticks by using taxonomic keys, then pooled ticks by species, sex, development stage, study site, and animal host, as previously reported (*4*). We spiked each pool, consisting of 1–6 ticks, with a predefined amount of MS2 bacteriophage for monitoring nucleic acid extraction, reverse transcription PCR (RT-PCR), and nucleic acid amplification (*5*). We used MagMAX Viral/Pathogen Ultra Nucleic Acid Isolation Kit (Thermo Fisher Scientific, https://www.thermofisher.com) to purify nucleic acids. We tested each sample by using 2 real-time RT-PCRs, 1 targeting the large (L) RNA segment (*2*) and 1 targeting the small (S) RNA segment (*6*). We used the SuperScript IV One-Step RT-PCR System Kit (ThermoFisher) to design 28 CCHFV-specific pairs of primers to amplify the S, medium (M), and L segments (Appendix, https://wwwnc.cdc.gov/EID/article/30/5/23-1742-App1.pdf). We sequenced PCR products by using S5 Ion Torrent technology (ThermoFisher). We determined the best model by using the maximum-likelihood method and performed phylogenetic analyses by using MEGA6 software (*7*) (Figure).

During June 2022–July 2023, we collected 5,165 ticks from 465 cattle and grouped ticks into 1,491 pools. Tick species consisted of 2,390 (46.27%) *Rhipicephalus bursa*, 1,103 (21.35%) *Hyalomma marginatum*, 750 (14.52%) *Boophilus annulatus*, 507 (9.81%) *Hyalomma scupense*, 238 (4.60%) *Haemaphysalis punctata*, 127 (2.45%) *Ixodes ricinus*, 48 (0.92%) *Rhipicephalus*

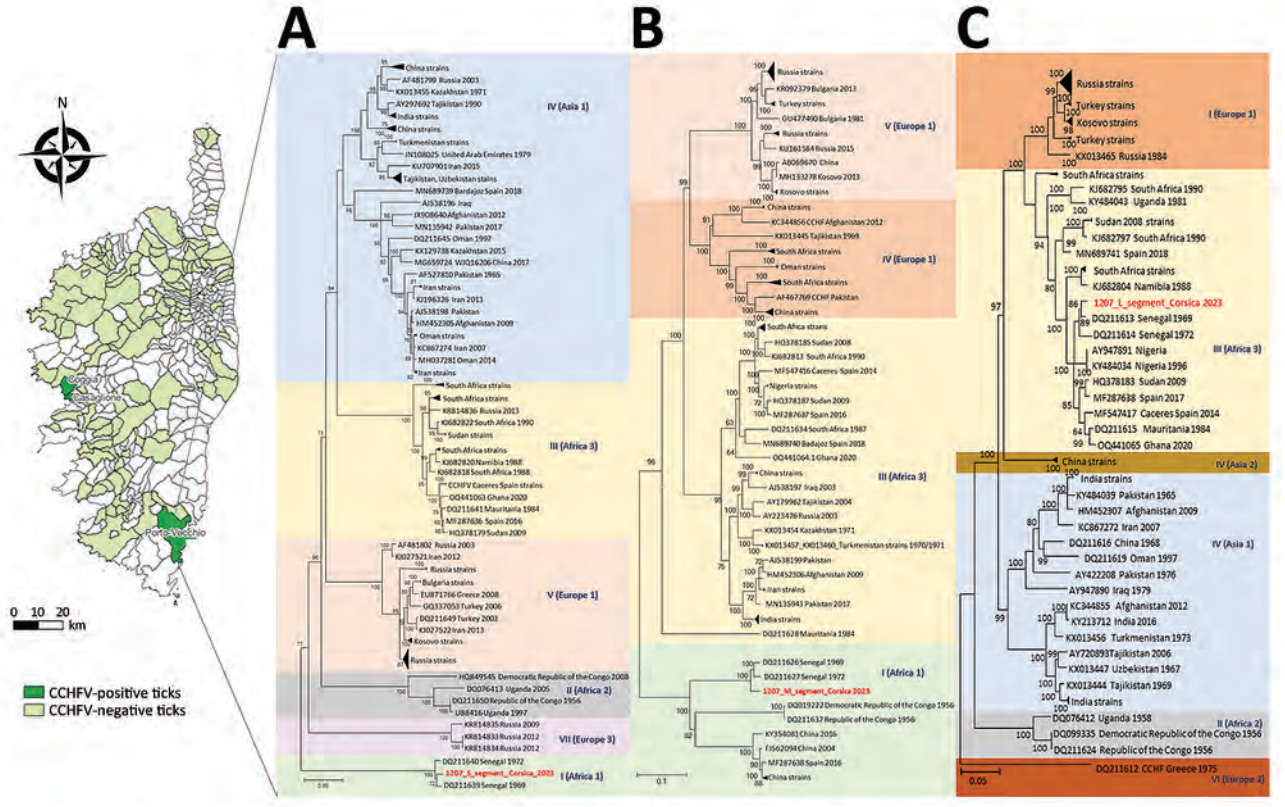

Figure. Phylogenetic analysis of Crimean-Congo hemorrhagic fever virus in ticks collected from cattle, Corsica, France, 2023. Map at left shows locations of cattle from which ticks were collected at the slaughterhouses of Ponte Leccia in the north and Cuttoli-Corticchiatto in the south during 2022–2023. Phylogenetic trees show small (A), medium (B), and large (C) RNA segments CCHFV strains. Red font indicates strains detected from Corsica; other sequences are named by GenBank accession number, geographic origin, and sampling year. Evolutionary analyses were conducted in MEGA6 (https://www.megasoftware.net) after best model determination. The optimal tree is shown for each fragment. Trees were constructed using the maximum-likelihood method based on sequences on the small (Tamura-Nei model), medium (general time-reversible model), and large (Tamura-Nei model) segments of the virus. All positions with <95% sequence site coverage were eliminated (i.e., <5% alignment gaps, missing data, or ambiguous bases were allowed at any position [partial deletion option]). Results of bootstrap test (1,000 replicates) are shown next to the branches. Genotypes are indicated by Roman numerals (*8*) with the equivalent clade nomenclature (*9*): I, West Africa (Africa 1); II, Central Africa (Africa 2); III, South and West Africa (Africa 3); IV, Middle East/Asia, divided into 2 groups Asia 1 and Asia 2; V (Europe 1), Europe/Turkey (Europe 1); VI, Greece (Europe 2); VII (Europe 3). Scale bars indicate nucleotide substitutions per site. CCHFV, Crimean-Congo hemorrhagic fever virus; L-RNA, large segment of CCHFV RNA.

Table. Description of Crimean-Congo hemorrhagic fever virus in tick pools collected from cattle, Corsica, France, 2023*

Cattle ID nos.	Cattle origin	Collection date	CCHFV–positive pool nos.	CCHFV assay, Ct		Tick species	Tick sex	No. ticks per pool
				L segment	S segment			
2478	Coggia	2022 Sep 27	417	IND	IND	*Haemaphysalis punctata*	F	1
6069	Coggia	2022 Sep 27	418	IND	IND	*H. punctata*	M	1
4376	Casaglione	2023 May 9	1252	IND	IND	*Rhipicephalus bursa*	M	6
			1253	IND	IND	*R. bursa*	M	6
4371	Casaglione	2023 May 9	1233	40.8	IND	*Hyalomma marginatum*	M	6
4039	Porto-Vecchio	2023 May 9	1204	35.9	IND	*R. bursa*	M	6
			1205	34.7	IND	*R. bursa*	F	6
			1206	34	IND	*R. bursa*	F	6
			1207	31.9	40	*R. bursa*	M	6
			1208	34.2	IND	*R. bursa*	M	6
			1209	33.7	IND	*R. bursa*	F	6
			1210	33.5	IND	*R. bursa*	M	6
			1211	32.9	IND	*Hyalomma marginatum*	M	6
			1212	34.7	40	*R. bursa*	M	6
			1213	33.2	IND	*Hyalomma marginatum*	F	6
			1214	33.1	IND	*R. bursa*	F	6
			1215	33.8	IND	*R. bursa*	F	6
			1218	34.2	IND	*Hyalomma marginatum*	M	4
			1219	35	IND	*Hyalomma marginatum*	F	6
			1220	35.1	IND	*Hyalomma marginatum*	M	3
			1221	34.1	IND	*R. bursa*	M	6
			1222	36.5	IND	*R. bursa*	M	6
			1223	35.7	IND	*Rhipicephalus sanguineus*	M	1
			1224	37.5	IND	*R. bursa*	F	1
Total			24 pools					119

*Pools of ticks were tested with quantitative reverse transcription PCR of the L and S segments of CCHFV RNA. A total of 24 pools comprising 119 ticks were tested CCHFV-positive from 5 animals. CCHFV, Crimean-Congo hemorrhagic fever virus; Ct, cycle threshold; ID, identification; IND, indeterminate (weakly positive); L, large; S, small.

sanguineus, and 2 (0.03%) *Dermacentor marginatus*. A total of 24 (1.70%) pools collected from 5 cattle from southern Corsica tested positive by the L-RNA assay (Table). Nineteen of the 24 tick pools were collected from 1 animal (no. 4039) (Table). Partial sequences for S (1,340 bp), M (4,894 bp), and L (11,275 bp) segments were obtained from animal nos. 2478 (pool 417) and 4039 (pool 1207) (Table). The effective detection of CCHFV genome is strongly supported by the formal exclusion of contamination because no CCHFV strain or genome had been previously processed in the laboratory, the PCR systems used can distinguish genomic RNA from the positive control (*6*), and the CCHFV sequences obtained were original and unambiguous.

The obtained S and M segment sequences constituted a monophyletic group belonging to genotype I (Africa 1), whereas the L segment sequence grouped with genotype III strains (Africa 3) (Figure). The sequences of all 3 segments of the CCHFV from Corsica are closely related to 2 sequences from Senegal corresponding to strains identified in the 1970s and likely represent strains reassorted in Senegal. Whether those strains are typical of strains from Senegal or have been circulating in other parts of Africa requires additional investigations.

Our results suggest that CCHFV strains circulating in Corsica and Spain have distinct origins. In Spain, genotype III is the most widespread and is most often detected in *H. lusitanicum* ticks (*2*), a species not yet identified in Corsica. Trans-Saharan migratory birds carrying *H. marginatum* ticks are the most likely source of CCHFV strains entering Corsica (*6*). Examination of the main bird migration routes suggests that 2 different migratory corridors link Spain and Corsica to Africa; mainly, but not exclusively, West Africa for Spain and Central Africa for Corsica (*6*). Those migration routes also could explain the different origin of CCHFV strains circulating in Corsica and in Spain.

Our results provide evidence for established CCHFV circulation in Corsica because detection occurred at 2 distinct sites in the southeastern and central western parts of the island. In addition, our results provide evidence for infection in cattle because multiple CCHFV-positive ticks were found on the same animal. CCHFV detection in feeding ticks is indicative of virus circulation within the cattle population but does not elucidate the role of ticks in virus transmission. Our results must be interpreted by considering previous serologic evidence of CCHFV circulation in cattle in Corsica (*3*), the presence of competent vectors locally (*4*), and recent reports of CCHFV detection in southern mainland France (*10*). The threat of possible continuous expansion and circulation of the virus over Western Europe should not be disregarded. Healthcare professionals and other groups at risk for infection, including hunters and farmers, should be informed about CCHFV circulation in Corsica.

Acknowledgments

We thank the staff of the slaughterhouses for their help in collecting ticks from cattle. We thank Gregory Mollé, Laurence Thirion, Pierre Combe, and Cecile Baronti for the production and validation of diagnostic reagents.

This work was supported in part by the VHFMODRAD project (no. 823666, call H2020-JTI-IMI2-2015-08-single-stage) of the H2020 program by the Innovative Health Initiative (IHI) agency of the European Commission; by the European Commission European Virus Archive Global project (EVA GLOBAL, grant agreement no. 871029) of the Horizon 2020 Research and Innovation Programme; and by Centre de Coopération Internationale en Recherche Agronomique pour le Développement (provision of service no. E2F03F6F). The reagent material was provided by the European Virus Archive-Marseille (EVAM) under the label technological platforms of Aix-Marseille University.

About the Author

Ms. Kiwan is a PhD student at the Unité des Virus Emergents, University of Corsica Pascal Paoli and Aix-Marseille University, France. Her primary research interests focus on tickborne viruses via a One Health approach.

References

1. Lorenzo Juanes HM, Carbonell C, Sendra BF, López-Bernus A, Bahamonde A, Orfao A, et al. Crimean-Congo hemorrhagic fever, Spain, 2013–2021. Emerg Infect Dis. 2023;29:252–9. https://doi.org/10.3201/eid2902.220677
2. Sánchez-Seco MP, Sierra MJ, Estrada-Peña A, Valcárcel F, Molina R, de Arellano ER, et al.; Group for CCHFv Research. Widespread detection of multiple strains of Crimean-Congo hemorrhagic fever virus in ticks, Spain. Emerg Infect Dis. 2021;28:394–402. https://doi.org/10.3201/eid2802.211308
3. Grech-Angelini S, Lancelot R, Ferraris O, Peyrefitte CN, Vachiery N, Pédarrieu A, et al. Crimean-Congo hemorrhagic fever virus antibodies among livestock on Corsica, France, 2014–2016. Emerg Infect Dis. 2020;26:1041–4. https://doi.org/10.3201/10.3201/eid2605.191465
4. Cicculli V, Maitre A, Ayhan N, Mondoloni S, Paoli JC, Vial L, et al. Lack of evidence for Crimean-Congo hemorrhagic fever virus in ticks collected from animals, Corsica, France. Emerg Infect Dis. 2022;28:1035–8. https://doi.org/10.3201/eid2805.211996
5. Ninove L, Nougairede A, Gazin C, Thirion L, Delogu I, Zandotti C, et al. RNA and DNA bacteriophages as molecular diagnosis controls in clinical virology: a comprehensive study of more than 45,000 routine PCR tests. PLoS One. 2011;6:e16142. https://doi.org/10.1371/journal.pone.0016142
6. Estrada-Peña A, D'Amico G, Fernández-Ruiz N. Modelling the potential spread of *Hyalomma marginatum* ticks in Europe by migratory birds. Int J Parasitol. 2021;51:1–11. https://doi.org/10.1016/j.ijpara.2020.08.004
7. Tamura K, Stecher G, Peterson D, Filipski A, Kumar S. MEGA6: Molecular Evolutionary Genetics Analysis version 6.0. Mol Biol Evol. 2013;30:2725–9. https://doi.org/10.1093/molbev/mst197
8. Chamberlain J, Cook N, Lloyd G, Mioulet V, Tolley H, Hewson R. Co-evolutionary patterns of variation in small and large RNA segments of Crimean-Congo hemorrhagic fever virus. J Gen Virol. 2005;86:3337–41. https://doi.org/10.1099/vir.0.81213-0
9. Carroll SA, Bird BH, Rollin PE, Nichol ST. Ancient common ancestry of Crimean-Congo hemorrhagic fever virus. Mol Phylogenet Evol. 2010;55:1103–10. https://doi.org/10.1016/j.ympev.2010.01.006
10. Anses – National Agency for Food, Environmental and Occupational Health Safety. Crimean-Congo hemorrhagic fever: first detection of the virus in cattle farms in southern France [in French] [cited 2023 Dec 18]. https://www.anses.fr/fr/content/fievre-hemorragique-crimee-congo-detection-virus-elevages-bovins

Address for correspondence: Alessandra Falchi, Unité des Virus Emergents, IRD 190-Inserm 1207, University of Corsica Pascal Paoli and Aix-Marseille University, Laboratoire de Virologie, Faculté des Sciences, Campus Grimaldi, Corte 20250, France; email: falchi_a@univ-corse.fr

Deforestation and Bovine Rabies Outbreaks in Costa Rica, 1985–2020

Christie Jones, Amanda Vicente-Santos, Julie A. Clennon, Thomas R. Gillespie

Author affiliation: Emory University, Atlanta, Georgia, USA

DOI: https://doi.org/10.3201/eid3005.230927

In Latin America, rabies virus has persisted in a cycle between *Desmodus rotundus* vampire bats and cattle, potentially enhanced by deforestation. We modeled bovine rabies virus outbreaks in Costa Rica relative to land-use indicators and found spatial-temporal relationships among rabies virus outbreaks with deforestation as a predictor.

Costa Rica has benefited from effective vaccination campaigns to eliminate canine rabies virus infections. Still, the virus has endured, spread by vampire bats (*Desmodus rotundus*) to cattle, with rare but documented transfer from bats to humans (*1*,*2*). To determine how anthropogenic disturbance affects

rabies virus incidence and risk in this system, we investigated the relationship between land-use change and documented bovine rabies virus outbreaks in Costa Rica during 1985–2020.

Since 1985, the National Animal Health Service of Costa Rica (SENASA) has conducted rabies virus surveillance on domestic animals, confirming outbreaks of ≥1 cases by using fluorescent antibody testing (*3*). We mapped bovine rabies outbreaks during 1985–2020 reported by SENASA with neighboring land-use data by using QGIS 3.16.2 (QGIS, https://qgis.org). Ten outbreaks from the initial SENASA report (n = 119) were removed because of inaccurate location data, leaving 109 outbreaks for our study.

To evaluate outbreak probability and distribution, we used kernel density estimations with the QGIS default bandwidth to create spatial probability estimations on the basis of known outbreaks. We used a kernel function that smoothed and interpolated probabilities across the study area. We used a kernel radius of 10 km, the maximum vampire bat foraging range, limiting interpolation to the determined area (*4*). We applied a Kulldorff retrospective space-time scan with an elliptical spatial scan by using SaTScan version 9.7 (SaTScan, https://www.satscan.org) to detect the number of outbreak locations in space and time (*5*).

We applied logistic regression by using a generalized linear mixed model R-package (https://cran.r-project.org/web/packages/lme4/lme4.pdf) to evaluate the effects of land-use factors on bovine rabies virus outbreak locations compared with random control locations (n = 119). We set the district as a random effect to account for spatial effects. We set the number of control points to match the true number of SENASA-reported outbreaks. We created control locations by using the random points function in QGIS and by using the 2005 and 2017 agricultural land-use data to bind nonoutbreak samples to areas that could house cattle. We matched controls temporally to outbreaks on the basis of the proportion of outbreaks before and after 2006.

For each outbreak and control location, we used district-level human population density and cattle population density as explanatory variables. We used the distance to and area of forest cover from each outbreak and control location within a 10-km buffer of the location. For outbreaks and control events up to

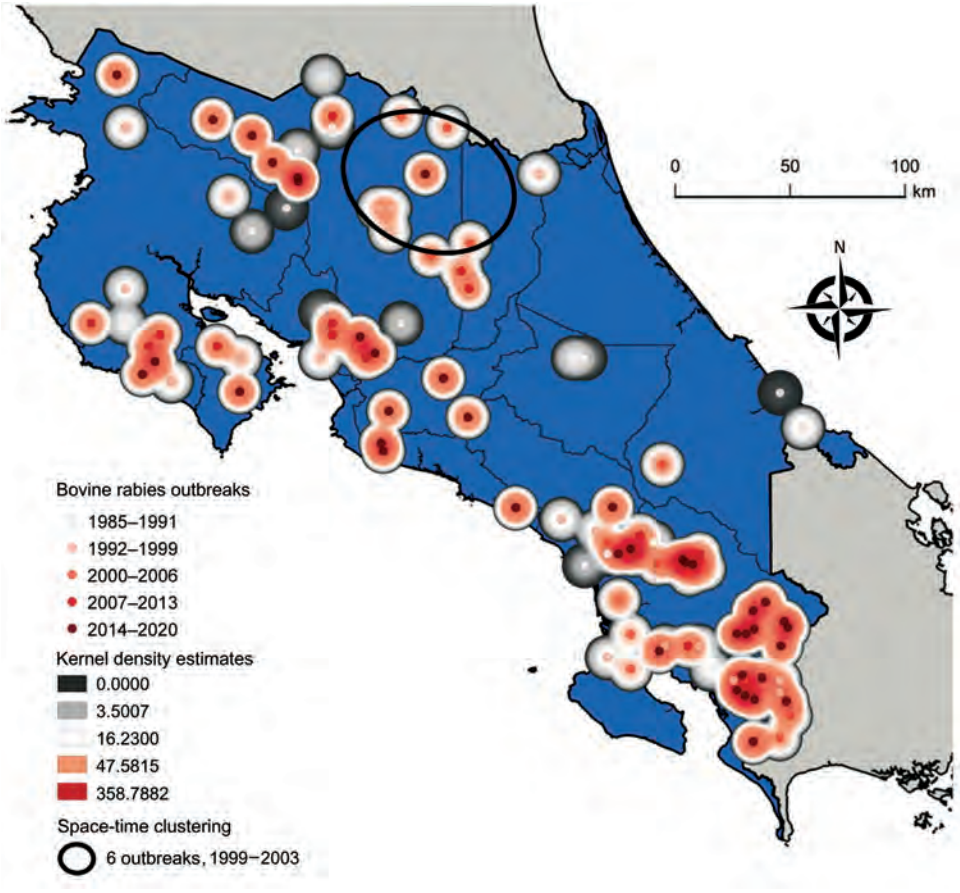

Figure. Kernel density estimations and Kulldorff space-time scan results for 109 bovine rabies outbreaks, Costa Rica, 1985–2020. Scan was limited to a 10-km distance from the epicenter of an outbreak to account for *Desmodus rotundus* vampire bat foraging ranges, enabling the detection of outbreak locations in space and time. Kernel density estimations were interpolated by using GeoDa version 1.18.0 (http://geodacenter.github.io), and the Kulldorff scan was implemented in SaTScan (https://www.satscan.org). The bovine rabies outbreak data is from the National Animal Health Service of Costa Rica. Map was created by using QGIS version 3.16.2 (https://qgis.org).

Table. Statistical relationship between bovine rabies virus outbreaks and relative variables of distance to forested areas, human density, and cattle density, Costa Rica, 1985–2020*

Relative variable	Estimate	SE	t-value	p value
Distance to forest	4.33×10^{-4}	3.32×10^{-1}	1.95	0.05†
Human density	-3.93×10^{-5}	1.93×10^{-5}	–1.53	0.13
Cattle density	-3.76×10^{-5}	3.23×10^{-5}	–0.93	0.35

*Results of a generalized linear mixed model regression analysis used to determine a statistical relationship between deforestation, human and bovine density, and bovine rabies outbreaks using data from the National Animal Health Service of Costa Rica, the 2014 Atlas of Costa Rica aerial photograph, the 2018 National Territorial Information System aerial photograph, population data, and population density estimates based on growth trends.
†p-value ≤0.05 is considered statistically significant.

2014, we calculated forest cover by using the 2014 aerial photograph from the Atlas of Costa Rica (http://www.kyriosoft.com/atlas). For outbreaks after 2014, we used a 2018 aerial photograph from the National Territorial Information System (https://www.snitcr.go.cr). We used human population data from 2011 for all detections up to 2011. After 2011, we used a human population density estimate based on national growth trends (*6*). We used a similar approach for cattle density data based on a dataset from 2014 (*7*).

Outbreaks occurring in the northern provinces of Alajuela and Heredia clustered on the basis on their statistically significant closeness in both location and time of occurrence (6 outbreaks during 1999–2003; log likelihood ratio 7.52; p = 0.035) (Figure). The increased number of outbreaks in southern Puntarenas Province may be because of repeated emergence given the lack of space-time clustering (Figure).

We found a positive association between the distance to forested areas and bovine rabies virus outbreaks (generalized linear mixed model estimate 4.33×10^{-4}, SE 3.32×10^{-1}; Z-value 1.95; p = 0.05) (Table). Each 1-km increase in distance from forested areas increased the probability of an outbreak by 4%. This finding aligns with our understanding of *D. rotundus* bat feeding preferences and rabies virus transmission risk. Decreased forested roosting site proximity appears to increase *D. rotundus* bat feeding behavior on cattle (*8*). Human and cattle densities were not associated with bovine rabies outbreaks (Table). Because human population data were unavailable until 2011 and cattle population data unavailable until 2014, the effect of those population densities may be skewed because agricultural intensification in Costa Rica has undergone major changes during the study period (*9*).

Our results show an association between deforestation and bovine rabies virus outbreaks, highlighting the importance of considering negative health effects in risk assessments for forest conversion proposals (*10*). Our results indicated the southern region of Costa Rica has the highest probability of bovine rabies outbreaks, indicating the need for localized, preventative interventions in the south. On the basis of recent findings, we must caution against bat culling as a response to this threat, because disrupting bat dispersal in unexpected ways may increase the spread of the rabies virus (*2*). Because rabies virus remains endemic in Latin America, an increased focus on integrating spatial, dietary, and surveillance data for *D. rotundus* bats is needed to provide additional insights into land-use effects on the persistence and spread of the rabies virus.

Acknowledgments

We thank Mariano Arroyo of the National Animal Health Services of Costa Rica for data access.

About the Author

Ms. Jones is a recent graduate of the joint Environmental Sciences and Environmental Health Bachelor of Science–Masters of Public Health Program at Emory University, Atlanta, Georgia. Her primary research interests are the application of one health and planetary health approaches to mitigating zoonoses.

References

1. Badilla X, Pérez-Herra V, Quirós L, Morice A, Jiménez E, Sáenz E, et al. Human rabies: a reemerging disease in Costa Rica? Emerg Infect Dis. 2003;9:721–3. https://doi.org/10.3201/eid0906.020632
2. Viana M, Benavides JA, Broos A, Ibañez Loayza D, Niño R, Bone J, et al. Effects of culling vampire bats on the spatial spread and spillover of rabies virus. Sci Adv. 2023;9:eadd7437. https://doi.org/10.1126/sciadv.add7437
3. Hutter SE, Brugger K, Sancho Vargas VH, González R, Aguilar O, León B, et al. Rabies in Costa Rica: documentation of the surveillance program and the endemic situation from 1985 to 2014. Vector Borne Zoonotic Dis. 2016;16:334–41. https://doi.org/10.1089/vbz.2015.1906
4. Rocha F, Ulloa-Stanojlovic FM, Rabaquim VCV, Fadil P, Pompei JC, Brandão PE, et al. Relations between topography, feeding sites, and foraging behavior of the vampire bat, *Desmodus rotundus.* J Mammal. 2020;101:164–71. https://doi.org/10.1093/jmammal/gyz177
5. Kulldorff M, Heffernan R, Hartman J, Assunção RM, Mostashari F. Space-time permutation model: a space-time permutation scan statistic for the early detection of disease outbreaks. PLoS Med. 2005;2:216–24. https://doi.org/10.1371/journal.pmed.0020059
6. National Institute of Statistics and Censuses. District population estimates and projections 2000 to 2025. 2014

[cited 2023 Jul 1] https://inec.cr/wwwisis/documentos/INEC/Estimaciones%20y%20Proyecciones/Estimaciones_Proyecciones_Distritales_2000-2025_2014.pdf
7. National Institute of Statistics and Censuses. VI National agricultural census: characteristics of farms and producers [in Spanish]. 2015 Jul [cited 2023 Jul 1] https://admin.inec.cr/sites/default/files/media/reagropeccenagro2014-ti-006_6.pdf
8. Fleischer R, Jones C, Ledezma-Campos P, Czirják GÁ, Sommer S, Gillespie TR, et al. Gut microbial shifts in vampire bats linked to immunity due to changed diet in human disturbed landscapes. Sci Total Environ. 2024;907:167815. https://doi.org/10.1016/j.scitotenv.2023.167815
9. Jadin I, Meyfroidt P, Lambin EF. International trade, and land use intensification and spatial reorganization explain Costa Rica's forest transition. Environ Res Lett. 2016;11:035005. https://doi.org/10.1088/1748-9326/11/3/035005
10. Gillespie TR, Jones KE, Dobson AP, Clennon JA, Pascual M. COVID-clarity demands unification of health and environmental policy. Glob Change Biol. 2021;27:1319–21. https://doi.org/10.1111/gcb.15508

Address for correspondence: Thomas Gillespie, Emory University, 400 Dowman Dr, Ste E510, Atlanta, GA, 30307, USA; email: thomas.gillespie@emory.edu

Novel Patterns in High-Resolution Computed Tomography in Whipple Pneumonia

Hui Li, Jiajia Wu, Xiaojun Mai, Wan Zeng, Shuping Cai, Xiuji Huang, Chunxia Zhou, Jin Li, Qin Jiang, Chunliu Lai, Canmao Xie

Author affiliation: The Seventh Affiliated Hospital, Sun Yat-sen University, Shenzhen, China

DOI: https://doi.org/10.3201/eid3005.231130

With the use of metagenomic next-generation sequencing, patients diagnosed with Whipple pneumonia are being increasingly correctly diagnosed. We report a series of 3 cases in China that showed a novel pattern of movable infiltrates and upper lung micronodules. After treatment, the 3 patients recovered, and lung infiltrates resolved.

Whipple pneumonia is a rare, chronic, multiorgan disease, with symptoms including arthritis, diarrhea, and weight loss. Diagnosis is traditionally confirmed by a histologic examination of a small bowel biopsy (*1*). The causative pathogen is *Tropheryma whipplei* bacteria, initially identified from the aortic valve of an endocarditis patient in 2000 (*2*). The bacterium was successfully cultured again in 2012 by using a sample of bronchoalveolar lavage fluid (BALF) from a pneumonia patient with an acute pulmonary infection (*2*). By using special culture systems, laboratories can grow positive staining or immunofluorescence detectable bacteria within a macrophage or fibroblast cell in 40–60 days. Metagenomic next-generation sequencing (mNGS) is a useful tool for diagnosis.

We report 3 patients in China diagnosed with *T. whipplei* pneumonia by using BALF mNGS (Vision Medicals Company, http://www.visionmedicals.com) screening during July 2021–December 2022. The patients had unique radiologic patterns, including upper lung gathering of micronodules forming a galaxy sign, and slightly movable infiltrates before, during, and after treatment.

Patient 1 was a 46-year-old man with a productive cough and a 5-year history of lung abnormality. His lung lesions gradually increased over time, and we found gathering micronodules forming a galaxy sign on the right upper lung (Appendix Figure 1, https://wwwnc.cdc.gov/EID/article/30/5/23-1130-App.pdf). *T. whipplei* bacteria was the only pathogen we recovered from BALF screened by using mNGS.

Patient 2 was a 67-year-old man with progressive dyspnea, productive cough, poor appetite, and weight loss. Repeated high-resolution computed tomography (CT) showed gradual increase of diffused micronodules gathering on the upper right lung for 6 months before diagnosis (Figure, panel A). Lesions in the upper right lung also showed movement. After bronchoscopic examination, *T. whipplei* bacteria was the only pathogen we recovered from BALF. Our histologic examination of the lung biopsy showed increased foamy macrophages within the alveolar space and thickened alveolar septal (Figure, panel B); neutrophils were the predominant cell type seen.

Patient 3 was a 57-year-old man with complaints of cough and chest tightness. We found diffuse ground-glass micronodules in the left upper lung (Appendix Figure 2). We performed mNGS of BALF and found *Cryptococcus* spp. yeast and *T. whipplei* bacteria. We treated the patient with fluconazole. Six months later,

the patient was readmitted to our hospital because of chest tightness and dry cough. We repeated mNGS, and *T. whipplei* bacteria was the only pathogen identified.

The lung tissue from all 3 patients was negative for periodic acid-Schiff and anti-acid staining. We performed an enteroscopic examination on the patients 2 and 3; both were negative. We treated the 3 patients with intravenous ceftriaxone (2 g/d) for 2 weeks, then we began combination therapy of minocycline and hydroxychloroquine for an extended period. All 3 patients responded well to treatment, and chest CT showed improvement of lung lesions.

We conducted a literature review for similar cases. We systematically reviewed PubMed for "T. whipplei" or "Whipple's disease" and "pneumonia" for the period July 2021–December 2022. We included literature for analysis if they provided individual patient and imaging data. We defined acute pulmonary infection by classic clinical manifestation and opacity on a chest radiograph or a CT scan. A total of 97 patients with Whipple pneumonia were mentioned. CT findings were available for 14 patients from 7 studies (2–8). The CT findings included bilateral alveolar consolidation, mass, nodule with

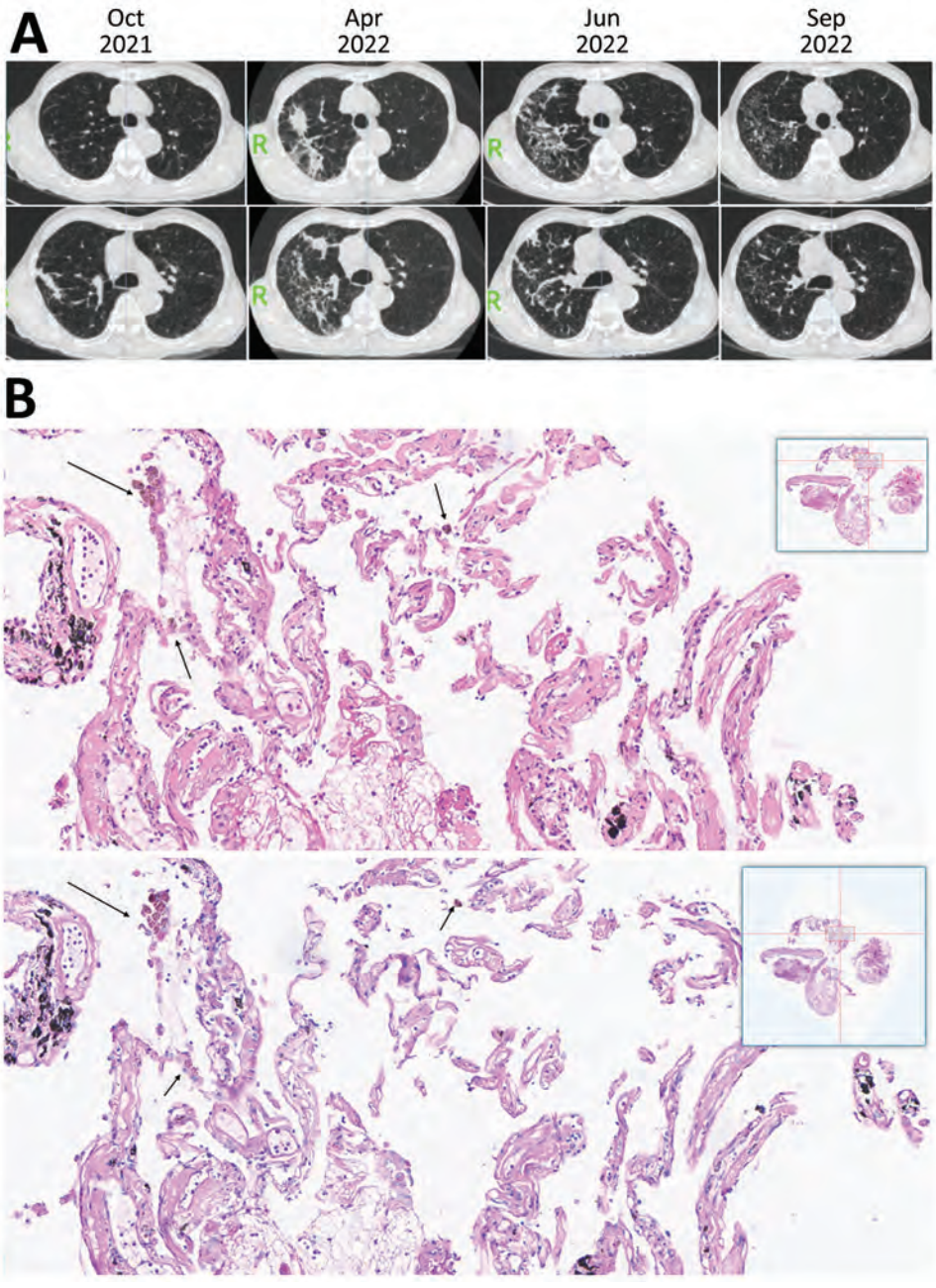

Figure. High-resolution computed tomography imaging and histology findings of the lung biopsy from a 67-year-old patient in China who had *Tropheryma whipplei* pneumonia. A) High-resolution computed tomography imaging showing gradual increase of diffused micronodules gathering in the upper right lung 6 months before diagnosis. In October 2021, micronodular and cord-like consolidation were seen on the upper right lung. In April 2022, the lesions were seen changing on both range and pattern and forming movable properties. In June 2022, the lesions were changed and scattered compared with lesions observed in April 2022. In September 2022, lesions were absorbed after 3 months of combined therapy consisting of minocycline and hydroxychloroquine. B) Magnified portion of slide showing histologic findings from the lung biopsy of the patient. The top image shows increased foamy macrophages within alveolar space, thickened alveolar septal and collagen deposition. The top image stain is hematoxylin and eosin staining, with arrows indicating foamy macrophages that have phagocytosed carbon pigment; the bottom image is periodic acid-Schiff staining and is negative for foamy macrophages. Insets show the entire histology slide.

Table. Categorized data from previously published studies on high-resolution CT findings, symptoms, inflammatory indicators, and immune status in patients with *Tropheryma whipplei* infection*

Study (reference)	Patient age, y/sex	CT findings	Symptoms	Inflammatory indicators	Patient immune status
Fenollar et al. (*2*)	70/F	Diffuse bilateral micronodular involvement, mediastinal lymphadenopathy	Nocturnal sweats, fever, dyspnea, myalgia, arthralgia, diarrhea	Unremarkable leukocyte and CRP levels	Immunocompetent
Stein et al. (*3*)	24/M	Right upper lobe pneumonia and bilateral alveolar condensation	Dyspnea, productive cough, high-grade fever	Elevated leukocyte and CRP levels	HIV
Zhang and Xu (*4*)	26/M	A thick-walled cavity in the left upper lung	Breathing-related chest pain	Unremarkable leukocyte and CRP levels	Immunocompetent
Kelly et al. (*5*)	31/M	Several discrete nodules	Dry cough with progressive weight loss, malaise, poor appetite	Elevated ESR	Immunocompetent
Li et al. (*6*)	39/F	Diffuse bilateral ground glass opacity and consolidation	Coughing, dyspnea, low-grade fever	Elevated neutrophil and CRP levels	Immunocompetent
Canessa et al. (*7*)	60/F	Alveolar consolidation in the left lower lobe, pleural effusion	Diarrhea, progressive dyspnea, dry cough, weight loss	Unknown	Unknown
Lin et al. (*8*)	Mixed	Nodular type: ground glass nodules or solid nodules; pneumonia type: focal or patchy mixed density shadow; other manifestations: cavity, cystic, or pleural effusion.	Respiratory symptoms, weight loss, fever, rare gastrointestinal symptoms	Unremarkable leukocyte and CRP levels	Unknown

*CRP, C-reactive protein; CT, computed tomography; ESR, erythrocyte sedimentation rate.

cavitation, ground-glass opacity, and diffuse micronodules (Table). Mediastinal lymphadenopathy was described in 1 patient. Therapeutic outcomes were described in 5 patients, and no patients died from pneumonia. Only 1 patient had a comparative chest CT before and after treatment. No patients demonstrated movable lung infiltrates.

A 17-year-long retrospective study identified 36 patients with positive PCR results of *T. whipplei* bacteria; of those, 8 patients had pulmonary involvement, and only 3 patients had abnormalities in chest imaging (*9*). Another study showed that 6.1% (88/1,430 samples) of BALF samples were positive for *T. whipplei* bacteria; 58 patients had pneumonia, and *T. whipplei* bacteria was identified as the causative pathogen for 9 patients (*10*). One study analyzed the characteristics of 70 patients positive for *T. whipplei* bacteria in BALF detected by mNGS in which *T. whipplei* was the only pathogen recovered for 20 patients (*8*); in that study, 15 patients received therapy, and 6 patients improved after treatment (*8*). In our study, *T. whipplei* bacteria was the only pathogen in 2 patients and was repeatedly detected in the third patient. In our patients, the infiltrates exhibited movable changes over time before, during, and after treatments. Histologic examination of case 2 showed a collagen and carbon deposition within lung tissue without any history of coal mine exposure, suggesting that *T. whipplei* bacterial infection can cause chronic infection and scar formation, eventually leading to granulomatous-like changes within lung tissue. All 3 patients symptoms improved after receiving the first-line treatment recommendation of minocycline and hydroxychloroquine (*1*).

In conclusion, Whipple pneumonia is increasingly recognized when mNGS is used. We report a relatively unique feature of CT findings in patients with Whipple pneumonia and provide support for choosing combination treatment using minocycline and hydroxychloroquine.

About the Author

Dr. Li is a respiratory diseases specialist at the Seventh Affiliated Hospital, Sun Yatsen University. Her research interests include the mechanisms of respiratory infection and lung injury.

References

1. Boumaza A, Ben Azzouz E, Arrindell J, Lepidi H, Mezouar S, Desnues B. Whipple's disease and *Tropheryma whipplei* infections: from bench to bedside. Lancet Infect Dis. 2022;22:e280–91. https://doi.org/10.1016/S1473-3099(22)00128-1
2. Fenollar F, Ponge T, La Scola B, Lagier JC, Lefebvre M, Raoult D. First isolation of *Tropheryma whipplei* from bronchoalveolar fluid and clinical implications. J Infect. 2012;65:275–8. https://doi.org/10.1016/j.jinf.2011.11.026

3. Stein A, Doutchi M, Fenollar F, Raoult D. *Tropheryma whipplei* pneumonia in a patient with HIV-2 infection. Am J Respir Crit Care Med. 2013;188:1036–7. https://doi.org/10.1164/rccm.201304-0692LE
4. Zhang WM, Xu L. Pulmonary parenchymal involvement caused by *Tropheryma whipplei*. Open Med (Wars). 2021;16:843–6. https://doi.org/10.1515/med-2021-0297
5. Kelly CA, Egan M, Rawlinson J. Whipple's disease presenting with lung involvement. Thorax. 1996;51:343–4. https://doi.org/10.1136/thx.51.3.343
6. Li W, Zhang Q, Xu Y, Zhang X, Huang Q, Su Z. Severe pneumonia in adults caused by *Tropheryma whipplei* and *Candida* sp. infection: a 2019 case series. BMC Pulm Med. 2021;21:29. https://doi.org/10.1186/s12890-020-01384-4
7. Canessa PA, Pratticò L, Sivori M, Magistrelli P, Fedeli F, Cavazza A, et al. Acute fibrinous and organising pneumonia in Whipple's disease. Monaldi Arch Chest Dis. 2008;69:186–8.
8. Lin M, Wang K, Qiu L, Liang Y, Tu C, Chen M, et al. *Tropheryma whipplei* detection by metagenomic next-generation sequencing in bronchoalveolar lavage fluid: a cross-sectional study. Front Cell Infect Microbiol. 2022;12:961297. https://doi.org/10.3389/fcimb.2022.961297
9. Duss FR, Jaton K, Vollenweider P, Troillet N, Greub G. Whipple disease: a 15-year retrospective study on 36 patients with positive polymerase chain reaction for *Tropheryma whipplei*. Clin Microbiol Infect. 2021;27:910.e9–13. https://doi.org/10.1016/j.cmi.2020.08.036
10. Lagier JC, Papazian L, Fenollar F, Edouard S, Melenotte C, Laroumagne S, et al. *Tropheryma whipplei* DNA in bronchoalveolar lavage samples: a case control study. Clin Microbiol Infect. 2016;22:875–9. https://doi.org/10.1016/j.cmi.2016.07.010

Address for correspondence: Hui Li, the Seventh Affiliated Hospital, Sun Yatsen University, 628 Zhenyuan Rd., Shenzhen, China; email: huil36@163.com; Canmao Xie, the Seventh Affiliated Hospital, Sun Yatsen University, 628 Zhenyuan Rd., Shenzhen, China; email: xiecanmao@163.com

Detection of Influenza D Antibodies in Dogs, Apulia Region, Italy, 2016 and 2023

Claudia Maria Trombetta, Serena Marchi, Maria Giovanna Marotta, Ana Moreno, Chiara Chiapponi, Emanuele Montomoli, Gianvito Lanave, Michele Camero, Vito Martella

Authors affiliations: University of Siena, Siena, Italy (C.M. Trombetta, S. Marchi, M.G. Marotta, E. Montomoli); VisMederi Research srl, Siena (C.M. Trombetta, E. Montomoli); Istituto Zooprofilattico Sperimentale della Lombardia e dell'Emilia-Romagna, Brescia, Italy (A. Moreno, C. Chiapponi); VisMederi srl, Siena (E. Montomoli); University of Bari, Valenzano, Italy (G. Lanave, M. Camero, V. Martella)

DOI: https://doi.org/10.3201/eid3005.231401

Dogs are known to be susceptible to influenza A viruses, although information on influenza D virus (IDV) is limited. We investigated the seroprevalence of IDV in 426 dogs in the Apulia region of Italy during 2016 and 2023. A total of 14 samples were positive for IDV antibodies, suggesting exposure to IDV in dogs.

Influenza D virus (IDV) was first identified from swine exhibiting influenza-like symptoms in 2011 in the United States (*1*). IDV RNA or antibodies have been detected worldwide in several animal hosts, including cattle, swine, small ruminants, camelids, and wild ungulates, although cattle are the main reservoir (*2*).

Because of social interactions, dogs are known to occasionally transmit pathogens to humans. In addition to being susceptible to canine influenza A viruses, dogs seem susceptible to common human influenza viruses and to avian viruses. Antibodies to influenza C virus (ICV) have been reported, suggesting that dogs may be naturally infected by ICV (*3*). However, information on the susceptibility of dogs to IDV is lacking.

We estimated the seroprevalence of IDV in household adult dogs on a total of 426 serum samples collected in 2016 (n = 169) and in 2023 (n = 257) in the Apulia region, Italy. The samples were collected by veterinary offices either for presurgical evaluation (n = 361) or for routine analysis (n = 65). We tested the samples in duplicate by using a hemagglutination inhibition (HI) assay against 2 IDV strains, D/bovine/

Table 1. Serum testing for influenza D virus results showing HI and VN assay titers of dog samples collected in 2016 in the Apulia region, Italy*

	D/bovine/Oklahoma/660/2013		D/swine/Italy/199724–3/2015	
Sample no.	HI	VN	HI	VN
4	10–10	<10	<10	<10
66	80–80	160–160	80–80	10–10

*Samples were tested against 2 strains of IDV, D/bovine/Oklahoma/660/2013 (D/660 lineage) and D/swine/Italy/199724–3/2015 (D/OK lineage). For calculation purposes, titers below the detectable threshold of 10 were expressed as <10. HI, hemagglutination inhibition assay; VN, virus neutralization assay.

Oklahoma/660/2013 (D/660 lineage; (provided by Prof. Feng Li, University of Kentucky) and D/swine/Italy/199724–3/2015 (D/OK lineage; obtained from the European Virus Archive). We tested the HI-positive samples and a subset of negative samples by virus neutralization (VN) assay. We analyzed the IDV-positive samples collected in 2023 for the presence of ICV antibodies (human influenza C/human/Victoria/2/2012 virus; provided by Victorian Infectious Diseases Reference Laboratory, Melbourne, Victoria, Australia), although the 2016 samples could not be screened because of the limited residual volume (Appendix Figure 1, https://wwwnc.cdc.gov/EID/article/30/5/23-1401-App1.pdf). We considered an IDV antibody titer ≥10 a positivity cutoff for the HI and VN assays (*4*).

Our screening of the 2016 samples for HI (Table 1) resulted in 2 samples (2/169; 1.2% [95% CI 0.05%–4.5%]) testing positive for the D/660 lineage. One of the 2 samples (1/169; 0.6% [95% CI 0.0%–3.6%]) was also positive for the D/OK lineage by HI. Only the sample with double HI reactivity was also positive in the VN assay. For the samples collected in 2023, a total of 12 samples (12/257; 4.7% [95% CI 2.6%–8.1%]) were positive for D/660 lineage by HI, and none of the samples were positive for D/OK lineage (Table 2). The 2023 samples positive for HI were also tested in VN, and only 5 serum samples (41.7%) possessed neutralizing antibodies for D/660 lineage. The HI titers of the positive samples ranged from 10 to 160. The VN titers of the positive samples ranged from 10 to 80 (Table 2). Five of the 12 HI-positive samples tested positive for antibodies against ICV (Table 2).

Our findings provide evidence of dog exposure to IDV at a low prevalence. Because most animals were household dogs, the source of exposure remains uncertain. Because our study was based on serologic investigations, any correlation between IDV infection and clinical signs in dogs could not be inferred. IDV infection in horses is subclinical, whereas in other animal species, IDV is associated with respiratory disease (*5*). Our findings are also partially in line with surveillance data from Europe and Italy suggesting the emergence of a D/660-like clade after the mid-2010s (*6*). In our study, none of the samples collected in 2023 reacted against D/OK, likely reflecting the epidemiology of IDV in susceptible animals in the Apulia region.

Although phylogenetic analyses have suggested that IDV is more closely related to ICV (≈53% homology of hemagglutinin-esterase fusion protein) than to influenza A and B viruses, no cross-reactivity was observed between IDV and human ICV by HI assay (*7*–*9*). To assess this potential issue caused by the genetic relatedness between IDV and ICV, the IDV-positive samples were also tested for ICV, and 5 samples did react against ICV. Four samples showed HI titers

Table 2. Serum testing for influenza D virus results showing HI and VN assay titers of dog samples collected in 2023 in the Apulia region, Italy*

Sample	D/bovine/Oklahoma/660/2013		D/swine/Italy/199724–3/2015		C/human/Victoria/2/2012
no.	HI	VN	HI	VN	HI
5	10–10	<10	<10	<10	40–40
18	10–10	20–20	<10	<10	<10
35	10–20	<10	<10	<10	<10
45	10–10	<10	<10	<10	<10
50	20–20	<10	<10	<10	20–10
55	40–40	10–10	<10	<10	80–80
98	10–10	<10	<10	<10	<10
118	10–10	20–20	<10	<10	40–40
137	160–160	80–80	<10	<10	<10
167	10–10	<10	<10	<10	80–80
183	20–20	<10	<10	<10	<10
216	20–20	20–20	<10	<10	<10

*Samples were tested against 2 strains of IDV, D/bovine/Oklahoma/660/2013 (D/660 lineage) and D/swine/Italy/199724–3/2015 (D/OK lineage), and against 1 strain of influenza C virus, C/human/Victoria/2/2012. For calculation purposes, titers below the detectable threshold of 10 were expressed as <10. HI, hemagglutination inhibition assay; VN, virus neutralization assay.

higher for ICV than for IDV, suggesting the possibility of cross-reactivity between IDV and ICV. Other serologic studies have investigated the antibody prevalence of IDV and ICV in animal populations (*8*–*10*), showing that serum reactivity in HI can vary among different IDV lineages and possibly between IDV and ICV. The combination of HI and VN assays may represent a good proxy of IDV circulation in animal hosts.

Our findings indicate that household dogs are exposed to IDV, potentially acting as a source of infection for humans. Although IDV does not seem to cause major forms of illness in humans and currently IDV is not regarded as an important public health threat, the possibility that some IDV strains may acquire the ability to evolve and adapt in the human host should not be disregarded. This potential risk could be higher in settings where there is more viral pressure, such as in groups with occupational exposure.

This publication was supported by the European Virus Archive GLOBAL project that received funding from the European Union's Horizon 2020 research and innovation program (grant agreement no. 871029).

Author contributions: conceptualization (C.M.T. and M.C.); formal analysis (S.M.); investigation (S.M. and M.G.M.); resources (C.M.T., G.L., M.C., and V.M.); data curation (S.M.); writing, original draft preparation (C.M.T. and V.M.); writing, review and editing (C.M.T., S.M., M.G.M., A.M., C.C., E.M., G.L., M.C., and V.M.); supervision (C.M.T. and S.M.); project administration (C.M.T.); and funding acquisition (C.M.T.).

Conflicts of interest: C.M.T. is an external consultant of VisMederi Research srl. E.M. is founder and chief scientific officer of VisMederi srl and VisMederi Research srl.

About the Author

Dr. Trombetta is an associate professor of hygiene and public health at the University of Siena. Her primary research interests include zoonotic viruses, infectious disease, and vaccine-preventable diseases.

References

1. Hause BM, Ducatez M, Collin EA, Ran Z, Liu R, Sheng Z, et al. Isolation of a novel swine influenza virus from Oklahoma in 2011 which is distantly related to human influenza C viruses. PLoS Pathog. 2013;9:e1003176. https://doi.org/10.1371/journal.ppat.1003176
2. Gaudino M, Moreno A, Snoeck CJ, Zohari S, Saegerman C, O'Donovan T, et al. Emerging influenza D virus infection in European livestock as determined in serology studies: are we underestimating its spread over the continent? Transbound Emerg Dis. 2021;68:1125–35. https://doi.org/10.1111/tbed.13812
3. Manuguerra JC, Hannoun C. Natural infection of dogs by influenza C virus. Res Virol. 1992;143:199–204. https://doi.org/10.1016/S0923-2516(06)80104-4
4. Saegerman C, Salem E, Ait Lbacha H, Alali S, Zouagui Z, Meyer G, et al. Formal estimation of the seropositivity cut-off of the hemagglutination inhibition assay in field diagnosis of influenza D virus in cattle and estimation of the associated true prevalence in Morocco. Transbound Emerg Dis. 2021;68:1392–9. https://doi.org/10.1111/tbed.13805
5. Sreenivasan CC, Uprety T, Reedy SE, Temeeyasen G, Hause BM, Wang D, et al. Experimental infection of horses with influenza D virus. Viruses. 2022;14:661. https://doi.org/10.3390/v14040661
6. Gaudino M, Chiapponi C, Moreno A, Zohari S, O'Donovan T, Quinless E, et al. Evolutionary and temporal dynamics of emerging influenza D virus in Europe (2009–22). Virus Evol. 2022;8(2):veac08.
7. Trombetta CM, Montomoli E, Di Bartolo I, Ostanello F, Chiapponi C, Marchi S. Detection of antibodies against influenza D virus in swine veterinarians in Italy in 2004. J Med Virol. 2022;94:2855–9. https://doi.org/10.1002/jmv.27466
8. Nedland H, Wollman J, Sreenivasan C, Quast M, Singrey A, Fawcett L, et al. Serological evidence for the co-circulation of two lineages of influenza D viruses in equine populations of the Midwest United States. Zoonoses Public Health. 2018;65:e148–54. https://doi.org/10.1111/zph.12423
9. Trombetta CM, Marchi S, Manini I, Kistner O, Li F, Piu P, et al. Influenza D virus: serological evidence in the Italian population from 2005 to 2017. Viruses. 2019;12:30. https://doi.org/10.3390/v12010030
10. Salem E, Cook EAJ, Lbacha HA, Oliva J, Awoume F, Aplogan GL, et al. Serologic evidence for influenza C and D virus among ruminants and camelids, Africa, 1991–2015. Emerg Infect Dis. 2017;23:1556–9. https://doi.org/10.3201/eid2309.170342

Address for correspondence: Claudia Maria Trombetta, Department of Molecular and Developmental Medicine, University of Siena, Aldo Moro 2, 53100, Siena, Italy; email: trombetta@unisi.it.

Detection of OXA-181 Carbapenemase in *Shigella flexneri*

Ghulam Dhabaan,[1] Hassan Jamal,[1] Danielle Ouellette, Sarah Alexander, Karen Arane, Aaron Campigotto, Manal Tadros, Pierre-Philippe Piché-Renaud

The Hospital for Sick Children, Toronto, Ontario, Canada (G. Dhabaan, H. Jamal, S. Alexander, K. Arane, A. Campigotto, M. Tadros, P.-P. Piché-Renaud); University of Toronto, Toronto (G. Dhabaan, H. Jamal, S. Alexander, K. Arane, A. Campigotto, M. Tadros, P.-P. Piché-Renaud); King Abdulaziz University, Jeddah, Saudi Arabia (H. Jamal); Western University, London, Ontario (D. Ouellette)

DOI: https://doi.org/10.3201/eid3005.231558

We report the detection of OXA-181 carbapenemase in an azithromycin-resistant *Shigella* spp. bacteria in an immunocompromised patient. The emergence of OXA-181 in *Shigella* spp. bacteria raises concerns about the global dissemination of carbapenem resistance in Enterobacterales and its implications for the treatment of infections caused by *Shigella* bacteria.

Shigella flexnerii infection leads to shigellosis, an acute gastrointestinal disease. Shigellosis affects socioeconomically disadvantaged and densely populated communities that have unsafe water, poor sanitation, and poor hygiene (*1*). *Shigella* spp. bacteria are major contributors to acute bloody diarrhea worldwide, adding to disease numbers and death in children under 5 years of age (*2*). The emergence of multidrug-resistant *Shigella* strains is a concerning trend. Multidrug-resistant strains resist multiple first-line oral antimicrobials (i.e., ampicillin, trimethoprim/sulfamethoxazole, and ciprofloxacin). The situation is further complicated by enzyme-mediated β-lactam resistance in *Shigella* bacteria, further impacting empiric therapy and making the isolates extensively drug-resistant (*2*). Although extensively drug-resistant isolates have remained susceptible to carbapenem therapy, carbapenem resistance in *Shigella* spp. through imipenemase-type metallo-β-lactamase, New Delhi metallo-β-Lactamase, and Verona integron-encoded metallo-β-lactamase has been reported (*3*,*4*).

We report a case of OXA-181–producing *S. flexneri* bacteria recovered from the stool of an immunocompromised patient with B-cell acute lymphoblastic leukemia (B-ALL). OXA-181 is a subtype of the OXA-48–like carbapenemase enzymes, classified as an Ambler class D β-lactamase, that primarily hydrolyzes penicillins and carbapenems. Those enzymes are usually transmitted on plasmids and are typically associated with Enterobacterales such as *Klebsiella pneumoniae* and *Escherichia coli* bacteria (*5*).

A 2-year-old girl, born in a rural area near Hyderabad, India, was diagnosed with standard-risk B-ALL. Her chemotherapy treatment was complicated by 2 episodes of culture-negative febrile neutropenia and acute gastroenteritis. Her diarrhea was presumed to be allopurinol-induced and was managed with supportive care. Her care team discovered evidence of a B-ALL relapse. The patient recovered from the fever and diarrhea, and her family immigrated to Canada, where the patient was admitted to a hospital to establish care for her relapsed B-ALL.

The patient was afebrile and did not have diarrhea until day 3 in the hospital, when she had onset of febrile neutropenia, nonbloody diarrhea, and abdominal pain. In accordance with the hospital's infection prevention protocol, we collected a stool sample for carbapenemase-producing Enterobacterales (CPE) screening. It exhibited growth of non–lactose fermenting colonies on the OXA side of a Chromid Carba Smart plate (bioMérieux, http://www.biomerieux.com), which we confirmed to be *S. flexneri* bacteria type 2a by using a biochemical panel and serotyping. We performed a stool PCR by using Seegene Allplex GI-EB gastrointestinal multiplex assay (SeeGene Inc., https://www.seegene.com) that showed the presence of *Shigella* spp. bacteria and astrovirus. We also isolated *S. flexneri* bacteria from a stool culture by using molecular detection (Appendix).

We began treatment for febrile neutropenia with piperacillin/tazobactam and vancomycin, in addition to azithromycin because of the detection of *S. flexneri* bacteria from the patient stool samples. Both isolates from the CPE screen and stool culture demonstrated a similar susceptibility profile (Table 1). Although the meropenem MIC was susceptible according to Clinical and Laboratory Standards Institute breakpoints, it was higher than 0.12 mg/L, the CPE screening cutoff in our laboratory protocol (*6*). We used the CARBA-5 assay (NG Biotech, https://www.ngbiotech.com) to further evaluate the antibiotic susceptibility, and the results indicated the presence of an OXA-48–like enzyme. The Public Health Ontario Laboratory verified the presence of OXA-48–like gene by using multiplex PCR (*7*). Because of the azithromycin resistance, we modified the treatment to trimethoprim/sulfamethoxazole.

[1]These authors contributed equally to this article.

Table 1. Antibiotic-susceptibility results using 4 different methodologies for the *Shigella flexneri* bacteria cultured from an immunocompromised patient, Canada*

Antibiotic	BD Phoenix,† mg/L	Broth microdilution, mg/L	Agar dilution, mg/L	CLSI breakpoints for susceptibility, mg/L	Kirby–Bauer disk diffusion, mm
Azithromycin	NA	NA	≥32	≤8	NA
Ceftriaxone	0.5	0.5	NA	≤1	28
Ceftazidime	0.5	1	NA	≤4	30
Ertapenem	>1	1	≤0.5	≤0.5	24
Meropenem	0.5	0.5‡	≤0.12	≤1	24
Ciprofloxacin	2	>2	NA	≤0.25	NA
TMP/SMX	≤0.5	2/38	NA	≤2/38	NA
Colistin	NA	NA	≤0.25	≤2§	NA

*CLSI, Clinical and Laboratory Standards Institute; NA, not available; TMP/SMX, trimethoprim/sulfamethoxazole.
†Becton Dickinson, https://www.bd.com.
‡Lowest concentration for meropenem on methodology used (Gram negative sensititer panel).
§Intermediate susceptibility.

After treatment, the patient experienced rapid defervescence and resolution of the diarrhea. We repeated the stool culture after 2 weeks of treatment, and the culture resulted in no growth of *S. flexneri* bacteria.

We conducted whole-genome sequencing (Appendix). We extracted DNA from the bacterial isolate by using easyMag (bioMérieux) and sequenced on a GridION system with a R10.4.1 flow cell (Oxford Nanopore Technologies, https://nanoporetech.com). We analyzed data with MinKNOW 23.04.5 (Oxford Nanopore Technologies) to construct a consensus genome. We analyzed the isolate's genome and plasmid with the Comprehensive Antibiotic Resistance Database (CARD) (http://arpcard.mcmaster.ca), identifying 5 resistance genes on the plasmid (Table 2), including OXA-181 with ≥95% identity and length within the plasmid. The plasmid has a size of 91,956 bp and carries all the genes for the resistance profile (Appendix). We deposited the plasmid gene sequence into GenBank (accession no. PP417752).

Given the low-hydrolytic activity of OXA-48–like enzymes, microbiology laboratories face difficult challenges in accurately detecting these enzymes in Enterobacterales. The Clinical and Laboratory Standards Institute breakpoints for meropenem are not suited for CPE surveillance, potentially missing OXA-48–like producers (*8*). Our laboratory has adopted a meropenem MIC breakpoint of >0.12 mg/L for CPE screening, in line with European Committee on Antimicrobial Susceptibility Testing recommendations (*9*). This approach is crucial for identifying isolates that require further CPE investigation, especially considering the reduced activity of OXA-48–like enzymes against cephalosporins.

Identification of an OXA-181 carbapenemase in a plasmid carried by *S. flexneri* bacteria is an alarming finding and concerning for the spread of this resistance profile in densely populated low- and middle-income communities. The detection of OXA-181 in *Shigella* spp. bacteria increases concerns about the broad dissemination of carbapenem resistance among other Enterobacterales (*10*). This finding emphasizes the need for vigilant and targeted surveillance for CPE in at-risk patients.

Table 2. Antibiotic-resistance genes detected within the plasmid recovered from a *Shigella flexneri* bacteria cultured from an immunocompromised patient sample, based on the Comprehensive Antibiotic Resistance Database,* Canada

Gene	Phenotypic resistance
OXA-181	Carbapenems
qnrS1	Fluoroquinolones
mrx	Macrolides
mphA	Macrolides
ermB	Macrolides

*Available at http://arpcard.mcmaster.ca.

Dr. Dhabaan is finishing his clinical microbiology fellowship at the University of Toronto. His interests include leveraging artificial intelligence alongside genomics and clinical data to advance infectious disease management.

References:

1. World Health Organization. Water, Sanitation and Hygiene (WASH) [cited 2024 Feb 26]. https://www.who.int/health-topics/water-sanitation-and-hygiene-wash.
2. Centers for Disease Control and Prevention Health Alert Network. Increase in extensively drug-resistant shigellosis in the United States [cited 2024 Feb 26]. https://emergency.cdc.gov/han/2023/pdf/CDC_HAN_486.pdf
3. Abdelaziz NA. Phenotype-genotype correlations among carbapenem-resistant Enterobacterales recovered from four Egyptian hospitals with the report of SPM carbapenemase. Antimicrob Resist Infect Control. 2022;11:13. https://doi.org/10.1186/s13756-022-01061-7
4. Thamizhmani R, Rhagavan R, Sugunan AP, Vijayachari P. VIM- and IMP-type metallo-β-lactamase-producing *Shigella* spp. in childhood diarrhea from Andaman Islands. Infect Dis (Lond). 2015;47:749–50. https://doi.org/10.3109/23744235.2015.1022874
5. Pitout JDD, Peirano G, Kock MM, Strydom KA, Matsumura Y. The global ascendency of OXA-48-type carbapenemases. Clin Microbiol Rev. 2019;33:e00102–19. https://doi.org/10.1128/CMR.00102-19
6. Clinical & Laboratory Standards Institute. Performance standards for antimicrobial susceptibility testing: thirty-third

informational supplement (M100-S33). Wayne (PA): The Institute; 2023.
7. Public Health Ontario. CPE – carbapenemase producing Enterobacteriaceae – Confirmation [cited 2024 Feb 26]. https://www.publichealthontario.ca/en/Laboratory-Services/Test-Information-Index/CPE-confirmation
8. Fattouh R, Tijet N, McGeer A, Poutanen SM, Melano RG, Patel SN. What is the appropriate meropenem MIC for screening of carbapenemase-producing Enterobacteriaceae in low-prevalence settings? Antimicrob Agents Chemother. 2015;60:1556–9. https://doi.org/10.1128/AAC.02304-15
9. European Committee on Antimicrobial Susceptibility Testing. EUCAST guideline for the detection of resistance mechanisms and specific resistances of clinical and/or epidemiological importance. Version 2.0. 2017 Jul [cited 2024 Feb 26]. https://www.eucast.org/resistance_mechanisms
10. Baker S, Scott TA. Antimicrobial-resistant *Shigella*: where do we go next? Nat Rev Microbiol. 2023;21:409–10. https://doi.org/10.1038/s41579-023-00906-1

Address for correspondence: Pierre-Philippe Piché-Renaud, The Hospital for Sick Children, 555 University Ave Toronto, ON M5G 1X8, Canada; email: pp.piche-renaud@sickkids.ca

SARS-CoV-2 IgG Levels as Predictors of XBB Variant Neutralization, Israel, 2022 and 2023

Yaniv Lustig, Michal Canetti, Victoria Indenbaum, Yovel Peretz, Yael Weiss-Ottolenghi, Ili Margalit, Keren Asraf, Tal Levin, Neta Zuckerman, Enosh Tomer, Michal Mandelboim, Ram Doolman, Noam Barda, Gili Regev-Yochay

Author affiliations: Sheba Pandemic Research Institute, Ramat-Gan, Israel (Y. Lustig, M. Canetti, Y. Peretz, Y. Weiss-Ottolenghi, I. Margalit, N. Zuckerman, G. Regev-Yochay); Tel-Aviv University Faculty of Medical and Health Sciences, Tel Aviv, Israel (Y. Lustig, M. Canetti, I. Margalit, M. Mandelboim, G. Regev-Yochay); Central Virology Laboratory, Public Health Services, Ministry of Health, Ramat-Gan (Y. Lustig, V. Indenbaum, T. Levin, N. Zuckerman, E. Tomer, M. Mandelboim); The Dworman Automated-Mega Laboratory, Ramat-Gan (K. Asraf, R. Doolman); ARC Innovation Center, Ramat-Gan (N. Barda); Ben-Gurion University of the Negev, Be'er Sheva, Israel (N. Barda)

DOI: https://doi.org/10.3201/eid3005.231739

Although a vaccine against SARS-CoV-2 Omicron-XBB.1.5 variant is available worldwide and recent infection is protective, the lack of recorded infection data highlights the need to assess variant-specific antibody neutralization levels. We analyzed IgG levels against receptor-binding domain–specific SARS-CoV-2 ancestral strain as a correlate for high neutralizing titers against XBB variants.

Since the beginning of 2023, SARS-CoV-2 Omicron XBB variants have led as the cause of global SARS-CoV-2 infections (*1*,*2*). SARS-CoV-2 mRNA vaccines based on the ancestral variant were shown to be less effective against Omicron variants, with reduced neutralization efficiency (*3*,*4*). Because of this reduced neutralization efficiency, updated mRNA vaccines, like the monovalent XBB1.15 vaccine, were developed and distributed (*5*). High levels of neutralizing and receptor-binding domain (RBD) binding IgG levels are known to be correlated with protection from infection or severe disease (*6*,*7*). The evasiveness of Omicron variants against neutralizing antibodies induced by vaccination or infection with previous variants demonstrated the importance of determining variant-specific neutralizing antibodies (*4*). In this study, we investigated the utility of measuring RBD IgG levels against the SARS-CoV-2 ancestral (wild-type [WT]) strain to predict titers of XBB-specific neutralizing antibodies.

During February 2022–August 2023, we obtained 1,070 samples from 373 study participants at Sheba Medical Center in Ramat Gan, Israel, and tested the samples for levels of IgG against WT-RBD and XBB-specific neutralizing antibody levels (Appendix, https://wwwnc.cdc.gov/EID/article/30/5/23-1739-

Table. Sex, age range, and COVID-19 history of patient participants who provided samples for testing IgG against SARS-CoV-2 ancestral strain and Omicron XBB-specific neutralizing antibody levels in 2022 and 2023, Israel*

Variable	Value
Sex	
F	251 (67)
M	122 (33)
No. COVID-19 vaccinations received	
0	1 (0.3)
1	13 (3.5)
2	5 (1.3)
3	102 (27)
4	215 (58)
5	36 (9.7)
6	1 (0.3)
No. COVID-19 infections	
0	227 (61)
1	120 (32)
2	22 (5.9)
3	3 (0.8)
4	1 (0.3)

*Values are no. (%) except as indicated.

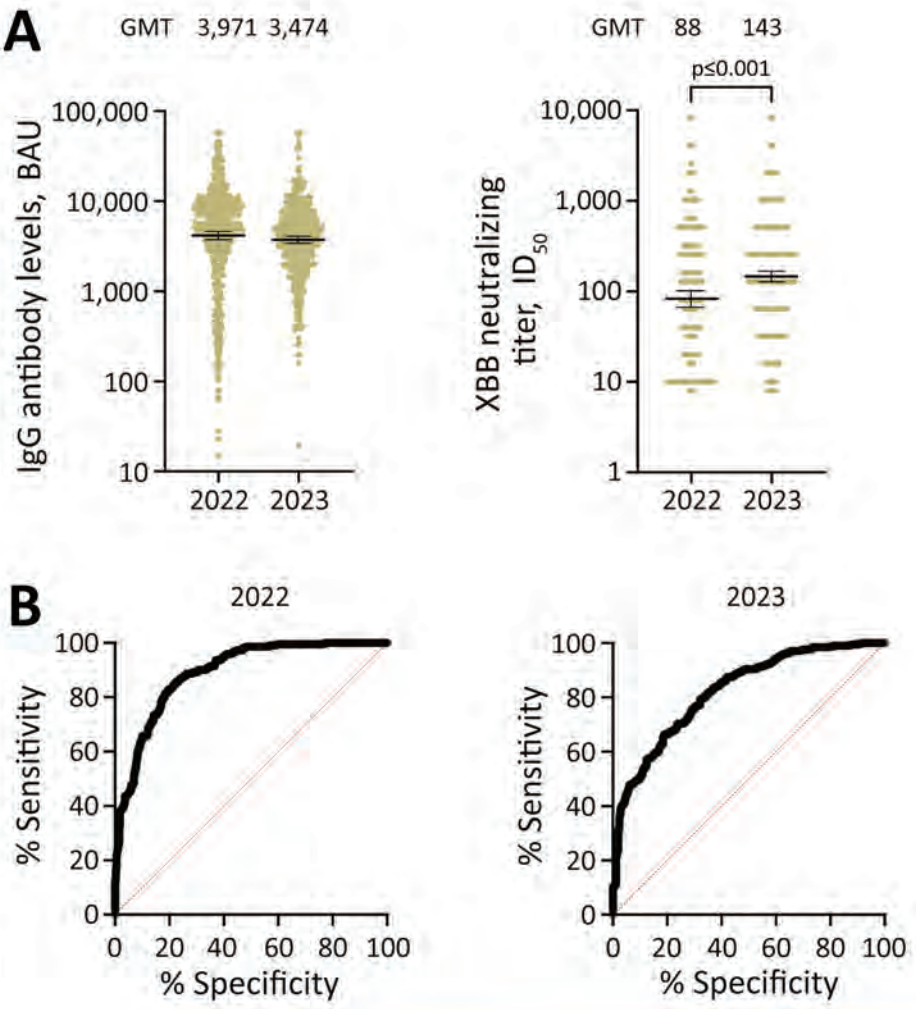

Year	Cutoff (BAU)	Sensitivity (95% CI)	Specificity (95% CI)
2022	>8,712	66% (59–72)	90% (87–93)
2023	>6,278	51% (44–58)	90% (85–93)

Figure. Binding IgG and neutralizing titer levels from samples collected in 2022 and 2023 from patient participants at the Sheba Medical Center, Israel, and the prediction of SARS-CoV-2 Omicron XBB neutralization by RBD-WT IgG levels from those samples. A) Scatter plot analyses of 1,071 WT IgG and XBB-specific neutralizing titers in samples obtained from healthcare workers during 2022 and 2023. Horizontal lines indicate GMTs; error bars indicate 95% CIs. GMT of each timepoint is indicated. B) ROC curves showing the diagnostic value of WT IgG levels for high (titer ≥250) XBB-specific neutralization levels. Sensitivity and specificity determinants for specific cut off levels are shown. BAU, binding antibody unit; GMT, geometric mean titer; ID_{50}, 50% inhibitory dilution; RBD, receptor-binding domain; ROC, receiver operating characteristic; WT, SARS-CoV-2 ancestral (wild-type) strain.

App1.pdf). Most of the study participants were vaccinated ≥3 times with the BNT162b2 (Pfizer-BioNTech, https://www.pfizer.com) or mRNA1273 (Moderna, https://www.modernatx.com) vaccines, and 39% were previously infected (Table; Appendix Table). Because XBB variants were only marginally circulating in Israel during 2022 but were the dominant variants during 2023 (Appendix Figure 1), we examined antibody levels separately for 2022 and 2023. Although IgG levels against WT virus were lower in 2023 (geometric mean titer of 3,474 binding antibody units [BAU] [95% CI 3,093–3,902] in 2022 vs. 3,971 BAU [95% CI 3,496–4,511] in 2023), 50% inhibitory dilution neutralizing antibody titers against XBB were significantly higher (geometric mean titer of 88 [95% CI 75–1,040] in 2022 vs. 143 [95% CI 121–168] in 2023) 2 (Figure 1, panel A).

We assessed the correlation between WT IgG and XBB neutralizing antibody levels. Although a strong correlation between RBD IgG and neutralizing antibody titers was maintained in both years, a stronger correlation was detected in 2022 (repeated measures correlation of 0.54 [95% CI 0.46–0.60]) compared with 2023 (repeated measures correlation of 0.31 [95% CI 0.17–0.44]). The regression co-efficient between IgG and neutralizing antibody levels was different for 2022 and 2023 (Appendix Figure 2). We found the expected

value of XBB specific neutralizing antibody titers for IgG of 7,000 BAU was 156 in 2022 and 276 in 2023.

We investigated if the correlation between WT IgG and XBB neutralization levels could be applied to predict persons with high XBB neutralization titers. A titer of 50% inhibitory dilution ≥1:250 was considered to be high neutralizing. US Food and Drug Administration guidelines consider titers of 50% inhibitory dilution ≥1:250 as eligible for transfusion as COVID-19 convalescent plasma (*8*,*9*). We found 36% of samples in 2022 and 46% of samples in 2023 had 50% inhibitory dilution ≥1:250. The area under the receiver operating characteristic curve was 0.89 (95% CI 0.87–0.92) for 2022 and 0.82 (95% CI 0.79–0.86) for 2023, suggesting a good discrimination between high and low titers based on WT IgG levels. Requiring a specificity of 90%, the receiver operating characteristic analysis showed a sensitivity of 66% (95% CI 59%–72%) for WT IgG levels >8,712 BAU in 2022 and a sensitivity of 51% (95% CI 44%–58%) for WT IgG levels >6,278 BAU in 2023 (Figure 1, panel B).

The results of our study show that measuring IgG against the SARS-CoV-2 ancestral strain (WT-RDB) can predict the presence of high neutralizing antibody levels against current circulating variants. We focused on the prediction of neutralizing antibodies against XBB variants because it was the immune antigen present in the vaccines available during the study period. We found that significantly higher XBB neutralizing antibody titers, but lower WT-RBD IgG levels were detected in samples obtained during 2023 compared with 2022. One explanation is that increased exposure to XBB-related variants in 2023 led to the development of XBB-specific antibodies paired with waning WT IgG levels. Our regression co-efficient analysis showed that samples obtained in 2022 had higher mean WT IgG levels than in 2023, despite having similar XBB neutralizing levels. The WT IgG level cutoff that can predict XBB-specific high neutralizing antibodies with 90% specificity was lower in 2023 compared with 2022.

The continued waves of COVID-19 infections together with SARS-CoV-2 vaccinations have diversified the immune protection of humans worldwide. Vital public health actions to prevent COVID-19 infections include prioritizing vaccination on the basis of known immunity, estimating the immune status of the population, ensuring COVID-19 convalescent plasma has high neutralizing antibodies, and investigating the effects of updated vaccines in persons with varying levels of neutralizing antibodies. Our results show that, regardless of any knowledge of previous SARS-CoV-2 infections, WT IgG levels are correlated and can predict XBB-specific neutralizing antibody titers.

About the Author

Dr. Lustig is the director of the Israeli Central Virology Laboratory of the Ministry of Health at Sheba Medical Center. His primary research interest is characterization of the immune response against emerging viral pathogens.

References

1. Chatterjee S, Bhattacharya M, Nag S, Dhama K, Chakraborty C. A detailed overview of SARS-CoV-2 omicron: its sub-variants, mutations and pathophysiology, clinical characteristics, immunological landscape, immune escape, and therapies. Viruses. 2023;15:167. https://doi.org/10.3390/v15010167
2. Miller J, Hachmann NP, Collier AY, Lasrado N, Mazurek CR, Patio RC, et al. Substantial neutralization escape by SARS-CoV-2 omicron variants BQ.1.1 and XBB.1. N Engl J Med. 2023;388:662–4. https://doi.org/10.1056/NEJMc2214314
3. Accorsi EK, Britton A, Fleming-Dutra KE, Smith ZR, Shang N, Derado G, et al. Association between 3 doses of mRNA COVID-19 vaccine and symptomatic infection caused by the SARS-CoV-2 omicron and delta variants. JAMA. 2022;327:639–51. https://doi.org/10.1001/jama.2022.0470
4. Nemet I, Kliker L, Lustig Y, Zuckerman N, Erster O, Cohen C, et al. Third BNT162b2 vaccination neutralization of SARS-CoV-2 omicron infection. N Engl J Med. 2022;386:492–4. https://doi.org/10.1056/NEJMc2119358
5. Regan JJ, Moulia DL, Link-Gelles R, Godfrey M, Mak J, Najdowski M, et al. Use of updated COVID-19 vaccines 2023–2024 formula for persons aged ≥6 months: recommendations of the advisory committee on immunization practices—United States, September 2023. MMWR Morb Mortal Wkly Rep. 2023;72:1140–6. https://doi.org/10.15585/mmwr.mm7242e1
6. Bergwerk M, Gonen T, Lustig Y, Amit S, Lipsitch M, Cohen C, et al. Covid-19 breakthrough infections in vaccinated health care workers. N Engl J Med. 2021;385:1474–84. https://doi.org/10.1056/NEJMoa2109072
7. Garcia-Beltran WF, Lam EC, Astudillo MG, Yang D, Miller TE, Feldman J, et al. COVID-19-neutralizing antibodies predict disease severity and survival. Cell. 2021;184:476–488.e11. https://doi.org/10.1016/j.cell.2020.12.015
8. McDyer JF, Azimpouran M, Durkalski-Mauldin VL, Clevenger RG, Yeatts SD, Deng X, et al. COVID-19 convalescent plasma boosts early antibody titer and does not influence the adaptive immune response. JCI Insight. 2023;8:e167890. https://doi.org/10.1172/jci.insight.167890
9. US Food and Drug Administration. 2021. COVID-19 convalescent plasma EUA decision memo 02052021 [cited 2021 Dec 27]. https://www.fda.gov/media/141480/download

Address for correspondence: Yaniv Lustig, Central Virology Laboratory, Sheba Medical Center, 2 Sheba Way, Ramat-Gan, Israel; email: yaniv.lustig@sheba.health.gov.il

Sporotrichosis Cluster in Domestic Cats and Veterinary Technician, Kansas, USA, 2022

Ian Hennessee, Erin Barber, Erin Petro, Stephanie Lindemann, Bryan Buss, Amanda Santos, Lalitha Gade, Shawn R. Lockhart, D. Joseph Sexton, Tom Chiller, Mitsuru Toda

Author affiliations: Centers for Disease Control and Prevention, Atlanta, Georgia, USA (I. Hennessee, B. Buss, A. Santos, L. Gade, S.R. Lockhart, J. Sexton, T. Chiller, M. Toda); Republican Valley Veterinary Clinic, Saint Francis, Kansas, USA (E. Barber); Kansas Department of Health and Environment, Topeka, Kansas, USA (E. Petro, S. Lindemann); Nebraska Department of Health and Human Services, Lincoln, Nebraska, USA (B. Buss)

DOI: http://doi.org/10.3201/eid3005.231563

We describe a feline sporotrichosis cluster and zoonotic transmission between one of the affected cats and a technician at a veterinary clinic in Kansas, USA. Increased awareness of sporotrichosis and the potential for zoonotic transmission could help veterinary professionals manage feline cases and take precautions to prevent human acquisition.

Sporotrichosis, an implantation mycosis caused by fungi in the genus *Sporothrix*, affects humans and other mammals. Although cat-transmitted sporotrichosis caused by the highly transmissible *Sporothrix brasiliensis* species is an increasing concern in Latin America (*1*), *S. brasiliensis* has not been detected in the United States, and cat-transmitted *Sporothrix schenckii* is rarely reported (*2*,*3*). We describe a cluster of sporotrichosis cases involving 2 domestic cats and zoonotic transmission between one of the affected cats and a veterinary technician in Kansas, USA.

In August 2022, a pregnant, 2-year-old, indoor-outdoor cat was brought to a veterinary clinic in northwest Kansas with an ulcerated lesion on her distal paw thought to be from a cat fight. She was initially treated with amoxicillin-clavulanic acid, but the wound worsened over the next month and additional ulcerated lesions developed along the rest of the forelimb (Figure, panel A).

The veterinarian performed an impression smear, which revealed cytology consistent with *Sporothrix* (Figure, panel B). The cat was treated with 10 mg/kg itraconazole and meloxicam in addition to amoxicillin-clavulanic acid. The cat improved on antifungal medication and gave birth to 2 healthy kittens in September 2022 (Figure, panel C). However, lesions reappeared after 1 month and began to extend up the limb. Treatment was adjusted to include terbinafine at 30 mg/kg, but the lesions continued to worsen and spread to the other 3 limbs. The cat was humanely euthanized, and the remains were cremated.

In November 2022, a veterinary technician caring for cat 1 at the clinic received a puncture wound through the glove from the cat's infected paw. A small blister developed at the puncture site approximately 2 weeks after the scratch (Figure, panel D). The blister quickly ulcerated, and the technician developed sporotrichoid lymphadenopathy up her arm (Figure, panels E, F). The technician began a treatment of cephalexin and then switched to 200 mg oral itraconazole twice daily and doxycycline. Cultures completed at Nebraska Medical Center were positive for *Sporothrix* spp., and an isolate was sent to the US Centers for Disease Control and Prevention (CDC) for identification. The isolate was identified as *S. schenckii* based on Sanger sequencing of the calmodulin gene (Appendix, https://wwwnc.cdc.gov/EID/article/30/5/23-1563-App1.pdf). Whole-genome sequencing showed the isolate clustered with historical *S. schenckii* isolates from the United States (bootstrap value of 100%) (Appendix Figure). The technician completed 8 months of oral itraconazole and recovered.

In February 2023, cat 1's owners brought another indoor-outdoor cat from the same property to the veterinary clinic with similar lesions. Cytology revealed *Sporothrix*. Cat 2 underwent a 4-month regimen of itraconazole 10 mg/kg, and the lesions healed.

This report describes a cluster of feline sporotrichosis cases in 2 indoor-outdoor cats and zoonotic transmission between 1 of the cats and a veterinary technician. The disease course of cat 1 highlights the potential severity of feline sporotrichosis. Early diagnosis of sporotrichosis and early treatment initiation with appropriate antifungal drugs can improve outcomes and help prevent transmission to other cats or humans (*4*). Cytology and culture should be considered for wounds or lesions that fail to respond to antibiotics. Itraconazole should be given to cats with food to improve absorption, and potassium iodide in combination with itraconazole can improve treatment efficacy in cats with multiple or extensive lesions or in treatment refractory cases (*5*,*6*).

This sporotrichosis cluster raised concerns that *S. brasiliensis* could be the etiologic agent. *S. brasiliensis* has increasingly been reported in Latin America (*1*), and 3 cases were recently reported in the United Kingdom, highlighting the potential for international spread (*7*). However, the etiologic agent in our report

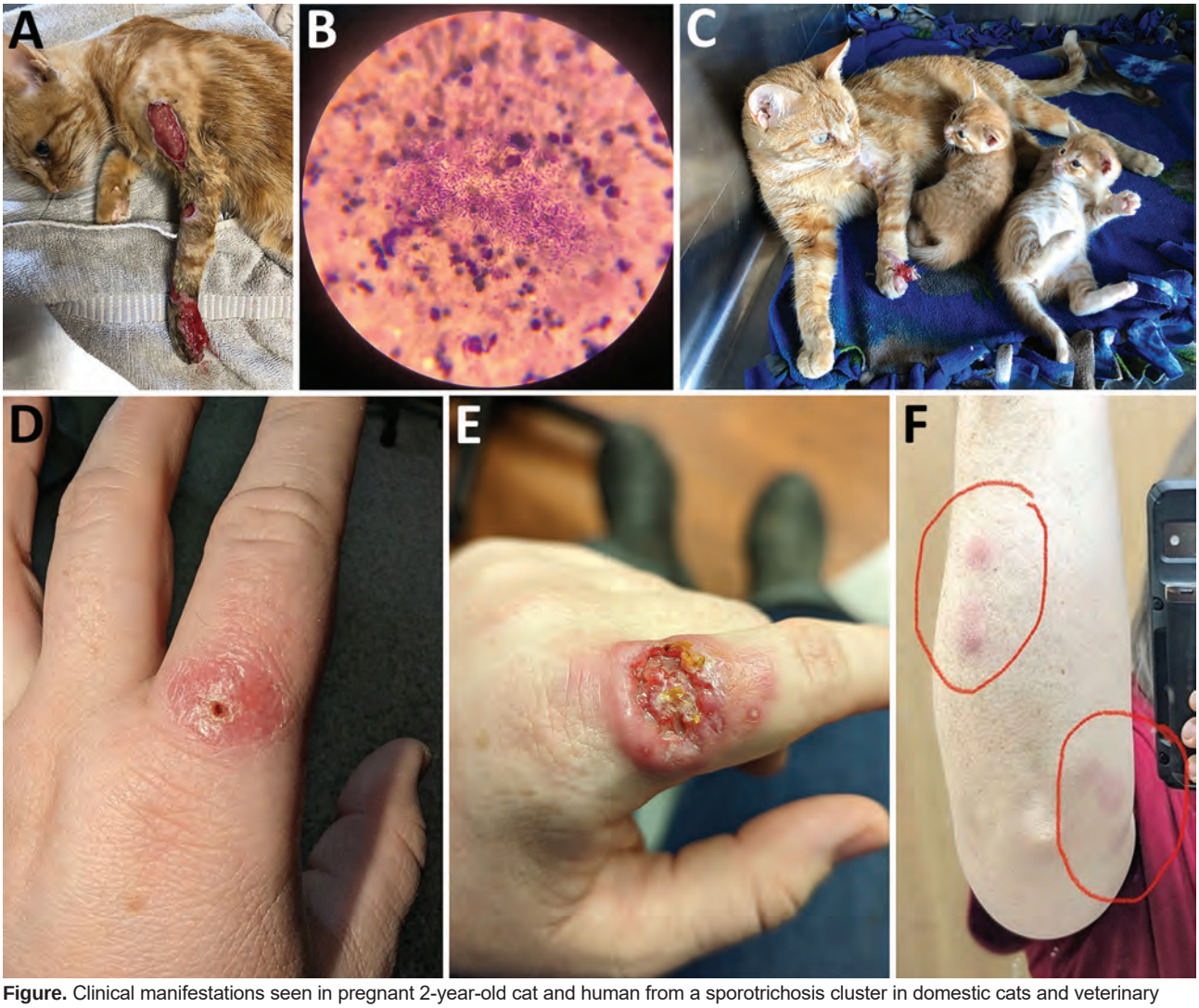

Figure. Clinical manifestations seen in pregnant 2-year-old cat and human from a sporotrichosis cluster in domestic cats and veterinary technician, Kansas, USA, 2022. A) Severe lesion on cat 1 in August 2022; B) cytological examination from cat 1's lesions showing numerous cigar-shaped yeasts consistent with *Sporothrix*; C) image of cat 1 with kittens and improved lesion in September 2022; D) lesion on the finger of a veterinary technician who had contact with cat 1; E) ulcerated and more severe lesion on technician's finger after X days; F) lymphadenopathy on technician's arm. Cat 1 initially was treated with antibiotics in August 2022 and lesions improved on antifungal therapy. However, the cat's lesions returned and worsened in October 2022, after discharge from the facility. In November 2022, a veterinary technician developed a small lesion 1 week after being poked through the glove by a claw on cat 1's infected paw. Lymphadenopathy progressed up the technician's arm (red circles, panel F) in a sporotrichoid pattern along dermal and lymphatic vessels.

was *S. schenckii*, which is typically acquired through traumatic contact with plant matter. Although rare, cat-transmitted *S. schenckii* cases have been reported in the United States and Southeast Asia (*2*,*3*,*8*).

To reduce zoonotic transmission risk, veterinary professionals should wear examination gloves when handling cats with suspected sporotrichosis and take precautions to avoid scratches or bites (*9*). Wounds from scratches or bites should be washed promptly with soap and water (https://www.cdc.gov/healthypets/pets/cats.html). Persons who have close contact with a cat with sporotrichosis should seek healthcare promptly if they develop lesions or sporotrichoid lymphadenopathy (*1*,*3*).

This report was limited by a lack of detailed exposure information for how the cats acquired sporotrichosis. Nevertheless, keeping cats indoors is recommended to prevent environmental acquisition of sporotrichosis (*1*,*2*). Risk factors for feline acquisition of sporotrichosis likely resemble those for humans, including traumatic inoculation or wound contamination with hay, roses, or sphagnum moss, or bites or scratches from other cats (*9*,*10*). Intact male, free-roaming cats might be at increased risk for

sporotrichosis (*10*). Cats with sporotrichosis should be kept indoors and apart from other cats in the home to reduce the potential for further transmission. In conclusion, increased awareness of sporotrichosis in cats and the potential for zoonotic transmission could help veterinary professionals more quickly recognize and treat feline cases and take precautions to prevent human acquisition in the veterinary setting.

Acknowledgments

We gratefully acknowledge the cat owners as well as the veterinary technician who shared her experience for this report. We also acknowledge Dr. Karen Wu for facilitating the initial connection between the Kansas veterinary office and CDC.

This activity was reviewed by CDC and was conducted consistent with applicable federal law and CDC policy (e.g., 45 C.F.R. part 46, 21 C.F.R. part 56; 42 U.S.C. §241(d); 5 U.S.C. §552a; 44 U.S.C. §3501 et seq).

About the Author

Dr. Hennessee is an Epidemic Intelligence Service Officer with the Mycotic Diseases Branch, Division of Foodborne, Waterborne, and Environmental Diseases, National Center for Emerging and Zoonotic Infectious Diseases, Centers for Disease Control and Prevention, Atlanta, Georgia, USA. His research focuses on the epidemiology, prevention, and control of emerging infectious diseases.

References

1. Rossow JA, Queiroz-Telles F, Caceres DH, Beer KD, Jackson BR, Pereira JG, et al. A One Health approach to combatting *Sporothrix brasiliensis*: narrative review of an emerging zoonotic fungal pathogen in South America. J Fungi (Basel). 2020;6:247. https://doi.org/10.3390/jof6040247
2. Rees RK, Swartzberg JE. Feline-transmitted sporotrichosis: a case study from California. Dermatol Online J. 2011;17:2. https://doi.org/10.5070/D30459K1JB
3. Reed KD, Moore FM, Geiger GE, Stemper ME. Zoonotic transmission of sporotrichosis: case report and review. Clin Infect Dis. 1993;16:384–7. https://doi.org/10.1093/clind/16.3.384
4. de Miranda LHM, Silva JN, Gremião IDF, Menezes RC, Almeida-Paes R, Dos Reis ÉG, et al. Monitoring fungal burden and viability of *Sporothrix* spp. in skin lesions of cats for predicting antifungal treatment response. J Fungi (Basel). 2018;4:92. https://doi.org/10.3390/jof4030092
5. Reis ÉG, Schubach TMP, Pereira SA, Silva JN, Carvalho BW, Quintana MSB, et al. Association of itraconazole and potassium iodide in the treatment of feline sporotrichosis: a prospective study. Med Mycol. 2016;54:684–90. https://doi.org/10.1093/mmy/myw027
6. Gremião IDF. Martins da Silva da Rocha E, Montenegro H, Carneiro AJB, Xavier MO, de Farias MR, et al. Guideline for the management of feline sporotrichosis caused by *Sporothrix brasiliensis* and literature revision. Braz J Microbiol. 2021;52:107–24. https://doi.org/10.1007/s42770-020-00365-3
7. Barnacle JR, Chow YJ, Borman AM, Wyllie S, Dominguez V, Russell K, et al. The first three reported cases of *Sporothrix brasiliensis* cat-transmitted sporotrichosis outside South America. Med Mycol Case Rep. 2023;39:14–7. https://doi.org/10.1016/j.mmcr.2022.12.004
8. Yingchanakiat K, Limsivilai O, Sunpongsri S, Niyomtham W, Lugsomya K, Yurayart C. Phenotypic and genotypic characterization and antifungal susceptibility of *Sporothrix schenckii sensu stricto* isolated from a feline sporotrichosis outbreak in Bangkok, Thailand. J Fungi (Basel). 2023;9:590. https://doi.org/10.3390/jof9050590
9. Welsh RD. Sporotrichosis. J Am Vet Med Assoc. 2003;223:1123–6. https://doi.org/10.2460/javma.2003.223.1123
10. Crothers SL, White SD, Ihrke PJ, Affolter VK. Sporotrichosis: a retrospective evaluation of 23 cases seen in northern California (1987–2007). Vet Dermatol. 2009;20:249–59. https://doi.org/10.1111/j.1365-3164.2009.00763.x

Address for correspondence: Ian Hennessee, Centers for Disease Control and Prevention, 1600 Clifton Road NE, Mailstop H24-10, Atlanta, GA 30329, USA; email: xye0@cdc.gov

Burkholderia thailandensis Isolated from Infected Wound, Southwest China, 2022

Jin Li, Jishan Tan, Xingyun Xiong, Qiu Zhong, Weiping Lu

Author affiliations: Chongqing Medical University Affiliated Dazu Hospital, Chongqing, China (J. Li); Daping Hospital of Army Medical University, Chongqing (J. Li, Q. Zhong, W. Lu); General Hospital of Western Theater Command, Chengdu, China (J. Tan); Dazhu County People's Hospital, Dazhou, Sichuan, China (X. Xiong)

DOI: http://doi.org/10.3201/eid3005.230743

We report a clinical isolate of *Burkholderia thailandensis* 2022DZh obtained from a patient with an infected wound in southwest China. Genomic analysis indicates that this isolate clusters with *B. thailandensis* BPM, a human isolate from Chongqing, China. We recommend enhancing monitoring and surveillance for *B. thailandensis* infection in both humans and livestock.

Burkholderia thailandensis is a member of the *Burkholderia pseudomallei* complex and is generally considered nonpathogenic (*1*). Initially identified in Thailand, *B. thailandensis* was distinguished from *B. pseudomallei* by its ability to assimilate arabinose (*2*). Similar to *B. pseudomallei*, *B. thailandensis* is frequently found in soil and water, especially in rice paddies (*3*,*4*). Although invasive infections caused by *B. thailandensis* are rare worldwide, recent reports have documented cases of suppurative infections, such as wound infections, cellulitis, and tissue abscesses (*5*,*6*). Previously, we identified a strain of *B. thailandensis* BPM that caused a human infection in Chongqing, southwest China (*7*). In this study, we report another clinical isolate of *B. thailandensis* that we obtained in Dazhu, Sichuan, southwest China, from an infected wound resulting from a cut inflicted by a farm tool in 2022.

A 61-year-old male farmer who had untreated type 2 diabetes mellitus reported a 1-month history of pain and swelling in his left knee. He had injured the middle toe of his left foot with a plow a month earlier, and redness, swelling, and pain developed below the left knee joint. Despite a week of antimicrobial treatment at a local community health center, his symptoms did not improve. In December 2022, the patient began to experience weakness in his right lower limb, and he later fell, sustaining an injury to his left lower limb. During this period, he experienced lower-limb weakness and exhibited symptoms related to the central nervous system. He sought care and was admitted to the orthopedics department of Dazhu County People's Hospital (Dazhou, China) for treatment of a left lower-limb injury and a left-foot diabetic foot infection. However, because his central nervous system symptoms worsened, he was transferred to the neurology department and receive a diagnosis of osteomyelitis and demyelinating disease. *B. thailandensis* strain 2022DZh was obtained from a deep-tissue specimen during surgical debridement of the infected wound on the left foot (Appendix Figure 1, https://wwwnc.cdc.gov/EID/article/30/5/23-0743-App1.pdf). The initial empirical antimicrobial therapy consisted of cefradine. However, the hospital laboratory tested the isolate 2022DZh using the VITEK 2 COMPACT system (bioMérieux, https://www.biomerieux.com) and identified it as *B. pseudomallei*, leading to a switch to intravenous meropenem treatment (Appendix Table 1). Despite treatment with meropenem, the patient's condition continued to deteriorate; he died 3 days after applying for discharge.

Subsequently, the isolate 2022DZh was submitted to the laboratory for confirmatory identification.

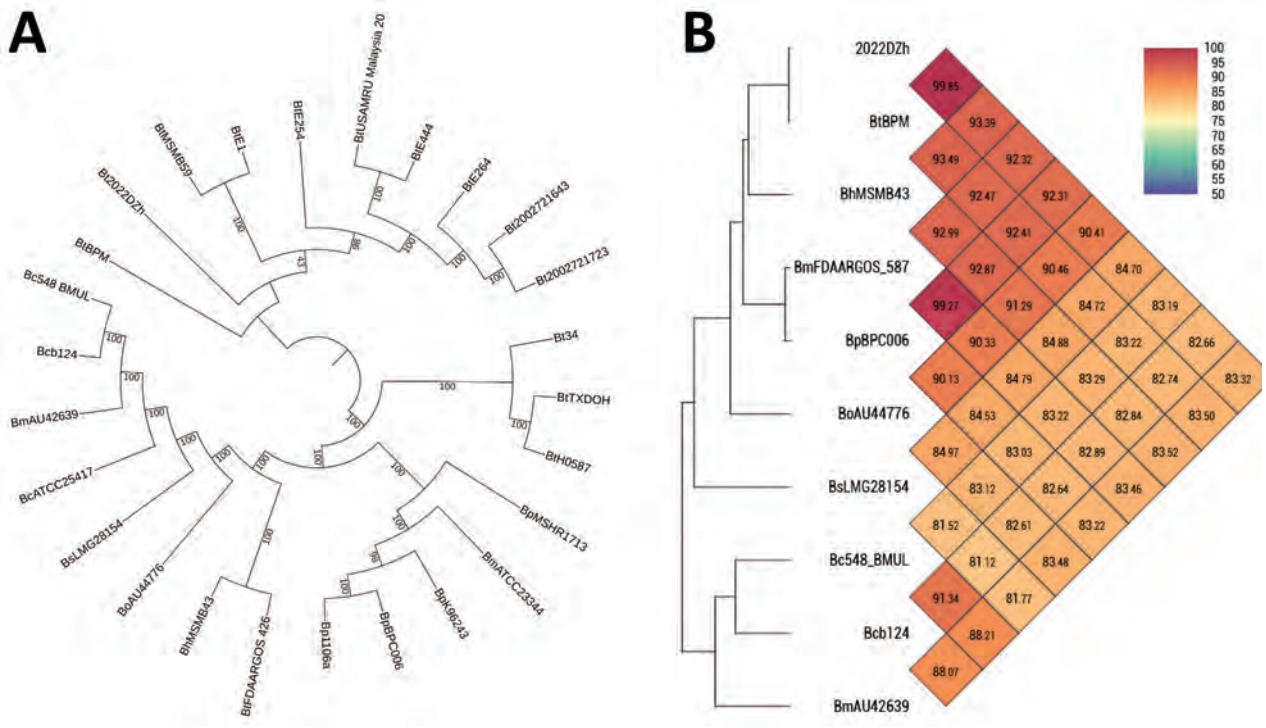

Figure. Analysis of the single-copy gene phylogenetic tree and average nucleotide identity for genomes of *Burkholderia thailandensis* 2022DZh from a patient in Dazhu, Sichuan, China, and other isolates from *Burkholderia* species. A) Single-copy gene phylogenetic tree created using the genomes of *B. thailandensis* 2022DZh and 25 other isolates from various *Burkholderia* species. B) Average nucleotide identity heatmap developed using genomes of *B. thailandensis* 2022DZh and 9 other isolates from various *Burkholderia* species.

Results of arabinose assimilation testing of isolate 2022DZh by API 20NE system (bioMérieux) were positive, consistent with the biochemical characteristics of *B. thailandensis* (Appendix Figure 2). We extracted DNA from the isolate 2022DZh for confirmation and further characterization. We performed 16S rRNA gene sequencing of 2022DZh using nucleotide BLAST (https://blast.ncbi.nlm.nih.gov/Blast.cgi), revealing 100% similarity with *B. thailandensis* BPM (Appendix Figure 3). The nucleotide sequences of the 2 chromosomes of isolate 2022DZh are >99.5% consistent with those of *B. thailandensis* E264 and *B. thailandensis* E254 (Appendix Table 2). We conclusively identified isolate 2022DZh as *B. thailandensis* based on our phenotypic and molecular data. We deposited the genome sequences of *B. thailandensis* strain 2022DZh into GenBank (accession nos. CP141809.1 and CP141811.1).

For phylogenetic analysis, we compared the genome of *B. thailandensis* 2022DZh with a reference panel of publicly available *Burkholderia* species genomes (Appendix Table 3). The single-copy gene phylogenetic tree analysis indicated that *B. thailandensis* 2022DZh clusters with *B. thailandensis* BPM (Figure, panel A). The results of average nucleotide identity revealed that *B. thailandensis* 2022DZh also clusters with *B. thailandensis* BPM; genome identity was 99.85%. However, when compared with *B. pseudomallei* BPC006, genome identity was 92.31% (Figure, panel B), consistent with the commonly used 95% threshold for distinguishing species. Through multilocus sequence type analysis (https://pubmlst.org/organisms/burkholderia-pseudomallei) (*8*), we determined that *B. thailandensis* 2022DZh and *B. thailandensis* BPM both belong to sequence type 76. In addition, there appears to be no known epidemiologic link between *B. thailandensis* 2022DZh and *B. thailandensis* BPM; they are geographically separated by a significant distance of ≈200 km (Appendix Table 3).

One limitation of this study is that we did not attempts to identify related isolates of *B. thailandensis* from environmental samples in this region of southwest China. Further studies are needed to identify the primary molecular mechanisms underlying the pathogenicity of *B. thailandensis* 2022DZh and to determine its molecular and evolutionary relationships with other strains of *B. thailandensis* (*9*).

In conclusion, our findings underscore that *B. thailandensis* can cause serious infections, and clinical practitioners should be aware of this type of infection (*10*). Therefore, we strongly recommend enhancing monitoring and surveillance for *B. thailandensis* infection in both humans and livestock.

This work was supported by the National Natural Science Foundation of China (82072348) and the Youth Project of the National Natural Science Foundation of China (82002113).

About the Author

Dr. Li is a researcher in the department of laboratory medicine, Daping Hospital, Army Medical University, Chongqing, China. His research primarily focuses on clinical microbiology and infectious disease.

References

1. Ronning CM, Losada L, Brinkac L, Inman J, Ulrich RL, Schell M, et al. Genetic and phenotypic diversity in *Burkholderia*: contributions by prophage and phage-like elements. BMC Microbiol. 2010;10:202. https://doi.org/10.1186/1471-2180-10-202
2. Lertpatanasuwan N, Sermsri K, Petkaseam A, Trakulsomboon S, Thamlikitkul V, Suputtamongkol Y. Arabinose-positive *Burkholderia pseudomallei* infection in humans: case report. Clin Infect Dis. 1999;28:927–8. https://doi.org/10.1086/517253
3. Birnie E, van 't Hof S, Bijnsdorp A, Mansaray Y, Huizenga E, van der Ende A, et al. Identification of *Burkholderia thailandensis* with novel genotypes in the soil of central Sierra Leone. PLoS Negl Trop Dis. 2019;13:e0007402. https://doi.org/10.1371/journal.pntd.0007402
4. Hall CM, Stone NE, Martz M, Hutton SM, Santana-Propper E, Versluis L, et al. *Burkholderia thailandensis* isolated from the environment, United States. Emerg Infect Dis. 2023;29:618–21. https://doi.org/10.3201/eid2903.221245
5. Gee JE, Elrod MG, Gulvik CA, Haselow DT, Waters C, Liu L, et al. *Burkholderia thailandensis* isolated from infected wound, Arkansas, USA. Emerg Infect Dis. 2018;24:2091–4. https://doi.org/10.3201/eid2411.180821
6. Glass MB, Gee JE, Steigerwalt AG, Cavuoti D, Barton T, Hardy RD, et al. Pneumonia and septicemia caused by *Burkholderia thailandensis* in the United States. J Clin Microbiol. 2006;44:4601–4. https://doi.org/10.1128/JCM.01585-06
7. Chang K, Luo J, Xu H, Li M, Zhang F, Li J, et al. Human infection with *Burkholderia thailandensis,* China, 2013. Emerg Infect Dis. 2017;23:1416–8. https://doi.org/10.3201/eid2308.170048
8. Tuanyok A, Mayo M, Scholz H, Hall CM, Allender CJ, Kaestli M, et al. *Burkholderia humptydooensis* sp. nov., a new species related to *Burkholderia thailandensis* and the fifth member of the *Burkholderia pseudomallei* complex. Appl Environ Microbiol. 2017;83:e02802–16. https://doi.org/10.1128/AEM.02802-16
9. Li J, Zhong Q, Li J, Chong HM, Wang LX, Xing Y, et al. Genomic features and virulence characteristics of a rare *Burkholderia thailandensis* strain causing human infection. J Med Microbiol. 2023;72:72. https://doi.org/10.1099/jmm.0.001688
10. Cossaboom CM, Marinova-Petkova A, Strysko J, Rodriguez G, Maness T, Ocampo J, et al. Melioidosis in a resident of Texas with no recent travel history, United States. Emerg Infect Dis. 2020;26:1295–9. https://doi.org/10.3201/eid2606.190975

Address for correspondence: Weiping Lu or Qiu Zhong, Department of Laboratory Medicine, Daping Hospital, Army Medical University, Chongqing, 400042, China; email: luweiping19710416@163.com or 410835830@qq.com

Reemergence of *Bordetella parapertussis*, United States, 2019–2023

Brooklyn A. Noble, Sarah S. Jiudice, Jay D. Jones, Tristan T. Timbrook

Author affiliations: bioMérieux, Salt Lake City, Utah, USA (B.A. Noble, S.S. Jiudice, J.D. Jones, T.T. Timbrook); University of Utah, Salt Lake City (T.T. Timbrook)

DOI: https://doi.org/10.3201/eid3005.231278

To determine changes in *Bordetella pertussis* and *B. parapertussis* detection rates, we analyzed 1.43 million respiratory multiplex PCR test results from US facilities from 2019 through mid-2023. From mid-2022 through mid-2023, *Bordetella* spp. detection increased 8.5-fold; 95% of detections were *B. parapertussis.* While *B. parapertussis* rates increased, *B. pertussis* rates decreased.

Whooping cough is a highly contagious, acute, respiratory illness caused by *Bordetella* spp. bacteria, primarily *B. pertussis* and *B. parapertussis*, and may be associated with complications such as pneumonia (*1*,*2*). Unlike *B. pertussis*, *B. parapertussis* is not notifiable in the United States because it is thought to be less prevalent and to cause milder symptoms than *B. pertussis* (*1*,*2*). Although isolation of *B. parapertussis* was uncommon in the United States before 2005, it has since been suggested that *B. parapertussis* infections are more common than previously recognized and may contribute to cases thought to result from vaccine failure (*1*,*3*). Our objective with this study was to detect recent changes in *B. pertussis* and *B. parapertussis* detection rates by using a cloud-based near real-time surveillance network.

We analyzed >1.43 million multiplex PCR results from 125 US facilities for January 1, 2019–July 31, 2023, for detection of *B. pertussis* or *B. parapertussis* (Table). Information on clinical manifestations, patient demographics, and confirmatory testing were not known. Facilities were primarily reference laboratories or hospitals, 12 of which were pediatric or contained a pediatric site, and all facilities used the BIOFIRE FILMARRAY Respiratory 2 (RP2) Panel, the BIOFIRE Respiratory 2.1 (RP2.1) Panel (bioMérieux, https://www.biomerieux.com), or both (*4*,*5*). The RP2 and RP2.1 tests detect nucleic acid of 21 (RP2) or 22 (RP2.1) pathogens commonly associated with respiratory infections and are identical, except the RP2.1 test can also detect SARS-CoV-2. Both tests detect *B. pertussis* (limit of detection of 1.0×10^3 CFU/mL) and *B. parapertussis* (limit of detection 4.1×10^1 CFU/mL) (*5*). Deidentified patient test results were captured by the BIOFIRE Syndromic Trends database, a cloud-based pathogen surveillance network (*6*). We excluded suspected verification, quality control, and proficiency tests (*6*).

We determined the total number of tests in the database and the number of those tests that detected *B. pertussis* or *B. parapertussis*, aggregated monthly (Figure, panel A), and detection rates (3-week centered rolling average) for *B. pertussis* and *B. parapertussis* (stacked) (Figure, panel B). During January 1, 2019–March 11, 2020 (before the COVID-19 pandemic), we observed that in the United States, the average

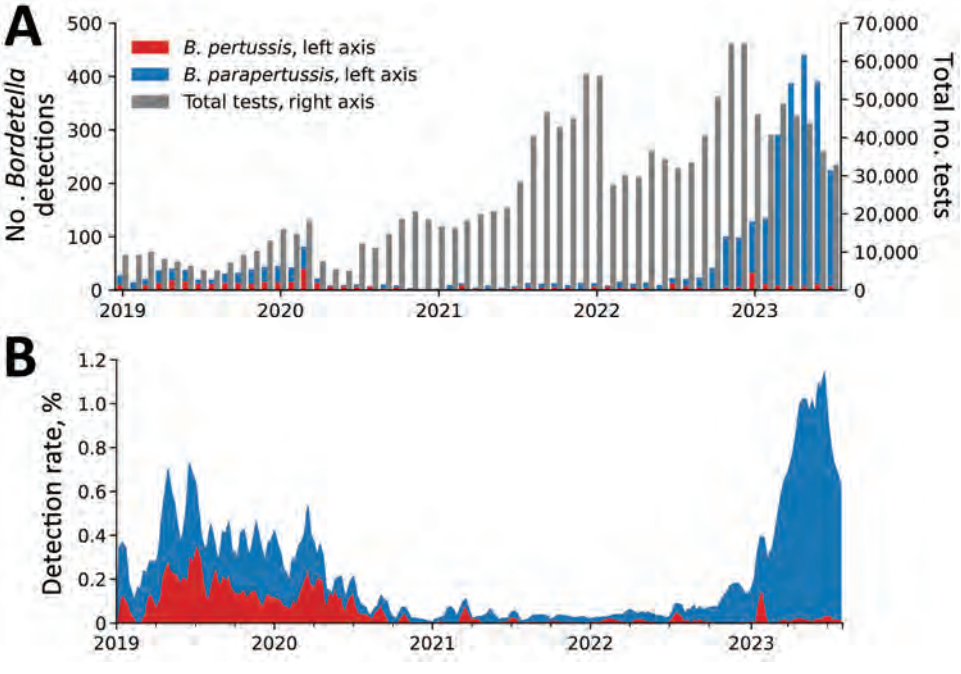

Figure. *Bordetalla pertussis* and *B. parapertussis* detection count and detection rates, January 2019–July 2023. A) Total number of tests and number of tests positive for *B. pertussis* or *B. parapertussis* per month. Scales for the y-axes differ substantially to underscore patterns but do not permit direct comparisons. B) Detection rate (3-week centered rolling average) for *B. pertussis* and *B. parapertussis*.

Table. *Bordetella parapertussis* testing, United States, 2019–2023*

Year, region	States	No. (%) tests performed		
		Facilities	RP2 tests	RP2.1 tests†
2019				
Midwest	IL, IN, KS, MI, MO, ND, NE, OH, SD, WI	19 (52.8)	49,226 (48.9)	0
Northeast	NY, PA	3 (8.3)	6,252 (6.2)	0
South	FL, SC, TX	6 (16.7)	13,109 (13.0)	0
West	AK, AZ, CA, ID, UT	8 (22.2)	31,989 (31.8)	0
2020				
Midwest	IL, IN, KS, MI, MO, ND, NE, OH, SD, WI	36 (45.0)	44,545 (27.3)	44,832 (27.5)
Northeast	NY, PA	5 (6.2)	1,988 (1.2)	1,511 (0.9)
South	AL, FL, GA, LA, SC, TN, TX, VA	18 (22.5)	9,208 (5.6)	17,352 (10.6)
West	AK, AZ, CA, CO, ID, OR, UT, WY	20 (25.0)	25,663 (15.7)	13,845 (8.5)
2021				
Midwest	IA, IL, IN, KS, MI, MO, ND, NE, OH, SD, WI	40 (39.2)	3125 (0.8)	137,322 (36.8)
Northeast	MA, NY, PA	6 (5.9)	0	37,207 (10.0)
South	AL, AR, FL, GA, KY, LA, MD, MS, SC, TN, TX, VA	31 (30.4)	405 (0.1)	124,544 (33.4)
West	AK, AZ, CA, CO, ID, MT, NM, OR, UT, WY	25 (24.5)	1,709 (0.5)	64,733 (17.4)
2022				
Midwest	IA, IL, IN, KS, MI, MO, ND, NE, OH, SD, WI	41 (36.9)	502 (0.1)	169,739 (33.9)
Northeast	MA, NJ, NY, PA, VT	8 (7.2)	0	65,602 (13.1)
South	AL, AR, FL, GA, KY, LA, MD, MS, NC, SC, TN, TX, VA	35 (31.5)	0	174,014 (34.8)
West	AK, AZ, CA, CO, ID, MT, NM, OR, UT, WA, WY	26 (23.4)	221	87,262 (17.5)
2023‡				
Midwest	IA, IL, IN, KS, MI, MO, ND, NE, OH, SD, WI	39 (34.8)	0	98,274 (31.7)
Northeast	MA, NJ, NY, PA, VT	8 (7.1)	0	51,160 (16.5)
South	AL, AR, FL, GA, KY, LA, MD, MS, NC, SC, TN, TX, VA	37 (33.0)	0	114,433 (36.9)
West	AK, AZ, CA, CO, ID, MT, NM, OR, UT, WA, WY	27 (24.1)	0	44,612 (14.4)

*Rates consider the total number for each year across all regions and test versions.
†The BIOFIRE RP2.1 test (bioMérieux, https://www.biomerieux-usa.com, authorized for emergency use in May 2020) is identical to the BIOFIRE RP2 test except for the addition of SARS-CoV-2. Use of the 2 test versions overlapped primarily during June–July 2020. During that time, comparison of detection rates of the 2 test versions did not show strong evidence of a statistically significant difference for *B. pertussis* (p = 0.16) or *B. parapertussis* (p = 0.72).
‡The 2023 data collection period was January–July.

(95% binomial CI) *B. pertussis* detection rates (0.14% [95% CI 0.12%–0.16%]) were slightly lower than the *B. parapertussis* detection rates (0.21% [95% CI 0.18%–0.23%]). From mid-2020 through late 2022, the detection rates of *B. pertussis* and *B. parapertussis* declined significantly; the combined rate remained <0.20%. In 2023 (January–July), we observed a marked increase in *B. parapertussis* detections; average detection rate was 0.65% (95% CI 0.62%–0.68%) and peaked mid-June at 1.3% (95% CI 1.1%–1.6%). We did not observe a similar increase in *B. pertussis* detections, for which the average detection rate in 2023 was 0.03% (95% CI 0.02%–0.04%).

Comparing recent (January 2023–July 2023) rates to rates from a commensurate prepandemic time frame (January 2019–July 2019), we observed an increase of 0.44% (95% CI 0.39%–0.49%) for *B. parapertussis* and a decrease of 0.12% (95% CI 0.09%–0.16%) for *B. pertussis*. Those findings lend evidence to a significant (p<0.001) national *B. parapertussis* increase and *B. pertussis* decrease; similar trends were observed in each US Census region. Of the 23 facilities with data for both time frames, the *B. parapertussis* detection rate increased for 20 facilities.

Co-detection of *B. pertussis* and *B. parapertussis* in the same test was rare, observed in only 9 tests (0.03% of tests positive for either *B. pertussis* or *B. parapertussis*) (Appendix Table, https://wwwnc.cdc.gov/EID/article/30/5/23-1278-App1.pdf). However, a virus was co-detected with 47.1% (95% CI 42.5%–51.7%) of *B. pertussis* and 66.2% (95% CI 64.4%–68.0%) of *B. parapertussis* detections.

In summary, we found that 95% of *Bordetella* spp. detected in the last year of the study (July 2022–July 2023) were *B. parapertussis*. The observed high incidence of virus co-detections along with previous data that found that clinical infection developed in <5% of those with *B. parapertussis* (compared with 75% of those with *B. pertussis*) may suggest that many of the observed *B. parapertussis* detections were subclinical (*7*). Although the reason behind the observed increase in *B. parapertussis* detections is unknown, Bhattacharyya et al. suggested that the erratic dynamics of whooping cough could be explained by interactions of *B. pertussis* and *B. parapertussis*, which oscillate out of phase through age-dependent convalescence (*8*). It is possible that secondary effects of the COVID-19 pandemic, such as decreased population immunity, affected this interaction, because incidence of many other respiratory illnesses also decreased during the pandemic, followed by atypical prevalence (*9*).

Testing and near real-time surveillance of *B. parapertussis* are needed to enhance prompt response to clinical outbreaks and contamination events, both of which have been reported (*1*,*10*). Determining the clinical implications of the observed *B. parapertussis* surge may help inform patient management and public health action.

The data obtained by bioMérieux are subject to the terms and conditions of a data-use agreement by and between bioMérieux and each facility participating in the BIOFIRE Syndromic Trends program. If a dataset is requested, bioMérieux will review such request internally to ensure that any disclosure does not conflict with bioMérieux obligations and restrictions set forth in the data-use agreement. Code available upon reasonable request.

All authors are employees of bioMérieux.

About the Author

Dr. Noble is a data scientist at bioMérieux, Salt Lake City, Utah. Her research interests include syndromic testing and spatiotemporal trends of infectious diseases.

References:

1. Watanabe M, Nagai M. Whooping cough due to *Bordetella parapertussis*: an unresolved problem. Expert Rev Anti Infect Ther. 2004;2:447–54. https://doi.org/10.1586/14787210.2.3.447
2. Faulkner A, Skoff TH, Martin SW, Cassiday PK, Tondella ML, Liang JL. Chapter 10: Pertussis. In: Manual for the surveillance of vaccine-preventable diseases [cited 2024 Apr 10]. A https://www.cdc.gov/vaccines/pubs/surv-manual/chpt10-pertussis.html
3. Cherry JD, Seaton BL. Patterns of *Bordetella parapertussis* respiratory illnesses: 2008–2010. Clin Infect Dis. 2012;54:534–7. https://doi.org/10.1093/cid/cir860
4. Leber AL, Everhart K, Daly JA, Hopper A, Harrington A, Schreckenberger P, et al. Multicenter evaluation of BioFire FilmArray respiratory panel 2 for detection of viruses and bacteria in nasopharyngeal swab samples. J Clin Microbiol. 2018;56:e01945–17. https://doi.org/10.1128/JCM.01945-17
5. BioFire Diagnostics LLC BioFire® Respiratory Panel 2.1 (RP2.1) de novo instructions for use. 2021 [cited 2024 Jan 12]. https://www.biofiredx.qarad.eifu.online/ITI/US/all?keycode=ITI0105
6. Meyers L, Ginocchio CC, Faucett AN, Nolte FS, Gesteland PH, Leber A, et al. Automated real-time collection of pathogen-specific diagnostic data: syndromic infectious disease epidemiology. JMIR Public Health Surveill. 2018;4:e59. https://doi.org/10.2196/publichealth.9876
7. Lautrop H. Epidemics of parapertussis. 20 years' observations in Denmark. Lancet. 1971;297:1195–8. https://doi.org/10.1016/S0140-6736(71)91713-2
8. Bhattacharyya S, Ferrari MJ, Bjørnstad ON. Species interactions may help explain the erratic periodicity of whooping cough dynamics. Epidemics. 2018;23:64–70. https://doi.org/10.1016/j.epidem.2017.12.005
9. Shaw D, Abad R, Amin-Chowdhury Z, Bautista A, Bennett D, Broughton K, et al. Trends in invasive bacterial diseases during the first 2 years of the COVID-19 pandemic: analyses of prospective surveillance data from 30 countries and territories in the IRIS Consortium. Lancet Digit Health. 2023;5:e582–93. https://doi.org/10.1016/S2589-7500(23)00108-5
10. Flipse J, Tromp AT, Bosman J, Ten Hove C, Beks H, Kortbeek T, et al. Pseudo-outbreak of *Bordetella parapertussis* caused by contaminated swabs in the Netherlands. Emerg Infect Dis. 2022;28:890–2. https://doi.org/10.3201/eid2804.212097

Address for correspondence: Brooklyn A. Noble, bioMérieux, 1201 S 4800 W, Salt Lake City, UT 84104, USA; email: brooklyn.noble@biomerieux.com

Sphingobium yanoikuyae Bacteremia, Japan

Yayoi Miyamatsu,[1] Ryutaro Tanizaki,[1] Satoko Yamada

Author affiliation: Ise Municipal General Hospital, Ise, Japan

DOI: https://doi.org/10.3201/eid3005.231514

We report a case of *Sphingobium yanoikuyae* bacteremia in an 89-year-old patient in Japan. No standard antimicrobial regimen has been established for *S. yanoikuyae* infections. However, ceftriaxone and ceftazidime treatments were effective in this case. Increased antimicrobial susceptibility data are needed to establish appropriate treatments for *S. yanoikuyae*.

The genus *Sphingomonas* was divided into 4 clusters, and *Sphingomonas yanoikuyae* was renamed *Sphingobium yanoikuyae* (*1*). *S. yanoikuyae* is a gram-negative, nonsporulating, strictly aerobic rod-shaped bacterium (*2*) widely distributed in natural environments, especially in water and soil, and is rarely a human pathogen (*3*). Although 1 case of *S. yanoikuyae* infection has been reported in the central nervous system (CNS) of a child (*4*), infections have not been reported in adults. We report a case of *S. yanoikuyae* bacteremia in an older man.

[1]These authors contributed equally to this article.

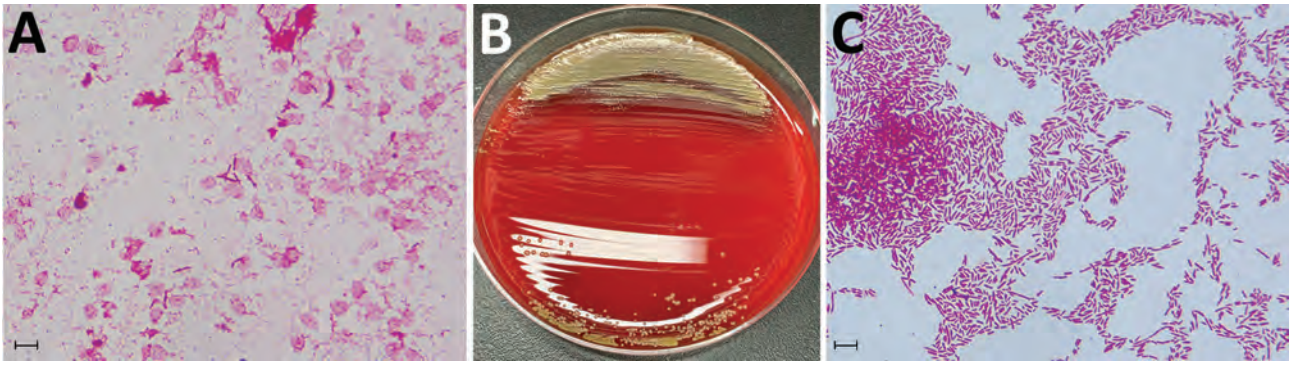

Figure. Identification of *Sphingobium yanoikuyae* bacteremia in 89-year-old man, Japan. A) Gram stain of the organisms growing in a blood sample incubated in a BACTEC Plus Aerobic/F Culture Vial (Becton Dickinson, https://www.bd.com). Scale bar is 10 μm. B) Colonies of *S. yanoikuyae* cultured on Trypticase Soy Agar with 5% Sheep Blood (Becton Dickinson). C) Gram stain of *S. yanoikuyae* bacteria from a colony obtained by subculturing positive blood culture fluid on Trypticase Soy Agar with 5% Sheep Blood at 35°C in an aerobic environment. Scale bar is 10 μm.

An 89-year-old man from Japan sought care at an emergency department because of fever and chills lasting 1 hour. He had been taking prednisolone (5 mg/day) for 6 years for interstitial pneumonia. He was alert, and his vital signs were as follows: body temperature, 38.6°C; heart rate, 71 beats/min; blood pressure, 112/64 mmHg; respiratory rate, 28 breaths/min; and blood oxygen saturation, 100% while breathing room air. Laboratory findings revealed elevated leukocyte count (16,100 cells/μL; reference range 3,300–8,600 cells/μL) and C-reactive protein level (4.16 mg/dL; reference range 0–0.14 mg/dL) but were otherwise unremarkable. Chest computed tomography revealed honeycombing and multiple reticular shadows in both lungs, unchanged from 5 months earlier. We suspected sepsis and administered intravenous ceftriaxone (2 g/24 h) after obtaining 2 sets of blood samples for culture. On day 2, the patient's fever subsided. On day 5, a blood culture sample yielded positive results after incubation in an aerobic BACTEC Plus Aerobic/F Culture Vial in a BACTEC FX system (Becton Dickinson, https://www.bd.com). Gram staining revealed small gram-negative rods (Figure, panel A) that we were unable to identify by using mass spectrometry (MALDI Biotyper; Bruker Daltonics, https://www.bruker.com). We subsequently cultured the positive blood culture fluid on Trypticase Soy Agar with 5% Sheep Blood (Becton Dickinson) at 35°C in an aerobic environment and identified *S. yanoikuyae* by using mass spectrometry of bacteria isolated on day 6 (Figure, panels B, C). Genetic analysis of a 1,402 nt 16S rRNA sequence revealed 99.5% homology with *S. yanoikuyae* (Appendix, https://wwwnc.cdc.gov/EID/article/30/5/23-1514-App1.pdf). We performed antimicrobial susceptibility testing by using the dilution method and a Neg MIC NF1J panel (Beckman Coulter, https://www.beckmancoulter.com) in accordance with Clinical and Laboratory Standards Institute (CLSI) criteria for other non-Enterobacterales bacteria (Table) (*5*). We determined the ceftriaxone MIC by using the Neg MIC EN 2J panel for Enterobacterales bacteria and Pos MIC 1J panel for gram-positive cocci (both Beckman Coulter). Although *S. yanoikuyae* was susceptible to ceftriaxone, we preferred to use antimicrobial drugs that were effective against glucose nonfermenting bacteria, which is the fermentation pattern exhibited by *Sphingomonas* spp. On day 6, we switched the antimicrobial to ceftazidime (1 g/8 h). We did not detect *S. yanoikuyae* in blood cultures at follow-up on days 6 and 11, indicating treatments were effective, and the patient's condition remained stable. However, severe aspiration

Table. Drug susceptibility pattern for *Sphingobium yanoikuyae* isolated from an 89-year-old man's blood sample in study of *S. yanoikuyae* bacteremia, Japan*

Antimicrobial drug	MIC†, μg/mL	Breakpoint MIC‡, μg/mL
Piperacillin/tazobactam	≤4/4	16/4
Ceftriaxone	4	8
Ceftazidime	2	8
Cefepime	≤1	8
Aztreonam	>16	8
Imipenem	1	4
Meropenem	4	4
Gentamicin	≤1	4
Tobramycin	≤1	4
Amikacin	≤4	16
Minocycline	≤1	4
Ciprofloxacin	≤0.25	1
Levofloxacin	≤0.5	2
Trimethoprim/sulfamethoxazole	≤1/19	2/38

*Drug susceptibility data according to Clinical and Laboratory Standards Institute criteria (*5*). MIC values for antimicrobial drugs, except ceftriaxone, were determined by using a Neg MIC NF1J panel (Beckman Coulter, https://beckmancoulter.com). The MIC value of ceftriaxone was determined by using Neg MIC EN 2J Enterobacterales and Pos MIC 1J gram-positive cocci panels (both Beckman Coulter).
†MIC for the isolate from 89-year-old case-patient.
‡Breakpoints for other non-Enterobacterales susceptible strains.

pneumonia developed on day 16, and he died of respiratory failure on day 17.

Within the genus *Sphingomonas*, *S. paucimobilis* is the most frequently reported cause of human infection (*6*), predominantly causing bacteremia, septicemia, peritonitis, lung infections, pneumonia, or urinary tract infections; 24 of 52 (46%) cases in published literature were of nosocomial origin (*7*). Thus, *Sphingomonas* spp. might be a chief cause of nosocomial infection in addition to other glucose nonfermenting bacteria. The *S. yanoikuyae* infection reported previously in a child was a nosocomial infection after head surgery (*4*). Although this case in an older man was not a nosocomial infection, he had been taking prednisolone for 6 years, which might have increased his infection risk.

No antimicrobial regimen has been established for treating *S. yanoikuyae* infections. The child who had a CNS infection received 28 days of intravenous meropenem and 5 days of intrathecal amikacin (*4*). A novel bacteria strain, CC4533, isolated from a contaminated Tris-acetate-phosphate agar plate used to grow *Chlamydomonas reinhardtii*, showed 99.55% DNA sequence identity to *S. yanoikuyae*; drug susceptibility testing indicated CC4533 was resistant to polymyxin B, penicillin, and chloramphenicol and sensitive to neomycin (*8*). We treated our patient with intravenous ceftriaxone and then ceftazidime. Cefepime, a 4th-generation cephalosporin, can penetrate the cerebral spinal fluid and has an additional quaternary ammonium group enabling penetration through the outer membrane of gram-negative bacteria, increasing effectiveness against β-lactamase–producing gram-negative bacilli (*9*). We selected ceftazidime, a 3rd-generation cephalosporin, because our clinical findings did not suggest a CNS infection, and *S. yanoikuyae* did not produce β-lactamase.

No breakpoints have been established for *Sphingobium* sp. bacteria; thus, we evaluated antimicrobial susceptibility according to CLSI criteria for other non-Enterobacterales bacteria (*5*). According to the dilution method, MIC values for ceftriaxone were >2 by using the Enterobacterales panel and ≤4 by using the gram-positive cocci panel. The ceftriaxone MIC for the isolate from this patient was 4, which is below the CLSI breakpoint of 8 for other non-Enterobacterales bacteria (*5*), indicating that the isolate was susceptible to ceftriaxone.

In conclusion, no standard antimicrobial treatment regimen has been established for *S. yanoikuyae*. Ceftriaxone and ceftazidime were effective treatments for *S. yanoikuyae* infection in this patient. Increased antimicrobial susceptibility data are needed to establish appropriate treatments for *S. yanoikuyae*.

Acknowledgments

We thank Editage (http://www.editage.com) for reviewing and editing this manuscript for English language.

About the Author

Dr. Miyamatsu is a physician in the Department of Internal Medicine and General Medicine, Ise Municipal General Hospital, Ise, Japan. Her primary research interest is general internal medicine.

References

1. Takeuchi M, Hamana K, Hiraishi A. Proposal of the genus *Sphingomonas* sensu stricto and three new genera, *Sphingobium, Novosphingobium* and *Sphingopyxis*, on the basis of phylogenetic and chemotaxonomic analyses. Int J Syst Evol Microbiol. 2001;51:1405–17. https://doi.org/10.1099/00207713-51-4-1405
2. Yabuuchi E, Yano I, Oyaizu H, Hashimoto Y, Ezaki T, Yamamoto H. Proposals of *Sphingomonas paucimobilis* gen. nov. and comb. nov., *Sphingomonas parapaucimobilis* sp. nov., *Sphingomonas yanoikuyae* sp. nov., *Sphingomonas adhaesiva* sp. nov., *Sphingomonas capsulata* comb. nov., and two genospecies of the genus *Sphingomonas*. Microbiol Immunol. 1990;34:99–119. https://doi.org/10.1111/j.1348-0421.1990.tb00996.x
3. Ammendolia MG, Bertuccini L, Minelli F, Meschini S, Baldassarri L. A *Sphingomonas* bacterium interacting with epithelial cells. Res Microbiol. 2004;155:636–46. https://doi.org/10.1016/j.resmic.2004.05.009
4. Guner Ozenen G, Sahbudak Bal Z, Bilen NM, Yildirim Arslan S, Aydemir S, Kurugol Z, et al. The first report of *Sphingomonas yanoikuyae* as a human pathogen in a child with a central nervous system infection. Pediatr Infect Dis J. 2021;40:e524. https://doi.org/10.1097/INF.0000000000003301
5. Clinical and Laboratory Standards Institute. Performance standards for antimicrobial susceptibility testing; thirty-third edition (M100-ED33). Wayne (PA): The Institute; 2023.
6. Laupland KB, Paterson DL, Stewart AG, Edwards F, Harris PNA. *Sphingomonas paucimobilis* bloodstream infection is a predominantly community-onset disease with significant lethality. Int J Infect Dis. 2022;119:172–7. https://doi.org/10.1016/j.ijid.2022.03.060
7. Ryan MP, Adley CC. *Sphingomonas paucimobilis*: a persistent gram-negative nosocomial infectious organism. J Hosp Infect. 2010;75:153–7. https://doi.org/10.1016/j.jhin.2010.03.007
8. Mitra M, Nguyen KM, Box TW, Gilpin JS, Hamby SR, Berry TL, et al. Isolation and characterization of a novel *Sphingobium yanoikuyae* strain variant that uses biohazardous saturated hydrocarbons and aromatic compounds as sole carbon sources. F1000Res. 2020;9:767. https://doi.org/10.12688/f1000research.25284.1
9. Bui T, Preuss CV. Cephalosporins. Treasure Island (FL): StatPearls Publishing; 2023 [cited 2024 Feb 3]. https://www.ncbi.nlm.nih.gov/books/NBK551517

Address for correspondence: Ryutaro Tanizaki, Department of Internal Medicine and General Medicine, Ise Municipal General Hospital, 3038, Kusubecho, Ise, Mie 516-0014, Japan; email: rtanizaki@hospital.ise.mie.jp

Vladimir Donatovich Orlovsky (1842–1914) *Harvest* (1882). Oil on canvas, 24.4 in x 39.4 in/62 cm x 100 cm. National Art Museum of Ukraine, Kyiv, Ukraine. Photo credit: Alfredo Dagli Orti. Digital image from Art Resource, New York, New York, USA.

A Looming Storm on the Horizon

Byron Breedlove

Ukrainian realist painter Vladimir Orlovsky was born in Kiev (now Kyiv), Ukraine, where he received his early artistic training. In 1861, he attended the Saint Petersburg Academy of Fine Arts. After graduating in 1868, Orlovsky earned a medal of recognition and monetary award for a series of paintings of Crimean landscapes, enabling him to travel and paint throughout Europe for the next 3 years. He later joined the Saint Petersburg Academy faculty and in 1878 was named a professor of art. His work was popular among the aristocratic class, including the Emperor of Russia, Alexander III.

According to the *Encyclopedia of Ukraine*, "In 1886 he returned to Ukraine, where he taught at the Kyiv Drawing School and helped found the Kyiv Art School. As Orlovsky gradually freed himself from academism, his works acquired a more natural composition, more confident lines, and a finer coloration." *Harvest*, this month's cover image, is one among "his famous depictions of the Ukrainian and Crimean countryside."

In *Harvest*, Orlovsky depicted workers on the Ukrainian steppe cutting grain with scythes. In the foreground, one worker bends and grasps the stalks as the other looks across the field. To their left are a brown jug and perhaps remains of a midday meal. The uncut grain twitches and bends, pressed by winds from the rainstorm swelling over the plains. A third person walking in the distance and the remote horizon revealed as a thin strip of light define the scale of the steppes. A maelstrom of purplish clouds laden with rain roils above the fields save an open space of blue sky tinged with white clouds that

Author affiliation: Centers for Disease Control and Prevention, Atlanta, Georgia, USA.

DOI: https://doi.org/10.3201/eid3005.AC-3005

illuminates the lower third of the canvas. Despite the pending storm, the workers seem untroubled and intent on their task.

An outbreak of a tickborne hemorrhagic disease documented in Crimea in 1944 may have occurred in a setting similar to the one in Orlovsky's painting. That disease, now called Crimean-Congo hemorrhagic fever (CCHF), is caused by infection with a tickborne *Nairovirus,* Crimean-Congo hemorrhagic fever virus (CCHFV), in the family Bunyaviridae. In an article in *Antiviral Research*, Dennis A. Bente and coauthors wrote that researchers investigating that outbreak in Crimea "were quickly able to link cases of the new disease to tick exposure. They noted that, because large areas of cultivated land had been abandoned during the German occupation, the population of hares and other wild hosts of *Hyalomma* ticks had increased, and soldiers and farm workers engaged in restoring agricultural production were suffering large numbers of tick bites."

Originally known as Crimean hemorrhagic fever, the disease acquired its current hyphenated name after identical symptoms were reported in the Democratic Republic of the Congo in 1969. It has been around much longer, of course, and researcher Chris A. Whitehouse reported that a hemorrhagic disease described by a 12th-century physician in the region today called Tadzhikistan was probably CCHF. As Whitehouse noted, CCHF is indicated by "the presence of blood in the urine, rectum, gums, vomitus, sputum, and abdominal cavity."

According to the World Health Organization (WHO), hosts for the ticks include many wild animals and domestic animals such as cattle, sheep, and goats; most cases of CCHF among humans have occurred among people working with livestock, including those preparing carcasses of infected animals. WHO also states, "Human-to-human transmission can occur resulting from close contact with the blood, secretions, organs or other bodily fluids of infected persons." Bente and his coauthors stated that CCHF "is the most widespread tick-borne viral infection of humans, occurring across a vast area from western China through southern Asia and the Middle East to southeastern Europe and throughout most of Africa." WHO considers CCHF a high-priority disease. The case-fatality rate is as high as 40%, and the disease is both difficult to prevent and challenging to treat.

Several articles in this issue address CCHF, including a three-part series, Crimean-Congo Hemorrhagic Fever Virus for Clinicians, by M.G. Frank et al., which addresses a trilogy of topics: diagnosis, clinical management, and therapeutics; virology, pathogenesis, and pathology; and epidemiology, clinical manifestations, and prevention. The authors report "lack of licensed effective therapeutic and prophylactic drugs, gaps in our understanding of CCHFV pathogenesis and immunology, and slow progression in development of CCHF medical countermeasures."

As temperatures increase around the world, could CCHF become the next storm brewing on public health horizon, like the dark clouds in Orlovsky's *Harvest*? CDC researcher Jessica Spengler and her coauthors wrote in a 2019 article, "Without question, frequency of disease reporting is increasing. Whether this represents expansion to new regions or changes to existing areas of sporadic circulation will continue to be challenging to differentiate. This rise could be due to increased awareness, but awareness is unlikely to be the only contributor."

Bibliography

1. Bente DA, Forrester NL, Watts DM, McAuley AJ, Whitehouse CA, Bray M. Crimean-Congo hemorrhagic fever: history, epidemiology, pathogenesis, clinical syndrome and genetic diversity. Antiviral Res. 2013;100:159–89. https://doi.org/10.1016/j.antiviral.2013.07.006
2. Centers for Disease Control and Prevention. Crimean-Congo hemorrhagic fever (CCHF) [cited 2024 Apr 3]. https://www.cdc.gov/vhf/crimean-congo
3. Encyclopedia of Art. Orlovsky Vladimir Donatovich (1842–1914) [cited 2024 Apr 3]. http://www.artsait.ru/art/o/orlovskyV/main.htm
4. Encyclopedia of Ukraine. Orlovsky, Volodymer [in Ukrainian] [cited 2024 April 3]. https://www.encyclopediaofukraine.com/pages/O/R/OrlovskyVolodymyr.htm
5. Frank MG, Weaver G, Raabe V; State of the Clinical Science Working Group of the National Emerging Pathogens Training and Education Center's Special Pathogens Research Network. Crimean-Congo hemorrhagic fever virus for clinicians—diagnosis, clinical management, and therapeutics. Emerg Infect Dis. 2024;30:30. https://doi.org/10.3201/eid3005.231648
6. Mehand MS, Al-Shorbaji F, Millett P, Murgue B. The WHO R&D Blueprint: 2018 review of emerging infectious diseases requiring urgent research and development efforts. Antiviral Res. 2018;159:63–7. https://doi.org/10.1016/j.antiviral.2018.09.009
7. Spengler JR, Bergeron É, Spiropoulou CF. Crimean-Congo hemorrhagic fever and expansion from endemic regions. Curr Opin Virol. 2019;34:70–8. https://doi.org/10.1016/j.coviro.2018.12.002
8. Whitehouse CA. Crimean-Congo hemorrhagic fever. Antiviral Res. 2004;64:145–60. https://doi.org/10.1016/j.antiviral.2004.08.001
9. World Health Organization. Crimean-Congo haemorrhagic fever [cited 2024 Apr 3]. https://www.who.int/news-room/fact-sheets/detail/crimean-congo-haemorrhagic-fever

Address for correspondence: Byron Breedlove, EID Journal, Centers for Disease Control and Prevention, 1600 Clifton Rd NE, Mailstop H16-2, Atlanta, GA 30329-4018, USA; email: wbb1@cdc.gov

EMERGING INFECTIOUS DISEASES®

Upcoming Issue
Respiratory Infections • June 2024

- Deciphering Unexpected Vascular Locations of *Scedosporium* spp. and *Lomentospora prolificans* Fungal Infections, France
- An Electronic Health Record–Based Algorithm for Respiratory Virus–like Illness
- SARS-CoV-2 Disease Severity in Children during Pre-Delta, Delta, and Omicron Periods, Colorado
- Effectiveness of 23-Valent Pneumococcal Polysaccharide Vaccine Against Invasive Pneumococcal Disease in Follow-Up Study, Denmark
- Sporadic Occurrence of Ensitrelvir-Resistant SARS-CoV-2, Japan
- Antibodies to H5N1 Influenza A Virus in Retrieving Hunting Dogs, Washington State, USA
- Evolution and Antigenic Differentiation of Avian Influenza A(H7N9) Virus, China
- *Burkholderia semiarida* as Cause of Recurrent Pulmonary Infection in Immunocompetent Patient, China
- SARS-CoV-2 in Captive Nonhuman Primates, Spain, 2020–2023
- Infection- and Vaccine-Induced SARS-CoV-2 Seroprevalence in Persons 0–101 Years of Age, Japan, 2023
- Evaluation of Humoral Immunity Elicited by XBB.1.5 Monovalent COVID-19 Vaccine

Complete list of articles in the June issue at https://wwwnc.cdc.gov/eid/#issue-309

Earning CME Credit

To obtain credit, you should first read the journal article. After reading the article, you should be able to answer the following, related, multiple-choice questions. To complete the questions (with a minimum 75% passing score) and earn continuing medical education (CME) credit, please go to http://www.medscape.org/journal/eid. Credit cannot be obtained for tests completed on paper, although you may use the worksheet below to keep a record of your answers.

You must be a registered user on http://www.medscape.org. If you are not registered on http://www.medscape.org, please click on the "Register" link on the right hand side of the website.

Only one answer is correct for each question. Once you successfully answer all post-test questions, you will be able to view and/or print your certificate. For questions regarding this activity, contact the accredited provider, CME@medscape.net. For technical assistance, contact CME@medscape.net. American Medical Association's Physician's Recognition Award (AMA PRA) credits are accepted in the US as evidence of participation in CME activities. For further information on this award, please go to https://www.ama-assn.org. The AMA has determined that physicians not licensed in the US who participate in this CME activity are eligible for *AMA PRA Category 1 Credits*™. Through agreements that the AMA has made with agencies in some countries, AMA PRA credit may be acceptable as evidence of participation in CME activities. If you are not licensed in the US, please complete the questions online, print the AMA PRA CME credit certificate, and present it to your national medical association for review..

Article Title

Crimean-Congo Hemorrhagic Fever Virus for Clinicians—Diagnosis, Clinical Management, and Therapeutics

CME Questions

1. You are seeing a 40-year-old man who works in on a ranch. He complains of 5 days of fever, malaise, and loose stools followed by a petechial rash over his back and shoulders for the past day. Which of the following diagnostic tests for Crimean-Congo hemorrhagic fever virus (CCHFV) would be most appropriate for him?

A. Viral culture
B. Reverse-transcriptase polymerase chain reaction (RT-PCR)
C. Serum immunoglobulin (Ig)M
D. Serum IgG

2. Which of the following statements regarding the laboratory assessment of suspected CCHF is most accurate?

A. RT-PCR remains reliable in the detection of CCHFV until around Day 15 of illness
B. The accuracy of real-time RT-PCR approaches 60% in identifying CCHFV
C. IgM becomes detectable within 3 days of infection with CCHFV
D. IgG remains detectable for ≥ 3 years

3. Which of the following statements regarding vaccination against CCHF is most accurate?

A. An inactivated CCHFV vaccine is available only in Bulgaria, but has not undergone human trials.
B. Randomized trials of the inactivated CCHFV vaccine have demonstrated vaccine efficacy of 50% in the prevention of CCHF
C. Higher anti-CCHF antibody titers correlate with vaccine efficacy against CCHF in animal models
D. Higher neutralizing antibody titers correlate with vaccine efficacy against CCHF in animal models

4. Which of the following statements regarding the treatment of CCHF is most accurate?

A. There is no specific antiviral therapy for CCHFV
B. Ribavirin has not been tested in randomized trials
C. Favipravir has been demonstrated to reduce mortality associated with CCHF in clinical trials
D. Plasmapheresis remains the treatment of choice for CCHF

Earning CME Credit

To obtain credit, you should first read the journal article. After reading the article, you should be able to answer the following, related, multiple-choice questions. To complete the questions (with a minimum 75% passing score) and earn continuing medical education (CME) credit, please go to http://www.medscape.org/journal/eid. Credit cannot be obtained for tests completed on paper, although you may use the worksheet below to keep a record of your answers.

You must be a registered user on http://www.medscape.org. If you are not registered on http://www.medscape.org, please click on the "Register" link on the right hand side of the website.

Only one answer is correct for each question. Once you successfully answer all post-test questions, you will be able to view and/or print your certificate. For questions regarding this activity, contact the accredited provider, CME@medscape.net. For technical assistance, contact CME@medscape.net. American Medical Association's Physician's Recognition Award (AMA PRA) credits are accepted in the US as evidence of participation in CME activities. For further information on this award, please go to https://www.ama-assn.org. The AMA has determined that physicians not licensed in the US who participate in this CME activity are eligible for *AMA PRA Category 1 Credits*™. Through agreements that the AMA has made with agencies in some countries, AMA PRA credit may be acceptable as evidence of participation in CME activities. If you are not licensed in the US, please complete the questions online, print the AMA PRA CME credit certificate, and present it to your national medical association for review.

Article Title

Crimean-Congo Hemorrhagic Fever Virus for Clinicians—Epidemiology, Clinical Manifestations, and Prevention

CME Questions

1. Which of the following statements regarding the epidemiology of Crimean-Congo hemorrhagic fever (CCHF) is most accurate?

A. CCHF is the most geographically widespread tickborne disease
B. There are about 100,000 cases of CCHF diagnosed worldwide each year
C. The primary vector of CCHF is the Amblyomma tick species
D. Healthcare workers are not a group at elevated risk for CCHF

2. Which of the following statements best characterizes the clinical course of CCHF?

A. Convalescent→recurrence→disseminated illness
B. Acute infection→subacute arthritis→tertiary features
C. Asymptomatic→hemorrhagic→myocarditis/pericarditis→late sequelae
D. Incubation→prehemorrhagic→hemorrhagic→convalescent

3. Which of the following statements regarding other clinical characteristics of CCHF is most accurate?

A. The typical incubation period is 2 to 4 days
B. Fever typically lasts 4 to 5 days
C. Severe headache is rare
D. The hemorrhagic phase usually last about 7 days

Emerging Infectious Diseases
Photo Quiz Articles

Volume 14, Number 9
September 2008

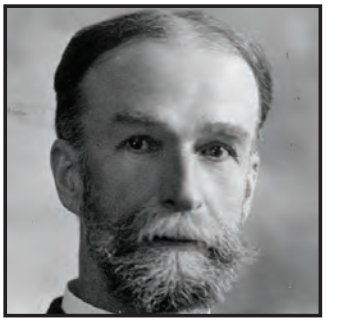

Volume 14, Number 12
December 2008

Volume 15, Number 9
September 2009

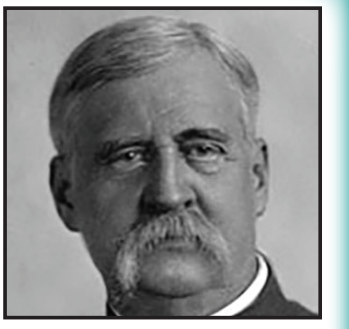

Volume 15, Number 10
October 2009

Volume 16, Number 6
June 2010

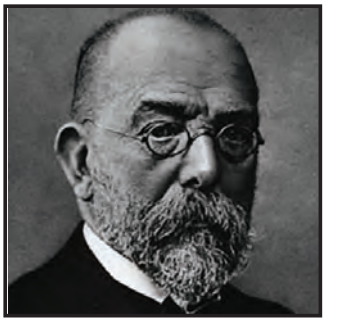

Volume 17, Number 3
March 2011

Volume 17, Number 12
December 2011

Volume 19, Number 4
April 2013

Volume 20, Number 5
May 2014

Volume 21, Number 9
September 2015

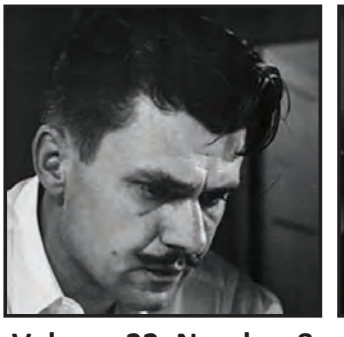

Volume 22, Number 8
August 2016

Volume 28, Number 3
March 2022

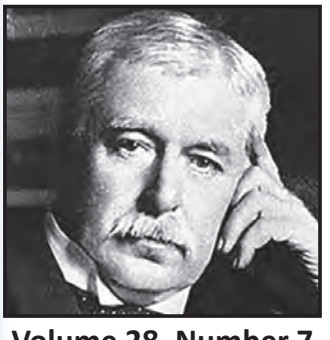

Volume 28, Number 7
July 2022

Click on the link below to read about the people behind the science.

https://bit.ly/3LN02tr

See requirements for submitting a photo quiz to EID.

https://bit.ly/3VUPqfj

EID Journal